EPA-650/2-75-016

JANUARY 1975

Environmental Protection Technology Series

SYMPOSIUM ON ELECTROSTATIC PRECIPITATORS FOR THE CONTROL OF FINE PARTICLES

Office of Research and Development
U.S. Environmental Protection Agency
Washington, DC 20460

RESEARCH REPORTING SERIES

Research reports of the Office of Research and Development, U. S. Environmental Protection Agency, have been grouped into series. These broad categories were established to facilitate further development and application of environmental technology. Elimination of traditional grouping was consciously planned to foster technology transfer and maximum interface in related fields. These series are:

1. ENVIRONMENTAL HEALTH EFFECTS RESEARCH
2. ENVIRONMENTAL PROTECTION TECHNOLOGY
3. ECOLOGICAL RESEARCH
4. ENVIRONMENTAL MONITORING
5. SOCIOECONOMIC ENVIRONMENTAL STUDIES
6. SCIENTIFIC AND TECHNICAL ASSESSMENT REPORTS
9. MISCELLANEOUS

This report has been assigned to the ENVIRONMENTAL PROTECTION TECHNOLOGY series. This series describes research performed to develop and demonstrate instrumentation, equipment and methodology to repair or prevent environmental degradation from point and non-point sources of pollution. This work provides the new or improved technology required for the control and treatment of pollution sources to meet environmental quality standards.

EPA-650/2-75-016

SYMPOSIUM ON ELECTROSTATIC PRECIPITATORS FOR THE CONTROL OF FINE PARTICLES

by

Charles E. Feazel, Editor

Southern Research Institute
2000 Ninth Avenue South
Birmingham, Alabama 35205

Contract No. 68-02-1308 (Task 14)
ROAP No. 21ADL-034
Program Element No. 1AB012

EPA Project Officer: Dennis C. Drehmel

Control Systems Laboratory
National Environmental Research Center
Research Triangle Park, North Carolina 27711

Prepared for

OFFICE OF RESEARCH AND DEVELOPMENT
U.S. ENVIRONMENTAL PROTECTION AGENCY
WASHINGTON, D.C. 20460

January 1975

EPA REVIEW NOTICE

This report has been reviewed by the National Environmental Research Center - Research Triangle Park, Office of Research and Development, EPA, and approved for publication. Approval does not signify that the contents necessarily reflect the views and policies of the Environmental Protection Agency, nor does mention of trade names or commercial products constitute endorsement or recommendation for use.

This document is available to the public for sale through the National Technical Information Service, Springfield, Virginia 22161.

ABSTRACT

The papers in these Proceedings were presented at the Symposium on Electrostatic Precipitators for the Control of Fine Particles, held at Pensacola Beach, Florida, September 30 - October 2, 1974, under the joint sponsorship of the Control Systems Laboratory of the Environmental Protection Agency and Southern Research Institute. The purposes of the symposium were to make available the results of recent research on electrostatic precipitators and to provide a forum for discussing applications of precipitators to dust-control problems of special interest. The papers were contributed by investigators active in the field of electrostatic precipitation. They describe recent advances in precipitator technology, especially in the control of fine particles (those less than 1-2 μm in diameter) in industrial emissions. Data such as fractional collection efficiency measurements are presented that can be used to help define the capability of precipitators for the control of fine particles. Techniques for the sizing and design of precipitators, including a theoretically-based mathematical model of precipitator performance, and the selection of power supplies to improve performance and reliability are discussed. Methods for combatting the problem of collecting high-resistivity fly ash from the combustion of low-sulfur coal that are described include the operation of precipitators at both lower and higher flue-gas temperatures than usual, and the conditioning of fly ash by injection of sulfur trioxide, ammonia, or sulfamic acid into the flue gas. Performance data are presented on precipitators for the control of fumes from kraft pulp-mill recovery boilers and on wet precipitators in aluminum reduction plants and other industrial applications. Research on electrostatic and radiation charging of fine particles, on corona quenching by particle space charge, and on charged-droplet scrubbers is discussed.

ACKNOWLEDGMENTS

Topics for the symposium were selected by the Symposium Committee, consisting of Sabert Oglesby (Symposium Chairman), James H. Abbott, Dennis C. Drehmel, Charles E. Feazel, and Leslie E. Sparks. Dr. Abbott and Dr. Drehmel also served as session chairmen. Other session chairmen were Alfred B. Craig and Grady B. Nichols. James H. Strickland was responsible for the meeting arrangements, and was assisted by Marilyn Greely and Lane L. Heinrich.

CONTENTS

	Page
ABSTRACT	iii
ACKNOWLEDGMENTS	iv
OPENING REMARKS Sabert Oglesby, Jr.	1
SYMPOSIUM OBJECTIVES Alfred B. Craig	3
SIGNIFICANCE OF PARTICULATE EMISSIONS John K. Burchard	
Abstract	5
References	12
EMISSION STANDARDS FOR PARTICULATES George W. Walsh	13
ROLE OF ELECTROSTATIC PRECIPITATORS IN PARTICULATE CONTROL—A RETROSPECTIVE AND PROSPECTIVE VIEW Harry J. White	
Abstract	17
Introduction	17
Growth and Applications	18
Technology	26
Problems and Correction	33
Future Outlook	36
References	38
A THEORETICALLY-BASED MATHEMATICAL MODEL FOR CALCULATION OF ELECTROSTATIC PRECIPITATOR PERFORMANCE John P. Gooch and Norman L. Francis	
Abstract	41
Introduction	41

	Page
Theoretical Background	42
Corrections to Theoretical Predictions	48
Description of Model	54
Results	56
Conclusions	63
Acknowledgments	64
References	64

ADHESIVE BEHAVIOR OF DUST IN ELECTROSTATIC PRECIPITATION
Gaylord W. Penney

Abstract	65

RESULTS OF FIELD MEASUREMENTS OF INDUSTRIAL PARTICULATE SOURCES AND ELECTROSTATIC PRECIPITATOR PERFORMANCE
Joseph D. McCain, John P. Gooch, and Wallace B. Smith

Abstract	79
Introduction	79
Measurement Methods	80
Results of Source Measurements	85
Conclusions	99
Reference	99

SOME ASPECTS OF ELECTROSTATIC PRECIPITATOR RESEARCH IN AUSTRALIA
Owen J. Tassicker

Abstract	101
Introduction	101
Pilot, Technical and Bench Scale Apparatus	102
Resistivity and Corona Parameters for Fly Ash	115
Complex Dielectric Constant	117
Adhesivity of Dusts	117
Electrode Evaluation	122
Gas Conditioning	124
References	127

SPECIFYING ELECTROSTATIC PRECIPITATORS FOR HIGH RELIABILITY
N. W. Frisch and D. W. Coy

Abstract	131
Introduction	131

	Page
Fuel Characteristics Specifications	133
Other Factors in Designing for Reliability	143
Conclusions	154
References	157
DESIGN AND APPLICATION OF HIGH-VOLTAGE POWER SUPPLIES IN ELECTROSTATIC PRECIPITATION H. J. Hall	
Abstract	159
Introduction	159
High Voltage Electrical Equipment	162
Operating Factors and Problems	176
References	189
PRECIPITATOR GAS FLOW DISTRIBUTION C. L. Burton and D. A. Smith	
Abstract	191
Introduction	191
Background	192
Field Visual Evaluation of Problem	195
Detailed Field Velocity Traverse	197
Precipitator Performance Analysis	206
Field vs Model Study Results	207
Final Model and Field Results	210
Conclusions and Recommendations	215
References	217
HOT-SIDE PRECIPITATORS A. B. Walker	
Abstract	219
References	227
"COLD-SIDE" ELECTRIC PRECIPITATORS FOR HIGH-RESISTIVITY FLY ASH REQUIRE DIFFERENT DESIGN PHILOSOPHY S. Matts	
Corona Current	229
Current Distribution	231
Summary: Requirements for Successful High Resistivity Operation	233
The European Design Concept	234

Page

SURFACE RESISTIVITY AND THE CHEMICAL COMPOSITION OF FLY ASH
Roy E. Bickelhaupt

Abstract 237
Introduction 238
Procedure 240
Results 242
Discussion 248
Acknowledgment 255
References 255

CONDITIONING OF FLY ASH WITH AMMONIA
Edward B. Dismukes

Abstract 257
Introduction 257
Summary of Investigations of Ammonia Conditioning 258
Investigation of Ammonia Conditioning in TVA Power Stations 260
Conclusions 283
Acknowledgments 285
References 285

CONDITIONING OF FLY ASH WITH SULFAMIC ACID
Edward B. Dismukes

Abstract 289
Introduction 289
Basis for Interest in Sulfamic Acid as a Conditioning Agent 290
Precipitator Tests of Sulfamic Acid as a Conditioning Agent 293
Fundamental Properties and Conditioning Mechanisms of Sulfamic Acid 302
Acknowledgments 312
References 313

SULFUR TRIOXIDE CONDITIONING
Ronald E. Cook

Abstract 315

Page

APPLICATION OF ELECTROSTATIC PRECIPITATORS FOR THE CONTROL OF FUMES FROM LOW ODOR PULP MILL RECOVERY BOILERS
John E. Paul

Abstract 327
Introduction 328
The Traditional Process 330
The Low-Odor Process 332
Low-Odor Precipitator Design 332
Economics 343
Summary 346
References 347

WET ELECTROSTATIC PRECIPITATORS FOR CONTROL OF SUB-MICRON PARTICLES
Even Bakke

Abstract 349
Introduction 349
Principle of Operation 351
Applications 355
Water Treatment 367
Power Consumption and Economics 368
Conclusions 368
References 368

CALCULATION OF THE CHARGING RATE OF FINE PARTICLES BY UNIPOLAR IONS
Wallace B. Smith and Jack R. McDonald

Abstract 371
Introduction 372
Theoretical Discussion and Results 376
Acknowledgments 392
References 392

THE EFFICIENCY OF ELECTROSTATIC PRECIPITATORS UNDER CONDITIONS OF CORONA QUENCHING
M. B. Awad and G. S. P. Castle

Abstract 393
Introduction 394
Review of Previous Work 395
Effect on Collection Efficiency 398
Experimental Set-Up 400
Results and Discussion 400

CONTENTS (continued)

	Page
Conclusions	404
Nomenclature	407
References	408

RADIATION CHARGING: A NOVEL WAY TO ELECTRICALLY CHARGE FINE PARTICLES
Robert Jennings Heinsohn, Samuel H. Levine, Robert A. Fjeld, and Gary W. Malamud

Introduction	409
Historical Review	410
Radiation Charging System	411
Phenomenological Description	414
Ion Generation	415
Analytical Predictions	423
Preliminary Experiments	431
Discussion and Conclusions	439
Nomenclature	443
Acknowledgment	444
References	444
Appendix	445

COLLECTION OF AEROSOL PARTICLES BY ELECTROSTATIC DROPLET SPRAY SCRUBBERS
Michael J. Pilat

Abstract	447
Introduction	448
Theoretical Calculation of Particle Collection Efficiency	448
Experimental Measurements	449
Results of Laboratory Tests	455
Field Testing of U. of W. Electrostatic Scrubber	455
Acknowledgments	457
References	457

CHARGED DROPLET SCRUBBING FOR FINE PARTICLE CONTROL
C. W. Lear, W. F. Krieve, and E. Cohen

Abstract	459
Introduction	459
Charged Droplet Scrubbing Devices	460
Experimental Approach	470
Results	472
Summary	482
References	484

CONTENTS (continued)

	Page
CLOSING COMMENTS Dennis C. Drehmel	485
METRIC CONVERSION FACTORS	487

OPENING REMARKS

Sabert Oglesby, Jr.
Southern Research Institute
Birmingham, Alabama

Developments in the control of emissions of particulates from industrial sources have been accelerated within the past few years as a result of regulations which require greater reliability and a higher level of control. Developments in the field of electrostatic precipitation have provided a better theoretical understanding of collection mechanisms and increased understanding of application problems.

The rapidity with which information is becoming available makes it desirable to bring together researchers, users, and manufacturers of electrostatic precipitators on a frequent basis to exchange research data and experience so that more effective applications can be made to control particulate emissions.

This symposium is the second to be sponsored by the Environmental Protection Agency, the first being held in Birmingham in 1970.

The purposes of this symposium are to make available the results of EPA-supported research on electrostatic precipitators and to provide a forum for discussing applications of precipitators to dust control problems of special interest, as well as other research and development efforts.

The papers to be presented cover a wide range of subjects from studies of a highly theoretical nature to those of practical application. A major thrust of the symposium will be toward defining the capabilities of electrostatic precipitators for the control of particles of less than about 1-2 μm diameter.

It has been shown that it is particles in this size range that constitute the greatest interest from the standpoint of health effects and visibility. It is also these small particles that represent the most severe collection problem.

A second topic to be considered is the factors related to more reliable installations of precipitators. One of the major concerns of the precipitator industry has been the proper sizing and design of precipitators to meet the widely varying conditions resulting from the variety of physical and chemical properties of dusts from industrial sources. Costs of providing control equipment are high at best, and improper design of control equipment adds disproportionately to that cost.

A review of the papers to be presented at this symposium will show that much new material is presented which it is hoped will provide a more effective means of controlling particulate emission to the atmosphere.

SYMPOSIUM OBJECTIVES

Alfred B. Craig
Environmental Protection Agency
Research Triangle Park, North Carolina

The Control Systems Laboratory (CSL) of the Environmental Protection Agency has been developing improved technology for the control of particulate emissions from stationary sources for nearly 20 years. Starting about three years ago, emphasis has been gradually shifted to the study of fine particulate which we define as solid or liquid particles less than about three microns in diameter. Rationale for this shift in emphasis will be covered in Dr. Burchard's paper, the next on our program.

In an effort to increase interest in fine particulate control technology within private industry and academic circles, CSL has established the following series of symposia covering all facets of this subject:

1. SEMINAR ON ELECTROSTATICS AND FINE PARTICLES

   National Environmental Research Center
   Research Triangle Park, North Carolina

   September 6-7, 1973

2. SYMPOSIUM ON THE USE OF FABRIC FILTERS FOR THE CONTROL OF SUBMICRON PARTICULATES

   Boston, Massachusetts

   April 8-10, 1974

3. FINE PARTICLE SCRUBBER SYMPOSIUM

   San Diego, California

   May 28-30, 1974

4. SYMPOSIUM ON ELECTROSTATIC PRECIPITATORS FOR THE CONTROL OF FINE PARTICLES

   Pensacola, Florida

   September 30-October 2, 1974

5. FINE PARTICLE GENERATION AND MEASUREMENT SYMPOSIUM

   (Tentative)

   Spring 1975

The basic objectives of each of these symposia have been to:

1. Bring together in one location many of the leading authorities in the subject field of technology;

2. Present a comprehensive series of technical papers covering the broader areas of the subject technology;

3. Establish a forum for in-depth discussions of all facets of the control of fine particulates by the subject technology;

4. Stimulate new ideas for the development of new or improved techniques for control of fine particulates.

A review of the list of attendees at this meeting and the program arranged by Sabert Oglesby and Southern Research Institute indicates that we should quite ably meet all of these objectives at this symposium covering the use of Electrostatic Precipitators for the control of fine particulates for stationary sources.

SIGNIFICANCE OF PARTICULATE EMISSIONS

John K. Burchard
Environmental Protection Agency
Research Triangle Park, North Carolina

ABSTRACT

The advancement of technology relating to particulate emissions is pointed out as a significant aspect of this Nation's air pollution control efforts. Important factors include the ability of particulates: to cause poor visibility, to constitute a health hazard, to act as transport vehicles for gaseous pollutants, and (for some) to be highly active both chemically and catalytically. Attention is drawn to fine particulates (those with diameters less than about 3 microns) as an object of special attention within the general problem area. Recent EPA evaluations have indicated the effectiveness, under proper conditions, of advanced precipitators for fine particulate control.

The American public's general awareness of air pollution as an ever-increasing problem dates back (with a few notable exceptions) only as far as the early 1950's. It was an awareness prompted by increasing concern over decreasing visibility and acrid odors; by the alarming increase in the number of smog-plagued areas, both urban and rural; and by the prevalence of illnesses—even deaths—linked to air pollution episodes.

It is understandable then that the clearly evident problem of controlling the emission of pollutants to our atmosphere, as well as other environmental concerns, developed into full-blown national issues in the mid-1960's. These issues, entering the political arena, prompted passage of the Clean Air Act of 1967 and the major strengthening amendment of 1970. In December of that same year the Environmental Protection Agency came into being; also at about this time, various ecology groups were either established or escalated their activities, making their voices heard (and their influence felt) at many levels of both government and industry.

Although the general consensus appears to be that these events have, for the most part, been for the good of our Nation, there admittedly have been excesses of action, inaction, and over-reaction. But even these excesses have proven valuable in focussing attention on specific needs, including those for more advanced control technology, and for more definitive pollutant data.

Typical of the air pollution control problems complicated by inadequate data are those associated with particulate matter, specifically those which we refer to as "fine particulate."

I wish, of course, that a precise quantitative response could be given to the question "How significant are particulate emissions?", but this is just not possible given the current state of knowledge.

We in EPA's Control Systems Laboratory feel that controlling particulate emissions is indeed highly significant. Some indication of this is given by the fact that our budget in this area has risen from approximately $0.5 million in Fiscal Year 1971 to over $5 million in Fiscal Year 1975, or about an order of magnitude increase in the last few years. Admittedly, basing significance on expenditures by a single government laboratory is unfair both quantitatively and qualitatively. For one thing, it represents nowhere near the actual national annual expenditure for particulate control technology advancement. Other government groups, as well as industrial segments, are contributing significantly to advancing our knowledge in this area.

Even if my numbers were all-inclusive, to cite them as proof of the significance of the problem would be erroneous and involve circular logic. We think the problem is serious, so we allocate "X" number of dollars to solve it. Then, we turn around and say, "Look, the problem must be serious; we have spent "X" number of dollars trying to solve it."

Obviously the significance of the particulate problem cannot be measured solely on such a basis. The real criteria of significance include the ability of particulates to cause poor visibility, to constitute a health hazard, to act as transport vehicles for gaseous pollutants, and (in many cases) to be highly active both chemically and catalytically.

An indication of the complexity of the particulate emissions problem, especially from the standpoint of control systems, is the fact that this symposium on electrostatic precipitation for the control of fine particles is the fourth of the series sponsored by our Laboratory in the past year and mentioned previously.

Throughout these meetings you will note the emphasis on fine particulate which, for the sake of consistency, we have defined as liquid or solid particles with diameters less than about 3 microns. This trend of emphasis on fine particulate came about several years ago, following the release of a pair of EPA-funded milestone reports:

A study on electrostatic precipitator systems in 1970;[1] and a study of particulate pollutant systems in 1971.[2]

These reports validated the significance of controlling particulate emissions, documented the ability of electrostatic precipitators to collect particulates (other than submicron in size), and indicated areas in which work was still required to extend the applicability of electrostatic precipitators to the elusive submicron particles.

Among the work areas recommended in the 1970 report were:

> Refinement of the simplified electrostatic precipitator (ESP) performance model developed by Southern Research Institute to show the interrelationships between variables that influence performance.
>
> Better definition of the role of turbulence and electric wind.
>
> A study of spark propagation.

Development of quantitative data to relate reentrainment to dust resistivity.

Determination of the effect of dust layer on corona generation.

Better definition of the most desirable conditions for corona generation at temperatures of 1500°F (800°C) and at pressures of 100 to 200 psi (7-14 kg/cm^2).

Investigation of high resistivity problems.

Determination of optimum conditions for handling high-resistivity dusts.

Solution of problems relating to the application of ESP's in specific areas and industries, and to the overall acceptance of ESP's.

But we are not basing our particulate programs on 1970 and 1971 dated information. A more recent (May 1974) report[3] concludes succinctly:

> "Presently available equipment for the control of particulate emissions from stationary sources has achieved limited success in the control of fine particulates (i.e., less than or equal to 3 micron diameter particles). This limited ability of existing control equipment to collect fine particulates means that if we are to achieve significant control in this area an aggressive, well-conceived research and development program will be required to improve existing equipment and develop new techniques."

Since this meeting deals specifically with electrostatic precipitation, one of the control techniques cited in the May report, it is important to note that the report indicated that significant collection of fine particulates "should be possible" using electrostatic precipitators. The report states:

"Electrostatic forces between charged particles and collecting bodies can be quite effective for the collection of particulates. To secure rapid and efficient deposition of particles, forced charging of particles should be used... Particle migration velocities calculated from theoretical equations for field and diffusion charging indicate that migration velocities in the range of 2 cm/sec should be realized for fine particles in electrostatic precipitators operating with reasonable electric fields, charge densities, and residence times."

I mentioned previously the health hazards associated with particulates; complicating this problem is the fact that the health effects case against submicron particulates is not crystal clear. Fine particulates represent a large category of pollutants (rather than being a single pollutant) with a common set of size, transport, and behavioral characteristics. Once dispersed, they behave (depending on their size) like something between coarse particles and gases: they remain suspended and diffuse, are subject to Brownian motion, follow fluid flow around obstacles, and can penetrate deep into the respiratory system.

Specifically, and based on limited information available from mathematical models and experimentation, particles larger than 5 microns are deposited in the nasal cavity or nasopharynx, whereas increasing numbers of smaller particles are deposited in the lungs, where over 50% of the number of particles between 0.01 and 0.1 microns penetrating the pulmonary compartment are deposited. This ability of particulates to penetrate the respiratory system and be captured is mainly a function of their geometry, rather than their chemical properties.

This contrasts with the resulting health effects of the fine particulates which have been captured, since such adverse effects are almost completely dependent on their chemical or toxic nature except for long fibrous materials. It is this contrast that makes it unwise to generalize on health effects. When discussing health effects of fine particulates, specific materials must be considered.

The principal effect on health is through inhalation and direct attack on the respiratory system. This may result in short term irritant effects, or longer term damage such as silicosis, asbestosis, chronic bronchitis, and emphysema. In all these cases the respiratory system is directly impaired.

A second mechanism of adverse effects involves the respiratory system indirectly as a significant route of entry for non-respiratory toxicants. In this case, substances which are deposited in the respiratory system are translocated to the gastro-intestinal system by muco-ciliary transport and are swallowed. They may then exert a primary toxic effect directly or be absorbed and translocated to other tissues to exert secondary harmful effects.

Because of the present scarcity of knowledge concerning the health effects of specific pollutants and combinations of pollutants, it will take years to develop the data base necessary to quantify the exact dose/response characteristics of fine particulates. Sufficient information does exist, however, to conclude that fine particulates must be controlled to fairly stringent levels if public health is to be properly protected.

As indicated earlier, EPA has taken an active part in developing solutions to some of the problems relating to fine particulate control. To extend measurement capabilities to extremely small particulates, EPA recently funded the use of a series of diffusion batteries coupled with condensation nuclei counters, to provide concentration and size distributions over the size range from about 0.01 to 0.3 micron. Interesting information about control of fine particulate is already being gathered, using these new measurement techniques. Four tests on high efficiency electrostatic precipitators have shown fractional efficiencies better than 90% (in some cases better than 98%) all the way down to 0.1 micron.

These and other similar tests indicate that certain currently available devices—including electrostatic precipitators—can effectively control fine particulates under the right conditions. However, it should be emphasized that the range of applicability of conventional precipitators to control fine particulates is limited: they are most effective on particulates of a fairly narrow range of electric resistivity; at both higher and lower resistivities, control efficiency drops off. Unfortunately, most low-sulfur coals produce high-resistivity fly ash, so that switching to low-sulfur Western coals decreases the sulfur oxides problem, but increases the particulate control problem.

Although the data has not been fully analyzed, EPA recently completed testing of a "hot-side" precipitator on a Western coal-fired power plant. Preliminary indications are that it is a very efficient collector of fine particulate. Work is also underway on conditioning agents to reduce the resistivity of fly ash from low-sulfur coal thereby alleviating the problem noted above. Also initial work on the improvement of charging sections for electrostatic devices is promising for all dusts, regardless of resistivity.

EPA is not restricting its efforts, but is intensively studying all facets of the very complicated fine particulate problem. These studies include characterization of the chemical composition and toxicology of particulates as a function of particle size and industrial source. As would be expected, chemical composition varies dramatically depending on source. For example, particulate emissions from an open-hearth furnace have been found to be about 90% iron oxide, while particulate from a cement plant was 40% calcium oxide, 20% silicon dioxide, 10% iron oxide, and the remainder other metallic oxides.

Fly ash from fossil fuel burning varies markedly in composition depending on the source of coal and degree and type of combustion. In addition to substantial quantities of oxides of silicon, aluminum, iron, and calcium, as many as 30 to 40 additional elements are present in trace to significant quantities. Most exist at constant levels in all particle sizes, although some of the more toxic elements appear in increasing concentrations with decreasing particle size.

The complexity of sources of fine particulate emissions, and the physical and chemical characteristics of the particles, as well as of the off-gases bearing them, complicate the development of adequate control technology. In addition to studying the application of currently available control techniques, we are continually evaluating numerous new concepts and novel devices. In the long run, we believe it will be necessary to develop a number of different techniques for control of the wide diversity of sources, and wide variety of types, of fine particulate.

In conclusion, although there have been significant improvements in our Nation's air, a massive effort is still needed to meet the air quality standards. Many areas of the country have ambient levels which still exceed the primary standards for the six "criteria" pollutants; this situation is worse for particulates than for any other major pollutant. These problems, combined with the special problems of fine particulate control, make it clear that EPA, industry, and the control equipment manufacturers, working together, have a difficult and challenging task.

Improved electrostatic precipitation will be an important step toward the successful accomplishment of this important task.

REFERENCES

1. Oglesby, S., Jr., and G. B. Nichols. A Manual of Electrostatic Precipitator Technology. Southern Research Institute, Contract CPA 22-69-73, National Air Pollution Control Administration. 1970. Part I. Fundamentals. NTIS PB 196380. 322 p. Part II. Application Areas. NTIS PB 196381. 875 p. Selected Bibliography of Electrostatic Precipitator Literature. NTIS PB 196379. 154 p. An Electrostatic Precipitator Systems Study. NTIS PB 198150. 65 p.

2. Particulate Pollutant Systems Study. Midwest Research Institute, Contract CPA 22-69-104, Environmental Protection Agency. 1971. Volume I. Mass Emissions. NTIS PB 203128. 372 p. Volume II. Fine Particle Emissions. NTIS PB 203521. 335 p. Volume III. Handbook of Emission Properties. NTIS PB 203522. 607 p.

3. Control Technology for Fine Particulate Emissions. Midwest Research Institute, for Environmental Protection Agency. Publication Number EPA-650/2-74-027. May 1974.

EMISSION STANDARDS FOR PARTICULATES

George W. Walsh
Environmental Protection Agency
Research Triangle Park, North Carolina

The Emission Standards and Engineering Division is responsible for the promulgation of standards of performance under Section 111 and national emission standards for hazardous pollutants under Section 112 of the Clean Air Act. The Division also serves as a primary source of technical expertise in defining stationary source control measures for State implementation plans. Different criteria are applied when defining stationary source emission standards depending on which Section of the Clean Air Act is being implemented. For State implementation plans we are generally concerned with reasonably available control for existing sources. Standards of performance which reflect the best systems of emission reduction are promulgated under Section 111 of the Act. Under Section 112, the criterion is one of providing an ample margin of safety to protect public health from incapacitating or irreversible illness. Standards under Section 112 can reflect any degree of control as long as an ample margin of safety to protect public health is provided. In practice, therefore the Emission Standards and Engineering Division spends its time delineating what can be accomplished in the way of emission reduction by different types of control systems—sometimes for EPA standards, sometimes as support to State/local agencies. What we need to better accomplish this job are equations that really work.

Dr. Burchard has emphasized the importance of controlling fine particulate matter to achieve present national ambient air quality standards and quite possibly to achieve and maintain national ambient air quality standards and/or hazardous pollutants standards defined specifically for fine particulates. Electrostatic precipitators will undoubtedly play a major role in these control efforts. Your

dedication and commitment to improving the art of precipitator design, operation, and maintenance is, therefore, a vital factor in protecting the Nation's health and air environment. Your success in applying your skills and knowledge will be reflected in the frequency with which EPA identifies electrostatic precipitators as the best system of emission control for standards of performance under Section 111 of the Act. I can make this statement because of the three ways of setting standards for stationary sources under the Clean Air Act, Section 111 is the only approach available at this time.

As defined in the Act, standards of performance only apply to new facilities, and must "reflect the application of the best system of emission reduction." The term "best system of emission reduction" was chosen to emphasize the concept that good pollution control practice considers the selection of raw materials, the manufacturing process, performance of the control device, and disposal of collected materials. Under Section 111 the potential exists for the application of new technology, provided one can demonstrate that the standards are achievable. This is an important aspect relative to the control of fine particulates. Cost is a factor to be considered, but a cost/benefit analysis is not mandatory. According to Congress, the costs must be reasonable in terms of the economics of the industry for which standards are being set.

Since standards of performance must reflect "the best system of emission reduction," our data base is always limited. A purist philosophy leads to the conclusion that the standards should be based on a single system. The word "reflects," however, provides some relief and the "consideration of costs" provides increased maneuverability. Nonetheless, we are clearly not attempting to define averages nor the most probable emission rates given the application of some generic control device to a large number of sources. We do, however, attempt to define the standards in such a way that two or more control systems can achieve the specified emission limits. To take advantage of this policy we need equations that allow the calculations that will demonstrate performance capability; especially, if an industry has exhibited a tendency to use one type of control device.

Standards of performance do not need to distinguish between total particulate matter and fine particulate matter. As a result, the standards can be used to control fine particulates prior to adoption of a national ambient air quality standard or hazardous pollutant standards. For example, standards for electric arc furnaces, basic oxygen furnaces, and cement kilns are really controlling fine particulate matter. In these cases the allowable emission rates are so

low that it is necessary to control sub-micron size particles to be in compliance. For most sources of particulate matter, therefore, standards of performance tend to define the limits of technology for fine particulates. Increased standard setting by way of standards of performance thus defines a regulatory base for possible future actions under State implementation plans or hazardous pollutants standards.

A limit does exist, however, beyond which standards of performance cannot progress unless costs of control are reduced or a specific regulatory program for fine particulates is initiated. This limit is established by the reasonableness of regulations which impact smaller and smaller increments of the total mass of pollutants emitted. That is, cost-effectiveness places a practical limit on the degree to which standards of performance for total particulates reflect the limits of technology for fine particulates.

The establishment of a specific regulatory program to control fine particulates does, of course, provide a different justification and removes that limit. Also, reduced costs make it possible to lower the performance standards and thus increase the degree of fine particulate control. This is an area wherein continued research and development, coupled with imaginative application, could make the electrostatic precipitator more competitive with bag filters and scrubbers.

Another factor which limits fine particulate control—and one which this symposium should help solve—is related to our ability to predict collector performance. The need for a predictive capability cannot be overemphasized. It is critical to standard setting under any Section of the Clean Air Act and is vital if we are to take advantage of technology transfer from one industry to another. Predictive capability is obviously important when setting standards for emerging industries, where existing plants are not available for study.

Predictive capability will also be important if an ambient standard for particulates is promulgated. Imagine the types of questions that will be asked by State/local agencies as they begin to formulate State implementation plans. Imagine the questions raised by industry as it tries to comply. Many of these questions will focus on particulate formation in the atmosphere, natural particulates and fugitive dusts. Eventually, questions will be raised concerning the upgrading of existing control devices and/or how to design new control systems. For the most part none of these questions have been answered with any degree of specificity—we have been able to bypass them by dealing in generalities. The potential economic impact of a national ambient air quality

standard for fine particulates is of such great magnitude that generalities will not, and should not, be allowed.

The main points of my remarks are these:

- The need to control fine particulates already exists.

- Standards of performance tend to accomplish this goal, although written for total emissions.

- There is a limit beyond which standards of performance cannot go without a formal regulatory effort to control fine particulates.

- When such a program is initiated, predictive capability will be critical to the development of implementation plans or hazardous pollutant regulations.

It would seem, therefore, that increased emphasis should be placed on field studies and laboratory research which will enable the engineers to make the calculations to provide the answers to management's questions on how to achieve the established goals within the established times without wrecking the establishment. In summary, we need equations that work.

ROLE OF ELECTROSTATIC PRECIPITATORS IN PARTICULATE CONTROL— A RETROSPECTIVE AND PROSPECTIVE VIEW

Harry J. White
Consultant
Carmel, California

ABSTRACT

The paper presents an overall view of the growth, applications, technology, problem areas, and future outlook of the electrostatic precipitation process as the major instrument for high efficiency control of fine particle emissions in heavy industry in the United States.

Growth in applications and the trends toward very high collection efficiencies are shown. Broader aspects and highlights of precipitator technology are examined, together with some of the more prominent recent developments and advances in the field. The changing character of precipitator design from the rather casual function of the past to a serious enterprise involving high performance and high financial stakes is brought out. Precipitator problems and strategies for correction are covered as an important phase of the technology.

INTRODUCTION

Primary purpose of this paper is to present an overall view of the growth, applications, current technology, problems, and future outlook of electrostatic precipitation as the major instrument for high efficiency control of particulate emissions in heavy industry in the United States.

Application of electrostatic forces to separate suspended particles from gases was already known in the 18th century, and was further elaborated by numerous experimenters in the 19th century. However, successful development and application of the electrical gas cleaning method to industrial air pollution control problems had to await the pioneer efforts and genius of Cottrell in the early years of the present century. Cottrell's developments and contributions during the years 1907-1912 opened the way for the rapid growth and expansion of the electrical process which soon followed. The descriptive term "electrical precipitation" was originated by Cottrell to designate the process and was widely used for many years, although later generations have adopted the less precise terminology "electrostatic precipitation".

Other pioneer contributors following the lead of Cottrell in advancing the technology and applications of the process include especially W. A. Schmidt, Evald Anderson, H. Welch, W. Deutsch, and H. Rohmann. The range of investigations and accomplishments in this era were remarkable for their scope and insight. Much of the work had a quality of distinction and character now unfortunately rare.

GROWTH AND APPLICATIONS

The Cottrell process developed rapidly during the 1910-1920 era in the non-ferrous smelting industry, as an effective countermeasure in the desperate legal struggle then under way against suits for fume damage to forests and vegetation. Other gas cleaning methods, such as huge settling chambers, and filtration through woolen bags, had proved ineffective in solving the smelter fume problems. Although precipitators were applied in the smelting field initially to abate the serious smoke nuisance, it was soon found that recovery of the valuable copper, lead, and zinc oxides and other compounds previously lost out of the stacks in the form of dusts and fumes more than paid for the recovery costs, and in many cases returned substantial profits. Many of these precipitators were large installations, the largest being the two million cfm unit at Anaconda built in 1919.

Precipitators also played an important role in the solution of the serious sulfur dioxide problems created in smelters by sulfide ore roasting and other operations. The Ducktown, Tennessee and Trail, British Columbia cases were classic examples of such damage.[1] The most successful system for controlling sulfur dioxide emanations proved to be thorough removal of particulates from the smelter gases followed by conversion of the sulfur dioxide to sulfur trioxide and high-

quality sulfuric acid. In many instances the acid was marketed at a profit, to the developing fertilizer industry, instead of representing a financial loss as originally feared by smelter operators.

Other early applications of great importance to the development of the electrical method took place in the cement industry, chemical plants and processes, steel industry, and in the detarring of fuel gases. Thus, by the early 1920's electrical precipitation was well established and in wide use in heavy industry.

Major growth and development of electrostatic precipitation since these pioneer efforts came initially from applications to other existing industrial air pollution problems and later from technological advances in various industrial fields which gave rise to new gas cleaning problems. Increasingly stringent air pollution control legislation, especially in recent years, has not only expanded the fields of application, but has also required new levels of efficiency and performance. Examples of developing technology leading to large new fields of precipitator application are the introduction of powdered-coal-fired boilers in electric power generation, the fluidized catalyst process in gasoline production, and basic oxygen furnaces in the steel industry. Economic recovery of valuable materials has also played a role as, for example, the recovery of soda ash in kraft paper mills, recovery of expensive catalyst dust in the fluidized catalyst process and, on a more exotic level, recovery of silver and gold dust in minting operations.

Several comprehensive surveys of the major applications of precipitators in the United States have been made, the most recent in 1970.[2,3,4] Such surveys are becoming more difficult to make with confidence, because of the proliferation of precipitator vendors and the changing and uncertain plans of precipitator users. Projections of future demands for precipitators are especially difficult because of uncertainties in air pollution control requirements and schedules, the confusions of the energy crises, and other current unknowns, but substantial increased application of precipitators seems unquestionable.

Table 1 shows a summary of precipitator applications in the United States. Fly-ash collection in pulverized-coal-fired power plants is by far the most important field, comprising some 75 percent of the total in terms of volume of gas treated. This is followed by metallurgical, cement, and paper mill applications, each in the five to ten percent range. All other fields combined account for less than five percent, although individually they may be of great

Table 1. SUMMARY OF UNITED STATES PRECIPITATOR INSTALLATIONS IN MAJOR FIELDS OF APPLICATION, 1907-1970

Application	First installation	Total precipitators	Total gas flow cfm millions[a]	Percent total gas flow
Electric power industry (fly ash)	1923	1330	530	75.3
Metallurgical: copper, lead, and zinc	1910	250	18	
iron and steel	1919	340	40	
aluminum	1949	80	6	
		670	64	9.1
Cement	1911	300	42	6.0
Gypsum	1930	70	2	0.2
Paper mills	1917	230	35	5.0
Chemical industry	1907	700	14	2.0
Detarring of fuel gases	1915	700	6	0.8
Municipal incinerators	1965	10	2	0.3
Petroleum fluidized catalyst	1942	42	4	0.6
Carbon black	1926	90	3	0.6
Totals		4142	702	100.0

[a]Although it is the policy of the Environmental Protection Agency to use the metric system for quantitative descriptions, English units are used in some of the papers in these proceedings in order to avoid confusion. Readers who are more accustomed to metric units may refer to the table of conversion factors at the end of the proceedings.

importance and some, such as municipal incinerators, are growing areas of application. Precipitator application as a whole has historically grown at a rather rapid pace, as illustrated in Figure 1. It is also evident that fly-ash precipitation has been the dominant field for many years. Although only rough estimates of the particulates collected by precipitation are possible, calculations based on the gas volumes treated and particle concentrations for the various fields show a total of the order of 100 million tons per year for all applications, of which fly ash amounts to some 45 million tons per year.

Precipitator collection efficiency trends are of basic interest in reflecting levels of air pollution control and the cleanliness of industrial gas emissions. These trends are shown in Figure 2 for fly ash precipitators, and in Figure 3 for cement kiln and paper mill recovery furnace precipitators. Trends for maximum and average efficiencies are given for fly ash, and average efficiencies for cement and paper mills. The averages are weighted in accord with the gas volumes represented. The rapid increases in efficiencies are especially evident for the past five to ten years, coinciding with greater public awareness and increasingly stringent air pollution control legislation. Currently, virtually all precipitators are being designed for 99 percent or better collection efficiency. Efficiencies at these levels are sufficient in many cases to provide virtually clean stacks as observed by eye.

The overall growth of electrostatic precipitator applications in the United States is remarkable when both the increases in cfm capacity and in collection efficiency are taken into account. A precipitator designed for 99 percent efficiency, for example, will be at least two to three times larger than one for 90 percent efficiency. On this basis, the per annum rate of growth of new precipitator capacity is of the order of 20 times greater for the 1965-1970 era as compared with the 1945-1950 era. A graph portraying annual sales of precipitators in the United States in recent years is shown in Figure 4.

Newer trends in precipitator applications which may be mentioned include the following:

1. Use of precipitators ahead of the air preheaters in power plants to collect fly ash at high temperatures of 600 to 800°F as a means of avoiding high resistivity problems in plants burning low sulfur coals. This precipitator arrangement has become known colloquially as a "hot" precipitator.

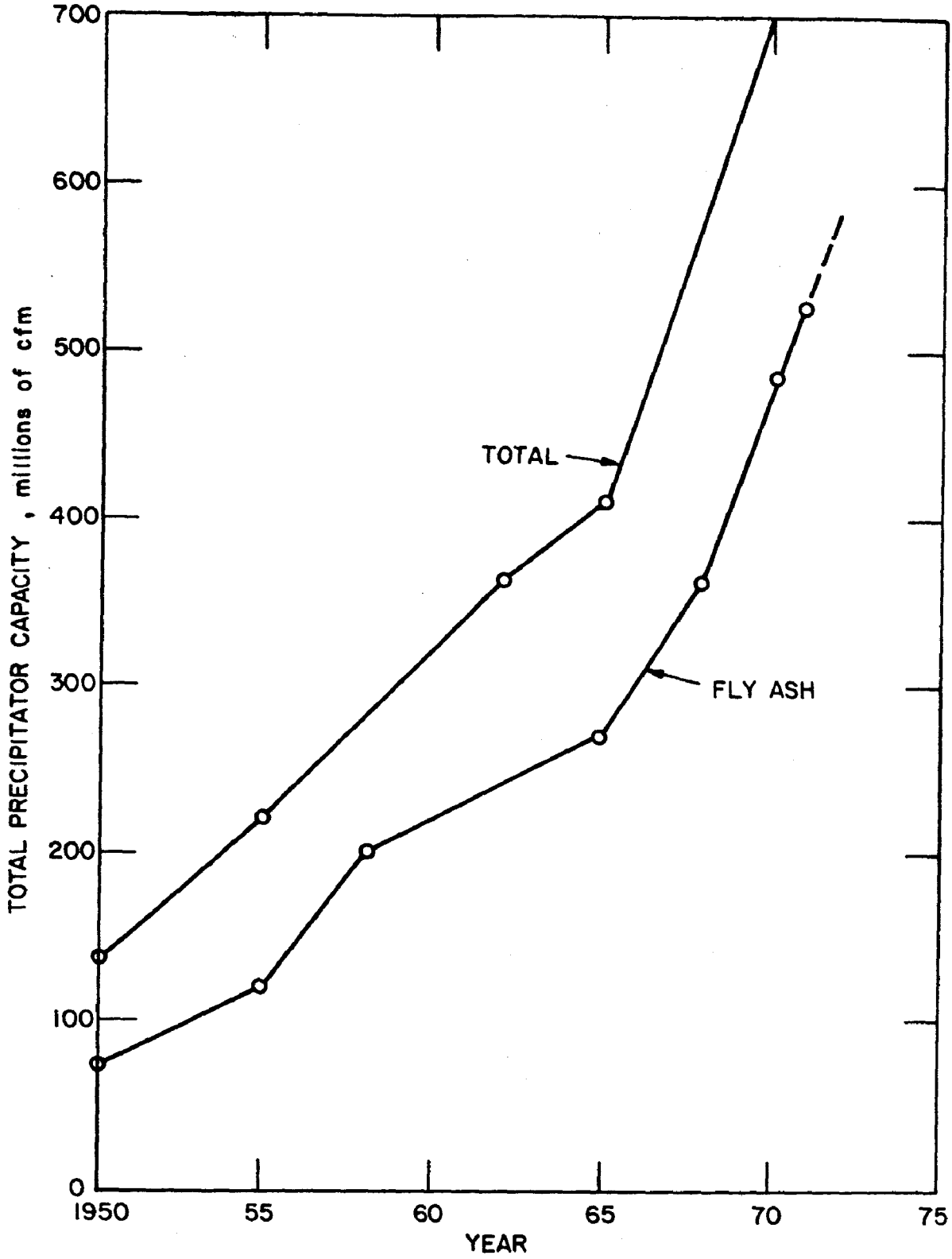

Figure 1. Growth in total and fly-ash precipitation capacity since 1950

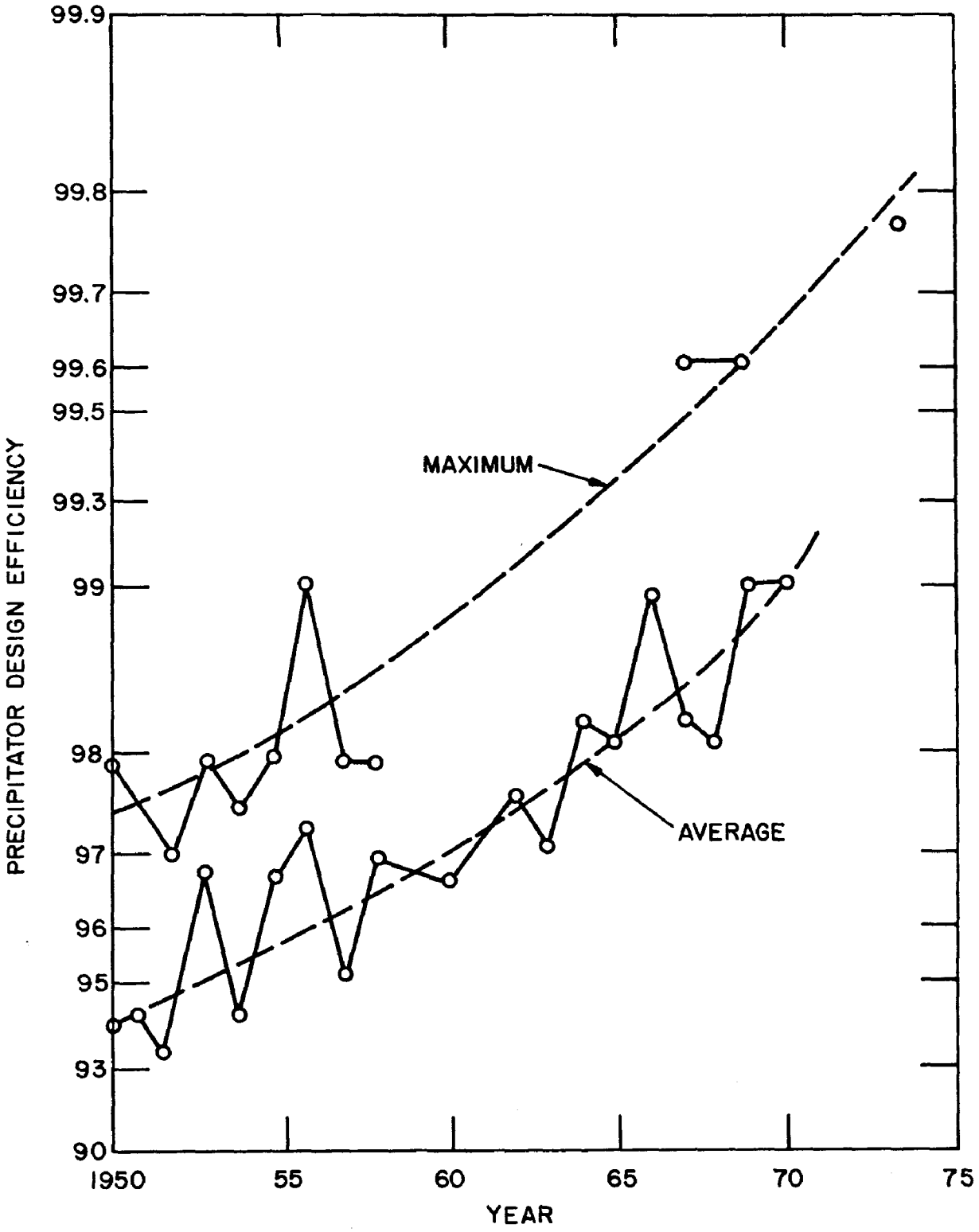

Figure 2. Efficiency trends for fly-ash precipitators

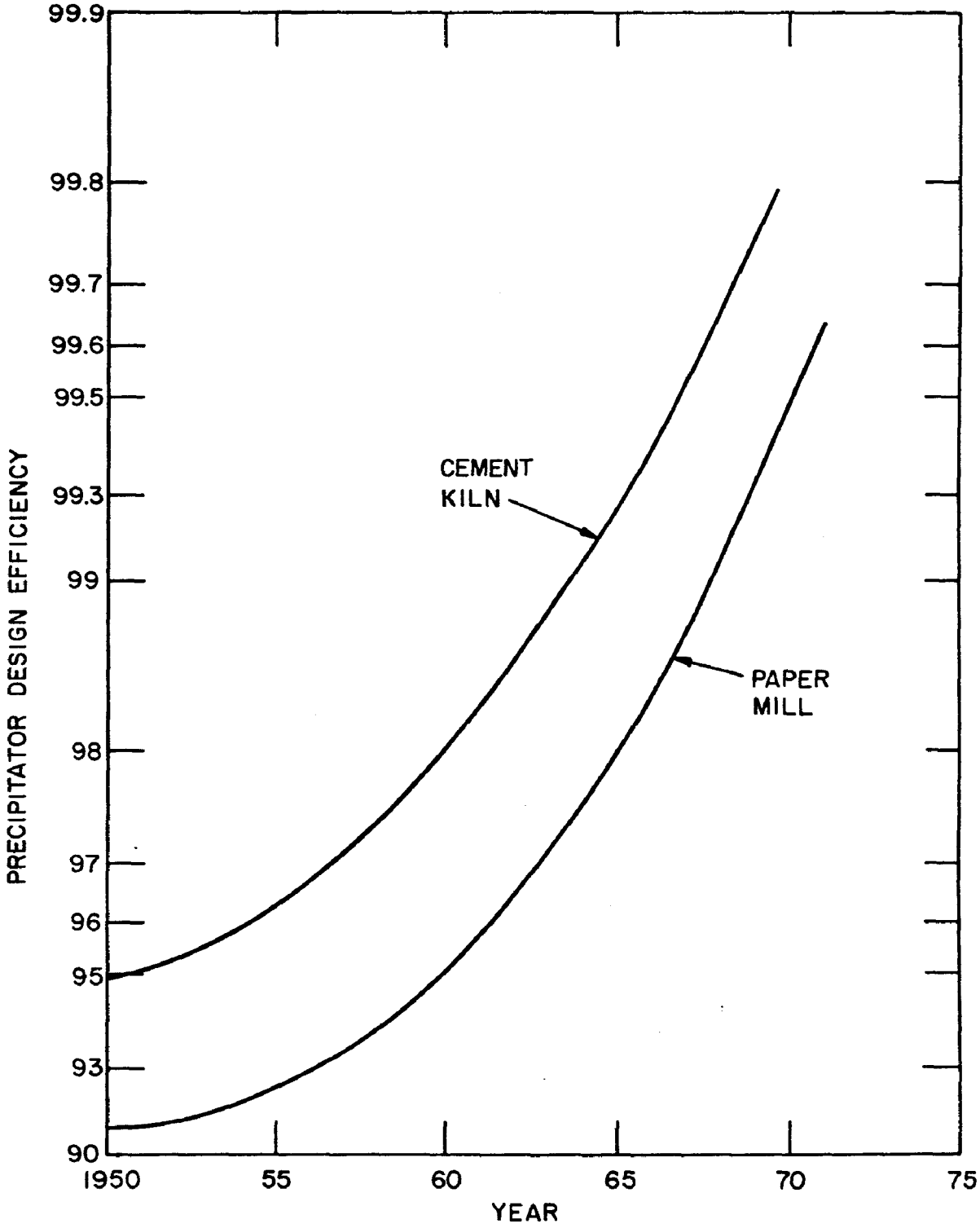

Figure 3. Efficiency trends for cement kiln and paper mill precipitators

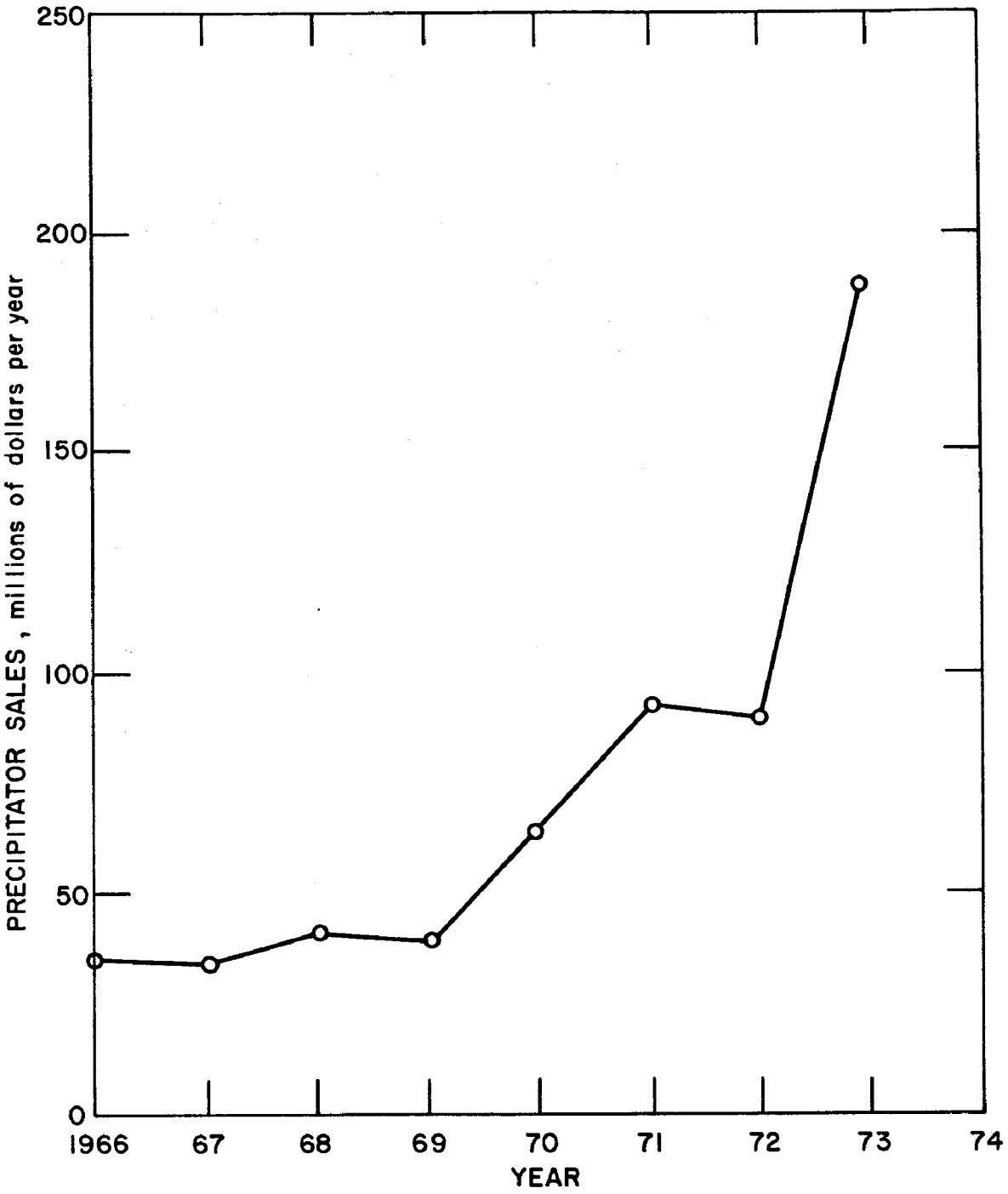

Figure 4. Annual sales of precipitators in the United States

2. Changing from wet-bottom to dry-bottom precipitators in paper mills using odor-free recovery boilers. The dry-bottom designs require relatively large hoppers and are usually equipped with scraper mechanisms to effectively remove the very low-density collected dust characteristic of the process. Relatively low precipitation gas velocities, good gas distribution, and larger hopper capacities are necessary to avoid the "snowing" problem.

3. Changes in steel-making technology from open-hearth to basic oxygen furnaces (BOF) involve cooling and humidifying the gas ahead of the precipitator. High resistivity can be a problem for part of the BOF cycle. Very high collection efficiencies of 99.5 percent or higher are required because of the high concentrations and fineness of the particles.

4. Use of wet precipitators in aluminum reduction plants to reduce particle emissions from the reduction furnaces to the level of invisibility and to collect mist carry-over from scrubbers preceding the precipitators. Outlet concentrations of particulates as low as 0.002 grain per cu ft have been reported with this arrangement.[5]

5. The increasing use of municipal incinerators in the United States has resulted in a growing new field of precipitator application in this country, although incinerator precipitators have been used in Europe for some time.

6. Development work has been conducted over the past several years to meet the demand for precipitators to clean gases at high temperatures and pressures, up to 1700°F and 100 lb per sq in., respectively,[6] for application to newer industrial processes such as magnetohydrodynamic (MHD) power generation and coal gasification.

TECHNOLOGY

Experience over many years shows that cleaning of industrial gases presents complex problems arising from the fineness of the particles, their high concentration in the gases, and the huge volumes of hot and frequently corrosive gases that must be treated. The gas cleaning systems used must be highly reliable, provide consistently high performance, and be relatively insensitive to process conditions. High

collection efficiencies of submicron particles are especially important because these particles account for most of the visibility of stack emissions, and may also be injurious to health. The gas cleaning problem is multiplied because these fine particles are also hardest to separate from the carrier gases. These difficult factors, coupled with the increasing size and complexity of modern industrial plants, require the fullest use of known technology, as well as attainment of new levels of technology, if air pollution goals are to be met.

Despite the obvious need, there are no easy methods for the efficient collection of fine particles from large-scale industrial processes. The variety and complexity of industrial operations usually precludes routine application of even long-established particle collection methods. Most gas cleaning problems require their own analyses and equipment designs if desired performances are to be achieved.

The choice of basic processes for the effective removal of fine particles from gases is essentially limited to electrostatic precipitation, filtration, and high-energy scrubbing. Of these, electrostatic precipitation has the largest application in terms of volume of gas cleaned and mass of particles collected. Electrostatic precipitation also differs fundamentally from the other two processes in that the separation forces are electrical and are applied directly to the particles themselves, rather than indirectly through the gas stream. The electrical process has the inherent capability of capturing submicron particles at high efficiency with relatively low energy consumption and small pressure drop through the gas cleaning system.

This marked capability of removing fine suspended particles from gases at high efficiency and relatively low energy consumption is the major reason for the extensive use of precipitators, which are relatively expensive devices, in industrial gas cleaning. Much cheaper mechanical methods can be used for particle sizes above a few microns diameter.

While both theory and experience show that the particle collection rate for electrostatic precipitators decreases somewhat with decreasing particle size, it is also found to reach a minimum for particles of a few tenths micron diameter and then to increase substantially for the superfine particles of less than a few tenths micron diameter.[7]

Field experience over many years has shown that there have been many highly successful precipitator installations, but also many cases where precipitators have failed to meet performance goals, sometimes by large margins. These deficiencies are, in this author's view, usually attributable to

failure to take a sufficiently broad systems view of air pollution and environmental problems in plant design and operation. This can result in underestimates of requirements, in inattention to engineering design and construction of the gas cleaning equipment, and in questions concerning the obligation of precipitator vendors to provide adequate equipment. Also, the level of attention to environmental problems by some industrial companies has been minimal.

Precipitation technology is far from an exact and unified field. It has long presented a peculiar dichotomy of theory and practice, with several schools of thought in existence, ranging from pure empiricism to a high degree of reliance on scientific methods. The theory and principles underlying the field have been largely codified and are available in the technical and scientific literature.

On the other hand, the documentation of the practice, as represented by records of the large body of accumulated field experience, has been for the most part fragmented in the files of precipitator vendors, users, and individual engineers, and therefore not available to the public. These files are often regarded as containing trade secrets, even though their actual value may be highly questionable. Considerable efforts have, however, been made in the past few years toward codifying and making the field experience generally available[3] as a strategic means of improving air pollution control.

The advantages of a recognized scientifically based precipitation technology are readily apparent in terms of sound engineering design, development of performance standards, equipment evaluation, and as a basis for major improvements through systematic research and development. Some efforts toward unification and development of technical standards have been made by an industry trade group,[8] but currently most of the investigative work in this country is being carried on by contract research institutes under Environmental Protection Agency sponsorship,[9] to a lesser extent by universities, and in rare instances by precipitator users.

DESIGN

A fundamental task in precipitation technology is the design of optimum precipitator systems for given applications. The design of such systems should take into account relevant technical, economic, legal, and public relations factors, but this broad approach is seldom followed in practice as yet, and precipitator designs are usually based only on technical

and cost criteria. For example, the broad overall evaluation of collector equipment should include the large costs which can be incurred as a result of being forced to curtail production because of excessive particulate emissions from deficient collector equipment, yet this is seldom done even though for the case of a large power plant, for example, these costs can run into tens of thousands of dollars per day. The necessity of adding retrofit collection equipment to make up deficiencies or to meet higher air pollution control standards may also need to be considered. Clearly, these broader issues are the province of precipitator users, but precipitator manufacturers should be conversant with them.

Nevertheless, despite the narrow perspective, precipitator design has changed in character during the past several years from a rather routine and casual function to a more serious enterprise involving high performance and high financial stakes. This change has been forced by the implementation of stringent air pollution control standards which require not only substantially invisible stack emissions for new units, but have also added enforcement provisions which can curtail or even shut down entire production units, if that is necessary, to comply with emission standards. The latter factor, in effect, adds a new dimension to the particulate collection problem because of the very large costs and disruptions which can result from plant production losses. In a sense, precipitator design is now of the same importance as that of the production equipment itself.

Under current competitive bidding conditions, the precipitator design problem most often reduces to developing a design to meet a set of equipment performance specifications and requirements at presumably the lowest cost to the customer. There have been attempts to standardize precipitator bidding and evaluation practices in the United States.[10] However, actual purchase specifications may range from elementary statements covering hardly more than gas flow and required collection efficiency to comprehensive documents specifying basic design parameters, details of construction, and the like. The latter practice is the outgrowth of users' attempts to insure satisfactory performance and to protect themselves against deficient equipment.[11] Unfortunately, some of the most essential physical and chemical properties of the particles and gases which influence precipitator performance are seldom specified, and frequently are not known. The most conspicuous example is the resistivity of the particles. Even in those cases where these properties can be measured in existing plants and used for equipment design purposes, the measurements are seldom made, or even requested by either purchaser or seller.

The basic design problem for precipitators is the determination of the principal parameters for precipitator sizing, electrode arrangement, and electrical energization needed to provide specified levels of performance. Ancillary factors such as rappers, gas flow control methods, dust removal systems, and performance monitoring must also be considered.

Various design methods and philosophies are used in practice for the design of fly-ash precipitators. These range from empirical design by analogy based on previous operating experience with similar installations to more sophisticated methods based on theory and fundamental principles. Design by analogy can be applied successfully to applications such as collection of sulfuric acid mist for which conditions change little from installation to installation but is not viable for applications such as fly-ash collection where particle and gas properties tend to be highly variable because of major differences in coals, furnaces, and operation. There have been many examples in practice of fly-ash precipitators supposedly designed for high efficiencies of 95 to 99 percent which in actual operation turn out to do no better than 50 to 90 percent. Costly changes and additions to the original installations are then necessary to bring performance up to guarantee requirements.

Pilot precipitators are often used in the case of existing plants, or where new processes are being developed, as a means of determining design of full-scale precipitators. The main problem here is the scale-up factor to be used, since it is well known that pilot units operate much better per unit size than do those of commercial size. The scale effect is chiefly attributable to differences in electrical energization and gas flow, with the former usually being the more important factor. In general, pilot precipitator data should be supplemented as fully as possible by basic data on the particle and gas properties, and especially by resistivity information.

Precipitator designs might, in principle, be deduced from theory alone if all the significant variables were known. But this is not the case in practice, and it is necessary to specify some of the basic design parameters primarily from field experience. Recently, theoretical techniques have been advanced by the development of a computer model for precipitator design and performance analysis.[12] Although still in the developmental stage, this approach shows much promise for future practical engineering use.

Basic parameters used in precipitator design, together with the numerical values used for fly ash, are summarized in Table 2. It is to be noted that the values of these

Table 2. RANGE OF BASIC DESIGN PARAMETERS IN PRACTICE FOR FLY-ASH PRECIPITATORS

Parameter	Symbol	Range of values
Duct spacing	S	8-12 in.
Precipitation rate	w	0.05-0.6 ft/sec
$\frac{\text{Collection surface}}{1000\ \text{cfm}}$	$\frac{A}{V}$	100-800 ft^2/1000 cfm
Gas velocity	v	4-8 ft/sec
Aspect ratio	$\frac{L}{H}$	0.5-1.5 $\frac{\text{length of ducts}}{\text{height of ducts}}$
$\frac{\text{Corona power}}{1000\ \text{cfm}}$	$\frac{P_c}{V}$	50-500 watts/1000 cfm
$\frac{\text{Corona current}}{\text{sq ft plate area}}$	$\frac{I_c}{A}$	5-70 microamps/ft^2
Plate area per electrical set	A_s	5,000-80,000 ft^2/el set
No. of H.T. sections in gas flow direction	N_s	2-8
Degree of H.T. sectionalization	$\frac{N}{V}$	0.4-4 $\frac{\text{H.T. bus sections}}{100{,}000\ \text{cfm}}$

parameters will vary with particle and flue gas properties, with gas flow, and with required collection efficiency. The highly important precipitation rate parameter w achieved in actual operation depends strongly on such quality factors as accuracy of precipitator electrode alignment, uniformity and smoothness of gas flow through the precipitator, rapping of the electrodes, and the size and electrical stability of the rectifier sets. These factors have to do with the mechanical and electrical quality of the precipitator, and experience shows that deficiencies in quality often exist in these areas. Therefore, allowance needs to be made for them in the design process. Other design factors that need to be considered in addition to the basic parameters are the following:

1. Corona electrodes: type and method of supporting.

2. Collecting electrodes: type, size, mounting, mechanical and aerodynamic properties.

3. Rectifier sets: ratings, automatic control system, number, instrumentation and monitoring provisions.

4. Rappers for corona and collecting electrodes: type, size, range of frequency and intensity settings, number, and arrangement.

5. Hoppers: geometry, size, storage capacity for collected dust, number, and location.

6. Hopper dust removal system: type, capacity, protection against air inleakage and dust blow-back.

7. Heat insulation of shell and hoppers, and precipitator roof protection against weather.

8. Access doors to precipitator for ease of internal inspection and repair.

9. Provisions for obtaining uniform, low-turbulence gas flow through precipitator. This will usually require a high-quality gas flow model study made by experienced people in accord with generally accepted techniques, with full report to precipitator purchaser before field construction.

10. Quality of field construction of precipitator, including adherence to electrode spacing and rigidity requirements.

11. Warranties: performance guarantees, payment schedules, adequate time allowance for performance tests, penalties for non-performance.

12. Support insulators for high-tension frames: type, number, reliability. Air venting, if required.

13. Inlet and outlet gas duct arrangements.

14. Structure and foundation requirements.

Although precipitator design technology has undergone little fundamental change in recent years, there have been a number of hardware changes and trends which should be pointed out. Most important is the use of much larger precipitators for fly-ash collection, made necessary by the higher gas flows and higher particle removal efficiencies required. The precipitator sizes have been made even larger by the concurrent trend toward more conservative designs to reduce risks and avoid penalties for non-performance. Other design trends worthy of note include: (1) use of higher plates, exceeding 40 ft in many cases, and made to reduce floor space requirements and to reduce overall costs; (2) use of very high current rectifier sets up to 3000 to 4000 mA or even more, presumably for economic reasons; (3) an increasing preference by some users for internal rotating hammer-type rappers which reportedly in some cases at least give less trouble than external types; (4) an increasing preference by some users for stiff corona electrodes over suspended wire types, again because of reportedly less trouble; (5) renewed interest in wet precipitators for use in combination with wet scrubbers or wet systems for removal of particulates and contaminant gases.

PROBLEMS AND CORRECTION

Experience has shown that problems of some magnitude are encountered in a significant percentage of precipitators. These problems fall into three major categories: fundamental, mechanical, and operational. The underlying causes of poor performance are attributable to deficiencies in one or more of these primary areas. Examples of fundamental problems are high resistivity particles, poor gas flow, and deficient electrical energization. Mechanical problems include, for example, poor alignment of the electrodes, breakage of corona wires by fatigue or by electrical burning, and air inleakage to the hoppers. Operational problems commonly encountered include poor electrical set adjustments,

shorted corona sections (caused by broken wires, for example), overloading the precipitator by excessive gas flow, and failure to empty hoppers of collected dust. A more complete list of the most frequently encountered problems is as follows:

Fundamental Problems

1. High resistivity particles
2. Re-entrainment of collected particles
3. Poor gas flow
4. Insufficient or unstable rectifier equipment
5. Insufficient number of corona sections
6. Improper or incompatible rapping
7. Gas velocity too high
8. Aspect ratio too small
9. Precipitator size too small

Mechanical Problems

1. Poor electrode alignment
2. Distorted or skewed collecting plates
3. Vibrating or swinging corona wires
4. Excessive dust deposits on corona electrodes and/or collecting plates (sometimes cemented on)
5. Formation of dust mountains in precipitator inlet and outlet ducts
6. Gas turning vanes and/or gas distribution screens plugged with dust
7. Air inleakage into hoppers, shells, or gas ducts
8. Gas sneakage around precipitation zones and/or through hoppers

Operational Problems

1. Full or overflowing hoppers
2. Shorted corona sections (broken wires, etc.)
3. Rectifier sets or controls poorly adjusted
4. Precipitator overloaded by excessive gas flow
5. Precipitator overloaded by excessive dust concentration
6. Process upsets (poor combustion, steam leaks, etc.)

Commonly, these factors are intertwined, which may complicate the identification and correction of problems.

Diagnosis and cure of problem precipitators proceed most smoothly and expeditiously by making use of scientific and systematic methods. Bitter experience shows that erratic methods, offhand judgments, and random guesses (which are

not infrequently used in the hope of finding quick and easy solutions) seldom pay off and are likely, instead, to greatly increase both time and expense.

HIGH RESISTIVITY[13]

Although high resistivity has been a troublesome problem from the earliest years of electrostatic precipitation, the incidence of the problem has been greatly increased in recent years because of the wider use of low-sulfur coals in the electric power industry.

Methods for dealing with the high resistivity problem in the precipitation of fly ash include: conditioning with SO_3, collection at high temperatures of 600 to 800°F, collection at low temperatures of the order of 220 or 230°F, use of very large precipitators, and, quite recently, the possibility of conditioning the ash by addition of small quantities of sodium compounds such as Na_2CO_3 to the coal being burned.

The role of sodium in increasing the conductivity of fly ash is an interesting one and the subject of considerable recent and on-going research.[14,15] The effect of sodium content on fly-ash resistivity in some typical cases is shown in Table 3. It is observed that high sodium content results in low resistivity ash, and vice versa. Research shows that the increased conductivity is due to sodium ion migration through the fly-ash particles, and is effective at gas temperatures above about 350°F.

Table 3. EFFECT OF SODIUM CONTENT ON RESISTIVITY OF FLY ASH

Power plant	Coal analysis S %	Coal analysis Na_2O %	Flue gas Temp. °F	Fly ash Na_2O %	Fly ash Resist. ohm-cm
1	0.25	0.01	350	0.3	2×10^{12}
2	0.25	0.40	350	2.4	5×10^{10}
3	0.54		350	5.6	3×10^{9}

The overall outlook is for continued growth of electrostatic precipitation as the major method for high efficiency cleaning of industrial gases. This expectation is based on the long record of past growth of precipitation applications, the fundamental ability of electrostatic precipitators to meet the newer air pollution control objectives of effectively removing fine particles in the micron and submicron range, and the ability to perform this function with relatively low expenditure of energy and with high reliability.

New applications will undoubtedly develop because of the ready adaptability of precipitators to a wide variety of conditions, but there seems little question that fly ash collection will continue to be the largest field of application. Continued growth seems inevitable because the huge coal resources of the United States, coupled with the manifold problems associated with alternate energy sources, make it almost certain that coal will remain the major fuel for electric power production in this country for many years to come. Proposed methods for converting coal to a "clean" fuel by removing ash and sulfur before burning, and thereby rendering cleaning of the combustion gases unnecessary, appear to be only in the experimental stage at present. Displacement of electrical precipitation by other gas cleaning methods for fly-ash collection is, of course, possible, but entails many problems, not the least of which are high consumption of energy and questions concerning high efficiency removal of submicron particles.

Requirements under the Clean Air Act to greatly reduce sulfur dioxide emissions from fossil-fuel-fired power plants have complicated air pollution control in the electric power industry, and no clearly acceptable solutions for the necessary sulfur dioxide reduction seem as yet to be in sight. The trend toward much greater use of low-sulfur coals as a means of reducing sulfur dioxide is very evident, and this trend complicates precipitator application because of the potential high resistivity problems with these coals. Of the various possible solutions, the use of the so-called "hot" precipitator has gained the widest acceptance, a trend that is likely to continue.

Where low-sulfur coal is insufficient to reduce sulfur dioxide emissions to control standard levels, or where higher sulfur coal is burned, removal of sulfur oxides from the flue gas is necessary. Wet precipitator systems, which combine particulate and sulfur oxide removal, are under investigation and if successfully developed would probably have large

application in coal-fired power plants because of potential advantages of relatively low energy consumption, very high particulate removal efficiencies and reduced mist or water carry over beyond the collector system as compared to other wet systems.

Further developments in the science and technology of electrostatic precipitation are to be expected. Promising areas, in addition to wet precipitator systems for power plants already mentioned, include better understanding of superfine particle collection, and development of computer design models and methods capable of providing optimum precipitator designs for specific installations on a cost/benefit analysis basis.

Despite the importance of new developments, an even greater need exists to make better use of the science and technology already known. The lack of such use has, in some cases, hampered growth and created needless problems in the design and operation of precipitators.

Although variations in design practices are to be expected, the record shows that more than a few precipitators have been designed and constructed with disregard for fundamentals and engineering principles well documented in the published literature. Investigations of such installations reveal weaknesses such as: deficient electrical energization; poor gas flow; precipitators sized too small for the high resistivity particles encountered; high dust losses resulting from improper rapping, from gas sneakage around electrodes, and from hopper sweepage; misaligned electrodes, unshrouded corona wires; and so on. Because of these problems it may be expected that there will be further use by purchasers of restrictive specifications and severe penalties for failure to meet performance guarantees.

A closing remark regarding the impact of recurring energy crises on industrial air pollution control and efforts may be in order at this point. The uncertainties of oil and natural gas fuel resources, the growing dependence in the United States on coal for electric power production, and panic reactions, have led to an attitude in some quarters of jettisoning hard-won air pollution control legislation and enforcement. Under the guise of such simplistic issues as "energy versus clean air", questions are often raised about technical and economic feasibility, and temptation may be strong to scuttle environmental controls. Without attempting to make sweeping judgment, this author believes that sacrificing or compromising control of particulate emissions is unjustified and against the public interest, because of the

proved technical ability which we now possess to deal with most of these problems, including high-efficiency cleaning of flue gases from power plants burning so-called "dirty" coal.

REFERENCES

1. Swain, R. E. Smoke and Fume Investigations, a Historical Review. J. Ind. Eng. Chem. 41:2384-2388, November 1949.

2. White, H. J. Fifty Years of Electrostatic Precipitation. (Presented at Air Pollution Control Association Golden Jubilee Meeting. June 1957.)

3. Oglesby, S., Jr., and G. B. Nichols. A Manual of Electrostatic Precipitator Technology. Southern Research Institute, Contract CPA 22-69-73, National Air Pollution Control Administration. 1970. Part I. Fundamentals. NTIS PB 196380. 322 p. Part II. Application Areas. NTIS PB 196381. 875 p. Selected Bibliography of Electrostatic Precipitator Literature. NTIS PB 196379. 154 p. An Electrostatic Precipitator Systems Study. NTIS PB 198150. 65 p.

4. Walker, A. B., and R. E. Brown. Statistics on Utilization, Performance, and Economics of Electrostatic Precipitators for Control of Particulate Air Pollution. In: Proceedings of the Second International Clean Air Congress, Englund, H. M., and W. T. Beery (eds.). New York, Academic Press, 1971.

5. Byrne, J. L. Fume Control at Harvey Aluminum. (Presented at Air Pollution Control Association Meeting. Spokane. November 1970.)

6. Brown, R. F., and A. B. Walker. Feasibility Demonstration of Electrostatic Precipitation at 1700°F. J. Air Pollut. Contr. Assoc. 21:617-620, October 1971.

7. McCain, J. D., K. M. Cushing, and W. B. Smith. Measurement of the Fractional Efficiency of Pollution Control Devices. Southern Research Institute. (Paper No. 74-117, presented at Air Pollution Control Association 67th Annual Meeting. Denver. June 9-13, 1974.)

8. The reference here is to the Industrial Gas Cleaning Institute.

9. Most of the research and development work referred to is being done at Southern Research Institute.

10. Industrial Gas Cleaning Institute, Publications EP-4 and EP-5, 1968.

11. Consolidated Edison was the pioneer in establishing firm specifications for precipitators, including minimum design parameters, beginning some 20 years ago. TVA has increasingly turned to this approach over the past several years, as described by the following paper:
Greco, J., and J. A. Hudson. Specifications for High Efficiency Electrostatic Precipitators for Coal-Fired Steam-Electric Generating Plants. Tennessee Valley Authority. (Presented at Fourth Annual Industrial Air Pollution Control Conference. Knoxville. March 1974.)

12. Gooch, J. P., and N. L. Francis. A Theoretically-Based Mathematical Model for Calculation of Electrostatic Precipitator Performance. In: Proceedings, Symposium on Electrostatic Precipitators for the Control of Fine Particles. Pensacola Beach. September 30-October 2, 1974.

13. A comprehensive treatment of this phase of precipitation technology is given in the following paper:
White, H. J. Resistivity Problems in Electrostatic Precipitation. J. Air Pollut. Contr. Assoc. 24:314-338, April 1974.

14. Bucher, W. E. A Study of the Bulk Electrical Resistivity Characteristics of Fly Ash from Lignite and Other Western Coals. M. S. Thesis, University of North Dakota, Grand Forks, 1970.

15. Bickelhaupt, R. E. Electrical Volume Conduction in Fly Ash. J. Air Pollut. Contr. Assoc. 24:251-255, March 1974.

A THEORETICALLY-BASED MATHEMATICAL MODEL FOR CALCULATION OF ELECTROSTATIC PRECIPITATOR PERFORMANCE

John P. Gooch and Norman L. Francis
Southern Research Institute
Birmingham, Alabama

ABSTRACT

A mathematical model is described which relates collection efficiency to precipitator size and operating parameters. Procedures are given for calculating particle charging rates, electric field as a function of position in wire-plate geometry, and the theoretically expected collection efficiencies for various particle sizes and precipitator operating conditions. Methods are proposed for empirically representing the losses in collection efficiency caused by non-uniform gas velocity distributions, gas by-passage of the electrified regions, and particle reentrainment due to rapping of the collection electrodes. Incorporation of these proposed techniques into a mathematical model of precipitator performance results in reduction of the theoretically calculated overall collection efficiencies. The reduced efficiencies are compared with those obtained from measurements on precipitators treating flue gas from coal-fired generating stations. The effects of changes in particle size distributions on calculated collection efficiencies obtained from the mathematical model are also presented.

INTRODUCTION

This paper summarizes work conducted at Southern Research Institute concerning the development of a mathematical model for simulating electrostatic precipitator performance. The approach which has been taken is to define the collection efficiency under ideal conditions in terms of precipitator geometry and operating parameters for dusts of various sizes and properties. Empirical corrections to the theoretical

performance are then made to account for non-uniformity of gas flow, reentrainment, and by-passage of dust laden gas through non-electrified regions above and below the collection plates.

The incentive for using a theoretical approach lies in the ability to account for the variations in both dust properties and precipitator operating parameters in a logical and orderly fashion. Methods which are exclusively empirical can lead to serious miscalculation in collection electrode area requirements for a specific installation. A theoretical approach offers the potential for increased confidence in design and in cost savings by preventing under-sizing on the one hand and over-sizing on the other. The accuracy of predictions obtained from such an approach is subject to the accuracy with which the properties comprising the independent variables are measured, the degree to which the theoretical relationships describe precipitator operation, and the precision with which the factors that correct for non-ideal conditions can be modelled and determined. At present, it is necessary to use assumed values for parameters describing non-ideal conditions. Comparisons between predicted and measured performance using the relationships described in this paper and the limited amount of applicable test data indicate that the model in its present stage of development is useful in developing performance curves that relate efficiency to specific collecting area under various conditions.

THEORETICAL BACKGROUND

The fundamental steps in the precipitation process are particle charging, particle collection, and the removal and disposal of the collected material. Particle charging is accomplished by a source of charge carriers in the presence of an electric field which drives the charge carriers to the particulate. Collection of the charged particulate occurs as the electric field drives the particles to a collecting electrode, where they are held by mechanical and electrical forces. Removal of the collected material is accomplished by the application of a force to the collecting electrode in such a manner that the collected ash is dislodged, and falls into a receiving hopper for subsequent transport to a disposal system.

In order to calculate the theoretically expected performance of an electrostatic precipitator, it is necessary to calculate particle charge as a function of particle size, residence time, and precipitator operating conditions. Field charging theory adequately describes experimentally observed particle charge values for particles larger than 2.0 μm with moderate to high values of applied electric field. Calculation of particle charge for diameters exceeding 2.0 μm is

therefore relatively straightforward if the precipitator operating conditions are adequately defined. For particle diameters less than 2.0 μm, the calculation of particle charge is complex, and has been the subject of considerable effort by a number of investigators. A more detailed discussion of particle charging theories is given in a paper by Smith and McDonald.[1]

The expression currently used in the model for particle charging calculations is given below in differential form:

$$\frac{dq}{dt} = \frac{N_0 e b q_s}{4\varepsilon_0}\left(1 - \frac{q}{q_s}\right)^2 + \pi r^2 e \tilde{v} N_0 \exp\left(-\frac{qe}{4\pi\varepsilon_0 r k T}\right) \qquad (1)$$

where q_s is a modified saturation charge given by

$$q_s = 4\pi\varepsilon_0 (r + \lambda)^2 E_0 \left(1 + 2\,\frac{K-1}{K+2}\,\frac{(r)^3}{(r+\lambda)^3}\right) \qquad (2)$$

in which
q = charge, coul
N_0 = free ion density, no/m^3
e = electronic charge, coul
ε_0 = permittivity of free space, coul^2/N-m^2
E_0 = electric field, volt/m
b = ion mobility, m^2/volt-sec
$\tilde{v}$ = mean thermal speed of ions, m/sec
r = particle radius, m
k = Boltzmann's constant, J/°K
T = temperature, °K
t = time, sec
K = dielectric constant
λ = an adjustable parameter

This expression is similar to one developed by Cochet.[2] Although the above expression represents the charging of submicron particles with sufficient accuracy to be useful in calculating precipitator performance, there are indications that the relationships developed by Smith and McDonald describe the charging process more accurately. Therefore, it may be desirable to incorporate their calculation procedure into the model at a later date.

The value of electric field used for the particle charging calculations is simply the average value between the discharge and collecting electrodes. In order to calculate the velocity of charged particles near the collecting electrode, however, it is necessary to compute the local electric field values in this region of space. A review of previous work

on this problem indicated that the most promising method of calculation was a numerical technique introduced by Leutert and Böhlen.[3] The equations which must be solved are given in two dimensions, written in discrete form:

$$\frac{\Delta^2 V}{\Delta X^2} + \frac{\Delta^2 V}{\Delta Y^2} = -\frac{\rho}{\varepsilon_0} \tag{3}$$

and

$$\rho^2 = \varepsilon_0 \left(\frac{\Delta V}{\Delta X} \frac{\Delta \rho}{\Delta X} + \frac{\Delta V}{\Delta Y} \frac{\Delta \rho}{\Delta Y} \right) \tag{4}$$

where V = potential, volts

ρ = space charge, coul/m^3

X = distance perpendicular to gas flow from wire to plate

Y = distance parallel to gas flow from wire to wire

A computer program based on these equations was written and incorporated into the model as a subroutine. In order to check the accuracy of the calculation procedure, the computer program has been used to calculate potential profiles and electric fields based on the geometry and operating conditions given for electric field measurements reported in the literature.

Figure 1 shows calculations based on the geometry and operating conditions reported by Penney and Matick[4] and their experimental results. Fairly good agreement is found for the potential profiles from the wire to the plate and from a point midway between wires to the plate. Also the field near the plate (the slope of the potential curve) is in excellent agreement. As a result of these and other comparisons between computed and measured results it was concluded that Leutert and Böhlen's technique provides a basis for computing electric fields in the region of interest adjacent to the collecting electrode.

If the particle charge and the electric field adjacent to the collecting electrode have been calculated, the next step in calculating theoretical collection efficiency is the calculation of electrical drift velocity, or migration velocity resulting from the coulomb and viscous drag forces acting upon a suspended particle. For particle sizes in

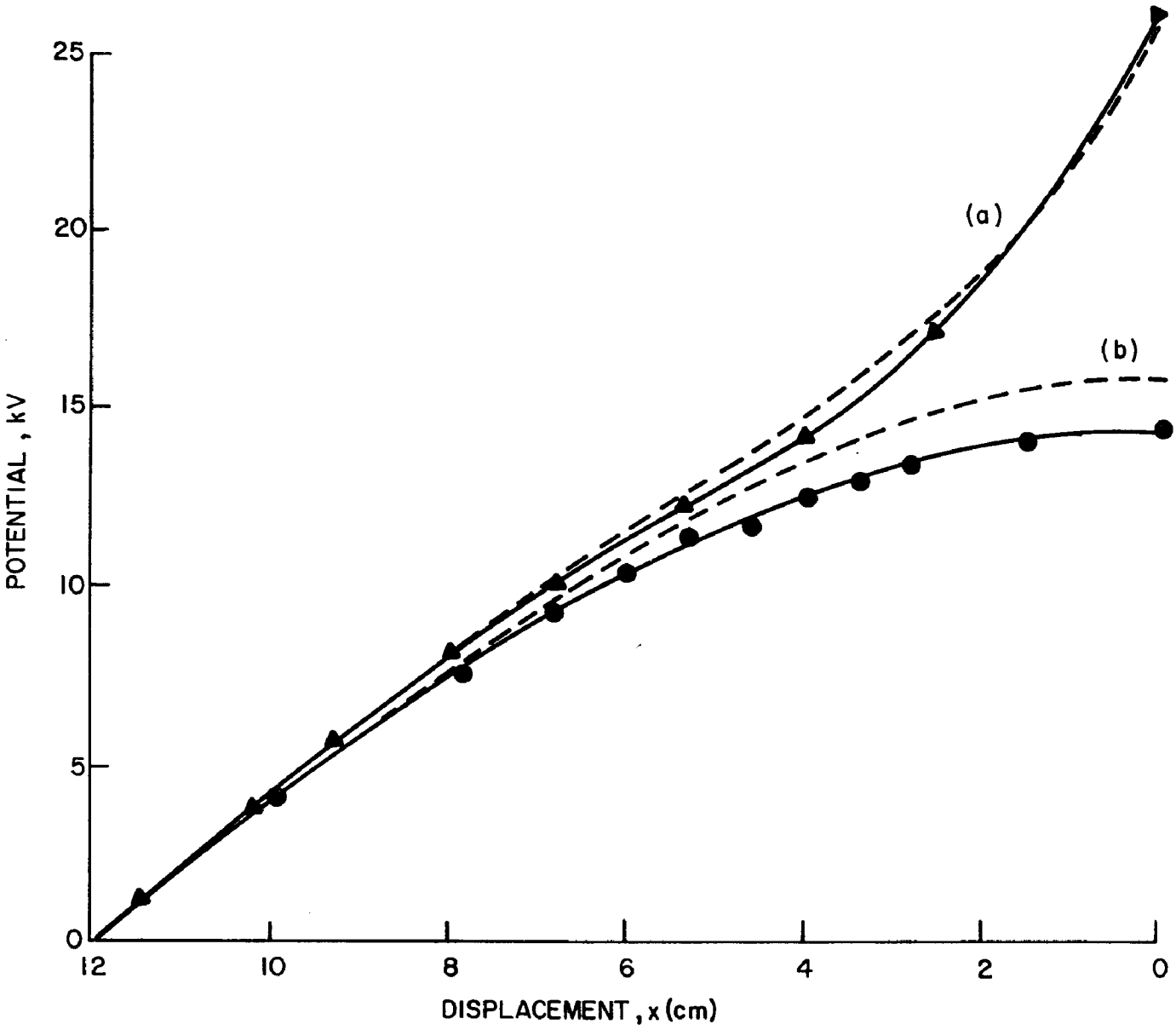

Figure 1. Potential profiles in a wire plate precipitator

(a) x=0 corresponds to the wire, x=12 cm the plate. Solid line, Penney and Matick (experimental). Dashed line, Southern Research Institute (calculated).

(b) x=0 corresponds to a point midway between wires, x=12 cm the plate. Solid line, Penney and Matick (experimental). Dashed line, Southern Research Institute (calculated).

the size range of interest, the acceleration time is negligible and the migration velocity is given by

$$w = \frac{qE_pC}{6\pi r\mu} \qquad (5)$$

where w = migration velocity of a particle of radius r, m/sec

E_p = electric field near collecting electrode, volt/m

C = Cunningham correction factor

μ = gas viscosity (kg/m-sec)

Gas flow velocities in most cases of practical interest are between 0.60 and 1.8 m/sec, while theoretical migration velocities for particles smaller than 6.0 μm are usually less than 0.3 m/sec. The path of these smaller particles therefore tends to be dominated by the turbulent motion of the gas stream in the interelectrode region. The classical equation for describing particle collection in electrostatic precipitators under turbulent flow conditions was derived by Deutsch and gives collection efficiency as a function of gas volume flow, collection area, and migration velocity:

$$\eta = 100\ [\ 1 - \exp\ (-A_pw/Q)\ ] \qquad (6)$$

where η = collection efficiency of a particle of radius r, %

A_p = collecting area, m^2

Q = gas volume flow, m^3/sec

The assumptions on which the derivation of this equation is based are:

(1) Gas turbulence provides sufficient mixing to establish a uniform particle concentration at any cross section of the precipitator.

(2) The gas velocity through and across the precipitator is uniform except for a boundary layer near the wall.

(3) The particle migration velocity near the collecting surface is constant for all particles and small compared with the average gas velocity. This implies that the equation is strictly applicable only to a monodisperse particulate with a diameter less than about 6 to 10 μm.

(4) There are no disturbing effects, such as reentrainment, back corona, etc.[5]

White[6] has reported a series of experiments using oil fumes under experimental conditions that were consistent with all of the above assumptions. The results indicate that the Deutsch equation adequately describes the collection mechanism for particulate in an electrostatic precipitator under idealized conditions. It has been common practice, however, to attempt to use the Deutsch equation to correlate field data obtained under conditions which violate most of the assumptions on which the original derivation was based. The correlation procedure usually involves solving the Deutsch equation as written below:

$$w_p = \frac{Q}{A} \ln \left(\frac{100}{100-\eta_0} \right) \qquad (7)$$

where w_p = precipitation rate parameter, m/sec

η_0 = overall mass collection efficiency, %

The quantity w_p can vary widely due to variations in the particle size distribution of the particulate and the operating conditions of the precipitator.

The approach which has been used in our work for calculating theoretical particle collection efficiencies consists of the following steps:

(1) Migration velocities are calculated for representative particle sizes as a function of electrical conditions for length increments in the direction of gas flow through the precipitator.

(2) The Deutsch equation is used to calculate the number of particles in each size band (the particle size distribution is represented by a histogram) which are collected in each incremental length.

(3) The collection efficiency of each representative particle size is determined by summing over the length of the precipitator. The overall mass collection efficiency is obtained by summing the mass of particles collected in each size band of the histogram.

CORRECTIONS TO THEORETICAL PREDICTIONS

In the preceding section, a basis for calculating theoretical collection efficiencies has been described. This section will discuss some of the non-idealities which exist in full-scale electrostatic precipitators and describe calculation procedures for estimating the effects of such conditions on predicted collection efficiencies. The factors which have been considered are:

(1) Gas velocity distribution

(2) Gas sneakage

(3) Rapping reentrainment

EFFECT OF GAS VELOCITY DISTRIBUTION

Although it is widely known that a poor velocity distribution gives a lower than anticipated efficiency, it is difficult to apply a numerical description for gas flow quality. This discussion will describe an approach to the calculation of degradation of performance based upon the velocity distribution, the theoretical or ideal efficiency, and the Deutsch equation.

The Deutsch equation can be rearranged to allow calculation of the corrected penetration of a given size particle as a function of the efficiency expected with a uniform velocity and the actual velocity distribution. This can be accomplished as follows:

(1) Calculate a constant k from the efficiency predicted under ideal conditions:

$$k = u_a \ln \frac{1}{1 - \eta/100} \tag{8}$$

(2) Calculate the mean penetration:

$$p = \frac{1}{Nu_a} \sum_{i=1}^{N} u_i \ (1 - \eta_i/100) \tag{9}$$

$$p = \frac{1}{Nu_a} \sum_{i=1}^{N} u_i e^{-\frac{k}{u_i}} \tag{10}$$

where u_a = average velocity, m/sec

p = corrected penetration fraction of a given size particle

N = number of points or channels with a given velocity

u_i = point values of velocity

η_i = point values of efficiency

For any practical velocity distribution and efficiency, the mean penetration obtained by summation over the velocity traverse will be higher than the calculated penetration based on an average velocity. If an apparent migration velocity for a given particle size is computed based upon the mean penetration and the Deutsch equation, the result will be a value lower than the value used for calculation of the single point values of penetration. The ratio of the original migration velocity to the reduced migration velocity is a numerical measure of the performance degradation caused by a non-uniform velocity distribution. An expression for this ratio may be obtained by setting the penetration based on the average velocity equal to the corrected penetration obtained from a summation of the point values of penetration, and solving for the required correction factor, which will be a divisor for the migration velocity.

The correction factor "F" may be obtained from:

$$\exp\left(-\frac{k}{F}\cdot\frac{1}{u_a}\right) = \frac{1}{Nu_a}\sum_{i=1}^{N} u_i \exp\left(-k/u_i\right) = p \qquad (11)$$

Therefore

$$F = -\frac{k}{u_a(\ln p)} \qquad (12)$$

Whether the quantity F correlates reasonably well with statistical measures of velocity non-uniformity is yet to be established. A limited number of traverse calculations seem to indicate a correlation between the factor F and the normalized standard deviation of the velocity traverse. Figure 2 shows F as a function of the ideal efficiency for several values of gas velocity standard deviation. These curves were obtained by computer evaluation of equation 12, and the data on which the calculations are based were obtained from Preszler and Lajos.[7] The standard deviations have been normalized to represent a fraction of the mean. The overlapping of the curves for standard deviations of 1.01 and 0.98 indicates that the standard deviation alone does not completely determine the relationship between F and collection efficiency.

GAS SNEAKAGE AND DUST REENTRAINMENT

Gas sneakage occurs when gas by-passes the electrified areas of an electrostatic precipitator by flowing through the hoppers or through the high voltage insulation space. Sneakage can be reduced by frequent baffles which force the gas to return to the main gas passages between the collection plates. If there were no baffles, the percent sneakage would establish the minimum possible penetration because it would be the percent volume having zero collection efficiency. With baffles, the sneakage re-mixes with part of the main flow and then re-by-passes in the next unbaffled area. The limiting penetration due to sneakage will therefore depend on the amount of sneakage gas per section, the degree of re-mixing, and the number of sections.

If we make the simplifying assumption that perfect mixing occurs following each baffled section, a simple expression may be derived which relates penetration to the fractional amount of sneakage per section, the ideal efficiency, and the number of stages over which the by-passage is assumed to occur.

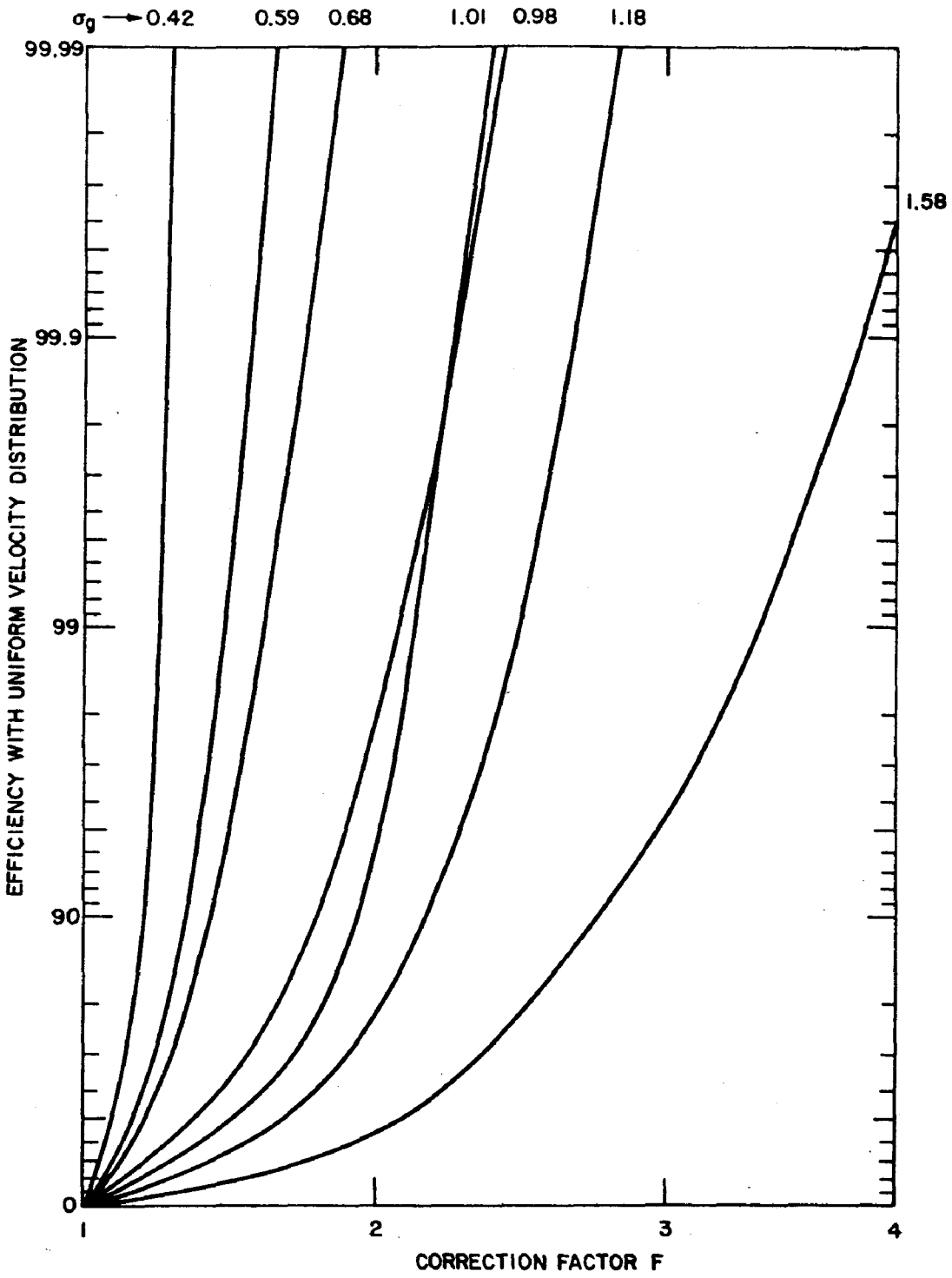

Figure 2. "F" as a function of ideal efficiency and gas flow standard deviation (σ_g)

The expression is:

$$Ps = \left[S + (1-S)(1-\eta/100)^{1/N_s}\right]^{N_s} \qquad (13)$$

where p_s = penetration corrected for sneakage

S = fractional amount of gas sneakage per section

N_s = number of baffled sections

η = collection efficiency of a given particle size obtained with no sneakage.

Rapping reentrainment is concerned with the amount of material that is recaptured by the gas stream after being dislodged from the collection plates by rapping. If we make the simplifying assumptions that a fixed fraction of the collected material of a given particle size is reentrained, and that the fraction does not vary with length through the precipitator, an expression can be derived identical in form to that obtained for gas sneakage:

$$p_R = \left[R + (1-R)(1-\eta/100)^{1/N_R}\right]^{N_R} \qquad (14)$$

where p_R = penetration corrected for reentrainment

R = fraction of material reentrained per section

N_R = number of stages over which reentrainment is assumed to occur

η = collection efficiency of a given particle size obtained with no reentrainment.

Figure 3 shows the effect on resultant efficiency for a given particle size of various degrees of reentrainment for a four-section precipitator with the indicated values of no-reentrainment efficiency.

Since both the expressions for reentrainment and sneakage result in a reduction of the expected collection efficiency under ideal conditions, it is possible to define a correction factor for the Deutsch equation, which is a divisor for the migration velocity, analogous to that defined for the effect of a non-uniform gas velocity distribution. The expression for the correction factor is, in terms of reentrainment:

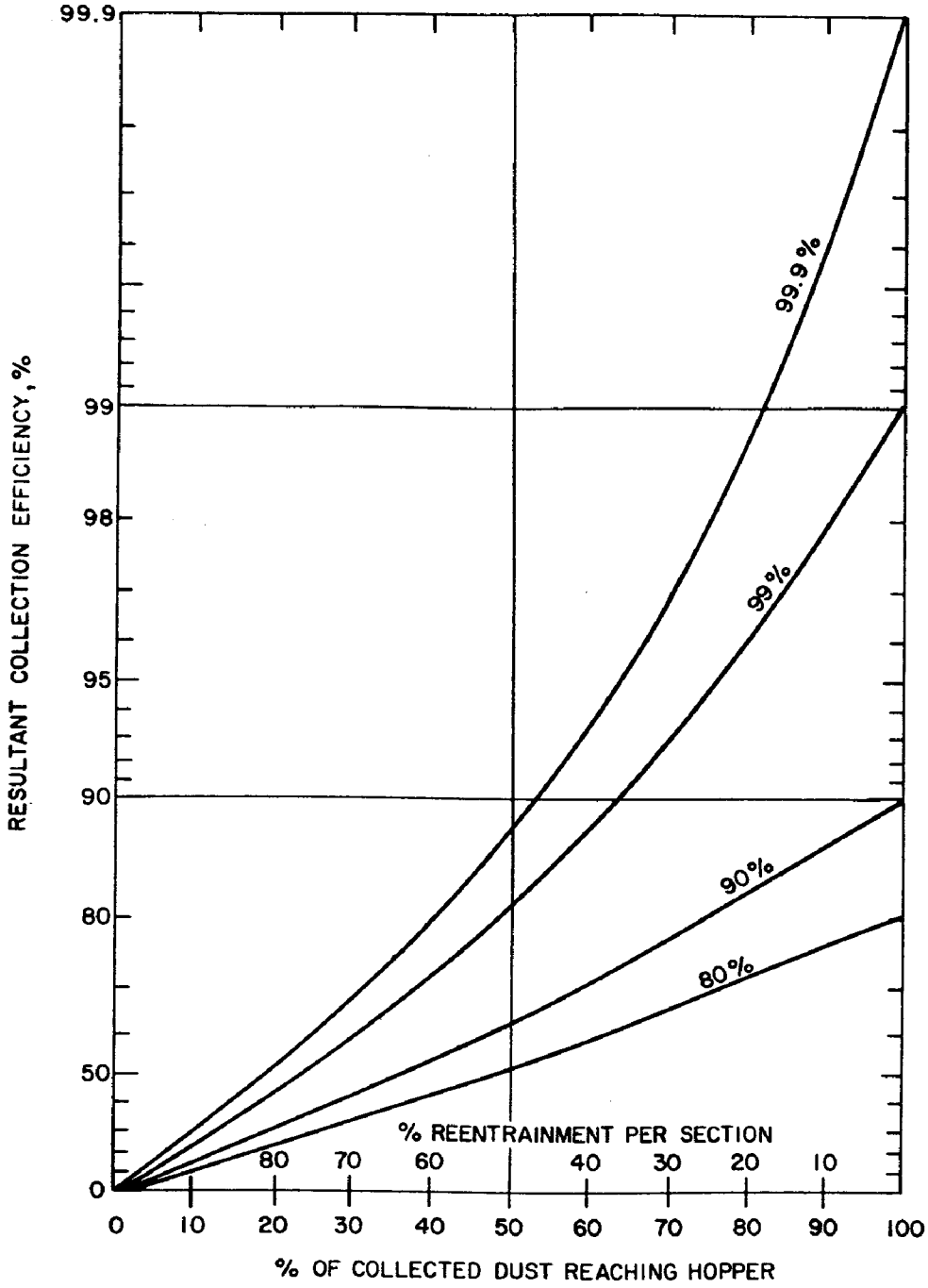

Figure 3. Effect of reentrainment on the efficiency of a four-section precipitator designed for a no reentrainment efficiency, as indicated for a monodisperse particulate

$$B = \frac{\ln (1 - \eta/100)}{N_R \ln \left[R + (1-R)(1-\eta/100)^{1/N_R}\right]} \qquad (15)$$

The foregoing expressions for reentrainment and gas sneakage are over-simplifications, but it is believed this analysis will be useful by providing a basis for estimating the order of magnitude of efficiency losses caused by these phenomena. If experimental data on these losses become available, it should be possible to develop more sophisticated models.

DESCRIPTION OF MODEL

Figure 4 gives a simplified block diagram of the precipitator model computer program. The program is structured around three major loops, the outermost of which is a direct iteration that converges on the overall mass efficiency. An initial estimate of overall mass efficiency is required because the space charge on the particulate at any point in the precipitator is a function of the particle charge and the number of particles remaining in the gas. The program contains a calculation procedure which estimates the effect of particulate space charge on the average free ion density and the electric field near the collecting electrode. The second major loop includes the calculations which must be performed in each incremental length, and the innermost loop contains the calculations dependent on particle size. After the theoretical collection efficiencies for each particle size have been obtained, the program calculates an effective migration velocity for each particle size from the relationship:

$$w_e = \frac{Q}{A} \ln \left(\frac{100}{100-\eta}\right) \qquad (16)$$

where η is again the collection efficiency of the particle size under consideration. At this point, a table of ideal or theoretical efficiencies and effective migration velocities is available for the representative particle sizes in the histogram of the particle size distribution. The program then evaluates the correction factors for gas velocity and reentrainment-sneakage, and calculates reduced effective migration velocities and collection efficiencies for each particle size. Overall mass efficiency is obtained by summing over the particle size distribution.

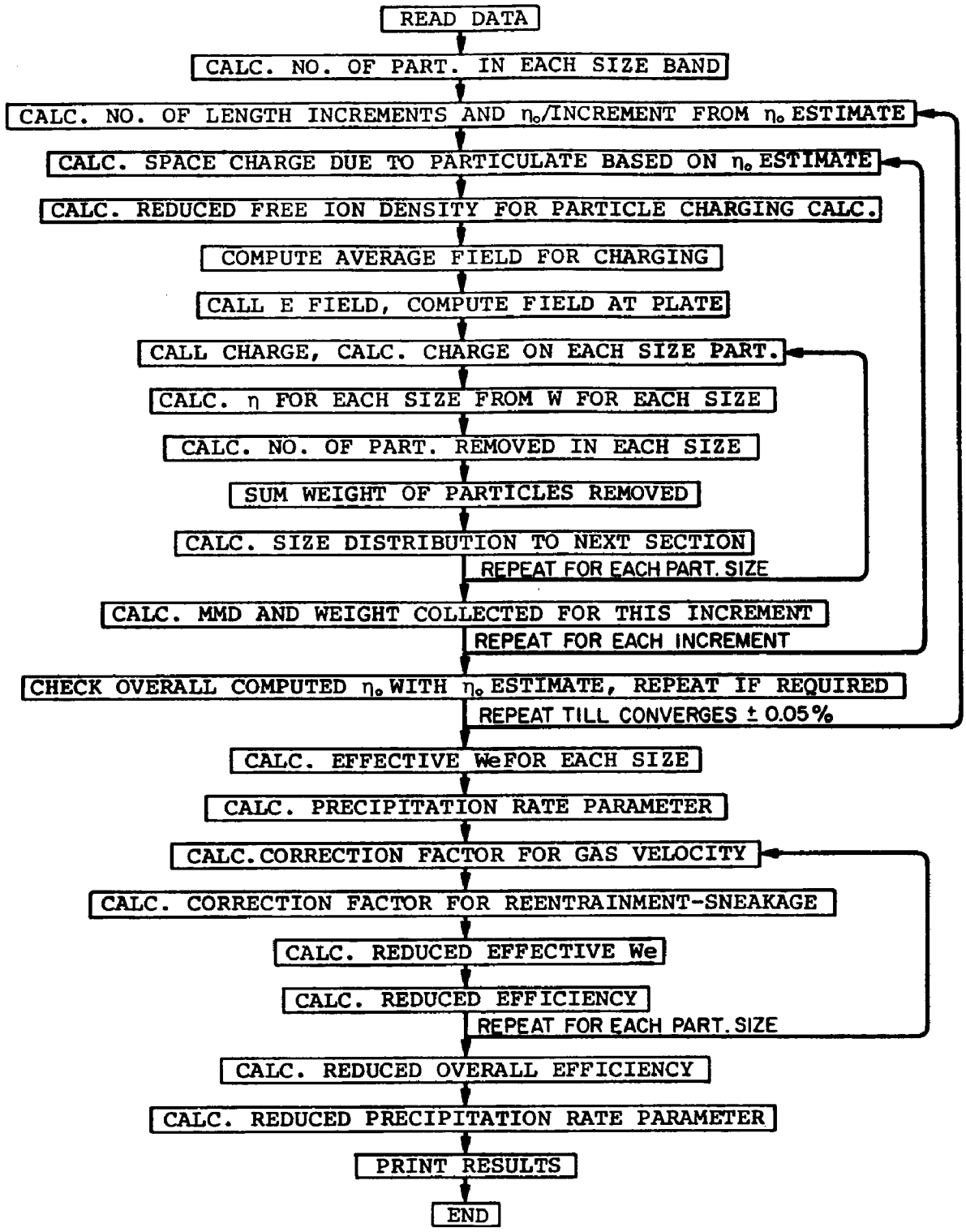

Figure 4. Simplified flow diagram of precipitator model

RESULTS

For the purpose of developing typical performance relationships for electrostatic precipitators collecting coal fly ash, a representative particle size distribution and secondary voltage vs current relationship were chosen for input data to the computer model. Operating current densities from 5 to 40 nA/cm^2 were selected. Theoretical values of effective migration velocity as a function of particle size are given in Figure 5. The values shown were computed with a specific collection area of 200 $ft^2/1000$ cfm. Particle charging dynamics become significant at the lower current densities, and the indicated values for effective migration velocities would decrease somewhat if the program were executed with a lower value of specific collecting area.

If the previously discussed corrections are utilized in the computer model, the predicted values of overall mass efficiency are reduced to the range of values obtained from field measurements. Figures 6, 7, and 8 provide comparisons between test data from coal fired power boilers and computed values of efficiency as a function of specific collection area for the indicated current densities. It can be seen that the theoretical overall mass efficiency curves are consistently higher than the field data. The value of 0.68 for the normalized gas velocity standard deviation represents a poor gas velocity distribution, and it can be seen that this has a major effect on predicted performance. It should be noted that the correction factors for gas velocity were obtained from an empirical fit to the data in Figure 2, which is based on a pilot-plant gas flow study. Similar data from full scale units would probably produce significantly different relationships between efficiency, standard deviation, and the quantity F. Since reentrainment and sneakage effects are estimated with identical mathematical expressions, these effects were combined by assuming 10% loss per stage over four effective stages.

The relationships presented in Figures 6, 7, and 8 are based on 9-inch plate to plate spacing, and a secondary volt-amp curve and particle size distribution considered to be typical for a coal-fired power boiler.

As an illustration of the trends predicted by the program, the effect of changes in particle size distribution are presented in Figures 9 and 10. These calculations are based on the assumption that the change in space charge suppression of corona current with size distribution is not a significant factor. This assumption is valid only if the dust loading in the fine particle range is not unusually large.

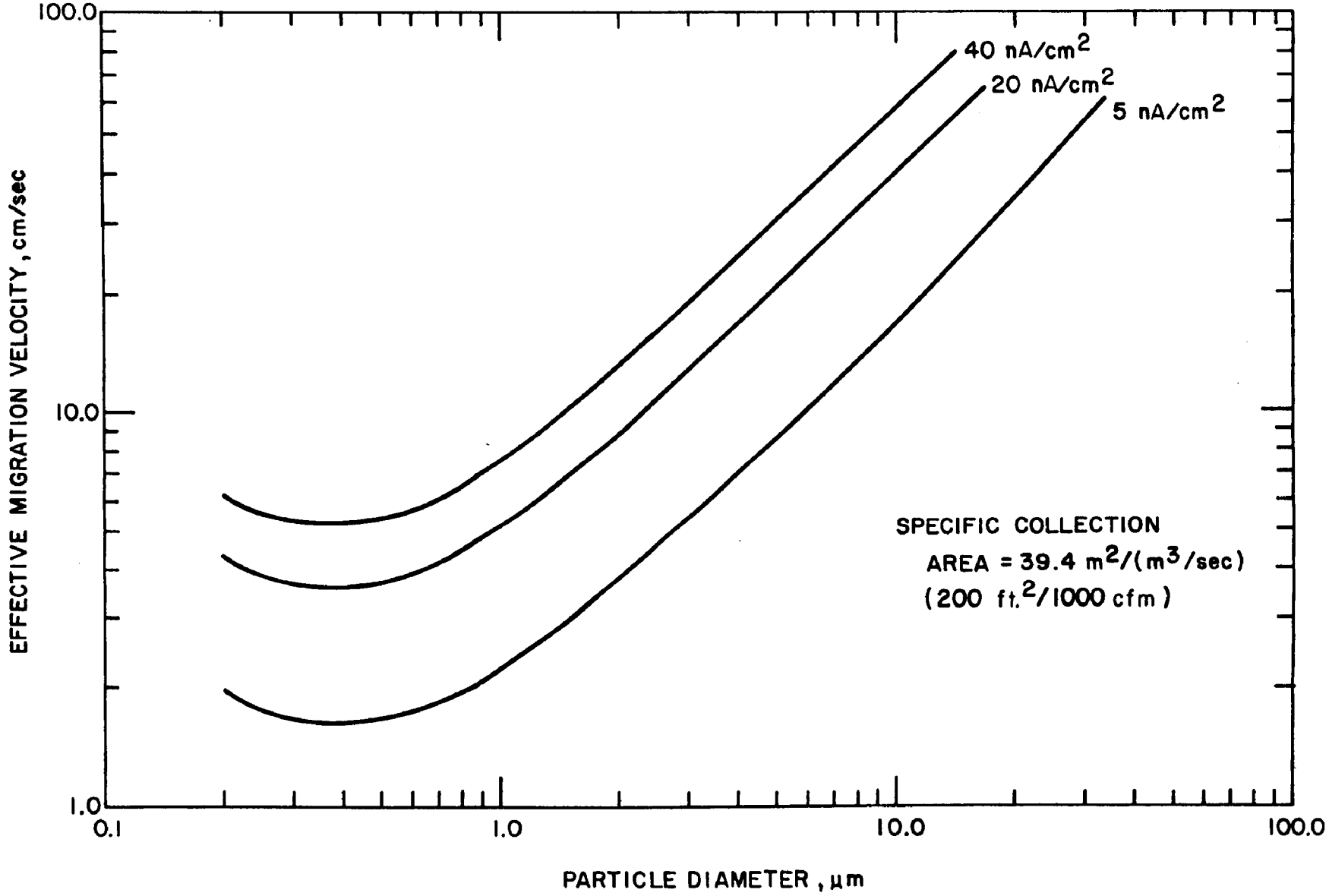

Figure 5. Theoretical effective migration velocity as a function of current density and particle size

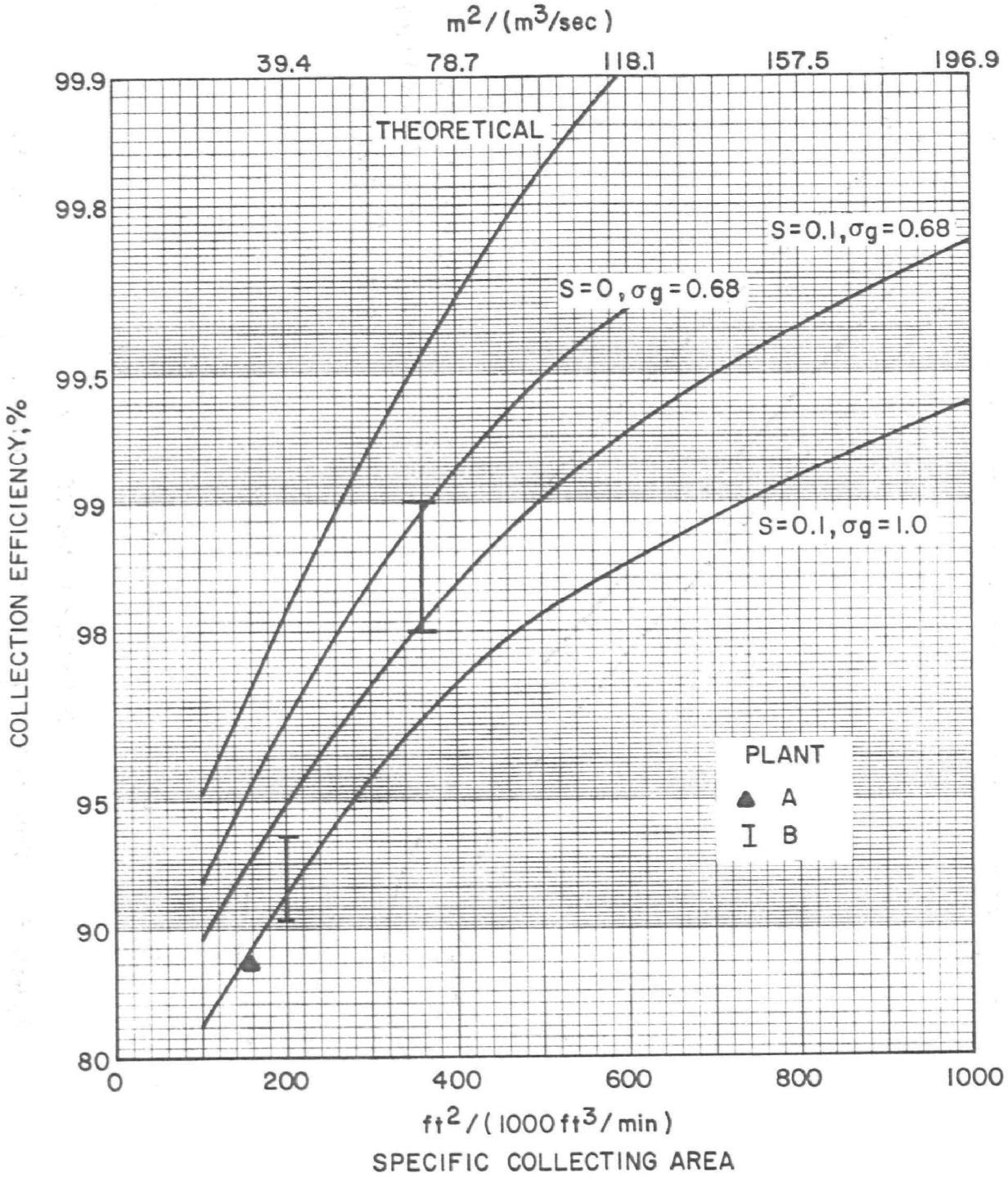

Figure 6. Computed performance curves at 5 nA/cm^2

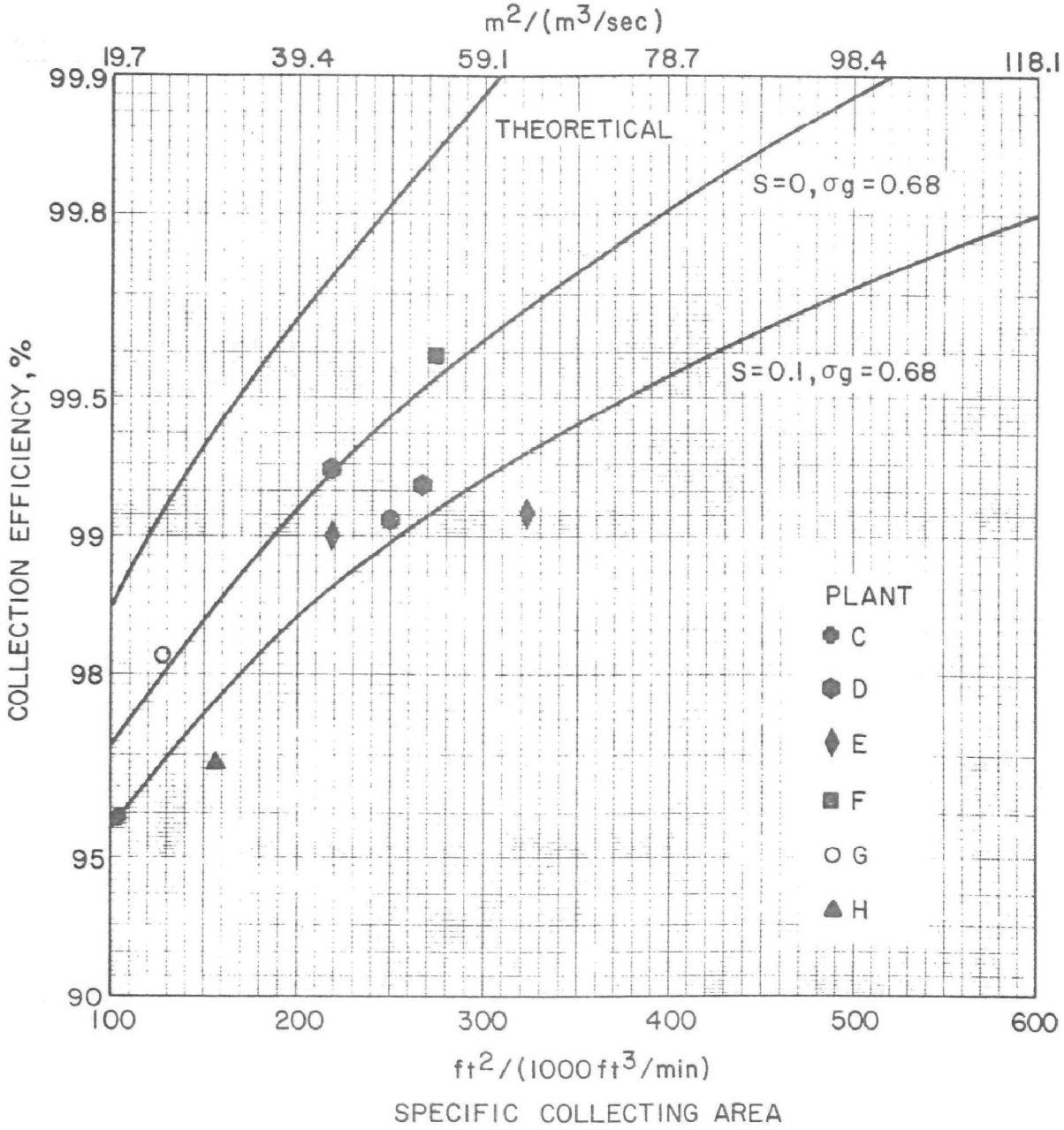

Figure 7. Computed performance curves at 20 nA/cm^2

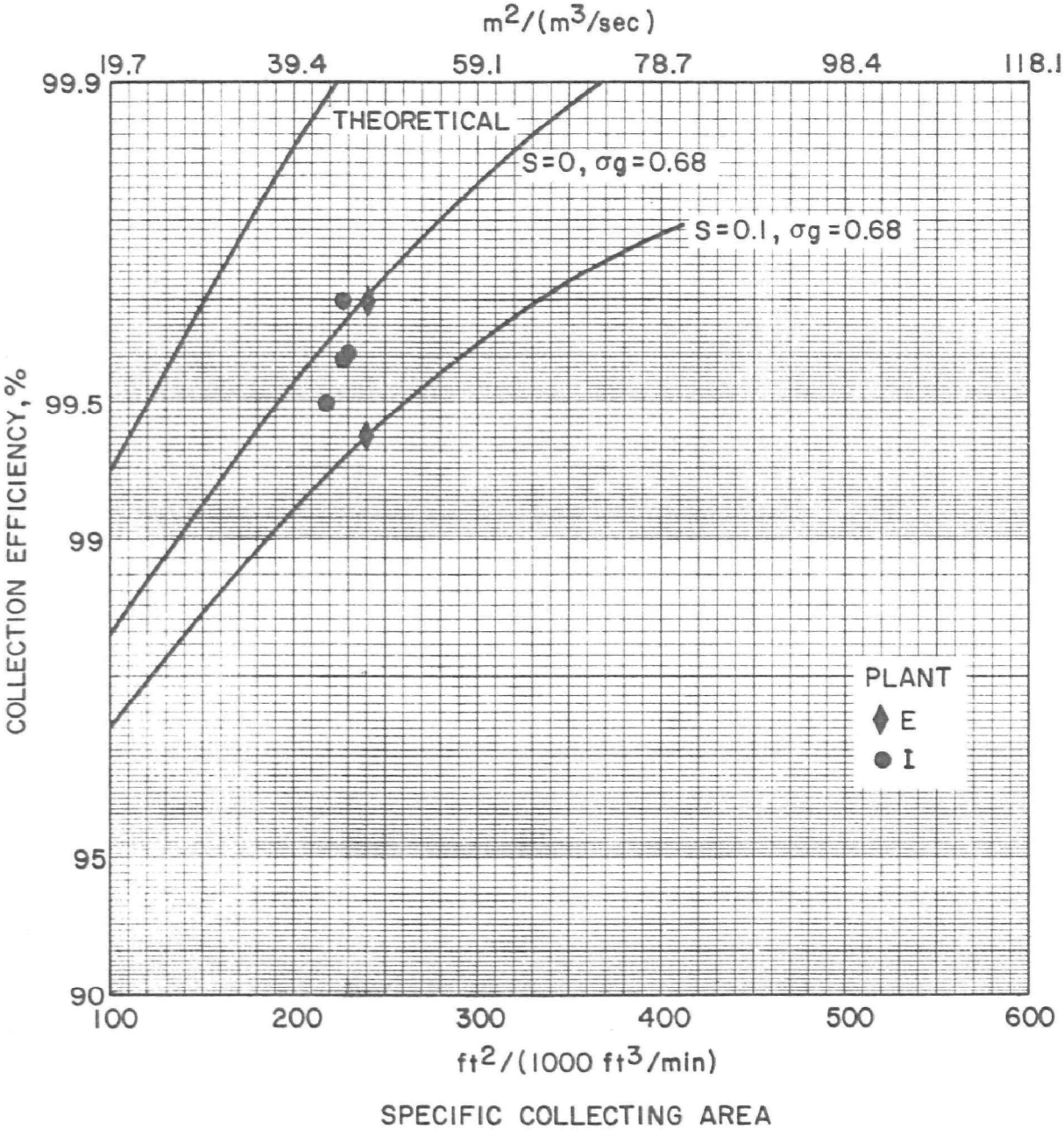

Figure 8. Computed performance curves at 40 nA/cm^2

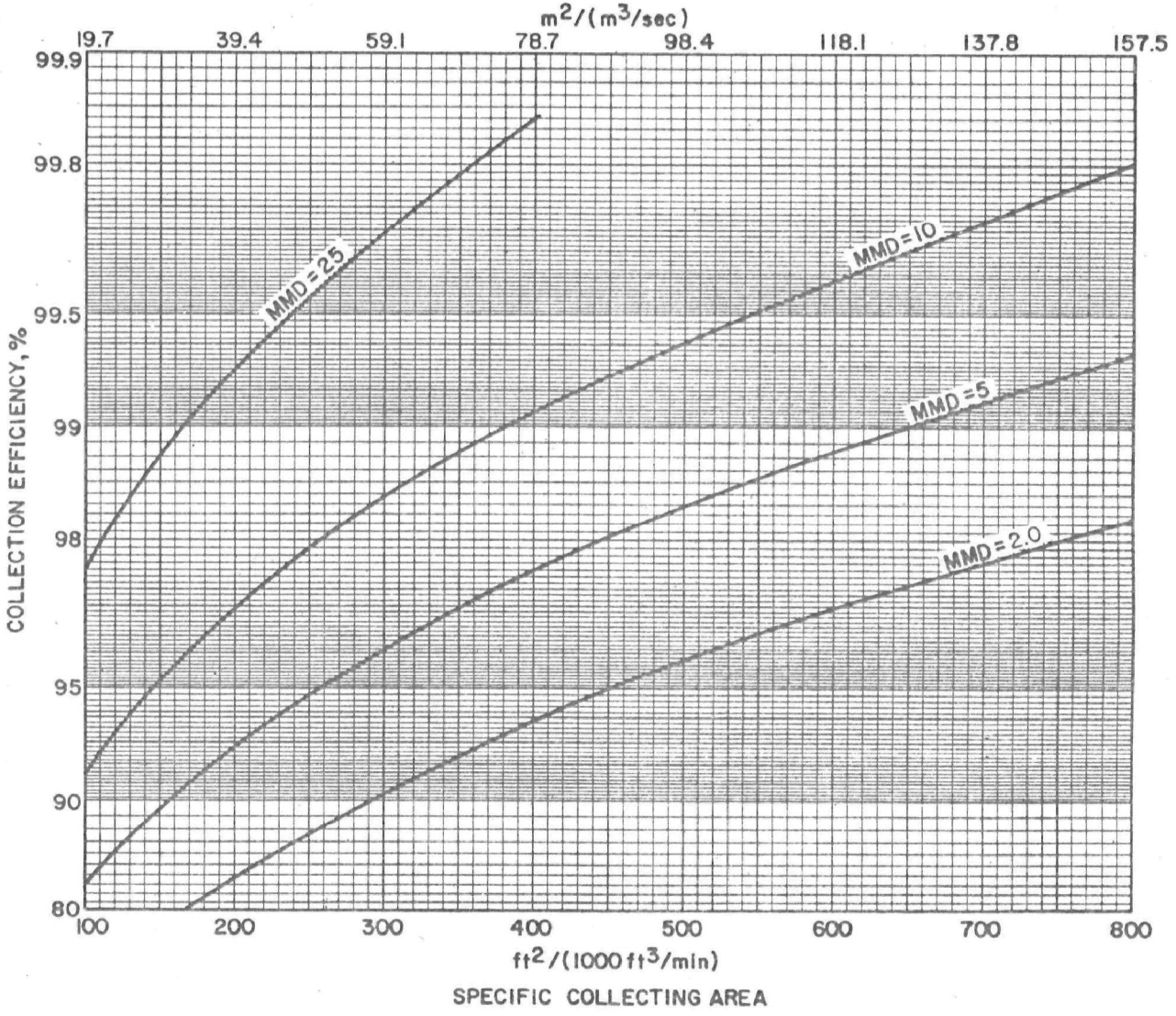

Figure 9. Effect of mass median diameter on computed performance (σ_p = 2.8)

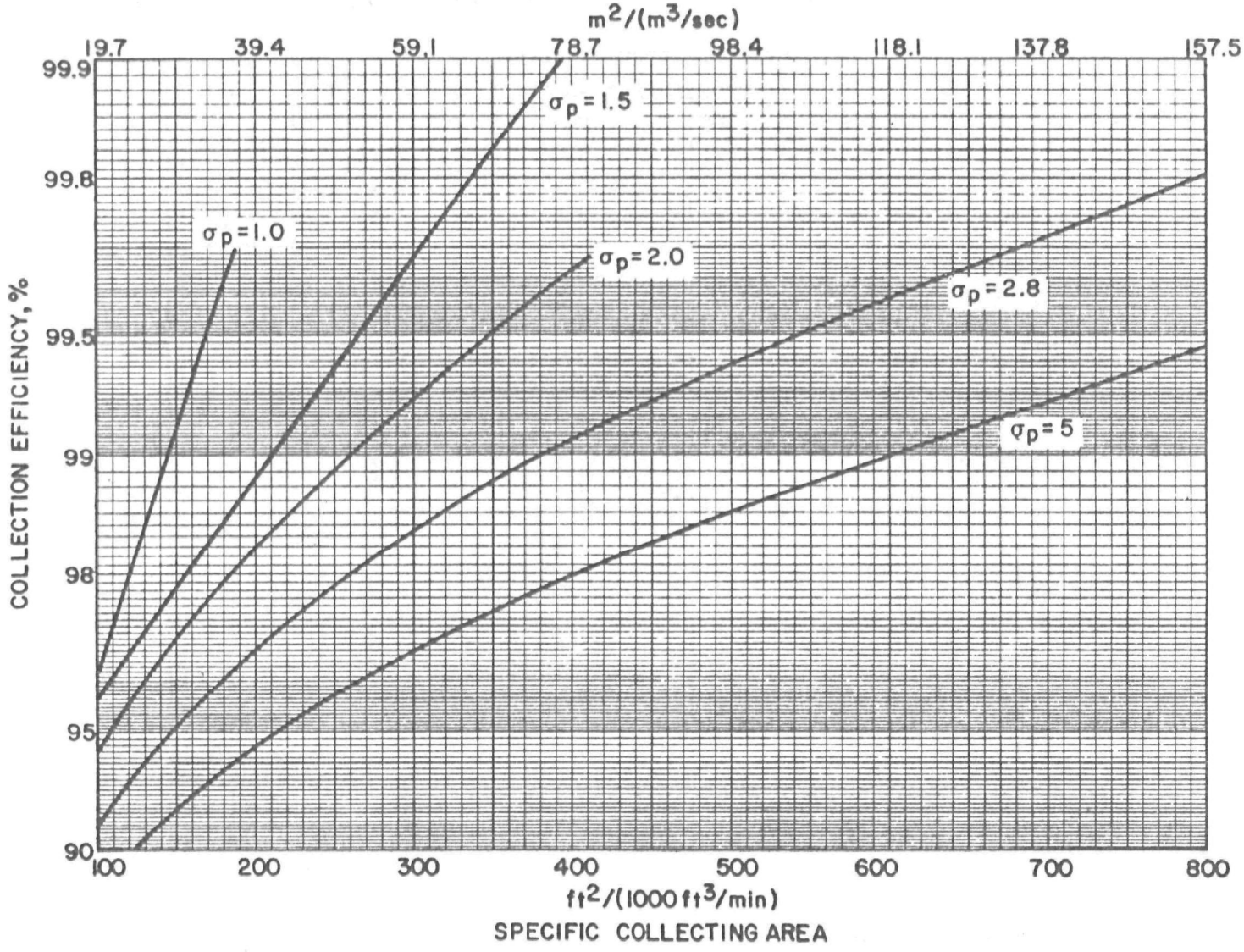

Figure 10. Effect of particle size distribution standard deviation on computed performance (MMD = 10 μm)

Log normal particle size distributions with mass median diameters of 25, 10, 5, and 2 μm and a geometric standard deviation of 2.8 were used as input data to the computer model along with a current density of 20 nA/cm^2, a gas velocity standard deviation of 0.68, and a reentrainment-sneakage factor of 0.1 over 4 stages. The results from these computer simulations are given in Figure 9. As would be expected, the computed performance is a strong function of the mass median diameter of the distribution.

It is also of interest to examine the variation in predicted performance caused by varying the standard deviation of a log normal size distribution with a given mass median diameter. Figure 10 presents results from computer simulations using a log normal particle size distribution with a mass median diameter of 10.0 μm and standard deviations ranging from 1.0 (a monodisperse distribution) to 5.0. Figure 10 indicates that predicted performance decreases with increasing values of particle size standard deviation. This decrease results from the influence of the increasing proportions of fine particulate which are present with the larger values of standard deviation. Note that the use of a monodisperse distribution with a diameter of 10.0 μm gives results vastly different from those obtained with realistic values of standard deviation.

CONCLUSIONS

Calculation of overall collection efficiency of polydisperse particulate in an electrostatic precipitator from theoretical relationships gives results considerably higher than those obtained from performance measurements on full-size units for coal-fired power boilers. Corrections to the idealized or theoretical collection efficiency to estimate the effects of non-uniform gas flow, rapping reentrainment, and gas by-passing the electrified sections reduce the overall values of calculated efficiency to the range of values obtained from field measurements. These calculations suggest that the theoretical model may be used as a basis for quantifying performance under field conditions if sufficient data on the major non-idealities become available.

ACKNOWLEDGMENTS

The work described in this paper was supported by the Environmental Protection Agency. The electric field and particle charging subroutines of the computer model were developed by Dr. Wallace B. Smith, Head of the Physics Section, Southern Research Institute.

REFERENCES

1. Smith, W. B., and J. R. McDonald. Calculation of the Charging Rate of Fine Particles by Unipolar Ions. In: Proceedings, Symposium on Electrostatic Precipitators for the Control of Fine Particles. Pensacola Beach. September 30-October 2, 1974.

2. Cochet, R. Laws of Charging of Fine (Submicron) Particles. Theoretical Studies, Recent Controls, Particle Spectra. Colloques Internationaux C.N.R.S. No. 102:331-338, 1960.

3. Leutert, G., and B. Böhlen. The Spatial Trend of Electric Field Strength and Space Charge Density in Plate-Type Electrostatic Precipitators. Staub-Reinhalt. Luft (in English). 32:27-33, July 1972.

4. Penney, G. W., and R. E. Matick. Potentials in DC Corona Fields. Trans. Amer. Inst. Elec. Eng. 79, Part I:91-99, May 1960.

5. White, H. J. Industrial Electrostatic Precipitation. Reading, Mass. Addison-Wesley, 1963. p. 165.

6. White, op. cit., p. 185.

7. Preszler, L., and T. Lajos. Uniformity of the Velocity Distribution Upon Entry into an Electrostatic Precipitator of a Flowing Gas. Staub-Reinhalt. Luft (in English). 32:1-7, November 1972.

ADHESIVE BEHAVIOR OF DUST IN ELECTROSTATIC PRECIPITATION

Gaylord W. Penney
Carnegie-Mellon University
Pittsburgh, Pennsylvania

ABSTRACT

In 2-stage precipitators particles are driven to the collecting plates by electrostatic forces but then the electrostatic force reverses and tends to pull the particles off so that dust is held on the collecting electrodes only by adhesion.

In Cottrell or single-stage precipitators the corona current can provide a significant force tending to hold the collected dust to the electrode provided that the resistivity of the dust is 10^{10} ohm-cm or more. Adhesion is still essential in the collection of lower resistivity dust and is of vital importance in the transfer of dust from the collecting electrodes to the hopper. As the dust falls from the plates to the hopper dust must be held in agglomerations or chunks as it falls.

There are many peculiarities in the adhesive behavior of eletrostatically collected dust. A better understanding of this adhesive behavior is essential if we are to improve the transfer of dust from the collecting electrodes to the hopper.

The term "adhesion" will be used to include forces between dust particles and the collecting surface and also forces between adjacent dust particles. If we regard a deposit of dust as homogeneous then I should say that cohesive forces hold the dust particles together. However I tend to regard most dust deposits as non-homogeneous. So for simplicity, the word "adhesion" will be used in a general sense and will include forces holding particles to each other as well as holding particles to the collecting electrodes.

My introduction to electrostatic precipitation (ESP) was the development of the Westinghouse Precipitron. This is a 2-stage precipitator used for cleaning ventilating air. In this device air passes through a corona region where the dust receives a positive charge but most of the dust is removed by the electric field between parallel plates. The positive charge interacts with the field to drive dust particles to the grounded or negative plates, but then the initial positive charge leaks off and is replaced by the negative induced charge. Thus the dust is deposited by electrostatic forces, but then the force reverses and tends to pull the dust off from the collecting plates so that the dust is held only by adhesion. This development of the Precipitron occurred in the 1930's. This was before smoke control and much of the pollution in Pittsburgh came from the incomplete combustion of soft coal. There was enough tarry material to give good adhesion and so the particulates could be effectively collected in a 2-stage precipitator. However attempts to use 2-stage precipitators for fly ash and many similar dry dusts have usually been unsuccessful.

In a single-stage or Cottrell precipitator, the dust is collected in the corona region. The corona current can provide a force holding the dust to the collecting plate. If the resistivity is 10^{10} ohm-cm or more, this holding force may be of the order of one-half gram per cm^2. However, if this electrostatic force was the only thing holding dust to the plates, the dust would fall off whenever the power was turned off. But if you have ever looked into a power plant ESP when it is shut down it is very evident that there are strong adhesive forces holding dust to electrodes. A startling example is the deposit of dust on the corona wires. In theory particles should be repelled from the wires. Yet one often observes dust deposits over 1 in. in diameter hanging to the wires in spite of the fact that there are rappers which are intended to keep wires free of dust. A surprising characteristic of these dust deposits is that they hang tenaciously to the wires and yet after the dust is shaken off it seems to exhibit almost no adhesion. The dust can be pressed at 100 $lb/in.^2$ or more yet exhibit no adhesion. Thus there is something peculiar about this adhesion.

The Deutsch equation is widely used to describe the efficiency of an ESP. It is a simple relation giving precipitator efficiency in terms of collecting area, gas flow rate, and the electrically induced velocity at which charged particles migrate or drift toward the collecting electrode. This drift velocity can be calculated from fundamentals and yet ESP performance cannot in general be predicted from fundamentals especially with dry dusts. Instead the Deutsch equation is normally used to correlate measured efficiencies. In any given test the collecting area is known, and the air flow and the efficiency can be measured. Then if the Deutsch relation is assumed to apply, this drift velocity can be computed. However, when determined in this way, I think that it should be given some other name, e.g., correlation coefficient, because this calculated number has little relation to the velocity with which individual particles drift toward the collecting electrode.

Since the amount of charge on particles and the consequent electrostatic drift velocity are subject to reasonably good calculation, and since the Deutsch equation is generally accepted as describing the precipitation process, it seems reasonable to ask, "Why cannot precipitator efficiency be predicted by substituting this calculated drift velocity into the Deutsch equation?" The Deutsch equation depends on several simplifying assumptions which do not represent actual conditions in precipitators and so errors occur when this simple equation is applied to real conditions. In my opinion, the most serious of these errors lies in the complete neglect of the question of adhesion. The derivation assumes that a particle is collected when it touches the collecting electrode. It can be shown that, even in the absence of rapping, particles do not necessarily remain where they are first deposited.

However the major importance of adhesion is in moving the dust from the collecting surface to the hopper. If when the surface was rapped dust came off in its original fine state almost none of it would reach the hopper. The effective transfer of dust to the hopper is almost entirely dependent on the formation of chunks or agglomerations of dust which can effectively fall with a minimum of reentrainment.

Korn working with a fine quartz fiber under a microscope has done pioneering work on the adhesion of individual particles. However, his studies did not explain the peculiar behavior of groups of particles in a precipitator, for example, the deposits on wires show such high adhesion and yet once the deposit is disturbed there seems to be no adhesion.

One method for measuring the adhesion of electrostatically deposited dust is to deposit dust on a small test surface and then to mount the test surface in a centrifuge and gradually increase the speed until dust flies off. This speed can be converted to force in "g's". Then by determining the weight and area of the deposit, the force in g/cm^2 can be computed. Figures 1-5 illustrate some of these things. I said that dust particles do not always remain where they first touch the collecting electrode.

Figure 1 is a photograph showing the path of a quartz particle as it is precipitated. The background is black and not illuminated so that only the particle is seen. The light beam which illuminates the particle is chopped so that one sees a series of dashes each 1/1000th second long. The velocity can then be determined from the length of a dash. This shows a 225 μm silica particle being precipitated onto a clean metal plate. Note that the particle bounces off with about one-half of the velocity at which it struck.

Figure 2 shows a large fly ash particle under otherwise similar conditions. Note that the fly ash particle, which is largely coke, is not as elastic so that it does not bounce as high. Notice the series of hops much like a golf ball bouncing along the ground.

Figures 3-5 show attempts to precipitate larger (225 μm) particles onto a layer of previously deposited dust. Figure 3 shows the deposit of fine particles before the large particles were precipitated onto it.

Figure 4 shows the dust deposit when 225 μm particles were deposited with an air velocity of only 108 ft/min. Note the many craters where large particles struck. At this low air velocity most of the large particles come to rest relatively near to the point where they struck.

Figure 5 shows an attempt to precipitate the same large particles but at an air velocity of 800 ft/min. Note the long craters where the large particles struck. At this high air velocity all of the large particles are carried well downstream from the point where they struck. At this velocity attempting to precipitate one gram of large particles could knock off about one gram of the previously deposited fine particles. Of course if the precipitator were long enough both the large particles and the fine particles knocked off would eventually be precipitated.

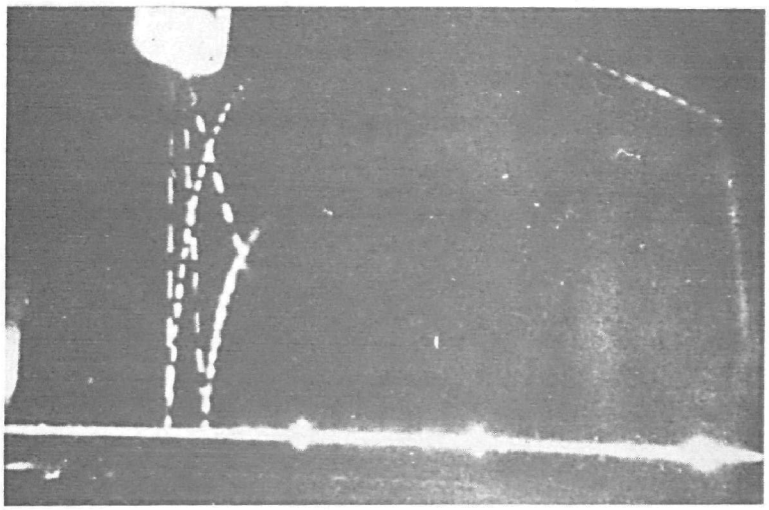

Figure 1. Path of a quartz particle being precipitated

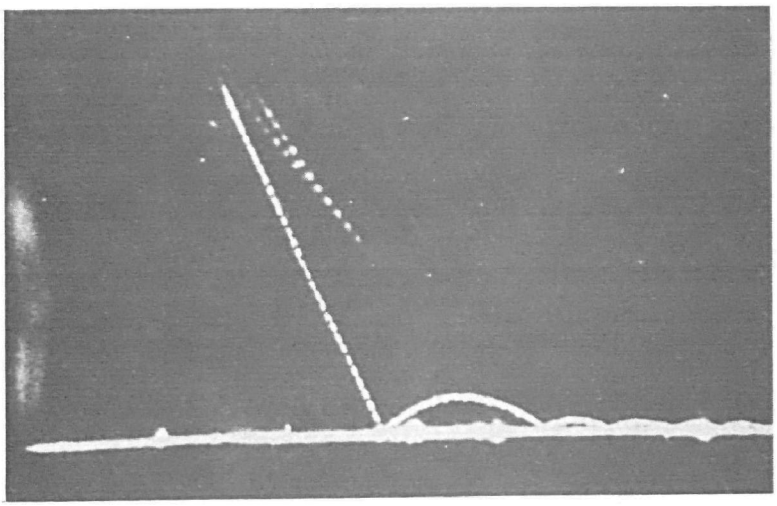

Figure 2. Large fly ash particle being precipitated

Figure 3. Precipitation of 225-μm particles onto layer of previously deposited dust

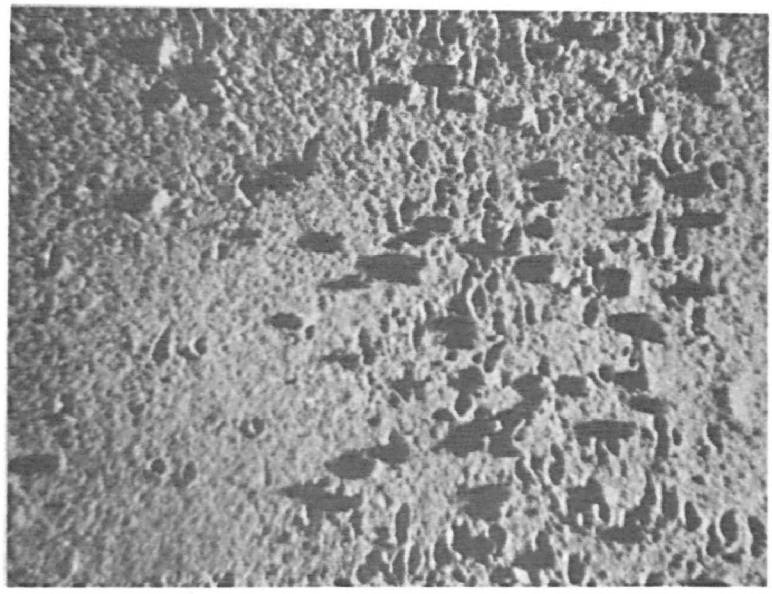

Figure 4. Deposition of 225-μm particles with air velocity 108 ft/min

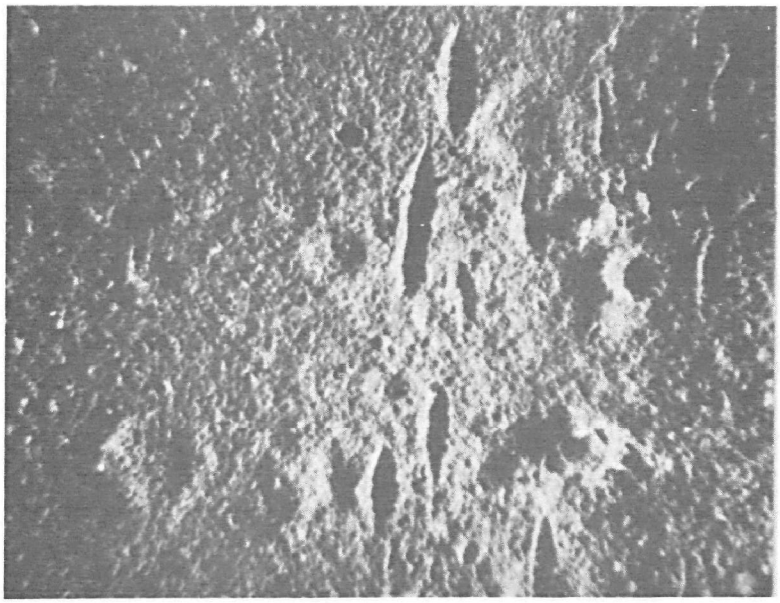

Figure 5. Deposition of 225-μm particles with air velocity 800 ft/min

The dislodging of dust from the plates in such a manner that it will fall to the hopper with a minimum of reentrainment is a subject that seems to be avoided in the literature. Little is known about it, probably because it is difficult to observe and measure.

Many older rapping systems utilized heavy hammer blows which dislodged the dust but caused a cloud of dust, or puff, to go up the stack. This was very visible and therefore highly objectionable. To avoid these puffs so called continuous rapping was developed. Rather light blows to a small section were used with the location of these blows continuously rotated over the various sections of the precipitator. This system avoided the very visible clouds or puffs of dust. However whenever I have had an opportunity to look into a power plant precipitator at shut down it is very evident that the dust is not effectively removed from the collecting surfaces.

In a precipitator thick deposits of dust often build up. Looking into a precipitator after a long period of operation one often sees irregular dust deposits up to 1 or 2 cm in thickness. Adjacent to a thick deposit will be a thin layer of dust where a deposit has broken loose.

Current must be conducted through the layer of collected dust. It can do this until the breakdown voltage of the dust is reached which is typically 10,000 to 20,000 volts/cm. At this point minute sparks occur through the dust layer. These result in back-corona and may trigger streamer pulses which result in sparkover.

Suppose the resistivity of the dust is 10^{12} ohm-cm and its puncture voltage is 15 kV/cm. Then the permissible current $I = E/R$ is $1.5 \times 10^{4}/10^{12}$ or 1.5×10^{-8} A/cm^2. Suppose one adjusted the corona current to this value. Then the voltage drop in a 2-cm layer would be 15 kV/cm or 30 kV while in the adjacent 1-mm thickness, it would be 1.5 kV. It is obvious that such a drop would seriously distort the electric field so that the current density would not be uniform. Current would concentrate at this thin dust layer so that the average current density would have to be reduced to avoid back-corona.

Rapping force is often specified in terms of maximum acceleration (so many times gravity). The figure of 50 g's is often to be used. By itself this is very incomplete information; 50 g's could describe a high frequency wave motion propagated from the hammer blow. This would have relatively little effect. On the other hand 50 g's at 2 cycles per second would almost certainly destroy the entire precipitator.

In addition to theoretical objections to thick dust deposits there is the practical experience that precipitators operate relatively efficiently for a few hours after being shut down and thoroughly cleaned out. From such reasoning one can make a strong case for mechanically as well as electrically sectionalizing a precipitator. In this way a section could be dampered off and vigorously rapped to remove any heavy dust deposits without reentrainment. This would of course add to the cost for a given size. So information on the possible gain is needed to indicate whether the cost can be justified by the improved performance. This indicates a need for more basic work on adhesion.

The contact potential theory of adhesion appears to explain many of the peculiar adhesive properties of electrostatically deposited dust. The theory assumes that, with most dust particles, the work function is not uniform over the surface of the particle so that there is a contact potential difference. Contact potentials must cancel out, or add to zero, around any closed circuit. Thus contact potentials are not important in usual electric circuits and so most engineers are not familiar with the subject. However, wherever there is a contact potential difference between two surfaces there is an electric field. If the spacing between the two surfaces is small, the field may be high and so there may be a large

effect on the motion of ions or small charged particles. Our first tests to study adhesion were made using talc particles. Talc is a crystalline material which tends to fracture along crystal planes. Opposite crystal faces have different work functions and so there is a contact potential difference between opposite faces. If this is true a particle would behave like a dipole in an electric field (Figure 6). This diagram represents the theory in its simplest form.

Dipolar particles would be oriented by the electric field. With negative corona the particles are deposited on the positive electrode with the negative side of the particle against the positive electrode. The top of the particle is positive so that the negative side of the next particle contacts the positive side of the first particle. Thus there are coulomb forces holding particles together. If this theory is correct there should be a contact potential difference between a sample of dust precipitated using negative corona and a similar sample precipitated using positive corona. Contact potential difference cannot be measured by an ordinary meter because such potential differences must cancel out around any closed circuit. A method of measurement proposed by Lord Kelvin is used to measure these contact potential differences. If we deposit one sample of dust using negative corona and then a second deposit of the same dust but using positive corona we do find that there is a contact potential difference between the negative corona deposit and the positive corona deposit.

As described thus far the contact potential theory appears to be fairly simple. Actual dusts usually behave in a much more complicated manner. The work function of a material is dependent on layers of gas absorbed on the surface as well as on the internal atomic structure. It appears that some particles behave like dipoles but in general most particles behave as though there were differences in contact potential rather randomly distributed over the particle surface. High adhesive forces can still result because if the particles are deposited one at a time they can be oriented by coulomb forces so that positive areas are adjacent to negative areas. In this manner high adhesive forces can be produced in mechanically deposited dust. Depositing dust on a porous filter and depositing it in a centrifuge have both produced about the same degree of adhesive force as when the same dust was precipitated in an electric field. However when precipitated in an electric field there always seems to be some difference in contact potential between dust deposited on the anode and the dust deposited on the cathode indicating that there is some orientation by the electric field.

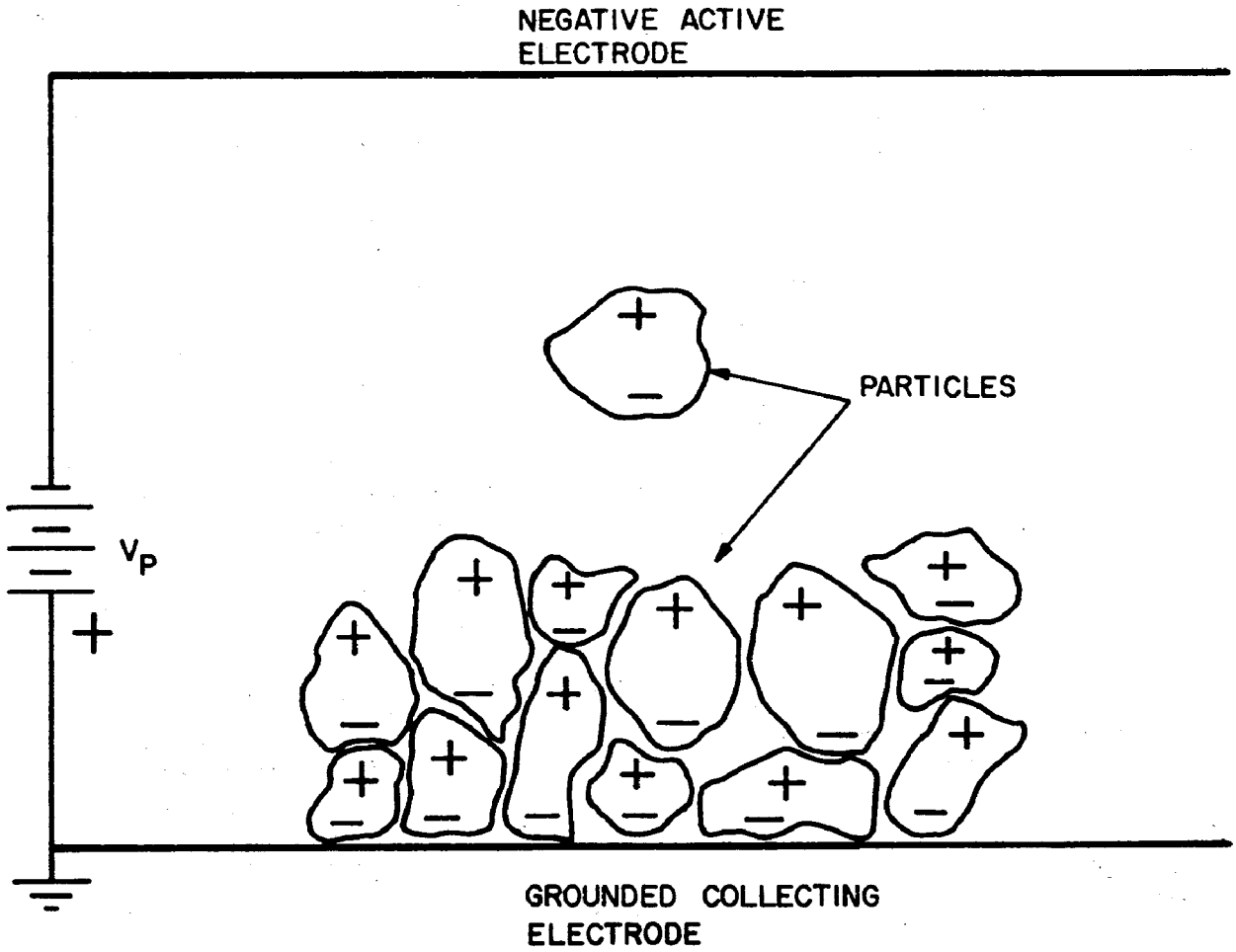

Figure 6. Dipolar particles in an electric field

There are many other puzzling aspects to the theory. Dalmon and Tidy at Leatherhead, England, made tests which appeared to be in conflict with our first paper and so they said they had disproven the theory. However, they apparently had not seen our second paper which showed measurements similar to theirs. So the question seems to be one of interpretation and not of experimental facts.

According to theory, adhesion due to differences in contact potential should be effective for particles of a few microns or less but should be relatively ineffective for large particles.

Figure 7 shows the measured adhesive force as a function of particle size. For the larger sizes (above 40 μm diameter) the separation was by screening so that a given sample could consist of a rather narrow range of sizes. Below 37 μm the stated size is the largest particle in the sample. The 10 μm point was for a sample from which the larger particles were removed by a cyclone. This separation was not very exact. For the points below 10 μm the larger particles were removed by an elutriator which appeared to effectively remove almost all particles above the stated size. The behavior of larger particles in a precipitator seems to need much further study.

Adhesion is important in holding dust to the collecting electrode but a more important function is to hold dust together into chunks or agglomerations, as the dust falls from the collecting surface to the hopper. This transfer of the dust to the hopper has received relatively little attention largely because it is difficult to study. Over the years we made several unsuccessful attempts to obtain useful information. But recently we developed a promising method. A test surface is rapped at some height above a horizontal moving collecting surface. The timing of the rapping blow is synchronized with a particular position of the moving collecting surface. Then knowing the velocity of the collecting surface, the time required to fall can be calculated from the position of the dust on the collecting surface. When fine particles were precipitated in the corona discharge under conditions such that no dust was pulled off and redeposited, the deposits had a high adhesive force.

The high adhesion could be measured by tests in the centrifuge or in the dust fall apparatus. When tested in the dust fall apparatus a major fraction of this dust fell a

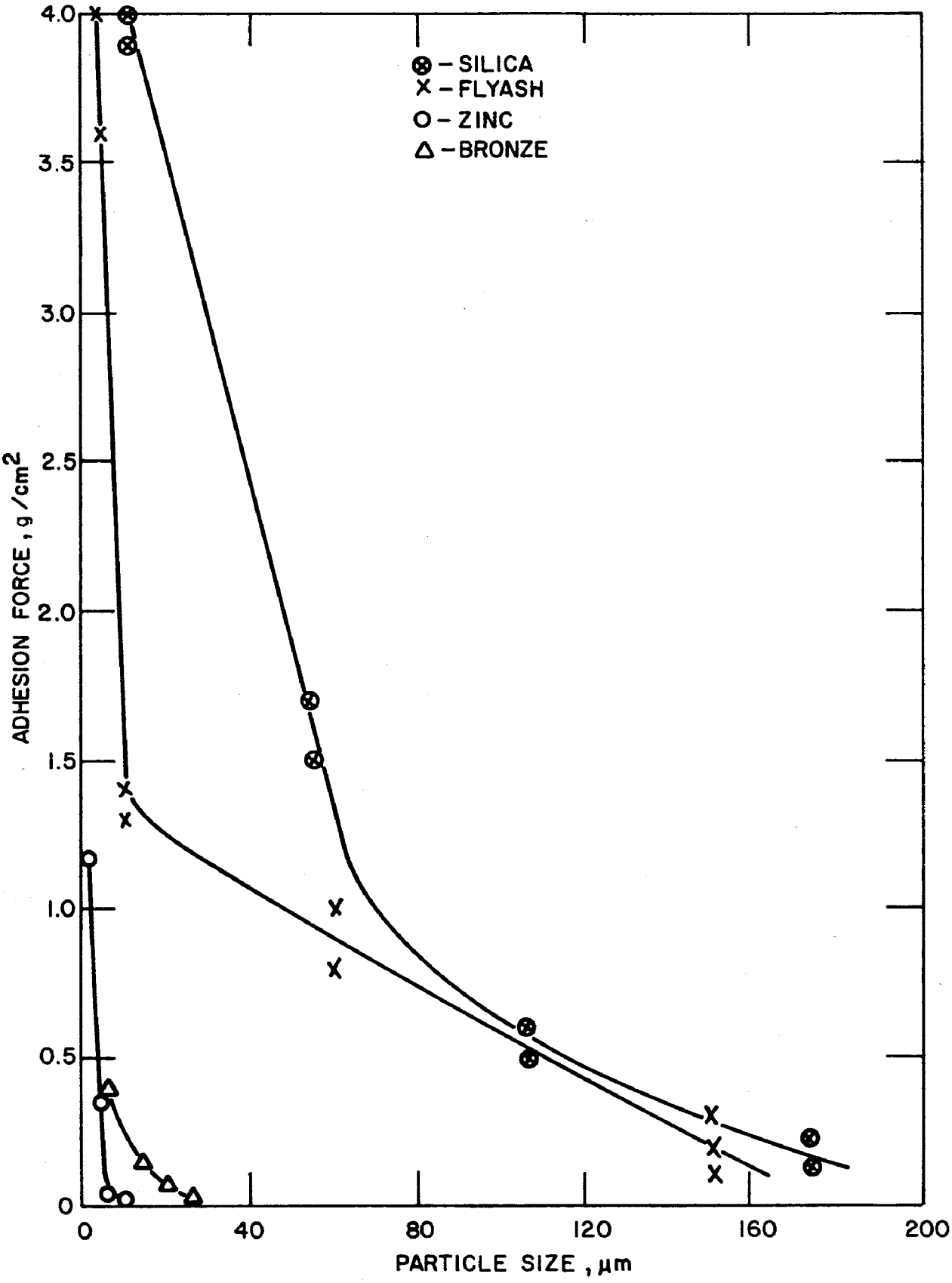

Figure 7. Measured adhesion force as a function of particle size

distance of 4 ft with very little reentrainment. On the other hand at a location where there was negligible corona current and where much of the dust consisted of agglomerations resulting from dust dislodged and carried downstream, this dust deposit showed a low adhesive force and when tested in the dust fall apparatus, most of this dust had a velocity of fall less than 2.5 ft/sec. Thus if it were falling in a precipitator where the gas velocity was 5 ft/sec its resultant angle of motion would be less than 27° from the horizontal.

In summary both theory and experiment indicate that for fine particles there is a mechanism that depends on the relative orientation of the particles. The resulting adhesive force is materially greater than the forces due to the applied electric field. Thus in a two-stage precipitator where the electrical force reverses and tends to pull the particle off, the dust can still be held by adhesive forces. In this meeting we are primarily discussing single stage industrial precipitators. Here there is the possibility of removing larger particles by a mechanical collector located ahead of the ESP. But this may change the resistivity of the dust as well as the adhesive behavior. Therefore quantitative information is needed so as to properly balance the various effects and to know how to adjust rapping mechanisms to compensate for changes in adhesive behavior.

One may argue that we merely need to make empirical tests and then copy the best behavior. But it is my belief that precipitator performance is too complicated for this method to be successful. If we do not understand the basic mechanisms, mistakes in interpreting empirical tests are almost certain to occur. White in discussing precipitator energization says, "An empirical approach to the question merely leads to hopeless confusion because field data, when presented uncritically, may be cited to support almost any point or conclusion."

There are other definitive tests that can be made to distinguish between theories and to evaluate the extent to which a given theory applies. I believe that such fundamental or basic research should be conducted in parallel with the empirical tests so that results of both can be compared.

RESULTS OF FIELD MEASUREMENTS OF INDUSTRIAL PARTICULATE SOURCES AND ELECTROSTATIC PRECIPITATOR PERFORMANCE

Joseph D. McCain, John P. Gooch, and Wallace B. Smith
Southern Research Institute
Birmingham, Alabama

ABSTRACT

This paper presents results of source size distribution measurements over the size range from 0.01 μm to 5 μm for six classes of particulate sources and fractional efficiency measurements on five full scale electrostatic precipitators and one pilot scale precipitator.

The precipitators all showed moderately high to high particulate collection efficiencies for particles having diameters larger than a few micrometers or smaller than a few hundredths of a micrometer and a minimum in collection efficiency for particles having diameters of a few tenths of a micrometer.

INTRODUCTION

In the control of particulate emissions to the atmosphere, the emphasis has historically been on reducing the mass of material discharged. Recent studies, however, have indicated that small particles, defined as those less than 2 μm in diameter, have a greater impact on visibility, health, and water-droplet nucleation than larger particles, even though this size range may constitute a small fraction by weight of the particulate matter in a typical flue gas. Moreover, the long retention time in the atmosphere of the small particles makes them a more significant problem of control than the larger particles which have so far received the greatest attention. As a result of these considerations, the Environmental Protection Agency has been sponsoring research with the objectives of measuring and enhancing the performance of control devices in the small particle range.

The increasing emphasis on control of fine particulate emissions from industrial sources has resulted in a concomitant need for both improved source size distribution information and control device performance in collecting fine particulate. Southern Research Institute has, over the past several years, undertaken research programs for various governmental and industrial sponsors aimed at (1) devising, improving, or adapting techniques for the measurement and characterization of fine particulates, (2) obtaining source size distribution measurements, and (3) determining fractional collection efficiencies of various pilot-scale and full-scale particulate control devices installed on industrial sources. This paper presents results of source measurements on a variety of industrial sources and results of fractional efficiency determinations made on one wet and five dry electrostatic precipitators.

MEASUREMENT METHODS

Three measurement techniques were used in obtaining the information presented in this paper: (1) cascade impactors (inertial sizing devices) for obtaining size distributions on a mass basis over the range of sizes from about 0.3 μm to 5 μm, (2) optical single particle counters for obtaining particulate concentration information on a number basis over the size range from about 0.3 μm to 2.0 μm, and (3) diffusional sizing for obtaining information on a number concentration basis over the size range from 0.01 μm to 0.2 μm.

Detailed discussions on the application and limitations of the three methods used in obtaining the data presented in this paper are in publication elsewhere; hence, only a brief description of measurement methods will be given here.

Diffusional sizing is accomplished by passing a particulate-laden sample gas stream through a diffusion battery, a series of small tubes or narrow rectangular flow channels. Because of their high diffusivities, smaller particles migrate more rapidly, through Brownian motion, to the walls of the channels than do larger particles; any particle contacting the walls is assumed to adhere. Thus, a diffusion battery acts as a size-selective filter preferentially removing small particles and passing larger particles in a predictable fashion. By passing the sample gas stream through a series of such batteries, progressively removing larger and larger particles, one can obtain the desired size distribution data. The range of applicability of the method is from about 0.005 μm to about 0.2 μm. The residual particulate concentration of the sample

stream as it emerges from the successive batteries is measured with a condensation nuclei counter. Electrostatically induced losses of particles within the diffusion batteries can be substantial with a highly charged aerosol; therefore, some form of charge neutralization must be used prior to passing the aerosol through the diffusion batteries.

Optical particle counters operate by passing particles individually through a small illuminated view volume and detecting the particle by the light scattered as it passes through the illuminated zone. Size discrimination is based on the intensity of the light scattered by the particle, larger particles generally producing light pulses of greater intensity than smaller particles; however, in addition to its size, the shape and optical properties of the particle will also affect its light scattering properties.

In order to use either the optical particle counters or the condensation nuclei counters, extractive sampling and extensive dilution of stack gases are required because of instrumental saturation effects at high particulate concentrations and instrumental sample temperature limitations. Typical dilution factors used in the field work described in this paper ranged from about 1:10 to 1:2000, depending on the nature of the source and whether the measurement was made before or after a control device. The sample is dried simultaneously with dilution by recirculating the filtered dilution air through condensers and drying tubes. In this way, the concentrations of moisture and other condensable vapors in the sample are reduced by approximately the same fraction as the particle concentration. Although line losses can be a problem in out-of-stack sampling, it may be shown that they are not serious for particles having sizes between 0.01 and 2 μm with sampling lines of reasonable length.

The optical counters employ parallel counting into the various size ranges and provide real time monitoring capability; however, the diffusional method as presently implemented requires a large number of sequential measurements and is not well adapted to obtaining data on a source with frequent process variations. A sample of the real time capability of the optical system is illustrated in Figure 1. Because of the size and complexity of the total optical/diffusional measurements system, the data reported in this paper, with few exceptions, represent single point samples rather than full spatial averages as would be obtained by traverse sampling. The degree to which the data properly represent the process or device being characterized is dependent on the amount of mixing of

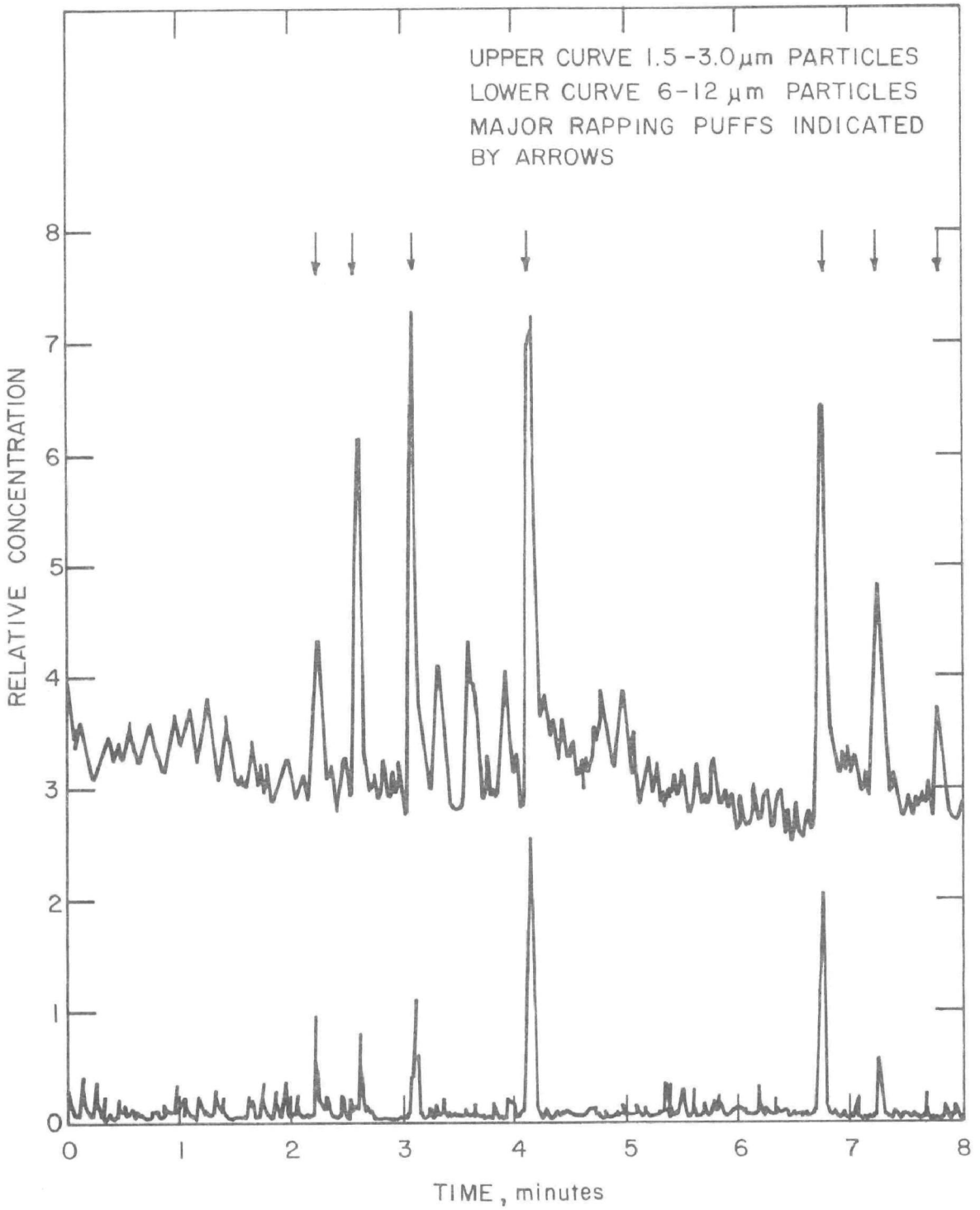

Figure 1. Relative concentrations of particles in two size ranges between and during rapping puffs as observed at the exit of a cold side precipitator collecting fly ash from a coal fired boiler

the process exhaust gases that occurred upstream of the sampling point and the uniformity of the concentration and size distribution of the effluent particulate across the exit plane of the control device.

The data from cascade impactors are obtained on a "mass within a size interval" basis; the stage size cutoffs are determined by the operating characteristics of the particular impactor and on the shape and densities of the particles. For many purposes, the stage cutoffs are calculated on the basis of the behavior of unit density spheres, in which case the sizes quoted are so-called "aerodynamic diameters". However, for control-device modeling purposes, or for predicting plume opacities, the stage fractionation sizes are often based on an assumption of spherical particles having a density either equal to the density of the primary parent material from which the aerosol is formed or from a measured value of a true mean density of the particles. The diameters based on the latter assumptions, Stokes diameters, generally permit better correlations to be obtained with the optical properties of the particulate, i.e., plume opacities, and better represent the particles insofar as predicting charging dynamics within electrostatic precipitators is concerned. The sizes used for presenting the data in this paper are based on the estimated true density of the particles. Approximate conversions of the particle sizes reported here to aerodynamic diameters can be made by multiplying the indicated size by the square root of the assumed particle density. The densities used in calculating particle diameters for the impactor data in this paper are given in Table 1. The data from cascade impactors reported in this paper generally were obtained by approximations to traverse sampling rather than single point samples, although in some locations the relatively small duct dimensions as compared to the impactor dimensions dictated the use of single-point sampling.

Figure 2 shows composite size distributions obtained with all three techniques at the inlet and outlet of an electrostatic precipitator installed on a coal-fired boiler. For the purpose of making this composite, the impactor data was transformed from a mass per size interval basis to number basis assuming the particles were spheres having a density of 2.3 g/cm^3. The agreement among the methods in the size intervals over which the methods overlap appears to be reasonably good.

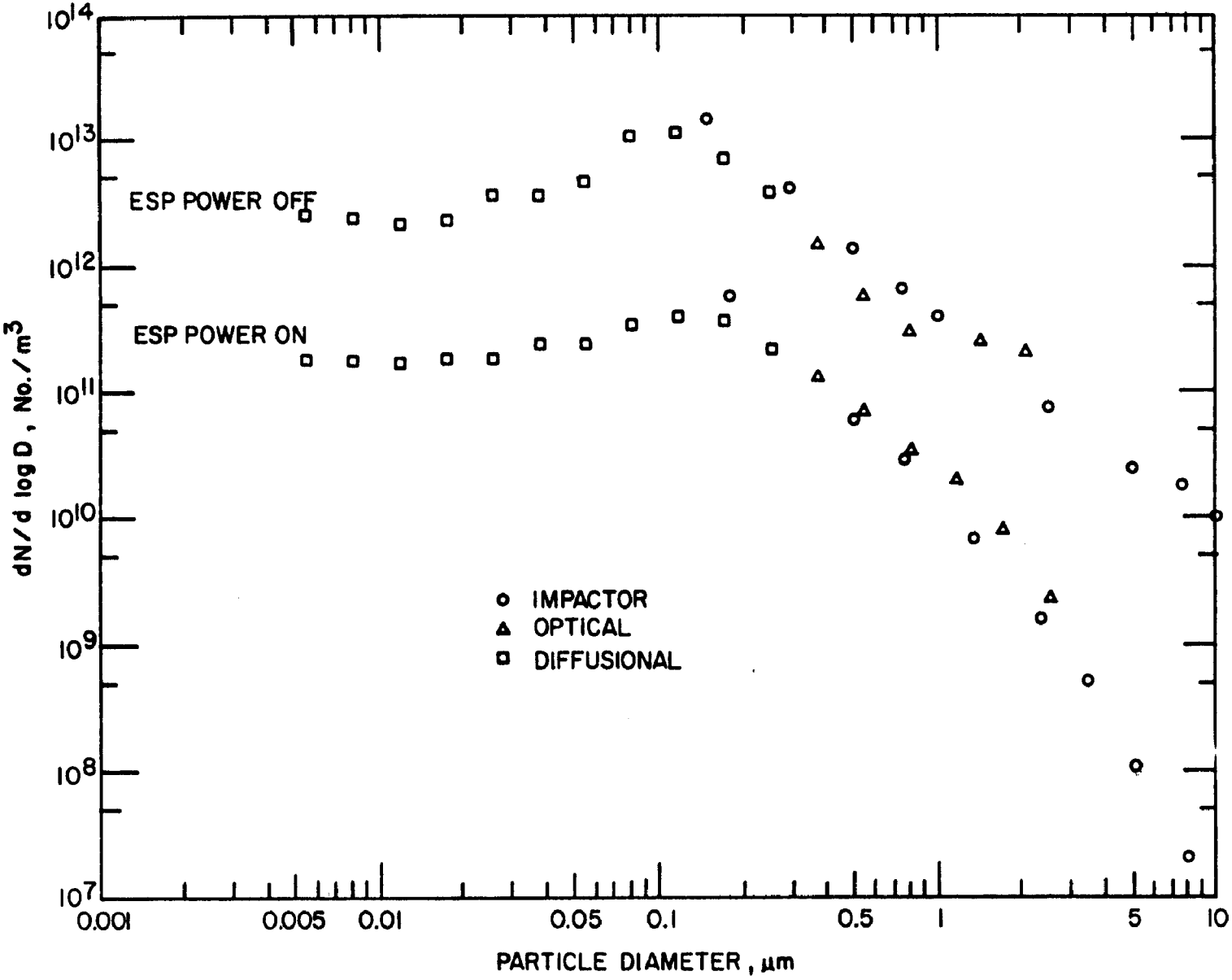

Figure 2. dN/d log D vs. D at inlet and outlet of electrostatic precipitator installed on a coal-fired power boiler

Table 1. ESTIMATED PARTICLE DENSITIES USED FOR IMPACTOR DATA

Source	Particle density g/cm^3
Coal-fired boiler	2.3
Open hearth furnace	5.2
Kraft recovery boiler	1.46
Submerged-arc ferro-alloy furnace	4.5
Packed bed SO_2 scrubber	1.77
Aluminum reduction furnace	2.0

RESULTS OF SOURCE MEASUREMENTS

Typical results of measurements of particulate size distributions using optical and diffusional methods are shown in Figures 3 and 4. These are the results of measurements made on process effluents at the inlets to control devices. The data are presented in terms of the concentrations by number of particles having diameters larger than the indicated sizes. Figure 3 shows data from three coal-fired utility boilers, and Figure 4 shows data from three metallurgical processes and two SO_2 scrubbers.

Similar control device inlet data as obtained with cascade impactors are shown in Figures 5 and 6. In these cases, the data are presented in terms of cumulative concentrations of particulate by mass for particles smaller than the indicated sizes. The densities used in calculating the impactor stage cutoff diameters were given in Table 1. Because of increasingly large sampling errors resulting from deviations from isokinetic sampling and, as a rule, the use of a less than desirable number of sampling points in obtaining the impactor data, the size distributions presented here are arbitrarily cut off at a diameter of 5 μm. This does not imply that particles larger than 5 μm were not present in any of the samples—in fact, in many cases the total particulate mass loading was dominated by particles having a greater size; rather, we do not believe that our data for sizes larger than 5 μm are valid representations of the true size distribution. Figure 5 shows data collected on several pulverized

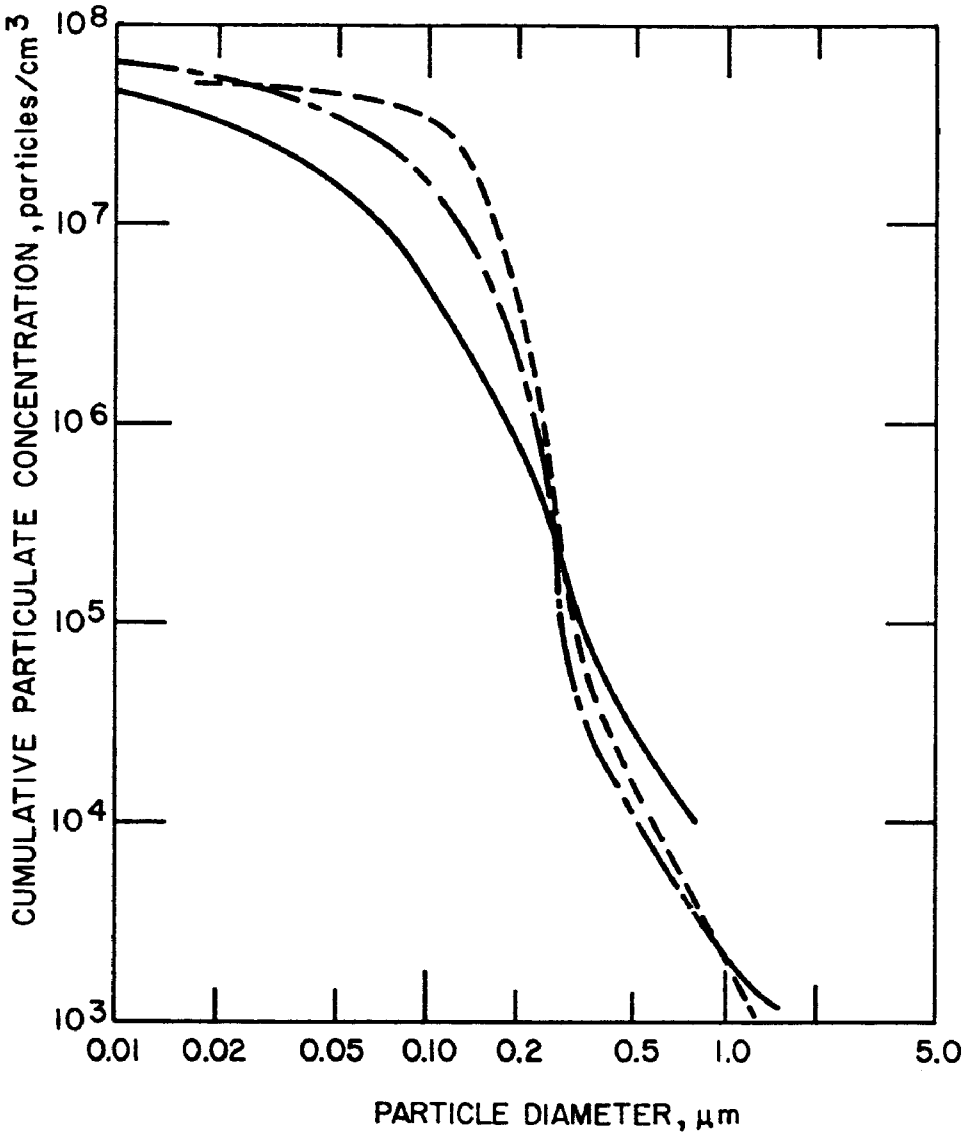

Figure 3. Typical size distributions of particulate emissions from coal fired boilers as measured by optical and diffusional methods

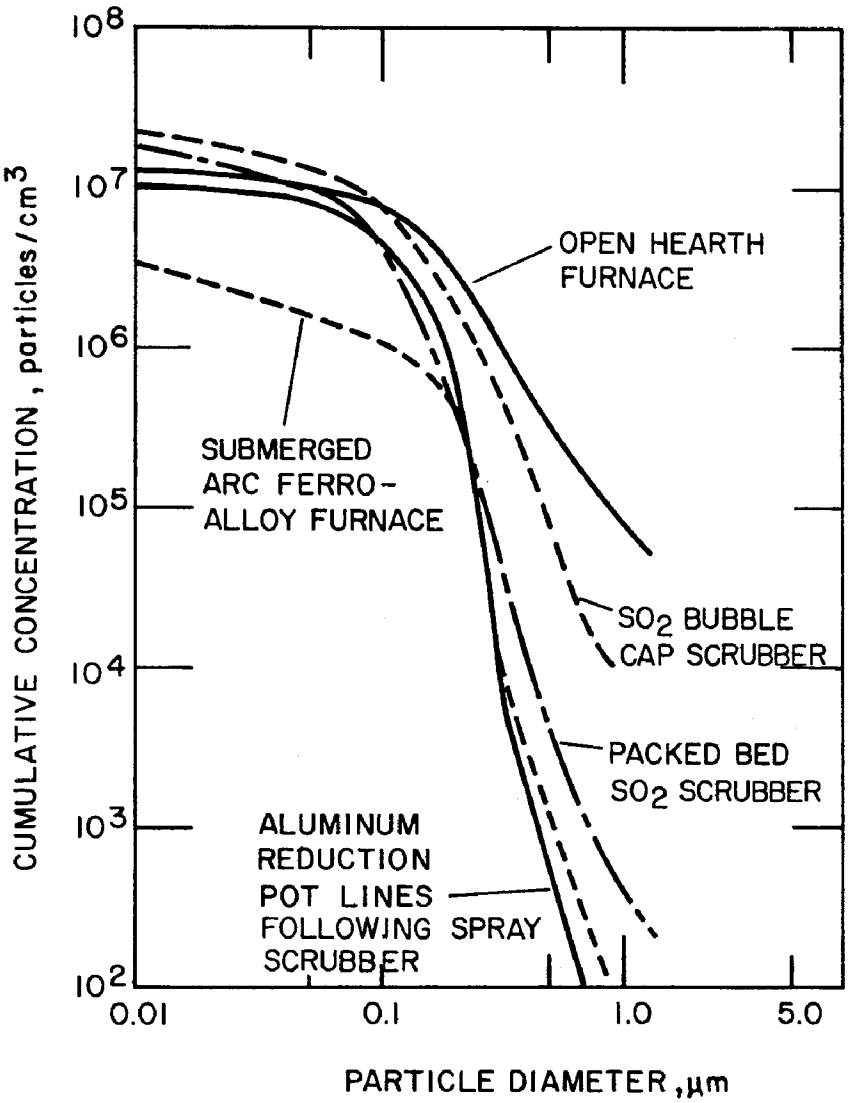

Figure 4. Cumulative size distributions on a number basis for various industrial particulate sources as measured by optical and diffusional methods

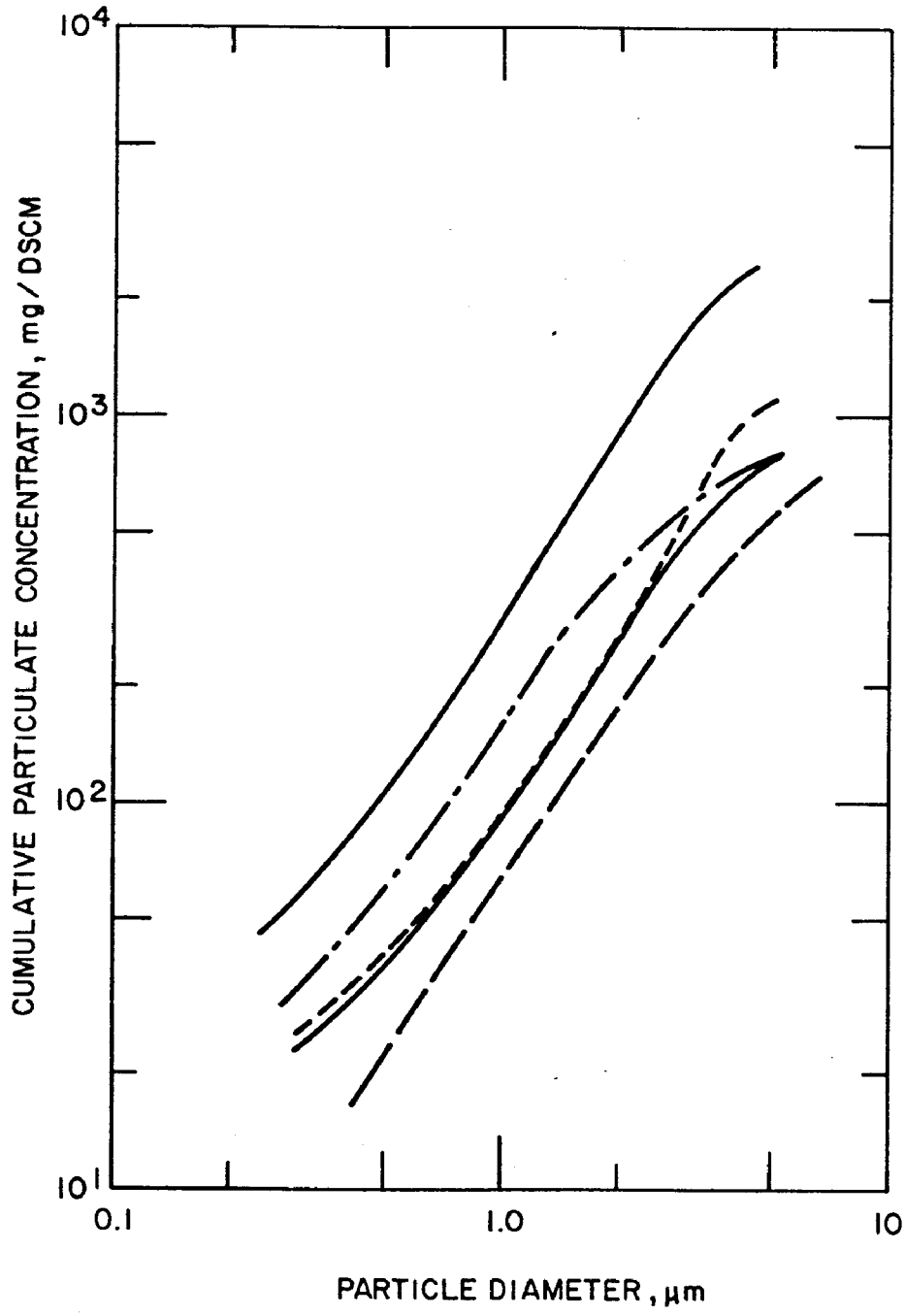

Figure 5. Size distributions by mass for five pulverized coal utility boilers as measured using cascade impactors

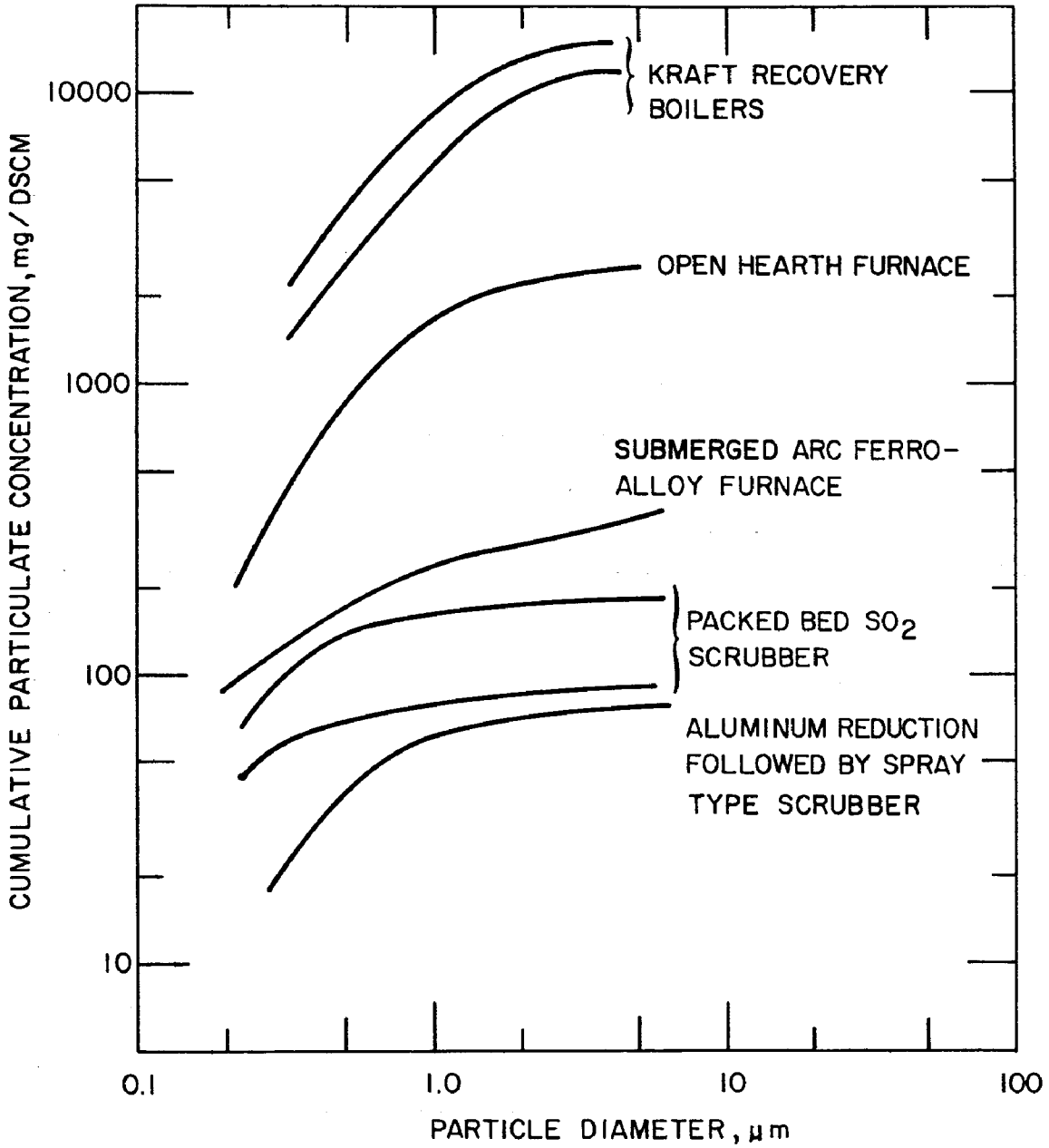

Figure 6. Size distributions by mass for various industrial particulate sources as measured using cascade impactors

coal-fired utility boilers. Figure 6 shows data from two Kraft recovery boilers, three metallurgical furnaces, and an SO_2 scrubber operated at two liquor concentrations. The dominant factor causing the variations in the mass size distribution among the pulverized coal boilers is probably the ratio of the percentage of ash to thermal energy content per unit weight of the fuel. A high ash-low heating value fuel will result in higher particulate loadings than are obtained from burning coal with low ash and high heating value.

Table 2 gives the operating conditions and the overall mass efficiency for the five precipitator installations for which fractional efficiencies are given. The fractional efficiency data are presented in Figures 7, 8, 9, 10, 11, and 12.

Table 2. PRECIPITATOR OPERATING CONDITIONS AND MASS EFFICIENCY

Installation	Specific collecting area, m^2/m^3 sec	Temperature, °C	Average current density nA/cm^2	Overall mass efficiency, %
A	56	156	22	99.6
B	55	141	16	98.1
C	47	157	30 (upper set) 10 (lower set)	99.8
D	67	160	16	98.3
E	85	335	35	99.3
F	59	41	30	96.2

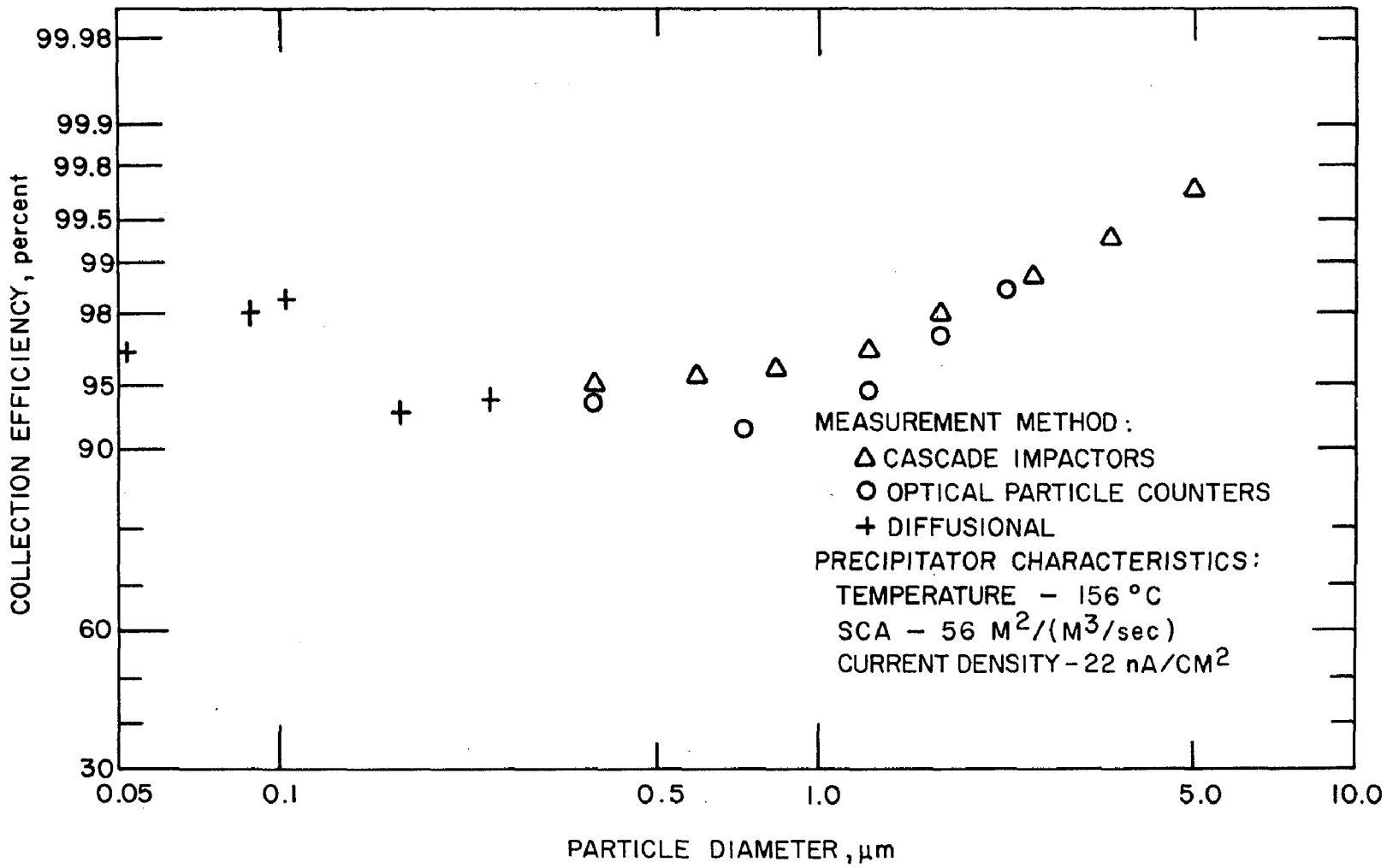

Figure 7. Measured fractional efficiencies for a cold side electrostatic precipitator with the operating parameters as indicated, installed on a pulverized coal boiler (Installation A)

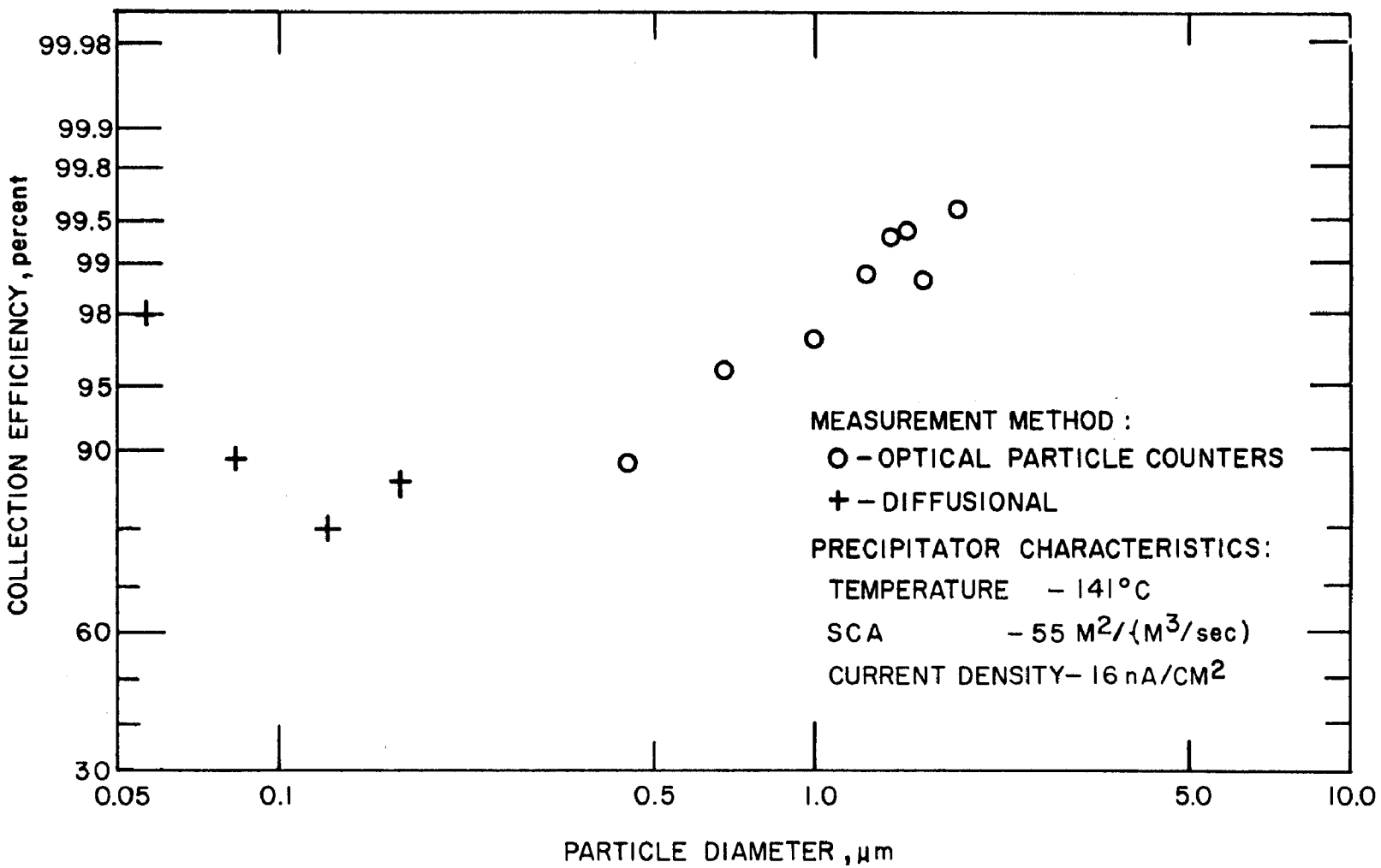

Figure 8. Measured fractional efficiencies for a cold side electrostatic precipitator with the operating parameters as indicated, installed on a cyclone type coal boiler (Installation B)

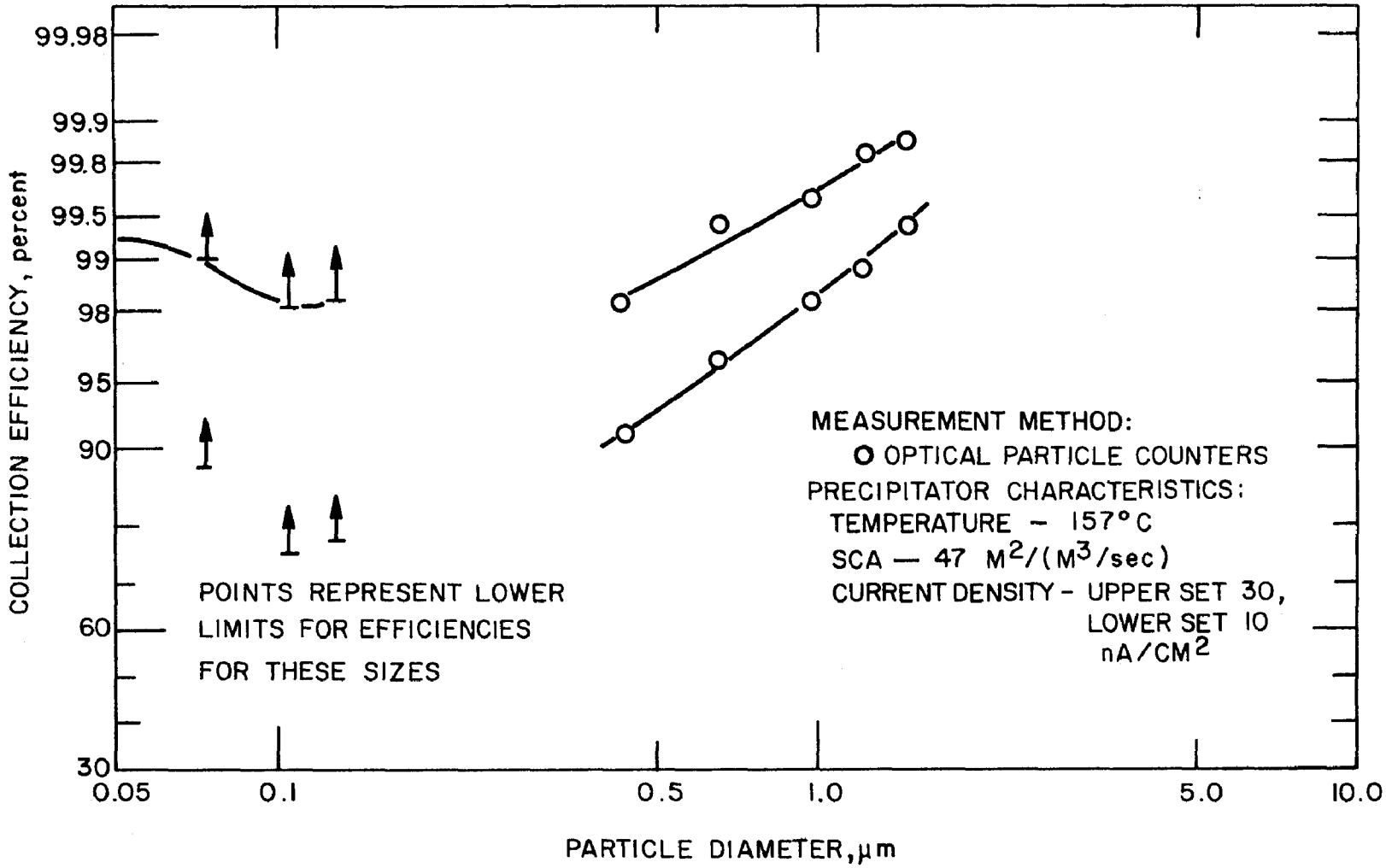

Figure 9. Measured fractional efficiencies for a cold side electrostatic precipitator with the operating parameters as indicated, installed on a pulverized coal boiler (Installation C)

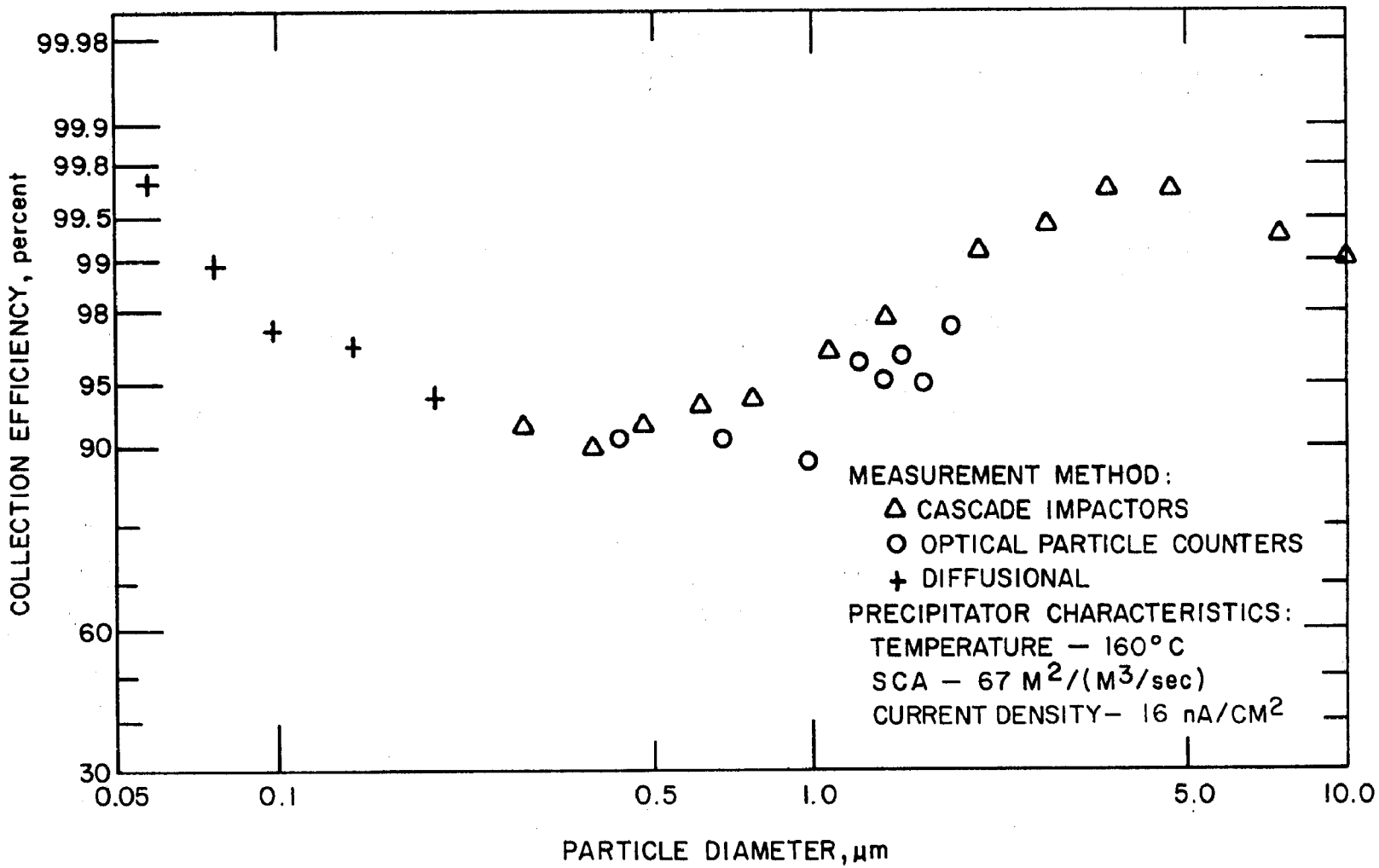

Figure 10. Measured fractional efficiencies for a cold side electrostatic precipitator with the operating parameters as indicated, installed on a pulverized coal boiler (Installation D)

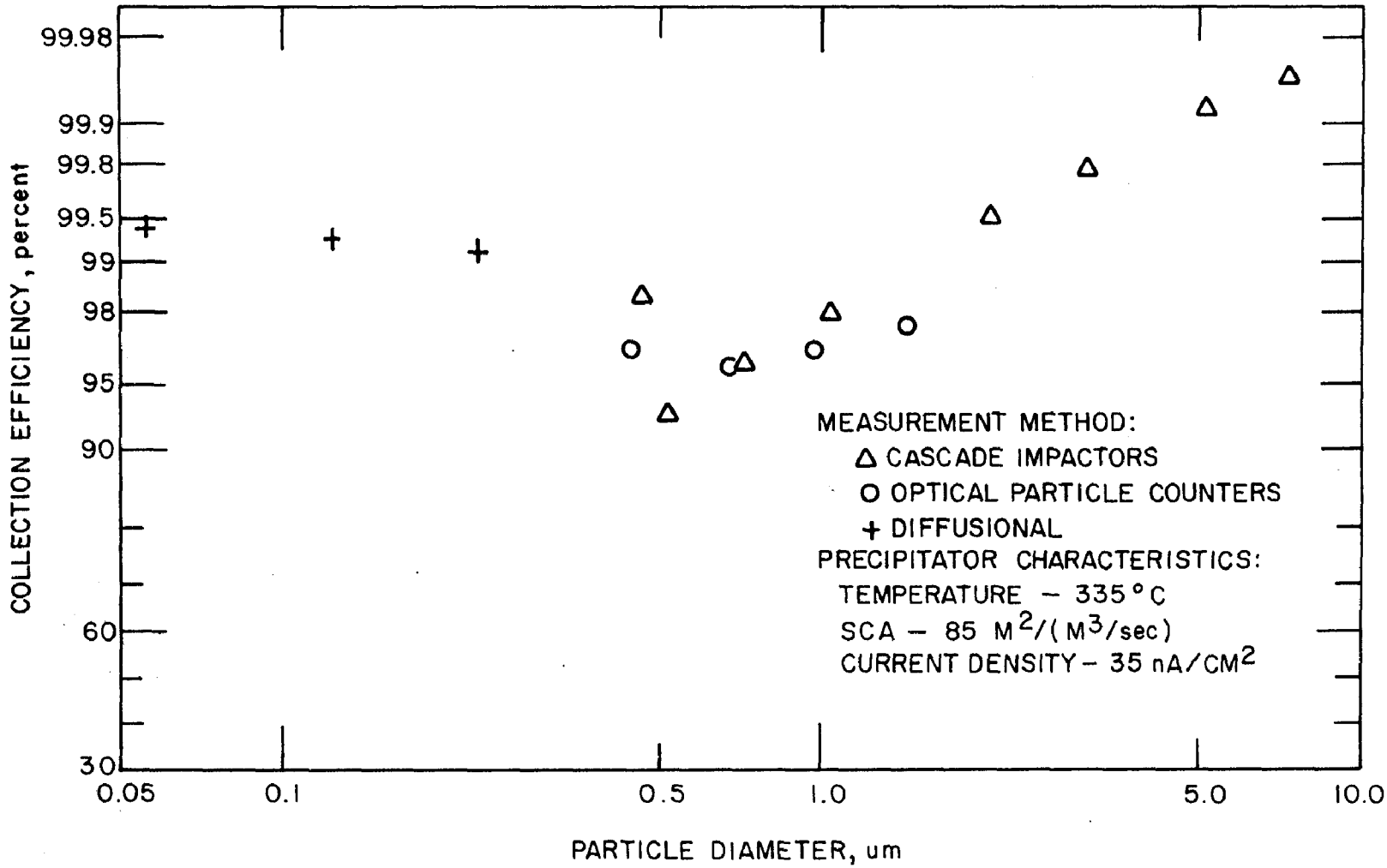

Figure 11. Measured fractional efficiencies for a hot side electrostatic precipitator with the operating parameters as indicated, installed on a pulverized coal boiler (Installation E)

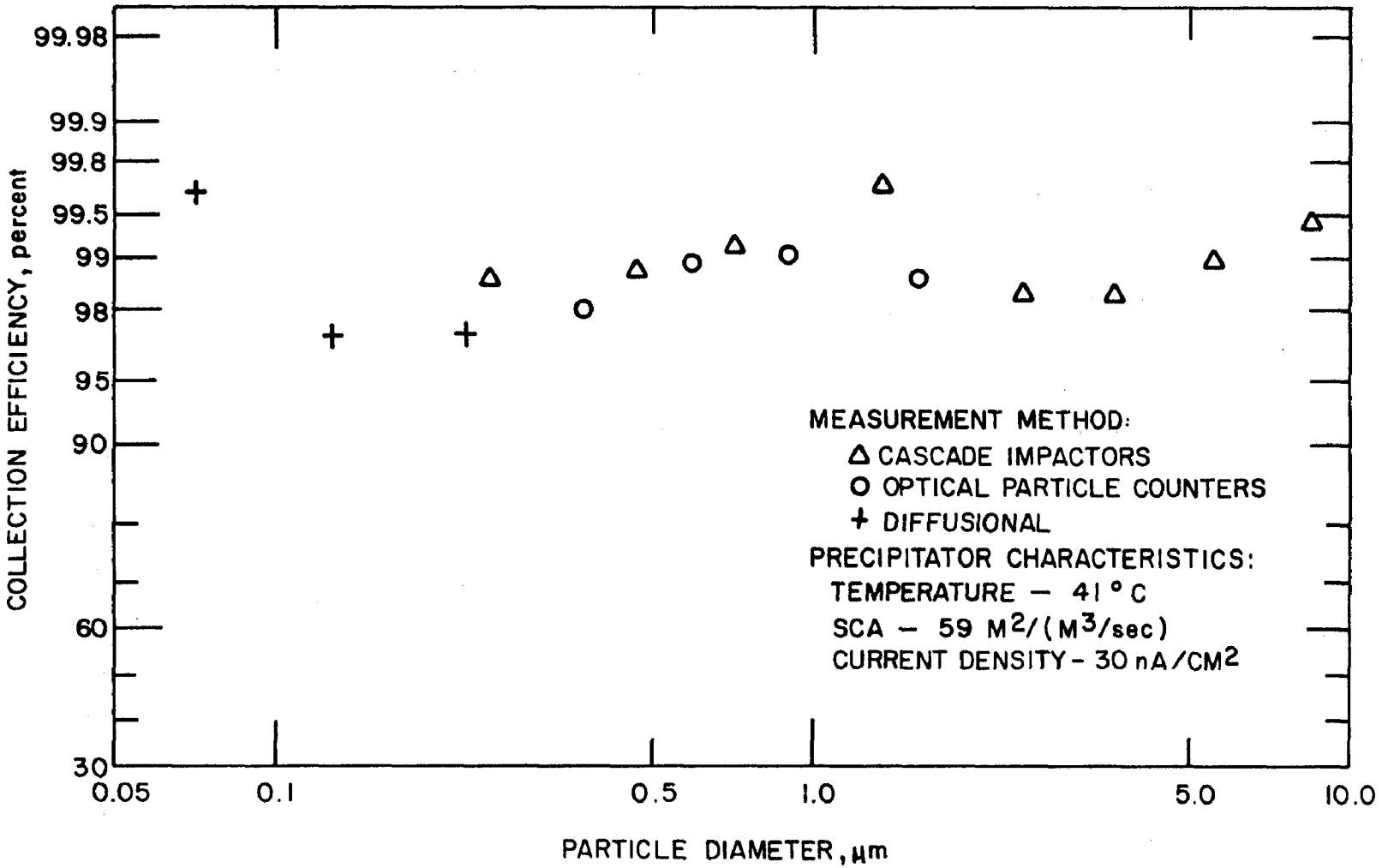

Figure 12. Measured fractional efficiencies for a wet electrostatic precipitator with the operating parameters as indicated, installed downstream of a spray type scrubber on an aluminum reduction potline (Installation F)

The data presented in Figure 7 (Installation A) indicate that the collection efficiency for particles smaller than 0.1 μm in diameter decreases from about 98% at 0.1 μm to about 96% at 0.05 μm and about 78% at 0.03 μm (not shown). This decrease may be an artifact resulting from the manner in which the measurements were made. Inlet concentrations of particulate matter for the optical and diffusional measurements were estimated by determining outlet concentrations with the precipitator power supplies deenergized. For particle sizes less than 0.1 μm, agglomeration rates may have been very high during the transport time from the inlet to outlet sampling plane of the precipitator, resulting in underestimation of the inlet concentrations and thus, underestimation of the precipitator collection efficiency for particles in this size range. Impactor measurements were made by taking a traverse at both the precipitator inlet and outlet. Fair agreement is indicated for the efficiencies determined by inertial and optical methods. The data used in preparing Figure 2 was obtained at this location. This installation is a pulverized-fuel power boiler operating with a coal of moderate sulfur content. There was no indication of performance degradation resulting from back corona due to high dust resistivity.

Installation B (Figure 8) is a cyclone-type boiler which also burns coal of moderate sulfur content. The increase in collection efficiency for particles smaller than 0.1 - 0.5 μm is more pronounced than that shown for Installation A, and there is no indication of decreasing efficiency with decreasing particle size below 0.1 μm. Both inlet and outlet diffusional and optical measurements were made at this location. The overall collection efficiency of this installation as reported in Table 2 was measured at a different time with a higher volumetric flow rate through the precipitator than that at the time the fractional efficiency determinations were made.

Figure 9 presents lower-limit efficiency data obtained at Installation C, which burns a high-sulfur coal, for particle sizes from 0.05 to 0.15 μm, and optically determined efficiency values for particle sizes from 0.4 to 1.5 μm. A highly non-linear variation of particle concentration with dilution ratio as measured with the condensation nuclei counters was encountered at the precipitator outlet at the values of dilution ratio required to obtain sufficient material for diffusional sizing. This nonlinearity was apparently caused by a condensation phenomenon, probably of sulfuric acid within the dilution system, and prevented diffusional sizing at the outlet. Therefore, lower limits of collection efficiencies for particles in the size range of 0.01 to

0.15 μm were computed by assuming that all the particles counted at the outlet were of uniform size, and then using the inlet concentration of particles at the size under consideration in the relationship

$$\text{minimum efficiency} = \left(\frac{\text{inlet-total outlet}}{\text{inlet}}\right) \times 100$$

There was no evidence of the condensation problem with the optical counter measurements. The data in Figure 9 illustrate the pronounced effects of precipitator electrical conditions on the collection efficiency achieved - a threefold increase in current producing a much more than proportional decrease in the exit particulate concentrations.

Installation D (Figure 10) is a pilot-scale precipitator which was treating a side stream of flue gas from a utility boiler burning a low-sulfur coal. It can be seen that agreement between inertially and optically determined fractional efficiencies at this installation is poor. It should be noted that no corrections were made to the optical data for differences in refractive index between fly ash and the polystyrene latex used for calibrating the instrument, and this may account for some of the indicated disagreement. Corrections of this type are difficult because fly ash particles of differing composition may differ in refractive index. Figure 10 also indicates that the functional form of the efficiency versus particle-size relationship for particle sizes greater than about 3.0 μm deviates from theoretical predictions, which indicate a continuously increasing efficiency with particle size in this size range. Reentrainment and gas sneakage (passage of a portion of the gas stream through a region other than the volume between the electrodes) are possible explanations for the relatively low measured values.

Installation E (Figure 11) is a hot-side precipitator installed on a pulverized-coal boiler burning a southwestern (low-sulfur) coal. The generally better electrical conditions and a higher specific collecting area than in the previous examples result in generally higher collection efficiencies than were found in most of the previous cases.

The data shown in Figure 12, Installation F, were obtained on a wet precipitator installed downstream of a spray-type scrubber on an aluminum reduction pot-line. In this installation, the precipitator walls are irrigated by collecting mists produced by liquor spray nozzles located in the region above the collection electrodes. Because the inlet concentration is so very low for all particle sizes larger than

2 μm (see Figures 4 and 6), evaporative residues from any, even slight, carryover from the irrigation sprays will result in anomalously low efficiencies for these sizes—that is, the exit loading may be decoupled from the inlet for all particle sizes larger than about 2 μm. Therefore, the apparent decrease in the fractional efficiency between 1 μm and 5 μm should probably be disregarded.

Although the results presented here show reasonably high electrostatic precipitator collection efficiencies for particle sizes smaller than 2 μm, the data do not necessarily indicate that mass-emission standards are met at the values of specific collecting area used during the tests. For instance, the Federal standard for new fossil-fuel fired steam generators requires that particulate emissions be no greater than 0.1 $lb/10^6$ Btu. For a plant burning a coal with 12% ash, with a thermal energy release of 12,000 Btu/lb, an electrostatic precipitator would be required to collect about 98.8% by weight of the particulate matter leaving the furnace, assuming that 80% of the ash leaves in the flue gas. Some states have more stringent requirements than the Federal standard.

CONCLUSIONS

These data sets indicate that a minimum in the collection efficiency vs. particle size relationship occurs in the size range between 0.1 to 0.5 μm. Such a minimum is predictable from theoretical considerations, and the increasing collection efficiency shown for particles smaller than 0.2 μm suggests that electrostatic precipitation is a promising means of collecting extremely fine particles. For particle sizes smaller than 0.05 μm, however, collection efficiency may be limited by considerations of charging probability. The efficiencies shown in Figures 7 through 12 are indicative only of the specific collecting area and electrical conditions of the individual precipitators tested. Higher minimum collection efficiencies than the ones measured would be expected to occur with higher values of specific collecting area or more favorable electrical conditions.

REFERENCE

1. McCain, J. D. Methods for Determining Particulate Mass and Size Properties: Laboratory and Field Measurements. In: Proceedings, Symposium on the Use of Fabric Filters for the Control of Submicron Particulates, Seale, L. M. (ed.). Boston. April 8-10, 1974. p. 179-199. Publication Number EPA-650/2-74-199.

SOME ASPECTS OF ELECTROSTATIC PRECIPITATOR RESEARCH IN AUSTRALIA

Owen J. Tassicker
Electric Power Research Institute
Palo Alto, California

ABSTRACT

In Australia, research and development into electrostatic precipitator performance has been taking place, mainly, but not wholly, in relation to the electric power utility industry. Special interest has centered around back-ionization resulting from the high-resistivity fly ash prevalent amongst the low-sulfur coals found there. Work has proceeded on full-scale, pilot-scale, and bench-scale apparatus. Resistivity, adhesivity, and the permittivity of fly ash has been studied. Back-ionization has been mitigated by both gas conditioning and special energization.

INTRODUCTION

Some of the more significant Australian research being conducted into the electrostatic precipitation of fly ash from stack gases is reviewed. Work is proceeding on laboratory and technical-scale combustors to produce fly ash; laboratory macro and micro analyses of ashes; electrical conductivity and back-corona producing tendency; adhesivity of ashes; pilot-scale precipitators; chemical precipitants; electrode geometry and electric fields; and development of regression equations to predict precipitator performance.

The coals involved, mostly with less than 1% sulfur, vary from bituminous to lignites and have ash contents of from 1% to 30%.

The laboratories and utilities involved are the Australian Coal Industries Research Laboratories (ACIRL); Division of Mineral Chemistry of the Commonwealth Scientific and Industrial Research Organization (CSIRO); Electricity Commission of New South Wales (ECNSW); Herman Central Scientific Laboratories of the State Electricity Commission of Victoria (SECV); and Wollongong University College (WUC).

Broadly, the research activity falls into three categories: investigations aimed at elucidating fundamental processes, pragmatic studies for the refurbishing of existing installations, and specific experiments when a new plant is under design.

PILOT, TECHNICAL AND BENCH SCALE APPARATUS

Several different approaches have been developed for the sizing of proposed new precipitator installations, particularly when a new coal is to be fired. These vary all the way from pilot scale through technical scale down to bench scale investigations.

PILOT PLANT TESTS BY ECNSW

In collaboration with several manufacturers the Electricity Commission of New South Wales has conducted many pilot-scale plant investigations.[1,2] The aim of these tests has been to provide manufacturers with direct sizing information for new boiler installations firing pulverized coal. From 10 to 30,000 tonnes (tons) of coal is mined from the new seam under investigation and trucked to a suitable power station. The actual site of the cut is carefully chosen after extensive bore-core analyses, typical examples of which are shown in Table 1. Firing and testing take place over several weeks.

Table 1. CHEMICAL COMPOSITION OF SOME AUSTRALIAN COAL AND FLY ASH
(Dry Air Basis)

State	New South Wales			Victoria
Coal field	Western	Southern	Northern	Deep South
Seam	Lithgow	Wongawilli	Bayswater	Yallourn
Colliery	Newcom	Huntley	Ravensworth	No. 4 Cut
Coal analysis:				
Calorific value, Btu /lb	11,040	9,720	9,130	6,830
Volatile matter, %	29.1	22.8	23.4	33.7
Fixed carbon	45.9	43.3	43.0	30.1
Moisture	7.0	1.1	4.0	35.0
Ash	17.9	32.8	30.0	1.2
Sulfur:				
Total	0.58	0.42	0.36	0.16
Pyritic		0.06	0.12	0.00
Sulfate		0.00	0.00	0.01
Organic		0.36	0.24	0.15
Ash analysis:				
SiO_2	63.1	65.0	57.8	17.2
Al_2O_3	26.8	25.0	28.9	48.5
Fe_2O_3	0.59	7.24	4.71	8.6
CaO	0.51	0.33	1.76	1.7
MgO	0.30	0.48	1.70	10.3
Na_2O	0.12	0.07	0.50	4.0
K_2O	2.52	1.01	1.27	0.6
SO_3	0.30	0.20	1.35	6.9
TiO_2	0.88	0.60	1.10	2.3
Combustible	4.6	—	—	—

Typically, the pilot plant specification might be:

Stages:	Three, with separate full wave, 60 kV 20mA energization.
Collecting plates:	2 m x 1.6 m, a total of 25.6 m^2 (275 ft^2) per stage.
Electrode spacing:	25 cm plate to plate.
Discharge Electrode:	80 m (260 ft) per stage.
Rapping:	Tumbling hammer rapping for receiving and emitting electrodes.

This pilot plant, in conjunction with a 50 kW preheater, has been used over the range of temperatures: 80 to 315°C (200 to 600°F) at a single boiler installation--a most important facility. The pilot plants used, having normal commercial electrode spacings, therefore show the same V-I corona characteristics as the full scale plant. The resistivity of these fly ashes measured in the laboratory and in the field is extremely high, between 10^{10} and 10^{13} ohm-m at 150°C. The V-I corona characteristic becomes quite distorted by comparison with the clean electrode curve as indicated in Figure 2. If the precipitator is operated beyond the knee of the curve, the extra power input does not assist the precipitation process and is thus wasted.

An important outcome of the ECNSW tests is illustrated in Figure 1. The efficiency at a constant A/Q when tested as a function of temperature, typically behaves in the fashion depicted, passing through a minimum around 175°C and reaching a maximum around 320°C (a result only obtained when the precipitator is consistently energized at the maximum voltage).

In a number of respects, the pilot precipitator gives reliable sizing data for the full scale plants. Several other utilities, namely the Southern Electric Authority of Queensland, the Northern Electric Authority of Queensland and (though definitely not part of Australia!) the New Zealand Electricity Department[3] have all used the pilot plant facility in collaboration with the ECNSW to aid in sizing new installations.

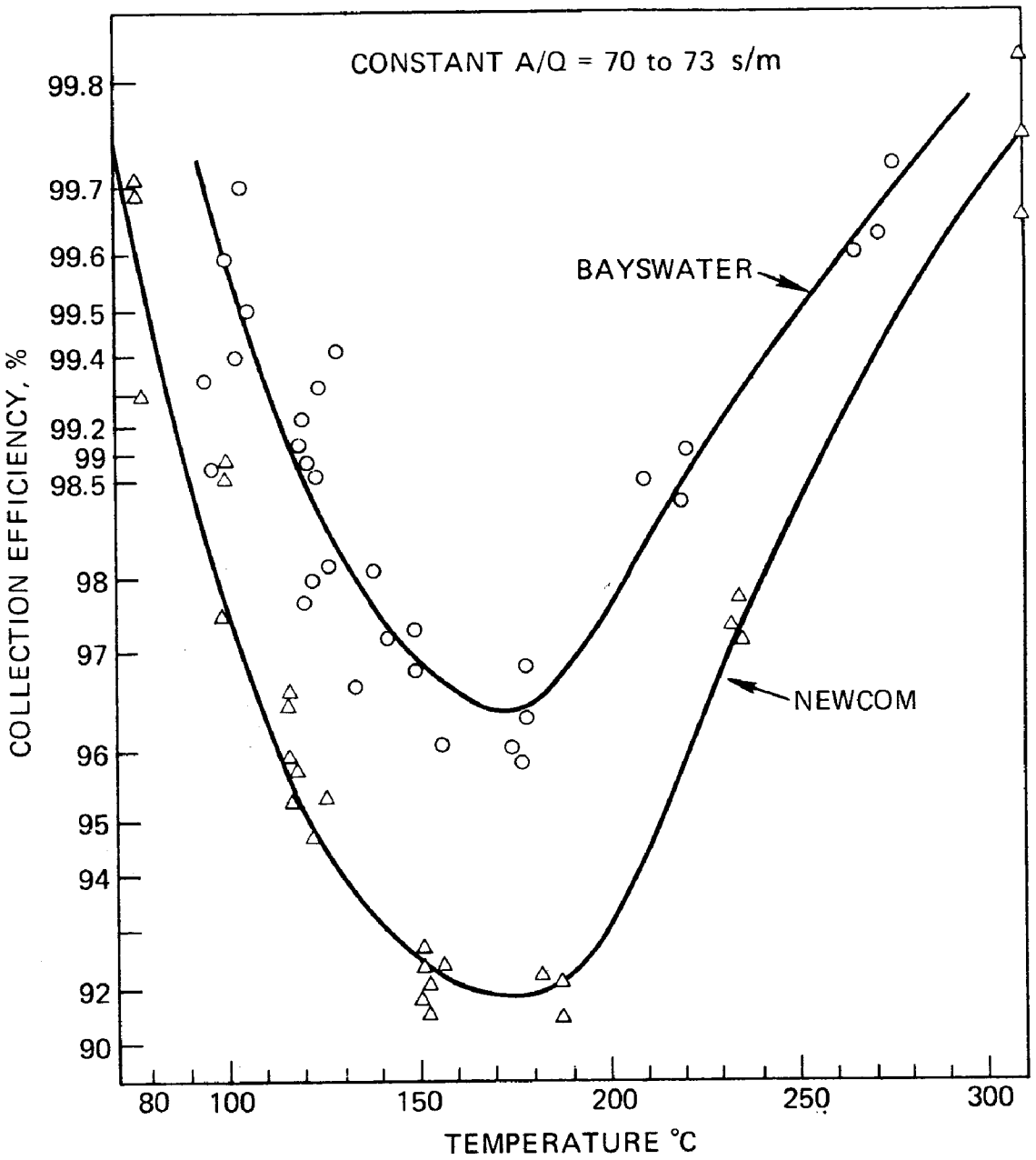

Figure 1. Temperature and efficiency. At a fixed specific collecting area of 70-73 s/m, the collection efficiency depends upon temperature, with a minimum around 175°C (after Watson, Lamb, Blecher, et al.[1,2])

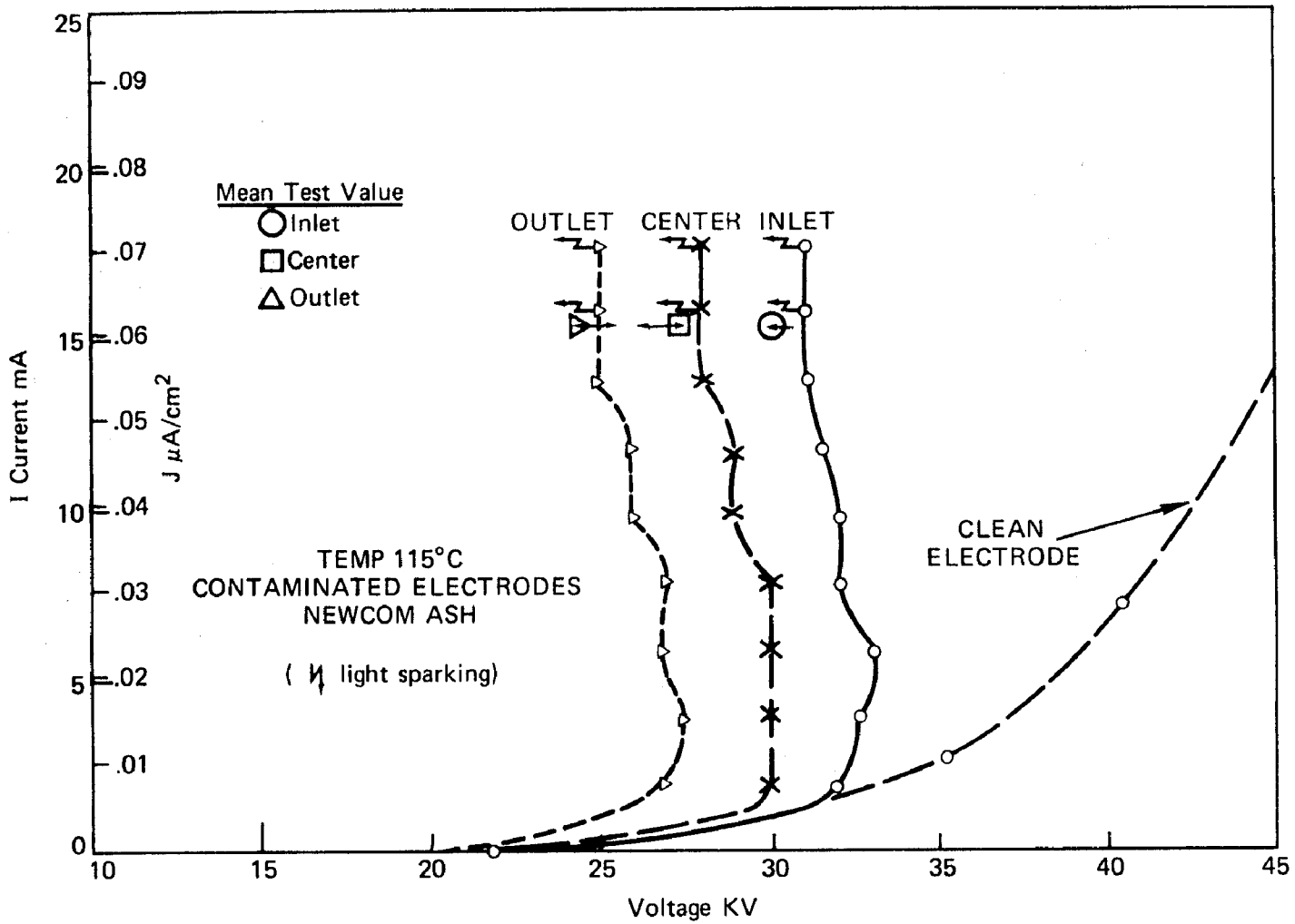

Figure 2. V-I corona characteristics for the pilot plant. The three zones are each contaminated with high resistivity low-sulfur fly ash. The curves are distorted by comparison with the clean electrode characteristic, a clear symptom of back corona. Higher voltages are sustained in the earlier stages due to space charge carried on the dust.

CORRELATION AND REGRESSION ANALYSIS OF PILOT PLANT TESTS

A statistical correlation and regression analysis has been performed by Tassicker on 169 pilot plant tests.[4] The dependent variable was taken as effective migration velocity, as defined by the exponential equation:

$$\eta = 1-e^{-\bar{w}\ (SCA)}$$

A number of plant parameters (independent variables) were examined but found to contribute little to the reduction in variance and were consequently omitted.

Resistivity, SCA and temperature entered strongly into the regression analysis, which finally gave a multiple correlation coefficient R = 0.899. More details will be reported later. While the resulting equation successfully models the curves of Figure 1, and several other features of the experimental results, cautious optimism is appropriate. For an initial study, the results are encouraging--more work along these lines is required to put it on a solid foundation. There is some promise here of being able to size a precipitator in terms of the resistivity of the ash, temperature, and flue-gas composition.

CSIRO COMBUSTOR/TECHNICAL SCALE PRECIPITATOR

The CSIRO Division of Mineral Chemistry at North Ryde, Sydney, has an extended technical-scale pulverized-coal-fired/combustion rig followed by an electrostatic precipitator. Two furnaces are available—a down-fired and a horizontally-fired unit.

The down-fired "U" shaped refractory furnace pre-heated by town gas has a concentric tube burner firing up to 30 kg/hr of pulverized coal. The combustion chamber, 0.76 m square in cross-section, is operated with controlled excess air at a heat release rate of up to about 1.6×10^5 w/m^3 (15,000 $Btu/ft^3/hr$). Water cooled heat exchangers at the furnace outlet enable precipitator temperatures of 200°C to be attained.

The tubular precipitator immediately following the heat exchanger has typical commercial electrodes of 25 cm diameter for the receiving electrode and a concentric straight emitter of 3 mm diameter. Precipitator length is 3 m, giving a fixed collection area of 2.34 m^2.

The collector and emitter are rapped normally and in shear respectively by tumbling hammers at two-minute intervals. The plant is thus roughly comparable to the Bureau of Mines facility at North Dakota.

Some scores of low-sulfur coals have been fired and the ash collected in this facility. While the objective of the plant is not to exactly reproduce full-scale conditions, it is considered that a ranking of one coal against another is possible. In this way, forewarning of precipitation difficulties with an unfamiliar coal can be given and some guidance on plant parameters may be offered. A comparison, made by McLean[5] and the writer, of the performance of the CSIRO rig, the ECNSW pilot-plant and the full-scale plant is shown in Table 2.

Table 2. COMPARISON OF EMV - NO GAS CONDITIONING
Temperature = 120°C (250°F) SCA = 51 s/m (260 ft^2/kcfm)

	Effective migration velocity, m/s		
Coal field	CSIRO	Pilot precipitator	Full-size precipitator
Northern	0.085	0.085	0.070 - 0.085
Bayswater	0.079	0.075	0.074
Southern	0.054	0.030 - 0.042	0.025 - 0.035

In one particular case, three tons of coal from the Jim Bridger seam in Wyoming were fired in this rig. Electrical resistivity measured on ash from this furnace was almost identical to that measured on ash from the micro-combustor to be described in later paragraphs.

Several interesting results of a general nature have emerged from the CSIRO pilot plant studies.[6] Following Deutsch, they observe that for a single particle:

$$\log_e (1-\eta) = kdV^2 (A/Q)$$

k = function of dielectric constant of ash

d = diameter of particle

A/Q = specific collecting area

V = applied voltage

from which they plot $(A/Q)V^2$ as a function of collection efficiency η as shown in Figure 3. The utility of this plot is that it demonstrates the importance of voltage. If the voltage were set at 28 kV, the efficiency would be 99.1%, while if it were set at the sparkover value of 30kV, the efficiency would have risen to 99.55%. An increase of 2 kV in the applied voltage from 28 to 30 kV, exactly halves the amount of dust escaping from the precipitator. This emphasizes the importance of maximizing applied voltage.

The weight of opinion and experience in New South Wales [5,17,18] is that for coals with less than say 1% sulfur, other constituents dominate the conduction process in fly ash and little correlation is found between precipitability and sulfur content.

ACIRL WUC COMBUSTOR/PRECIPITATION FACILITY

The WUC and ACIRL have collaborated in a long series of investigations utilizing bench scale apparatus to characterize fly-ash from bore-core coal samples.[7]

The ACIRL fires pulverized coal from bore cores in a bench-scale laboratory micro-combustor, intended as far as is possible in such a scaled-down device, to model full-scale furnace dynamic thermal conditions. The apparatus comprises a mullite tube of 3.8-cm bore and 100-cm long, heated by

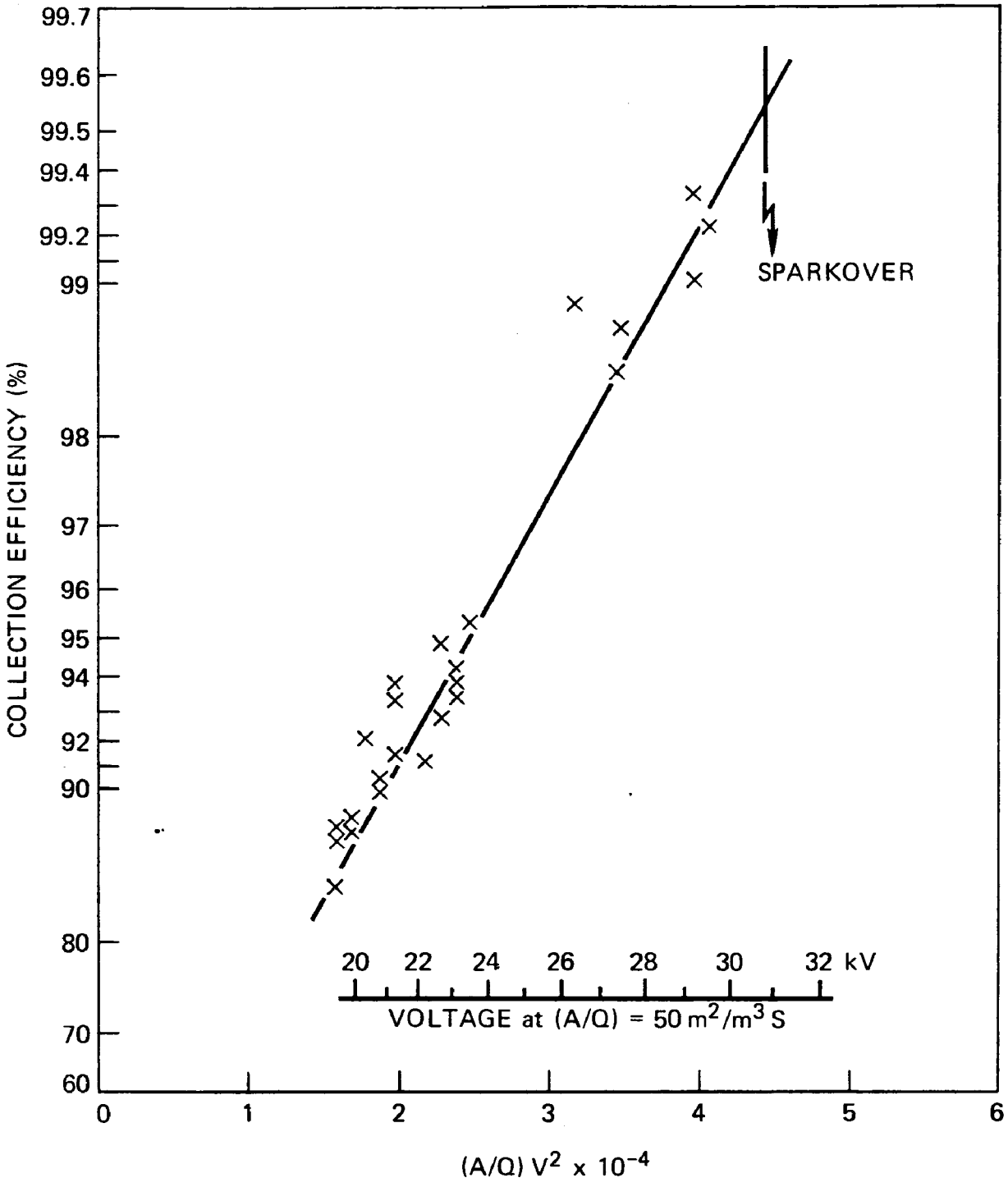

Figure 3. Precipitation characteristics of Great Northern seam fly ash in the CSIRO pilot plant. Illustrates the importance of the applied voltage on the collection efficiency. Maximum voltage attainable with this ash was 30 kV.
A/Q = specific collecting area
V = applied voltage

electrical elements. Feed gases which are closely metered are air, oxygen and propane. Pulverized coal is introduced to the feed gases in such a manner as to ensure good dispersion of particles and constant feed rate.

Studies were begun in the late 1960's, continuing to the present time to determine the degree of similarity between the micro-furnace ash and the ash from a full-scale boiler. A detailed review of the dynamics of the combustion of a coal particle in a full-scale furnace and the formation of fly-ash particles was therefore carried out. In establishing the validity of the micro-furnace ash, comparisons were made with the boiler fly ash, from some ten low-sulfur coals. The criteria for similarity were by microscopy, chemical and magnetic analysis, differential thermal analysis, electrical conductivity, and particle sizing. Correspondence continues to be encouraging.

Particle size from the micro-furnace is a little coarser than in a full-scale boiler; but when heavy particle drop out in the latter is accounted for, the correspondence is closer.

Using resistivity and corona data from 10-gram samples of ash from the micro-furnace, estimates of full-scale plant performance are made. Resistivity determined in a parallel-plate electrode apparatus conditioned with synthetic flue gas is used in the regression equation already discussed. The 95% probability band of the regression equation is rather broad at this stage of development, so that full-scale plant sizing deductions are on the borderline of the "ranking" and "quantitative" regimes.

Following on from the resistivity tests, the 10-gram sample of ash from the micro-furnace is fluidized and injected into a small precision cylindrical corona chamber where it is deposited on the outer electrode.[7] The corona V-I curves for the contaminated electrodes are then compared with the clean electrode curves and the amount of distortion is semi-empirically quantified to rank the precipitability of the ash.

An interesting recent case is depicted in Figure 4 where a new U.S.A. seam is under investigation. There are two levels in the seam known to be markedly different physically and chemically. Bore-core samples from the two seams were fired separately in the micro-furnace and the resistivities determined in an atmosphere of synthetic flue gas. The

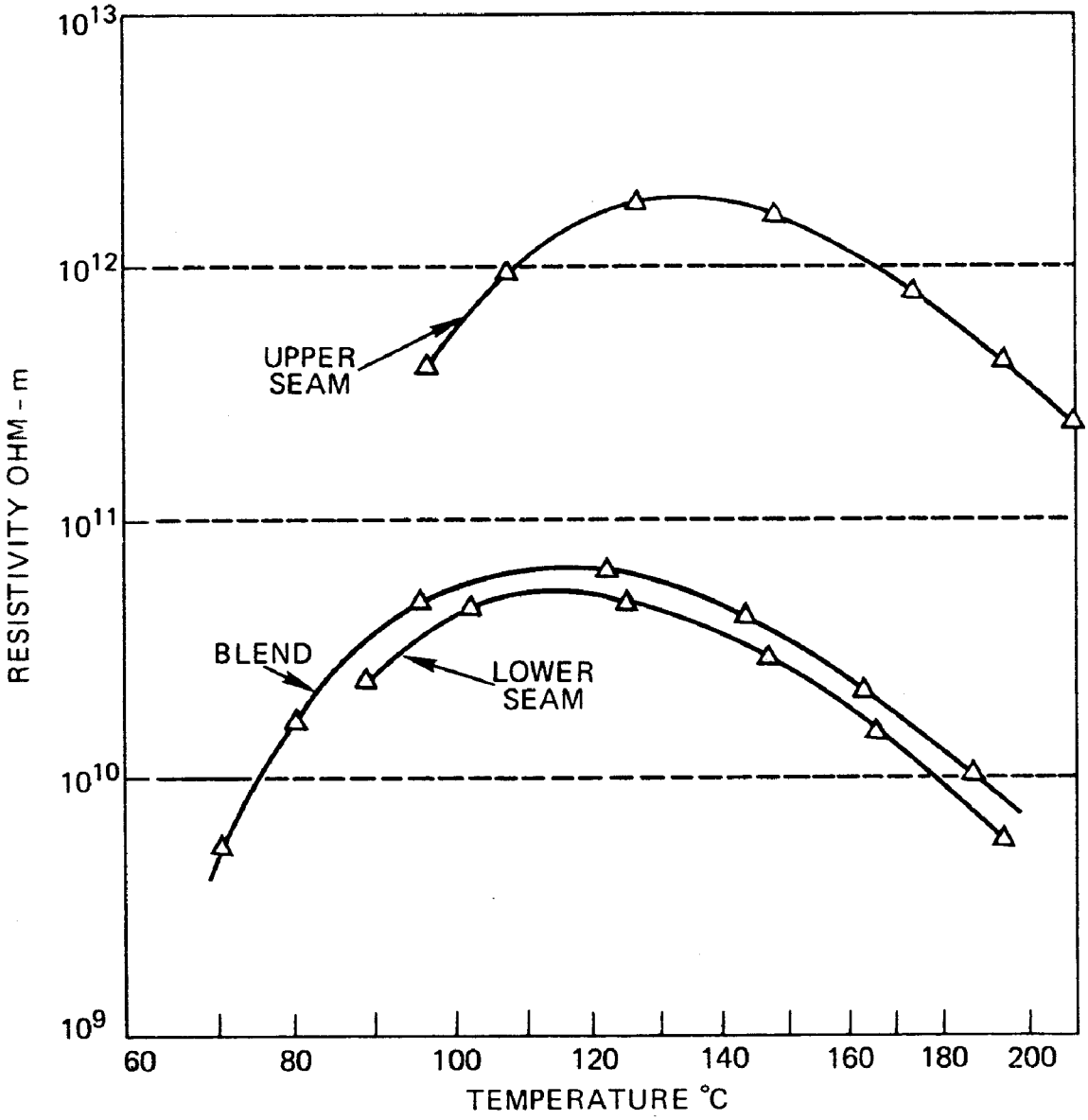

Figure 4. Resistivity of blended ash specimens. A new Montana seam with two separate levels is under investigation. Coals fired in laboratory micro-furnace. Upper seam fly ash was of higher resistivity than the lower seam. When the coals were blended, the resulting ash was closer to the lower seam properties. Constant electric stress = 4×10^5 V/m. Synthetic flue-gas conditioned.

upper seam gave rise to an extremely difficult ash, so it was decided to determine the outcome of blending the upper and the lower seams in a ratio of 78/22, and firing them in the micro-combustor. An inspection of Figure 4 shows that where the two specimens were blended and fired, the more conductive of the two species dominated to a surprising degree. This demonstrated that a blended mixture of the two coals, when fired in a boiler, would be a highly preferred procedure in this case.

The corona V-I characteristic determined in the laboratory apparatus is shown for this blended coal fly ash in Figure 5, in which for comparison, the clean electrode characteristic is also depicted. Such curves resemble those of Figure 2 already noted for the three-stage pilot plant.

By utilizing the micro-combustor together with the resistivity and cylindrical-geometry corona apparatus, the electrical properties of the fly ash from an unknown coal may be characterized quite closely.

SECV 35 kg/hr COMBUSTOR

The SECV 35 kg/hr laboratory combustor has been used for many studies on the extensive lignite deposits in that state, a typical composition of which is shown in Table 1, column 4. Though the combustor was originally installed in connection with boiler fouling studies, recently in a collaborative effort with WUC, electrical and adhesive properties of fly ashes produced by this combustor have been measured as well.

Coal was sampled from the conveyors to the Yallourn boilers simultaneously with isokinetic sampling of the inlet duct to the following precipitator installation. When both samples of dust were later taken to the laboratory and the resistivities measured over a wide range of temperatures and synthetic flue-gas moisture conditions,[7] the correspondence was remarkably close.

The conclusion was that from the limited tests conducted on these lignites, the 35 kg/hr laboratory combustor closely modelled all fly-ash properties including electrical and adhesivity parameters.

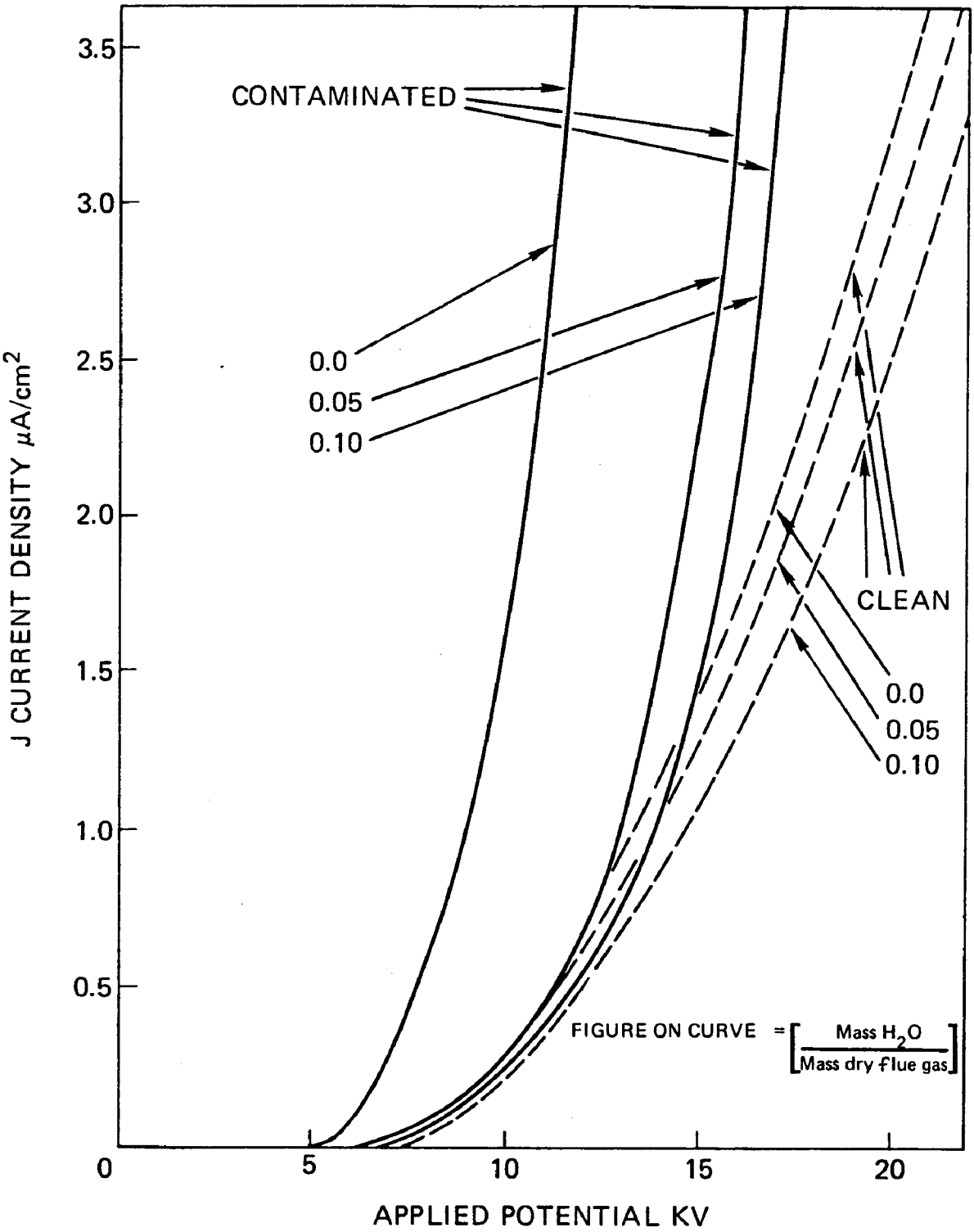

Figure 5. Corona V-I curves in a bench scale apparatus. The blended Montana ash is injected with synthetic flue gas into a precision cylindrical electrode bench-scale precipitator. The corona V-I curves are then measured using quality instrumentation, under both "clean" and "contaminated" electrode conditions for several different moisture contents in the flue gas.

Fundamental work on the electrical properties of a variety of fly ashes including lignites and sub-bituminous and bituminous coals from Australia, New Zealand and the U.S.A. has been carried out at Wollongong University College. In addition, various particulates from the iron and steel industry, copper smelters and cement kilns have been examined in the same apparatus.

Research has centered on the dc and ac conduction processes in fly ashes in both the bone-dry and gas-conditioned modes.

The back-corona inducing properties of such dusts have been intensively examined by contaminating various electrode assemblies such as the point-to-plane, parallel wire-in-duct, and concentric cylinder geometry. Such contaminated electrodes have been electrified with dc, ac, pulse, and special waveform energization.

Some interesting results have emerged as a result of these studies, a few of which may be cited. McLean[8,9] at WUC has examined conduction in bone-dry glasses, glass powders, and fly ashes in some detail, finding that generally the following holds:

Bone-dry

1. Bulk resistivity is independent of particle size.

2. All resistance occurs at the contacts between particles.

3. Compaction (or porosity) has a comparatively minor effect. If the packing is orthorhombic or tetrahedral or random, resistivity varies only by a factor of 2 or 3.

4. Pressure on the compacted layer plays a relatively small role, since resistivity varies as:

$$1/(\text{Pressure})^{1/3}$$

5. Temperature dependence of the powdered material, as expressed by the activation energy, is the same as for the solid material.

6. Powdered material generally deviates markedly from Ohm's Law, that is, resistivity is strongly field dependent.

7. For one specimen of Southern ash similar to that of Table 1, column 2, it was found that the resistivity could be expressed by:

$$\rho = 3000e^{10,210/T}\ e^{-0.77 \times 10^{-6}E}$$

where T = absolute temperature, °K
E = average field stress, mV/m

Moisture Conditioned[7]

1. The familiar inverted VEE curves, (for example Reference 5, Figure 7) are invariably obtained.

2. Some ashes show very much greater sensitivity to moisture than others.

3. To the left of the maximum, the conduction process is governed by the moisture conditioning and is directly proportional to the specific surface area of the dust.

4. Field dependency is still marked and may follow the same general pattern as the same ash in the dry condition.

5. There is the same relative insensitivity to mechanical pressure as in the bone-dry case.

Herceg[10] investigated the formation and mechanism of back-corona in highly resistive porous layers in some detail. By experimenting with porous papers, porous teflon filters as well as with ash layers, he found that the bi-ionization phenomena are basically the same in all these media. In order to represent the pulsed character of back corona, he developed a lumped parameter electronic model using solid-state circuitry. Resulting from these studies, Herceg has developed a form of asymmetrical waveform energization which entirely eliminates back corona.

COMPLEX DIELECTRIC CONSTANT

Studies on several species of dusts have been carried out at Wollongong University College[11] in order to determine the complex dielectric constant over a range of audio frequencies from 50 Hz to 50 kHz and of temperature 20°C to 220 C. Such investigations are important for electrostatic precipitators since the layer adhering to the collecting electrode forms a powder dielectric. The electrostatic precipitator behaves as a large lossy capacitor in which the dust is an important component. When subject to electrical transients, following for example a flashover, the device recovers with a time constant proportional to the real part of the effective dielectric constant. Furthermore, the complex dielectric constant is most important in determining the total adhesive forces on a deposited layer, including both the electrostatic component and the van der Waals component.

One uses the usual definition for the complex dielectric constant as:

$$\varepsilon(\omega) = \varepsilon'(\omega) - j\varepsilon''(\omega)$$

where it is understood that both the real component $\varepsilon'(\omega)$ and the lossy component $\varepsilon''(\omega)$ will be dependent upon the frequency, ω. Typical behavior of the component ε' as a function of temperature and frequency for a dry fly-ash similar in composition to that indicated in Table 1, column 3, is depicted in Figure 6.

ADHESIVITY OF DUSTS

Tassicker has reviewed and identified the forces of adhesion between a layer of dust which has been electrostatically deposited upon a substrate, under the conditions obtaining in an electrostatic precipitator. A full report of this work is being made elsewhere. The forces of adhesion and the rapping forces required to dislodge such a layer are the least understood phase of electrostatic precipitator operation.

ORIGIN OF ADHESIVE FORCES

The tensile strength of a compacted layer depends upon the particle-to-particle forces. These comprise London-van der Waals', triboelectric, capillary, surface dipole, and electric-field corona forces. The physical parameters

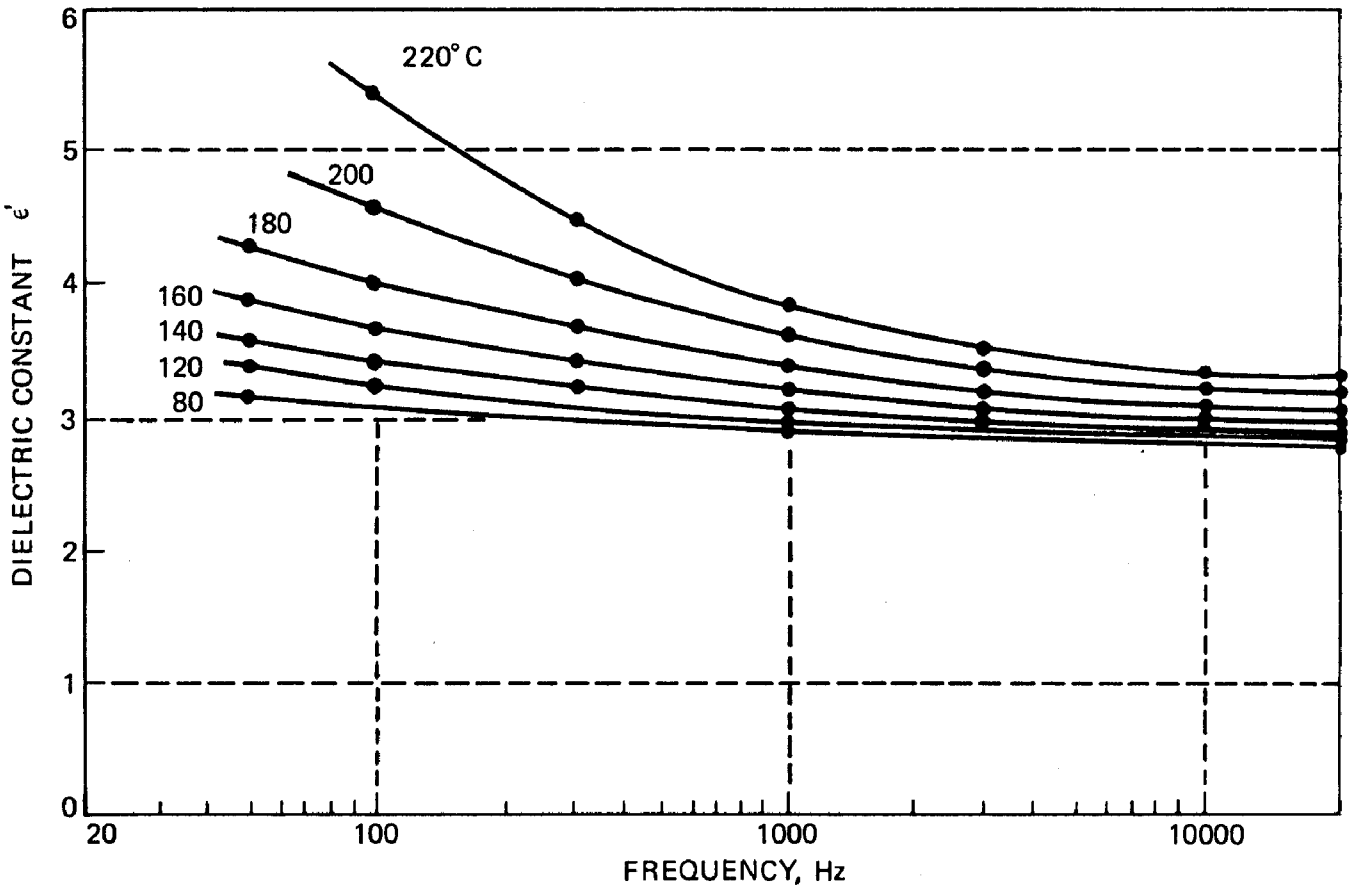

Figure 6. Dielectric constant of fly ash. Dielectric constant ε' of fly ash as a function of temperature and frequency. Generally similar behavior to vitreous, or glassy materials

which influence these component forces are particle diameter, porosity and compaction of the layer, complex dielectric constant from dc to ultra-violet frequencies, humidity in the gas, adsorbed surface dipolar molecules, work-function interfaces on the material, the electric field and current density in the gas space.

The tensile strength P is critically dependent upon the compaction of the layer as indicated by the expression:

$$P = H(\alpha_b/\alpha_s)^m$$

where (α_b/α_s) is the relative bulk density and H and m are empirical constants.

For a material with a given degree of compaction, the following equation applies:

$$P = (A_1/d) + (A_2/d) + 10^5\ (\varepsilon_0/2)[\varepsilon'(J\rho k)^2 - E_g^2]$$

where A_1 = van der Waals and dipole constant

A_2 = the capillary constant

ε_0 = permittivity of free space

ε' = relative permittivity of powder

J = current density in layer

ρ = resistivity of powder

k = constant from 1 to 20 depending upon particle elasticity

E_g = electric field in gas space,
$\simeq$ (applied potential)/(electrode spacing)

Thus, the capillary, van der Waals, and dipole components are always adhesive and inversely proportional to particle diameter. The electrical forces are adhesive for high resistivity particulates, but may become negative, i.e., detaching for low resistivity particles.

MEASUREMENT OF ADHESIVE FORCES

Separate measurement techniques have been used by Potter and Szirmai of the CSIRO and by Tassicker at WUC, for the determination of the strength of powder compacts:

(1) In the CSIRO methods,[12] at elevated temperature, stress is applied to the powder test-piece formed in the shape of two truncated cones joined at the 8 mm waist. The test piece is closely supported by metal and glass surfaces, except at the waist, where an unsupported height of approximately 0.01 mm corresponds to the eventual plane of brittle fracture. Tension is applied by slowly stretching a long metal spring attached vertically to the upper support of the powder test piece. Extension of the spring at fracture is measured and the tensile strength of the powder calculated directly. The method also allows a simultaneous shearing force to be applied up to tensile fracture, or the failure can be produced by shear alone, if desired. The capability of the method has been demonstrated by studying the tensile properties of various powders.

(2) The method used by Tassicker embodies a device known as a Precipifuge, which, as the name suggests, is a combined precipitator and centrifuge. As illustrated in Figure 7, there is an electrically screened (three terminal) rotating head connected to external, static transducers via a slip-ring assembly. The head is surrounded by a set of HT discharge electrodes, the whole being contained in a sealed corona chamber. Dusty gas is first admitted to the corona chamber with the head slowly turning. A layer of dust is thus electrostatically deposited on the head to a depth of a mm or so. The speed of the head is then raised in increments and the surface of the dust monitored by several transducers. The capacitance transducer is capable of resolving detachment of dust with very high sensitivity. The relationship between dust detached and adhesive strength of the deposit is:

$$P = (M/A)\ \omega_0^2 R \quad N/m^2$$

where (M/A) = mass detached per unit area

ω_0 = angular velocity at detachment

R = radius of centrifuge head

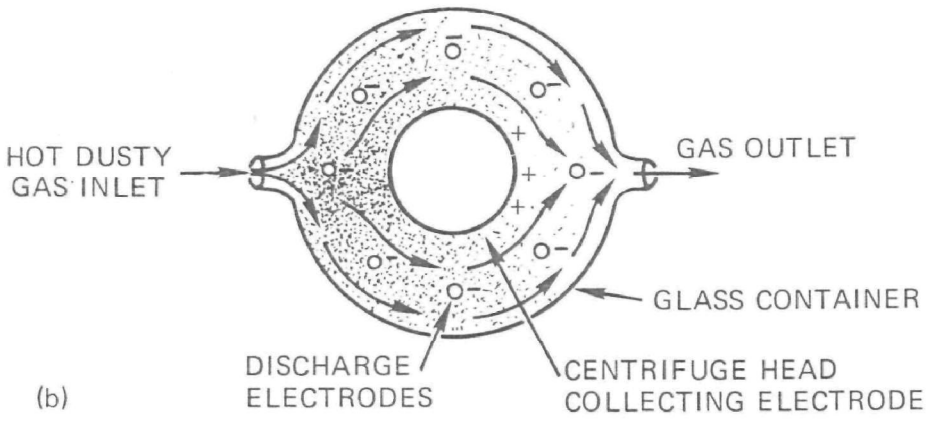

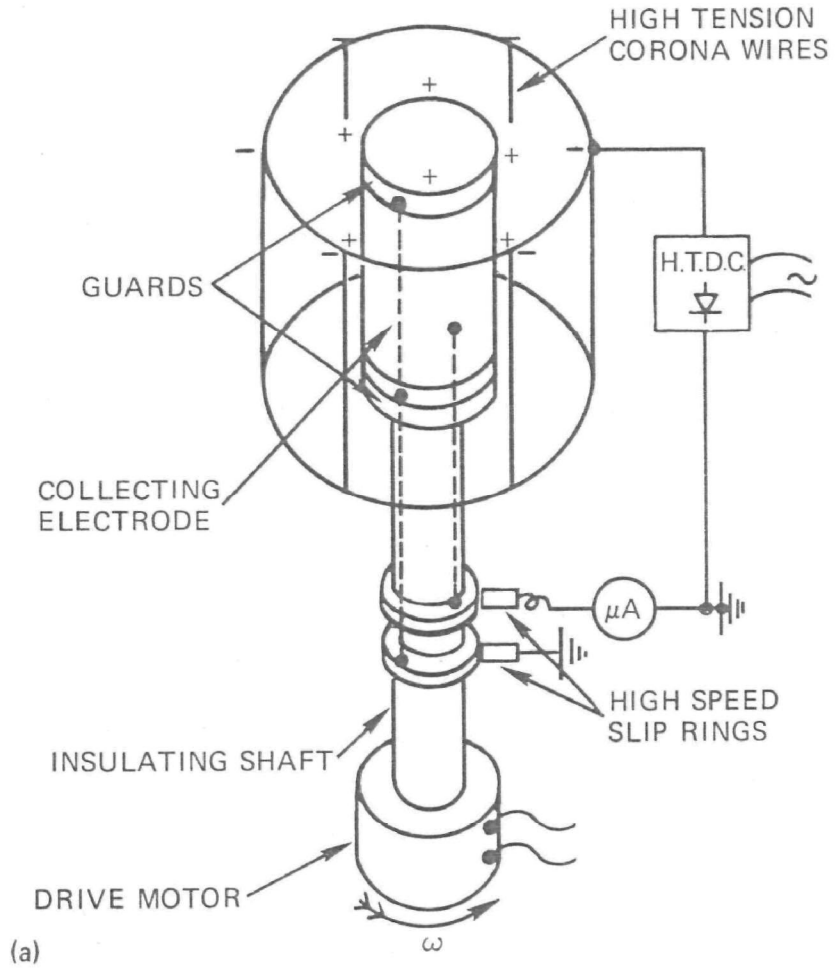

Figure 7. The Precipifuge. (a) Drive motor 0-10,000 RPM, high-speed screened slip-ring assembly guarded rotor head, high tension corona emitters; (b) Corona chamber, with options of gas inlet or vacuum

The adhesivity of the deposit may be determined with or without an electric field with or without corona current, in the presence of any gas or subject to a vacuum. By testing under a vacuum, the ash surface may be desorbed, and the effect of moisture or other adsorbed gases may be readily checked. Many fly-ash specimens have been examined by means of the Precipifuge.

ELECTRODE EVALUATION

BY BOUNDARY PROBE

In order to evaluate various electrode types, Tassicker developed an apparatus known as MABEL[13] (micro area boundary electrode) capable of measuring the electric field E_0 and current density J_0 over a collector electrode. It is capable of high mechanical resolution, since spatial accuracy of 0.5 mm is readily obtainable. Calibration of the probe is in terms of its mechanical dimensions, so that J may be determined to within ±1% and E to within ±5%.

The probe, as illustrated in Figure 8, comprises a small insulated circular area of about 1 mm diameter which is polished flat and set flush with the boundary. Without bias, the probe samples the current density at the point. When biased by V_b, the quiescent current I_0 is increased or decreased according to the relation:

$$I/I_0 = 1 + 4.75\ V_b/(d_m E_0)$$

where d_m is the mean probe diameter and E_0 the boundary unperturbed field. From this expression, E_0 may be readily determined, and the gas conductivity $\bar{\sigma}$ is E_0/J_0. The calibration is independent of carrier mobility and space-charge density.

In a more recent version of the device,[14] a three-terminal active probe has been developed, using an ac diagnostic signal and a modern impedance bridge as the transducer. In addition to J_0, E_0, and $\bar{\sigma}$, this device measures the complex dielectric constant of the ionized gas at a point on the electrode boundary.

By means of MABEL, many types of electrode emitters have been examined: cylindrical, point-to-plane, parallel wire-in-duct, barbed wire-in-duct, etc. Details of this work are being reported elsewhere. In addition, interesting fine structure in negative corona has been discovered.[15]

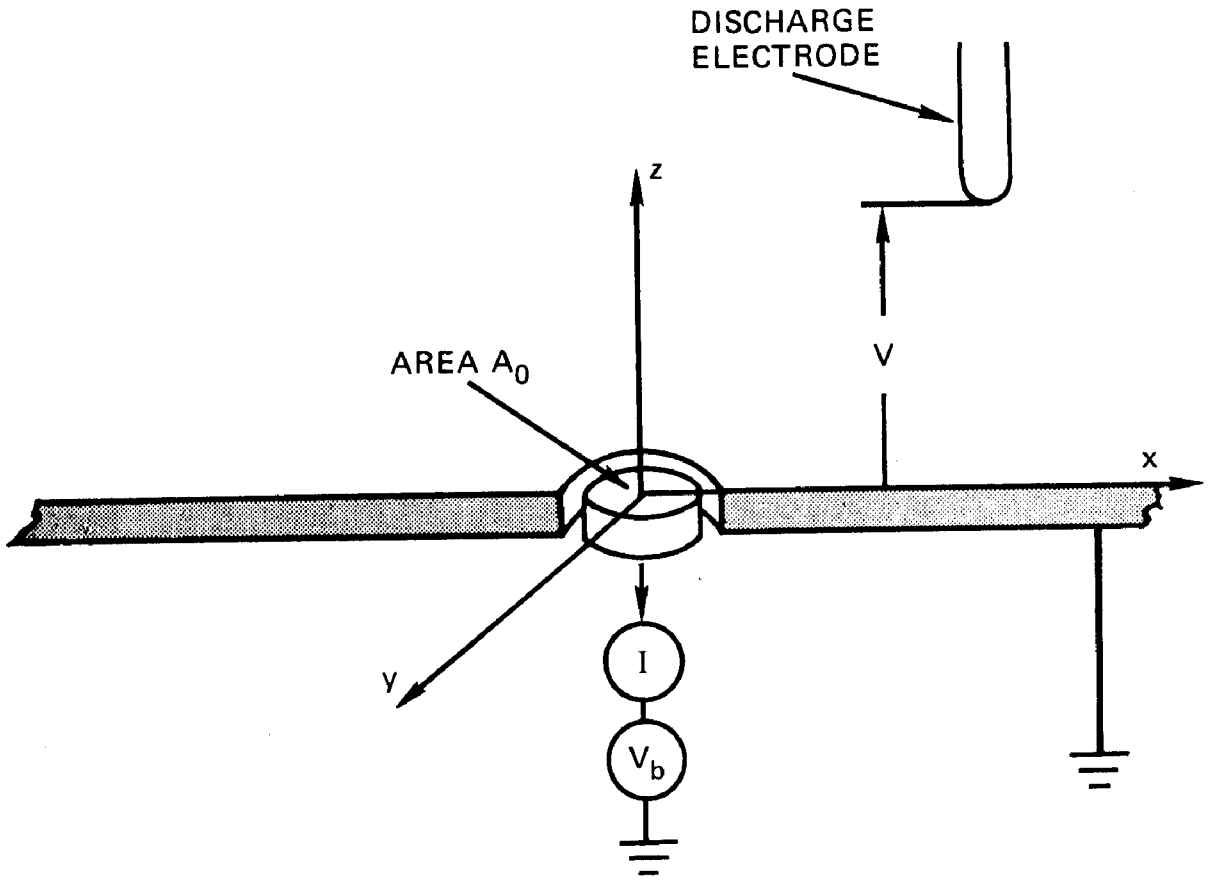

Figure 8. Micro area boundary electrode. MABEL measures the current density J_0 and electric field E_0 at the boundary of a corona system. HV discharge electrode is traversed relative to A_0 in the X-Y direction

GAS CONDITIONING

The ECNSW uses conditioning agents on a large number of its precipitator installations on a permanent basis in order to keep emissions within the Act.[16,17,18] Concentrated ammoniacal liquor (CAL) which is a by-product of steel works coke-ovens is the preferred additive, followed by sulfuric acid. Both agents are added in a few ppm. While most of these installations are in the nature of retrofits, one new installation has been sized for CAL conditioning following pilot plant testing.

There is clear evidence that the efficacy of ammonia is by improving the V-I corona characteristics of the flue-gas, rather than by any change in resistivity of the ash. By contrast, sulfuric acid conditioning has a large and persistent effect on the conductivity of the ash as illustrated in Figure 9. Conductivity was measured in the field and in the laboratory on the unconditioned ash. Following conditioning of the ash (Table 1, column 1) by sulfuric acid in a full-scale installation, the conductivity was again measured in situ. There are two orders of magnitude improvement in the conductivity. Interestingly, where the conditioned dust was tested about 24 hours later in the laboratory in a synthesized flue gas (but with no further acid), the enhanced conductivity persisted.

The results of gas conditioning on the collection efficiency have been spectacular in some cases, marginal in others. One particularly interesting case is depicted in Figure 10 (ash Table 1, column 2). Commissioning tests on the unconditioned dust in 1962-3 were dismal. Sulfur trioxide conditioning gave enhanced performance depending upon the amount and injection efficiency. Sulfuric acid conditioning in 1970 showed a little improvement. Ammonia additives in 1970 showed further benefit. Finally, in 1972, both steam and CAL were added and the installation has maintained +99% efficiency ever since - a striking result when compared with the unconditioned tests of 1962-3. Much of this pioneering work in gas conditioning has been under the direction of Kenneth S. Watson and Neville N. Lamb in collaboration with manufacturers. They have maintained informal contacts with fraternal utilities in several parts of the world.

More recently, the CSIRO, under Paulson, Potter and Kahne, have successfully used triethylamine on this same Wongawilli seam coal, obtaining collection efficiencies as good as, or superior to, those obtained with CAL, but with very much

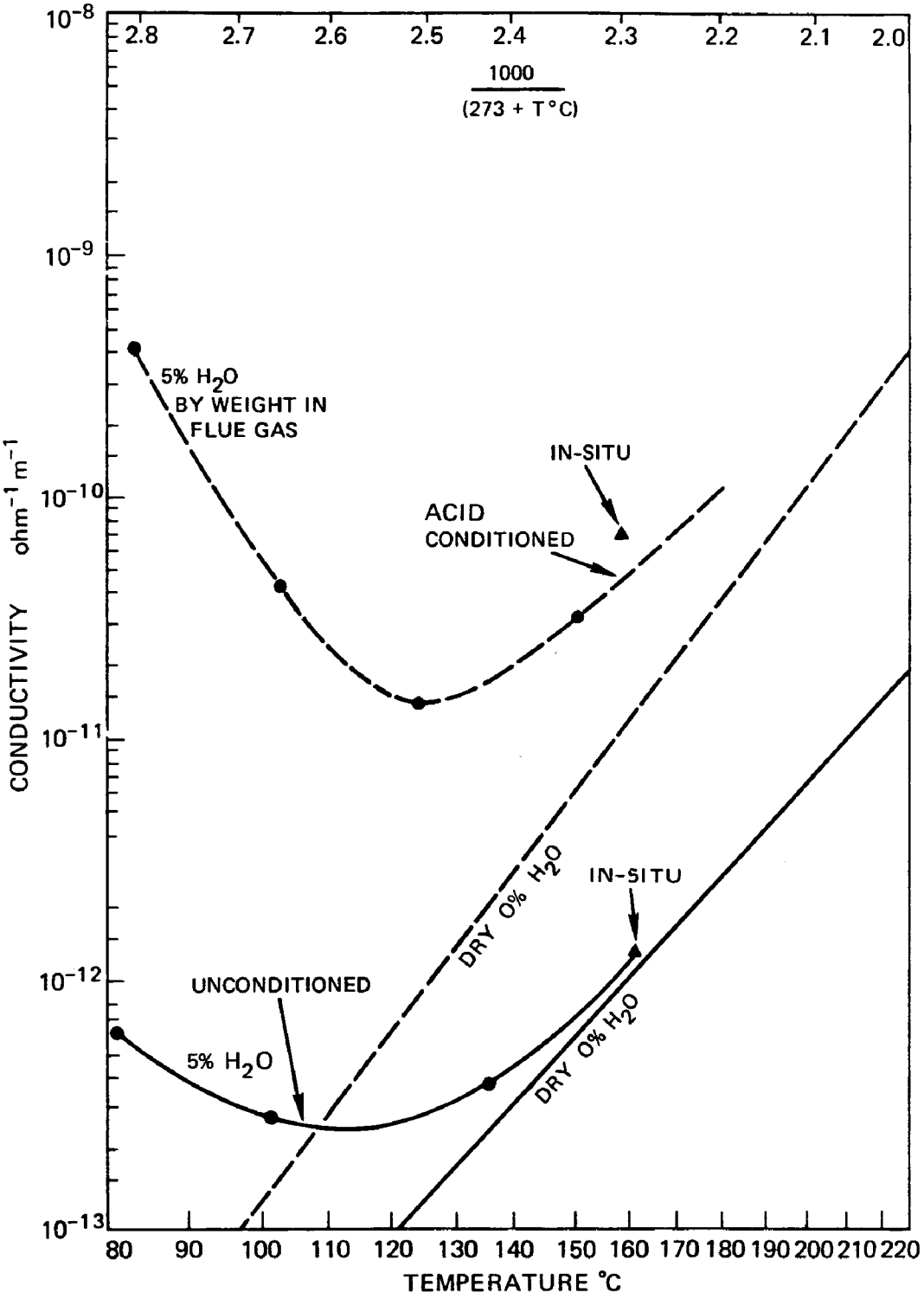

Figure 9. Sulfuric acid conditioning a high resistivity fly ash. Fly ash (Table 1, column 1) was tested in the field and later in the laboratory, both with and without sulfuric acid conditioning

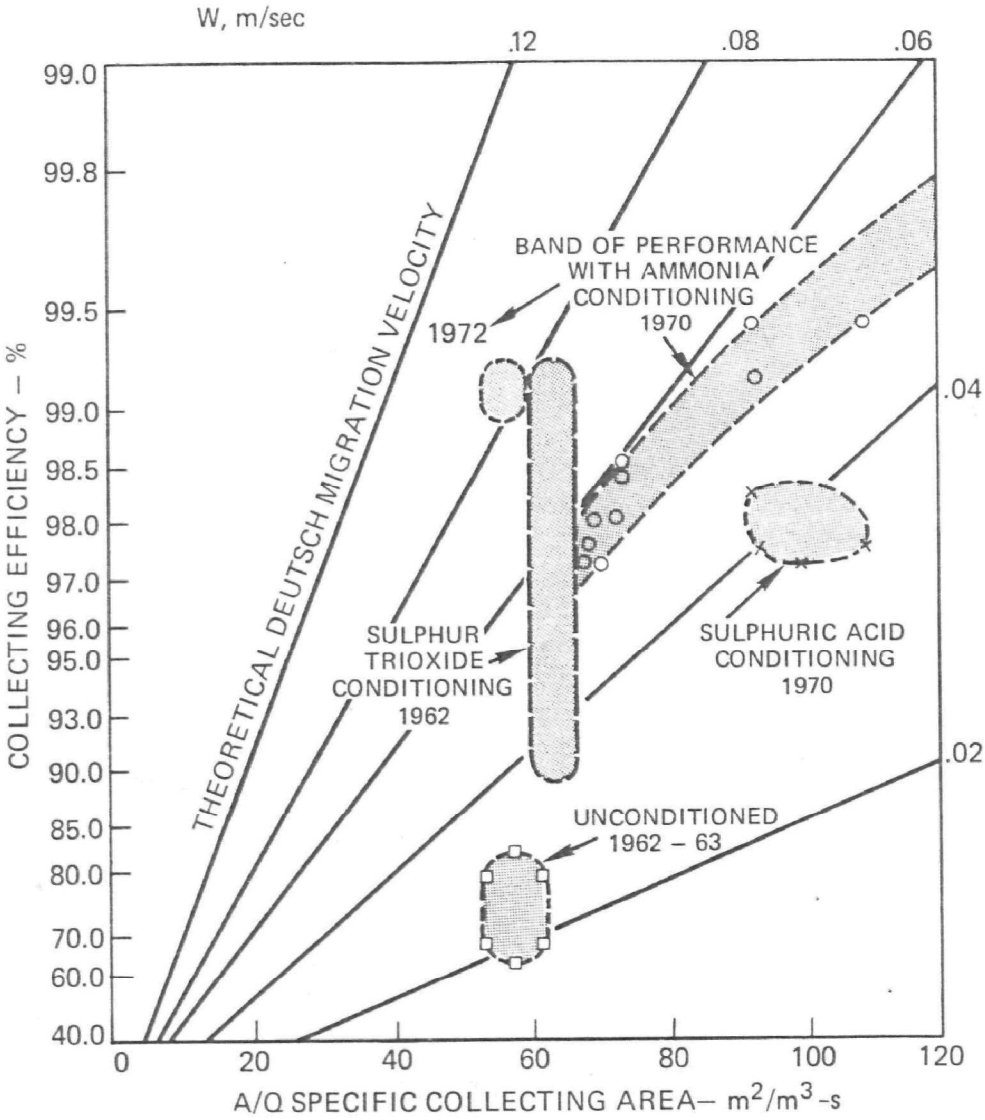

Figure 10. Precipitation performance with conditioning agents. Main plant shows poor performance with unconditioned dust, some improvement with acid conditioning, marked improvement with ammonia conditioning. After Kirkwood, Watson, Lamb, O'Brien, Blecher.

smaller quantities of additive. This is an interesting revival of the work of Dr. J. F. Chittum[19] with triethylamine at the Utah Oil Refining Company catalytic cracking plant in 1944. After an interval of 30 years, this chemical has had the same unqualified success--this time in treating what is possibly the most difficult low-sulfur fly ash found in Australia.

REFERENCES

1. Liddell Power Station, Investigation of Requirements for Electrostatic Precipitators. The Electricity Commission of New South Wales. Research Note No. 59. February 1967.

2. O'Brien, A., and A. N. Lamb. Wallerawang Power Station, Investigation of Requirements for No. 7 Boiler. The Electricity Commission of New South Wales. December 1969.

3. Mills, R. A., and O. J. Tassicker. Analysis of Pilot Plant Electrostatic Precipitator Testing in Connection with Huntly Power Station. In: Proceedings, International Clean Air Conference. Rotarua, New Zealand. February 1975.

4. Tassicker, O. J. Performance of Cold Side and Hot Side Electrostatic Precipitators Treating High Resistivity Fly Ash. Wollongong University College. (Presented at the Symposium on the Changing Technology of Electrostatic Precipitation. Adelaide. November 8, 1974.)

5. McLean, K. J. Survey of Australian Experience in Collecting High Resistivity Fly Ash with Electrostatic Precipitators. Contract 68-02-0245, Environmental Protection Agency. September 1972.

6. Paulson, C. A. J., and E. C. Potter. Reduction of Particulate Emissions to Air by Improved Assessment of Electrostatic Precipitators. (Presented at National Chemical Engineering Conference. Queensland. July 1974.)

7. Tassicker, O. J., and K. M. Sullivan. Estimation of Precipitator Performance for Collection of Fly Ash by Examination of Low Sulfur Coal Bore Cores. Wollongong University College. (Paper 73-311, presented at Air Pollution Control Association 66th Annual Meeting. Chicago. June 1973.)

8. McLean, K. J. Metal-Glass Contacts in High Electric Fields. Electron. Lett. (London). 5(4):72-73, February 1969.

9. McLean, K. J., and R. M. Huey. Influence of Electric Field on the Resistivity of a Particulate Layer. Proc. Inst. Elec. Eng. (London). 121:76-80, January 1974.

10. Herceg, Z., and R. M. Huey. Model for Corona Modes in Point-to-Plane Device with Coated Electrodes. Proc. Inst. Elec. Eng. (London). 120:394-399, March 1973.

11. Tassicker, O. J. The Temperature and Frequency Dependence of the Dielectric Constant of Power-Station Fly Ash. Staub-Reinhalt. Luft (in English). 31:23-28, August 1971.

12. Potter, E. C., and S. G. Szirmai. Measurements of Powder Strength at Elevated Temperatures by a New Method. (Presented at National Chemical Engineering Conference. Queensland. 1974.)

13. Tassicker, O. J. Boundary Probe for the Measurement of Current Density and Electric-Field Strength--with Special Reference to Ionized Gases. Proc. Inst. Elec. Eng. (London). 121:213-220, March 1974.

14. Tassicker, O. J. Determination of the Complex Dielectric Constant, Electric Field and Conductivity at the Boundary of an Ionized Gas. Proc. Inst. Elec. Eng. (London). (in press).

15. Tassicker, O. J. Measurement of Corona Current Density at an Electrode Boundary. Electron. Lett. (London). 5:285-286, 1969.

16. Tassicker, O. J. Experiences with an Electrostatic Precipitation Analyzer in the Evaluation of Difficult Dusts. In: Proceedings, International Clean Air Conference. Melbourne. May 1972.

17. Watson, K. S., B. P. Flanagan, and K. J. Blecher. Pilot Plant Testing as an Aid to Evaluating Precipitator Performance. (Presented at Institution of Electrical Engineers Colloquium. London. February 1965.)

18. Watson, K. S., and K. J. Blecher. Further Investigations of Electrostatic Precipitators for Large Pulverized Fuel Fired Boilers. In: Proceedings, Clean Air Conference. Sydney. August 1965.

19. Quoted in: Dismukes, E. B. A Study of Resistivity and Conditioning of Fly Ash. Southern Research Institute, Contract CPA 70-149, Environmental Protection Agency. February 1972. Publication Number EPA-R2-72-087. NTIS PB 212607. 138 p.

SPECIFYING ELECTROSTATIC PRECIPITATORS FOR HIGH RELIABILITY

N. W. Frisch and D. W. Coy
Research-Cottrell, Inc.
Bound Brook, New Jersey

ABSTRACT

Precipitators for utility applications must function reliably at high efficiency. However, often the conditions under which they are to function are poorly known. Some of these poorly defined conditions include relationship of plume opacity and quantitative emissions for the particular fuel, inadequately known temperature level and temperature variations due to air preheater operations, unknown gas velocity distribution, and especially absence of fuel characteristics data.

Various approaches, including statistical ones, are used to improve the reliability of the sizing under conditions of minimal information. In contrast, the ideal situation of having available extensive fuel data is also presented. Methods for handling temperature and gas velocity distributions are indicated. The optimum selection of redundancy is also discussed.

INTRODUCTION

Reliability of air pollution control equipment has become a key issue in the evaluation of competing control systems. The increased sophistication of customer requirements for reliable electrostatic precipitators is evident, even in

casual observation of their bid solicitations. Specific clauses frequently require design efficiencies to be achieved with a fraction of the precipitator collection area out of service. Performance tests are often required at the beginning of service, and one year after the unit has gone on stream. The initial performance tests may not be allowed until the unit has operated for a specified time period without shutdown for precipitator maintenance or adjustments. For the electric utilities, the search for system reliability is undoubtedly motivated by their need to avoid loss of generating capacity and revenues which result from breakdown of control equipment. The alternative of operating in defiance of emission regulations, risking financial loss through court action and loss of public sympathy, is certainly no more palatable.

Reliability in the broadest sense must encompass more than avoidance of equipment failures. Long-term successful operation of a precipitator is just as much dependent on being able to operate at original (or less demanding) design conditions. In general, recent environmental legislation has made it difficult for the utilities to maintain original design conditions. The new particulate regulations require higher collection efficiencies. Utilities have reacted by purchasing new and more efficient control equipment. Superimposed on the new particulate regulations are those for limiting sulfur oxides. While not directly forcing the use of low sulfur coals, the regulations have created a large scale movement in this direction. The particulate emission regulations and potential switches to low sulfur coals must be dealt with simultaneously to avoid another round of control equipment purchases. For pollution control equipment manufacturers to be responsive to these reliability requirements, it is essential that the customer be as definitive as possible about the long-term fuel situation.

The predominant present practice in specification writing is to submit a range of coal and ash analyses with, in some cases, typical values specified. While in the past precipitator sizings were specified primarily on the basis of sulfur content of the coal, this is no longer the case. Many more of the physical and chemical properties of the coal and ash are being used in the sizing process.

To Research-Cottrell, customer specification of "typical" or "average" values of coal and ash properties is becoming an unsatisfactory situation. Assessment of individual fuel and

ash analyses is preferred. The effects of limited fuel and ash analysis data on precipitator sizing and, consequently, overall reliability is demonstrated in a section of this paper.

Additionally, precipitator manufacturers are working to improve the electrical and mechanical reliability of their equipment. Recognizing that equipment failures do occur, however, and immediate repair is frequently not possible (especially with discharge electrode breakage), it is possible to avoid exceeding emission limitations between maintenance periods by including redundant capability in the precipitator design. Selection of redundant capacity must depend on anticipated failure and time between maintenance periods. Obviously, there is some optimum level of redundancy. Methodology for determining this level is presented in this paper.

The goal of much higher precipitator efficiencies is necessitating in-depth consideration of many more details than in the past. Temperature and gas velocity distributions in the gas stream entering the precipitator are important points. Good velocity distribution will maximize the efficiency for a given collector size. For precipitators operating in the temperature range of 250°F to 350°F, the extremes in temperature variation leaving the air preheater can produce zones of extreme performance in the precipitator as well.

It is unfortunate that many precipitator system specifications are written comprehensively in terms of construction details, but lack the kind of technical detail conducive to achieving reliable performance at high efficiencies. It is the intent of this paper to present approaches for improving reliability of design and a method for selecting the amount of redundancy built into the precipitator to accommodate equipment failure which may occur between maintenance periods. In the process, we hope to define the kind of detail that we, as one precipitator manufacturer, would like to see in the specifications to which we must respond. In particular, this paper addresses itself to fly ash collection for utility stations.

FUEL CHARACTERISTICS SPECIFICATIONS

Fuel characteristics, coupled with method of firing and operating temperature, largely influence the size of a precipitator required for a given installation. Specifications

offered by engineering consultants describe these fuel characteristics in varying degrees of adequacy, and it should be recognized by both the consultant and the utility that the adequacy of a precipitator offering is related directly to a detailed knowledge of fuel characteristics and variability of same.

A key element to long-term reliability is being certain that the fuel specifications presented in the solicitation are broad enough to encompass all potential fuel situations. This requirement at present is probably a most difficult one to meet. Competition among utilities for low sulfur coals has made it difficult in some cases to arrange long-term commitments with coal suppliers, and created much uncertainty about the consistency of fuel supply to a given plant.

The term "fuel specification" needs to be clarified. In dealing with anticipated problems of uncertain fuel supplies, some prospective customers choose to define their fuel expectations in terms of coal sulfur content. As a result, we receive coal specs which say 0 to 3% sulfur, 0.3% to 6% sulfur, eastern bituminous coal, western subbituminous low sulfur coal, etc. Information like this is almost worthless, except that it tells the equipment manufacturer the design must be conservative. These are not sufficient fuel specifications, since the information is only about sulfur content.

Fuel sulfur content in the high range 2% to 4% is of prime importance in cold precipitator sizing, but as sulfur content diminishes to 1% or less, chemical and physical properties of the ash become of much greater importance. For hot precipitators, fuel sulfur content is virtually of no value. The work of Shale[1] and of Bickelhaupt[2,3] serves to emphasize this point. Fly ash resistivity at elevated temperatures shows a strong dependency on sodium and also iron content. Further attempts to predict resistivity from ash properties and other variables are anticipated.

An adequate or broad "fuel specification" as used in this paper includes complete details (ultimate, proximate, and ash chemical analyses) about all potential fuel sources. A number of prospective customers and consultants do routinely provide this information. A continued trend into this direction would be most welcome.

An additional feature of the preferred fuel specification is inclusion of all available individual analyses for all potential fuels. Predominant present practice is to cite the maximum and minimum values for each constituent, and a

"typical" or average value (presumably these are not the same). If a number of analyses were obtained to derive the range of constituents, the individual analyses are of greater value to the equipment supplier than just the range. The importance of this point is treated in the examples below in which precipitators are sized for varying degrees of detail in fuel specifications. The variations in sizings demonstrate that selection of an optimum precipitator size is facilitated with detailed fuel information.

The example chosen for presentation is that of sizing a hot precipitator for a low sulfur western coal. This example was chosen because of the availability of a large number of coal and ash analyses which permit demonstration of techniques for handling a large amount of data. Additionally, in the hot case, unlike the cold situation, there is a well-defined and precise method[4] for sizing hot precipitators based upon ash composition.

To eliminate any misconceptions which may exist about sizing hot precipitators, there is sufficient variability among fly ashes to prevent any generalization about specific collection electrode area for a given collection efficiency. High temperature tends to minimize extreme variations in resistivity from ash to ash[5], but enough variation remains to produce precipitator size differences for given efficiencies.

Six examples follow which illustrate the effect of the specification on precipitator offering.

GENERAL FUEL SPECIFICATIONS CASE

No ash chemical analyses are available. Customer reports only that coal sulfur content will range from 0.3% to 6%, and the coals will be eastern bituminous or western subbituminous. A maximum gas rate, operating temperature, and design efficiency was specified. The example below indicates these levels.

Example: Case 1 - General Fuel Specification

Maximum gas volume - 3.656×10^6 acfm
Temperature - 780°F
Design Efficiency - 99.7%

In a case such as this, the customer is apparently relying on the precipitator manufacturer to select a precipitator to meet an insufficiently specified situation. The most

appropriate action is to go back to the customer for more information. Lacking that, the equipment supplier, in this case, may examine his fuel data bank and select a precipitator size (SCA) more conservative than the worst case in his files for the specified design efficiency, and hope that such a case does not exist. Alternatively, he may decline to bid.

The comparative sizings for all example cases are shown in Table 1.

WORST, WORST CASE

In this case, a range of fuel and ash analyses is specified with no indication of typical or average values. The sizing of the precipitator in this extreme case is based on selection of constraining values; i.e., maximum inlet concentration to determine highest required efficiency, maximum gas volume, and minimum iron and sodium contents. Following this procedure will usually result in a much too conservative precipitator size. The probability of all these conditions occurring simultaneously is insignificant.

Data for this case is summarized in the table below.

Example: Case 2 - Range of Fuels Specified - Worst Case Sizing

Maximum gas volume - 3.656×10^6 acfm
Temperature - 780°F
Efficiency (based on max. inlet conc.) - 99.84%
Minimum sodium content - 0.12%
Minimum iron content - 3.2%

AVERAGE ANALYSIS WITH RANGE OF FUEL ANALYSES CASE

A range of values for coal and ash analyses has been provided and an average value for the components specified. For this case, you begin to get some idea of how the sampling distribution of each constituent looks. Average values indicate whether the distribution is weighted towards higher or lower values. Precipitator sizing based on average values, however, may be too small to handle a large percentage of the cases which are likely to occur.

Table 1. COMPARISON OF PRECIPITATOR SIZES FOR VARYING DEGREES OF DETAIL IN FUEL SPECIFICATIONS

Case No.	Description	Temperature, °F	Gas volume, millions of acfm	Efficiency (EPA), %	Ash comp. Na_2O %	Ash comp. Fe_2O_3 %	Area, 10^6 ft^2
1	General fuel specifications	780	3.66	99.70	--	--	3.77
2	Worst case	780	3.66	99.84	0.12	3.18	2.85
3	Average case	760	3.50	99.67	0.34	6.70	1.24
4	Typical case	760	3.60	99.67	0.25	5.50	1.44
5	98% of samples 99% of samples 99.9% of samples	780	3.61	99.70	--	--	1.61 1.64 1.75
6	Most probable worst case	780	3.61	99.70	0.122	4.36	2.12

Example: Case 3 - Range of Fuels Specified - Average Case Sizing

Gas volume - 3.5×10^6 acfm
Temperature - 760°F
Efficiency (based on avg. inlet conc.) - 99.67%
Average sodium content - 0.34%
Average iron content - 6.7%

TYPICAL ANALYSIS WITH RANGE OF FUEL ANALYSES CASE

The customer has supplied range of values for the coal and ash analyses, and a set of analyses he has judged to be typical. Presumably, the criterion for selecting the typical data is the most frequently occurring value in the constituents considered critical to the precipitator selection. Specifications based on typical values occur frequently at present. The sizings from this data, however, are subject to the same weakness as sizings based on average data. The selected size may not achieve design efficiencies for a large percentage of the fuel because of random variation in the composition.

The table below summarizes the data for this case.

Example: Case 4 - Range of Fuels Specified - Typical Case Sizing

Gas volume - 3.57×10^6 acfm
Temperature - 760°F
Efficiency (based on typical inlet conc.) - 99.67%
Typical sodium content - 0.25%
Typical iron content - 5.5%

LARGE NUMBER OF FUEL ANALYSES CASE

For this case, the customer has supplied a large number of individual fuel and ash analyses in his solicitation. It is our intent to design the precipitator to handle a very high percentage (greater than 98) of the individual fuel analyses. Through a series of calculations—combustion, ash carryover, resistivities—precipitator collection areas can be determined for each fuel and the cumulative distribution can be plotted. The table below shows the conditions for this case. Figure 1 is the cumulative plot. By virtue of the cumulative plot, a precipitator sizing can be chosen to accommodate any desired percentage of the sampled fuel analyses. Use of this methodology assumes that no blending

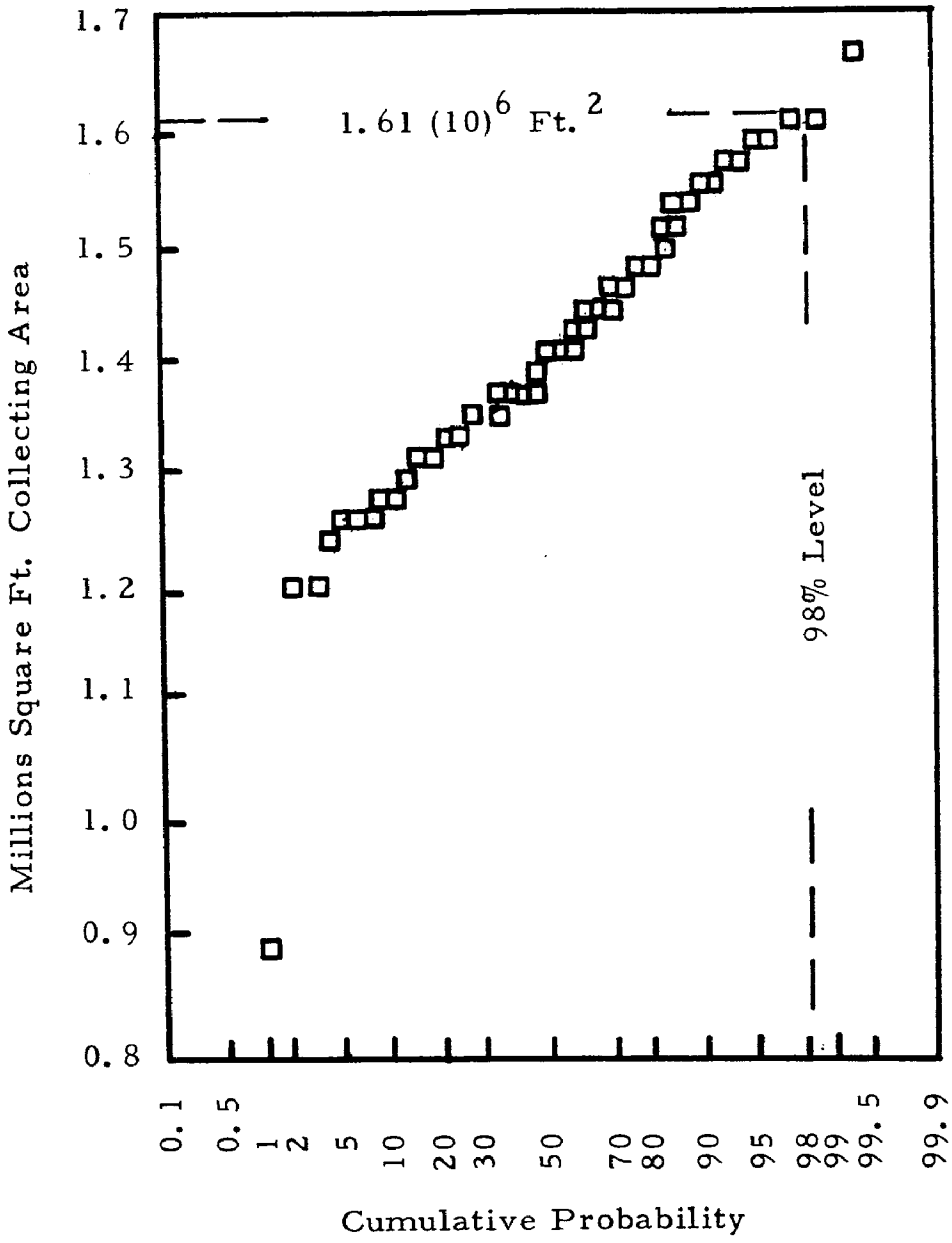

Figure 1. Normal plot of collection area for individual fuel samples

of the individual fuels occurs, and that any of the given fuels have an equal probability of becoming the fuel source for the boiler. If the latter assumption is incorrect, the method is easily modified by providing weighting factors for application to each fuel. The weighting factors will describe the probability assigned to the event that a particular fuel will be burned or the relative proportions of the total fuel supply the sample represents, or a combination of these depending on the specific case.

Providing the coal samples are truly representative of the coal seam, this method allows the designer with certainty to select a size which can handle a high percentage (98%-100%) of the fuels.

Additionally, the examination of a plot such as Figure 1 will indicate the possibility or advantage of adopting alternative policies to minimize the precipitator size requirements. Included are the possibility of fuel blending, operation at reduced load with a specific fuel segment or fuel segregation. In the latter cases, it is reasonably simple to define as part of the computer output, fuels with high ash resistivity, or high efficiency requirements, or even fuels mutually suitable for blending.

Example: Case 5 - Large Number of Fuel Sample Analyses Provided -
98% of Fuels Included in Sizing

Gas volume - 3.6×10^6 acfm
Temperature - 780°F
Efficiency (based on including 98% of inlet conc.) - 99.7%

To compensate for large variances in critical fuel and ash components, there is an additional useful method for analyzing the data and selecting values for sizing.

MOST PROBABLE WORST CASE

This approach is based on the generation of the distribution of important properties (sodium, iron, ash, etc.) that best represents the fuel supply. These distributions can even be developed with a limited number of fuel analyses, but the definition under these circumstances will be considerably broader than for the situation in which levels of 50, 100, or more individual analyses are available.

The parameters for Case 6 are shown:

Example: Case 6 - Large or Small Number of Fuel Sample Analyses Provided - Most Probable Worst Case (98% Probability Level)

Gas volume - 3.61×10^6 acfm
Temperature - 780°F
Efficiency (based on including 98% of inlet conc.) - 99.7%
Most probable worst sodium - 0.122%
Most probable worst iron - 4.36%

The use of this method permits us to compensate or correct for an imperfect knowledge of the true distribution of critical fuel and ash properties.

For this particular example, only two components, sodium and iron, of the ash were considered critical. The other important variables were relatively consistent. The analytical method can be extended, however, to the case of any number of critical variables, but it is not easily presentable graphically for more than two.

Briefly, the method analyzes the data in a manner which assumes that they are represented (with possible transformation of variable) by a bivariate normal distribution. The pertinent parameters (mean, standard deviation and correlation) which describe these distributions are generated, and it is then possible to pinpoint the most probable worst case (MPWC). This situation represents, in the general case of hot precipitator sizing, that fuel in the "true" population which will require the largest collecting area due to the combination of ash level (i.e., efficiency requirement), chemical composition of ash (i.e., resistivity level), and ultimate analysis (i.e., gas rate).

As noted for ease of understanding and due to limited ash variation, the present analysis is based on ash composition (Na_2O, Fe_2O_3) only. In this case, as in the previous one, it is necessary to define that proportion of the estimated population which is to be adequately treated by the precipitator system. In this case, the level was set at 98%.

Figure 2 is a plot of Na_2O and Fe_2O_3 concentrations in the ash samples. Individual data points are shown. The lower boundary of these values which encompasses 98% of the

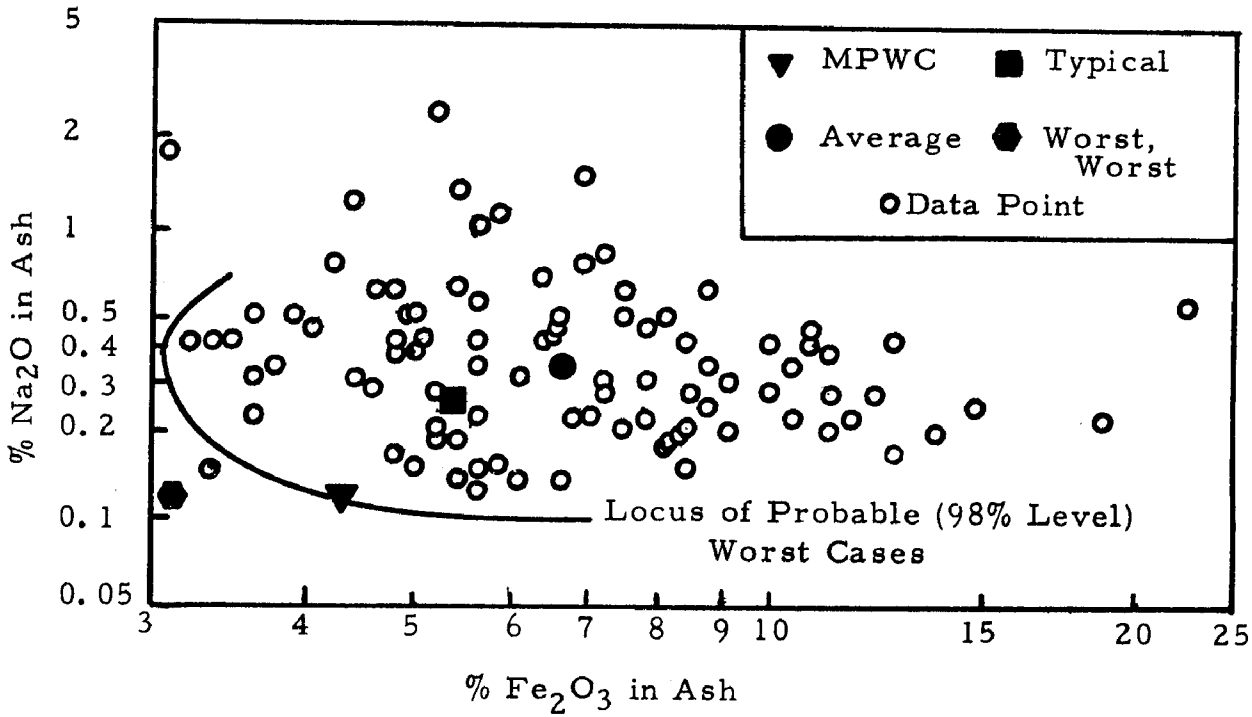

Figure 2. Na_2O-Fe_2O_3 plot showing compositions used for various sizing cases

estimated true distribution is shown. It is on this curve that the most probable worst case occurs. The latter point is noted.

Also shown in Figure 2 are the pertinent compositions related to the sizing for Cases 2, 3, and 4. The worst, worst case composition is clearly outside the lower boundary curve. The typical and average compositions are well within the curve, but inadequately describe much of the data.

Table 1 summarizes the recommended sizings for the six cases. Figure 3 shows the relative sizings graphically. Inadequate information (Case 1) and assumption of worst, worst situation conditions (Case 2) require inordinately large precipitator sizings. Average and typical composition sizings (Cases 3 and 4) require sizings that are somewhat modest with respect to handling all the fuel adequately. Case 5 is a good compromise; this precipitator offering is capable of handling 98% of the actual fuel samples. The most probable worst case size for this example may be excessively conservative, requiring 20%-30% additional area above Case 5.

OTHER FACTORS IN DESIGNING FOR RELIABILITY

There are other significant factors which should be considered in designing a unit for high reliability. Non-uniform temperature and velocity distributions in the precipitator can cause significant deterioration of performance below that expected for more ideal situations.

Additionally, the need for incorporation of redundant capacity in a precipitator system must be considered. Various approaches to these situations have been taken depending upon the controlling mechanism. Some of these approaches are discussed.

REDUNDANCY

Redundancy may be defined as the collecting area incorporated in the precipitator to compensate for the "normal" level of unavailable collecting area. The intent is clearly that the precipitator shall be capable of maintaining its design efficiency level at all times with infrequent periodic shutdowns corresponding largely to boiler outages.

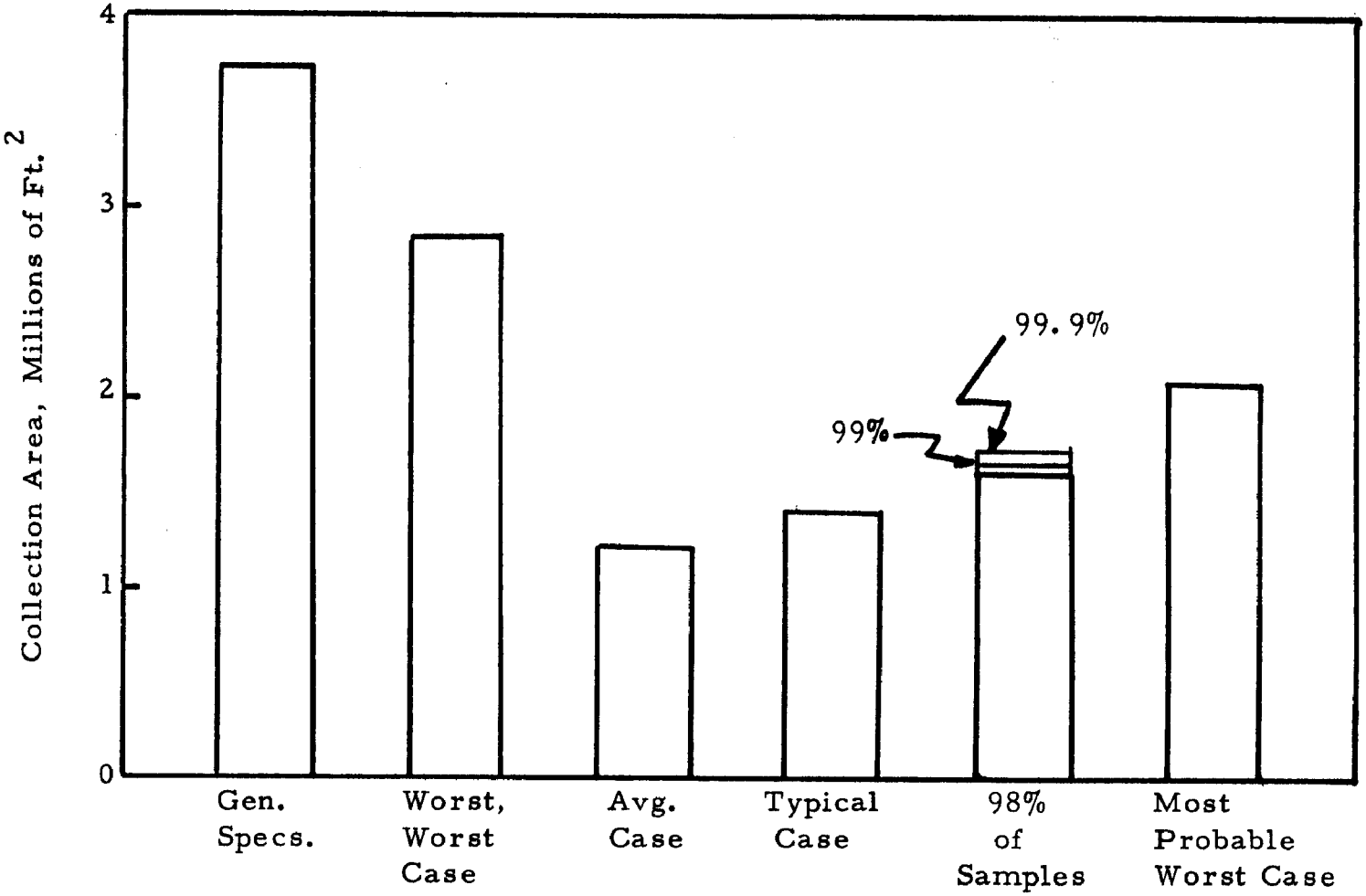

Figure 3. Comparison of sizings for various design specifications

The source of unavailable collecting area varies with precipitator design and service. Among the sources of difficulty are ash removal problems, discharge electrode failure, insulator failure, transformer-rectifier malfunction, etc., although the latter is generally quite small.

Approaches incorporated into specifications frequently include the requirement of demonstrating the design efficiency level with 10% to 14% of the precipitator collection area out of service. We prefer a somewhat more rational analysis for determining both the level of redundancy to be incorporated in a given precipitator design, and the optimum arrangement.

One of our analytical approaches is based on the assumed grounding of electrical sections due to discharge electrode failure. It is assumed in this conservative approach that (1) each discharge electrode failure results in the grounding of a section, (2) future electrode failures are unlikely to occur in previously grounded bus sections, and (3) grounded electrodes are not replaced except on a prescribed maintenance schedule. Clearly, these are extreme conditions, and predicted performance based on these hypotheses is likely to be exceeded in actual practice.

The performance of a precipitator depends upon the collection electrode area which an element of dirty gas stream sees. As the gas progresses along a passage, the incremental removal of dust decreases. Consequently, there is a significant difference in overall performance of a precipitator system, depending upon the location of grounded electrode sections. We have quantified these effects and use them in our reliability analysis programs.

In order to describe the electrical section failure pattern which will determine precipitator performance, say $\bar{t}$ months after the last maintenance, we must generate statistically the location of the failures. We do so by use of the random number generator technique which produces a quantity of random numbers equal to the number of broken electrodes. The latter is described by

$$N_f = [1-\exp(-Rt)]\, S \qquad (1)$$

where N_f is the total number of discharge electrodes failed

t is the time, months, since the last maintenance

R is the fundamental failure rate, (electrodes)/(wire-month)

S is the total number of discharge electrodes in the precipitator system

Each number is related to the location of an electrical bus section which becomes deactivated. Weighing factors can be assigned to account for a non-uniform probability of electrode failure which may occur in the precipitator. For each failure pattern, the operating efficiency is predicted. By repeated generation of a statistically significant number of failure patterns and related operating efficiency levels, it is possible to predict (with a high degree of confidence from the distribution of efficiency levels) a minimum efficiency level characteristic of the failure rate.

Figure 4 depicts the predicted collection efficiency of two precipitators with equal areas. Precipitator A is highly sectionalized in direction of gas flow, while B has only three fields in direction of flow. Both have the same number of transformer-rectifier sets (within 10%); each set is connected to about 15,000 ft.^{2} of collection area.

The abscissa represent the relative discharge electrode failure rate. The discharge electrode failure rate is expressed as grounded electrodes per installed electrode month of service relative to a base rate.

Curve A1 shows the relatively stable performance of the more highly sectionalized (in direction of gas flow) precipitator with a minthly maintenance schedule. A3 represents the performance with maintenance performed every three months. B1 shows the performance of the less highly sectionalized unit with a monthly maintenance schedule.

At relatively low failure rates, both units perform equally well. However, under adverse conditions favoring discharge electrode failure, or with extended maintenance frequency, Unit A tends to maintain its efficiency at design level. In fact for this situation, precipitator A will perform as well as B, even at a five-fold increase in failure rate.

The effect of electrical sectionalization on collection efficiency stability for a specific precipitator configuration is shown in Figure 5. The figure shows the benefit of

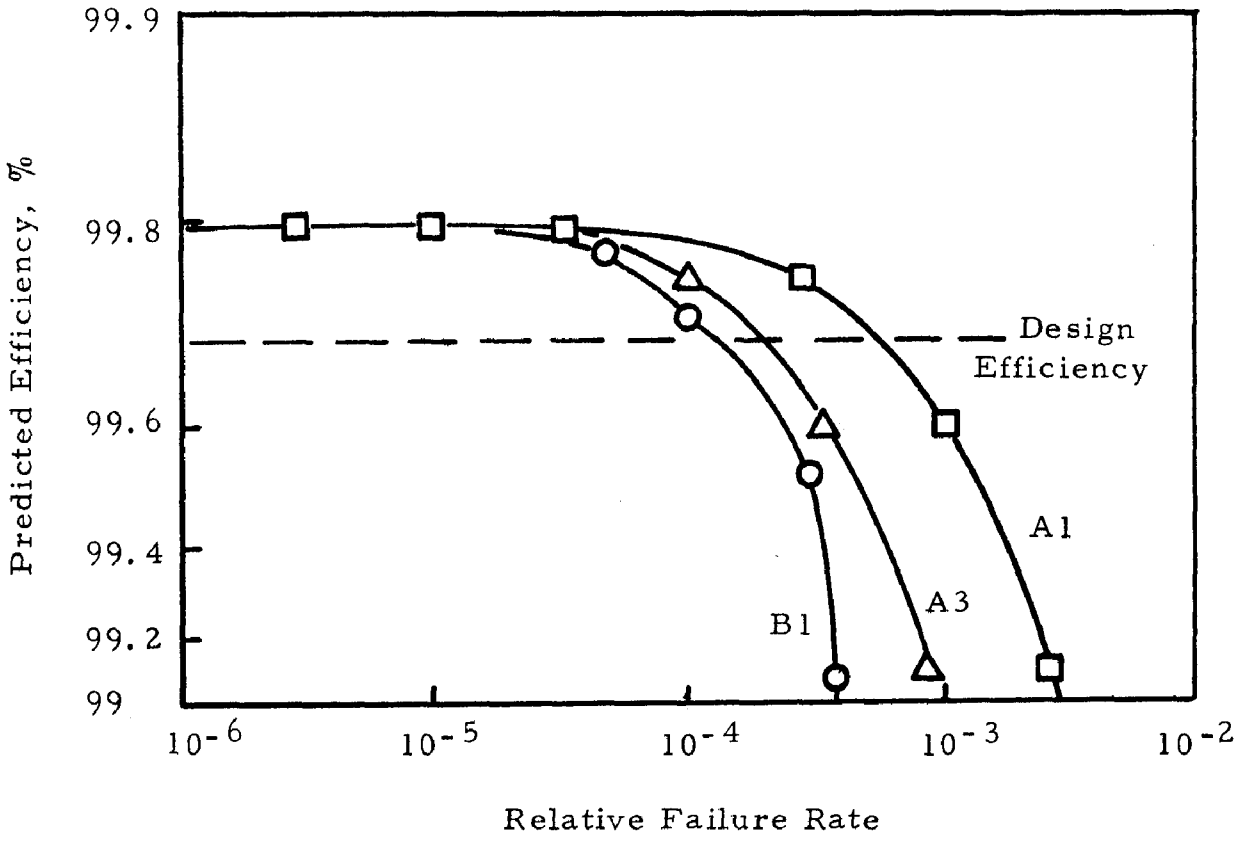

Figure 4. Predicted efficiency level versus precipitator configuration and maintenance policy

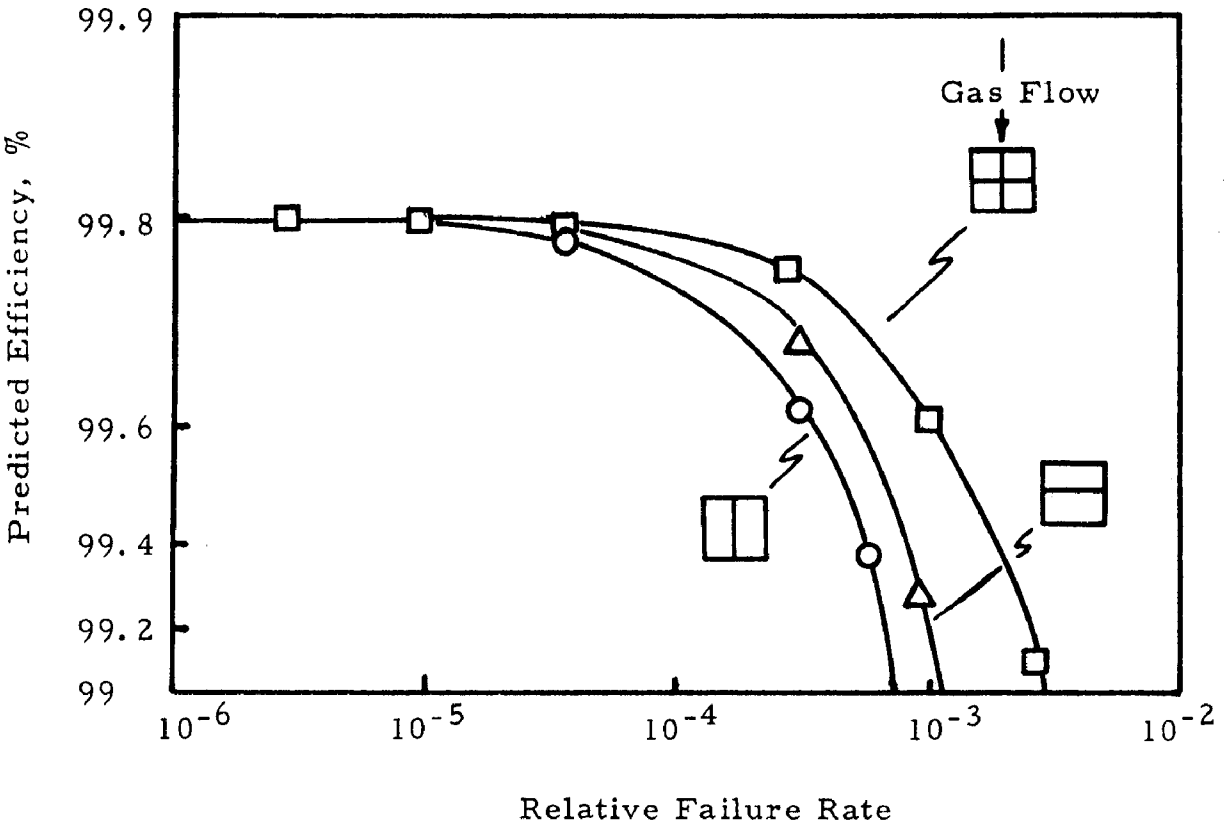

Figure 5. Predicted efficiency for various discharge electrode failure rates and electrical sectionalization

high electrical sectionalization of each mechanical section for maintaining high efficiency level. In particular, the sectionalization scheme which divides a mechanical section in two electrical bus sections in parallel, results in a relatively small number of in-series sections and, consequently, low reliability.

Patterns of predicted operating efficiency are of interest. Figure 6 shows the behavior of two precipitators of equal area performing on the same service. Precipitator C is highly sectionalized electrically, while precipitator D has only three electrical bus sections in the direction of gas flow. Precipitator C is more reliable in two senses: its efficiency level is closer to the 99.85% level at which the unit would operate without grounded sections, and also failure patterns generated produced a predicted efficiency level in a narrow band. On the other hand, precipitator D is less reliable, producing on the average three times the design level emissions. Moreover, on occasion, its poorly designed sectionalization configuration results in emissions as high as 12 times of design. In this particular case, the latter condition would be expected 5% of the time.

GAS FLOW DISTRIBUTION EFFECTS

It is sometimes necessary to design a precipitator system under space and other constraints such that gas flow distribution will be far from ideal. It is well known that non-uniform velocity distribution results in efficiency degradation when comparison is made with the uniform flow distribution case. For the case of plug flow with a distribution of velocities which approximates a normal distribution, the overall collection efficiency level which results in a large multi-duct precipitator may be approximated by:

$$\bar{\eta} = \frac{1}{\sqrt{2\pi}\ (\bar{\sigma}/V)} \int_{o}^{\infty} e^{-\frac{1}{2}[(\Psi-1)/(\sigma/\bar{V})]^2} \left[1-e^{\frac{\ell n(1-\eta_0)}{\Psi}} \right] \Psi d\Psi$$

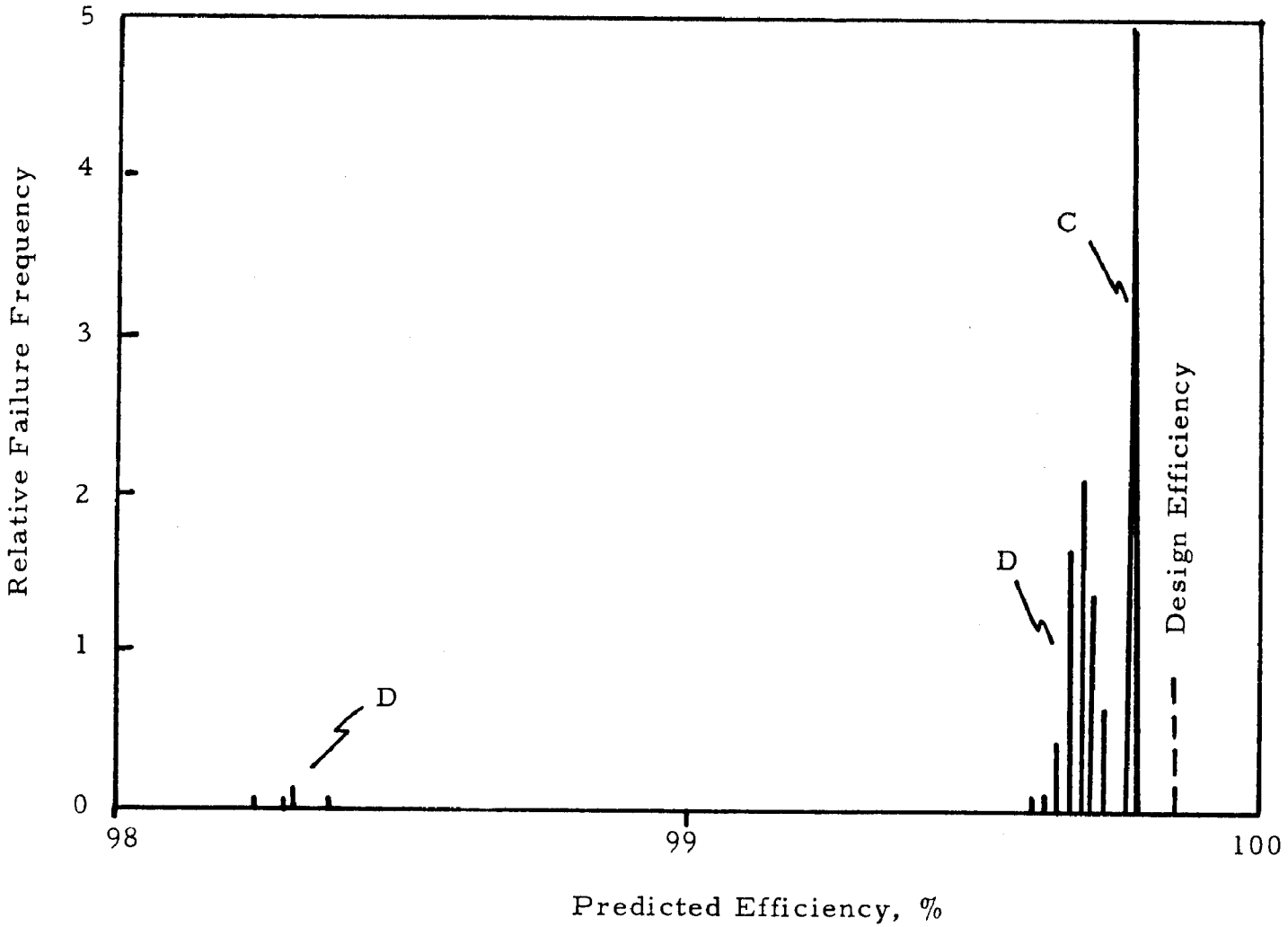

Figure 6. Predicted operating patterns for two precipitators

where $\bar{\eta}$ is the fractional efficiency obtained under non-uniform velocity distribution, characterized by a standard deviation σ and mean velocity $\bar{V}$.

η_0 is the fractional efficiency obtained under uniform velocity distribution conditions.

Ψ is an integration variable, equal to $V/\bar{V}$ where V is the variable duct velocity.

The expression is readily integrable numerically. Figure 7 is a plot of predicted operating efficiency versus $\sigma/\bar{V}$, the rms value. Relatively mild effects are predicted for this mechanism.

In actuality, many skewed velocity distributions have been observed in practice. Bimodal distributions do occur. Treatment in an analogous fashion by use of numerical methods is convenient.

It should be noted that the situation described by equation (2) is a relatively simple one. Much more severe aerodynamic situations which occur in actual precipitators cause massive increases in dust loss.

If conditions favor reentrainment (high conductivity ash, excessive rapping acceleration, etc.) then, of course, the effect of gas maldistribution can be quite severe. Various approaches can be employed. For the erosion situation, Figure 8 shows this calculated effect based on dust loss being proportional to $(V-V_0)^2$, where V_0 is the threshold velocity for reentrainment. It is assumed Deutschian losses are negligible. For the particulate case depicted, the threshold velocity was 90% of the average velocity. The effects shown are pronounced and serve to point out the need for quite strict tolerances on rms values for the reentrainment-controlling situation (note the difference in scale of Figures 7 and 8).

GAS TEMPERATURE DISTRIBUTION EFFECTS

Temperature affects electrostatic precipitator performance; generally, this effect is largely due to resistivity and the resulting changes in electrical energization. The effect is of smaller magnitude for elevated operation than for 250°F to 350°F operation, which depends upon surface conditioning effects largely due to adsorption of H_2O and SO_3 on the ash surface.

Air preheaters provide an outlet temperature which swings over a temperature range of about 65°F-100°F, depending upon rotary speed for the regenerator. The outlet tempera-

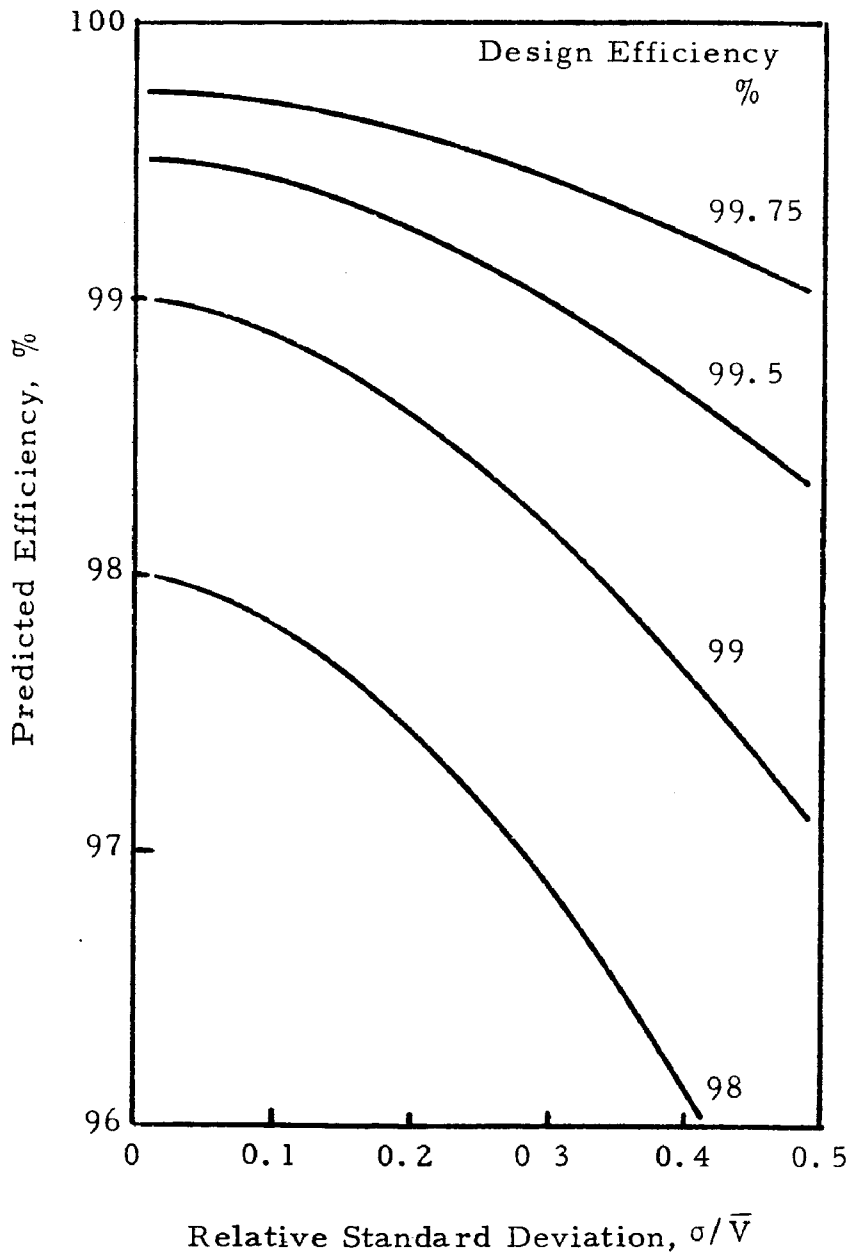

Figure 7. Predicted efficiency versus gas velocity relative standard deviation

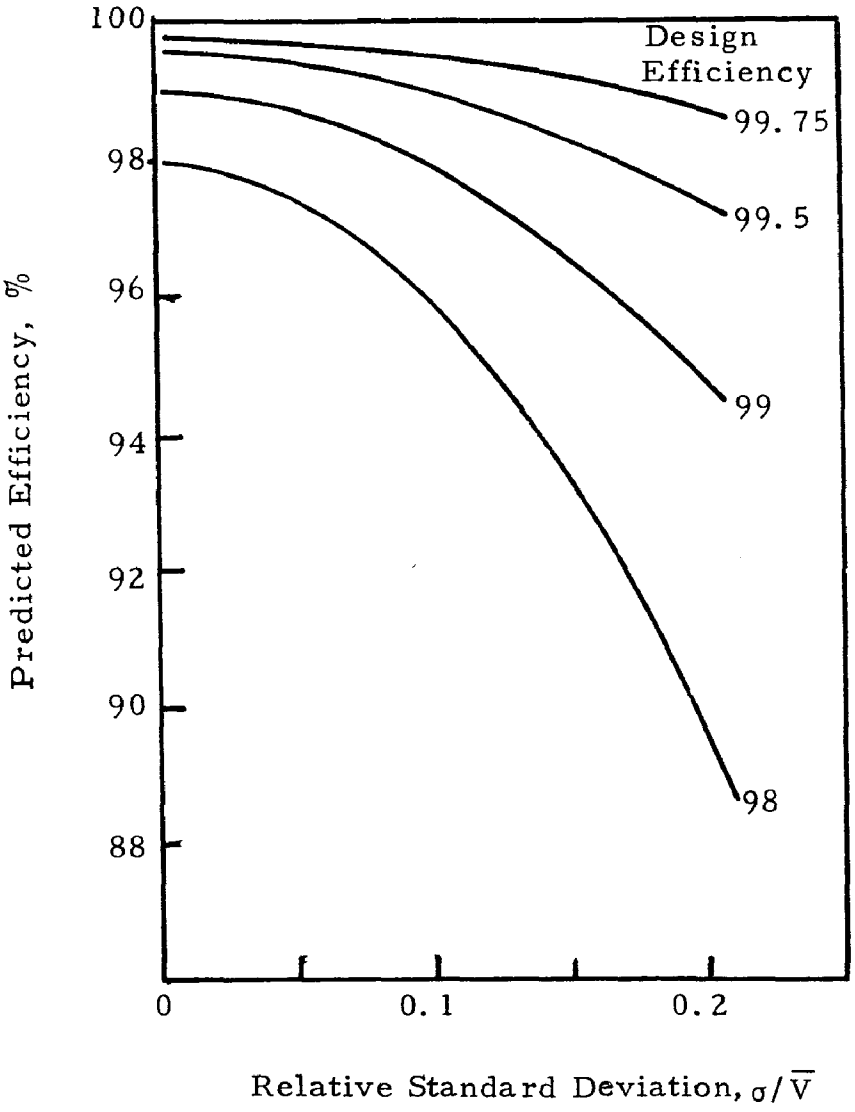

Figure 8. Predicted efficiency versus gas velocity relative standard deviation (erosion case)

ture is predictable, and generally available from the manufacturer of the air heater. It is possible for a given duct configuration to predict the effect of mixing on temperature distribution and, thus, approximate the inlet temperature distribution to the precipitator. Generally, this variation will reflect itself in the need for a larger precipitator than if the gas was uniform in temperature.

Figure 9 is an approximate representation of the extreme (highest and lowest) temperature levels actually measured at the inlet face of the precipitator. In this case, the average temperature was 293°F; the variation, over the inlet flue width, was 65°F, typical of the minimum spread seen at a precipitator inlet.

Figure 10 shows the calculated sizing, specific collecting electrode area required for various sectionalization approaches. For one electrical section in parallel, a sizing of 640 SCA is required. The power is limited severely here and, consequently, collection area operates at low utilization. As an increased number of electrical sections are placed in parallel, each smaller section operates nearer to optimum level, and the total area requirement is reduced. Very little savings result if more than four sections in parallel are used.

The area requirement for the uniform temperature case is somewhat lower than that needed for the highly sectionalized situation. In fact, more than 20% extra area is required with inadequate sectionalization compared to the uniform temperature situation.

CONCLUSIONS

Adequate fuel analysis data are required to design a reliable precipitator system. To attempt to specify a precipitator to treat all possible fuels will result in an excessively large unit. Average and "typical" fuel analyses are insufficient for sizing a precipitator to reliably treat a large proportion of the fuel population. The use of a large number (>30) of individual fuel samples, either for individual sizing or for the estimation of a parent population believed representative of the fuel samples, are more reliable approaches.

In addition to designing a precipitator based on the fuel population, it is important to incorporate in the design sufficient redundancy to permit sustained operation under conditions of electrical section and other failure. This redundancy is readily defined. Distribution effects, such

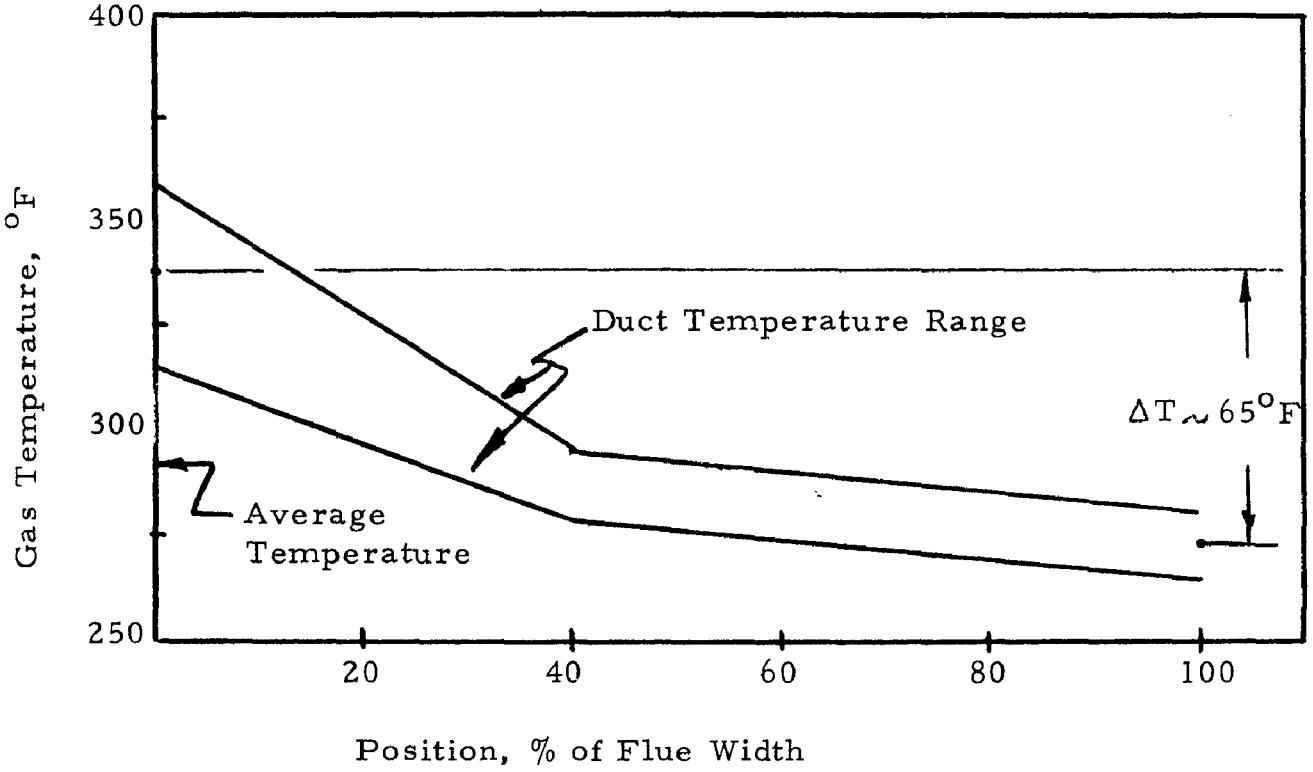

Figure 9. Temperature profile in inlet flue

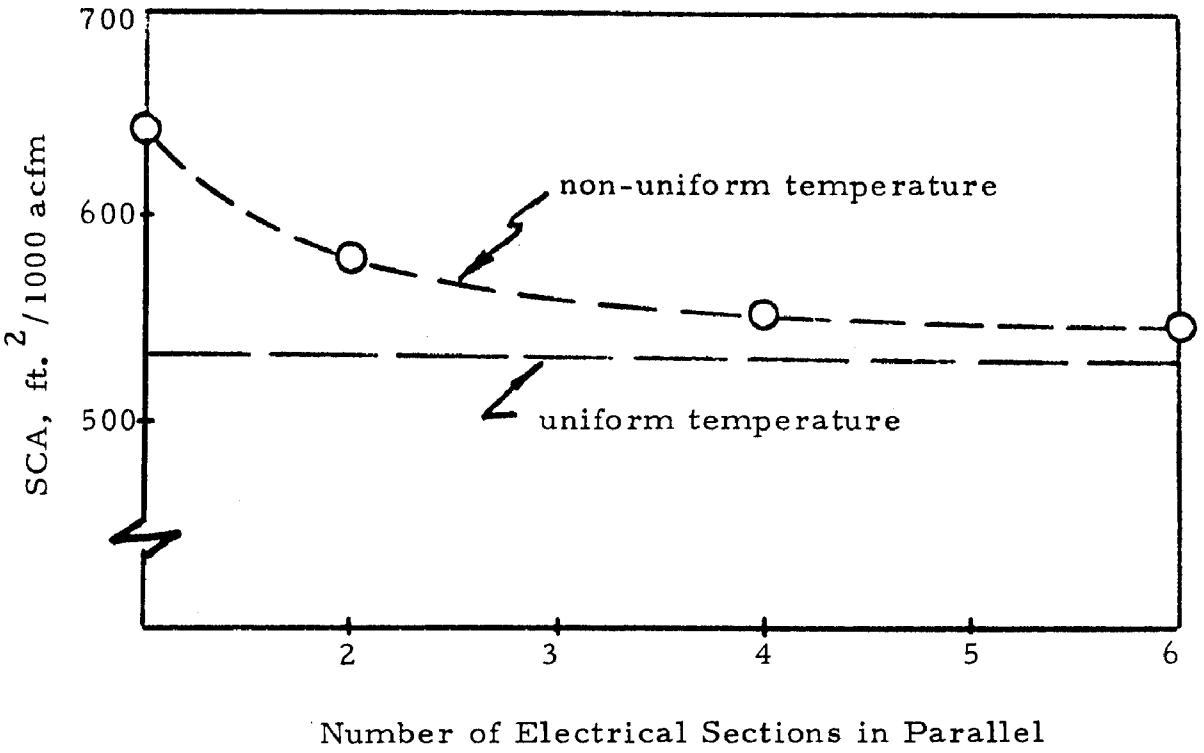

Figure 10. Effect of electrical sectionalization on SCA requirement

as those representing gas velocity, gas temperature, even dust concentration, can be significant in reducing the efficiency of a precipitator designed for high efficiency. Methods for adequately compensating for the effects are known, and should be applied.

REFERENCES

1. Shale, C. C., J. H. Holden, and O. E. Fasching. Electrical Resistivity of Fly Ash at Temperatures to 1500°F. Bureau of Mines, Washington, D. C. Report of Investigations 7041. 1968.

2. Bickelhaupt, R. E. The Influence of Ash Chemistry on the Volume Conduction of Fly Ash. Southern Research Institute. (Presented at Symposium on Control of Fine Particulate Emissions from Industrial Sources, U. S. - U. S. S. R. Working Group, Stationary Source Air Pollution Control Technology. San Francisco. January 15-18, 1974.)

3. Bickelhaupt, R. E. Electrical Volume Conduction in Fly Ash. J. Amer. Pollut. Contr. Assoc. 24:251-255, March 1974.

4. Frisch, N. W., and D. W. Coy. Sizing Electrostatic Precipitators for High Temperature Collection of Fly Ash. Research-Cottrell, Inc. (Presented at University of Colorado Conference on Hot Gas Precipitators. Denver. September 24, 1974.)

5. Walker, A. B. Experience with Hot Electrostatic Precipitators for Fly Ash Collection in Electric Utilities. Research-Cottrell, Inc. (Presented at American Power Conference. Chicago. April 29-May 1, 1974.)

DESIGN AND APPLICATION OF HIGH-VOLTAGE POWER SUPPLIES IN ELECTROSTATIC PRECIPITATION

H. J. Hall
H. J. Hall Associates, Inc.
Princeton, New Jersey

ABSTRACT

Proper electrical energization methods and equipment are the keys to successful electrostatic precipitation. The design, operation and application of conventional high voltage power supplies in this process are reviewed. Emphasis is on requirements and methods of achieving the high performance and reliability necessary in modern air pollution control systems. Typical field data on operations and effects in various precipitator applications, including high resistivity ash, high temperature, and/or high pressure gas treatment, are discussed.

INTRODUCTION

Today, as it was in the beginning, successful electrostatic precipitation depends primarily on proper high voltage energizing methods and equipment. These are the heart and life blood of the process which removes particles from gases by means of electric forces.[1] Fundamentally, a proper precipitator should be viewed as an effective and even an efficient device for generating and maintaining high electric fields in a very large volume of gas which may be flowing at rates up to several million cubic feet per minute. This is done by means of a unipolar corona discharge between suitable electrodes, such as co-planar wires or other small-radii type discharge electrodes centered between parallel plate ducts. The precipitator electrical equipment supplies the corona discharge with its gas ions and its electric fields for charging and collecting the particles suspended in the gas.

Overall design of the precipitator must be directed first to achieving and maintaining the optimum electrical environment so that each square foot of collecting electrode area can do its equal and effective share in continuously and reliably separating particles from the gas stream. In this light, it is easy to see the systems importance of knowing the physical, chemical and electrical properties of the dusts and gases to be treated; of good electrode alignment; of adequate sectionalization; of matching operating voltages and currents and waveforms to the application requirements; of having effective automatic controls and circuit design for electrical stability and reliability with changing loads, including sparking conditions; and of having suitable instrumentation for proper adjustment and trouble-shooting.

In this same bright light of maintaining an optimum electrical environment for high performance and reliability, we can readily appreciate the equally vital importance of these other complementary things: uniform gas and dust distribution at acceptable gas treatment velocities; adequate, controlled, and uniformly distributed rapping intensities to keep electrodes properly clean without excessive dust reentrainment; means and designs to eliminate excessive discharge electrode burning and breakage; preventing whipping discharge electrodes and swinging H. T. frame suspensions; adequate, reliable ash removal systems and instrumentation to prevent hopper over-filling, shorting out H. V. systems, clinker formations, and damage to electrode structures and alignment; high voltage insulator heating and cleanliness; maintaining hot ash for easy removal free of moisture condensation problems; elimination of hopper ash reentrainment; adequate insulation and protection from cold winds; tight gas seals and prevention of air inleakage; eliminating internal corrosion problems; thermal expansion control to prevent electrode misalignments and structure failures; easy access for routine inspections and maintenance; some spare precipitator capacity to maintain reasonable performance in spite of occasional equipment faults, system upsets, or normal variations in process operating factors. Why mention these factors in a paper on power supplies? It is simply because the electrical equipment, regardless of how and by whom it might have been specified and designed, does not operate by itself immune to its surroundings. All of the electrical, mechanical and process factors mentioned do indeed determine the quality of the electrical environment and the performance capability of the precipitator installation.

Thus, the precipitator is a finely balanced system by itself, but it is also a part of an even more complex total process system. The dust collector, as in the past, can no longer be treated as an evil adjunct to a production process; it has to be designed and operated for full, reliable performance as part of an integrated, harmonious whole. Although we can agree on the need for further improvements, new concepts, research and development on better ways of controlling and ensuring the right electrical environment in a precipitator, it is clear that the available tools and techniques relying on sound science and engineering experience must be brought to bear more broadly. On a cost-benefit basis, it pays to strive for excellence in electrical energization--where it counts. Remember that the collection efficiency increases exponentially as the product of the particle charging and the particle collecting electric field strengths. Failure to appreciate this fact and to pay attention to the primary purpose of ensuring the right electrical and gas flow environment has doomed many a competitively priced precipitator to abysmal failure and a costly field fix--not uncommonly even more than the cost of the original box.

Worldwide, there are probably 10,000 or more electrostatic precipitators in operation. Within the last ten years, about 10,000 electrical sets must have been built in the United States alone. In recent years, new capacity in large fly ash precipitators, by far the largest single application, has been added at the rate of several tens of millions of cubic feet per minute per year for collection efficiencies 99-99.8%. Thus, at this very moment there are a lot of electrical sets doing bad things: sets sparking uncontrollably with automatic controls not working or improperly designed; sets wishing they had the company of others for meeting required performance; sets with voltages and currents too low due to poor sectionalization or mismatching to load; corona currents maldistributed; wires misaligned, spark burning and breaking; sets out of service; sets with gross instabilities; sets making clinkers in full hoppers; sets struggling to get adequate corona current through dust layers that are too thick on discharge and collecting electrodes; sets sadly watching dust once collected being reentrained and lost; sets seeing dust in gases sneaking by and escaping the good electric fields. In addition, designers and specifiers, some of whom have never seen a precipitator and do not know what a real headache and cost item a real "trouble job" can be, are getting together to exercise empirical magic, or to inject a computer program with an arbitrary, if any, electrical input, or sometimes even with wrong data.

Out will come the numbers, and then it will be 2 to 3 years before the day of truth comes and they find out whether they guessed right or wrong. If it's wrong, then it will be somebody else's problem to fix it up; and how many more precipitators will have been specified in the same way before the tests are in on the first one?

Let us now consider some of the design, operating and application factors for high voltage electrical equipment in electrostatic precipitators.

HIGH VOLTAGE ELECTRICAL EQUIPMENT

BASIC SYSTEM AND ELEMENTS

Figure 1 shows the schematic diagram and basic circuit elements of conventional rectifier sets for electrostatic precipitators. The basic elements comprise a voltage control device or system, either manual or automatic; a series impedance which, in combination with the transformer impedance, is required to provide circuit stability under precipitator sparking conditions and to control voltage and current waveforms in the case of the linear reactor; a high voltage, step-up transformer of special design; and a high voltage, bridge rectifier circuit. In addition, appropriate overload and transient protection, instrumentation, and circuit breakers are used. For automatic control, networks from signal sensing circuits feeding closed-loop type control systems are employed. All automatic systems are equipped with a manual control switch for testing and troubleshooting. Input is typically from a 460 V ±5%, 1 Ph, 60 Hz line. Output voltages are typically rated 70-105 kilovolts peak (kV_p), 45-67 kV dc, negative polarity. Either two half-wave (HW) outputs, or a single full-wave (FW) output to the precipitator sections, are used with concentric pipe and guard conductors between power supply and the precipitator. Just about all industrial precipitators operate within the range 30-105 kV_p, with 40-70 kV_p being the most common.

HISTORICAL DEVELOPMENT

Historical trends in usage of the various element components are indicated in Figure 1. General periods of development in the USA may be noted as follows:[1,2,3]

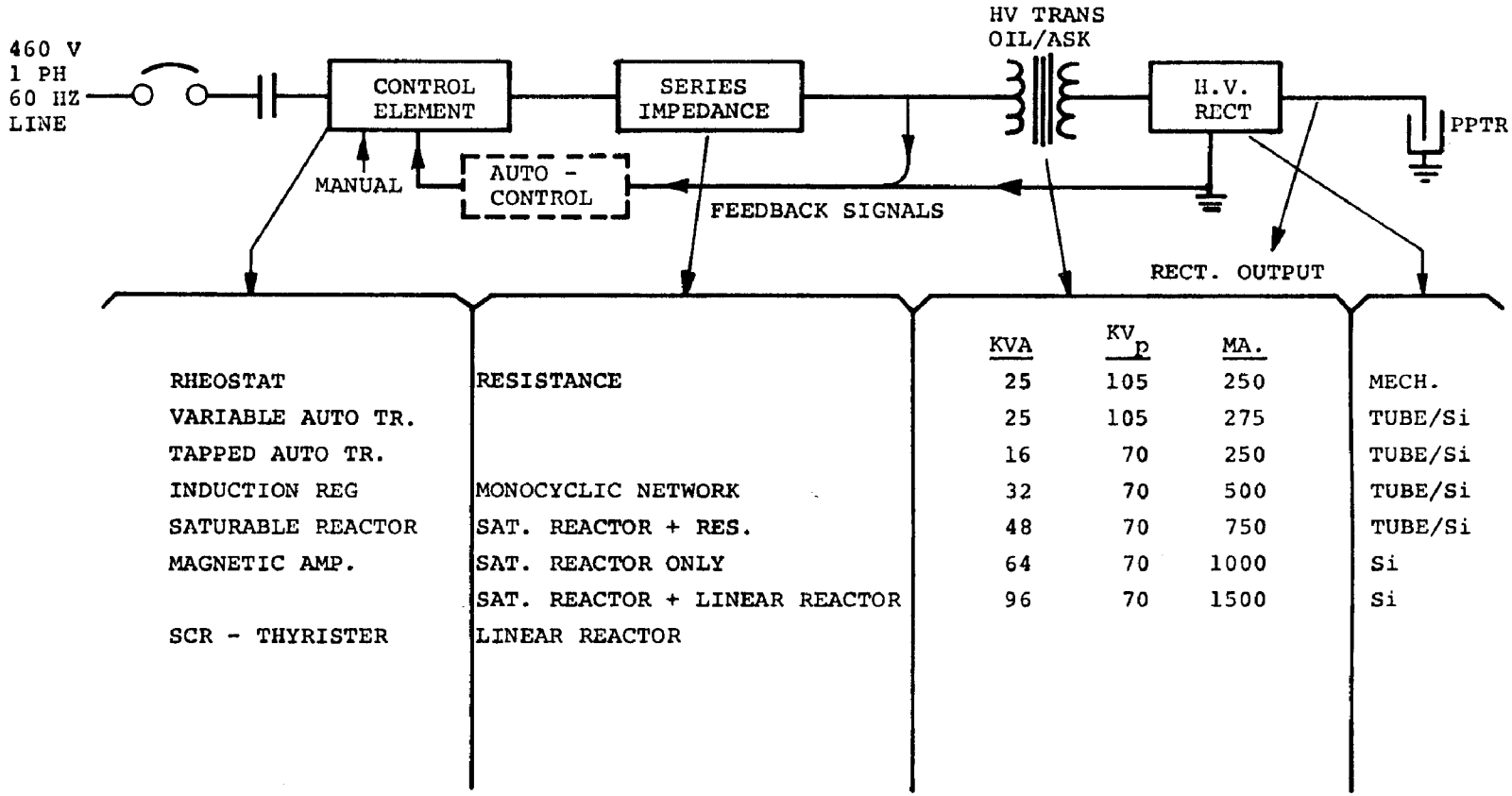

		KVA	KV_p	MA.	
RHEOSTAT	RESISTANCE	25	105	250	MECH.
VARIABLE AUTO TR.		25	105	275	TUBE/Si
TAPPED AUTO TR.		16	70	250	TUBE/Si
INDUCTION REG	MONOCYCLIC NETWORK	32	70	500	TUBE/Si
SATURABLE REACTOR	SAT. REACTOR + RES.	48	70	750	TUBE/Si
MAGNETIC AMP.	SAT. REACTOR ONLY	64	70	1000	Si
	SAT. REACTOR + LINEAR REACTOR	96	70	1500	Si
SCR - THYRISTER	LINEAR REACTOR				

Figure 1. Schematic diagram showing elements of precipitator rectifier sets and their historical usage

Modern sets use SCR control with linear reactor; silicon diode HV rect; output ratings 70-105kV_p, 250-1500 + mA dc; automatic control.

1906-1950 Precipitation as a batch process, empirical design, and large growth of many different, major industrial applications, moderate efficiencies required 90-95%. Mechanical rectifiers, generally with simple rheostat manual control; low power 250 mA dc sets, either double HW (beginning in 1932), or single FW electrical output, generally small size individual sections (4-10,000 ft^2 collecting area per set).

1950-1960 Precipitation becomes a continuous process with the introduction of continuous, intensity controlled rapping in 1948. Major use of vacuum tube HV rectifiers;[4] increasing use of automatic voltage control based on an optimum average precipitator sparking rate, first introduced in 1949,[5] and commercially adapted a few years later to saturable reactor or magnetic amplifier type controls;[6] growth of high power rectifier sets to 1000-1500 mA dc sizes and use of very large sections energized by individual sets. Increasing emphasis on research and development, foundations of instrumentation techniques and sound scientific methods of design and analysis. The first HV silicon diode rectifier set was designed in 1955-56 and its application was reported by Willison[7] in 1958.

1960-1970 Background to modern age of precipitation with introduction of computer techniques and the commercial use of the modern, solid state, SCR type automatic voltage control system with linear reactor in 1965;[8,9] universal use of silicon diode HV rectifiers; application of linear reactors to the stabilization of certain unreliable saturable reactor control systems (1963); high temperature/high pressure applicability of precipitation established[8,10,11] at least to ranges 800-930°C or at gas pressures 800-900 psia; use of high pressure cleaned process gas as dielectric medium for HV transformer design to eliminate high pressure feed through bushings;[8] development of more sophisticated automatic voltage control techniques using fast computer-type logic circuitry and printed circuit boards capable of stable rectifier set operation at threshold or very low sparking rates over a wide range of loads; introduction to USA market of the "European" type

precipitator design with stiff frame discharge electrodes, wider ducts, individual plate rapping, 4 point HV frame suspension, conservative sizing and rugged construction.

1970- Modern age of electrostatic precipitation with new and more critical requirements in electrical energization and overall performance to meet strict regulations and more severe standards of excellence by new market influences.

APPLICATION TRENDS

Developments and trends in the electrical energization of precipitators were reviewed in a recent paper.[2] Of special interest for modern applications are the following factors:

1. High performance and high reliability are of primary importance. Collection efficiencies in the 99.0-99.8% range must be continuously maintained—even with a few sections out of service. Air Pollution Control regulations are stringent and enforced.

2. Large gas volume flow rates and large size precipitators.

   a. Specific collecting surface areas 350-900+ ft^2/1000 acfm; two to five or more million actual cubic feet of gas per minute (acfm) treated.

   b. Collecting plate heights 9.15-11.0 meters (30-36 ft) in USA type designs; 12-15 meters (40-50 ft) in typical European type designs. It is a long way down to the hoppers.

   c. Average gas treatment velocities approximately 1-1.7 meters/sec (3-5.5 ft/sec).

3. Use of very large size individual sections—unfortunate in some cases; correspondingly large electric energy storage with serious transient disturbances, high peak currents on sparking, easy wire burning, difficult alignment problems, hard to maintain ideal electrical environment.

4. Increasing use of larger size individual rectifier sets 100-130 kVA (1500-2000 mA dc) operating from single phase, alternating current source. The

larger the set, the lower its internal impedance and the more critical become problems of circuit stability, arc suppression and automatic control--particularly when operated on sparking loads at less than about 50% rated capacity.

5. Growth of high resistivity ash problems with increasing use of low sulfur coals and Western coals with high CaO, possible low Na_2O contents. Great variability in fuel sources and properties is common today. Low temperature 150-180°C precipitators are current density limited. Careful overall designs are required to effectively use the highest possible current densities, uniformly distributed. This is especially important where large inlet cross-sections are involved with gas temperature variations ±50°F from average value. Increasing use of hot precipitators (350-450°C gases) to avoid ash resistivity problems require an entirely different approach to electrical equipment specifications.

6. Superiority and universal use of solid-state silicon HV rectifiers and solid state, SCR type automatic control systems in electrical equipment. The old saturable reactor type controls are now obsolete.

7. Growing emphasis on high performance for very fine particles <3 micrometer in size, including submicron particles. Precipitators can cope, but more work must be done; this means higher power densities and a closer approach to an ideal electrical environment, or else larger size equipment.

8. Increasing activity in development of coal gasification processes involving fine particle removal from hot, high pressure gases (800+ °C, 100-300 psia).

9. Significant influence of "European" type precipitator designs in the USA market. The wider ducts operate at higher voltages and lower currents than do standard USA 23 cm (9 in.) ducts. In high ash resistivity cases, the lower currents, if properly distributed, are more nearly matched to operating requirements limited by the current density.

10. Upgrading and modernization of older precipitator installations to meet more stringent regulations has been a big factor since about 1968-70. Addition

of new sets with greater sectionalization to increase corona power capability and replacement of older, manual control sets by modern equipment has provided substantial improvements in precipitator performance--particularly with the synergistic effects available with concomitant improvements in gas flow distributions, rapping and the use of shrouded discharge wire electrodes.

MODERN SYSTEM REQUIREMENTS AND OPERATION

General

Table 1 summarizes salient design and operating requirements for modern high voltage electrical equipment of the conventional type.

Figure 2 shows the schematic circuit diagram of a modern HV rectifier set with SCR (Silicon-Controlled-Rectifier) type automatic control. The combination with linear reactor provides good stability on either FW or HW operation and at high power. Sophisticated solid-state, automatic, voltage and current-limit control, with multiple signal feedback loops can provide good regulation and fast response to transient disturbances.

The use of a properly sized linear reactor yields good current-waveform control so that full, rated dc output current can be made available. Peak current during sparking is also limited to achieve stability and to prevent excessive discharge wire burning and breakage. Proper design also eliminates spark bursting and excessive arcing tendencies.

Automatic voltage control is typically based on maintaining an optimum, average precipitator sparking rate which must be adjustable according to application and dust concentration--usually in the range 5 or 10 to about 75 sparks per minute--proceeding from outlet to inlet sections. Excessive sparking in outlet sections must be avoided, for the gains obtained by increasing voltage can be rapidly offset by dust losses due to voltage offtime and from spark blasting and reentrainment of dust on the plates. Other effective methods of automatic control may be based, for example, on maintaining essentially a controlled sparking-threshold level where voltage is regulated in small increments with adjustable ramp recovery close to desired operating level.

Table 1. DESIGN AND OPERATING REQUIREMENTS FOR MODERN HV ELECTRICAL EQUIPMENT IN ELECTROSTATIC PRECIPITATION

Item	Specification
1. Of first importance	High reliability & stability under transient sparking conditions and occasional short-circuit load.
2. Precipitator operating voltage, kV_p	30-100+ (40-65 kV_p most common)
3. Precipitator current density, mA/1000 ft^2	10-100+
4. Precipitator voltage waveform	Pulsating, negative polarity full wave or double half-wave
5. Precipitator load	Capacitive - 0.02 to 0.125 μFD/section
6. Line input	460/480 V, 1 Ph, 60 Hz most common variation ±5% line voltage
7. Rectifier circuit, standard sets	Single phase, FW bridge, silicon diodes
8. Rated output voltage, R load	70 kV peak, 45 kV dc average - most common, 105 kV peak, 67.5 kV dc average
9. HV transformer	400 V/53 kV rms or 400 V/78 kV rms
10. Individual set capacity, kVA	15 to 100
11. Rated dc output current, mA	250 to 1500+ per set (R load)
12. Transformer-rectifier insulation	Oil/askarel convection cooling
13. Duty	Continuous - outdoor or indoor installation
14. Ambient temperature	50°C max for TR oil-filled tank 55°C max for control cabinet
15. Voltage control	Automatic control essential based either on optimum avg sparking rate (adjustable), or nominally at spark threshold
16. Voltage control range	Essentially zero to 100% rated output. Modern systems use SCR type control with linear reactor in HV transformer primary
17. Current limit - no sparking	Automatic limit at rated primary current. Full rated current availability independent of voltage
18. Peak current limit during sparking	2 to 2.5 times normal peak current in the best systems

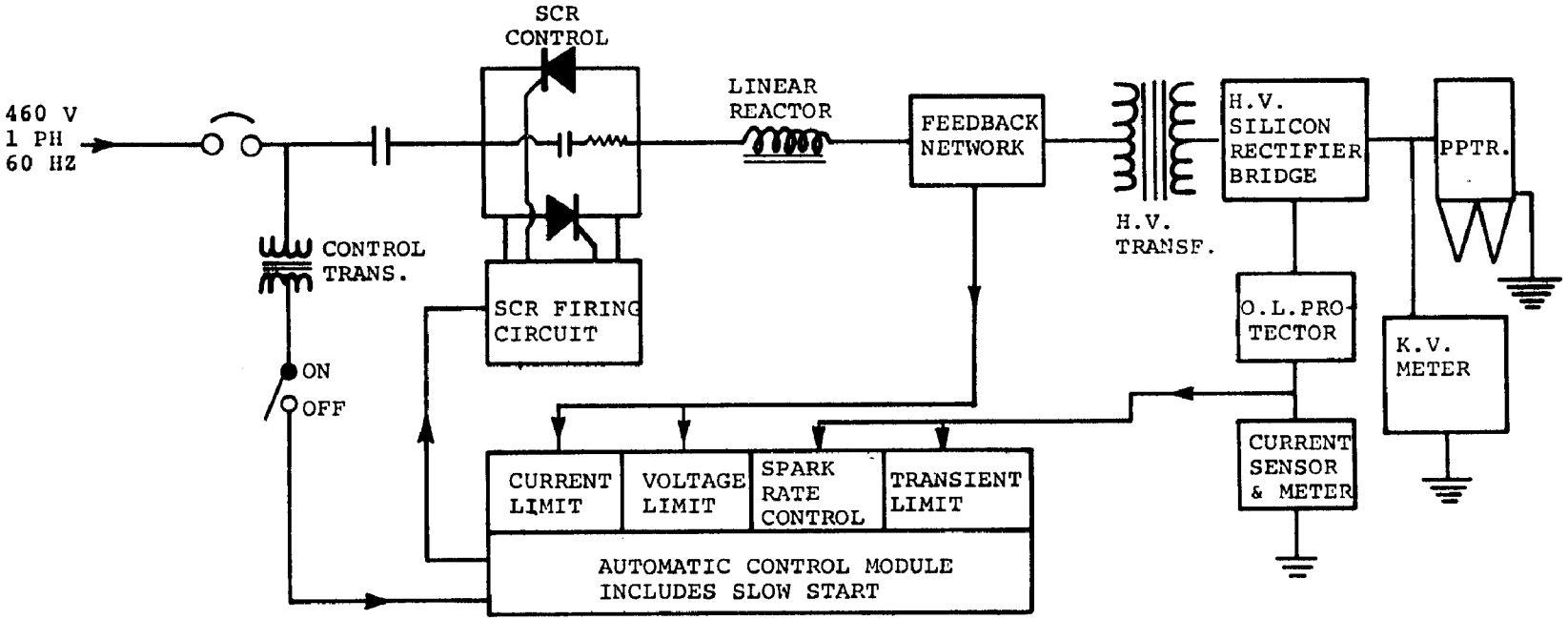

Figure 2. Schematic diagram - modern HV rectifier set with SCR type automatic control for electrostatic precipitators

Availability

There are about a dozen major suppliers of industrial electrostatic precipitators in the United States, and half of them supply the so-called European type design based on technology from England, Sweden, Germany, or Switzerland. The dozen are well known and include American Air Filter Co., Babcock and Wilcox, Belco Pollution Control Corp., Buell Division of Envirotech, Koppers Co., Lodge-Cottrell, Inc., Peabody Holmes, Pollution Control Walther, Precipitair Pollution Control, Research-Cottrell, Inc., Universal Oil Products (Air Correction Division), and Wheelabrator-Frye.

The sources of high voltage electrical equipment for precipitators are more limited. To the best of my knowledge, there are the following categories:

1. In-house — all electrical equipment designed and made by precipitator supplier. These include Research-Cottrell, Inc. and Pollution Control Walther (via Helena Corp.). Buell is also essentially in this category--buys only HV transformer core and coil.

2. Hybrid — Purchase of HV transformer (usually General Electric or Westinghouse) to specification and supplies control unit to own design made either in-house or at a separate local company.

3. Industrial — HV transformer and controls made by General Electric or Westinghouse.

4. Commercial — Several suppliers of ordinary high voltage power supplies for testing, calm loads, etc. offer equipment for precipitation. They often lack the sophisticated knowledge so necessary for performance and reliability in this difficult service. Attempts to save money this way usually backfire at very high cost.

Specifications, photos and data are thus generally available. Typical oil filled transformers weigh 2400 lbs at 16 kVA to about 4000 lbs at 100 kVA. Askarel non-flammable fluids increase weight about 1000 lbs. Modern control cabinets are typically about 1000 lbs or less, front access.

Electrical equipment must be good. Forsaking all others, use only the highest quality materials and workmanship in sound designs by experienced people knowledgeable in the special requirements and vagaries of electrostatic precipitators.

Voltage and Current Waveforms

Figure 3 illustrates typical precipitator voltage and current waveforms. Saturable reactor type control systems usually have somewhat peaked current waveforms with fractional current conduction periods from about 0.35 to 0.70 depending upon design and operating level. In the larger sizes, maximum value of about 0.55 is common unless care is taken in matching load to reactor size. Available maximum dc corona current on precipitator load may be typically 80-85% of nominal rated values based on a resistance load.

Current waveforms with modern SCR-linear reactor systems are capable of control to suit the particular conditions. Fractional conduction of about 0.86, with normal HV transformer design, yields full rated average currents on a precipitator load. Maximum rectifier set utilization is achieved with full range voltage control and a high degree of stability.

Voltage waveforms are illustrated for FW, HW, and pulse energization without sparking. With sparking, the precipitator voltage falls to zero, usually near the peak voltage, and with a good system design, the voltage will recover normally ½ to 1 cycle of the supply line.

Figure 4 shows typical load current ratios as a function of current conduction in the SCR type control. Figure 5 illustrates current conduction as a function of load—100% rated load corresponds to rated primary rms current and rated dc load current.

Like most power equipment, power supplies for precipitators work best at 70% or more of their rated capacity.

Comparison Between Saturable Reactor and SCR Type Controls

Table 2 summarizes some comparisons between the saturable reactor and the SCR-linear reactor type automatic controls for precipitators. Some saturable reactor systems in smaller sizes (up to ∿40 kVA) do have good response, particularly with relatively high forcing resistance in the dc control circuit, and frequently with some additional series resistance in the transformer primary circuit for improved stabilization.

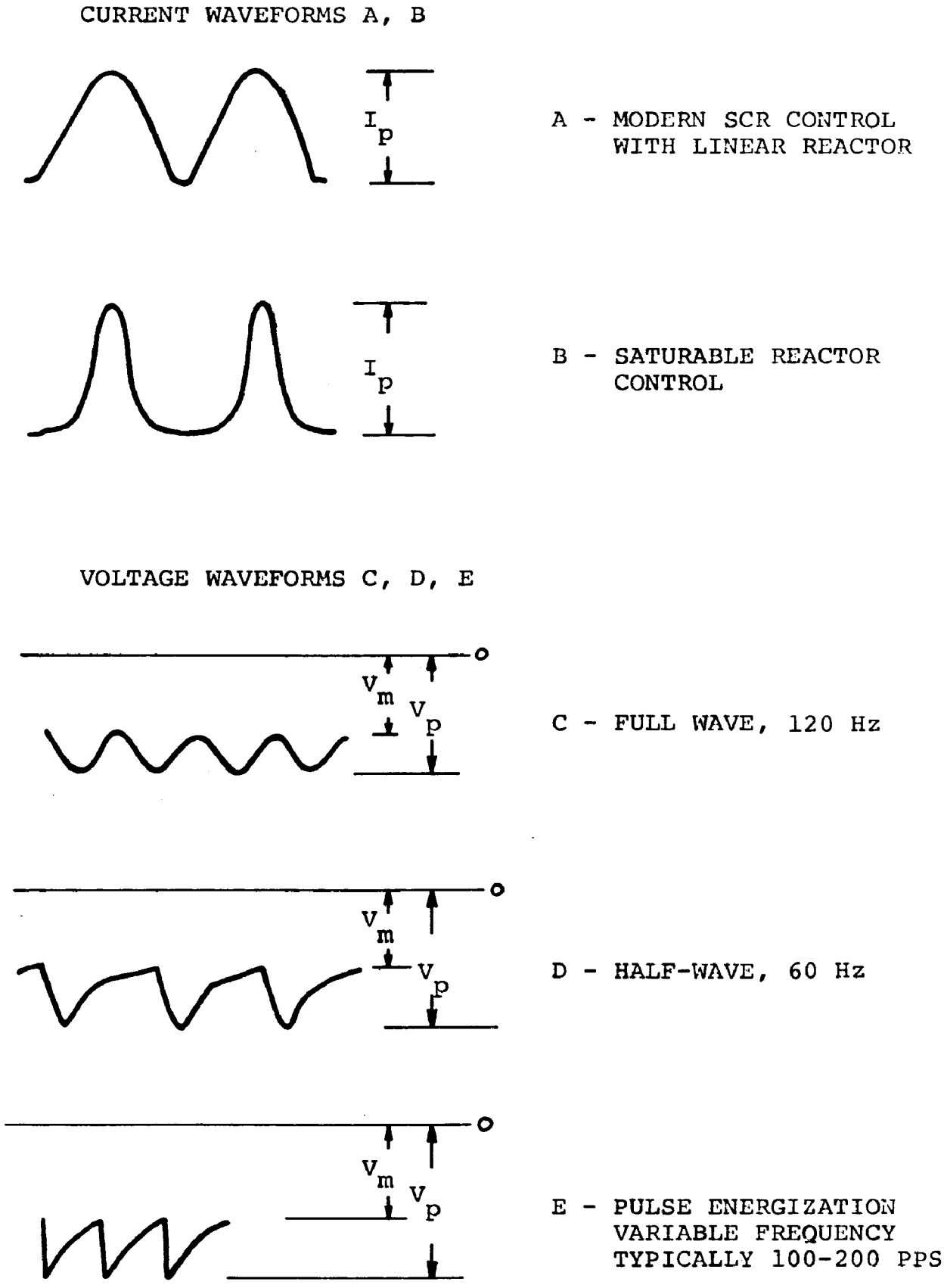

Figure 3. Typical precipitator current and voltage waveforms

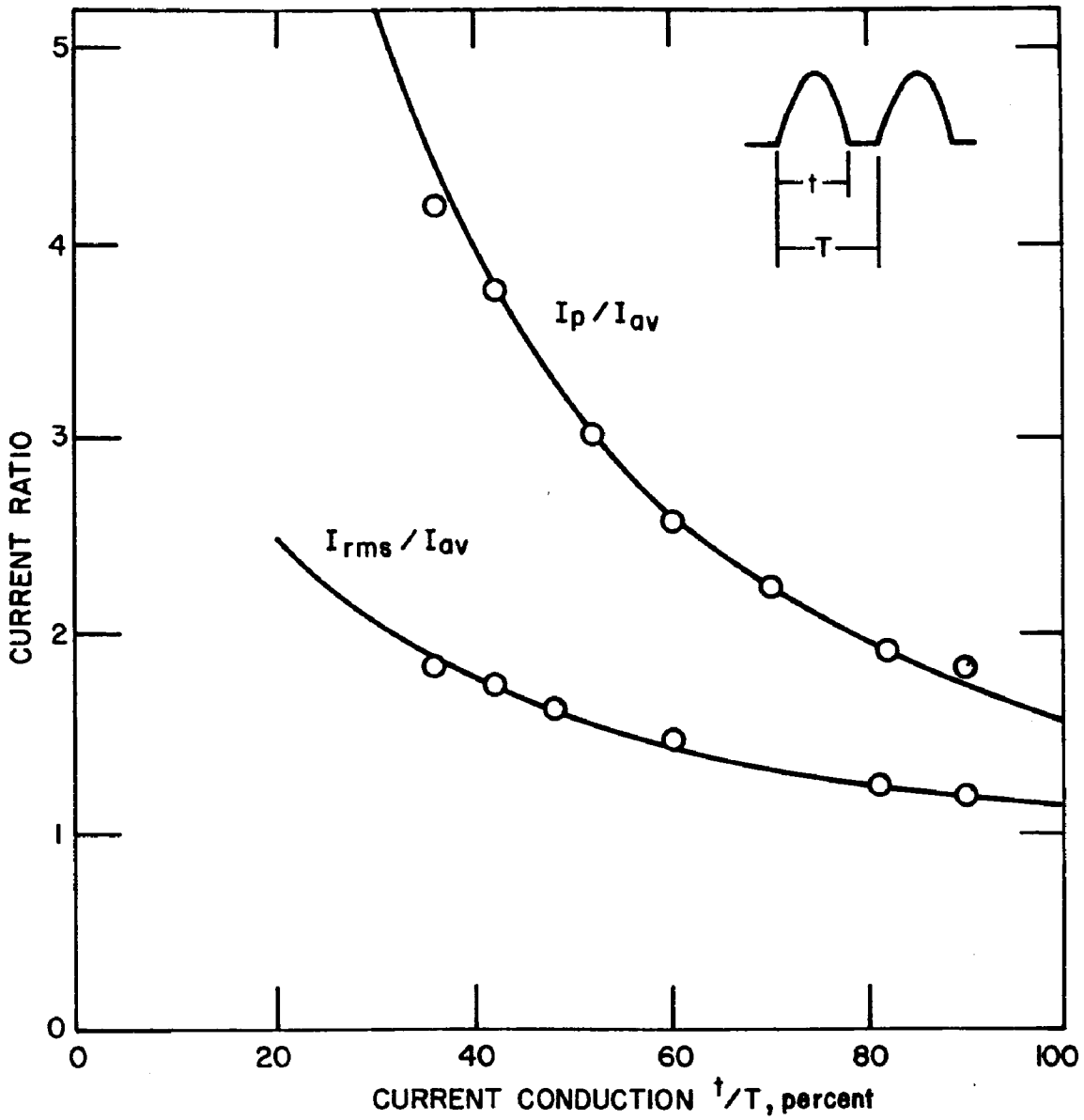

Figure 4. Typical load current ratios as a function of current conduction period for SCR type, automatic control system for electrostatic precipitators

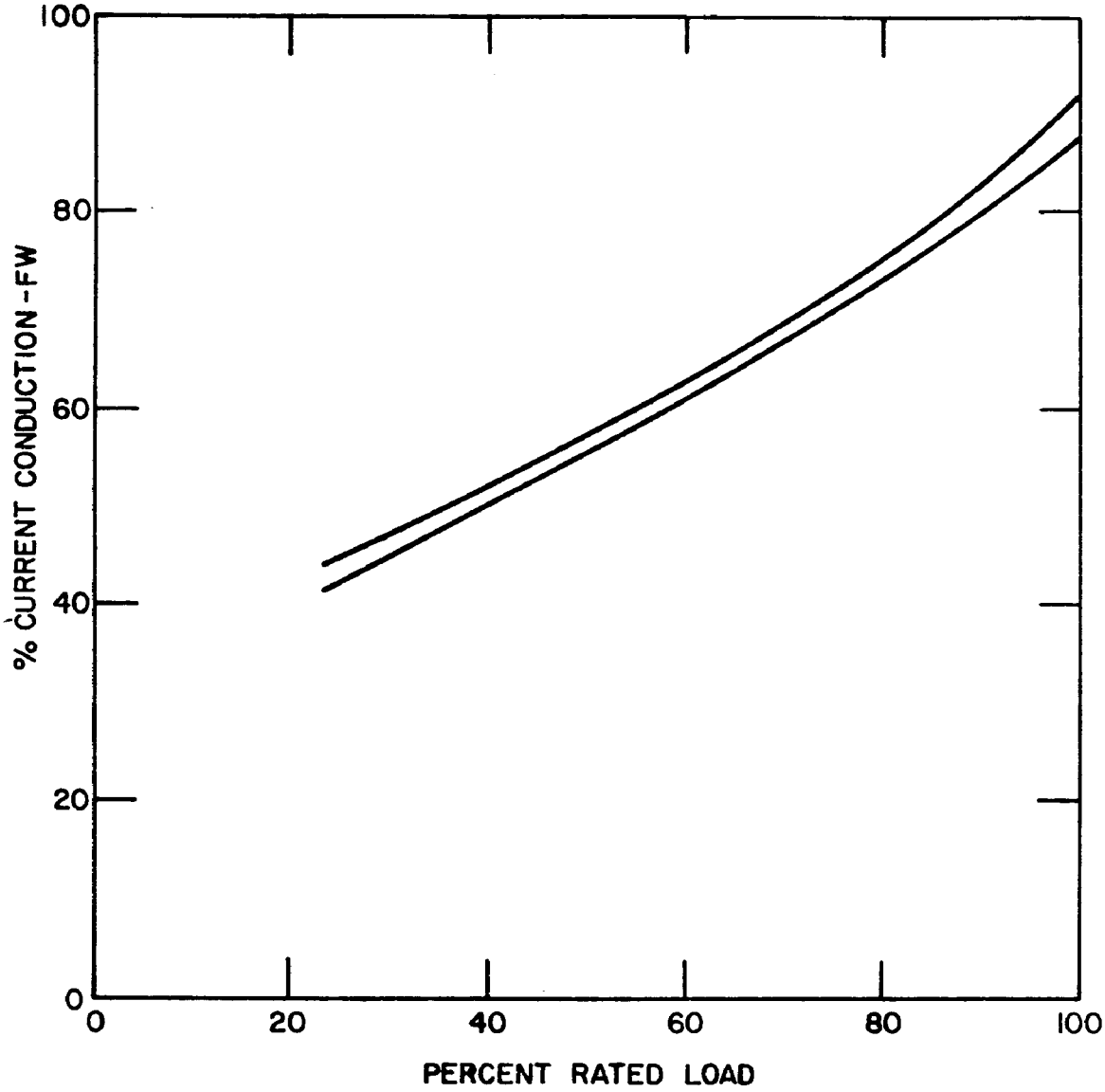

Figure 5. Typical load current fractional conduction as a function of load level—SCR type control system

Table 2. SOME COMPARISONS BETWEEN SATURABLE REACTOR AND SCR TYPE AUTOMATIC CONTROL SYSTEMS FOR ELECTROSTATIC PRECIPITATORS

Item	Standard 3 leg-core saturable reactor	SCR
1. Control range voltage and current	Typically 50-100% rating, max	0-100% rated output
2. Transient response		
a. Recovery, normal sparking	up to 30 cycles or more of supply line	<1 cycle
b. Recovery, arcing or bursting	may be several sec up to 30 sec	<0.15 sec
3. Operation on HW	poor, especially in high power sets	good, independent of power level
4. Spark suppression and recovery to eliminate bursting	poor	excellent
5. Direct current available, % rated	∿75-85	100
6. Heat loss, relative	1.0	0.25 or less
7. Overall efficiency system	poor to fair	good to excellent
8. Relative size of control	1.0	0.6
9. Relative weight, control system	1.0	∿0.5 or less
10. Field wiring	extra for separately mounted reactor	all equipment in single cabinet of uniform size

OPERATING FACTORS AND PROBLEMS

VOLTAGE-CURRENT CHARACTERISTICS

The corona voltage-current characteristics for electrostatic precipitators are controlled basically by the gas and dust load, by the electrode geometry and alignment and by the size of the individual section energized. The most important properties of the gas are density and chemical composition. The density factors are molecular weight and, importantly, temperature and pressure. Among the critical factors in chemical composition are the presence or absence of strongly electronegative gases such as SO_2 and SO_3, halogen compounds, etc., and the amount of water vapor. Some amount of normal electronegative gases, typically such as O_2, CO_2, CO, H_2O, must be present in order to produce negative gas ions. Water vapor increases the dielectric strength and usually raises operating voltages. The dust influences operating characteristics according to its resistivity, particle size and concentration. Medium to high concentrations of very fine particles, for example, can quench corona through space charge effects. Acid mist precipitators are notorious for strong current quenching; we note similar effects with fly ash or other precipitators where inlet sections operate at relatively high voltage and low currents, whereas outlet sections, with cleaner gas, operate with lower voltages at greatly increased currents. Sometimes current is exhausted, or limited by rectifier set rating long before sparking potential can be reached.

Figure 6 illustrates some general characteristics. It is interesting to note that over a very wide range of gas temperatures and pressures and for different applications, precipitator practical operating voltages are conveniently in the range 15-80 kV_{av} at average corona current densities from about 10 to 300 $mA/1000\ ft^2$ collecting area. Somewhat above corona starting voltages, the current density typically increases as the 3 to 4.5 power of the voltage (commonly 3.5 to 4th power). These and other factors lead to the following conclusions:

1. Power supply designs required are within easy practical levels of voltage and current.

2. It is most important that the electrical equipment ratings be properly matched to load requirements. Note that high temperature (low gas density) requires high current and power densities at modest voltages.

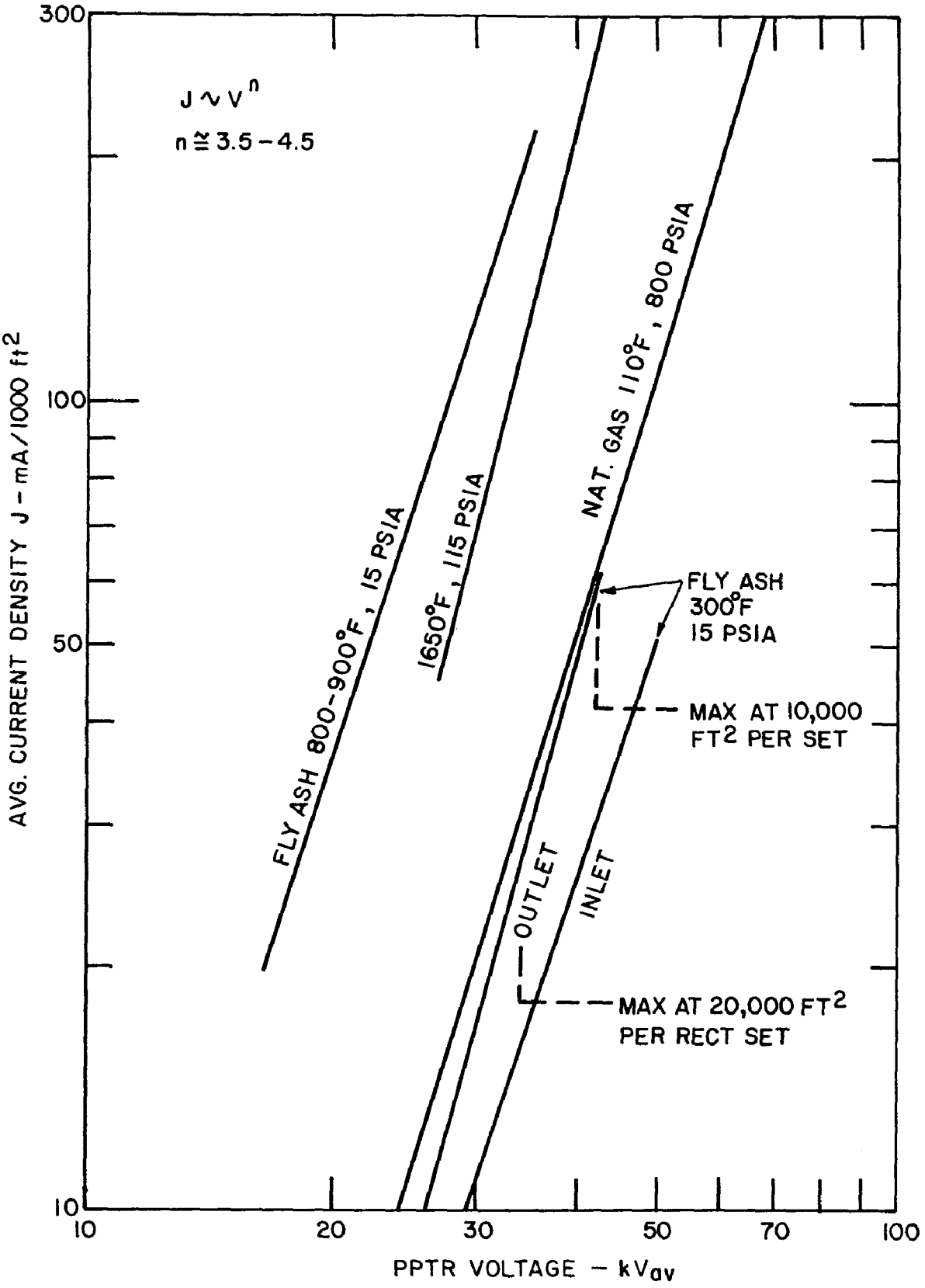

Figure 6. Typical precipitator voltage-current density characteristics over a wide range of gas temperatures, gas pressures and applications

3. Since current increases rapidly with voltage, automatic control is essential and incremental adjustments must be relatively small, <1% of the operating level. It turns out that sparking rates also increase very rapidly with voltage[5] and the larger the area/set, the faster the increase. Hence, to maintain proper stability in automatic control systems, very close control of the voltage is necessary if anything approaching optimum electrical environment is to be achieved.

4. Since the collecting electric field strength varies about as the square root of the current density, it is useful to view an electrostatic precipitator as a current dominated device. It turns out that the effective precipitation rate parameter, $\underline{w}$, can increase about as the 0.75 power of the current density if we assume that the particle charging electric field varies at least as the average field (V/S) where V is the average operating voltage and S is the interelectrode spacing. Figure 7 illustrates a calculation for typical, high performance fly ash precipitators. The results are generally supported by field experience. Low values of J (7-20 mA/1000 ft^2) are typical of high resistivity ash cases. Note that to get precipitation rates of 8-10 cm/sec at 725°F requires high current densities 70-90 mA/1000 ft^2, again in agreement with experience.

5. In precipitator operation, a premium in performance is available for uniform current distribution at highest possible levels, continuously maintained; hence, our concern with all the factors mentioned in the Introduction to this paper.

Figure 8 illustrates typical voltage-current characteristics on a five-field fly-ash precipitator without ash resistivity problems. This again points up the importance of matching electrical equipment to load requirements.

SOME OPERATING AND APPLICATION PROBLEMS

The following paragraphs summarize some common operating and application problems.

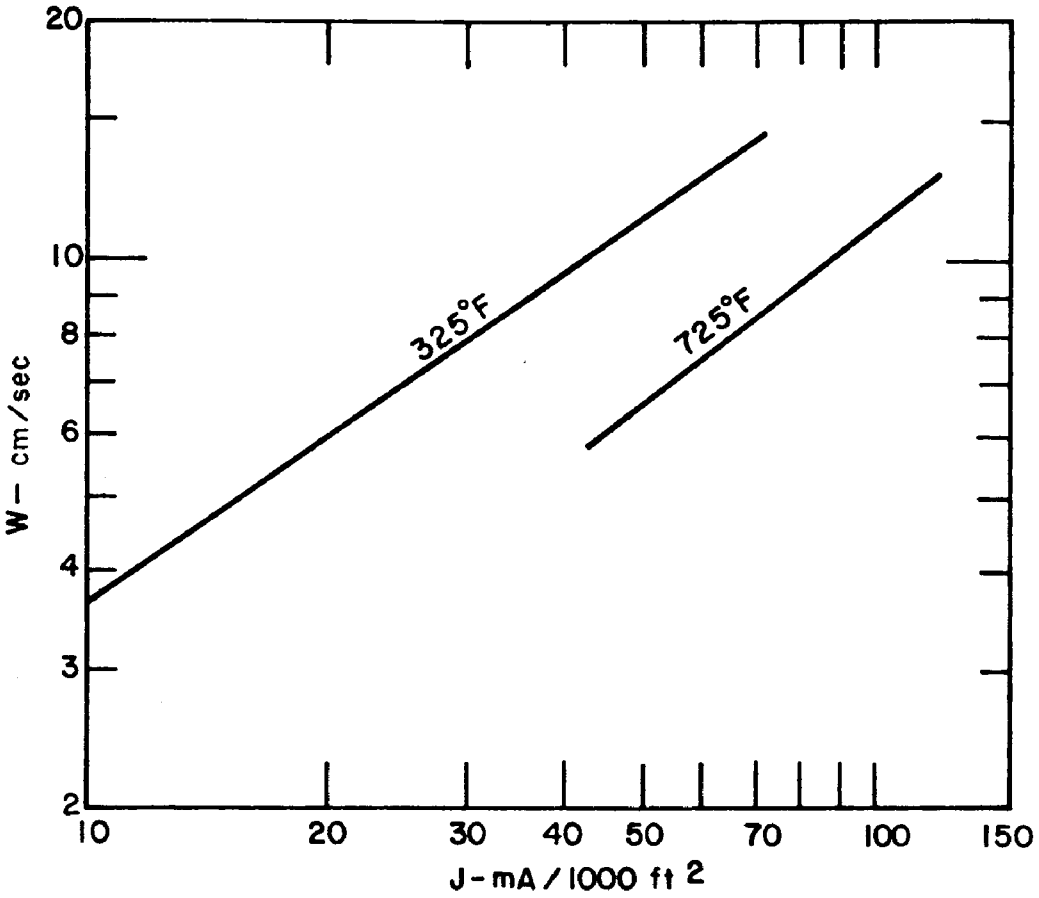

Figure 7. Average effective precipitation rate parameter, w, as a function of average current density, calculated for typical high performance fly ash precipitators

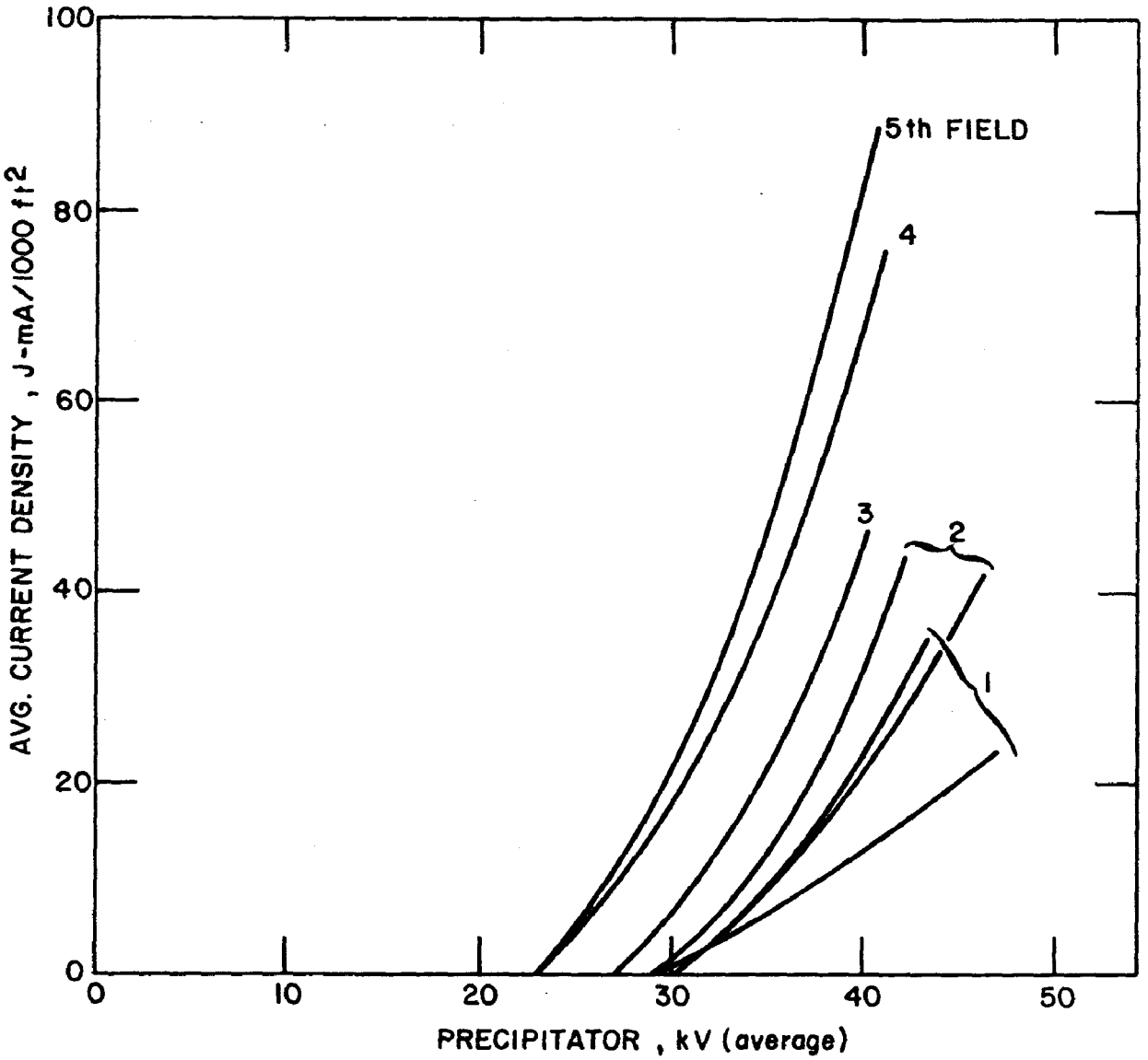

Figure 8. Typical fly ash precipitator voltage-current characteristics, five fields in series, no ash resistivity problem

1. Mismatched power supply to load

   a. Precipitator underpowered—too few electrical sets, sets of wrong capacity, too much collecting area energized from single set.

   b. Failure to fully appreciate effects of gas density and temperature on required operating levels. Figure 9 illustrates typical reduction in operating voltage with gas temperature. Remember, however, that while the voltage goes down the current demands are going up. At high pressures the reverse can occur.

   c. Too large a rectifier set on an application not requiring the current capacity. This is a common thing where 1500 mA saturable reactor sets, for example, are operating on high resistivity ash at perhaps 100 mA. This leads to loss of control, horrendous sparking and poor results.

2. Electrode gross misalignment—possibly due to full hoppers having bent structures, a sloppy construction job, thermal expansion problems, etc. Whatever cause, no decent performance can be achieved without straightening it out.

3. Localized sparking—insufficient operating voltage levels. This can be caused by a number of things such as--electrode misalignment, poor discharge electrode design (use of shrouds at top and bottom of wires can help significantly), localized high current density due to improper rapping, cold air inleakage, etc.

4. Poor sectionalization design and loss of performance. Table 3 illustrates some effects on available operating voltages and currents as a function of amount of collecting area energized per rectifier set. Large gains in performance in a given size precipitator are indeed possible. It is a matter of incremental performance gains versus cost. If an average electrical set installed costs about $15,000 and the cost of a precipitator is about $5.00 per sq ft collecting area, then one electrical set would be the equivalent of about 3000 sq ft of collecting area. On this basis using a few more sets with less total area would be beneficial in many cases.

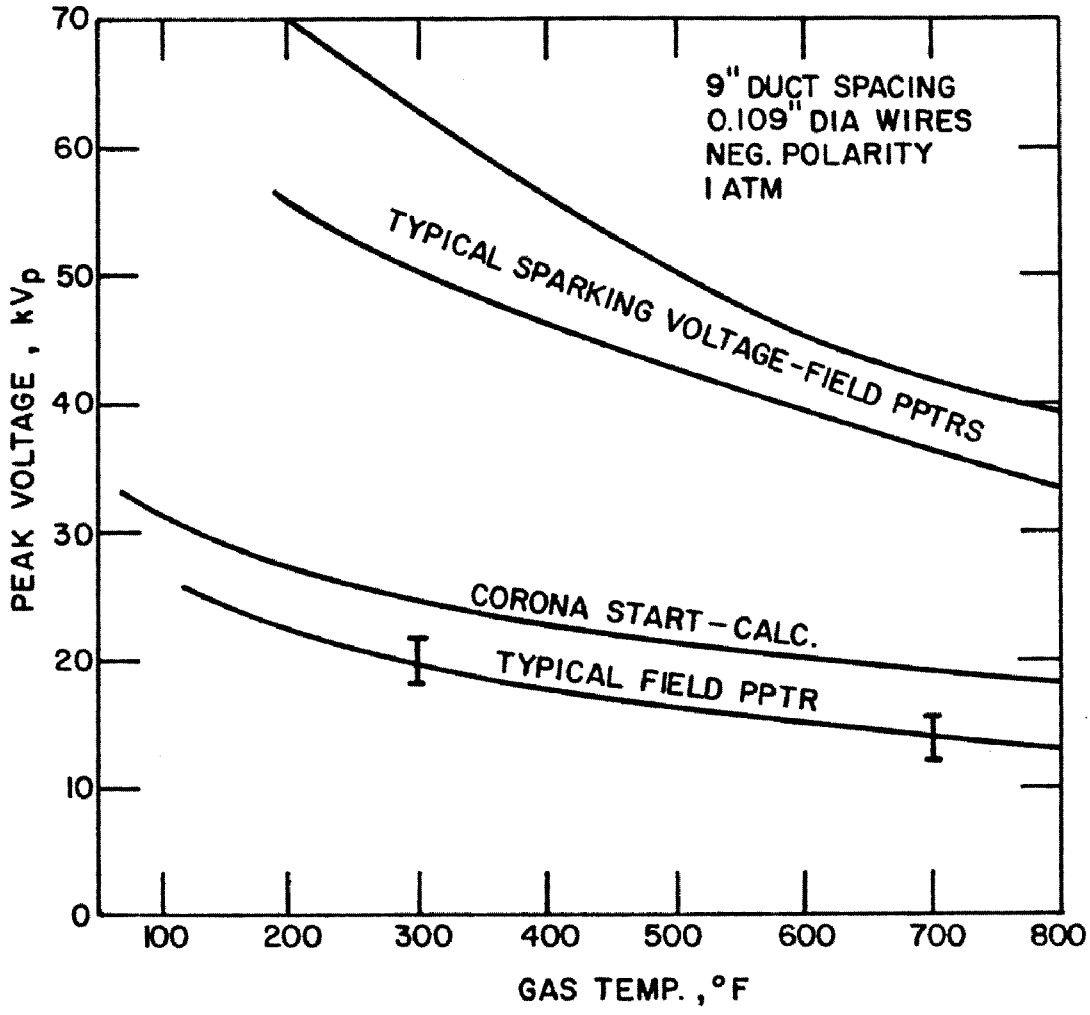

Figure 9. Typical precipitator operating voltage as a function of gas temperature

Table 3. PRECIPITATOR SECTIONALIZATION AND CONTROL EFFECTS

Control	ft^2 Area per set	kV_{av}	mA/1000 ft^2	kW	Wave	Fields
Low resistivity $<10^{10}$						
SR	13,400	31.6	78	33	FW	2
SCR-1	13,400	37.5	88	44.4	FW	2
SCR-2	12,600	33.2	92	37.2	FW	3
High resistivity $\sim 10^{11}$						
SR	13,400	24.5	28.4	9.3	FW	1
SR	26,800	24.8	26.5	17.6	FW	1
SR	26,800	22.7	13.4	8.2	HW	1

Effects for FW saturable reactor control

Location	ft^2 Area per set	kV_{av}	mA/1000 ft^2	P_c kW	Watts/ft^2 P_c/A
Inlet	71,280	31	10.4	22.6	0.32
Center	35,640	30.8	14	15.4	0.43
Outlet	35,640	36.75	13.2	17.3	0.48
Center	17,820	39.5	19.1	13.4	0.75

5. Unstable performance of saturable reactor controls on sparking load. This can be particularly bad on HW energization. It can also be a problem on FW with the larger size sets. Measures for stabilization include addition of an appropriate series linear reactor as shown in Figure 10. This increases current conduction period as illustrated in Figure 11 and reduces the ratio of HV transformer secondary current, I_{rms}, to average dc load current, I_{av}. At the same time additional corona power becomes available, if needed, within the ratings of the rectifier set. Most importantly, however, with sparking loads, the usual tendency for such systems to burst spark--self perpetuating sparking on several consecutive cycles--can be eliminated. Figure 12 illustrates comparative current waveforms for SCR and standard saturable reactor controls under normal transient, occasional sparking and under highly unstable burst type spark tendencies which, if uncontrolled, would lead to severe arcing. The third waveform from top shows effects of partial saturation of the transformer core on a spark initiated at B with several alternate half cycle sparks following each other until recovery. Note that the alternate current pulses A are at first missing altogether then gradually appear, getting progressively stronger towards normal level. Actually, this transient disturbance can last for periods of many more cycles than that shown. The effect comes from normal ac waveform from transformer secondary being elevated momentarily so that say the positive half cycles are lifted to a peak voltage about twice normal while the negative half cycles barely reach the zero axis. This explains the high voltages and spark current peaks on the one hand and the missing or low current pulses on the other hand.

6. Interference between sections on HW energization. One frequently hears that HW energization provides increased sectionalization, hence better performance and greater reliability. This is one of those subtile half truths. The two sections are not independent and what happens in one side can be coupled into the other side through the common transformer-rectifier set. Figure 13 illustrates the effect on a dual beam scope picture. The sparking section can induce sparking on the normally non-sparking section.

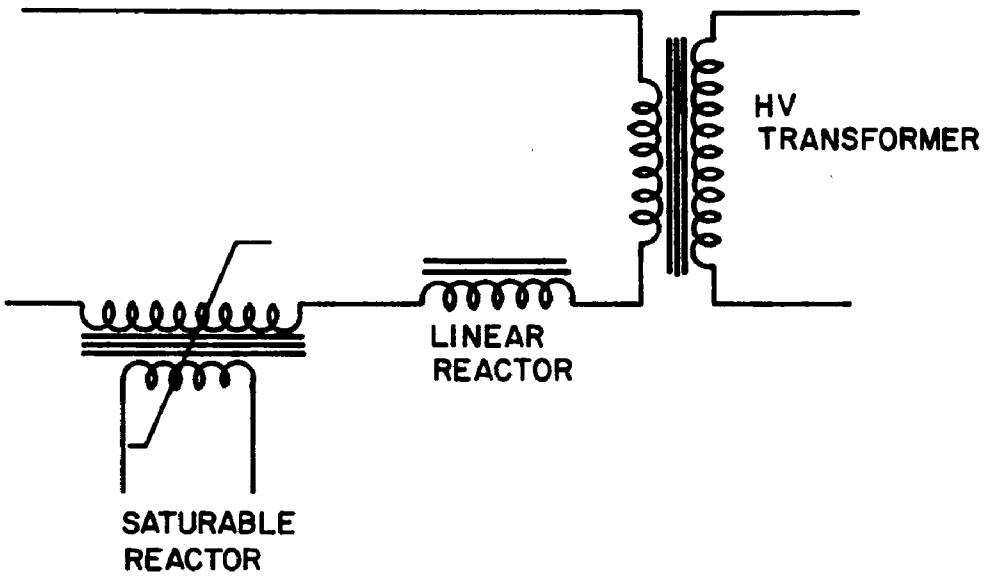

Figure 10. Method of stabilizing operation of saturable reactor type controls with series linear reactor

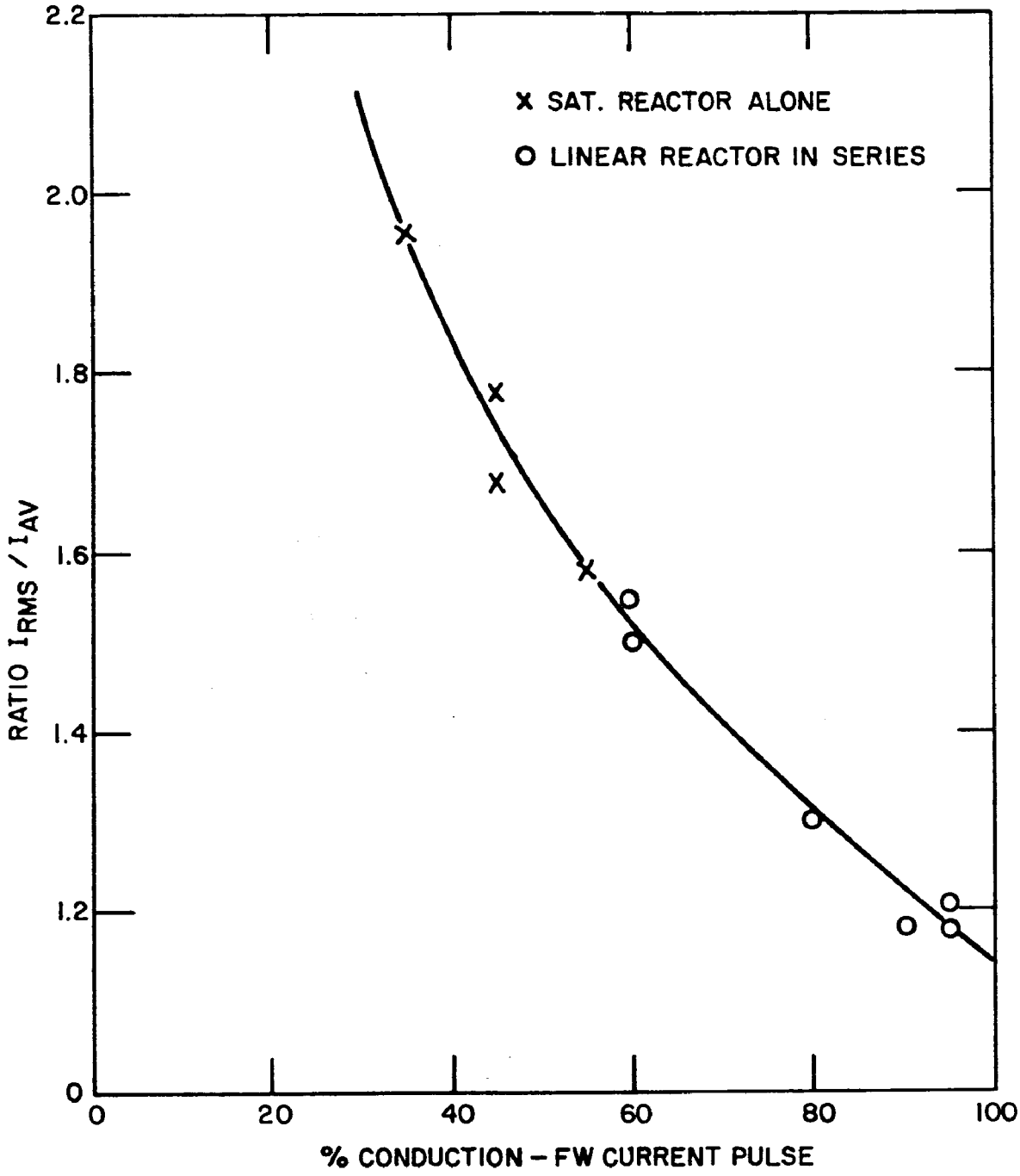

Figure 11. Ratio of HV transformer secondary current form factor as a function of fractional current conduction and effects of adding linear reactor in series with a saturable reactor

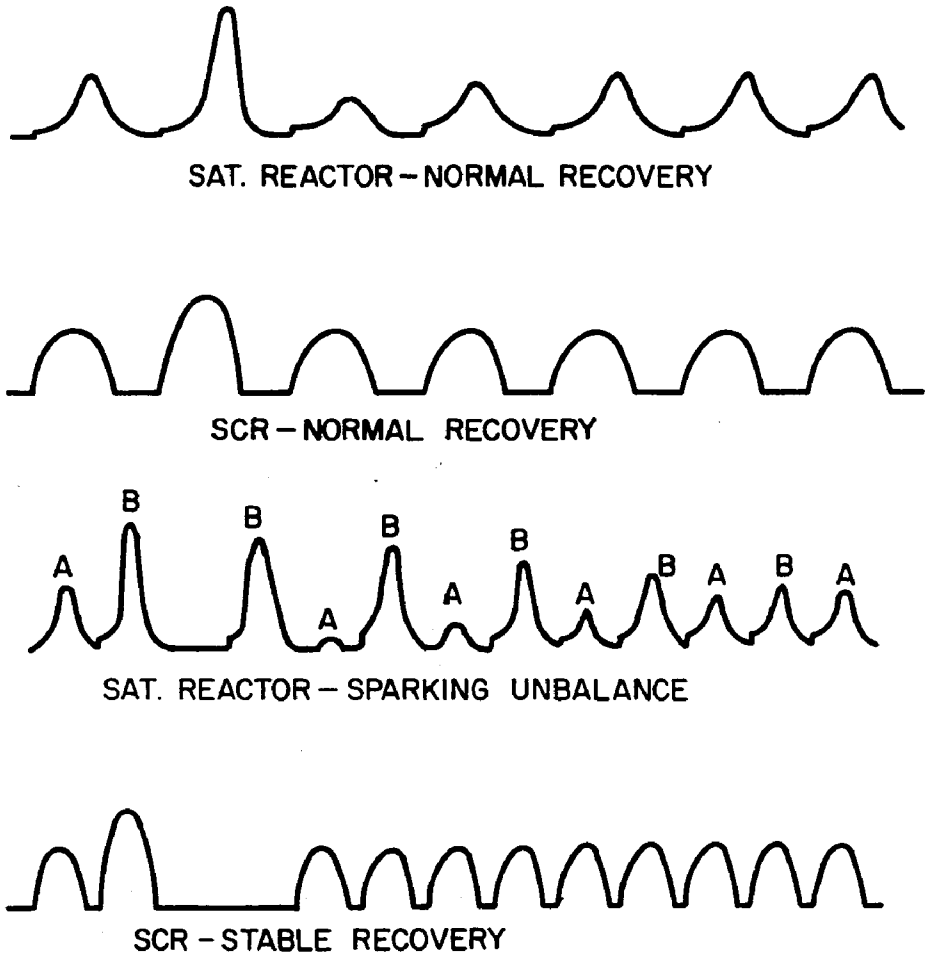

Figure 12. Typical current waveforms illustrating response to normal, transient sparking and to heavy sparking for saturable reactor and SCR type control systems on precipitator rectifier sets

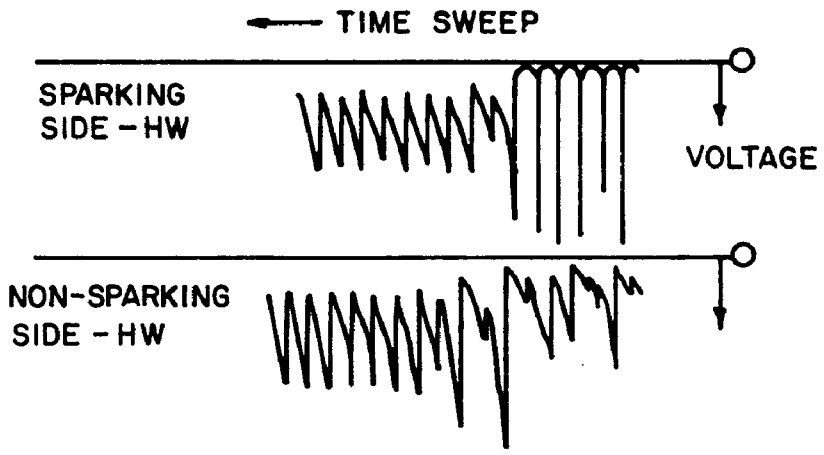

Figure 13. Voltage waveforms on dual beam oscilloscope showing induced sparking on normally non-sparking section with HW energization

Although there are many other interesting things that could be discussed, we have run out of space in this brief treatment of a fairly complex subject with many interrelated aspects. We come out by the same door wherein we entered--high performance and reliability in electrostatic precipitators of the future will begin with good electrical energization and equipment. The extent to which the electrical design achieves its purpose in providing an optimum electrical environment will depend upon good mechanical and gas transport design done with care and fine appreciation for high standards of excellence.

REFERENCES

1. White, H. J. Industrial Electrostatic Precipitation. Reading, Mass., Addison-Wesley, 1963. 376 p.

2. Hall, H. J. Trends in Electrical Energization of Electrostatic Precipitators. In: Proceedings, Electrostatic Precipitator Symposium. Birmingham, Southern Research Institute, February 1971. p. 77-116.

3. Hall, H. J. Trends in Electrostatic Precipitation and Industrial Gas Cleaning. Chem. Eng. Progr. 59:67-72, September 1963.

4. Hall, H. J. High Voltage Rectifier Tube Operation in Industrial Precipitation Equipment. Winter Issue, Machlett Cathode Press. Springdale, Connecticut, Machlett Laboratories, 1950-1951.

5. Hall, H. J. An Automatic Voltage Control System for Electrical Precipitators. Trans. Amer. Inst. Elec. Eng. 73, Part I:124-127, May 1954.

6. Van Hoesen, H. E., H. J. White, and H. J. Hall. Automatic Control of Electrical Precipitation Rectifiers. Trans. Amer. Inst. Elec. Eng. 77, Part I:126-128, March 1958.

7. Willison, R. E. The Application of Silicon Rectifiers to Electrostatic Precipitator Power Supplies. Direct Current:248-251, March 1958.

8. Hall, H. J., J. B. Eaton, Jr., R. F. Brown, and W. C. Brown. Removal of Lube Fume Raises Line Efficiency [The application of precipitators to cleaning high pressure pipeline natural gas]. Oil Gas J. 66:109-117, September 9, 1968.

9. Hall, H. J., and R. Jakoplic. Method and Apparatus for Automatic Voltage Control of Electrostatic Precipitators. U. S. Patent 3,507,096, April 1970.

10. Robinson, M. Electrostatic Precipitation. In: Air Pollution Control, Strauss, W. (ed.). New York, Wiley-Interscience, 1971. p. 283-298.

11. Brown, R. F., and A. B. Walker. Feasibility Demonstration of Electrostatic Precipitation at 1700°F. Research-Cottrell, Inc. (Paper 70-27, presented at Air Pollution Control Association 63rd Annual Meeting. St. Louis. June 14-18, 1970.)

PRECIPITATOR GAS FLOW DISTRIBUTION

C. L. Burton and D. A. Smith
Combustion Engineering, Inc.
Windsor, Connecticut

ABSTRACT

An electrostatic precipitator, furnished on a 500-MW tangentially-fired steam generator burning coal, was to collect 99.5% of the fly ash being generated in the furnace of this unit. Preliminary measurements indicated that the installation was not meeting its collection guarantee. Precipitator outlet flue dust distribution indicated that poor gas flow distribution might be one of the causes of the low performance. When observation ports were installed in the outlet flue to permit a direct visual evaluation of the problem, it was found that high velocity jets were present in the collecting electrodes, and that hopper sweepage was present.

A model study along with velocity distribution measurements of the installation were authorized. Flow analysis indicated that the field and model correlated well. Extensive changes were made in the model, which eliminated or minimized the high velocity jets and hopper sweepage. After these changes were made in the field installation, it was able to achieve the required dust collection efficiency.

INTRODUCTION

Back in the middle 1960's, there was a general feeling that the electrostatic precipitator had reached its peak capabilities in dust collection efficiency. It appeared that efficiencies in the range of 99.0 to 99.5% were the practical

limit to be expected. This paper describes two 1964-1965 precipitator installations that were designed for a fly ash-collection efficiency of 99.6%. These installations went on-line in 1968 and only could achieve collection efficiencies of 98.8 to 99.1%. Many studies were made. Mechanical remedies, electrical remedies, and gross gas flow corrections were attempted without improving the performance.

Finally, an in-depth study of gas-flow distribution was initiated. It was shown that the gas-flow distribution was significantly poorer than the Industrial Gas Cleaning Institute (IGCI) specifications.[1] Gas duct modifications were then made that improved gas distribution to a level better than IGCI. Subsequent dust collection efficiency tests proved that these installations were capable of performing at levels higher than the required efficiency.

Good gas-flow distribution is a necessity if precipitators being sold today at 99.5 to 99.9% collection efficiency guarantees are to realize their designed performance levels. The IGCI gas-flow criteria are based on the requirements and experience of the 1950's, while today's high performance precipitators require gas flow significantly better than IGCI specifications. The improved levels of gas-flow distribution that can be achieved are described here.

BACKGROUND

The installations being reported on have the following specifications:

Collection efficiency	99.6%
Gas volume treated	1,530,000 acfm @ 260°F
Collecting plate area	270,400 sq ft
Contract coal	
Ash	12.2% dry
Sulfur	3.65% as-fired

The efficiency achieved during the first three years of operation was measured several times and ranged from 98.8 to 99.1%. The inability to meet the performance guarantee prompted an in-depth study to define the cause of and develop a solution to the problem. Because the costs associated with a complete gas-flow analysis of an existing installation are high, preliminary observations to confirm the existence of potential gas-flow problems were conducted to justify further

large expenditures. A brief description of the various types of inexpensive techniques used to justify a detailed analysis is given below.

Figure 1 is a side elevation of the entire precipitator complex for Unit A. Gas leaves the Ljungstrom^{R} air preheater and is divided between the two precipitators of the double deck installation. During initial operation, gas-flow traverses were conducted to determine the gross division of gas between the precipitators. Detailed velocity traverses were also conducted in the vertical outlet flue leaving the upper precipitator, and in the inlets to the i.d. fans. The gas flow passing through the lower precipitator was determined by subtracting the measured gas flow leaving the upper precipitator from the measured gas flow entering the induced draft (i.d.) fan inlets. These initial tests showed that approximately 54.5% of the gas was going through the lower precipitator with the remainder going to the upper precipitator. This imbalance in gas flow had been previously predicted by a 3 dimensional air model. This model study had been conducted to develop the gas flow vaning needed to ensure adequate gas-flow distribution through each precipitator. Based on the recommendation of this model study, a perforated plate was installed in the vertical portion of the flue just before the turn into the lower precipitator. The turning vanes (Figure 1) shown in the inlet to the upper and lower precipitators and in the outlet of the upper precipitator also were installed based on recommendations from this same model study.

The velocity traverses conducted at the inlets to the i.d. fan also revealed a lateral imbalance of gas flow across the precipitators. Figure 2 shows the results of these tests. The north i.d. fan was receiving 9% more flow than the south but, more importantly, the inboard legs of each fan received more flow than the outboard legs. These imbalances were not predicted by the air-model test because complete geometric similarity had not been maintained in the model beyond the outlet of the lower precipitator.

Finally, when dust samples were taken in the inlet to each i.d. fan to check performance, it was found that 88% of the total dust collected in each inlet was collected in sample port #1 as noted in Figure 3.

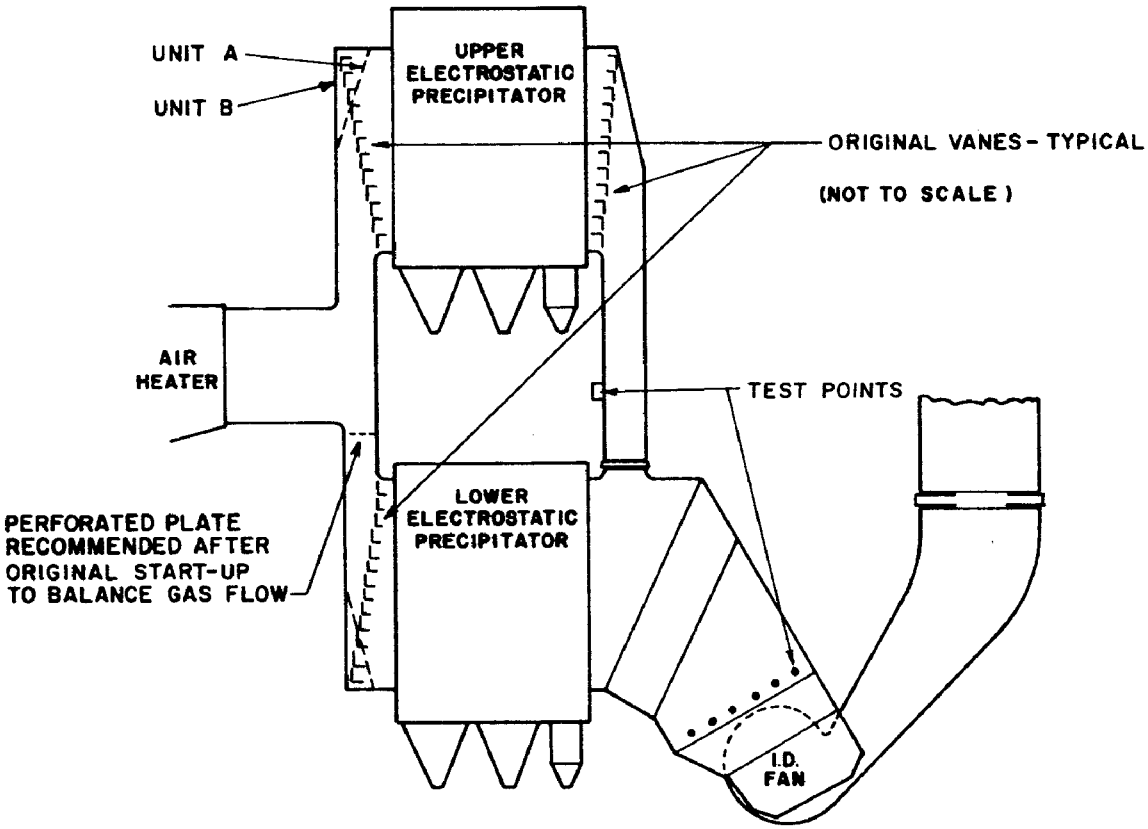

Figure 1. Side elevation of electrostatic precipitator

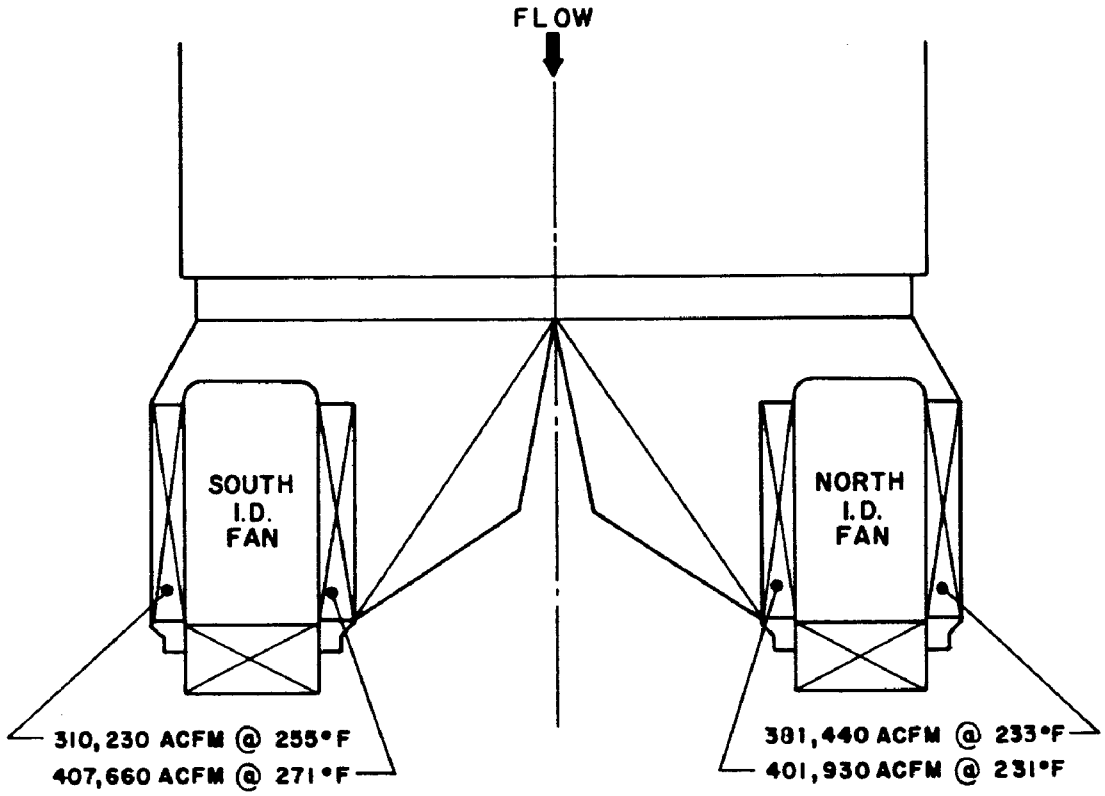

Figure 2. Gas-flow imbalance, outlet flues and i.d. fans (Unit A)

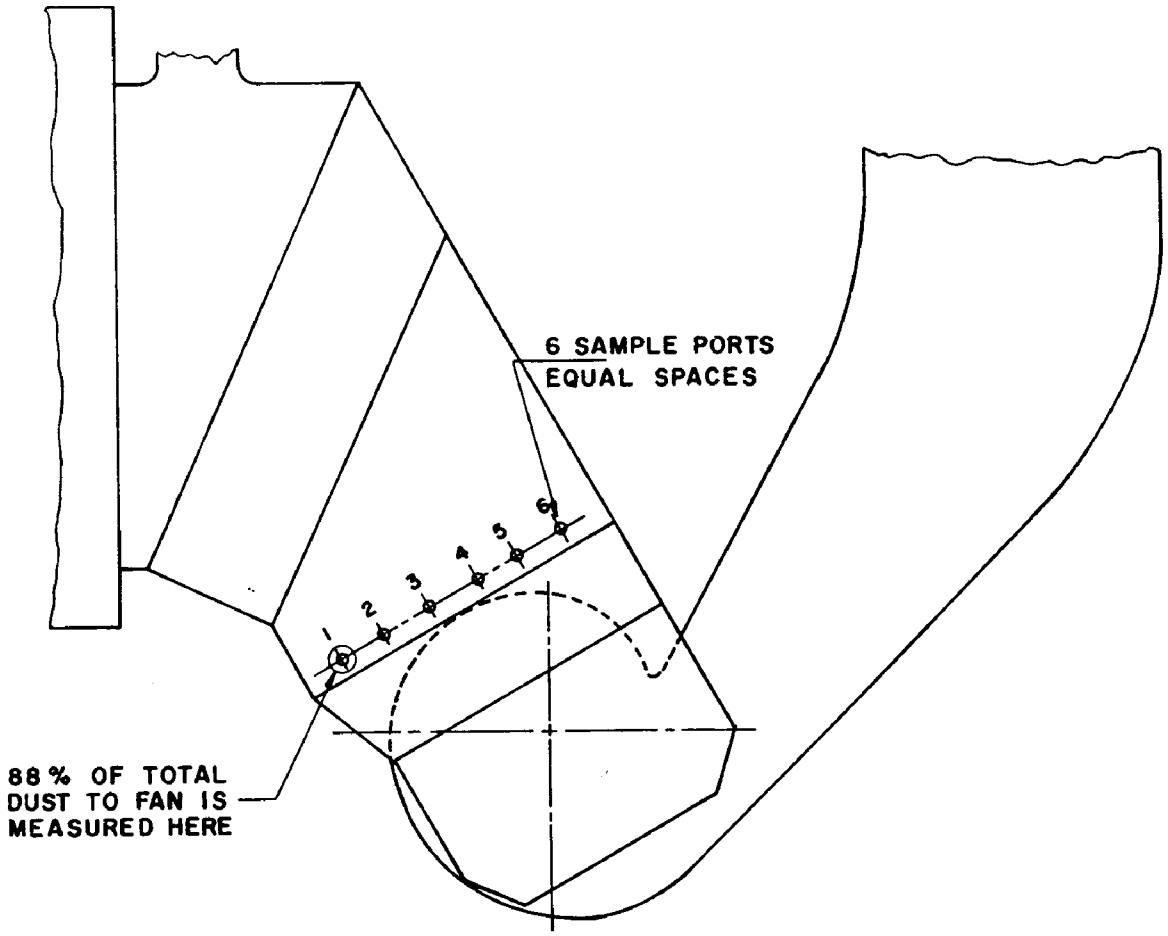

Figure 3. Side elevation of i.d. fans (Unit A)

FIELD VISUAL EVALUATION OF PROBLEM

Based on this history of gas-flow related problems, a decision was made to conduct detailed field evaluations. As shown in Figure 4, four eight-inch diameter observation ports were installed in the roof and side wall of the lower precipitator on the north side of the unit. The system was operated at full load and high intensity lights were used to illuminate the gas flow zones of interest through these ports.

These observations pointed out dramatically the effects of poor gas flow distribution on precipitator performance. Although initial short term observations showed no apparent problems, extended observations revealed that huge clouds of dust would suddenly appear in the lower precipitator outlet. Careful observation of this phenomenon revealed that these

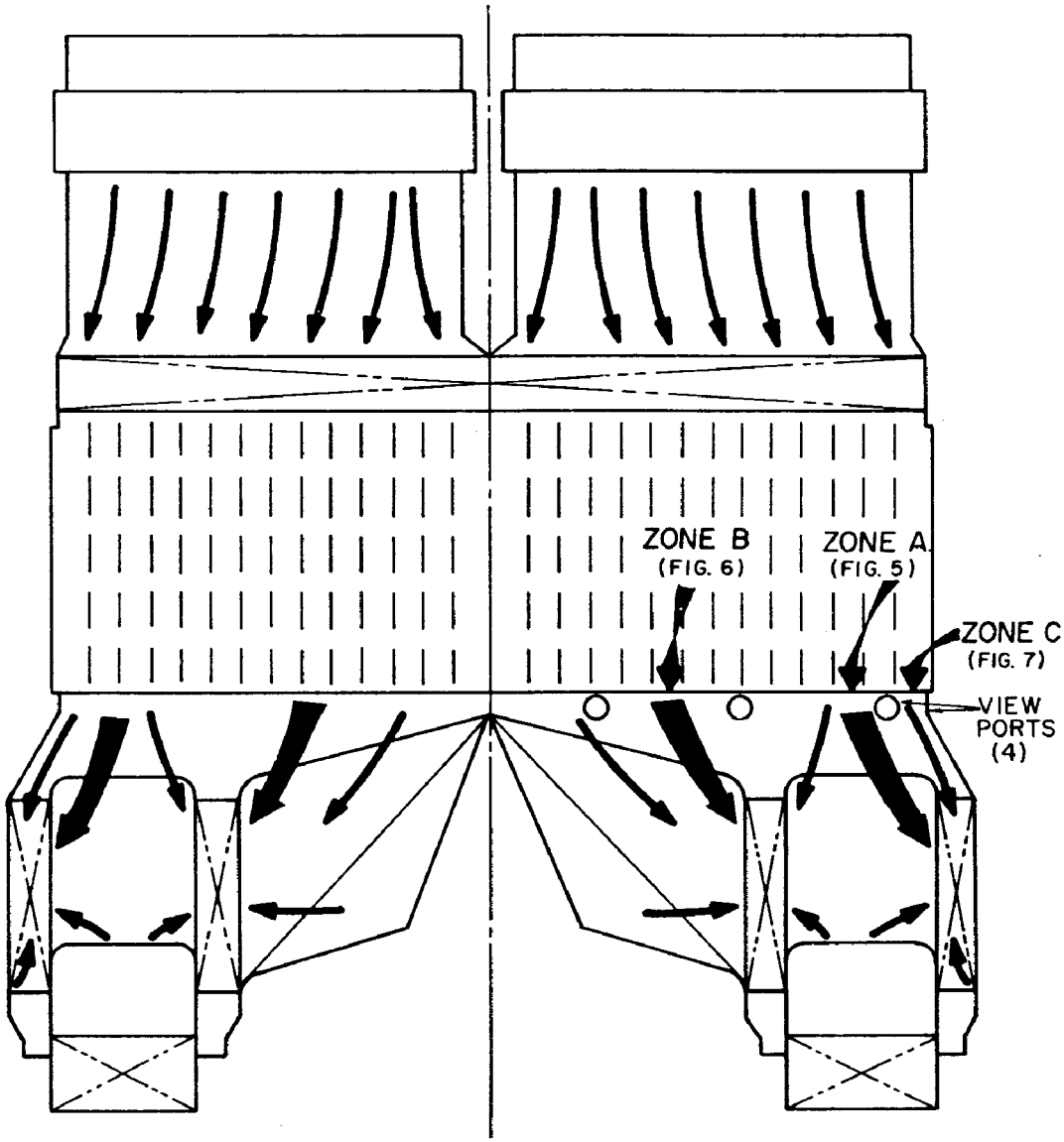

Figure 4. Gas-flow patterns, plan view of outlet flues (Unit A)

eruptions were occurring only in limited areas of the precipitator, and usually occurred when one or more collecting electrodes in these areas were being rapped. At first, it was thought that plate rappers were occasionally rapping entire precipitator lanes at once, but this proved not to be the case. The dust eruptions would occur only when the plates in the immediate vicinity of either of the i.d. fan inlet boxes were rapped.

To further define the problems observed through the observation ports, the unit was taken out of operation and detailed internal inspections of both the inlet and outlet flues of each precipitator were made. A skilled observer, by careful observation of polishing and deposition on internal pipe

struts, vanes, and dampers can define areas of flow separation, reverse flow, and extremely high or low velocity in great detail.

The flow arrows shown in Figure 4 show the result of this type of flow mapping. The inlet and outlet of the upper precipitator showed no unusually high or low velocity zones. The situation for the lower precipitator was quite different. Several feet of fly ash were found in the bottom of the flue entrance of the lower precipitator, with the two lowest turning vanes actually buried in fly ash.

The outlet flue of the lower precipitator also exhibited areas of high velocity and dust dropout. Figures 5, 6, and 7 are photographs taken in the outlet flue of the lower precipitator showing some of these areas of erosion and dust dropout. Figure 5 shows an area approximately four precipitator ducts wide, adjacent to the outboard leg of the north i.d. fan, where the surfaces of the collecting electrodes have been swept clean by the high-velocity jets created by the pressure gradient of the i.d. fan. Figure 6 shows a similar situation opposite the inboard leg of the same fan while Figure 7 shows an area of hopper sweepage and subsequent drifting of fly ash in the outlet flue. Previous experience indicated that velocities of 10 to 15 ft/sec would be required to produce the collecting electrode polishing shown in Figures 5 and 6.

These phenomena were repeated in the south half of the precipitator, but the problems appeared less severe because of the lower gas flow through that half of the installation.

DETAILED FIELD VELOCITY TRAVERSE

Based on the results of the on-line observations and off-line inspection, it was obvious that the gas flow problems in this unit were a major contributing factor to its deteriorated performance. It was also apparent that the original model study did not reveal the unacceptable gas distribution found in the lower precipitator, probably because the outlet flues were not completely modeled. It was therefore concluded that a new 3-D air model study would have to be conducted to evaluate the various options available to remedy this situation. Since the original model study of this installation did not reveal any of the problems just described, it was decided that a complete velocity traverse of the inlets to both the upper and lower precipitators would be conducted. This information would then be used to check the as-built model results to insure an accurate representation of the problem.

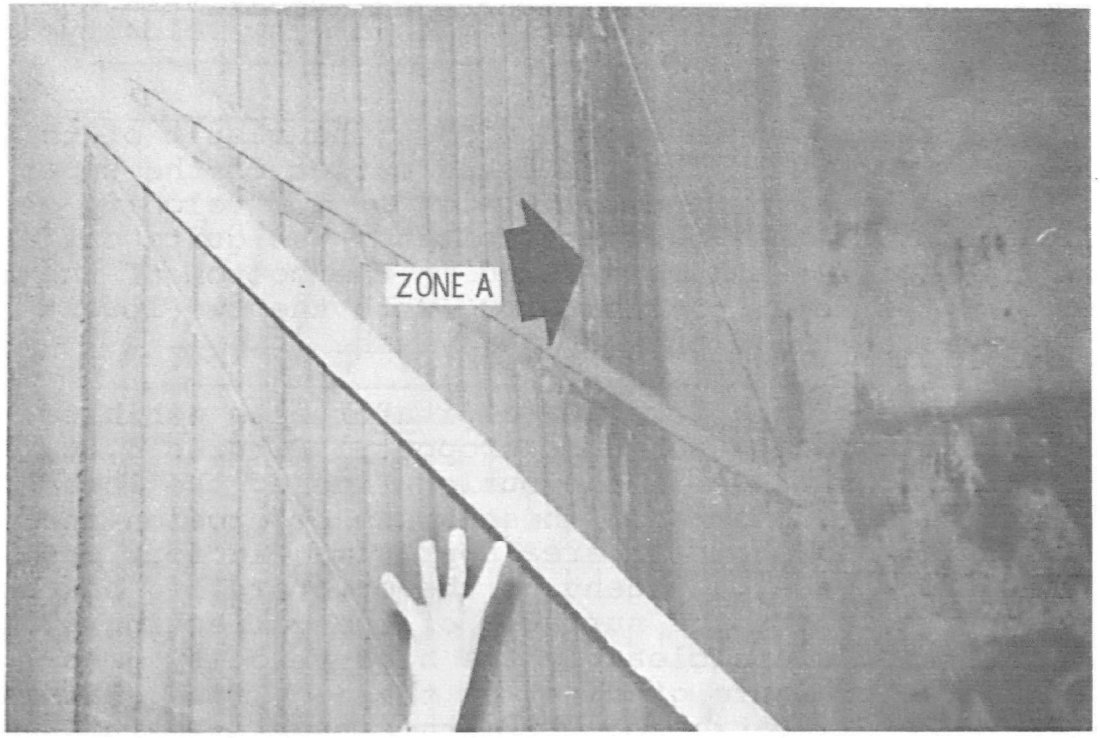

Figure 5. High velocity scrubbing, precipitator outlet, zone A

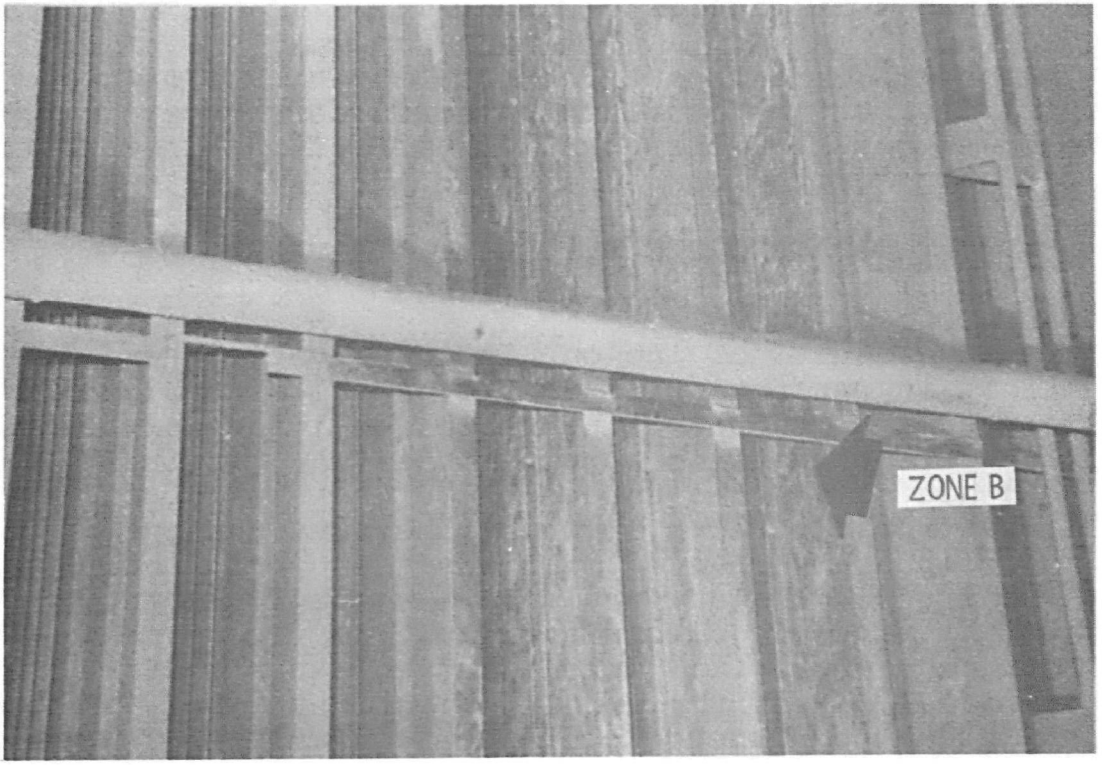

Figure 6. High velocity scrubbing, precipitator outlet, zone B

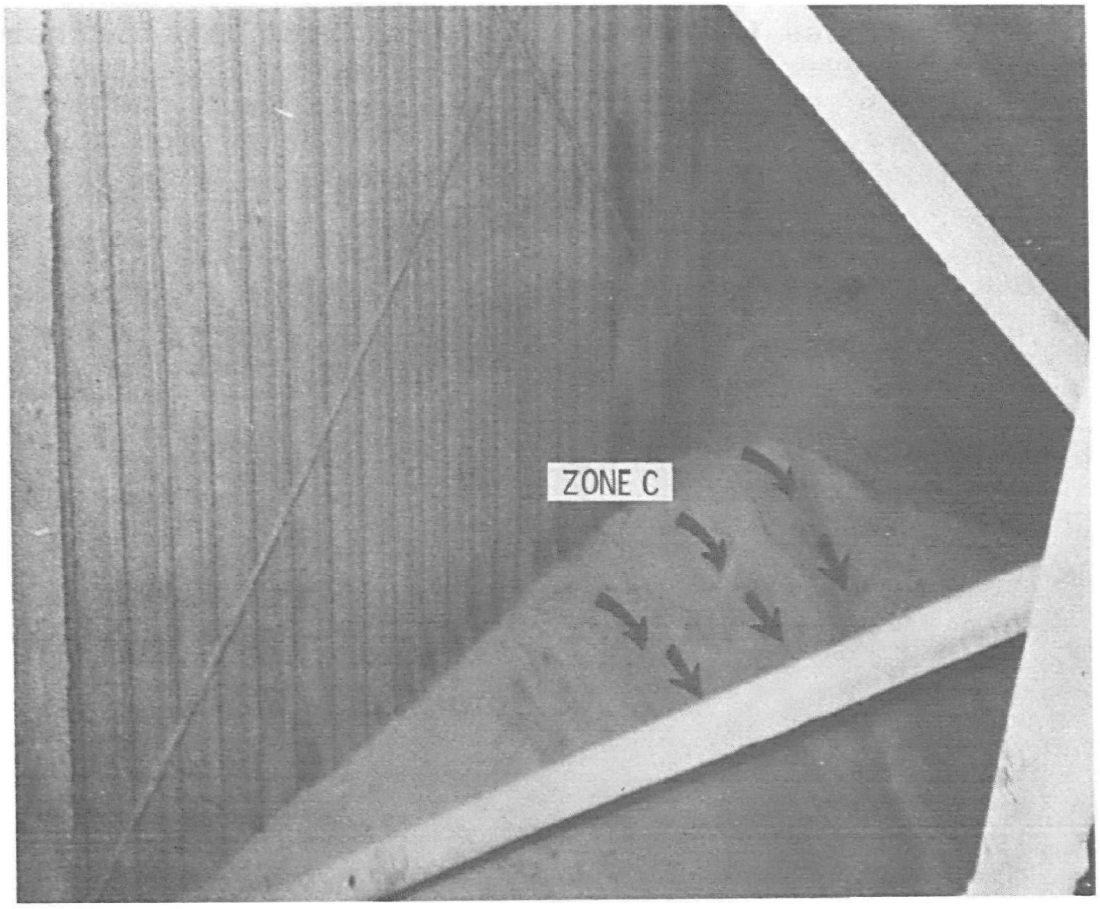

Figure 7. Hopper sweepage, precipitator outlet, zone C

Because of limited unit availability, the field velocity traverses could not be conducted on Unit A. They were, however, conducted on Unit B, a duplicate of installation A, which also had experienced performance problems of the same nature as Unit A.[2]

A quick walk-through of Unit B was conducted to ensure that the problems observed in Unit A were evident in Unit B. Unit B was then thoroughly cleaned before attempting to perform the field velocity traverses so that the traverses would be indicative of a new system.

TECHNIQUE

A heated thermocouple anemometer was used to obtain velocity data. The anemometer is basically a heat transfer device with a readout that is nonlinear with respect to velocity. Typically the relationship is

$$\text{Output} = f(V^{0.8})$$

The anemometer was traversed down the first two discharge electrodes of every 4th precipitator duct. Selected traverses were also obtained in the outlet of each precipitator. Figure 8 shows a sample of the data obtained from one precipitator duct.

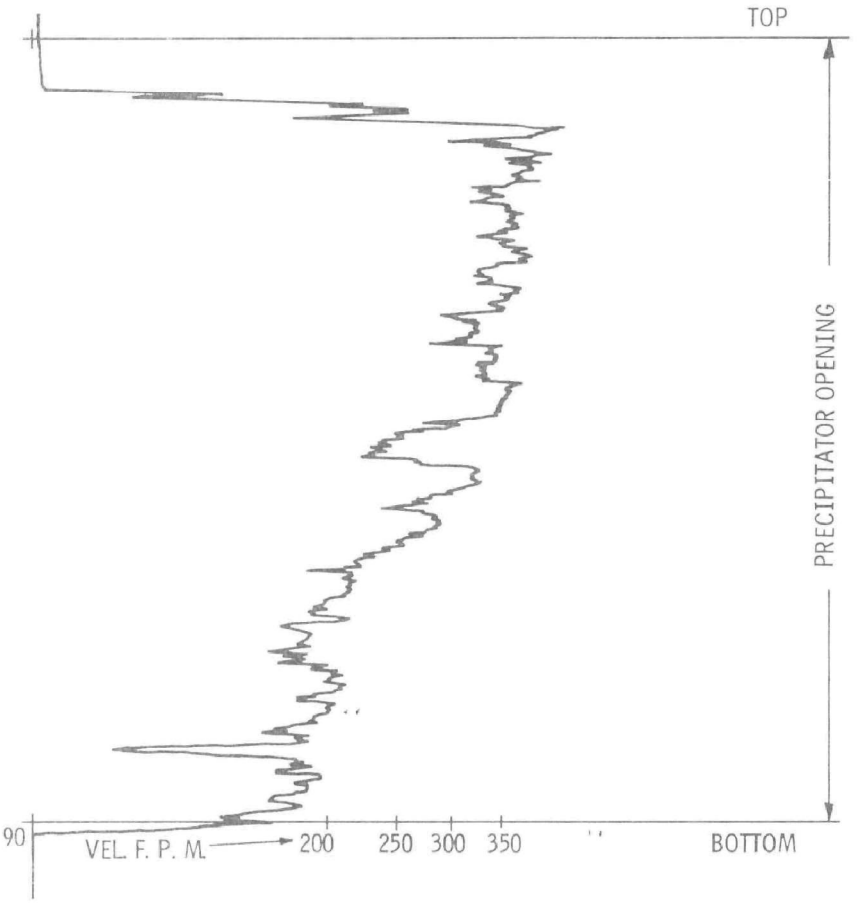

Figure 8. Lower precipitator inlet velocity profile duct 68 as measured with continuous traverse (Unit B)

The unit was operated on cold air at approximately 60% of design velocity. This provided a Reynolds' Number approximately equal to that which would be seen under actual full load operation. Figure 9 is an example of a typical field velocity profile after the velocity had been corrected back to a linear scale. Once all the data curves had been linearized, they were reduced to numerical form. An overlay grid was prepared of twenty equally spaced lines representing precipitator elevations. The overlay was placed over each linearized velocity profile and the value of the velocity

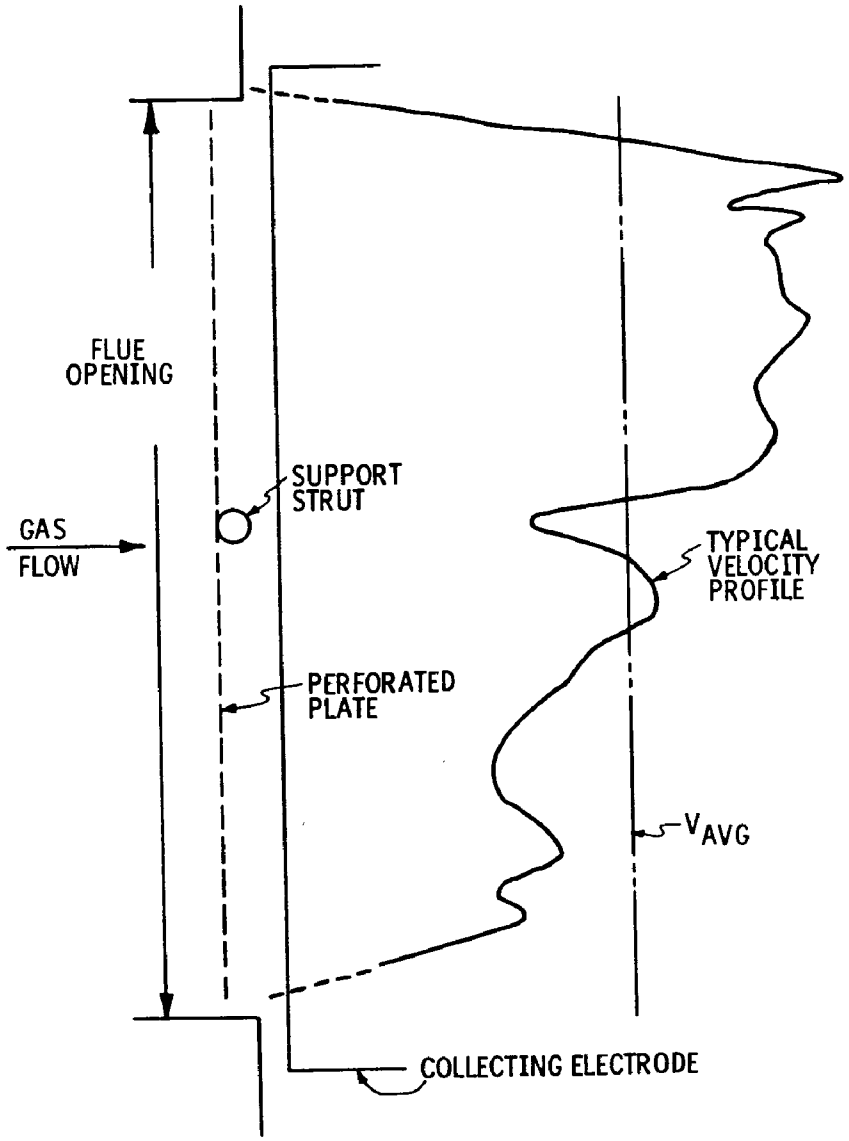

Figure 9. Typical measured velocity profile, as installed—lower precipitator inlet (Unit B)

profile at each evaluation was recorded as a point velocity. These velocity data points were then numerically averaged to establish an average vertical and horizontal velocity profile for each precipitator.

PRELIMINARY DATA REDUCTION

Figure 10 illustrates a simplified side elevation view of the upper and lower precipitators showing the average vertical

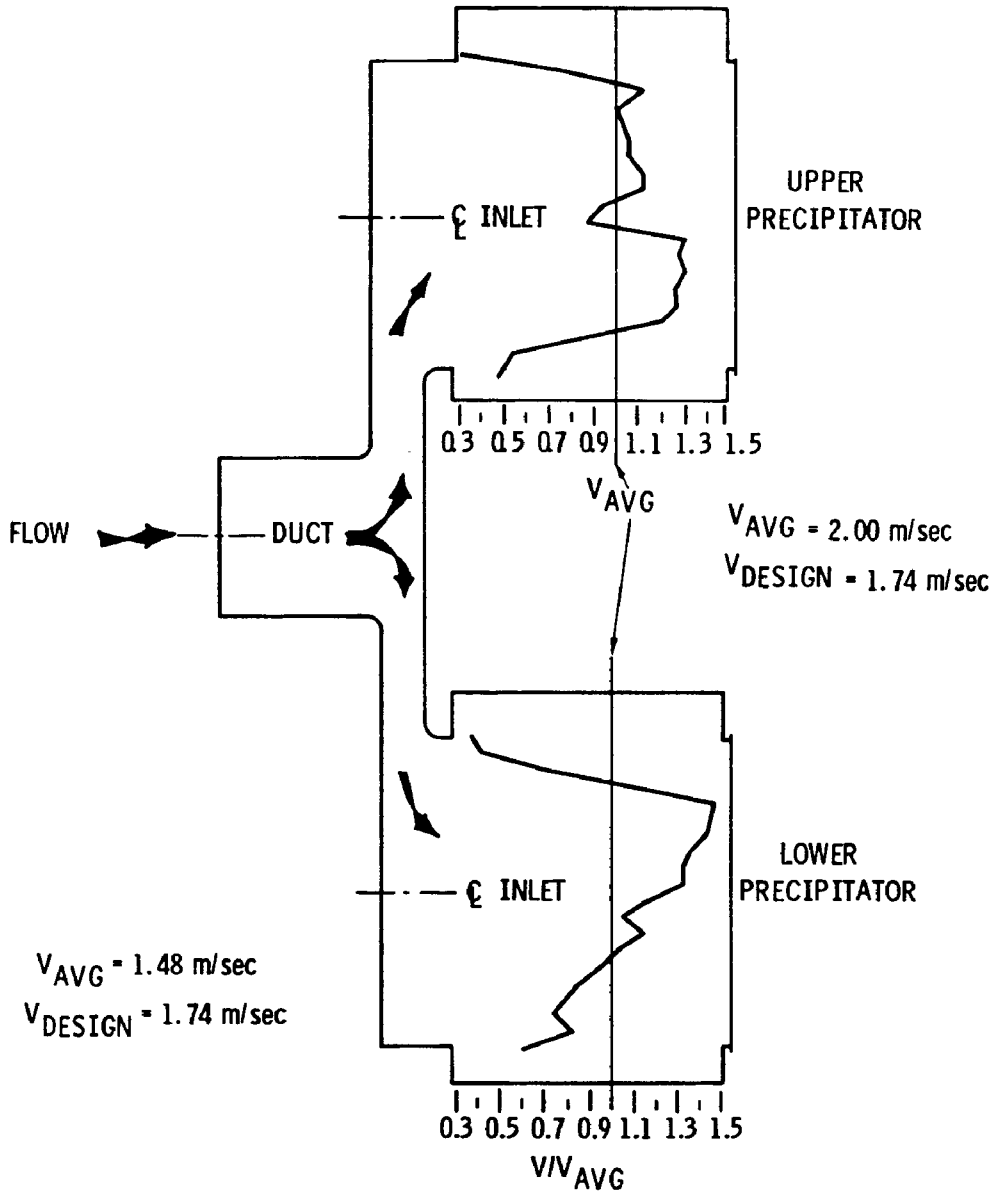

Figure 10. Average inlet velocity side elevation profiles—as installed (Unit B)

inlet velocity profile for each as obtained from the field test. It is important to note the skewness of the velocity profile in the lower precipitator and the imbalance of flow between the upper and lower precipitators. Approximately 58% of the gas was passing through the upper precipitator with the remainder passing through the lower. It should also be noted that this imbalance is not completely detrimental since previous field tests indicated that 80 to 90% of the dust went to the lower precipitator. If the design velocity had actually been met, the high velocity zones in the lower precipitator would have further reduced the efficiency of the overall system.

Figure 11 demonstrates the dramatic effect that the outlet flue has on the velocity profile leaving the lower precipitator. This points out the condition that must be eliminated if reentrainment and hopper sweepage in the lower precipitator are to be eliminated.

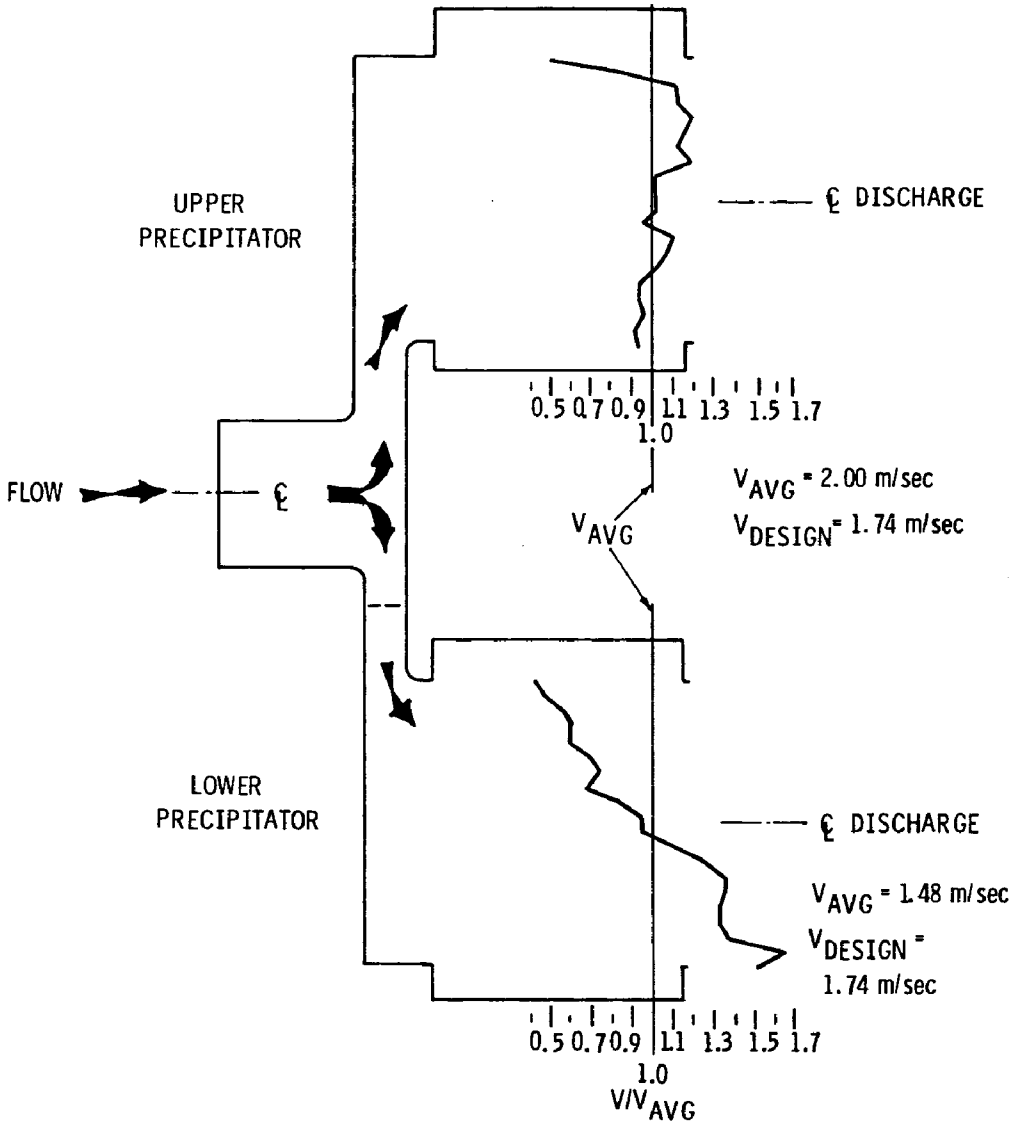

Figure 11. Average outlet velocity side elevation profiles—as installed (Unit B)

Figures 12 and 13 detail the statistical distribution of the data points taken in the upper and lower precipitators and compare these results with those recommended by the IGCI. The vertical bars of these histograms represent the percentage of the data points occurring at each velocity. The actual velocity values have been normalized (divided by the average velocity), following standard practice.

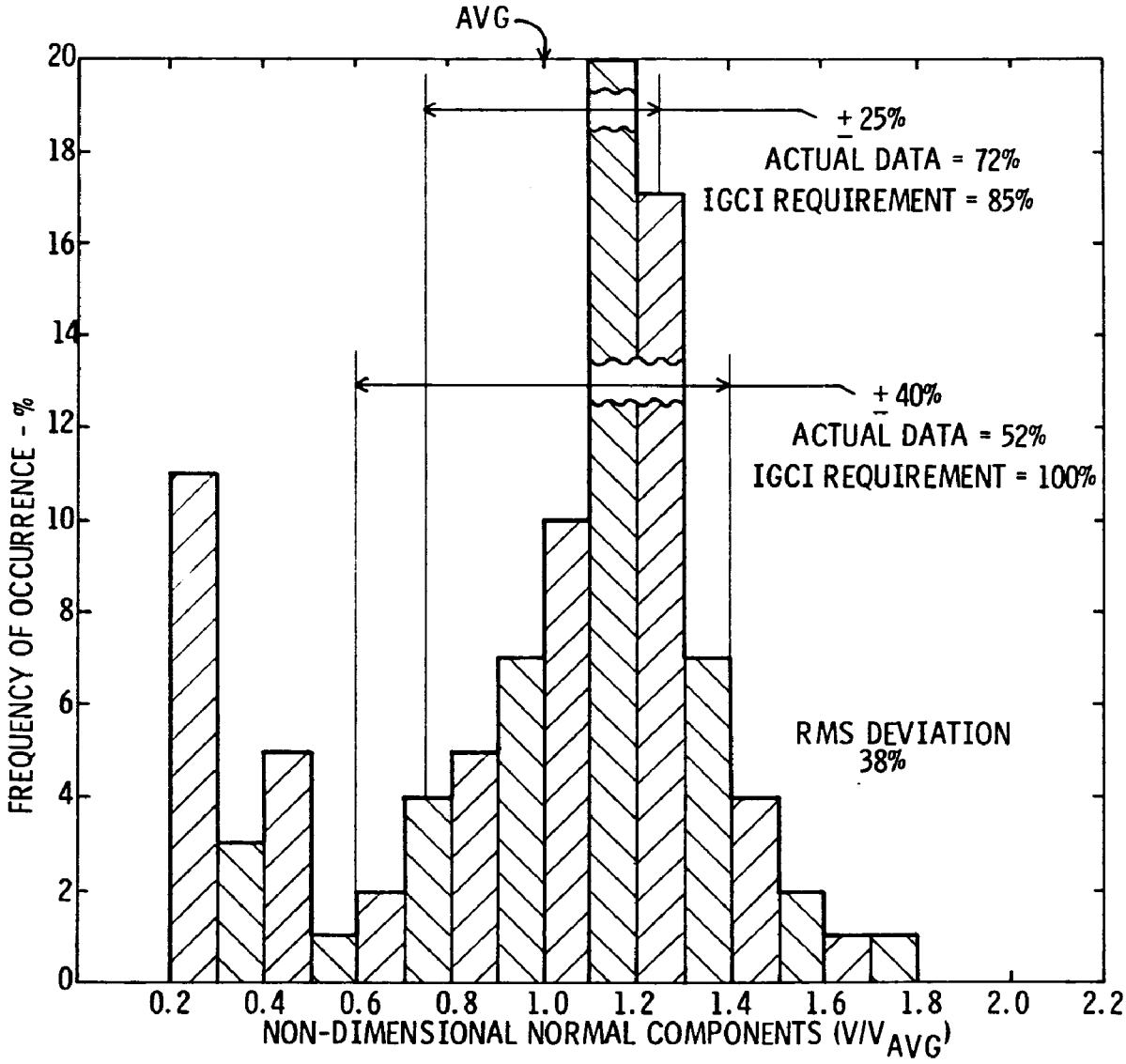

Figure 12. Histogram analysis of upper precipitator inlet velocity measurements (Unit B)

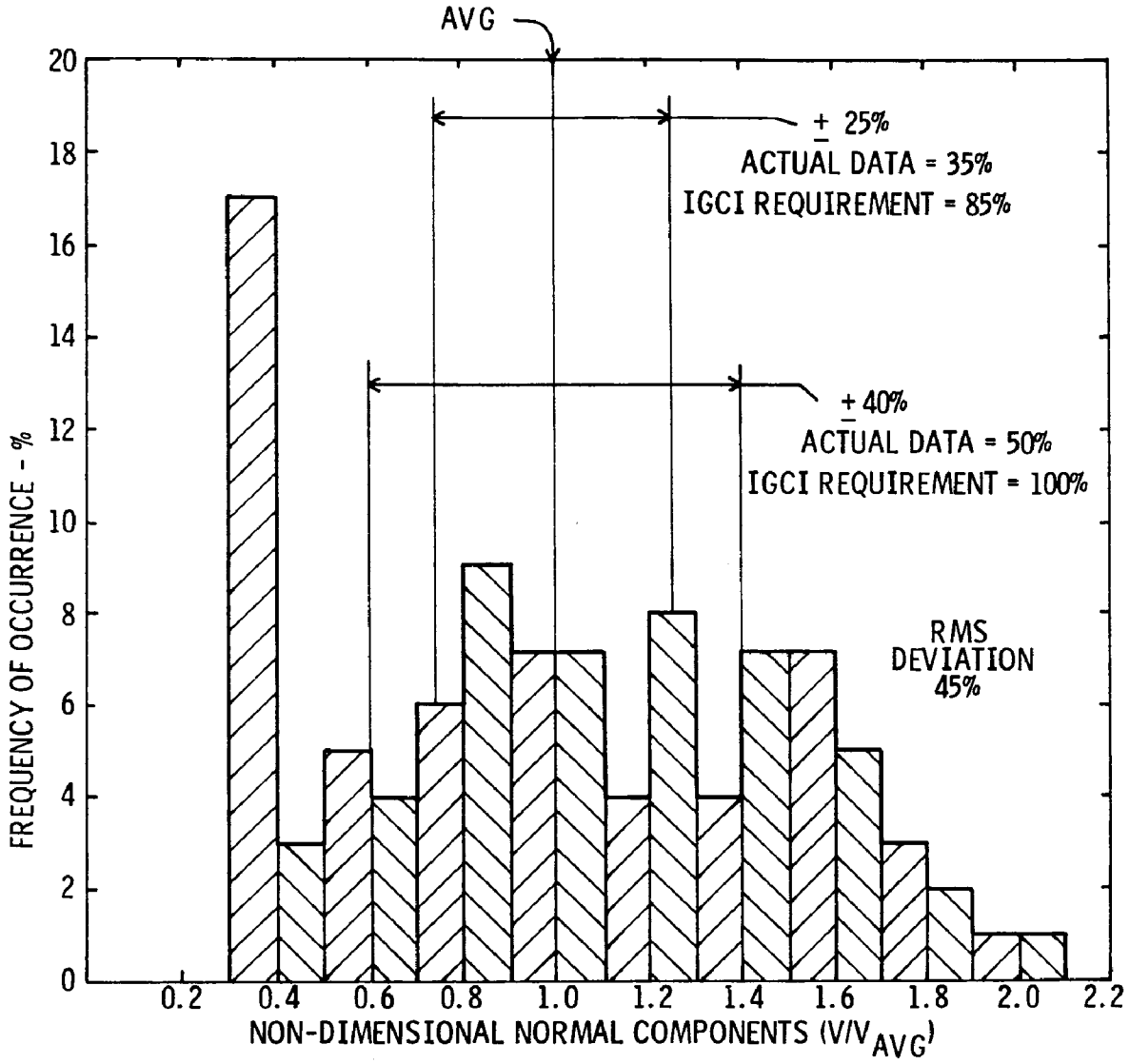

Figure 13. Histogram analysis of lower precipitator inlet velocity measurements (Unit B)

As can easily be seen, neither precipitator meets the IGCI requirements, with the upper precipitator approximately two times better than the lower precipitator.

PRECIPITATOR PERFORMANCE ANALYSIS

As of this time, it had been shown that there were severe gas-flow distribution problems associated with the poor performance of these precipitator installations. The actual significance, with respect to the precipitator efficiency, of the measured values of root mean squared (rms) deviation and the IGCI limits had not yet been evaluated. To justify further expenditures on correcting these gas-flow problems, it had to be shown analytically that gas flow was a major factor of the reduced precipitator performance.

To make an analytical study, a series of assumptions were made. The first was that the Deutsch-Anderson equation,

$$\text{Eff} = 1 - e^{-\frac{A}{V}w}$$

where A is precipitator collecting electrode area—sq meters (sq ft), V is actual gas volume being treated—cu meters per sec (cu ft/sec), w is precipitation rate—meters per sec (ft/sec), could be applied to the problem.

The second assumption was that the design value of w included the effects of nonperfect gas-flow distribution as identified by the IGCI limits.

The third and final assumption was that a standard rms deviation of 25% could be substituted for the IGCI limits. With these assumptions, an efficiency can be calculated for a given sized precipitator that would then represent the efficiency for perfect gas flow or 0% rms deviation. This efficiency would be greater than that guaranteed for IGCI conditions. In like manner, the effective w for perfect gas flow would be greater than the guaranteed w.

The results of such assumptions are as follows:

Contract:	efficiency	= 99.60%
	w	= 0.163 m/sec (0.521 ft/sec)
0%rms:	efficiency	= 99.76%
	w	= 0.178 m/sec (0.571 ft/sec)

This new value of w, at 0% rms, was then used with the volume flow rates and velocity distribution of Figures 10, 12, and 13 which were corrected for on-line operating conditions. The resultant Deutsch-Anderson efficiency was then calculated to be 99.29% as opposed to the 98.8 to 99.1% range indicated by the preliminary stack measurements. This result indicated that a significant improvement in performance could be obtained by correcting precipitator inlet gas flow distribution back to 25% rms (or IGCI limits). Further, it was obvious that an additional improvement in efficiency could be obtained by correcting the lower precipitator outlet gas flow distribution shown in Figures 7 and 11. However, no quantitative evaluation of the hopper sweepage was attempted.

FIELD VS MODEL STUDY RESULTS

Periodically, the authors are questioned as to the ability of a model study to quantitatively predict the performance of full-sized installations. Generally, it is accepted that a model study can produce, at the best, only qualitative results. It is our opinion that proper attention to details—in both the model and the prototype—will produce a one-to-one correlation between the model and the field.

A properly made model requires a high level of dimensional accuracy and should be complete from the air preheater at the model inlet to the stack or i.d. fan at the model outlet in the case of a "cold" precipitator. For a "hot" precipitator, the model should include the steam generator economizer at the model inlet and the air preheater at the model outlet. Practically all deviations in measured gas flow between field and model can be attributed to a change in the design of the prototype (after the completion of the model study) or to constructional distortions of the gas-flow control devices during installation.

A case in point can be made by reviewing Figure 14. This figure presents an analysis of the gas-flow distribution across the width of the lower precipitator inlet on a duct basis. The results are normalized and plotted as the ratio of measured duct flow to the calculated average duct flow over the precipitator width. The heavier curve (squares) is the flow distribution as measured in the prototype (and previously analyzed for vertical distribution in Figure 10). The lighter curve (circles) is the distribution as derived from the model study at the same test plane.

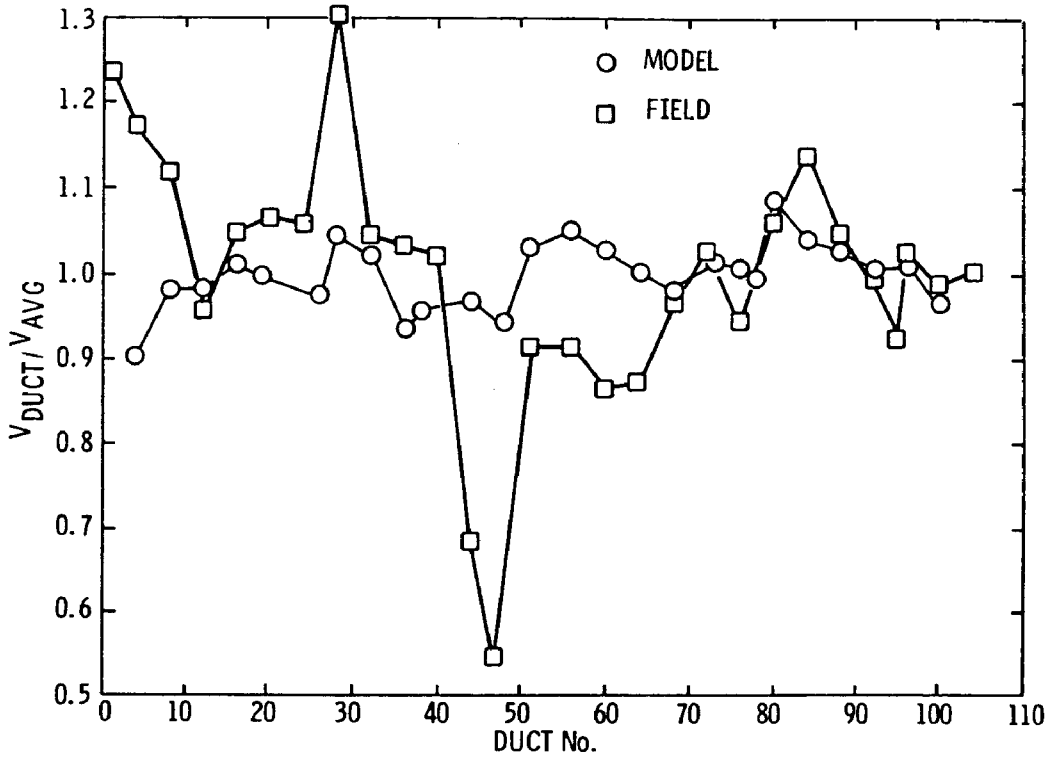

Figure 14. Lateral gas flow distribution, lower precipitator inlet, uncorrected (Unit B)

The model results are within the bounds of experimental error. The deviations are mainly due to a combination of instrumentation error and small variations in model collecting-duct spacing. However, two zones—one at ducts 28, 32 and one at ducts 80, 84—of higher velocity are noted. These higher velocities are traced from the inboard breechings of the i.d. fans back to the precipitator inlet.

In the case of the field data of Figure 14, three zones of initial non-correlation were noted. They are ducts 2, 4, and 8; duct 28, and ducts 44 and 48, all in the north half of the prototype. The field results of the south half were considered to be within reason with duct 84 responding to effects of the south i.d. fan. These results led to a reinvestigation of the field installation to identify the sources of these widely deviating flow rates.

The subsequent field inspection required that temporary access be made available downstream of the inlet flue turning vanes and between the two inlet perforated plates. The source of the high flow ducts, noted above, was immediately apparent. The precipitator and flue inlet perforated plates had been

installed in panels 3 feet to 4 feet wide by 10 feet high. These panels had been clipped together for alignment to maintain the effect of a large single-piece perforated plate. Some clips had not been installed while others had broken loose permitting the adjacent plates to buckle over their 10 ft height. Where a 1-inch gap had been desired, gaps of 4 to 8 inches were found. Figure 15 is a photograph of the start of one of these gaps in the flue perforated plate. Similar gaps were found in the precipitator perforated plates. This is not uncommon; this particular type of erection defect has been found in many installations. The gaps of the units reported here were oriented such that they accounted for the high flows in the ducts noted in the field data of Figure 14.

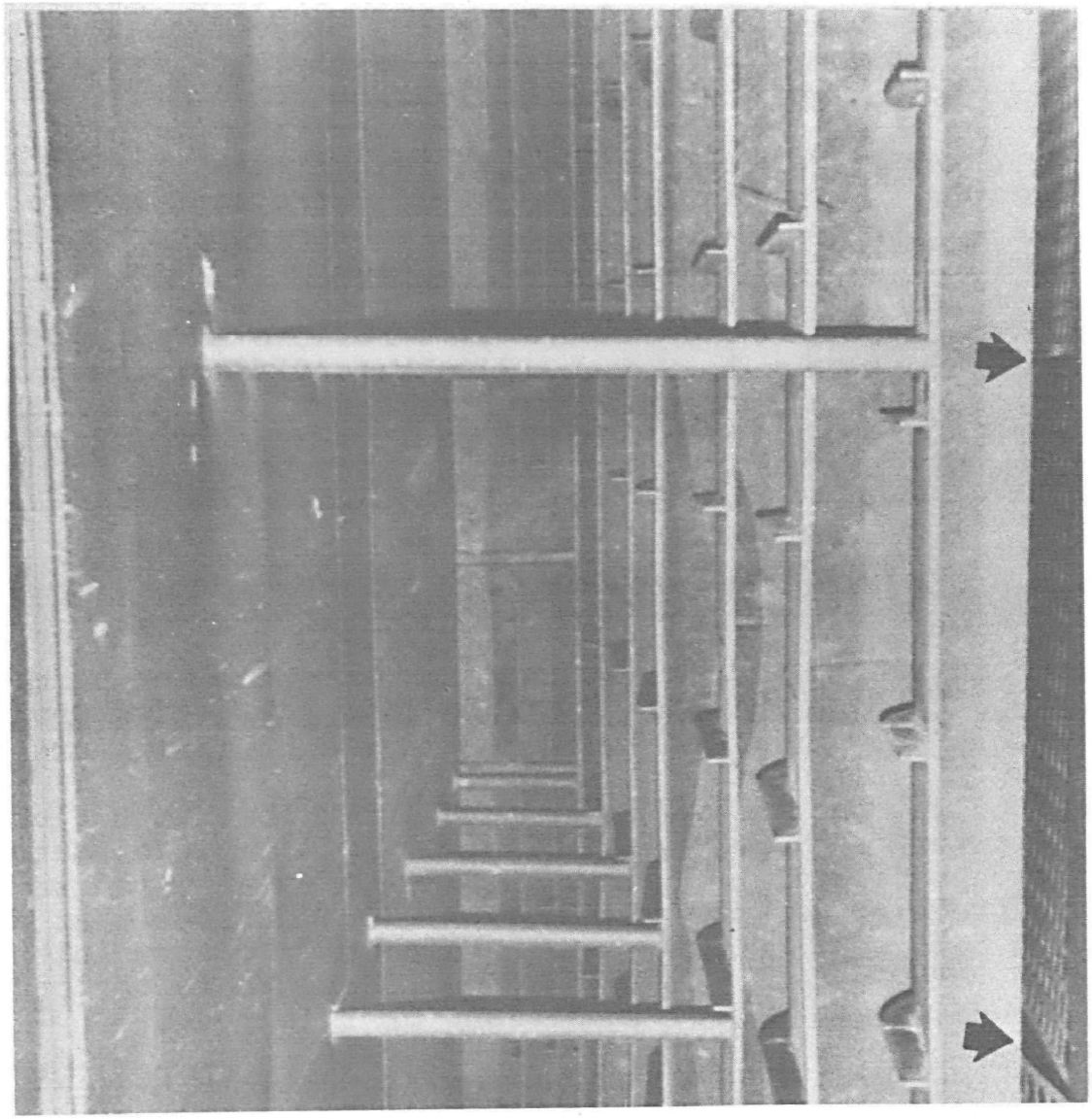

Figure 15. Buckled perforated plates, precipitator inlet

A gap in the flue perforated plate, in the area of ducts 48 to 50, created a jet that moved northward between the two sets of perforated plates. This jet then responded to a combination of a gap in the precipitator inlet perforated plate, in the area of duct 28, and the effects of the north i.d. fan, to create the high velocity measured in that duct.

Similarly, the high velocities measured in ducts 2, 4, and 8 were created by a 4-inch gap between the end of the flue and precipitator perforated plate and the north wall of the flue. This gap was the result of cumulative inaccuracies in hanging the plate panels.

All the perforated plate panels, both flue and precipitator inlet, were rehung, aligned, and clipped so as to present a flat plate structure to the gas flow. Attention to these details brought the installations up to the same levels of geometric accuracy as had been built into the model.

Similar observations and results on the ability to obtain a good correlation between the model and the prototype are given in Figures 16 and 17, which have been reproduced from Reference 3. In the case of Unit C, Figure 16, the rms deviation for the model was 16% and for the field 14%. The maximum velocities measured were 117% for the model and 114% for the field. Unit D, Figure 17, with a different air heater arrangement, produced rms deviations of 23% for the model and 20% for the field. The maximum measured velocities were 120% for the model and 112% for the field.

FINAL MODEL AND FIELD RESULTS

Based on the above, it was decided to proceed with the model study to determine the design of the flow corrective devices and produce an optimized flow field in the precipitators.[4]

Because of the very close coupling between the inlet-flue expansion turn and the precipitator, it was decided that "ladder vanes" would be used to replace the inlet radius vanes. Ladder vanes are a series of flat surfaces that are oriented perpendicular to the direction of the turn inlet gas flow. The optimum positioning of these vanes can only be done under actual flow conditions or in a model.

Unit B inlet flues were already squared off as shown in Figure 1 and would readily accept the ladder vanes. Unit A

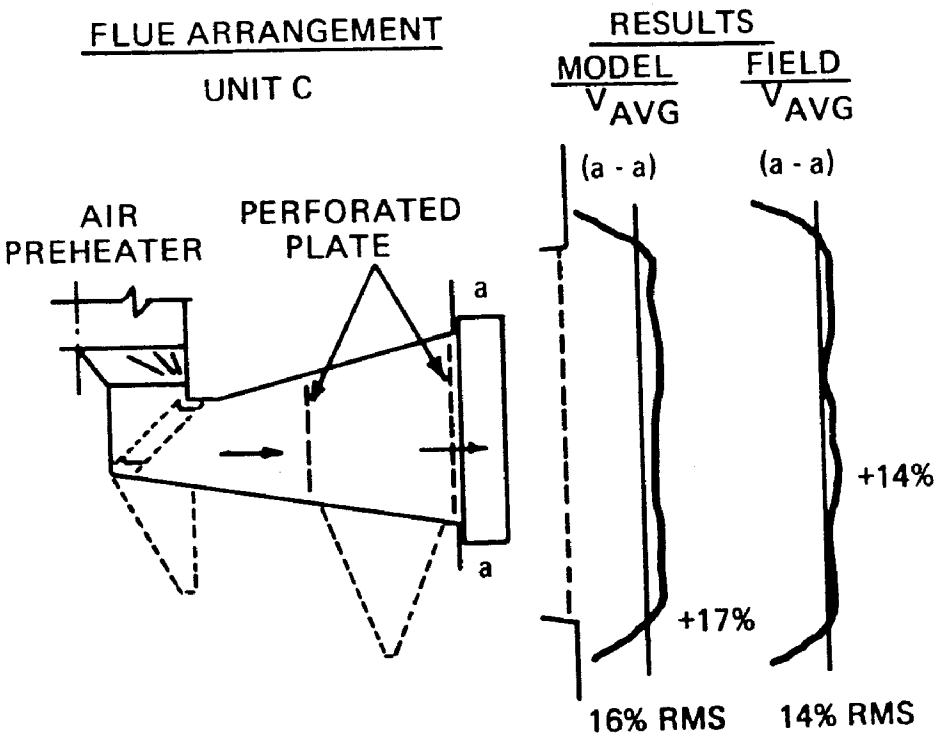

Figure 16. Field/model correlation, Unit C

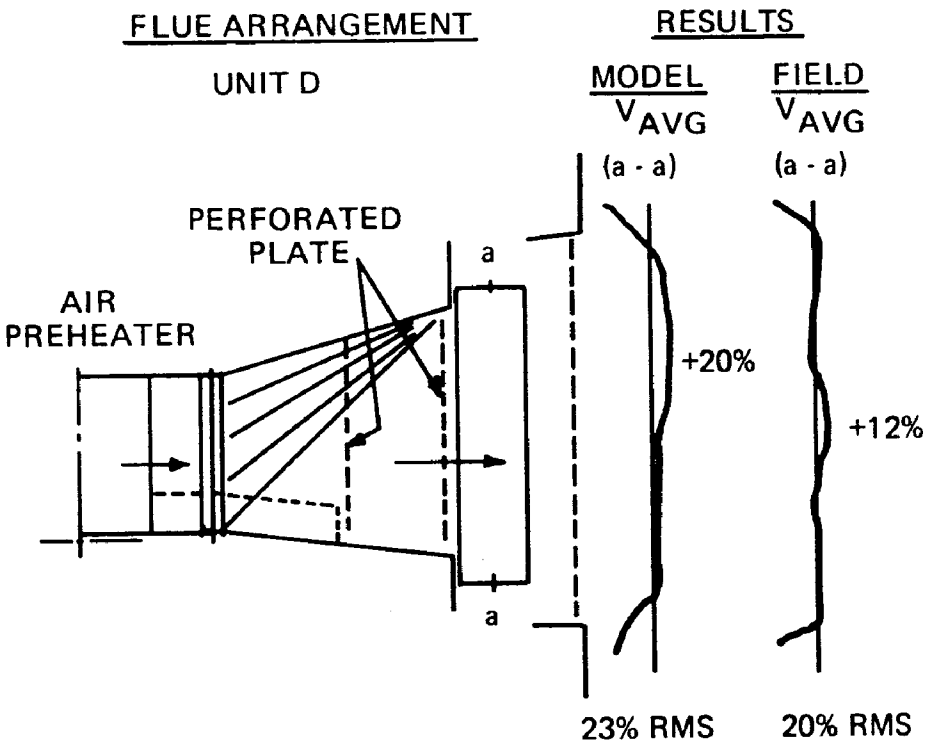

Figure 17. Field/model correlation, Unit D

inlet flues had cutoff outer corners. The Unit A flues would have to be rebuilt with square corners to accept the ladder vanes. The positioning of the inlet flue ladder vanes was then easily optimized in the model study. The model study also indicated that the floor of the lower precipitator inlet flue would be subject to potential fly ash dropout. It was, therefore, recommended that a dust blower be installed in this area to keep the flue clean.

A major problem that still remained was the correction of the lower precipitator outlet-gas-flow distribution. The upper precipitator outlet flue did not have to be changed once the inlet flue was corrected. The lower precipitator outlet was still experiencing both vertical (similar to Figure 10) and lateral (similar to Figure 2) gas-flow problems. It was again confirmed that this was the result of the close coupling of the lower precipitator to the i.d. fans.

Several approaches were made to solve this problem. It was finally noted that, during early prototype operation, the preferential flow through the lower precipitator had to be reduced by the installation of a third perforated plate in the lower inlet flue as shown in Figure 1. It was felt that, if this pressure-drop device could be placed at the lower precipitator outlet, a satisfactory decoupling of the i.d. fan and the precipitator could be obtained.

The installation of a perforated plate at the lower precipitator outlet was rejected. It was known that perforated plates installed at the precipitator outlet tended to plug due to the electrically grounded plate collecting the residual dust leaving the precipitator. Completely new rapping systems would have to be installed to keep this perforated plate clean. The solution was to install vertical structural shaped channels of standard dimensions, which would then form continuous vertical slots that would not plug. This satisfactorily decoupled the i.d. fan from the precipitator. The vertical slots were lined up with the center line of the precipitator ducts. The net free area required was found to be 15% open.

The net result of the above, i.e., the removal of the inlet flue flow biasing perforated plate, the installation of the inlet ladder vanes, and the installation of the 15% open "picket" fence at the lower precipitator outlet, produced a flow distribution slightly biased to the lower precipitator. The resultant corrected flow patterns are shown for the lower precipitator inlet in Figure 18 and the lower precipitator outlet in Figure 19. The gross improvement is noted when compared to Figures 10 and 11.

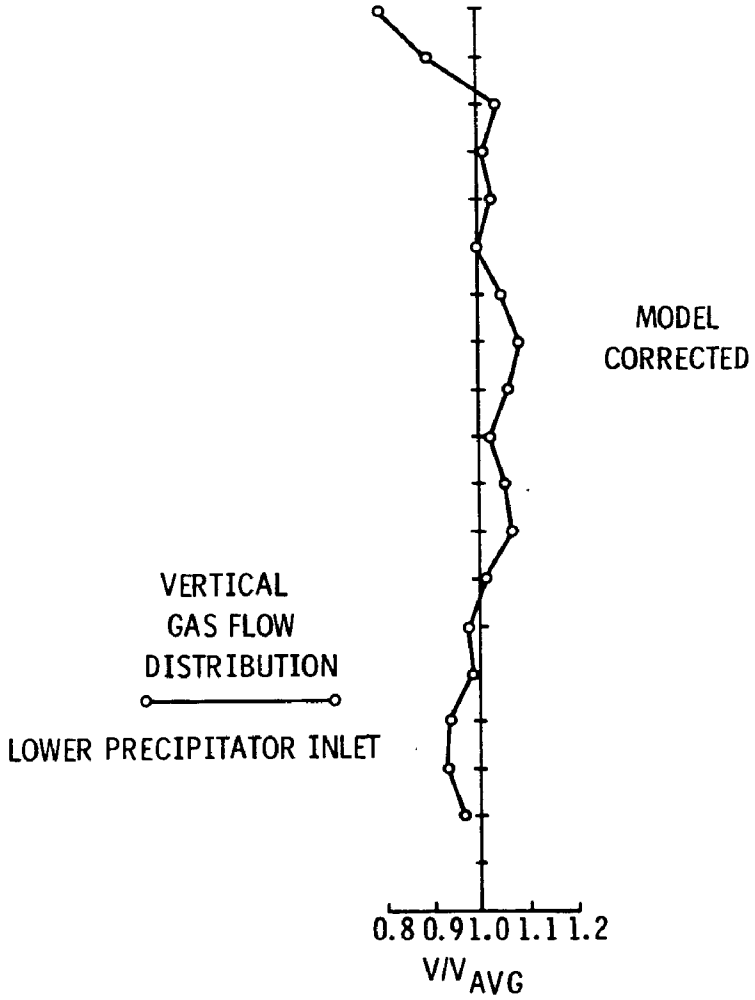

Figure 18. Vertical gas flow distribution lower precipitator inlet—model corrected

Further analysis of the corrected model study flow data produced the following results:

Lower Precipitator

Inlet: 10.6% rms Deviation
Outlet: 12.0% rms Deviation

Upper Precipitator

Inlet: 11.1% rms Deviation
Outlet: 9.2% rms Deviation

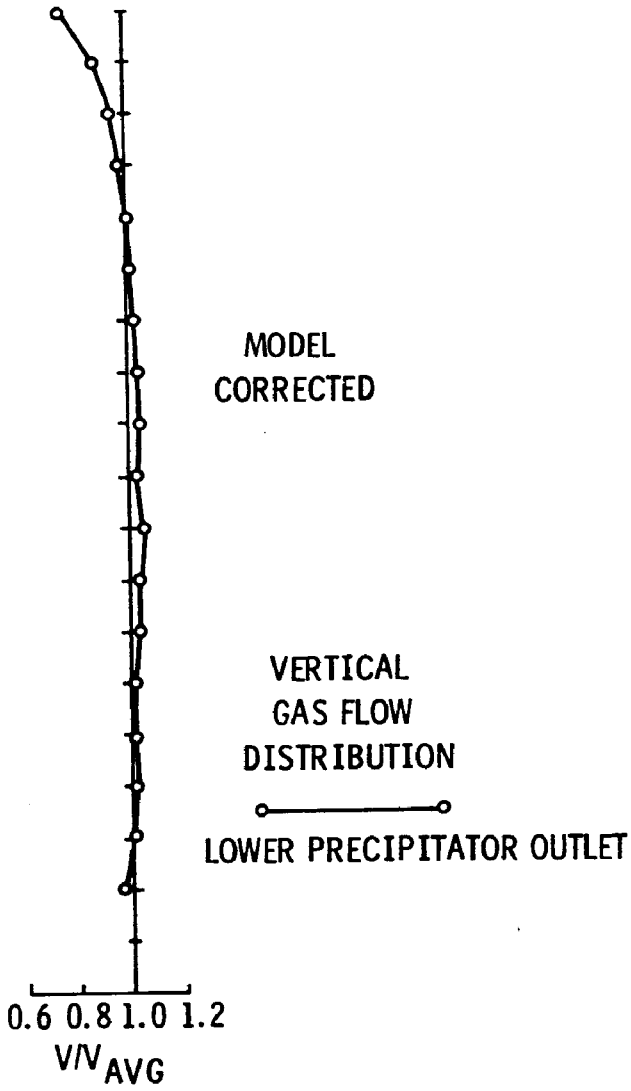

Figure 19. Vertical gas flow distribution lower precipitator outlet—model corrected

The data at the precipitator inlet was then evaluated in the same manner as in the detailed field velocity traverse to produce an anticipated precipitator efficiency of 99.76%. This represented a significant potential improvement over the originally indicated performance of 98.8 to 99.1%.

Because of these favorable results, the full-sized flues were modified in accordance with the model recommendations. The corrections were first made on Unit B, including the complete rehanging of the inlet perforated plates. Once this was completed, a fans-running walk-through inspection was

performed. None of the high-velocity jets or hopper sweepage of Figures 5, 6, or 7 could be found. Due to system load requirements, and the confidence levels established with model study results, a field follow-up velocity traverse was not performed.

The actual dust loading performance test was taken on Unit A. The unit had been permitted to operate for at least one month before testing. Three performance tests were run. All three tests produced equal to or better than required dust collection efficiencies. The final testing contractual agreements, the testing details, and analysis of these tests will be the subject of a subsequent paper.

CONCLUSIONS AND RECOMMENDATIONS

This paper has presented various techniques which can, and should be used in evaluating troubled precipitator installations. If poor gas-flow distribution is a contributing factor, the extent of the problem can readily be evaluated and appropriate remedial actions taken.

It is the authors' recommendation that gas-flow distribution be studied before the installation is built. Studies should be performed to produce standard flue designs for various repeating system geometries and precipitator flow quality requirements, i.e., 25% rms deviation for 98% efficiency or 15% rms deviation for 99+% efficiency. Any significant deviation from the standard flue geometries should be evaluated in a properly performed model study. The cost of a model study, during the design stages of a system, is significantly less expensive than finding and correcting the problems in the field. It has been our experience that correcting an existing installation can cost roughly ten times the cost of performing a design-stage model study.

It has been shown, through the study reported here, that model studies and the full-sized installations produced results which correlate well within the range of experimental error. This is a basic result of the design philosophies used in these systems. The cost of space in a power or industrial plant precludes that the flue be designed on aerodynamic, boundary layer or Reynolds' principles. The major draft losses and flow patterns are created primarily as a function of the typically cramped space allotted to the installation. The important factors in a model study are, then, complete

and accurate reproduction of the system geometry being studied and the proper modeling of the system flow fields and pressure gradients entering and leaving the model. Most of the time, this requirement is easily satisfied by including major system components (heat exchangers, fans, etc.) ahead of and following the model.

The present IGCI flow requirements are statistically reproducible, over the range of three standard deviations, by a 25% rms deviation flow field. It is the position of the authors that today's very large, very high-efficiency precipitator installations require gas-flow qualities significantly better than 25% rms deviation.

Precipitators of the 98.5% level and up to the 200 MW size can be, and have been sized, using the higher values of the precipitation rate "w". In the present instance, the design value of "w" was 0.163 m/sec (0.52 ft/sec). In actuality, the operating w was more like 0.04 m/sec (0.14 ft/sec). As shown in this paper, gas flow is quite important if the prototype systems are to achieve their design values of w. Further, as installations increase in size, and increase in collecting electrode height, it is even more important to achieve better than IGCI gas flow quality.

In further support of this position, an analysis by McCain et al.[5] shows that, as efficiency requirements move into the 99.5 to 99.9% levels, the design value of w must be made smaller to compensate for the more difficult collection of the rapidly reducing median particle size with increasing efficiency. This is partly due to the increased susceptibility of the very small particle sizes to gas-flow maldistribution and turbulence. A more general treatment of the problem is given by White.[6]

The results presented here, and in the previously quoted paper[3], show that rms deviations of 10 to 15% are achievable. It is, therefore, recommended that a minimum gas-flow quality, over the full height of the collecting electrode, of 15% rms deviation, be made part of present and future precipitator design requirements. If the gas flow is to be evaluated on the basis of the flue opening height, 10% rms deviation should be required.

REFERENCES

1. Industrial Gas Cleaning Institute Specification EP2. July 1973.

2. Report of Gas Velocity Distribution Field Test Unit B. Boyle Engineering Laboratories Co., Inc. August 8, 1972.

3. Burton, C. L., and R. E. Willison. Application of Model Studies to Industrial Gas Flow Systems. (Paper 59-A-280, presented at American Society of Mechanical Engineers Annual Meeting. Atlantic City. November-December 1959.) 9 p.

4. Report of Gas-Flow Tests in a Three Dimensional Model of the Precipitators and Precipitator Inlet and Discharge Flue Gas Ducts, Unit B. Boyle Engineering Laboratories Co., Inc. March 20, 1973.

5. McCain, J. D., K. M. Cushing, and W. B. Smith. Measurement of the Fractional Efficiency of Pollution Control Devices. Southern Research Institute. (Paper 74-117, presented at Air Pollution Control Association 67th Annual Meeting. Denver. June 9-13, 1974.)

6. White, H. J. Industrial Electrostatic Precipitation. Reading, Mass., Addison-Wesley, 1963. Chapter 8.

HOT-SIDE PRECIPITATORS

A. B. Walker
Research-Cottrell, Inc.
Bound Brook, New Jersey

ABSTRACT

Demands for high performance and reliability of electrostatic precipitators for collection of fly ash from low sulfur fuels have led to rapid escalation of sizes and uncertainties in sizings of cold-side precipitators. This has led to utilization of the so-called "hot-side" precipitator.

The underlying concept of hot-side precipitation is familiar to all attendees: avoidance of the necessity to operate the precipitator under high resistivity conditions. Data on in-situ measurements of resistivity of low sulfur fuel ash, as well as performance parameters of a number of operating installations, will be reviewed. These data will demonstrate the reduced sensitivity of hot-side precipitator sizing to fuel conditions. Other advantages of hot-side precipitators will be discussed.

Operating experience with hot-side precipitators has focused on structural problems which are peculiar to the larger, higher temperature installations. The nature and solution of these problems will be discussed.

General comparative economics of hot-side and cold-side precipitators as they relate to fuel properties will be reviewed.

The most widely adopted strategy for compliance with sulfur oxide regulations has been the use of low sulfur fuel. Thus, sulfur trioxide, one of the principal natural surface conditioning agents that we have traditionally relied upon to provide conductivity for good precipitator operation, has been drastically reduced. The result is that the chances of encountering high resistivity conditions in precipitators located at the cold end of the air preheater have also sharply increased. As an introduction to the panel discussion, I have been asked to present the so-called hot-side electrostatic precipitator approach to this problem.

Broadly speaking, we can take two courses: tailor the controllable design and operating conditions in the precipitator to control or avoid back corona while operating under high resistivity conditions; or tailor the operating conditions of the system in such a way as to avoid high resistivity conditions.

The first course involves continued use of the precipitator in its traditional location downstream of the air preheater. This approach involves some attempt, either by direct measurement or inference from operating data, at quantifying resistivity so that current densities and collected dust layer thicknesses can be adjusted to avoid back corona. And, since this approach involves operation at temperatures in the range of 270°F-350°F, where surface conduction is the dominant mechanism, it involves also a very detailed consideration of all of the variables which can affect surface conduction. This is an exceedingly complex situation, for it requires not only a knowledge of the relationship between many more fuel constituents than we have had to consider in the past, but also knowledge of the frequency of occurrence of these constituents. Thanks to the work of many here today, we are beginning to understand more clearly the role of many of these constituents, and that very small quantities can have a significant influence. But we still have to go some way before we can state with confidence that we can predict the occurrence of these constituents over the life of the plant. The result is that this alternative very often leads us to what might be termed a "worst case-brute force approach;" select the worst possible combination of fuel conditions one might encounter and design the precipitator to operate under these conditions. This typically means low current density, high rapping density and/or intensity, and high specific collecting area. In short, very large, expensive precipitators.

The alternative approach, of tailoring the operating conditions of the system to avoid high resistivity operation, involves three sub-approaches: chemical conditioning of the fuel prior to or during combustion, chemical conditioning of the flue gas and/or fly ash after combustion, and temperature conditioning. In spite of its evolutionary nature, chemical conditioning should remain a viable alternative. There is too prevalent a tendency today to categorically reject this option. This is not in the interest of most cost-effective solution of difficult fuel situations. Others later today will discuss chemical conditioning.

With regard to temperature conditioning, we again have two alternatives: avoid high resistivity by further reducing precipitator operating temperatures, or increase temperatures and rely on electronic rather than surface conduction. Both must be considered feasible and have been used, but the former requires operation close to the dewpoint, greatly increasing the chances of condensation, corrosion, and fouling in the precipitator, air heaters, and ash removal system. Variation in fuel sulfur, which affects acid dewpoint, is a further complicating factor which, again, leads to a worst case design philosophy; this puts a limit on how far down one can go in temperature to avoid high resistivity.

So, we deduce that a most attractive alternative is the hot-side precipitator. The critical questions are whether high resistivity will really be avoided, and whether the elimination of high resistivity will outweigh the disadvantages of increased gas volume, reduced peak field strengths, and increased complexity of the thermal/structural design which go along with higher temperatures.

From the process point of view, the balance appears clearly on the side of hot precipitators. Many in-situ resistivity measurements on a variety of low sulfur fuels, some of which are considered the worst from a cold-end collection standpoint, have clearly supported expectations from fundamental considerations and demonstrated the reduced frequency of occurrence of high resistivity at typical air heater inlet temperatures (see Figure 1).[1] This data is from 13 cases of source and fuel combinations. Boiler sizes ranged from 15 MW to 800 MW, with 9 of the 13 cases being PC units. Fuel compositions were all under 0.91% sulfur, but covered a wide range of other critical variables such as ash content, Na_2O, SiO_2, CaO, and MgO, which have been shown to affect mass emission concentration and collectibility characteristics

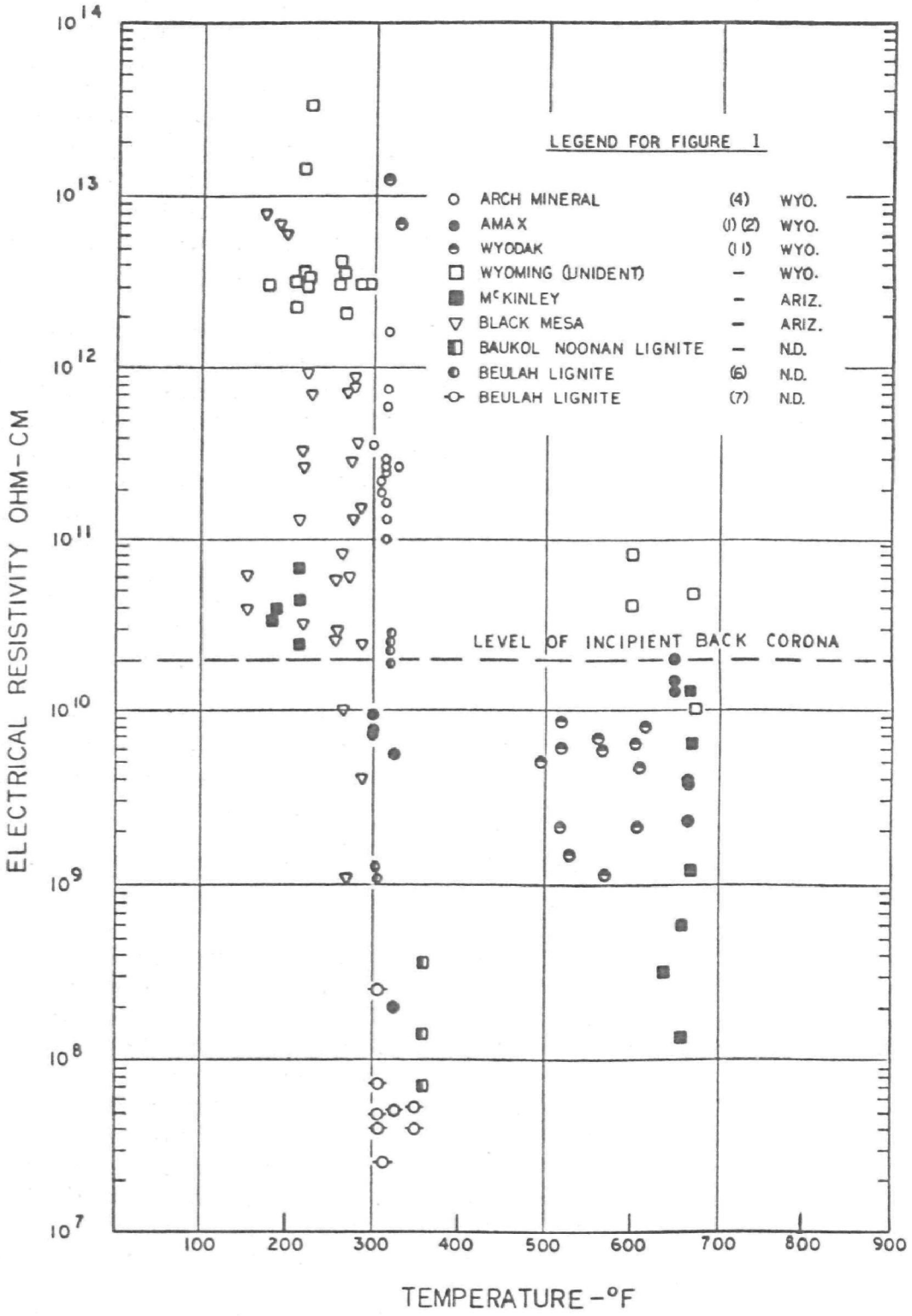

Figure 1. In-situ bulk electrical resistivity measurements on a variety of western fuels

of the particulate. The cases, therefore, represent a rather broad cross section of low sulfur fuel operating situations. The effect of temperature increase in lowering and converging values of resistivity is clearly evident. At 300°F, the values ranged over seven orders of magnitude; while at temperatures above 600°F, the range is limited to three orders of magnitude and 90% of the measurements were below levels where one would expect to encounter back corona.

This reduced sensitivity to fuel is further substantiated[2] by about 100,000 MW-months of operation on some 40 hot-side precipitators where design performance levels well in excess of 99% have been achieved consistently, and where required specific collection areas at the 99% level fall in a relatively narrow band between about 220 and 290 sq ft/1000 acfm (Deutsch-Anderson emv 7.5-10.5 cm per sec) (see Figure 2). This compares to typical sizings for the same fuels and efficiencies on cold-end units, which range from 400 to over 1000 sq ft /1000 acfm (Deutsch-Anderson emv of 3.0 cm per sec to over 15 cm per sec).

The typical hot-side precipitator does, as one would expect, operate at lower voltages. But, if properly designed, it operates at much higher current densities; it is characterized by relatively high power density, stable, current limited operation with sparking usually confined to inlet sections where dust concentrations are high. Thus, the process expectations derived from fundamental considerations have been largely realized.

The practical operating characteristics of the large majority of the hot precipitator installations have been good. Discharge electrode life seems equivalent to or better than cold-end precipitators. Material is easily rapped off collecting electrodes because adhesion forces are much reduced at higher temperatures. High temperature operation has reduced the occurrence of hopper buildup.

If any weakness has emerged in hot-side precipitators, it has had to do more with structural design than process aspects. Actual failure to the gas tight integrity of the shell on a few of the larger, higher temperature units has occurred. These failures have been traced to inadequate provision for differential thermal expansion between the lower shell and support structure, and between the precipitator shell and roof housing. These problems have been recognized and have been, or are being corrected with provisions for differential movement of the precipitator on its support structure, proper insulation, and adhering to proper design stresses, particularly in regions where some temperature gradients cannot be

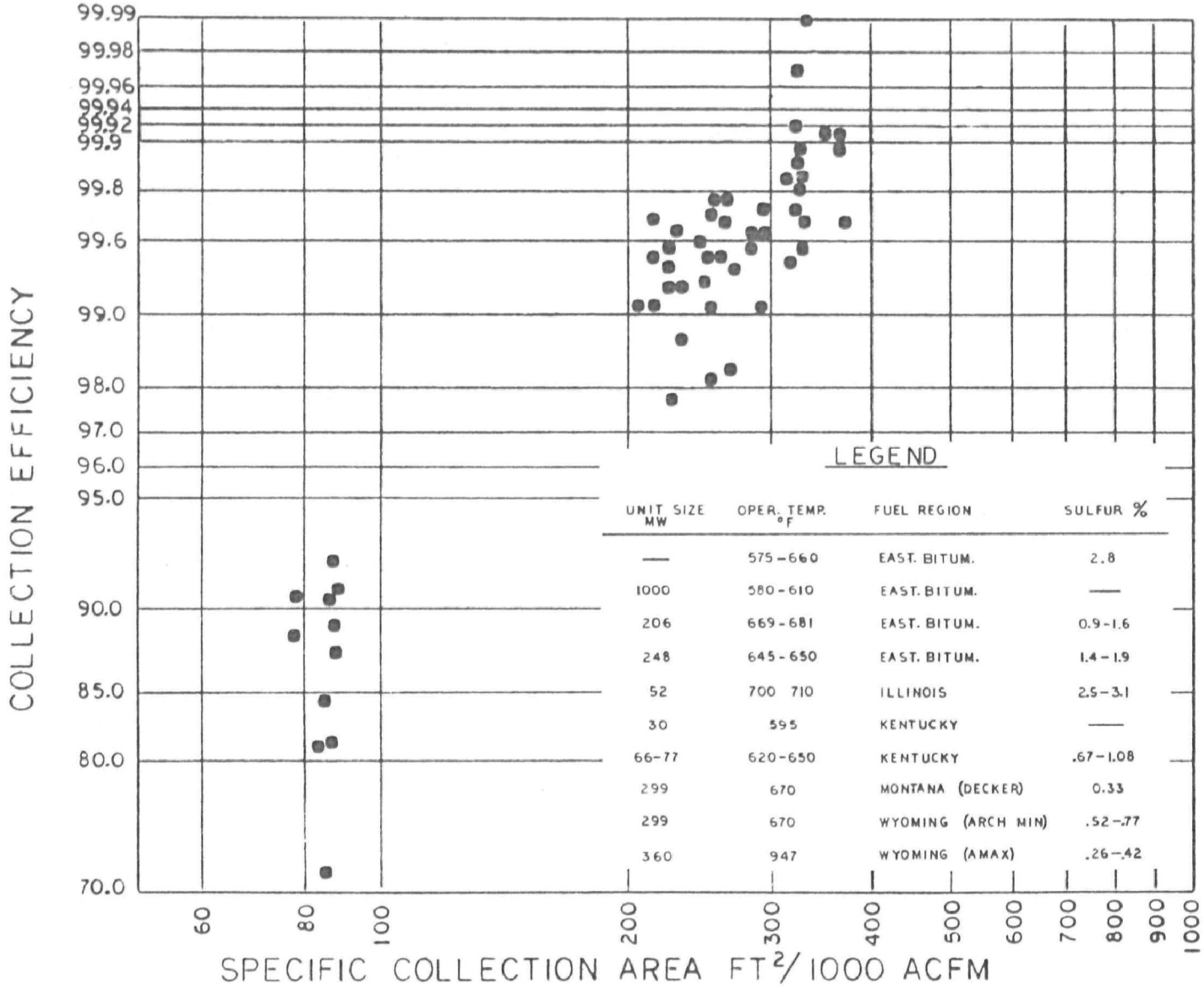

Figure 2. Actual performance on hot electrostatic precipitators to date

avoided. It should be emphasized that these problems have occurred in a small minority of installations, but this experience points up the need for careful thermal/structural designs.

The overall implications of our experience can be shown by a generalized comparison of costs per kW for hot and cold precipitators (see Figure 3). The data for hot-side precipitators includes extra costs associated with high temperature material and design stress considerations. These run about 8%-15%, depending on temperature. The cold-side data is based upon the range of sizings that would be expected under the same variety of fuels. The upper boundary would be typical of a most difficult ash; i.e., resistivity 10^{13} ohm-cm and low power density operation to minimize back corona. The lower would be typical of an optimum situation; i.e., resistivity 10^{8} to 10^{9} ohm-cm and operation at maximum power density. It should be understood that these are overall average costs to the operator on an erected flange-to-flange basis, and may vary ±20%. But they are sufficiently accurate to illustrate the point: if one can achieve the ideal resistivity situation at air heater outlet temperatures, the cold precipitator will be the more economic choice. On the other hand, if the uncertainty of the fuel supply over the life of the plant suggests that operation under high resistivity conditions cannot be avoided, which is the majority of the situations today, then we find ourselves designing cold-side precipitators for some anticipated worst case. This puts us on the upper boundary of the cold precipitator cost curve and, clearly, the hot-side precipitator is more economical.

One can sum up the hot-side case as follows:

1. From a high efficiency standpoint, hot-type precipitators are highly reliable and can be designed with a much higher degree of certainty than cold precipitators because the probability of encountering high resistivity operating conditions is sharply reduced.

2. Hot-type precipitators have an economic advantage over cold-end units under situations where the cold-end units must be designed for operation under high resistivity conditions.

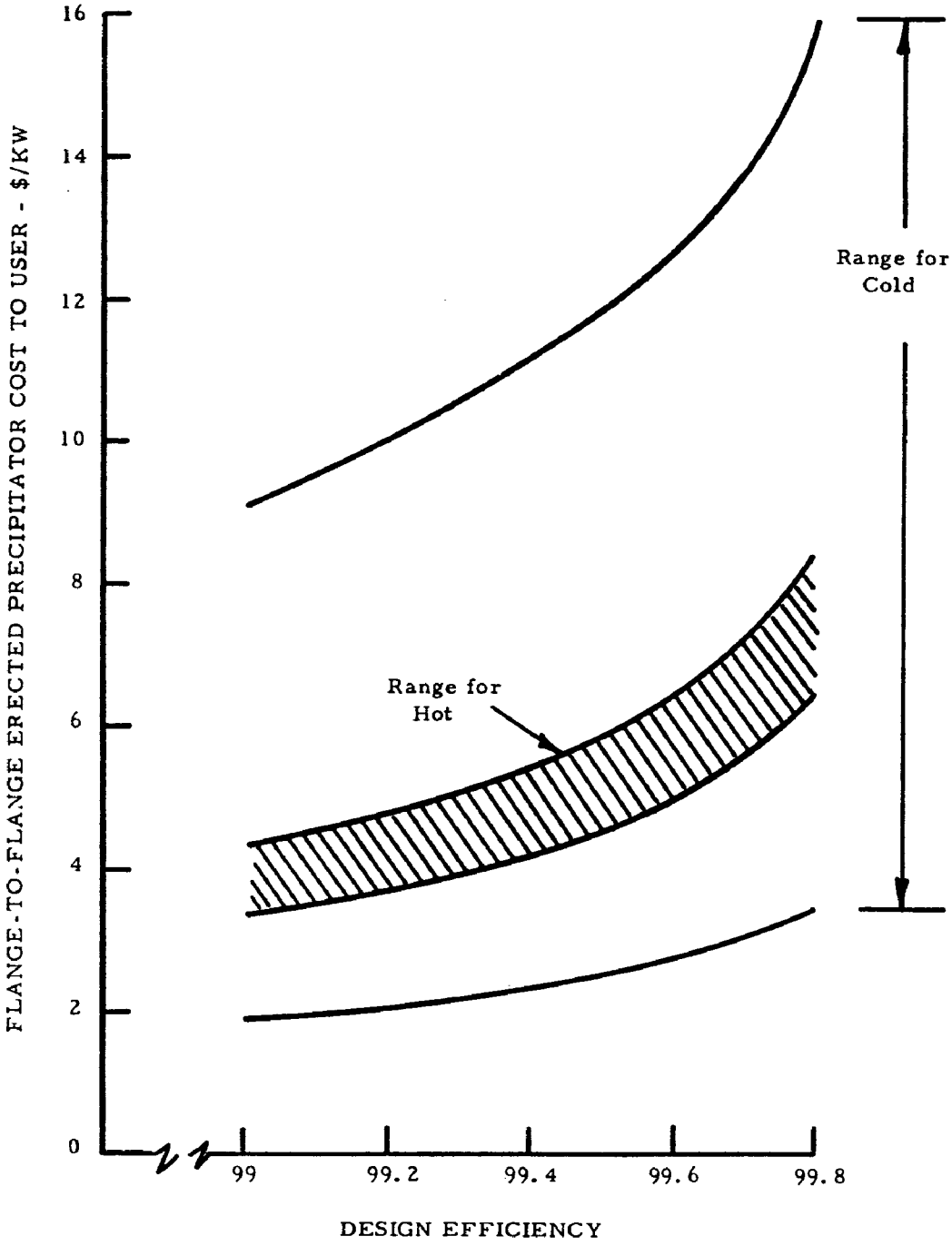

Figure 3. Approximate cost to user for flange-to-flange erected precipitators

Based upon typical bituminous coal firing at 25% excess air and heat rate of 10,000 Btu/kW

3. Hot-type precipitators appear to have a performance reliability advantage over cold precipitators in high resistivity situations because of stable, non-sparking electrical operation and ease of ash removal.

Thus, hot-side precipitators are the most cost-effective solution to reliable high performance in situations where uncertainty exists regarding occurrence of high resistivity at air heater outlet temperatures.

REFERENCES

1. Walker, A. B. Characteristics and Electrostatic Collection of Particulate Emissions from Combustion of Low-Sulfur Western Coals. Research-Cottrell, Inc. (Paper 74-11, presented at Air Pollution Control Association 67th Annual Meeting. Denver. June 9-13, 1974.)

2. Walker, A. B. Experience with Hot Electrostatic Precipitators for Fly Ash Collection in Electric Utilities. Research-Cottrell, Inc. (Presented at American Power Conference. Chicago. April 29-May 1, 1974.)

"COLD-SIDE" ELECTRIC PRECIPITATORS FOR HIGH-RESISTIVITY FLY ASH REQUIRE DIFFERENT DESIGN PHILOSOPHY

S. Matts
AB Svenska Fläktfabriken
Sweden

It has become common to talk about electric precipitators in terms of European versus American design. They both contain similar amounts of design effort, but differ in design goal. The Europeans have designed for high reliability and low operating costs to the disadvantage of considerable extra initial expenditure. The Americans have successfully designed for lowest possible initial cost. The two different design goals reflect customer preferences. Recent legislation has increased the American interest in the European design.

To explain the European reasoning (at least several brands of it), it is necessary to start with a refresher of some of the underlying principles. I will assume, however, that the basic precipitator geometry is known.

CORONA CURRENT

The corona current is produced in the corona discharge along the discharge electrodes. This discharge is not continuously distributed, but occurs locally in a very large number of corona spots along the electrodes. Only when the number of spots is very large can we talk about an evenly distributed discharge. Assume a bus-section of discharge electrodes, where we increase the applied voltage from zero. At a certain voltage, the corona onset voltage, the first corona spot will occur somewhere within the section. At this moment, there is current available to charge the dust in

only one single spot in the entire section. Naturally, the collecting efficiency of this section is very low. As the voltage is increased more and more corona spots appear and the collection efficiency increases rapidly. Soon we reach a voltage, where the number of corona spots is so large that we can start talking about an evenly distributed discharge. So far the improvement in efficiency of the bus-section has been dramatic. Further improvement is obtained with higher voltages due to space charge effect and increased field strength, but the rate of improvement is very much lower. This explains the knee in the precipitator performance versus precipitator current curve, A in Figure 1. Normally a current density of 0.1 mA/m^2 (10 $\mu A/ft^2$) is ample to pass the knee. Curve B shows correspondingly the required collecting area to reach a specific efficiency. Once above the knee, doubling the current density may decrease the required collecting area by something like 25% with a corresponding cost reduction between 10 and 15%.

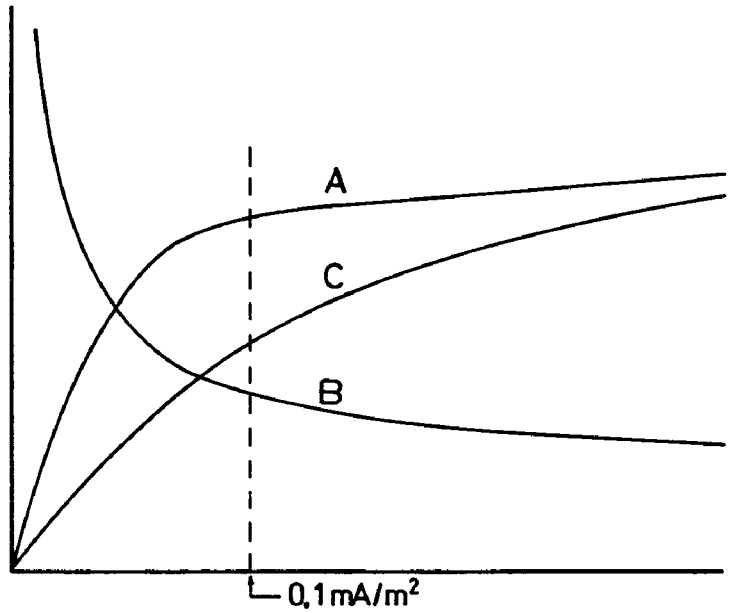

Figure 1. A, C. Precipitator efficiency vs. current
B. Required size vs. current

The higher levels of power input can usually be obtained only at greatly increased spark rate between the electrodes. The accompanying spark erosion increases the failure rate and therefore the required maintenance. The capitalized cost of

extra maintenance, power and electric hardware during the life of the plant easily exceeds the initial saving in precipitator size. As is the experience with all industrial equipment, it is not good economy to design the components for long-term operation near their theoretical limits.

CURRENT DISTRIBUTION

The steep part of curve A in Figure 1 was said to be due to uneven current distribution. This distribution can also be uneven for reasons other than low current density. Both poor discharge electrode design and uneven dust deposits will have this effect. Then curve C will be the result. This increases the current requirements and power cost. A good electrode design and efficient rapping is essential.

DUST RESISTIVITY

Figure 2 shows a collecting electrode with a deposited dust layer. Current flows from the discharge electrodes towards the collecting electrode and through the dust layer. An electric field is built up in the dust layer. Ohm's law states that

$$E = R.I$$

where E = field strength, kV/m
R = dust resistivity, ohm-meters
I = current density, A/m^2

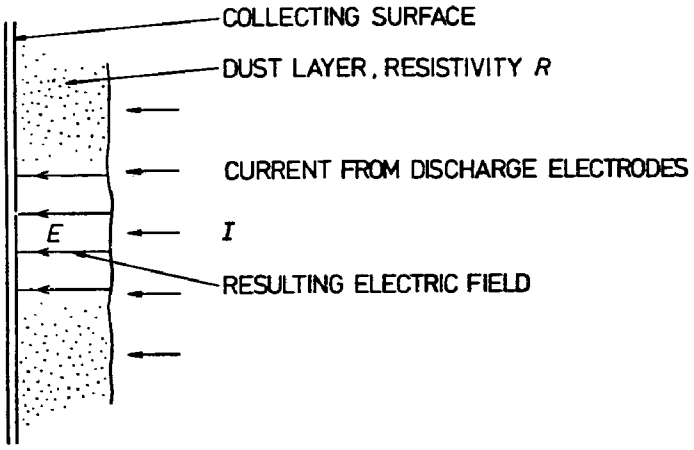

Figure 2. Field strength in dust layer

High field strength is obtained when the resistivity is high, but it is also obtained when the current density is high. The field forces hold the dust layer towards the collecting plate. Therefore high field forces require very high rapping accelerations to dislodge the dust.

By increasing the field strength, a point is soon reached where the dielectric strength of the dust layer is exceeded. A discharge occurs in the layer emitting large quantities of positive ions into the space between the electrodes. This is known as "back-corona". The positive ions reduce the useful negative charge acquired by the dust particles, and they therefore impair the efficiency of the precipitator.

Back-corona starts locally in spots where the current is higher than average. The positive ions attract more negative current from the corresponding parts of the discharge electrodes in a cumulative manner, and so "steal" from other parts already low in current. With poor current distribution back-corona starts at lower average current. Back-corona makes poor current distribution worse, a second way in which it impairs the precipitator efficiency.

The resistivity varies with the temperature and gas conditions. Figure 3 shows a typical characteristic. Curve A shows resistivity as a function of temperature measured in completely dry air. Curve B is typical of the result in stack gases. Below a certain temperature, the dust absorbs increasing amounts of moisture and therefore, the resistivity decreases quickly. Thus, in practice, the peak resistivity usually occurs around 150°C (300°F), i.e., close to normal operating temperatures after the air heater.

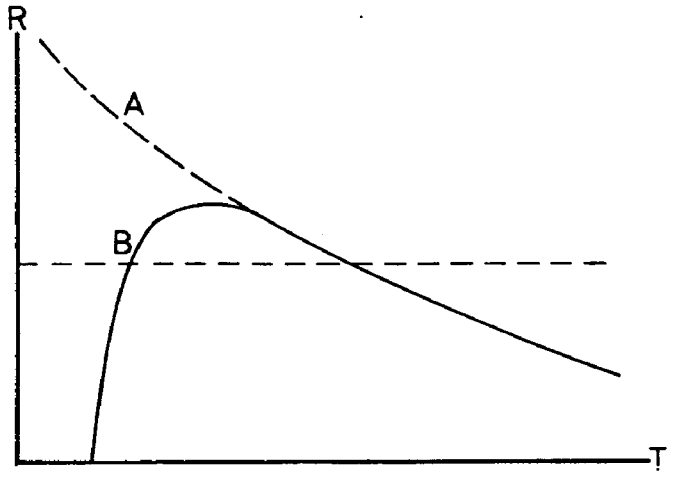

Figure 3. Resistivity R vs. temperature T

Curves A and B in Figure 4 show the normal precipitator performance as a function of temperature for a couple of different fly ashes, where resistivity is not a problem. The drop-off at high temperatures is due to increased gas viscosity and decreased dielectric strength of the gases. Now, if the dust resistivity is a problem, the precipitator performance deteriorates in the temperature range where peak resistivity occurs as indicated by Curve C. The severe deterioration at D is caused either by extremely high resistivity (not yet encountered by us in fly ash), or by poor current distribution (caused by poor electrode arrangement or rapping). In this case, operation at the high temperatures before the air heater is more successful. Several low sulfur coals from western USA and Canada have been tested in pilot scale precipitators. These tests indicate smaller total investment with precipitators on the cold side.

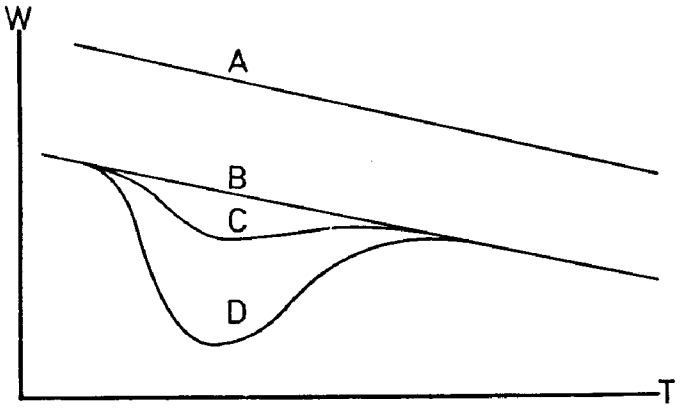

Figure 4. Migration velocity W vs. temperature T

SUMMARY: REQUIREMENTS FOR SUCCESSFUL HIGH RESISTIVITY OPERATION

1. Size the precipitator for the low current density range.

2. Select the electrode arrangement with the best current distribution.

3. Efficient rapping is needed to maintain the good current distribution.

Figure 5 shows a typical casing. It is designed for restricted deflection under load rather than fully utilizing the allowable stress in the material. This is to make sure that the electrode alignment remains perfect during all operating conditions. To avoid thermal distortion, the casing rests on the supporting structure via roller bearings or permanently lubricated slide plates. Non-lubricated slide bearings are not to be relied upon.

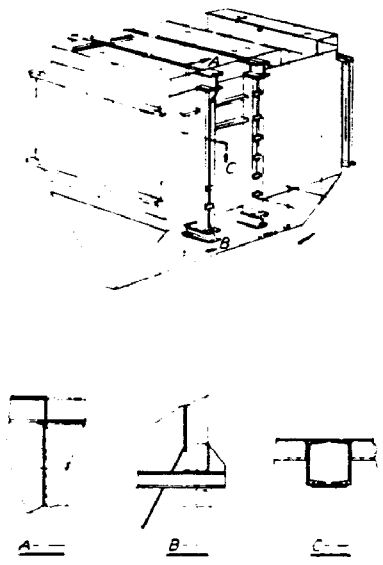

Figure 5. Precipitator casing

Figure 6 shows a typical collecting electrode arrangement. It is a curtain of narrow plate strips. Each strip is folded along the edges for mechanical stiffness. Each curtain is rapped by a separate hammer of the tumbling type. The rapping energy is transmitted to each of the strips via a rapping bar. Here are some reasons for the strip curtain design:

1. The manufacturing tolerances of each strip do not combine to produce excessive distortion of the curtain as a whole.

2. Since each strip can move relatively free of the others, thermal transients will not distort the curtain.

3. The rapping energy is introduced at several points on the curtain. The energy is transmitted to all parts of the curtain without undue concentration in a singular entrance point. The measured minimum rapping acceleration of a 3.6 m by 12.5 m (12 ft by 41 ft) curtain is 150 G's at the far corner! Acceleration rather than deflection is obtained. Therefore, the dust cake is not broken, only effectively dislodged. The dust reentrainment is kept low.

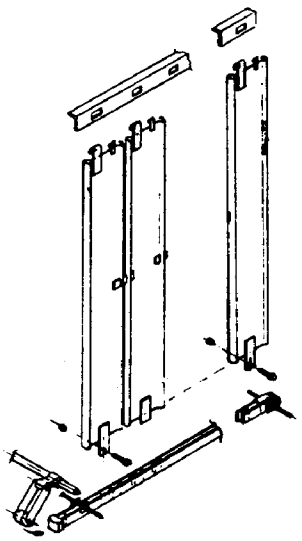

Figure 6. Collecting electrode plate strip curtain

The discharge electrodes are held in a framework, where top, bottom and intermediate frames are solidly connected together as shown in Figure 7. The whole frame is suspended from four insulators placed on the casing roof. It is so rugged that you can climb on it without moving it out of alignment. All framework swinging is eliminated. Due to the intermediate frames, each separate discharge electrode can be kept short. Therefore, electrode vibrations are limited. The rapping energy from the tumbling hammers is efficiently distributed due to the rigid framework and the tautness of the discharge electrodes.

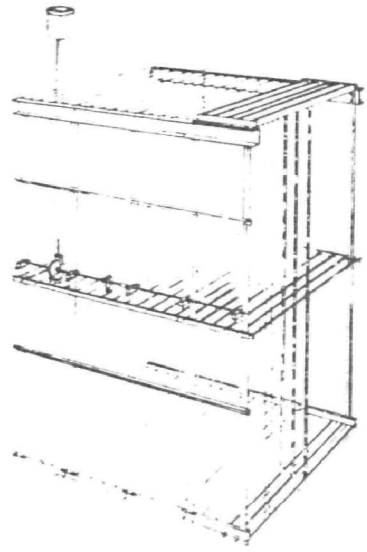

Figure 7. Discharge electrode frame work

The tumbling hammers are mechanically so rugged that they can be placed in the gas stream without problems. This means that the rapping forces can be applied at a point selected for best force distribution. The electrode supporting structures at the casing roof need not be flexible or strengthened to transmit rapping forces.

The dust concentration in the gases is obviously much higher in the front part of the precipitator than in the rear. The current distribution is influenced by the dust concentration. Where it is high, the current is suppressed. Therefore, it is necessary to subdivide the electrodes into several fields, separately energized. Dust buildup, however, is much more detrimental to the current distribution than is the dust concentration. Using the rigid discharge electrode frame-work, and its efficient rapping, larger bus-sections can be allowed. Therefore, European precipitators are usually less sectionalized than American. Unfortunately, this only partly decreases the price difference.

Many processes (e.g., cement and metallurgical plants) require the use of hot precipitators (up to 425°C or 800°F). Many precipitator manufacturers therefore have experience with hot operation. The choice between hot or cold pre-cipitators is not governed by temperature problems or adherence to a specific philosophy, but by necessity or economics. Using the European design, our experience is that the cold side precipitator is more economical than the hot side precipitator for American fly ashes encountered so far.

SURFACE RESISTIVITY AND THE CHEMICAL COMPOSITION OF FLY ASH

Roy E. Bickelhaupt
Southern Research Institute
Birmingham, Alabama

ABSTRACT

Resistivity was determined for a group of well characterized ashes representing both Eastern and Western coals. Data were taken between 60°C and 250°C in an environment of air containing approximately 9 volume percent water. Chemical transference experiments were conducted for two ashes having substantially different chemical compositions.

Chemical analyses of the transference specimens revealed a pronounced migration of alkali metal ions toward the negative electrode. It was observed that the surface resistivity was inversely proportional to the concentration of these ions and that the iron concentration influenced particularly the participation of potassium.

Surface resistivity is sensitive to the chemical composition of fly ash because the alkali metals serve as charge carriers. The conduction mechanism is probably analogous to that of glass. This viewpoint is compatible with the usual empirical observations regarding the effect of certain parameters on resistivity; for example, the interaction between ash and the environment.

INTRODUCTION

Electrical resistivity is one of the critical parameters influencing the collectability of fly ash by electrostatic precipitation. This paper discusses research designed to acquire additional knowledge about the surface conduction process. The pragmatic objective of this research is to ultimately obtain sufficient information so that resistivity might be predicted from the measurable chemical factors and conditioning agents might be objectively selected.

When resistivity is plotted on a logarithmic scale versus the reciprocal of absolute temperature, a curve resembling an inverted V results, upper curve, Figure 1. The high temperature leg is a straight line, illustrating the volume resistivity. It has been demonstrated[1] that volume resistivity is dependent on an ionic conduction mechanism in which sodium ions serve as the principal charge carriers. For a given ash chemistry, the volume resistivity is dependent on ash layer porosity, field strength, and temperature.

The low temperature leg represents the surface resistivity of the ash. If one interprets the surface and volume resistivities as a pair of parallel resistors, it becomes apparent that the low temperature portion of the curve joining the two legs (A to B) is governed by surface conduction. On the high temperature side of the maximum resistivity, the curve (B to C) is a resultant of both surface and volume conduction. For ashes having similar size distribution, packing density, and chemical composition, the surface resistivity is mainly dependent on the interaction between the environment and the ash. The environmental factors include temperature and the concentrations of gaseous and condensed phases in contact with the ash. Temperature influences the relative concentration of water vapor, the existence of a condensed phase and the reactivity between the ash and the environment.

It has been generally accepted[2] that surface conduction occurs by an electrolytic or ionic mechanism dependent principally on the physical and chemical adsorption of certain species on the ash surface to produce a conducting film. This implies that conduction is governed by the electrolysis of the adsorbed species and that the component ions serve as charge carriers.

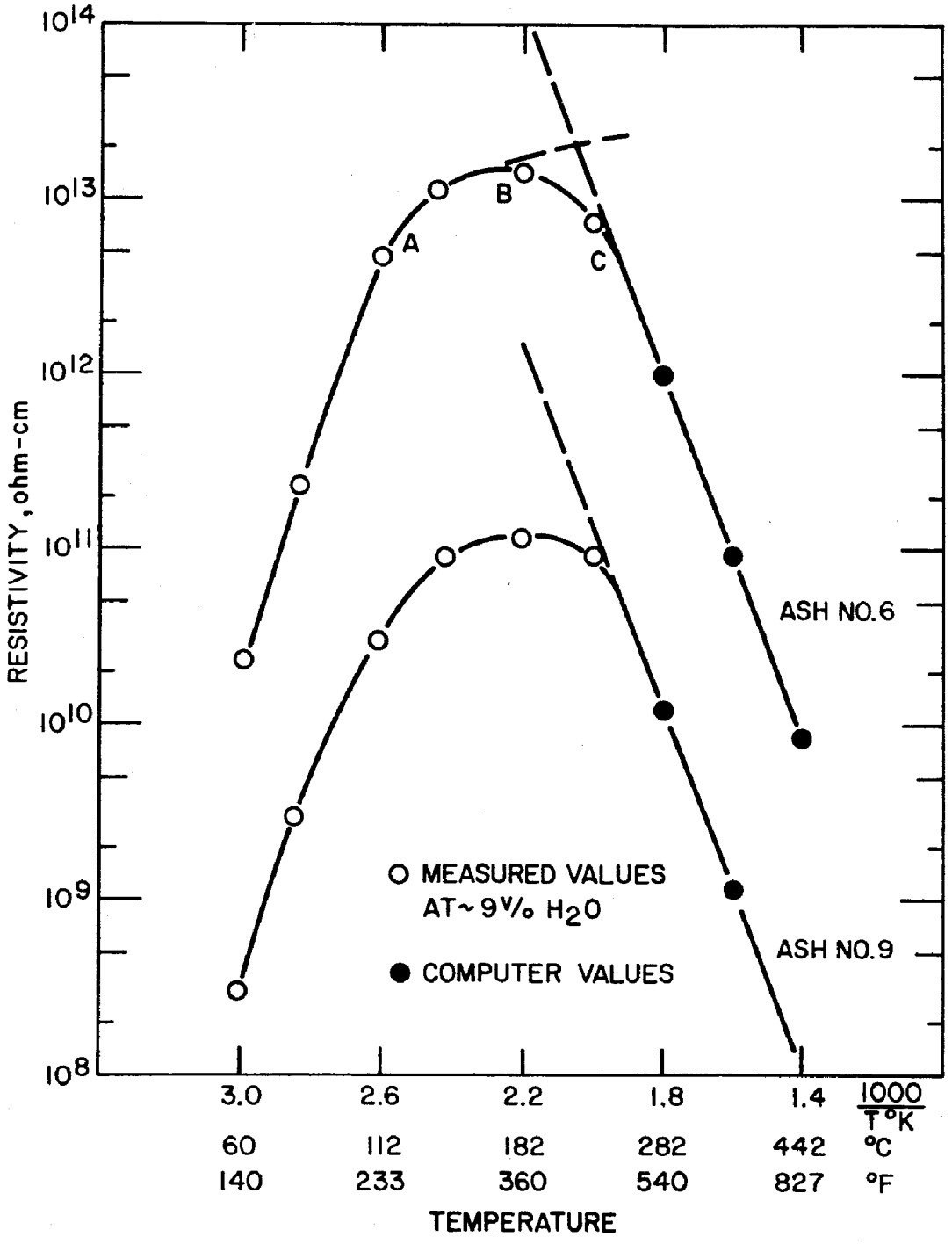

Figure 1. Typical resistivity data as a function of reciprocal absolute temperature

It is herein proposed that surface conduction takes place by an ionic mechanism in which the alkali metal ions serve as the principal charge carriers. This emphasizes the role of ash composition with respect to the concentration of alkali metals and the inherent chemical durability of the ash. The role of the environment is not lessened in importance in that these factors control the release of the alkali metal ions.

This paper attempts to substantiate the above hypothesis and illustrate the role of the ash composition regarding the magnitude of surface resistivity.

PROCEDURE

Commercially produced fly ashes used in this research were selected to be both representative of Eastern and Western coals and to yield a significant variation in the concentration of the various elements. The chemical compositions are shown in Table 1 in weight percent as oxides. These ashes and the resultant resistivity specimens were also characterized with respect to particle size, density, porosity, shape, surface area, and crystalline content. It was found that the ashes principally consist of heterogeneous, spherical, glassy particles having a mass-median diameter of 8 to 30 microns. The resistivity specimens possessed a porosity of 50 to 70% and presented a surface area of about 1000 to 3000 cm^2/cm^3 of ash.

Resistivity determinations were made using an ASME PTC 28 apparatus[3] housed in an environmentally controlled chamber. An atmosphere of air containing about 9 volume percent water was used. Under a voltage gradient of about 500 V/cm, six or seven data points were obtained between 60 and 250°C using ascending temperature.

Chemical transference experiments were conducted in a manner generally similar to that for resistivity determinations except that the temperature was held at 60°C, a voltage gradient of about 2000 V/cm was used, and the tests were operated continuously for several hundred hours. The details regarding the procedures and equipment used in this work appear elsewhere.[4]

Table 1. CHEMICAL ANALYSES OF ASHES IN WEIGHT PERCENT

Ash No.	Li_2O	Na_2O	K_2O	MgO	CaO	Fe_2O_3	Al_2O_3	SiO_2	TiO_2	P_2O_5	SO_4[a]	Loss on ignition
1	0.02	0.32	3.10	1.04	2.62	20.50	19.60	46.40	1.69	0.60	1.56	2.10
2	0.01	0.35	2.36	1.66	3.72	16.10	17.80	43.30	1.27	0.36	0.93	10.30
3	0.03	0.38	3.34	1.29	1.04	9.70	25.90	49.90	1.98	0.32	0.29	4.40
4	0.03	0.20	0.26	5.76	22.60	4.25	21.00	38.80	1.19	0.32	0.97	0.33
5	0.01	1.84	0.20	12.75	31.00	11.20	14.80	22.00	0.60	0.39	2.19	0.41
6	0.01	0.25	0.89	1.88	11.10	3.71	23.60	55.60	1.56	0.14	0.22	0.74
7	0.04	0.33	3.88	1.57	0.77	10.01	27.50	51.40	1.79	0.32	0.25	1.50
8	0.04	0.29	2.69	0.98	0.64	9.12	29.10	52.00	2.55	0.42	0.15	1.40
9	0.01	2.31	0.91	1.04	12.10	4.23	25.10	49.60	1.39	0.19	0.21	0.45
11	0.02	1.77	1.13	1.93	6.36	4.61	24.60	53.70	1.49	1.06	0.75	1.49
12	0.01	0.25	0.81	2.57	13.30	4.66	23.60	53.60	0.88	0.19	0.19	0.00
14	0.05	0.38	2.99	1.42	1.00	10.91	26.70	49.10	1.87	0.41	0.29	3.20
15	0.03	0.43	2.58	1.00	0.62	5.63	28.10	49.60	2.29	0.39	0.44	0.58
17	0.04	0.28	2.25	1.04	4.55	24.70	21.20	39.80	1.24	0.31	0.43	5.49
18	0.02	1.28	0.78	3.22	9.14	4.85	19.50	55.10	1.79	0.35	0.72	0.93
19	0.02	1.83	1.19	0.94	5.18	3.81	27.16	57.27	1.05	0.17	0.40	0.60
20	0.07	0.27	2.72	0.76	0.38	3.88	29.78	52.74	1.88	0.18	0.28	7.08

[a]Soluble sulfate.

RESULTS

TRANSFERENCE DATA

The objective of this study was to determine whether an alteration in chemical composition occurs in the direction of the voltage gradient, thereby suggesting the participation of certain ions in the conduction process as charge carriers. Two ashes having exceedingly different chemical compositions but similar values for resistivity were selected for the transference study. A portion of the ash specimen was chemically analyzed before the test. After the specimen had been subjected to a 2000 V/cm voltage gradient for several hundred hours at 60°C in an atmosphere of air containing 9 volume % water, the ash was removed in several layers parallel to each other and perpendicular to the voltage gradient. These individual layers of ash were also chemically analyzed.

The data given in Table 2 illustrate the results of these experiments. An obvious migration of alkali metal ions can be seen. The alkali metal concentration has formed a gradient consisting of a value less than the original concentration at the positive electrode to a value greater than the original at the negative electrode. This suggests that the positive alkali metal ions served as charge carriers and were transported to the negative electrode. This type of concentration gradient was not developed for the other species analyzed.

Utilizing the relative changes in alkali metal concentration and the quantity of electricity passed during the experiment, it was estimated that a major portion of the charge could be accounted for by the change in composition. These data do not define completely the overall conduction process nor do they prove that no other ions participate. However, the data offer excellent evidence that alkali metal ions are important in surface conduction and that an attempt to analyze surface resistivity as a function of ash chemistry is justified.

RESISTIVITY DATA

The type of resistivity data taken in this research is illustrated in Figure 1. The open circles represent the measured resistivity data from this research. The closed circles were determined from a computer program[5] designed to predict volume resistivity as a function of ash chemistry, temperature, and porosity. These two ashes were

Table 2. CHEMICAL ANALYSES OF TRANSFERENCE EXPERIMENTS IN WEIGHT PERCENT

	Li_2O	Na_2O	K_2O	Fe_2O_3	CaO	MgO	SO_4[a]
Before test, Ash 1	0.017	0.31	3.00	21.0	2.6	0.91	1.7
At positive electrode	0.016	0.26	2.88	21.4	2.5	0.87	1.7
Elevation 1	0.017	0.29	2.96	21.2	2.4	0.88	1.7
Elevation 2	0.017	0.38	3.11	21.4	2.6	0.86	1.7
At negative electrode	0.045	0.54	3.80	21.6	2.5	0.87	1.5
Before test, Ash 9	0.01	2.54	0.94	4.2	12.6	0.97	0.24
At positive electrode	0.01	2.53[b]	0.88	4.2	12.3	0.95	0.25
Elevation 1	0.01	2.39	0.90	4.2	12.4	0.93	0.26
Elevation 2	0.01	2.47	0.90	4.2	12.8	0.97	0.24
At negative electrode	0.01	2.70	0.97	4.2	12.6	0.98	0.24

[a]Soluble sulfate.

[b]Probable error.

selected to illustrate the typical data because they are almost identical in every characterization except that ash 9 contains considerably more sodium. Therefore, it can be suggested that the two order of magnitude difference in surface and volume resistivity was due to a one order of magnitude difference in sodium concentration alone.

To analyze the resistivity data in terms of fly ash composition, the maximum surface resistivity of each ash was selected from curves like those in Figure 1. This particular resistivity value was chosen to avoid the effect of the variation in sensitivity to water vapor pressure among the ashes. It is emphasized that the use of resistivity values taken at a particular temperature or water vapor pressure would not alter the result of this research.

The as-measured maximum or peak surface resistivity was corrected to a common specimen surface area prior to analysis as a function of composition. Ancillary experiments showed that the measured resistance of an ash was inversely proportional to the surface area of the specimen provided ash chemistry was invariant with respect to particle size fraction. All resistivity data were corrected to a surface area of 2000 cm^2/cm^3. The surface area per unit volume of ash was calculated as the product of the number of particles in a unit volume and the particle surface area determined from the mass-median diameter of the ash. The number of particles in a unit volume was calculated[6] from:

$$N = \frac{1 - P}{\alpha d^3}$$

where N = number of particles (in one cc of resistivity specimen)

P = porosity fraction (determined for the resistivity specimen)

α = shape factor ($\pi/6$ spheres)

d = particle diameter (mass-median diameter of the ash)

Other investigators have observed the relationship between surface resistivity and a parameter defining available conducting surface. Dalmon and Tidy[7] related decreasing surface resistivity to increasing specimen bulk density for a specific ash in which case the ash chemistry, theoretical or true density, and particle size distribution were constant.

Since the transference experiments at 60°C indicate the alkali metal ions serve as charge carriers, one would intuitively expect an inverse correlation between surface resistivity corrected to a common surface area and the summation of the three alkali metal atomic concentrations. This correlation failed, indicating the influence of an additional parameter. The situation was clarified when the factors involved were independently examined.

The relationship between surface resistivities normalized to a given surface area and the combined lithium and sodium concentrations is shown in Figure 2. The result was similar to that obtained in a study of volume resistivity[5]. The constructed curve ties together the data for groups of Western ashes having low and moderate amounts of lithium plus sodium. Since the transference experiment showed only a minor migration of potassium for the Western ash and Figure 1 showed the pronounced influence of sodium on resistivity, it is suggested that Figure 2 reasonably illustrates the effect of the combined lithium and sodium.

An attempt to rationalize the lower resistivities for the Eastern ashes based on high potassium content failed. When all the resistivity data in Figure 2 are normalized to a constant value of 0.4 atomic percent lithium plus sodium, and plotted against potassium concentration, the lack of correlation was obvious. This is shown in Figure 3 where the resistivity data for the Western ashes are clustered at one level of resistivity and the data for the Eastern ashes are spread over two orders of magnitude for a narrow band of potassium concentrations. Since the transference data for the Eastern ash indicated a substantial migration of potassium, Figure 3 presents an incongruous result. If one compares the general order of resistivity values for the Eastern ashes in Figure 3 with the chemical compositions of Table 1, it becomes apparent that the iron concentration may be important.

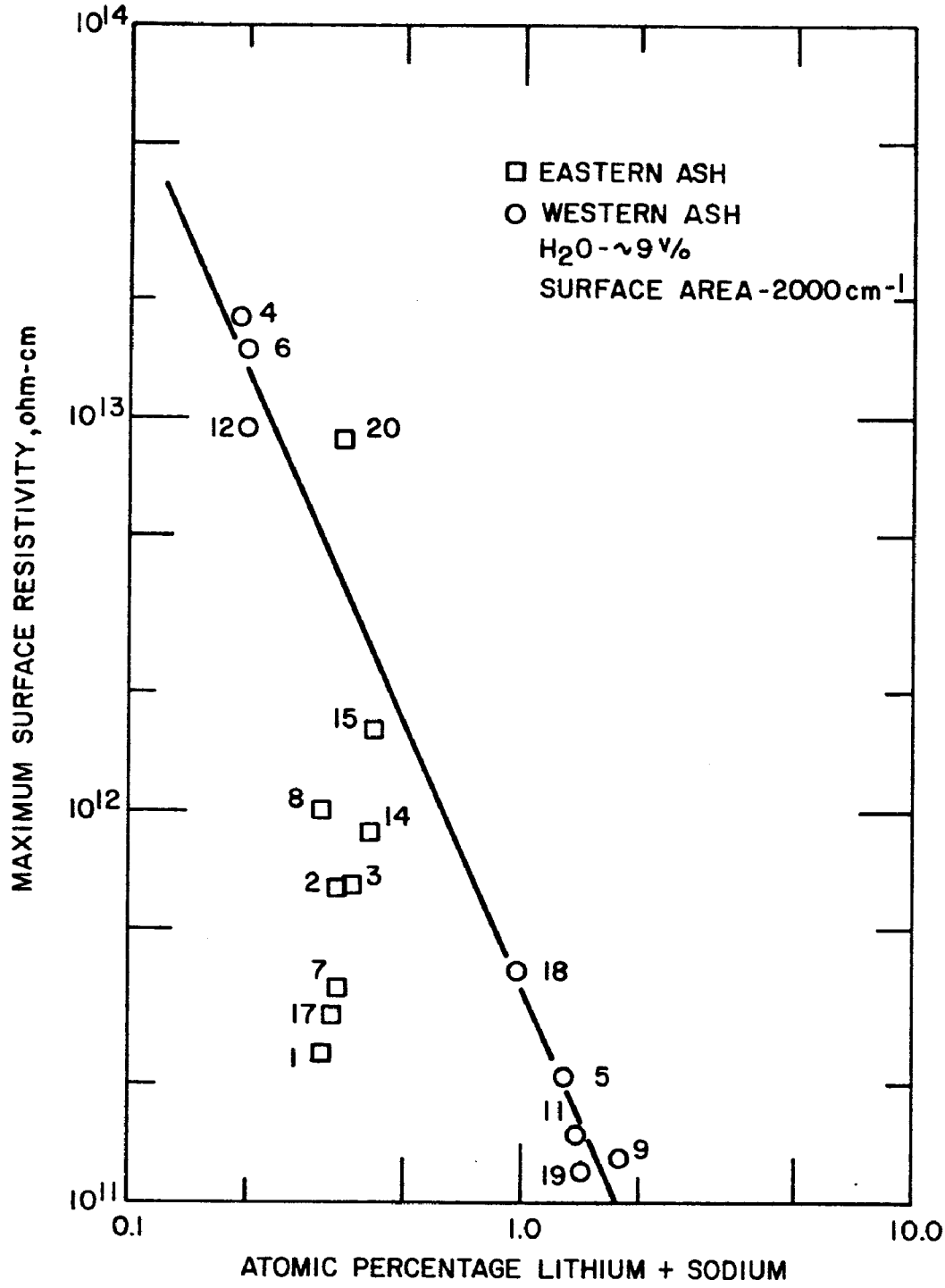

Figure 2. Maximum surface resistivity versus the combined atomic percentages of lithium and sodium

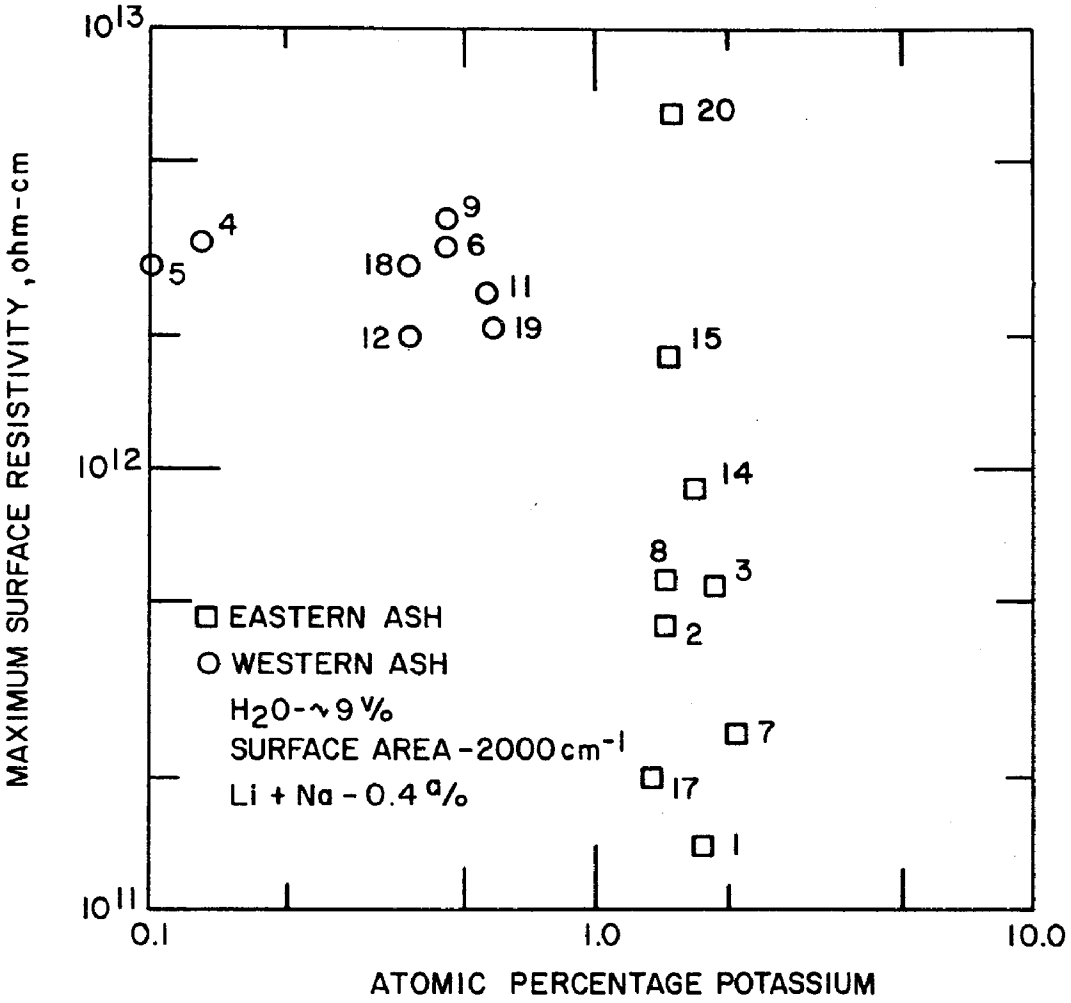

Figure 3. Maximum surface resistivity normalized to 0.4 atomic percent lithium plus sodium versus potassium concentration

In Figure 4 the resistivity data normalized to 0.4 atomic percent lithium plus sodium was plotted against the concentration of iron. A good pseudo-correlation is shown in that iron itself does not participate in the conduction process. It was deduced that iron affects the chemical solubility of the ash, thereby particularly influencing the release of potassium to serve in the conduction process. It was interesting to note that the Eastern ashes 20, 15, 14, 2 and 17 form a straight line. These ashes have similar compositions with the exception of iron content. Also, it was observed that ashes 5 and 7, deviating the most from the constructed line, have respectively the lowest and highest potassium concentrations.

In Figure 5 the relationship is shown for resistivities at constant lithium plus sodium concentration as a function of combined potassium and iron concentration. The correlation is reasonably good as shown; however, if one considers the individual data points with the proposed role of iron and ash solubility as a frame of reference, the correlation is excellent. First, the data for ashes 7 and 14 may represent the expected spread for this type of data. On the other hand, ash 7 contains the greatest amount of total alkali which may also affect ash solubility as well as supply charge carriers. Ash 1 contains by far the greatest amount of soluble sulfate for the high iron ashes and thereby may have lower resistivity due to increased reaction between ash and the environment. Ashes 15 and 20 contain a significant quantity of potassium but are low in iron, thereby limiting the release of potassium. Ash 5 containing a moderate amount of iron possesses very little potassium to support conduction.

DISCUSSION

SURFACE CONDUCTION

From the foregoing results, it has been observed that alkali metal ions migrate through the fly ash toward the negative electrode under the influence of an applied moderate voltage gradient and conditions suitable for surface conduction. This suggests that these ions have the role of charge carriers and therefore have a pronounced effect on the surface resistivity of the ash. Figure 1 illustrated the magnitude of the effect.

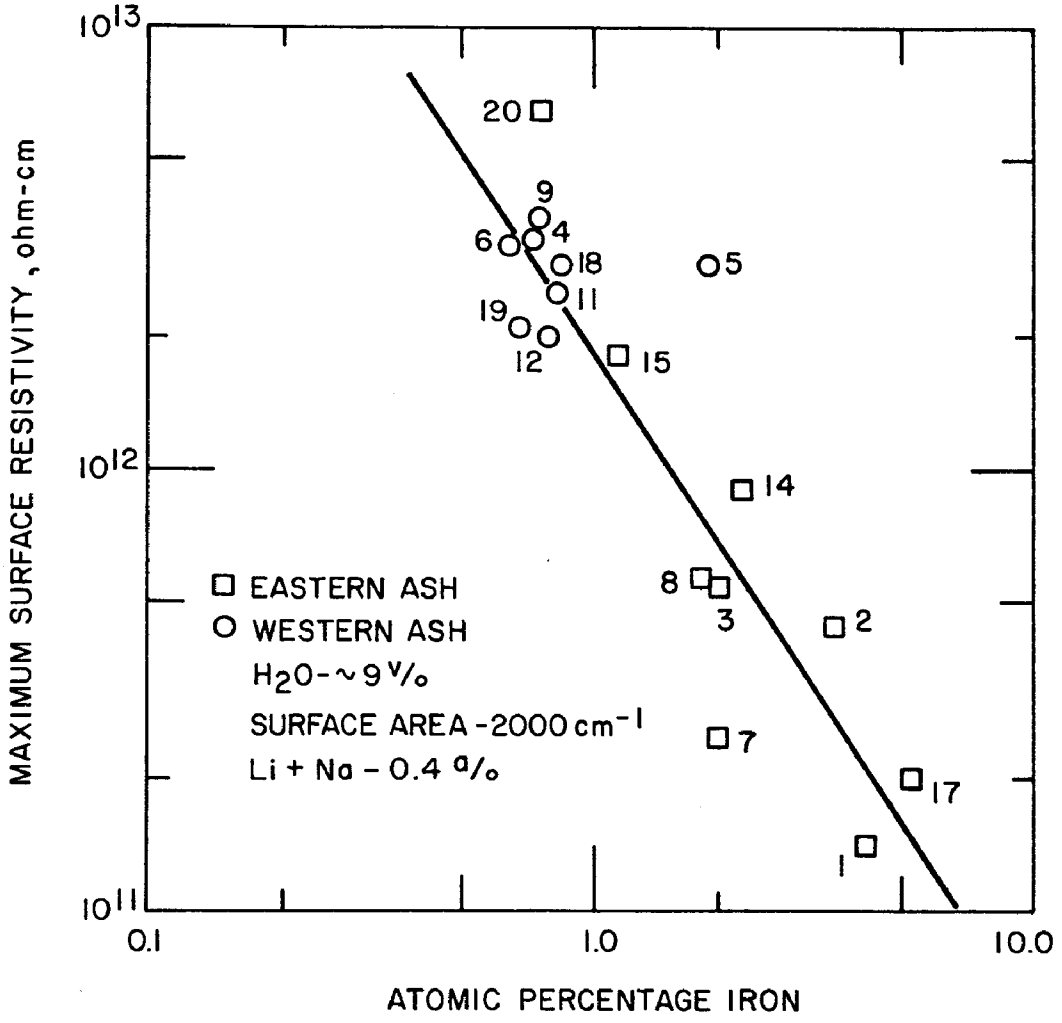

Figure 4. Maximum surface resistivity normalized to 0.4 atomic percent lithium plus sodium versus iron concentration

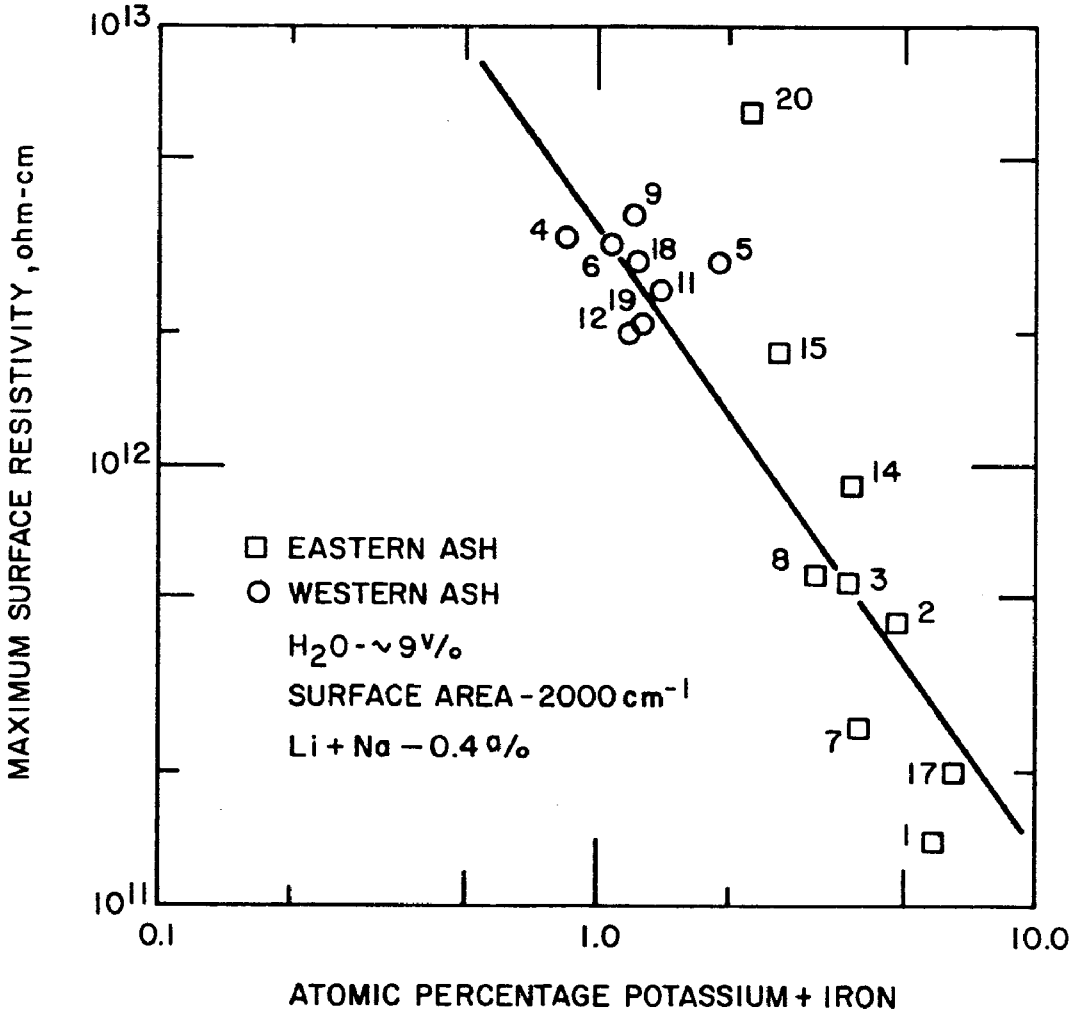

Figure 5. Maximum surface resistivity normalized to 0.4 atomic percent lithium plus sodium versus combined potassium and iron concentrations

Experiments[8] with fused accessory coal minerals have also illustrated the attenuation of resistivity due to the presence of alkali metals. In addition, Selle et al.[9] have demonstrated the decreasing surface resistivity of fly ash with increasing sodium concentration.

If the alkali metal ions serve as charge carriers, an inverse correlation should exist between resistivity and some measurement of the available carriers. Without knowledge about the degree of availability for the various carriers, the correlations were attempted using the total atomic concentrations of the alkali metal ions. A correlation between resistivity and the combined concentration of lithium and sodium was readily demonstrated. However, the effect of potassium alone or in combination with the other alkali metals was not detected. Since the transference experiments revealed a minor migration of potassium for one ash and a major contribution by this element for another ash, additional factors of potential influence were considered. It was deduced that the participation of the potassium as a charge carrier was related to the iron concentration of the ash. It is suggested that the presence of iron influences the reactivity between the ash and the environment promoting the dissolution of ash surface thereby releasing available potassium. Ancillary experiments have shown that the release of the alkali ions in the presence of water is enhanced for ashes of high iron content. Correlations between resistivity and iron concentration or iron plus potassium concentrations were obtained.

The following potential mechanism for the surface conduction of fly ash is suggested by this research. Under appropriate environmental conditions, the ash surface reacts with some agent (for example, water) capable of releasing alkali metal ions from the surface to act as charge carriers. The number of ions released is dependent on: the concentration of available alkali metal ions, the chemical durability of the ash in the hostile environment, the temperature, and the type and concentration of environmental species brought in contact with the ash surface. Tentatively, it would seem that the sodium is more readily released than the potassium. The latter apparently requires more vigorous interaction between the ash and the environment. Although this could be brought about by several of the above mentioned factors, the presence of iron probably by lowering the chemical durability of the ash has facilitated the participation of potassium.

The above discussion principally parallels the explanation of surface conduction for silicate glass. Since the main microconstituent in the ashes examined is a fused or glassy substance, this approach seems justified. Surface conduction for glass is usually explained[10] as an ionic migration of inherent alkali metal ions under the influence of an electric field. Clean, dry glasses containing monovalent cations have exceedingly high surface resistivity. In the presence of a humid environment, the resistivity decreases slowly at low partial pressures of water, and then rather rapidly as high relative humidity is approached. On the other hand, a very pure, clean siliceous glass maintains a high surface resistivity in a humid environment, indicating the importance of the alkali metals to the conduction process.

Glass containing alkali metal ions can react with water by ion exchange, forming metallic hydroxides (for example, NaOH) which further react with water forming mobile ions on the surface. This process is also in part responsible for the dissolution of glass in water. In addition to the ion exchange mechanism, the glass network itself can be destroyed by reaction with water as well as other agents. The dissolution of the network can permit the accelerated diffusion and migration of ions larger than sodium, for example potassium.

If the suggested surface conduction mechanism for fly ash is essentially correct, it places the role of ash chemistry in the proper perspective and allows one to more objectively consider problems regarding resistivity.

ESTIMATION OF RESISTIVITY

It is conceivable that the figures shown above can be used to estimate maximum surface resistivity from the chemical analysis of ash to anticipate problems for precipitators operating in the region of 150°C. Since the research represents an initial result, the utilization of these data should be approached with caution. Certainly the information will be improved upon with acquisition of additional laboratory data and field information.

A perusal of the individual data points, with respect to the correlations established, leads to the empirical suggestion that about 1.5 atomic percent iron is required to facilitate the participation of potassium in the conduction process. Using this observation, a correlation was developed between estimated resistivity values and

those determined in the laboratory. If the ash contained less than 1.5 atomic percent iron, the resistivity value from the curve in Figure 4 for the given iron concentration was determined. This resistivity value was located in Figure 2 at 0.4 atomic percent lithium plus sodium. The intersection of a line, through this point and parallel to the curve in Figure 2, with the ordinate of the known combined lithium and sodium concentration yielded the estimated maximum surface resistivity. For ashes containing more than 1.5 atomic percent iron, the same procedure was used except the starting point was Figure 5 using the combined iron and potassium concentration. The resultant relationship between estimated maximum surface resistivity and the laboratory measured values is shown in Figure 6.

The satisfactory correlation shown in Figure 6 was to be expected since the correlations illustrated in Figures 2, 4, and 5 were reasonably good. Keeping in mind that the resistivity numbers displayed are approximately an order of magnitude greater than those determined in the field, it was interesting to compare the available plant operating experiences with the estimated maximum resistivities. At the plants producing ash having an estimated resistivity $>1 \times 10^{12}$ ohm-cm, all had a high resistivity problem. No problem with high resistivity occurred at plants producing ash with an estimated resistivity of $<5 \times 10^{11}$ ohm-cm. Between these two resistivity values, problems have occurred.

On the positive side, this technique is tailored to a maximum value and ashes possessing wide variations in chemistry, including soluble sulfate, were used. Negatively, the method does not take into account: (1) the magnitude of the effect of water vapor pressure (which at the temperature considered is known to vary with the specific ash), (2) the variation in resistance related to surface area—however, this can be included, and (3) the effect of field strength on resistivity.

It is hoped that this technique of resistivity estimation will be improved upon and that the variation in sensitivity of resistivity to water vapor among ashes and the effect of field strength will be explored. It would be of interest to test the technique for a great many ashes for which all critical parameters are accurately available.

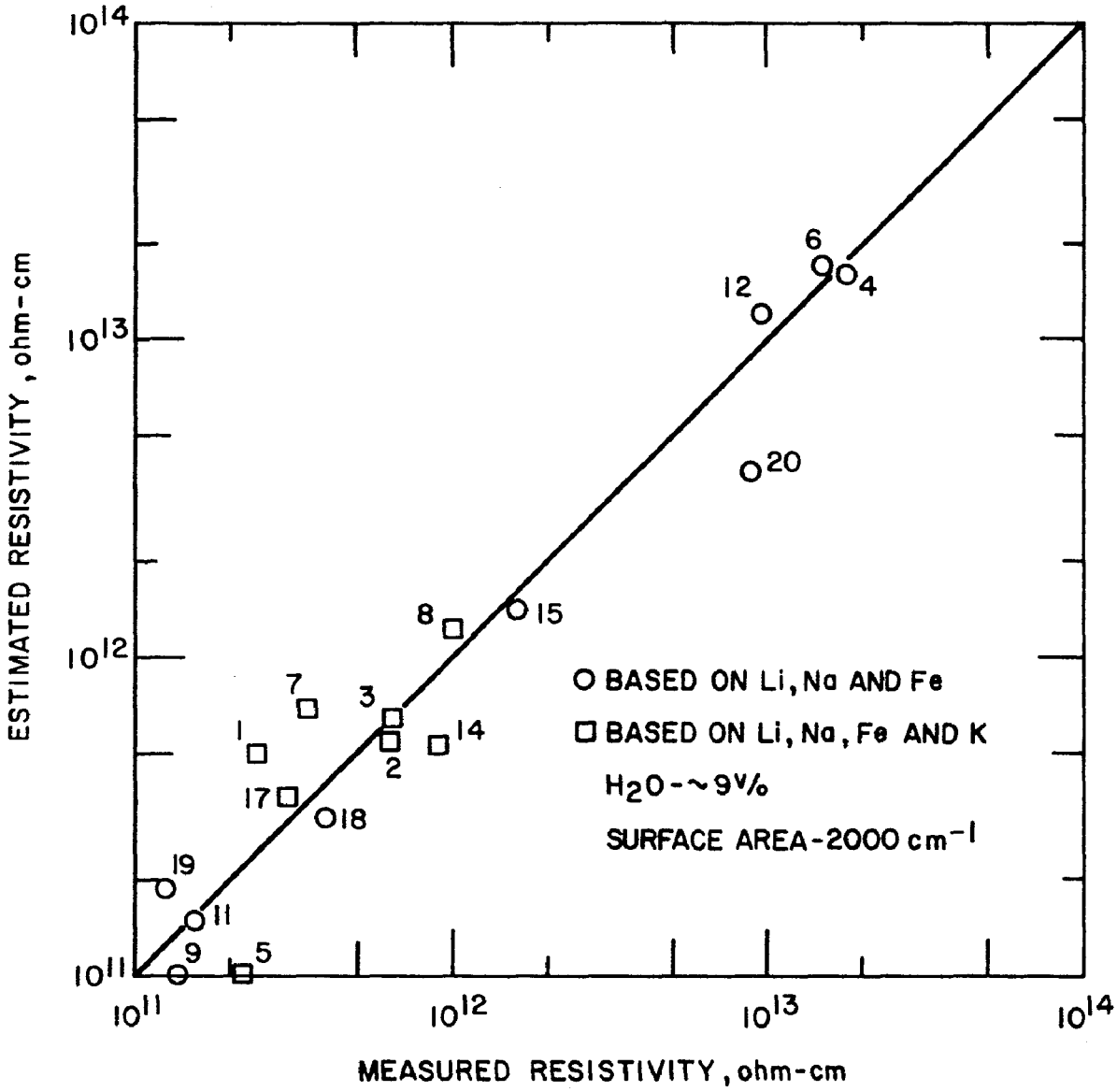

Figure 6. Correlation between estimated and measured maximum surface resistivity

ACKNOWLEDGMENT

The author gratefully acknowledges the sponsorship of this research by the Environmental Protection Agency, Research Triangle Park, North Carolina under Contract No. 68-02-1303.

REFERENCES

1. Bickelhaupt, R. E. Electrical Volume Conduction in Fly Ash. J. Amer. Pollut. Contr. Assoc. 24:251-255, March 1974.

2. White, H. J. Resistivity Problems in Electrostatic Precipitation. J. Amer. Pollut. Contr. Assoc. 24:314-338, April 1974.

3. Determining the Properties of Fine Particulate Matter. Power Test Code 28, American Society of Mechanical Engineers, New York, 1965.

4. Bickelhaupt, R. E. Investigation of the Role of Ash Chemistry in Surface Conduction. Southern Research Institute, Contract 68-02-1303, Environmental Protection Agency. Report to be issued.

5. Bickelhaupt, R. E. Influence of Fly Ash Compositional Factors on Electrical Volume Resistivity. Southern Research Institute for Environmental Protection Agency. Publication Number EPA-650/2-74-074. July 1974.

6. Dallavalle, J. M. Micromeritics. New York, Pitman, 1948. p. 133.

7. Dalmon, J., and D. Tidy. A Comparison of Chemical Additives as Aids to the Electrostatic Precipitation of Fly Ash. Atmos. Environ. (Oxford, England). 6:721-734, October 1972.

8. Dalmon, J., and E. Raask. Resistivity of Particulate Coal Minerals. J. Inst. Fuel (London). 46:201-205, April 1972.

9. Selle, S. J., P. H. Tufte, and G. H. Gronhovd. A Study of the Electrical Resistivity of Fly Ashes from Low-Sulfur Western Coals Using Various Methods. U. S. Bureau of Mines. (Paper 72-107, presented at Air Pollution Control Association 65th Annual Meeting. Miami Beach. 1972.)

10. Doremus, R. H. Glass Science. New York, Wiley, 1973. Chapters 12 and 13.

CONDITIONING OF FLY ASH WITH AMMONIA

Edward B. Dismukes
Southern Research Institute
Birmingham, Alabama

ABSTRACT

This paper presents the results of an investigation of the conditioning of fly ash with ammonia in electrostatic precipitators of power plants operated by the Tennessee Valley Authority. It focuses attention primarily on the mechanisms of conditioning encountered under the particular circumstances available for study. No effect of ammonia on the electrical resistivity of fly ash was evident. Instead, the effect of ammonia appeared to be an enhancement of the space-charge component of the electric field used for charging and precipitating particles of fly ash. In addition, a second effect appeared to be an increase in the cohesiveness of precipitated ash and a reduction in the quantity of ash reentrained during electrode rapping. Data demonstrating the value of ammonia conditioning for lowering the emission of fly ash during three precipitator studies are presented. Reasons for the ineffectiveness of ammonia conditioning during a fourth precipitator study are discussed. In conclusion, a discussion is given of the effects to be expected from ammonia conditioning under circumstances different from those investigated experimentally, particularly with ammonia as a conditioning agent for fly ash from low-sulfur Western coal.

INTRODUCTION

"Conditioning agents" have been used for many years to improve the collection of particulate substances in electrostatic precipitators.[1-3] Normally, the use of a conditioning agent is expected to overcome the problems associated

with high electrical resistivity. However, in some instances, conditioning agents may be of value in overcoming other problems stemming from adverse particulate properties, one possibility being an unacceptably low resistivity.

The best known conditioning agent is sulfur trioxide or the chemically equivalent compound sulfuric acid. In most applications, sulfur trioxide is effective through the process of lowering electrical resistivity by surface deposition along with water vapor on gas-borne particles. In conditioning fly ash in power plants, it is useful in supplementing the small quantity of sulfur trioxide that is produced naturally when low-sulfur coals are used as fuels.[4,5] On the other hand, in some power plants where the coal is not especially low in sulfur content and the fly-ash resistivity is not low enough to be detrimental to electrostatic precipitation, the use of sulfur trioxide as a conditioning agent may be of value in increasing the cohesiveness of fly-ash particles and thus minimizing reentrainment losses from the collection electrodes. Evidence of sulfur trioxide conditioning through this mechanism has been reported in a publication from the Central Electricity Research Laboratories in Great Britain;[6] further evidence of this effect has been obtained in recent studies by Southern Research Institute and will be presented in a forthcoming report.[7]

Other conditioning agents that are not as well known as sulfur trioxide include ammonia, ammonium sulfate, and sulfamic acid. Of these three compounds, ammonia has been most widely used in the utility industry. Experience with ammonium sulfate and sulfamic acid has thus far been relatively limited,[8] as illustrated by the information on sulfamic acid that is to be summarized in an accompanying paper.[9]

SUMMARY OF INVESTIGATIONS OF AMMONIA CONDITIONING

The value of ammonia as a conditioning agent was reportedly discovered in 1942 in efforts to deal with the high electrical resistivity of catalyst dust in the petroleum industry.[3] Research on ammonia as a conditioning agent for this material (a mixture of silicate minerals) was carried out for several years thereafter by J. F. Chittum of the Western Precipitation Corporation (now a division of Joy Manufacturing Company).[10] Chittum's research showed that ammonia was effective in lowering the resistivity of the catalyst dust;

it showed, on the other hand, that sulfur trioxide was relatively ineffective for this purpose. Chittum concluded that because the dust was acidic the surface collection of the basic conditioning agent, ammonia, occurred more readily than the collection of the acidic agent, sulfur trioxide.

The use of ammonia as a conditioning agent for fly ash in coal-fired power plants apparently began after the use in the petroleum industry had become an established practice. Some of the early trials of ammonia conditioning by electric utilities were made in Australia, and the use of ammonia in that country apparently continues today. In 1966, Watson and Blecher reported the results of preliminary trials of ammonia as a conditioning agent for the high-resistivity fly ash that is produced from coals in certain locations in Australia.[11] They stated that an acidic ash at the Tallawarra plant required extremely high concentrations of sulfur trioxide for efficient collection but only moderate concentrations of ammonia (15 to 20 ppm in the flue gas) for equivalent results. Watson and Blecher gave little information from which the mechanism of ammonia conditioning at Tallawarra can be deduced. Specifically, they did not report comparative resistivity values of the ash with and without ammonia conditioning. However, they did report electrical data for a pilot-scale precipitator that indicate a lowering of resistivity by ammonia. After the precipitation of unconditioned fly ash was begun on clean electrodes, marked decreases in voltage and increases in current (earmarks of a high-resistivity dust undergoing back corona) were recorded; then, after ammonia was introduced, a gradual reversal of the initial changes in voltage and current was observed.

In 1968, Baxter of the Koppers Company reported successful trials of ammonia conditioning in various power plants in the United States.[12] The reason given for trying ammonia conditioning was an unsuccessful trial of sulfur trioxide similar to that cited by Watson and Blecher. Baxter's data show that in some plants the resistivity of fly ash was lowered from high prevailing values (1×10^{12} ohm cm) and that in other plants the resistivity was raised from low values (5×10^{8} ohm cm), with the final resistivity being a more desirable value of the order of 1×10^{10} ohm cm in either event. Baxter's data also show consistent increases in precipitator power consumption and decreases in particulate emission as results of ammonia conditioning.

In another paper published in 1968, Reese and Greco reported success in the use of ammonia as a conditioning agent for fly ash in a power plant operated by the Tennessee Valley

Authority.[13] Their work was done at one of the units of the Widows Creek plant where a high-sulfur coal is normally burned as the fuel and the precipitators operate around 130°C (270°F). They found that either of two methods provided the needed improvement in precipitator efficiency: (1) raising the gas temperature to about 155°C (310°F) or (2) injecting ammonia as a conditioning agent at a concentration around 15 ppm. It was concluded that either change in precipitation conditions overcame the performance-limiting factor of an abnormally low ash resistivity. The low resistivity was attributed to the high sulfur trioxide concentration and the low temperature, which led to excessive deposition of sulfur trioxide and water as a conductive acid film on the ash particles. The postulated increase in resistivity with increased temperature was consistent with the known dependence of surface conductivity on temperature.[1,2] The postulated increase in resistivity with added ammonia was attributed to a reaction between sulfur trioxide, ammonia, and water vapor to form a "smoke" of solid ammonium sulfate, which lowered the amount of acid deposited on the ash.

From recent studies of fly ash from low-sulfur coals, there have been unpublished reports that appear to support the conclusion that ammonia is capable of improving precipitator performance by lowering the resistivity of fly ash.[14] There have also been reports to the contrary, some failing to show either a significant improvement in precipitator performance or a change in resistivity[14] and one indicating that ammonia improves precipitator performance without changing resistivity measurably.[15] With ash from high-sulfur coals, the investigation covered in this paper and at least one other investigation[16] have failed to confirm that ammonia is capable of increasing resistivity significantly from abnormally low values, as reported by Baxter[12] and postulated by Reese and Greco.[13]

INVESTIGATION OF AMMONIA CONDITIONING IN TVA POWER STATIONS

PURPOSE AND SCOPE

The investigation of ammonia conditioning covered in this paper was undertaken during the period from 1972 to 1974 by Southern Research Institute but supported financially by the Tennessee Valley Authority and aided experimentally by the technical personnel of that organization. The primary purposes of the investigation were to clarify the mechanisms

by which ammonia acts as a conditioning agent for fly ash and thus to determine as far as possible the circumstances under which conditioning by ammonia will be beneficial. Although the investigation was primarily concerned with conditioning mechanisms, it was carried out at power plants where there was previous knowledge of the effectiveness of the conditioning process or where there were parallel experiments being conducted to determine the effectiveness.

TVA's interest in ammonia conditioning stems from the favorable results obtained by Reese and Greco at the Widows Creek plant with fly ash from high-sulfur coal.[13] One of the tasks of this investigation was to make renewed efforts to explain the results obtained at the Widows Creek plant and the similar results obtained at the Gallatin plant with a later installation of ammonia-conditioning facilities. Studies of both of these plants were made with high-sulfur coals from Eastern sources. Another task was to assist TVA in the evaluation of ammonia as a conditioning agent for fly ash from low-sulfur coals, also from Eastern sources. Accomplishment of the latter task involved studies at the Bull Run plant and at the Widows Creek plant, where a temporary change was made in the sulfur content of the coal used as the fuel.

POWER-PLANT CONDITIONS

For the various power plants investigated (all in the TVA system), the primary conditions that were deemed relevant to the mechanisms and effectiveness of ammonia conditioning are given in Table 1. The plant parameters listed in this table are the sulfur percentage in the coal, the average gas temperature in the precipitator, the naturally produced concentration of sulfur trioxide, and two of the properties of the fly ash: (1) the electrical resistivity at the precipitator temperature and (2) pH values of a slurry of the ash in distilled water at room temperature (weight ratio, 1 part of ash to 300 parts of water). The first value of pH is the value recorded after very brief contact of the ash with the water, and the second is the steady-state or equilibrium value recorded after extended stirring of the mixture. For those apparently anomalous instances where the first value is in the acidic range (pH <7) and the second is in the basic range (pH >7), the assumed explanation is that the low value reflects the presence of an acidic film on the ash surface which dissolves very rapidly and the high value reflects the presence of excess soluble base in the interior of the ash which dissolves more slowly. All of the data in Table 1 for sulfur trioxide

Table 1. POWER PLANTS IN THE TVA SYSTEM INVESTIGATED WITH AMMONIA CONDITIONING

Plant	Coal, % S	Gas temp °C	Gas temp °F	Normal SO_3 concn,[a] ppm	Normal fly-ash properties[a] ρ, ohm cm	pH[b] Initial	pH[b] Equil.
Widows Creek	0.9	132	270	5	4×10^{11}	<5.5	5.2
Bull Run	1.2	127	260	2	3×10^{10}	<5.5	4.5
Widows Creek	3.5	132	270	11	1×10^{8}	4.3	10.0
Gallatin	4.0	143	290	9	4×10^{8}	4.4	8.6

[a]Determined without ammonia injection.
[b]Determined after very brief contact of the ash with water of pH 5.5 ("Initial") and after extended stirring of the mixture ("Equil.").

and fly ash were determined with samples collected at the precipitator inlets without the injection of ammonia. Comparative data for samples collected during the injection of ammonia are given later in this paper.

Several observations from the data in Table 1 need to be emphasized. First, the two so-called low-sulfur coals, having sulfur contents of about 1.0% (before drying), would hardly be classified as such by investigators familiar with Western coals, for which sulfur contents around 0.5% are common. These fuels are justifiably referred to as low-sulfur coals only in contrast to the two other fuels, having sulfur contents of 3.5 and 4.0%. A second observation from Table 1 is that the low-sulfur coals differ further from typical low-sulfur Western coals in producing sulfur trioxide at significant concentrations and fly ash with only moderately high resistivities and acidic equilibrium pH values. Experience of investigators at Southern Research Institute has shown that with low-sulfur Western coals the naturally produced concentrations of sulfur trioxide are frequently undetectable (< 1 ppm), the resistivities of fly ash are often above 1×10^{12} ohm cm, and equilibrium pH values of fly ash are usually above 10.

It seems likely that variations in the overall chemical composition of fly ash, particularly variations in the percentage of calcium oxide, account for all of the differences noted in the fly-ash properties and the sulfur trioxide concentrations listed in Table 1. The percentage of calcium oxide in the fly ash from each of the low-sulfur coals burned in the TVA plants was 0.8%; percentages found in various analyses of ash from a number of different low-sulfur Western coals ranged from 6 to 22%. The percentages of calcium oxide in the two high-sulfur coals burned in the TVA plants were around 3%; these higher concentrations of calcium oxide may account for the disproportionately low sulfur trioxide concentrations and the much higher fly-ash pH values associated with these fuels, in contrast with the corresponding data for the two low-sulfur fuels. Presumably, at least part of the calcium oxide in fly ash is able to react with sulfur trioxide in flue gas, forming calcium sulfate as the product. If this assumption is correct, the availability of calcium oxide in fly ash may rank on par with the sulfur content of the coal as a factor determining the concentration of sulfur trioxide that is available for regulating the electrical resistivity of the ash, the crucial factor affecting precipitation efficiency.

The foregoing rather extensive commentary about the circumstances prevailing in the TVA power plants is intended to serve as a warning about applying the conclusions from the experimental data under substantially different circumstances. This warning is a keynote in the discussion of the conclusions later in this paper.

CONDITIONING HYPOTHESES AND RELATED EXPERIMENTAL DATA

Different hypotheses about the mechanisms of ammonia conditioning provide a convenient basis for presentation of the experimental data. The first hypothesis considered is the most widely held concept of gas conditioning: the use of ammonia produces favorable changes in the electrical resistivity of fly ash. Experimental data on resistivity are examined in this context. Two alternative hypotheses involving less commonly discussed conditioning mechanisms are then stated, and they are evaluated on the basis of other types of experimental data.

Hypothesis A (Conditioning by Resistivity Modification)

This hypothesis is expressed by the following statements.

> Ammonia alters the electrical resistivity of fly ash in a favorable direction. This agent lowers the resistivity if the value is too high, permitting the needed precipitation voltages and currents to be maintained without the deleterious effect of excessive sparking or back corona. The agent increases the resistivity if the value is too low, maintaining an electric force across the ash deposit that is large enough to keep reentrainment losses within acceptable limits.

Method of Determining Electrical Resistivity—

Making a meaningful determination of the electrical resistivity of fly ash is a task involving many difficulties. Various aspects of the problem of determining resistivity and the options that may be followed with respect to apparatus and procedure have been discussed by Nichols.[17] With this discussion as a reference, it should be sufficient to state that in this investigation a point-to-plane resistivity probe was inserted into the gas duct ahead of each precipitator and used for the collection of an ash sample and the measurement of resistivity *in situ* at an electric field approaching the breakdown strength of the collected ash.

Observed Values of Resistivity—

Representative values of the resistivity determined at each TVA plant with and without ammonia conditioning are listed in Table 2. The data obtained with no ammonia added are the same as the data in Table 1. The data obtained with ammonia injected at specified concentrations are listed for comparison. Except with 7 ppm of injected ammonia at the Bull Run plant, each value is the average of several determinations; the exception is the result of a single determination.

Table 2. RESISTIVITY VALUES FOR FLY ASH IN TVA POWER PLANTS WITH AND WITHOUT AMMONIA CONDITIONING

Plant	Coal, % S	Injected NH_3 concn, ppm	Fly-ash resistivity, ohm cm
Widows Creek	0.9	0	4×10^{11}
		10	4×10^{11}
Bull Run	1.2	0	3×10^{10}
		7	4×10^{10}
Widows Creek	3.5	0	1×10^{8}
		20	3×10^{8}
Gallatin	4.0	0	4×10^{8}
		20	3×10^{8}

Experience in determining resistivity leads to the conclusion that none of the apparent changes produced by ammonia injection is large enough to be experimentally significant. Even if the apparent changes were real, none would be great enough to be of practical consequence in determining the efficiency of fly-ash collection.

Precipitator Electrical Data Bearing on Possible Resistivity Changes—

Because of the difficulties encountered in determining electrical resistivity of fly ash, it is always uncertain whether the measured resistivity is representative of the ash deposited on the precipitator electrodes. To minimize this uncertainty, it is desirable to determine whether the

measured resistivity is consistent with the magnitude indicated by the secondary voltages and currents produced by the transformer-rectifier sets supplying the electrical sections of the precipitator.

Voltages and currents supplied by two of the electrical sets at the Gallatin plant are shown in Figure 1. Sets 4C1 and 4C4 referred to in this figure supply the first and final sections in a series of four progressing from the inlet to the outlet of Precipitator C of Unit 4 at the Gallatin plant. The four curves in the figure show the relationships between voltage and average current density with essentially clean collector electrodes; to remove ash from the electrodes before the electrical data were recorded, the electrodes were rapped overnight with the electrical sections deenergized. The two unbroken curves show the data obtained in the absence of injected ammonia. These two curves are located differently because the space-charge component of the electric field near the precipitator inlet is substantially greater than that near the outlet; the concentration of gas-suspended, electrically-charged particles of fly ash is higher nearer the inlet, and the ratio of the current carried by particles to the current carried by gaseous ions is higher at this location. The dashed curves show the results of experiments conducted during a brief interval with ammonia injected at a concentration of 20 ppm; these experiments were started immediately after the experiments without ammonia injection were completed. In terms of the quantity and quality of the ash deposited on the electrodes, the data obtained with and without ammonia injection should be comparable, for the electrical sections were not energized long enough to cause an appreciable accumulation of ash or a change in the ash between the experiments.

It is evident that the injection of ammonia caused shifts in the locations of the voltage-current curves for both electrical sections of the precipitator but that the shift was more pronounced for the inlet section than the outlet section. If the quantities of ash or the properties of the ash on the electrodes had differed appreciably in the experiments with and without ammonia injection, the shifts in the locations of the curves could be attributed to increased voltage drops through the deposited ash. These changes could have been the result of either an increase in the thickness of the deposit or an increase in the resistivity of the deposit after ammonia injection was started. However, the assumption that the quantity or the properties of the ash could have changed in the brief interval between

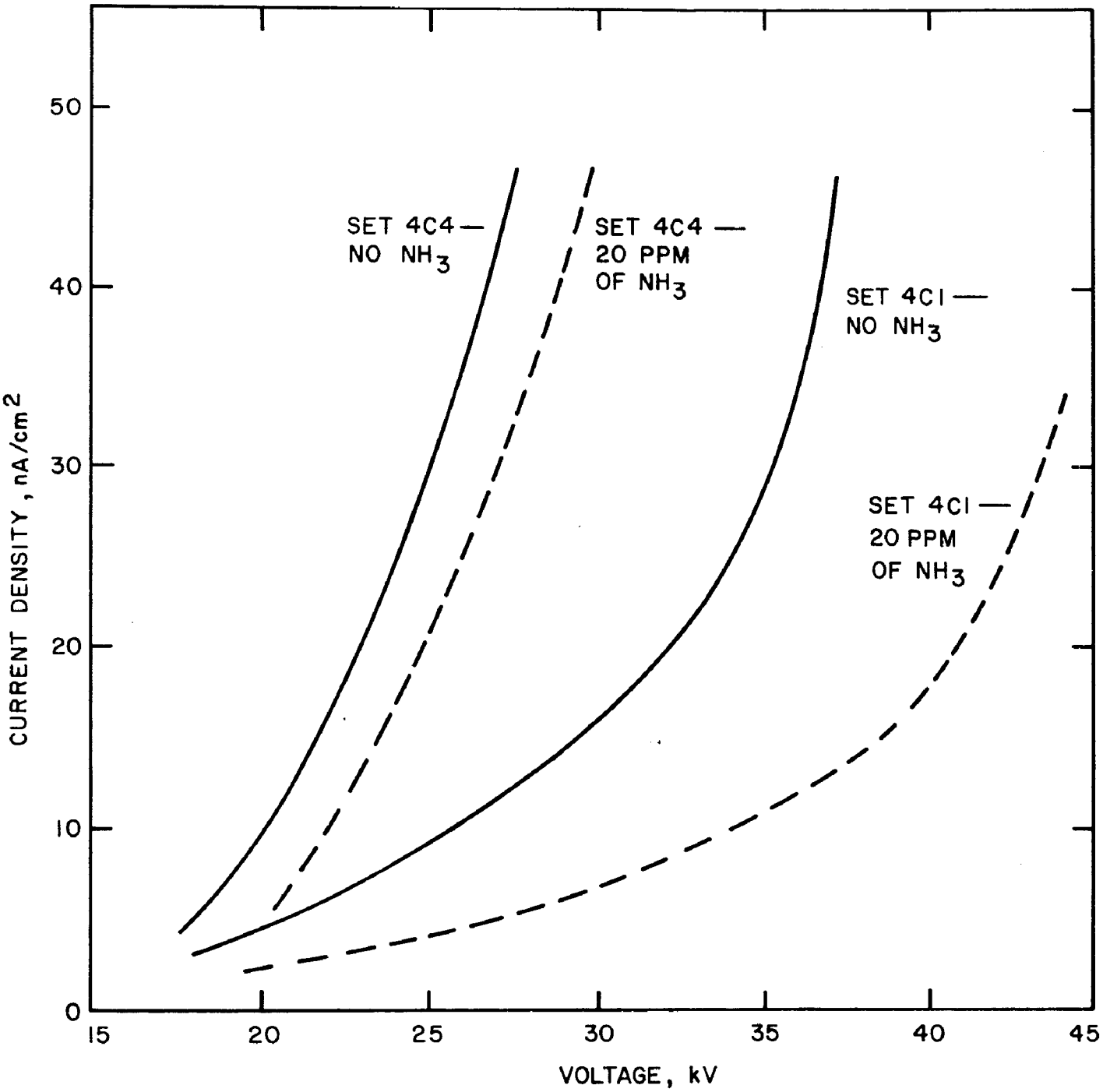

Figure 1. Relationships between voltages and current densities in the inlet and outlet electrical sections of Gallatin precipitator 4C with and without NH_3 injection

the experiments with and without ammonia injection seems to be untenable. Thus, a different explanation for the shift is necessary, and the most probable alternative explanation is that the addition of ammonia altered the electrical properties of the gas stream, not the resistivity of the fly ash. This phenomenon is referred to subsequently in this report as a space-charge effect.

Voltage-current curves similar to those for the Gallatin plant in Figure 1 were obtained in the other three TVA plants with both low- and high-sulfur coals. The similarity despite wide variations in the resistivity of unconditioned ash provides another basis for explaining the data in terms of a space-charge effect rather than a resistivity change with ammonia injected.

The secondary voltage in the inlet section of the Gallatin precipitator was recorded on one occasion through an interval of time when the injection of ammonia was started abruptly. The voltage recorded was that maintained automatically with the magnitude of the current or the spark rate limited. A reproduction of the recorder trace is shown in Figure 2. This figure shows that a very rapid increase of about 6 kV was brought about by the addition of ammonia and the increased voltage was sustained for 1 hr until the recorder was disconnected. The increase in voltage in such a brief interval of time almost surely was caused by the space-charge effect; it could not conceivably have been caused by a change in the resistivity of the ash deposited in the precipitator, for which the residence time has to be relatively long.

Rapid changes in voltage and also in current were observed as ammonia injection was started or stopped in all of the power plants investigated. Again, the electrical data strengthen the concept of a space-charge effect rather than a resistivity change in the fly ash.

Hypothesis B (Conditioning by a Space-Charge Effect)

This hypothesis is described as follows:

> Ammonia alters the electrical characteristics of the gas stream flowing between the corona wires and the collection electrodes. Specifically, it produces a space-charge enhancement of the electric field by which fly-ash particles are (1) initially charged and collected or (2) recollected following rapping reentrainment. The most probable process by which

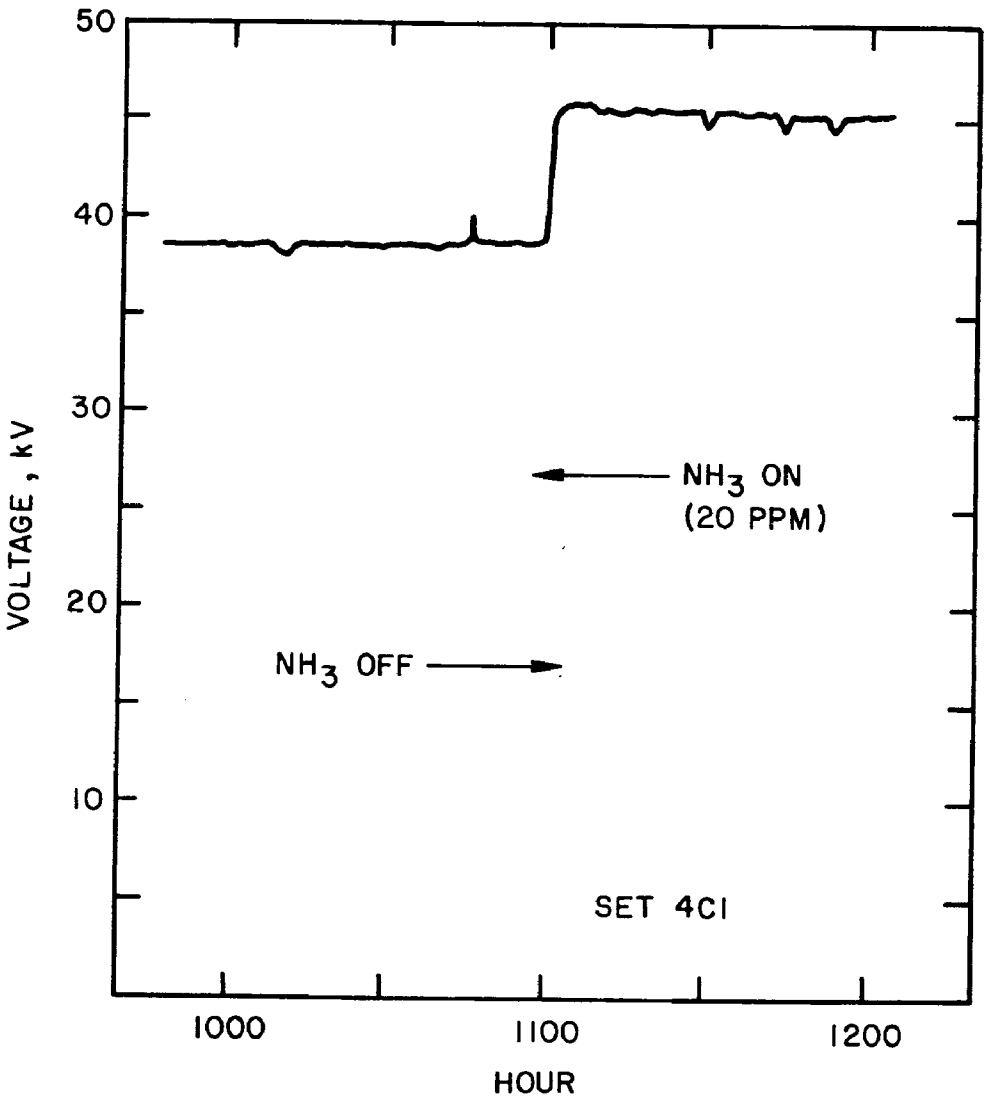

Figure 2. Rapidity of the effect of NH_3 injection on the voltage supplied to the inlet electrical field of Gallatin precipitator 4C

the space-charge effect occurs is reaction of the ammonia with the sulfur trioxide and water vapor normally present in flue gas to produce fine particles of ammonium sulfate or ammonium bisulfate and subsequent charging of the reaction product in the precipitator.

Several types of observations must be made if the foregoing hypothesis is to be substantiated experimentally. The types of experimental data required to support this hypothesis are described subsequently. If the specific process involving the formation of ammonium sulfate or ammonium bisulfate is to be an acceptable part of the hypothesis, the available thermodynamic data for the indicated reactants and products have to be favorable. Information published by Kelley et al.[18] for the relevant thermodynamic properties of the reactants and products does, in fact, warrant acceptance of the postulated chemical effects.

Precipitator Electrical Data—

The occurrence of the postulated space-charge effect will lead to shifts in voltage-current curves of the type previously shown in Figure 1. Moreover, the occurrence of this effect will lead to very rapid electrical changes as illustrated in Figure 2. It has been stated previously that electrical changes of the types illustrated in these two figures were observed in the investigation of each of the TVA power stations. Thus, the hypothesis of space-charge conditioning is supported by all of the precipitator electrical data.

Flue-Gas Concentrations—

The postulated reactions of ammonia with sulfur trioxide and water vapor by either of the proposed reactions are shown by the following two chemical equations:

$$2NH_3(g) + SO_3(g) + H_2O(g) \longrightarrow (NH_4)_2SO_4(s)$$

$$NH_3(g) + SO_3(g) + H_2O(g) \longrightarrow NH_4HSO_4(s,l)$$

The physical state of ammonium sulfate, the product of the first reaction, is the solid through a wide range of flue-gas temperatures. The physical state of ammonium bisulfate in the second reaction will be the solid below a temperature of about 144°C or the liquid above this temperature. There is some uncertainty about the phase-transition temperature of ammonium bisulfate; the indicated temperature of 144°C is based on the work of Kelley et al.[18]

If either of the above reactions occurs, the concentration of ammonia in flue gas downstream from the plane of injection will be lower than the concentration injection. Furthermore, either reaction will lower the concentration of sulfur trioxide normally present in the gas stream.

Concentrations of ammonia and sulfur trioxide found at the precipitator inlet in each TVA power plant are given in Table 3. Observed concentrations of ammonia were always well below the injected concentrations as predicted. Some of the data are anomalous in showing the presence of ammonia when the agent was not being injected; the probable reason for the unexpected presence of ammonia was bleeding of the agent from a leaky injection manifold or an ammonia-rich solid encrusted around the injection nozzles. Observed concentrations of sulfur trioxide were always lower with ammonia injection than without; thus, these data are also consistent with the theoretical predictions.

Table 3. CONCENTRATIONS OF AMMONIA AND SULFUR TRIOXIDE IN THE FLUE GAS OF TVA POWER PLANTS WITH AND WITHOUT AMMONIA CONDITIONING

Plant	Coal, % S	Injected NH_3 concn, ppm	Observed gas concn, ppm	
			NH_3	SO_3
Widows Creek	0.9	0	0.6	5
		10	0.8	1
Bull Run	1.2	0	<0.3	2
		7	<0.3	1
Widows Creek	3.5	0	<0.1	11
		20	<0.1	3
Gallatin	4.0	0	<0.1	9
		20	1.0	1

Losses of ammonia and sulfur trioxide from the gas stream may, in principle, be used to determine which of the two proposed reactions occurs. Any effort to draw conclusions about the method of reaction appears unjustified, however, for there is no basis for expecting the reactions to be complete within the time of contact allowed.

Fine-Particle Concentrations—

The postulated space-charge effect involving the presence of a charged aerosol of ammonium sulfate or ammonium bisulfate in a precipitator can only have significant magnitude if the limited quantity of the aerosol present occurs as fine particles, permitting a high concentration by number. The occurrence of the postulated effect can therefore be substantiated if an increase in the number concentration of fine particles can be demonstrated experimentally as a consequence of ammonia injection.

Use was made of a condensation-nuclei counter for comparing small-particle concentrations entering the precipitators with and without ammonia injection. The principle of operation of a condensation-nuclei counter is to cool a sample gas stream adiabatically to a temperature that is below the dewpoint of the water vapor present and thus to induce condensation of water vapor on the particles to be counted.[19] When the particles are enlarged by this process, they become detectable photoelectrically. In this investigation, use was made of a General Electric counter with sensitivity to particles smaller than 0.01 μm but not larger than 1.0 μm before growth. As an optional accessory, one or more diffusion batteries was used in the sampling line to the counter to remove particles smaller than specified sizes and thus to permit some degree of particle-size classification.

The condensation-nuclei counter was not used in the initial study at the Widows Creek plant when the low-sulfur coal was burned as the fuel. However, it was used in all subsequent studies, and it yielded the data shown in Table 4. The data give clear-cut evidence of the postulated increase in fine-particle concentrations as a result of ammonia injection. Presentation of the data in tabular form fails to convey one striking aspect of the observations made with the condensation-nuclei counter. As a recorder was used to monitor the response of the counter, quite sharp increases in particle concentrations were observed each time ammonia injection was started, and correspondingly sharp decreases occurred when injection was stopped.

The data in Table 4 were all determined at the precipitator inlets. Similar data not tabulated were also obtained at the outlets. The data from the outlets showed the rapid increase or decrease in particle concentrations that was observed at the inlets. However, the absolute concentration levels were lower at the outlets both with and without

Table 4. CONCENTRATIONS OF ULTRAFINE PARTICLES IN THE FLUE GAS OF TVA POWER PLANTS WITH AND WITHOUT AMMONIA CONDITIONING[a]

Plant	Coal, % S	Injected NH_3 concn, ppm	Particle concn, no./cm^3, vs. minimum size[b]		
			<0.010 μm	0.014 μm	0.050 μm
Bull Run	1.2	0	2.4×10^6	$<2.4 \times 10^6$	$<2.4 \times 10^6$
		5	9.8×10^6	8.9×10^6	3.1×10^6
Widows Creek	3.5	0	1.2×10^7	1.0×10^7	0.6×10^7
		20	3.1×10^7	2.9×10^7	1.7×10^7
Gallatin	4.0	0	2.2×10^7	1.7×10^7	-
		20	6.1×10^7	2.6×10^7	-

[a]Determined with a condensation-nuclei counter and diffusion batteries except at the Widows Creek plant during experiments with coal containing 0.9% sulfur.
[b]Maximum size detected, about 1.0 μm.

ammonia injection. This difference indicates that the particles formed from the ammonia were partly removed from the gas stream by electrostatic precipitation as were the particles of fly ash normally present. Finding this difference is important, for it indicates that the emission of fine particulate to the atmosphere is not increased in proportion to the quantity of ammonia used for conditioning. Actually, the quantity of particulate in the plume just beyond the top of the stack may be lower as a result of ammonia conditioning, for a reduction occurs in the quantity of sulfur trioxide that can undergo condensation to a mist of sulfuric acid as the evolved gases undergo cooling in the atmosphere.

Fly-Ash Chemical Constituents—

Loss of injected ammonia from the gas phase by reaction to form fine particles of ammonium sulfate or ammonium bisulfate should lead to the appearance of ammonia as a constituent of fly ash sampled from the gas stream at the inlet of a precipitator. Also, the loss of the reaction product from the gas stream during passage through the precipitator (indicated by the difference in the condensation-nuclei data obtained at the inlet and the outlet) should cause the appearance of ammonia in the precipitate deposited in the hoppers.

The results of determinations of ammonia dissolved from fly ash in aqueous slurries are given in Table 5. The data are for samples collected isokinetically from the flue gas entering the different precipitators; they show clearly that ammonia did become a significant constituent of each sample collected while the conditioning agent was being injected. The results of determinations of sulfur trioxide dissolved from the ash in the same slurries are included in the table; these data do not show a consistent effect of ammonia injection on the concentrations of sulfur trioxide present in the ash. (Although concentrations of sulfur trioxide are reported, this substance was determined as sulfate ion and was undoubtedly present in the ash in this form.) The equilibrium pH values of the ash-water slurries show no effect from the ammonia. Probably no pH effect should be seen, for soluble acid or soluble base other than ammonia was evidently always present in considerable excess.

Table 5. ANALYTICAL DATA FOR FLY ASH IN TVA POWER PLANTS INDICATING THE PRESENCE OF AMMONIA DURING CONDITIONING

Plant	Coal, % S	Injected NH_3 concn, ppm	Concn, %, of soluble ash constituents		pH (equil.) of ash slurry
			NH_3	SO_3	
Widows Creek	0.9	0	<0.01	0.22	5.2
		10	0.04	0.18	5.4
Bull Run	1.2	0	<0.01	0.31	4.5
		5	0.05	0.33	4.5
Widows Creek	3.5	0	<0.01	1.24	10.0
		20	0.12	1.31	10.0
Gallatin	4.0	0	<0.01	1.00	8.6
		20	0.21	1.40	8.6

Analyses of fly ash removed from the precipitator hoppers at the Bull Run and Widows Creek plants while ammonia conditioning was in progress showed the expected presence of ammonia. At Bull Run, about 0.04% of the collected material dissolved as ammonia. At Widows Creek during the experiments with high-sulfur coal as the fuel, about 0.05% of the ash was found as soluble ammonia.

Hypothesis C (Conditioning by Increasing the Cohesiveness of Fly-Ash Particles)

The concepts constituting this hypothesis are as follows:

> Ammonia increases the cohesiveness of fly-ash particles and thus lowers the reentrainment of ash deposited on the collection electrodes. This effect should be of greater consequence in improving the overall collection efficiency of low-resistivity ash than high-resistivity ash, because the much higher electric force across a deposit of the latter material will keep reentrainment losses from being excessive.

Basis for this Hypothesis—

There are several reasons for postulating that the use of ammonia as a conditioning agent increases the cohesiveness of fly ash. First, some of the trials of ammonia injection into the flue gas upstream from the air preheater have led to pluggage of the preheater.[12,13] Second, several observations made by TVA personnel in plants with ammonia injection downstream from the air preheater indicate that ammonia acts as a binder for fly-ash particles. One of these observations has to do with the accumulation of large rigid aggregates of solid material (known as "hornets nests") around the injection nozzles, which have been found to contain large quantities of ammonia (2.6% by weight in one analysis). Other observations have to do with problems of ash accumulation on induced-draft fans at the precipitator outlet and problems in ash removal from the precipitator hoppers. Third, photomicrographs of ammonia-conditioned ash in investigations by the Koppers Company have reportedly shown increased agglomeration of ammonia-conditioned ash particles through feather-like bridges thought to consist of ammonium sulfate.[20]

Still another qualitative reason for believing that ammonia increases the cohesiveness of fly ash was the difference in appearance of ash samples collected on the stages of a Brink impactor with and without ammonia conditioning at the Bull Run plant. The ash that had been conditioned with ammonia was deposited in fairly regular-shaped cones whereas the unconditioned ash was deposited with much more irregular scattering on the impaction surfaces.

Experiments by Dalmon and Tidy to determine quantitatively the cohesiveness of fly ash from a precipitator showed that ash conditioned with ammonium sulfate was much more cohesive

than unconditioned ash.[6] Although the conditioning agent in these experiments was ammonium sulfate rather than ammonia, the results produced by formation of ammonium sulfate during conditioning with ammonia could easily be the same.

Methods of Direct Laboratory Determinations of Cohesiveness—

Dalmon and Tidy based their determinations of cohesiveness on measurements of the mechanical force needed to rupture a compressed bed of fly ash. Fly ash from a precipitator was used to fill a cell consisting of two separable hemicylinders. One of the halves of the cell was fixed in position, but the other could be moved horizontally to rupture the bed of fly ash at a measured force per unit area.

Penney and Klinger described a different experimental method.[21] Fly ash was electrostatically deposited on small metal plates. The plates containing the deposited ash were then mounted on a centrifuge, and the centrifugal force needed to remove the ash from the plates was determined.

Both experimental methods may yield data of questionable significance for they fail to reproduce the environment prevailing in a full-scale precipitator. Dalmon and Tidy followed a procedure for simulating the water-vapor environment in a precipitator; however, they did not make any effort to simulate the temperature in a precipitator or to reconstitute the electrical forces present in electrostatically deposited ash, which Penney and Klinger found to be highly important. Penney and Klinger, on the other hand, made no effort to simulate either the gas environment or the temperature in a precipitator. Furthermore, they were unable to calculate the cohesive force as a single value characteristic of a given sample of fly ash, for different portions of their samples were always ruptured at different centrifugal speeds.

Methods of Indirectly Observing a Change in Cohesiveness as a Cause of Improved Precipitator Efficiency—

Because of the suspected deficiencies in the above-discussed experimental methods, observations relative to a change in cohesiveness as a conditioning mechanism during this investigation were made only by indirect methods. One method that was employed at each power plant was to use a light-obscuration device (a Bailey bolometer) to monitor the density of the stream of suspended fly ash escaping from the precipitator. The second method that was used only in the concluding experiments at the Gallatin plant

was to use an auxiliary photoelectric device (a Climet counter)[19] for monitoring the concentration of ash emitted from the precipitator in various size ranges.

By virtue of their responses in real time, both instruments were capable of showing the rate of change in the emission rate after the injection of ammonia was started or stopped. If the space-charge mechanism of conditioning were predominant, the range of change in the emission rate should be rapid. On the other hand, if a change in cohesiveness were either the predominant factor or an important contributing factor, the rate of change in the emission rate should be relatively slow, allowing time for an alteration in the properties of the ash present on the collection electrodes.

The Bailey bolometer was not always used as successfully as desired. The maintenance of optical components to keep them free of accumulated dust was sometimes lacking, and the nature of the response of the light detector to changes in the emission rate of fly ash from the precipitator was then obscured. However, under the substantially different conditions prevailing at the Widows Creek plant with low-sulfur coal and at the Gallatin plant with high-sulfur coal, the nature of the responses was seen fairly clearly. The recorded intensity of transmitted light increased much more rapidly at the Widows Creek plant than at the Gallatin plant as ammonia injection was started. This finding is, of course, consistent with that part of the hypothesis predicting that the overall efficiency of collecting a high-resistivity ash (about 4×10^{11} ohm cm at Widows Creek) would not be aided as much as the efficiency of collecting a low-resistivity ash (about 4×10^{8} ohm cm at Gallatin).

The slowness of the bolometer response at the Gallatin plant after ammonia injection was started or stopped is shown in Figure 3. This figure is a reproduction of the bolometer recorder chart for a period of several hours first with no ammonia injection, then with ammonia injection at a concentration of 20 ppm, and finally with ammonia injection discontinued. The wide oscillation of the recorder pen during the first period reflects the repeated emission of rapping puffs from the precipitator. This oscillation was gradually damped after ammonia injection was started, but little change was evident for at least 30 min. The oscillation was gradually intensified after ammonia injection was finally discontinued, but again little change was evident for 30 min.

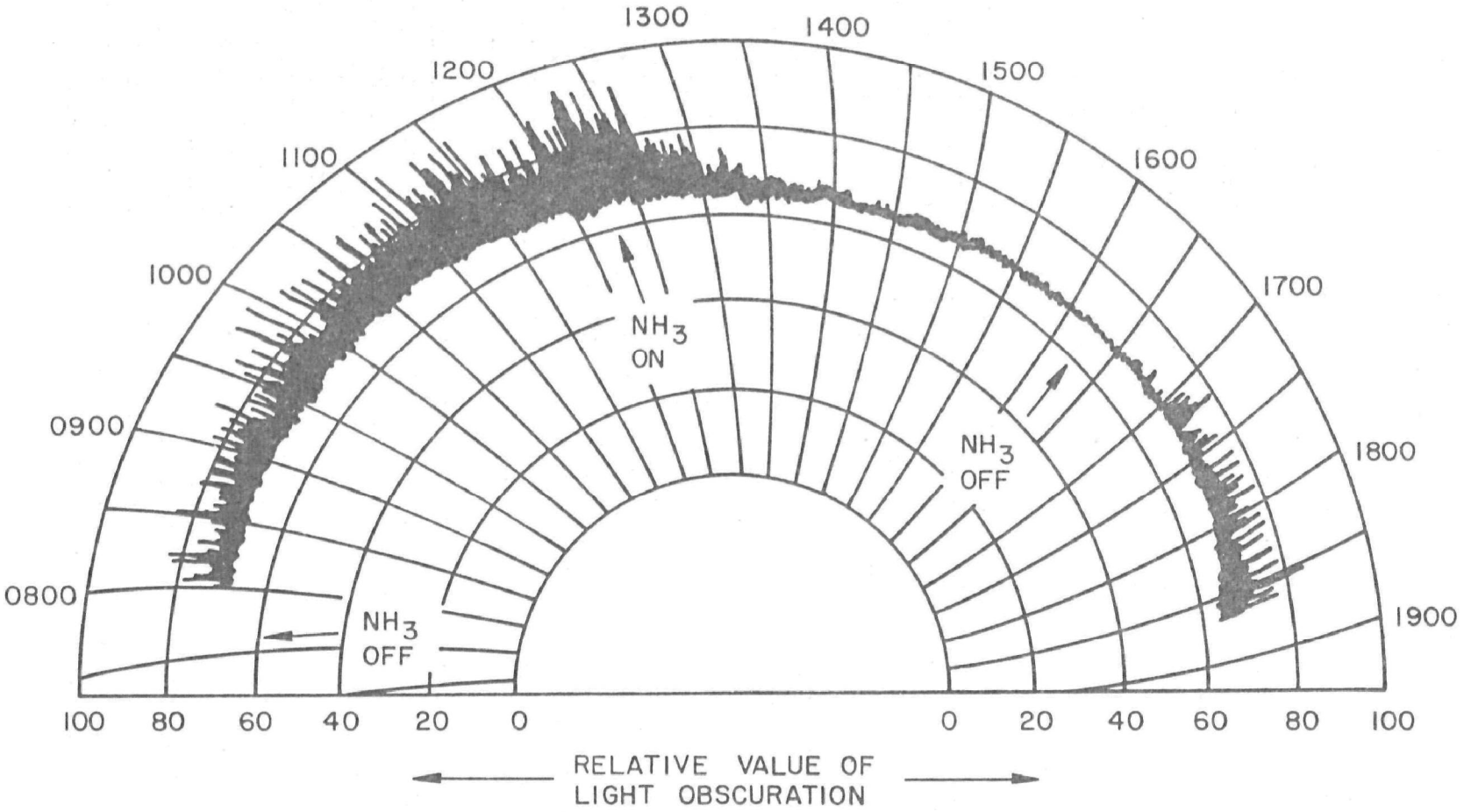

Figure 3. Effects of changes in NH_3 injection on the emission of particulate from Gallatin precipitator 4C as indicated by the Bailey bolometer

The effects of deenergizing the rappers with and without ammonia injection is shown in Figure 4. It is evident that deenergizing the rappers without ammonia injection gave reductions in particulate emission that were comparable to those achieved with injection. Clearly, therefore, rapping reentrainment was a severe cause of emission at the Gallatin plant. It is also evident that ammonia injection was effective in minimizing reentrainment while the rappers were in service, although ammonia injection only became gradually helpful for this purpose.

The data obtained with the Climet counter at the Gallatin plant are shown in Table 6. The data in the third group show the gradual decrease of particle concentrations between and during rapping events (especially the latter) that occurred after ammonia injection was started, the effect expected from the postulated importance of increased cohesiveness of the fly ash. Other data in this table confirm the conclusion given previously, that rapping reentrainment is a major factor contributing to the emission of fly ash from the Gallatin precipitator unless ammonia is used as a conditioning agent.

PRECIPITATOR EFFICIENCIES WITH AND WITHOUT AMMONIA CONDITIONING

Whereas the mechanisms of ammonia conditioning are of theoretical interest, the effect of the conditioning process on the efficiency of fly-ash precipitation is of immediate practical interest. The available information on the latter point is summarized in Table 7. This information includes inlet and outlet concentrations of fly ash and calculated precipitator efficiencies determined while other experiments at the Widows Creek plant were in progress with low-sulfur coal, as described in this paper. It gives efficiency data determined at this plant on an earlier occasion with coal of high sulfur content as the fuel (averaging 3.5%, the same as during the experiments described in this paper). Finally, the table gives outlet ash concentrations determined during an earlier investigation at the Gallatin plant with "high-sulfur" coal as the fuel, probably similar to the 4.0%-sulfur coal burned during the mechanism studies. No inlet concentrations were determined at Gallatin; thus, no efficiency values were calculated.

It is obvious from Table 7 that ammonia conditioning was of considerable benefit in improving the collection of fly ash in each instance. With respect to the data for the Widows

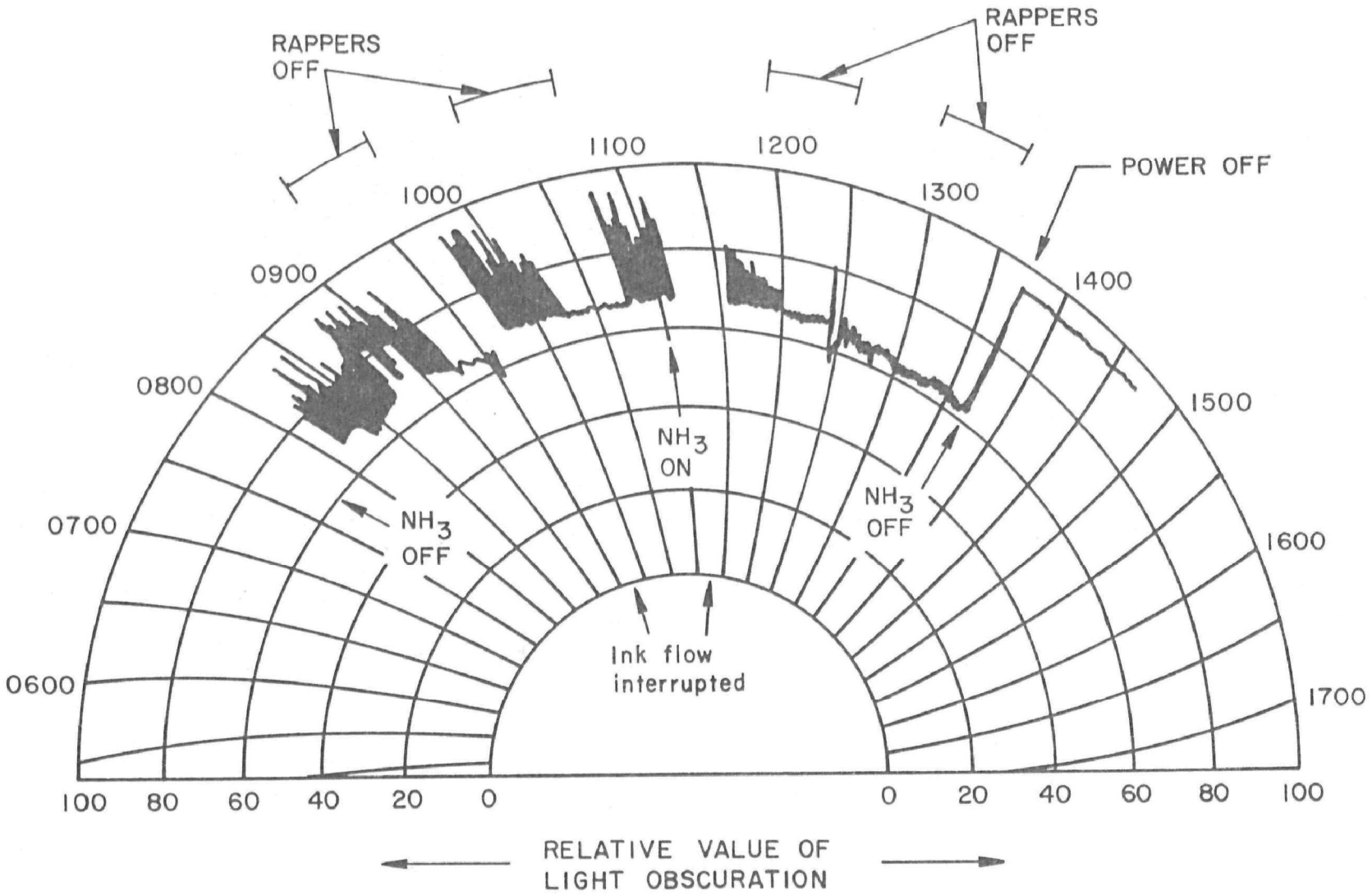

Figure 4. Effects of changes in NH_3 injection and electrode rapping on the emission of particulate from Gallatin precipitator 4C as indicated by the Bailey bolometer

Table 6. CONCENTRATIONS OF PARTICLES EMITTED FROM THE GALLATIN PRECIPITATOR WITH AND WITHOUT ELECTRODE RAPPING DURING INTERVALS WITH AND WITHOUT AMMONIA CONDITIONING[a]

Injected NH_3 concn, ppm	Electrode rapping	Duration of NH_3 injection, min	Particle concn, no./cm^3, vs. size range			
			0.5-2.0 μm		1.0-2.0 μm	
			Min[b]	Max[c]	Min[b]	Max[c]
0	On	-	1200	>4400	44	2600
0	Off	-	710	-	43	-
20	On	15	610	2700	80	1100
		26	380	2300	<4	38
		38	270	420	<4	38
20	Off[d]	62	250	-	<4	-
		85	250	-	<4	-

[a]Determined with the Climet particle counter.
[b]Recorded during intervals between rapping events in the outlet electrical section.
[c]Recorded during intervals of rapping in the outlet electrical section, repeated approximately every 30 sec.
[d]Discontinued 60 min after the injection of ammonia was started.

Creek plant, it is of some significance to add the comment that the efficiency data with low-sulfur coal are for a gas flow about 7% above the design level for the precipitator, whereas the data with high-sulfur coal are for a gas flow about 5% below the design level. The efficiency value found with unconditioned fly ash from high-sulfur coal at the higher gas flow was only about 72%, compared with 90% with unconditioned ash from low-sulfur coal. The efficiency for conditioned fly ash from high-sulfur coal at the high gas flow is apparently not known.

If efficiency determinations were made at the Bull Run plant with and without ammonia conditioning, the results are not available for inclusion in this paper. In any event, TVA evidently regarded ammonia conditioning at the Bull Run plant as unsuccessful, for the temporary facilities for ammonia conditioning have been dismantled and new permanent

Table 7. EFFECTS OF AMMONIA CONDITIONING ON THE EFFICIENCIES OF FLY-ASH COLLECTION IN TVA PRECIPITATORS

Plant	Coal, % S	Injected NH_3 concn, ppm	Fly-ash concn,[a] g/m^3		Efficiency, %
			Inlet	Outlet	
Widows Creek	0.9	0	15.2	1.54	90
		10	16.7	0.28	98
Widows Creek	3.5	0	-	-	87
		10	-	-	>99
Gallatin	High[b]	0	-	0.35	-
		18	-	0.07	-

[a]Expressed for a temperature of 0°C and a pressure of 1 atm (may be converted to concentrations in gr/ft^3 at the same conditions by division by the factor 2.3).
[b]Value not reported but assumed to be around 4.0%.

facilities for sulfur trioxide conditioning have now been installed instead. Some indications of the results achieved with ammonia conditioning at Bull Run were obtained with a Bailey bolometer. The chart recordings for the bolometer that were inspected by this speaker certainly did not indicate that the results achieved with ammonia were promising.

If, as it appears, ammonia was ineffective in improving the collection of fly ash at the Bull Run plant, it is important to understand why this was the case because of the marked similarities between the circumstances at this plant and at the Widows Creek plant when the latter plant used low-sulfur coal. Not only were the coals similar in sulfur content, but the fly ash had very nearly identical compositions, the sulfur trioxide concentrations in the flue gas were similar, and the gas temperatures differed by only 5°C (10°F). And, of course, ammonia conditioning was quite successful at the Widows Creek plant.

Failure of ammonia conditioning at the Bull Run plant was probably a result, in part, of unsatisfactory power-supply controls. Intensive sparking could not be avoided with the enhanced electric fields associated with the ammonia space-charge effect. Failure at Bull Run may also have been the result of electrode misalignment in the precipitator. In

the inlet electrical section, the onset of sparking during ammonia injection occurred at a voltage around 35 kV and an average current density below 10 nA/cm^2. In the inlet electrical section of the Widows Creek precipitator, the onset of sparking during ammonia injection did not occur until the voltage exceeded 40 kV and the average current density approached 30 nA/cm^2. The Bull Run precipitator has a narrower wire-to-plate spacing, which is nominally 11.4 cm (4.5 in.), compared with the Widows Creek precipitator, where the spacing is 12.7 cm (5.0 in.). However, misalignment rather than design spacing seems to be responsible for the lower electrical values attainable without sparking in the Bull Run precipitator.

CONCLUSIONS

This investigation has demonstrated that ammonia conditioning can improve the efficiency of fly-ash precipitation through two mechanisms, the first consisting of a space-charge effect and the second involving an increase in the cohesiveness of fly ash. The first mechanism was found to occur with fly ash having low to moderately high resistivities (1×10^8 to 4×10^{11} ohm cm). The second mechanism was found to be of definite significance only with fly ash of low resistivity (4×10^8 ohm cm). Evidence of each mechanism was obtained only under circumstances where the properties of the coal and the fly ash and the temperature of the flue gas permitted significant concentrations of sulfur trioxide (2 to 11 ppm) to be present in the flue gas. The reaction of ammonia with sulfur trioxide to produce ammonium sulfate or ammonium bisulfate appears to have been a key event in the occurrence of either type of conditioning process.

It is difficult to draw any conclusions about the mechanisms or the efficacy of ammonia conditioning of fly ash under circumstances differing markedly from those covered in this investigation. However, because of the possible value of ammonia conditioning of fly ash from low-sulfur Western coal, it is important to make tentative estimates of the results to be expected from ammonia in the type of environment that is associated with such a fuel. This type of environment may be characterized by a very low sulfur trioxide concentration (<1 ppm) and a very high fly-ash resistivity (>1×10^{12} ohm cm).

Lowering the concentration of sulfur trioxide will not necessarily prevent the occurrence of the space-charge effect. Even if the concentration is below 1 ppm, thermodynamic factors may still be conducive to the reaction with ammonia. Moreover, if the coal contains sufficient amounts of chloride salts, the hydrogen chloride produced as a constituent of the flue gas may supplant sulfur trioxide as a reactant with ammonia, producing a space-charge effect with small particles of ammonium chloride instead of ammonium sulfate or ammonium bisulfate. Another possible reactant, sulfur dioxide, is always present in flue gas at much higher concentrations than sulfur trioxide or hydrogen chloride; however, it is an unlikely reactant with ammonia because of the instability of ammonium sulfite and other chemical combinations of ammonia and sulfur dioxide at elevated temperatures.[22]

A question more fundamental than whether or not a space-charge effect can occur is whether the effect will be beneficial or detrimental to the performance of an electrostatic precipitator. If the electrical resistivity of the fly ash is high without ammonia conditioning, it will be difficult to reach the desired current density in the precipitator without incurring an undesirable rate of sparking. If the space-charge phenomenon occurs without a simultaneous reduction in the resistivity of the ash, the predominant effect may be simply an adverse reduction in the already low current density that can be maintained.

On the basis of present knowledge of conditioning, a reduction in the resistivity of fly ash appears to be essential if ammonia is to improve the precipitation efficiency of the ash from typical low-sulfur Western coals. The results of this investigation do not show whether this effect may occur with ash from this origin. To be sure, it is difficult to conceive of the adsorption of ammonia occurring efficiently on the surface of basic ash from Western coals. Unless adsorption occurs, ammonia cannot be expected to alter the resistivity. No resistivity data from other investigations known to this speaker have shown a convincing reduction in resistivity of this type of ash as a result of ammonia conditioning. On the other hand, precipitator electrical data have given distinct evidence that ammonia is capable of suppressing the phenomenon of back corona in electrode deposits of high-resistivity fly ash.

There continue to be unresolved questions about the mechanisms of ammonia conditioning and a need for further research in this area. One subject on which further research is

needed is the possible alteration of electrical resistivity. Another subject that needs consideration, at least from the speaker's point of view, is indicated by this question: Is it possible for ammonia to alter the electrical conditions in a precipitator by some process other than a space-charge effect or a reduction in fly-ash resistivity, whereby the evidence for suppressed back-corona may be explained?

ACKNOWLEDGMENTS

The financial support for this investigation was provided by the Tennessee Valley Authority through Research Agreement TV36921A. Some of the technical information presented in this paper was provided by members of the TVA technical staff, including J. R. Crooks, J. H. Lytle, W. M. McDonald, J. H. Roberts, and G. D. Whitehead.

Various members of the staff of Southern Research Institute made important contributions to the performance of the experimental work discussed in this paper. Major contributors to the experimental work were W. R. Dickson, J. D. McCain, and G. B. Nichols. Assistance was provided by J. P. Gooch, G. B. Nichols, and S. Oglesby, Jr., in the interpretation of the data.

REFERENCES

1. White, H. J. Industrial Electrostatic Precipitation. Reading, Mass., Addison-Wesley, 1963. p. 294-330.

2. Oglesby, S., Jr., and G. B. Nichols. A Manual of Electrostatic Precipitator Technology. Southern Research Institute, Contract CPA 22-69-73, National Air Pollution Control Administration. 1970. Part I. Fundamentals. NTIS PB 196380. p. 166-186.

3. Archer, W. E. Electrostatic Precipitator Conditioning Techniques. Power Eng. 76:50-53, December 1972.

4. Busby, H. G. T., and K. Darby. Efficiency of Electrostatic Precipitators as Affected by the Properties and Combustion of Coal. J. Inst. Fuel (London). 36:184-197, May 1963.

5. Dismukes, E. B. A Study of Resistivity and Conditioning of Fly Ash. Southern Research Institute, Contract CPA 70-149, Environmental Protection Agency. Publication Number EPA-R2-72-087. February 1972. NTIS PB 212607. 138 p.

6. Dalmon, J., and D. Tidy. The Cohesive Properties of Fly Ash in Electrostatic Precipitation. Atmos. Environ. (Oxford, England). 6:81-92, February 1972.

7. Dismukes, E. B. Conditioning of Fly Ash with Sulfur Trioxide and Ammonia. Southern Research Institute, for Environmental Protection Agency and Tennessee Valley Authority. Report to be issued, 1975.

8. Dismukes, E. B. Conditioning of Fly Ash with Sulfamic Acid, Ammonium Sulfate, and Ammonium Bisulfate. Southern Research Institute, Contract 68-02-1303, Environmental Protection Agency. Report to be issued, 1974.

9. Dismukes, E. B. Conditioning of Fly Ash with Sulfamic Acid. In: Proceedings, Symposium on Electrostatic Precipitators for the Control of Fine Particles. Pensacola Beach. September 30- October 2, 1974.

10. Chittum, J. F. Western Precipitation Corporation, Los Angeles, Calif. Unpublished data from studies in 1942-1945. (For excerpts, see Reference 1).

11. Watson, K. S., and K. J. Blecher. Further Investigation of Electrostatic Precipitators for Large Pulverized Fuel-Fired Boilers. Air Water Pollut. Int. J. (Oxford, England). 10:573-583, September 1966.

12. Baxter, W. A. Recent Electrostatic Precipitator Experience with Ammonia Conditioning of Power Boiler Flue Gases. J. Air Pollut. Contr. Assoc. 18:817-820, December 1968.

13. Reese, J. T., and J. Greco. Experience with Electrostatic Fly-Ash Collection Equipment Serving Steam-Electric Generating Plants. J. Air Pollut. Contr. Assoc. 18:523-528, August 1968.

14. Utility companies in the United States, Canada, and Spain. Information disclosed confidentially to Southern Research Institute, 1972-1973.

15. Tassicker, O. J. Wollongong University College, The University of New South Wales, Australia. Private communication, July 1972.

16. McLean, K. J. Environmental Protection Agency, Research Triangle Park, N. C. (present affiliation, Wollongong University College, The University of New South Wales, Australia). Private communication, May 1971.

17. Nichols, G. B. Techniques for Measuring Fly Ash Resistivity. Southern Research Institute, Contract 68-02-0284, Environmental Protection Agency. Report to be issued, 1975.

18. Kelley, K. K., C. H. Shomate, F. E. Young, B. F. Naylor, A. E. Salo, and E. H. Huffman. Thermodynamic Properties of Ammonium and Potassium Alums and Related Substances, with Reference to Extraction of Alumina from Clay and Alunite. Bureau of Mines, Washington, D. C. Technical Paper 688. 1946. p. 66-69.

19. McCain, J. D., K. M. Cushing, and W. B. Smith. Measurement of the Fractional Efficiency of Pollution Control Devices. Southern Research Institute. (Presented at Air Pollution Control Association 67th Annual Meeting. Denver. June 9-13, 1974.) 29 p.

20. Zarfoss, J. R. Environmental Elements Corporation (subsidiary of Koppers Company), Baltimore, Md. Private communication, May 1974.

21. Penney, G. W., and E. H. Klinger. Contact Potentials and the Adhesion of Dust. Trans. Amer. Inst. Elec. Eng. 81, Part I:200-204, July 1962.

22. St. Clair, H. W. Vapor Pressure and Thermodynamic Properties of Ammonium Sulphites. In: Fixation of Sulphur from Smelter Smoke. Bureau of Mines, Washington, D. C. Report of Investigations 3339. 1937. p. 19-29.

CONDITIONING OF FLY ASH WITH SULFAMIC ACID

Edward B. Dismukes
Southern Research Institute
Birmingham, Alabama

ABSTRACT

This paper is a review of recent investigations of the conditioning of fly ash with sulfamic acid. It discusses both a fundamental laboratory study of conditioning with sulfamic acid and various power-plant trials of this compound, most of which were conducted with a commercial blend of sulfamic acid with other chemicals. The data presented mainly relate to the practical question of how much improvement can be effected in the electrostatic precipitation of fly ash when the ash is conditioned with sulfamic acid. However, information related to the mechanisms of conditioning by this agent is analyzed, and tentative conclusions about the conditioning mechanisms are offered.

INTRODUCTION

The types of compounds employed as "conditioning agents" for fly ash in electrostatic precipitators are usually introduced as gases.[1] The most common examples of compounds introduced in this manner are sulfur trioxide and ammonia. Although these two compounds are stored as liquids (ammonia under pressure to maintain the liquid state), they are vaporized before injection into the gas stream entering a precipitator. Sulfuric acid, an alternative source of sulfur trioxide, is likewise vaporized before it is injected into a stream of flue gas.

Several compounds now being investigated as conditioning agents occur at normal temperatures and pressures as solids. Examples of these compounds are sulfamic acid, ammonium sulfate, and ammonium bisulfate.[2] They are injected into flue gas in the form of either a fine powder or an aqueous solution.

There is novelty in the use of sulfamic acid and the ammonium salts not only because of the physical form in which they are injected as conditioning agents but because of their chemical relationship to the better known conditioning agents, sulfur trioxide and ammonia. Sulfamic acid is a compound of sulfur trioxide and ammonia in 1:1 molar proportions as indicated by its formula, NH_2SO_3H. Ammonium sulfate and ammonium bisulfate contain the two parent compounds in 2:1 and 1:1 molar proportions, respectively, with water present as a third constituent. The customary formulas for these two salts and the corresponding formulas indicating their constitution in terms of the parent compounds are as follows:

Ammonium sulfate

$$(NH_4)_2SO_4 \text{ or } 2NH_3 \cdot H_2O \cdot SO_3$$

Ammonium bisulfate

$$NH_4HSO_4 \text{ or } NH_3 \cdot H_2O \cdot SO_3$$

BASIS FOR INTEREST IN SULFAMIC ACID AS A CONDITIONING AGENT

Much of the current interest in sulfamic acid as a conditioning agent for fly ash apparently originated with the thought that this compound would be a conveniently handled source of sulfur trioxide. Theoretically, sulfamic acid can be thermally decomposed to sulfur trioxide in hot flue gas, as indicated by the following chemical equation:

$$H_2NSO_3H \longrightarrow NH_3 + SO_3 \qquad (1)$$

The simultaneous interest in the related conditioning agents, ammonium sulfate and ammonium bisulfate, appears to stem from the possibility of decomposing these agents also to sulfur trioxide with ammonia and water vapor as associated products. Obviously, the flue-gas temperature would have to be above the range where the products of decomposition can recombine, as discussed in connection with ammonia as a conditioning agent.[3]

The handling of sulfur trioxide or its chemical equivalent, sulfuric acid, is difficult in a power plant because either compound is a highly corrosive and toxic liquid that must be vaporized before its injection into flue gas. The handling of sulfamic acid, on the other hand, is not the source of significant difficulty. As a solid compound, sulfamic acid is relatively noncorrosive and nontoxic. As previously stated, it can be injected into a flue-gas stream as a powdered solid or, alternatively, it can be dissolved in water and injected as an aqueous spray.

One trend of thought about the use of sulfamic acid has been described by Lowe of the Central Electricity Research Laboratories in Great Britain.[4] Lowe's publication indicates that interest was initially focused on sulfamic acid in the belief that this compound would serve as a convenient source of sulfur trioxide as shown in Equation 1. However, this publication reports the discovery that sulfur trioxide is only a minor product of the decomposition of sulfamic acid and that ammonium bisulfate is a far more significant product. The decomposition process yielding ammonium bisulfate is much more complex than that yielding sulfur trioxide, as discussed later in this paper. In any event, Lowe's publication indicates that promising results were obtained with sulfamic acid and with ammonium bisulfate and ammonium sulfate as alternative conditioning agents. The bisulfate can be obtained from partial decomposition of ammonium sulfate as well as sulfamic acid.

Interest in sulfamic acid as a conditioning agent has undoubtedly been stimulated by a recent publication by Dalmon and Tidy of the Central Electricity Research Laboratories.[5] This publication compares sulfamic acid and other novel conditioning agents with sulfur trioxide and ammonia. Dalmon and Tidy used a laboratory-scale precipitator for investigating various types of conditioning agents, which are classified below as to form at ambient temperatures.

- Gaseous compounds—sulfur trioxide, hydrogen chloride, and ammonia
- Liquid acid—sulfuric acid (injected at a concentration of 0.11 to 9.4 M in water)
- Solid compounds derived from sulfur trioxide and ammonia—sulfamic acid, ammonium sulfate, and ammonium bisulfate (injected as solids or solutes in aqueous solutions at concentrations of 0.23 to 1.8 M)

- Solid inorganic salts—sodium chloride, sodium sulfate, calcium chloride, and lithium iodide (injected as solutes in aqueous solutions at concentrations of 0.45 to 1.8 M)

The particulate substance conditioned with these agents was water-washed fly ash from a coal-fired power station. The gas stream containing the fly ash was produced by combustion of a low-sulfur paraffin and adjusted in composition by the addition of water vapor to reach a humidity level of about 8% by volume. The gas stream was essentially free of sulfur dioxide except when this gas was added deliberately to obtain a better approximation of the composition of flue gas from a low-sulfur coal.

Dalmon and Tidy reported that each additive to the gas stream improved the efficiency of fly ash collection in the absence of added sulfur dioxide, with the degree of improvement usually being controlled by the efficiency of uptake of the conditioning agent by the fly ash. They reported, however, that only a limited number of these additives improved the collection efficiency in the presence of added sulfur dioxide, which itself caused a significant improvement if added at concentrations of 100 to 300 ppm by volume (comparable to the concentrations found in flue gas from coal very low in sulfur content). The only additives effective in the presence of sulfur dioxide—that is, under the conditions better simulating a flue-gas environment—were sulfur trioxide, sulfuric acid, sulfamic acid, ammonium sulfate, ammonium bisulfate, and ammonia. Among these compounds, ammonia was effective only if hydrogen chloride was present in the gas stream. (It is possible that ammonia might have been effective if sulfur trioxide had been added in place of hydrogen chloride but ammonia was not evaluated with sulfur trioxide as a secondary additive.)

Successful trials of sulfamic acid have been made in full-scale power plants in both Great Britain and the United States. The trials in Great Britain have been made under the auspices of the Central Electricity Generating Board, which was responsible for the previously described work of Lowe, Dalmon, and Tidy.[4,5] The trials in the United States have been made by several utility companies that have employed a proprietary blend of sulfamic acid with other chemicals, which is available as a powder and as an aqueous solution.[6] Although sulfamic acid is clearly the predominant constituent of this commercial conditioning agent, the other minor constituents may play some role in the

activity of the agent. In this paper, sulfamic acid is regarded as the essential constituent, in view of the fact that the role of the other chemicals is not apparent.

PRECIPITATOR TESTS OF SULFAMIC ACID AS A CONDITIONING AGENT

PILOT-PLANT TESTS

In the pilot-plant precipitator tests performed by Dalmon and Tidy,[5] sulfamic acid was injected upstream from the precipitator at a temperature of about 400 or 165°C (750 or 330°F). At the higher temperature, the agent was injected either as a powder or as an aqueous solution (0.45 M); at the lower temperature, the agent was injected only in the aqueous form. The conditioned fly ash was then collected in the precipitator at a temperature of about 145°C (295°F).

Dalmon and Tidy made determinations and calculations of the following:

- Precipitator efficiency
- Precipitation rate parameter w_p (cm/sec)

$$w_p = -[\ln(1-E)]/k$$

where E = precipitator efficiency

k = 0.315 sec/cm (a constant based on the precipitator geometry and the flow rate of the gas stream)

- Uptake of sulfamic acid by the fly ash
- Sparkover voltage of the precipitator
- Electrical resistivity of the fly ash at the precipitated bulk density and at a constant bulk density of 0.975 g/cm^3

The investigators found that injection of sulfamic acid in solution was much more effective than injection of the agent as a solid. Using the solution method of injection, they found that the uptake of about 0.8% by weight produced the following desirable changes:

- Precipitation rate parameter—increased from 9.5 to 14 cm/sec
- Sparkover voltage—increased from 42 to 49 kV
- Resistivity—lowered from about 1×10^{14} to 1×10^{13} ohm-cm at a bulk density of 0.975 g/cm^3

Uptake of sulfamic acid by the fly ash was judged on the basis of the quantity of soluble sulfate ion found in the conditioned ash. The analysis of soluble constituents of the ash indicated that the sulfamic acid was decomposed to a sulfate, perhaps ammonium bisulfate as the initial product. However, little ammonium ion was found with the sulfate ion, and the explanation offered was that strong bases in the fly ash reacted with ammonium ion and allowed ammonia to be lost by volatilization. (Although the fly ash had been water-washed prior to use, it was highly basic, producing a pH of 11 in a 10%-by-weight slurry in water. No further information about the chemical properties of the ash was published.)

FULL-SCALE TESTS

The following paragraphs summarize information about trials of sulfamic acid in one British power station and in three American power stations. In the British station, the conditioning agent was presumably the ordinary commercial form of sulfamic acid. In each of the American stations, on the other hand, the agent was the proprietary material containing sulfamic acid as the major constituent.

Rugeley Power Station (Great Britain)

Dalmon and Tidy have given a brief summary of precipitator tests with sulfamic acid at the Rugeley Power Station in Great Britain.[5] They state that the conditioning agent was added to the flue gas ahead of the air preheater at a temperature of 500°C (about 930°F) by spraying an aqueous solution having a concentration of 1.3 M. The concentration thus injected in the flue gas was 20 ppm by volume, based on the assumption that complete volatilization occurred without decomposition (this assumption is used only as a convenient basis for comparing the rate of injection with the rates of injection of gaseous conditioning agents such as sulfur trioxide and ammonia). The emission of fly ash was reportedly lowered by 55%.

Cabin Creek Power Station (Appalachian Power Company)

The most extensive investigation of sulfamic acid in the American utility industry apparently has been made at the Cabin Creek Station of Appalachian Power Company, a subsidiary of American Electric Power Company. Cabin Creek Station is located in West Virginia, where state law requires a maximum dust emission rate of 0.09 mg/kcal (0.05 lb/10^6 Btu) but prohibits the use of sulfur trioxide as a conditioning agent to reach this emission rate when low-sulfur coal is burned to minimize sulfur dioxide emission. Thus, Appalachian Power Company undertook an investigation of sulfamic acid to determine whether use of this agent would permit compliance with the state requirements.

The utility company investigated sulfamic acid as a flue-gas additive when coals normally available were burned. The company also investigated this additive when certain "metallurgical" coals (low in ash content) were burned on an experimental basis, even though these coals were not available in sufficient amount for sustained use. Sulfur percentages in the various coals were in the range of 0.8 to 1.0% except in one instance where the value was 1.4%. Some of the results of the precipitator tests at Cabin Creek Station were published in a technical bulletin by the supplier of the sulfamic acid.[6] More extensive data from these tests were provided for publication in this paper by a representative of the American Electric Power Service Corporation.[7]

At Cabin Creek Station, sulfamic acid was injected as a powder into the flue gas produced in each of two boilers with rated loads of 50 MW (each boiler was one of a pair comprising one unit with a rated load of 100 MW). The site of injection was the duct upstream from the economizer, where the flue-gas temperature was approximately 625°C (1160°F). The treated gas stream then passed through a precipitator where the temperature averaged about 185°C (365°F) in one instance or about 160°C (320°F) in another instance. Coals from three different sources with ash contents of about 10% by weight were burned in one boiler, whereas coals from four other sources with ash contents of only about 6% were burned in the second boiler.

Table 1 summarizes the conditions under which sulfamic acid was investigated and gives comparative precipitator efficiencies with and without this additive. This table lists rates of sulfamic acid injection as a weight fraction of the rate of coal consumption. Calculations indicate that

Table 1. RESULTS OF PRECIPITATOR TESTS AT CABIN CREEK STATION WITH SULFAMIC ACID AS A FLUE-GAS ADDITIVE[a]

Coal			Boiler load, MW	Additive rate,[b] parts per 2000 parts of coal	Precipitator efficiency,[c] %
Type	% S	% Ash			
CI	1.4	9.7	48	1.1	98.6
			36	1.4	98.7
			33	2.0	99.1
C	0.9	10.4	32	0	91.0
			39	1.3	98.2
E	0.9	10.3	40	0	98.1
			44	1.1	97.2
			36	1.3	98.8
			42	1.6	99.0
ON	1.0	6.0	45[d]	0	95.3
			42	1.3	95.1
IC	1.0	5.7	51[d]	0	68.9
			50	0.5	88.2
			52	1.1	87.6
			52	2.0	94.0
AS	0.8	5.7	45[d]	0	95.3
			45	1.2	95.1
A	0.8	5.1	47[d]	0	78.6
			44	1.0	89.7
			45	1.8	84.6

[a]Most of the data presented are averages computed from the results of several tests.
[b]To calculate the approximate concentration in the gas stream in parts per million by volume, multiply the values listed by the factor 10.
[c]Average gas temperatures were 185°C with Coals CI, C, and E and 160°C with Coals ON, IC, AS, and A.
[d]Not reported but estimated from comparative values of the rate of steam production.

1 part of sulfamic acid to 2000 parts of coal corresponds to roughly 10 ppm by volume of the conditioning agent in the flue gas (based on the assumption of complete volatilization of the agent without thermal decomposition). The efficiency data indicate that conditioning with sulfamic acid produced favorable results with all of the coals except two (Coals ON and AS). However, an analysis performed by the Appalachian Power Company led to the conclusion that the only statistically significant improvement occurred with Coal IC.

For each of the coals investigated, a precipitator efficiency of 99% or greater is needed to satisfy the maximum dust emission level of 0.09 mg/kcal. From Table 1, it appears that the maximum additive rates used permitted this requirement to be approximated with Coals CI and E but not with the other fuels. The statistical study cited above led to the conclusion that the improvement in precipitator performance attained with sulfamic acid was not enough to meet the emission standard with coals of high emission levels and that it was inconsequential with coals of low emission levels.

Table 2 summarizes the results of fly ash analyses that were performed at the Cabin Creek Station. One of the most striking aspects of the analytical information is the loss-on-ignition data. These data indicate that the combustion efficiency in the boilers was always low but especially low when the low-ash fuels (Coals ON, IC, AS, and A) were burned. The oxide percentages show this primary difference: the low-ash coals had lower soda and lime contents but higher sulfur trioxide contents. Determinations of total sulfur trioxide, water-soluble sulfur trioxide, and pH were not always performed. However, the apparent effect of the conditioning agent on these ash properties was that the agent lowered the pH of ash from four of five coals and increased the soluble trioxide on the ash from three of four coals for which the data are available. These effects suggest that sulfur trioxide from decomposed sulfamic acid was deposited on the ash, although the occurrence of this effect is not consistently confirmed by the available data.

Table 3 shows the results of determinations of the concentrations of sulfur dioxide, sulfur trioxide, and ammonia at the outlet of the precipitator during the tests with Coals CI, C, and E. The concentrations of sulfur dioxide are about as expected from coals containing 0.9 to 1.4% sulfur considering the large excess of air that was present

Table 2. RESULTS OF FLY-ASH ANALYSES AT CABIN CREEK STATION WITH AND WITHOUT SULFAMIC ACID AS A FLUE-GAS ADDITIVE

Coal burned	LOI, %[a]	Constituent of fly ash[a]							Total SO_3, %[b]		Soluble SO_3, %[b]		pH[b]	
		Na_2O, %	K_2O, %	CaO, %	MgO, %	Al_2O_3, %	Fe_2O_3, %	SiO_2, %	w/o	w/	w/o	w/	w/o	w/
CI	10.3	0.7	0.3	3.8	-	(total, 38.2)		56.4	-	-	-	-	-	-
C	12.7	0.6	0.3	3.9	0.6	22.0	13.2	58.0	-	-	-	-	8.8	9.0
E	35.5	0.7	0.3	4.9	0.3	26.2	13.9	57.0	-	-	-	-	-	-
ON	39.4	Tr	0.6	Nil	Tr	29.2	18.1	51.4	-	-	0.3	0.6	7.8	5.8
IC	39.7	Nil	0.6	Nil	0.5	36.5	7.8	51.1	1.7	1.4	0.7	0.9	4.3	4.1
AS	49.3	0.2	0.4	Nil	0.2	38.9	4.9	50.5	1.6	1.9	1.2	1.5	5.4	4.6
A	40.5	Nil	0.3	Nil	0.3	35.1	3.7	59.3	1.3	1.0	0.8	0.8	4.7	4.4

[a]LOI indicates loss on ignition. Oxides percentages are for the ash after ignition. Tr indicates that only a trace was detected.
[b]The symbol w/ indicates that the additive was present, and the symbol w/o indicates its absence. Soluble SO_3 is the material dissolved in a 1% aqueous slurry. The pH value is for this slurry after 15 min of stirring.

in the gas stream. The concentrations of sulfur trioxide were all reported as "nil". The minimum concentration of sulfur trioxide that was detectable by the experimental method was not reported; however, it can only be concluded that the injection of the conditioning agent caused no perceptible increase in the concentration of effluent sulfur trioxide, despite the expected formation of this compound from the decomposition of sulfamic acid. Perhaps the most noteworthy aspect of the gas determinations is that ammonia was usually found during conditioning, showing that at least partial decomposition of the sulfamic acid did occur.

Table 3. RESULTS OF GAS ANALYSES AT CABIN CREEK STATION WITH AND WITHOUT SULFAMIC ACID AS A FLUE-GAS ADDITIVE[a]

Coal	Additive rate, parts per 2000 parts of coal	Gas concentrations, ppm		
		SO_2	SO_3	NH_3
CI	1.1	420	-	2.7
	1.3	414	Nil	2.8
C	0	332	Nil	Nil
	1.3	430	-	Nil
E	0	305	Nil	Nil
	1.1	316	Nil	0.3
	1.6	343	-	1.0

[a]The data presented are averages computed from the results of several determinations.

Mercer Station (Public Service Electric and Gas Company, New Jersey)

Favorable results from conditioning with sulfamic acid have been reported at the Mercer Station of the Public Service Electric and Gas Company in New Jersey.[8,9] One set of data published from this power station is summarized in Table 4. These data indicate that the injection of 1 part of conditioning agent per 2000 parts of coal brought the emission to a level below the maximum allowed by state law;[8] however, other data published for this station at a later time indicate that the preferred additive rate is 2.5 parts of conditioning agent per 2000 parts of coal.[9]

Table 4. RESULTS OF PRECIPITATOR TESTS AT MERCER STATION WITH SULFAMIC ACID AS A FLUE-GAS ADDITIVE[a]

Sulfur percentage in coal	Additive rate, parts per 2000 parts of coal	Emission rate, mg/kcal ($lb/10^6$ Btu)[b]
0.96	0	0.39 (0.22)
	0.50	0.11 (0.06)
	0.75	0.17 (0.09)
	1.00	0.09 (0.05)
	4.00	0.08 (0.05)
1.47	0	0.32 (0.18)
	1.20	0.13 (0.07)

[a]Mercer Station boiler rating, 300 MW. Additive injected at gas temperature of about 425 to 480°C (800 to 900°F).
[b]Emission allowed, 0.18 mg/kcal (0.1 $lb/10^6$ Btu).

A representative of the utility company has confirmed that the conditioning agent gives a distinct improvement in precipitator performance but has not agreed to release information beyond that summarized in Table 4.[10] This source of information has indicated that the use of sulfamic acid is continuing at the Mercer Station, whereas it has been discontinued at the Cabin Creek Station.

Station A (Unidentified Utility Company)

The Buell Division of Envirotech Corporation investigated sulfamic acid as a conditioning agent in two units of a power generating station designated as Station A.[11] These two units have power-generating capacities of about 25 MW and are equipped with electrostatic precipitators having design efficiencies of 95.0% in cleaning flue gas at temperatures of about 190°C (375°F). Neither precipitator operates at the design efficiency, however, when collecting fly ash from the coal that is now customarily used as a fuel at Station A.

The coal normally burned at Station A contains about 1% of sulfur and 9% of ash constituents. The fly ash produced from this coal typically has the composition given in Table 5. Laboratory measurements of the electrical resistivity of the ash indicate that the value is typically about 1×10^{12} ohm-cm at the gas temperature where the ash is collected in the precipitators.

Table 5. RESULTS OF FLY-ASH ANALYSIS AT STATION A

Constituent[a]	Percentage by weight
Na_2O	0.4
K_2O	2.5
MgO	0.7
CaO	1.4
Al_2O_3	27.0
Fe_2O_3	6.2
SiO_2	48.5
TiO_2	0.7
P_2O_5	0.3
SO_3	0.8

[a]Loss on ignition, 7.6%.

Sulfamic acid was investigated as a conditioning agent to determine whether it would allow the precipitators to reach or exceed their design efficiencies. In the two units of Station A, the conditioning agent was injected as a powder at locations upstream from the air preheaters where the estimated flue-gas temperatures exceed 600°C (1100°F). The injection rates ranged from 0.5 to 1.5 parts by weight of the conditioning agent for each 2000 parts by weight of the coal being burned. The performance of the precipitators with the conditioning agent present was based on determinations of efficiency in some of the tests and determinations of precipitator currents and observations of stack emission in other tests.

Efficiency data from four tests of one unit were made available by Buell for citation in this paper. With the feed rate of sulfamic acid set as 1 part of the agent to 2000 parts of coal, measured efficiencies were 96.1, 98.5, 98.8, and 99.1%. All of these efficiencies exceeded the design value of 95.0% as desired, and they were well above the values averaging about 90% without conditioning. Characteristically, injection of sulfamic acid increased the precipitator current and improved the appearance of the stack emission. The change in precipitator current implies that the electrical resistivity of the fly ash was lowered by the conditioning agent.

Buell appears to be satisfied with the performance of sulfamic acid as a conditioning agent except for one problem that it created: plugging of the air preheaters,

which are of the tubular type at Station A. This problem is regarded as severe enough to make sustained use of sulfamic acid impractical at this power station. Another reported disadvantage of sulfamic acid is its relatively high cost as a conditioning agent in comparison with sulfur trioxide or sulfuric acid.

FUNDAMENTAL PROPERTIES AND CONDITIONING MECHANISMS OF SULFAMIC ACID

PHYSICAL AND CHEMICAL PROPERTIES

The fundamental physical and chemical properties of sulfamic acid at both ambient and elevated temperatures are important in the use of this compound as a conditioning agent for fly ash. The properties at ambient temperatures are relevant in a practical sense to the methods used for handling the compound and injecting it into flue gas, which involve either the dry solid or an aqueous solution. The properties at elevated temperatures, on the other hand, are important theoretically in explaining the mechanisms by which the compound acts as a conditioning agent.

Ambient Temperatures

Pure sulfamic acid exists as a white crystalline solid at ambient temperatures.[12,13] It is quite stable through a wide range of temperatures, even up to its melting point of 205°C (401°F).[14,15] In contrast to sulfuric acid, to which it is structurally related, it is not a hygroscopic compound.[12]

The structural similarity of sulfamic and sulfuric acids is indicated by the formulas showing their functional groups: $H_2N\text{-}SO_2\text{-}OH$ and $HO\text{-}SO_2\text{-}OH$, respectively. Perhaps a more appropriate formula for sulfamic acid in the crystalline state is that of the bipolar ion, $^{+}H_3N\text{-}SO_2\text{-}O^{-}$.[14] Undoubtedly, the stability of this bipolar ion relative to that of the uncharged molecule accounts for the fact that sulfamic acid normally occurs as a solid, whereas sulfuric acid occurs as a liquid.

Sulfamic acid is readily soluble in water, dissolving to the extent of approximately 25 g in 100 g of water at 25°C

(77°F).[14,16] It behaves as a moderately strong electrolyte, thus conducting electricity readily in aqueous solutions.[12,14] For the process of ionization in water, shown by Equation 2, the

$$H_2NSO_3H \rightarrow H_2NSO_3^- + H^+ \qquad (2)$$

equilibrium constant at 25° is 0.101.[17] At a concentration of 0.1 M in water, sulfamic acid produces a pH of 1.25, only slightly higher than the pH of 1.00 that is produced by sulfuric acid at the same concentration.[12] Evidently, the dipolar ion mentioned above is far less important for sulfamic acid in solution than for the compound in the crystalline state.

The commercial blend of sulfamic acid with other chemical substances that is available in this country as a dry or dissolved solid obviously differs from pure sulfamic acid in some of its properties. This paper cannot give a comprehensive discussion of the difference in properties between the commercial and pure compounds because the complete composition of the commercial material has not been disclosed. However, analyses of the material supplied in solid form indicate that sulfamic acid accounts for about 90 wt-% of the material and that a hydrate of manganese sulfate ($MnSO_4 \cdot H_2O$) accounts for most of the balance.

Elevated Temperatures

At the elevated temperatures where sulfamic acid is used as a conditioning agent, the processes of melting, hydrolysis, and thermal decomposition may all be relevant to the mechanism of fly-ash conditioning. The importance of physical and chemical changes in the compound during the conditioning process has been stressed by various investigators. Lowe, for example, pointed out the original hypothesis that sulfamic acid serves as a source of sulfur trioxide through the reaction given previously in this paper:[4]

$$H_2NSO_3H \rightarrow NH_3 + SO_3 \qquad (1)$$

The supplier of the commercial form of sulfamic acid in this country stresses the importance of injecting this material at high temperatures to achieve volatilization,[6,8] but the nature of the volatilization process has not been described. Perhaps the manganese compound present in the

commercial material aids decomposition and thus volatilization of the sulfamic acid. The normal melting point of sulfamic acid is 205°C (401°F).[14,15] Up to this temperature, dry sulfamic acid appears to be stable. At elevated temperatures in the presence of water, however, the compound may undergo hydrolysis, yielding ammonium bisulfate as the product:

$$H_2NSO_3H + H_2O \rightarrow NH_4HSO_4 \qquad (3)$$

It is known that this process is accelerated as the temperature of sulfamic acid in aqueous solutions is increased.[14] It is possible that this process may also occur between dry sulfamic acid and water vapor at temperatures between the boiling point of water and the melting point of sulfamic acid. It is probable, therefore, that this process occurs to some extent when sulfamic acid is injected as a spray of an aqueous solution.

Various investigators have studied the thermal decomposition of sulfamic acid to fragments such as ammonia and sulfur trioxide. Halstead performed one of the most comprehensive studies, and his study was carried out with the purpose of explaining how sulfamic acid acts as a conditioning agent for fly ash.[15] Halstead reported that heating sulfamic acid in a stream of dry nitrogen causes little volatilization below the melting point or above the melting point up to a temperature of 323°C (613°F) but then produces considerable volatilization as the temperature increases to 467°C (873°F). The observed yield of sulfur trioxide is only about 0.2 mole per mole of sulfamic acid, rather than 1.0 mole as shown by Equation 1. The remaining sulfur in the starting material, about 0.8 mole, is released as sulfur dioxide as a result of an internal oxidation-reduction process in the residue that releases elemental nitrogen (N_2) along with the sulfur dioxide.

For a constant decomposition temperature of 397°C (747°F), Halstead concluded that molten sulfamic acid volatilizes through a series of decomposition reactions. The information given by Halstead is expressed by the reaction sequence given on the following page, which is based on one mole of molten sulfamic acid as the starting material. The first reaction (Equation 4) is the conversion of the melt to a molten mixture of two new compounds: a cyclic sulfur-nitrogen compound and ammonium bisulfate. The next reaction (Equation 5) evolves gaseous sulfur trioxide and again alters

$$1.000\ NH_2SO_3H(l)$$

$$\downarrow$$

$$\{0.083\ (NHSO_2)_6 + 0.500\ NH_4HSO_4\}(l) \quad (4)$$

$$\downarrow$$

$$0.167\ SO_3(g) + \{0.167\ NH_4HSO_4 + 0.0167\ (NH_4)_2S_2O_7 + 0.083\ (NH_2)_2SO_2 + 0.083\ NH_2(SO_2NH)_2SO_2NH_2\}(l) \quad (5)$$

$$\downarrow$$

$$\{0.083\ N_2 + 0.167\ H_2O + 0.250\ SO_2\}(g) + \{0.167\ (NH_4)_2SO_4 + 0.167\ NH_4HSO_4 + 0.083\ NH_2(SO_2NH)_2SO_2NH_2\}(l) \quad (6)$$

$$\downarrow$$

$$\{0.667\ NH_3 + 0.167\ NO_2 + 0.333\ H_2O + 0.583\ SO_2\}(g) \quad (7)$$

REACTION SEQUENCE FOR THE DECOMPOSITION OF SULFAMIC ACID ABOVE ITS MELTING POINT[15]

the composition of the melt, producing ammonium pyrosulfate and different sulfur-nitrogen compounds. Subsequently, a further reaction (Equation 6) evolves gaseous nitrogen, water, and sulfur dioxide and once more alters the composition of the melt. Finally, the residual melt remains constant in composition but evolves gaseous ammonia, nitrogen dioxide, water, and sulfur dioxide (Equation 7). When volatilization is complete, the net reaction is shown by the sum of Equations 4 through 7:

$$NH_2SO_3H(l) \rightarrow 0.167\ SO_3(g) + 0.833\ SO_2(g) \quad (8)$$
$$+ 0.500\ H_2O(g) + 0.083\ N_2(g) + 0.667\ NH_3(g) + 0.167\ NO_2(g)$$

Halstead did not report any information about the rates of the several reactions given above. However, rate data were obtained in the laboratory of American Electric Power Service Corporation for the volatilization of sulfamic acid in the commercial form used at the Cabin Creek Station.[7] A sample of this material was held for 1 hr at various temperatures and the cumulative losses in weight were determined, with the results shown in Table 6.

Table 6. RESULTS OF A VOLATILIZATION STUDY OF A COMMERCIAL FORM OF SULFAMIC ACID

Temperature, °C (°F)	Cumulative weight loss, %
100 (212)	0
200 (392)	0
400 (752)	6
500 (932)	10
600 (1112)	10 (+)
700 (1292)	11
900 (1652)	30

The above information bearing on the stoichiometry and the rate of decomposition of sulfamic acid may or may not be applicable to the decomposition of this compound when it is dispersed as a powder in hot flue gas. First, with regard to stoichiometry, the presence of significant concentrations of water vapor and oxygen in flue gas may suppress the formation of ammonium pyrosulfate (the anhydride of ammonium bisulfate, as shown in Equation 5), and the reduction of the

sulfur trioxide constituent of sulfamic acid to sulfur dioxide, as shown in Equations 6 and 7. Second, with regard to rate, the dispersion of a fine powder might lead to much more rapid decomposition than that indicated by the above loss-in-weight data, which presumably were obtained with bulk powder resting in some type of vessel in a laboratory furnace.

CONDITIONING MECHANISMS

It must be assumed that in the pilot-plant and full-scale investigations of sulfamic acid described earlier in this paper the lowering of the electrical resistivity of the fly ash was one probable mechanism of conditioning. It is also necessary, however, to consider a space-charge effect and an increase in the cohesiveness of the ash as alternative mechanisms, as discussed in connection with ammonia conditioning.[3]

Lowering of the Electrical Resistivity of Fly Ash

The laboratory experiments of Dalmon and Tidy[5] included measurements of the resistivity of fly ash, which indicated that the resistivity was lowered by sulfamic acid conditioning. On the other hand, the full-scale precipitator studies in this country did not, unfortunately, include any measurements of resistivity. These studies did, however, yield data on fly-ash composition and precipitator electrical parameters that suggest conditioning by a lowering of resistivity. A question of both practical and theoretical interest is what chemical substances could have been responsible for this effect in the widely varying temperatures at which the sulfamic acid was injected and the treated fly ash was collected.

Successful results have been reported with sulfamic acid injected as an aqueous spray at temperatures of 165, 400, and 500° (approximately 330, 750, and 930°F). Successful trials of sulfamic acid have also been reported with the injection of the powdered solid at temperatures ranging from about 400 to 625°C (750 to 1160°F). In view of the fact that the stability of sulfamic acid changes markedly through the range of temperatures that have been used for injection, different chemical substances undoubtedly participate in the conditioning of fly ash as the injection temperature is altered.

Low-Temperature Injection—

The lowest injection temperature that has been cited in this paper, 165°C (about 330°F), is below the melting point of sulfamic acid and also below the range of temperatures that is required for molecular fragmentation of the compound. At this temperature, therefore, injection of sulfamic acid in an aqueous solution may leave a residue of small particles of the original compound to be coprecipitated with the fly ash after the liquid water of the solution has evaporated. Alternatively, during the process of injection, the sulfamic acid may undergo hydrolysis to ammonium bisulfate as previously illustrated in Equation 3.

The coprecipitation of discrete particles of sulfamic acid and fly ash conceivably could have lowered the effective resistivity of the ash. The basis for this statement is Dalmon and Tidy's finding that the coprecipitation of discrete particles of fly ash and another conditioning agent, sodium chloride, lowered the resistivity of fly ash. Their publication includes the reproduction of a photomicrograph showing a large particle of fly ash partially coated with crystals of sodium chloride, all smaller than 1 μm in size.[5]

The formation of ammonium bisulfate and the coprecipitation of this compound with fly ash would undoubtedly have been a more effective process for lowering the resistivity. Above 144°C (291°F), ammonium bisulfate is a liquid that would spread over the surfaces of individual fly-ash particles, producing a continuous film of a conductive compound rather than a discontinuous coating of discrete crystals. (Different melting temperatures of the bisulfate have been reported by various investigators; here, the value cited is that reported by Kelley et al.[18], which seems to be the most reliable.)

The low-temperature conditioning of fly ash with sulfamic acid through the action of liquid ammonium bisulfate has been postulated as an explanation for the effectiveness of sulfamic acid in the work of Dalmon and Tidy.[19] A critical aspect of the circumstances under which sulfamic acid was employed by Dalmon and Tidy was the temperature of the precipitator, 145°C (about 295°F)—just above the reported melting point of ammonium bisulfate.

High-Temperature Injection—

All of the injection temperatures for sulfamic acid above 165°C (330°F) were above the melting point of the compound and thus capable of decomposing the compound through the

sequence of reactions shown. Injection of sulfamic acid as a powdered solid undoubtedly was followed to some degree by this sequence of reactions. Injection of the conditioning agent in an aqueous solution, on the other hand, conceivably could have produced ammonium sulfate by hydrolysis (Equation 3) as the water evaporated from the solution droplets.

The formation of some gaseous sulfur trioxide but, more importantly, the formation of a relatively large quantity of ammonium bisulfate at high temperatures (Equations 4 and 5) has been proposed as an explanation of sulfamic-acid conditioning with high-temperature injection.[19] Thus, the formation of ammonium bisulfate has been proposed as the key to the conditioning process at high temperatures as well as low temperatures of injection.

A matter of some concern that is related to the above conclusions is Dalmon and Tidy's failure to find ammonium and bisulfate ions on their conditioned fly ash in the 1:1 molar ratio that occurs in ammonium sulfate.[5] As previously pointed out in this paper, Dalmon and Tidy suggested that most of the ammonium ion was lost as ammonia gas as a result of the reaction between the surface film of ammonium bisulfate and basic constituents of the fly ash. Perhaps ammonium ion remained in the outermost layer of the deposit, which was not in physical contact with the basic constituents of the ash.

Conditioning through the Space-Charge Mechanism

It seems likely that conditioning by sulfamic acid through the space-charge mechanism will occur only if two temperature conditions are satisfied: (1) the compound is injected at a temperature that is high enough to cause molecular fragmentation to ammonia and sulfur trioxide as gaseous products and (2) the decomposition products subsequently reach a considerably lower temperature that permits the products to recombine in the presence of water vapor as fine particles of ammonium sulfate or ammonium bisulfate. If the injection temperature is low, molecular fragmentation will not occur, and only large particles with a low concentration by number will be introduced. On the other hand, if the temperature of the flue gas is not lowered sufficiently as the gas stream approaches the precipitator, recombination of the molecular fragments will not be thermodynamically possible. The kinetic studies of Halstead[15] indicate that the injection temperature would probably have to be above 300°C (575°F).

The thermodynamic data of Kelley et al.[18] indicate that the precipitator temperature would have to be as low as 195°C (about 385°F) if ammonia and sulfur trioxide at concentrations of the order of 10 ppm are to react and produce ammonium sulfate or the temperature would have to be even lower, 173°C (about 345°F), if they are to produce ammonium bisulfate as an alternative product.

Both temperature conditions were satisfied in most of the investigations of sulfamic acid described in this paper. The most outstanding exception occurred in the pilot-plant work of Dalmon and Tidy with the lower of two injection temperatures, 165°C (about 330°F).[5] Unfortunately, the available data do not provide any basis for determining whether the space-charge effect was a significant conditioning mechanism.

However, the problem of air preheater plugging that was encountered by Buell[11] is comparable to the problem encountered in some studies of ammonia conditioning when the site of ammonia injection was upstream from the air preheater.[20] The similarity of these problems with the two conditioning agents suggests a possible similarity of conditioning mechanisms.

Conditioning through the Mechanism of Increasing the Cohesiveness of Fly Ash

Ammonium bisulfate, one of the decomposition products of sulfamic acid, may act as a conditioning agent by increasing the cohesiveness of fly ash, particularly at precipitator temperature above 144°C (291°F) where the compound exists as a liquid. The importance of this process, however, cannot be assessed because of the lack of pertinent data.

ECONOMIC ASPECTS OF SULFAMIC ACID AS A CONDITIONING AGENT

Dalmon and Tidy made a comparison of the relative costs of sulfur trioxide, sulfuric acid, sulfamic acid, ammonium sulfate, and ammonium bisulfate as conditioning agents.[5] Their first basis of comparison was the purchase price per mole of sulfur trioxide theoretically available from one mole of each compound. Their second basis of comparison took into account the efficiency of pickup of each agent by fly ash as observed experimentally. The results of the comparisons are given in Table 7. The relative costs given in this table indicate that sulfamic acid and ammonium bisulfate have a decidedly

adverse competitive position resulting from both purchase price and effectiveness. Capital and operating costs were not taken into account in the above comparisons. Dalmon and Tidy pointed out that these items of cost would be much lower for any of the alternatives to sulfur trioxide that can be injected as sprays of dilute aqueous solutions or as powdered solids. Even so, these investigators regarded the direct costs of sulfamic acid and ammonium bisulfate as too great to be offset by lower capital costs; thus, they concluded that only sulfuric acid and ammonium sulfate would be competitive with sulfur trioxide.

Despite the unfavorable cost of sulfamic acid, significant success apparently is being achieved in marketing a blend of this conditioning agent with other compounds. One of the factors evidently responsible for this success, despite Dalmon and Tidy's conclusion to the contrary, is the comparatively low cost of an injection system for sulfamic acid.[9] Another consideration is the relatively noncorrosive quality of this compound and the resulting savings in maintenance and operating costs.

Table 7. RELATIVE COSTS OF SULFUR TRIOXIDE, SULFAMIC ACID, AND RELATED CONDITIONING AGENTS

Conditioning agent	Cost per mole purchased	Cost for effective use
Sulfur trioxide	1.0	1.0
Sulfuric acid	0.6	1.1
Sulfamic acid	5.7	11.4
Ammonium sulfate	1.1	2.4
Ammonium bisulfate	5.5	11.1

CONCLUSIONS

Investigations of sulfamic acid that are discussed in this paper indicate that this conditioning agent is a substitute for sulfur trioxide that is worthy of consideration by the electric power industry. Its primary advantages seem to be

ease in handling and freedom from hazard. Another advantage at present is that sulfamic acid can be used in some localities where the use of sulfur trioxide is prohibited; whether this advantage is justified in terms of a lesser amount of noxious material emitted from a power-plant stack seems, to this reviewer, to be uncertain on the basis of the limited present knowledge about the quantity and type of material contributed to stack emissions when either sulfamic acid or sulfur trioxide is used. A disadvantage associated with sulfamic acid that has been stressed by several utility representatives is the high cost of the chemical; this paper does not attempt to resolve the question of relative cost, but it does point out some of the factors that determine the ultimate relative cost of using sulfamic acid as a substitute for sulfur trioxide.

It seems clear that sulfamic acid will sometimes be less effective as a conditioning agent than may be desired. It is certainly true, however, that sulfur trioxide will not always be as effective as desired. Shortcomings of both agents may sometimes be attributed to factors that cannot be eliminated by any conditioning agent, such as poor gas distribution or excessive gas velocity in a precipitator. Shortcomings attributed to the agents themselves may actually arise from insufficient skill in adding the chemicals to a flue-gas stream in active chemical and physical states.

The mechanisms by which sulfamic acid acts as a conditioning agent are not clearly established. Some tentative conclusions about mechanisms based on indirect evidence are given in this paper. However, there are uncertainties in these conclusions that can only be resolved by further study.

ACKNOWLEDGMENTS

Financial support for this review of sulfamic acid as a conditioning agent was provided by the U. S. Environmental Protection Agency through Contract 68-02-1303. Sources of some of the information solicited during this review were Mr. E. B. Morris of American Electric Power Service Corporation, Mr. C. A. Gallaer of Buell Division of Envirotech Corporation, and Dr. Ira Kukin of Apollo Chemical Corporation. Other sources of information were Dr. J. Dalmon and Dr. W. D. Halstead of the Central Electricity Research Laboratories in Great Britain, who provided interpretations of some of their published data through personal communications.

REFERENCES

1. White, H. J. Industrial Electrostatic Precipitation. Reading, Mass., Addison-Wesley, 1963. p. 294-330.

2. Dismukes, E. B. Conditioning of Fly Ash with Sulfamic Acid, Ammonium Sulfate, and Ammonium Bisulfate. Southern Research Institute, Contract 68-02-1303, Environmental Protection Agency. Report to be issued, 1975.

3. Dismukes, E. B. Conditioning of Fly Ash with Ammonia. In: Proceedings, Symposium on Electrostatic Precipitators for the Control of Fine Particles. Pensacola Beach. September 30-October 2, 1974.

4. Lowe, H. J. Reduction of Emission of Pollutants—Recent Advances in Electrostatic Precipitators for Dust Removal. Phil. Trans. Roy. Soc. Ser. A. 265(1161):301-307, 1969.

5. Dalmon, J., and D. Tidy. A Comparison of Chemical Additives as Aids to the Electrostatic Precipitation of Fly-Ash. Atmos. Environ. (Oxford, England). 6:721-734, October 1972.

6. The Increase in Precipitator Efficiency by Use of Apollo PPA-30 with Low Sulfur Coals. Apollo Chemical Corporation, Whippany, N. J. Bulletin U-556. 1973.

7. Morris, E. B. American Electric Power Service Corporation, New York, N. Y. Private communication.

8. Kukin, I. The Practical Applications of Chemical Additives to Increase Electrostatic Precipitator Efficiency of Coal Fired Units. Apollo Chemical Corp. (Presented at Pennsylvania Electric Association Fall Meeting. October 18-19, 1973.) 9 p.

9. Chemical Helps Trap Flyash from Low-Sulfur Coal. Electric Light and Power. 52(7):20-21, April 1974.

10. Billings, J. Public Service Electric and Gas Company, Newark, N. J. Private communication.

11. Gallaer, C. A. Buell Division of Envirotech Corporation, Lebanon, Pa. Private communication.

12. Sautmyers, D., and R. Aarons. Sulfamic Acid and Sulfamates. In: Kirk-Othmer Encyclopedia of Chemical Technology, Volume 19, Standen, A. (ed.). New York, Wiley, 1969. p. 242-249.

13. Stecher, P. G. (ed.). Merck Index. Rahway, N. J., Merck and Co., 1968. p. 997.

14. Brasted, R. C. Comprehensive Inorganic Chemistry, Volume 8. Princeton, Van Nostrand, 1971. p. 215-227.

15. Halstead, W. D. Vaporization of Sulphamic Acid. J. Appl. Chem. Biotechnol. (London). 21:22-26. January 1971.

16. Linke, W. F. Solubilities—Inorganic and Metal Organic Compounds, Volume 1. Princeton, Van Nostrand, 1958. p. 1167.

17. King, E. J., and G. W. King. The Ionization Constant of Sulfamic Acid from Electromotive Force Measurements. J. Amer. Chem. Soc. 74:1212-1215, March 1952.

18. Kelley, K. K., C. H. Shomate, F. E. Young, B. F. Naylor, A. E. Salo, and E. H. Huffman. Thermodynamic Properties of Ammonium and Potassium Alums and Related Substances, with Reference to Extraction of Alumina from Clay and Alunite. Bureau of Mines, Washington, D. C. Technical Paper 688. 1946. p. 66-69.

19. Halstead, W. D. Central Electricity Research Laboratories, Leatherhead, England. Private communication.

20. Archer, W. E. Electrostatic Precipitator Conditioning Techniques. Power Eng. 76:50-53, December 1972.

SULFUR TRIOXIDE CONDITIONING

Ronald E. Cook
Commonwealth Edison Company
Chicago, Illinois

ABSTRACT

Burning of western low sulfur coal, to reduce sulfur oxide emissions, has resulted in decreased electrostatic precipitator collection efficiencies. In an effort to restore precipitator performance a flue gas conditioning program was established by the company.

This paper is a brief history of Commonwealth Edison Company's experience with sulfur trioxide as a flue gas conditioning agent. Testing at State Line Station has proven that sulfur trioxide conditioning can effectively be used to improve precipitator performance when burning low sulfur coals.

Although the first phase of the conditioning program is not completed, information has been gained which is being used as a basis in design and evaluation of future systems.

The reduction of sulfur oxide emissions from coal fired boilers to meet regulatory requirements can be accomplished in several ways. Some of these are:

1. Converting to low sulfur oil or fuel gas
2. Installing coal gasification plants
3. Using flue gas scrubbers
4. Changing to low sulfur coal

All of these methods have limitations from both an engineering and economic standpoint. The burning of low sulfur coal is one of the methods used by Commonwealth Edison to meet sulfur oxide emission standards.

The change to low sulfur coal, however, creates an electrostatic precipitator performance problem. Fly ash from burning Western low sulfur, low sodium coals has low surface electrical conductivity at normal boiler exhaust temperatures (133-177°C) (270-350°F). This high resistivity characteristic hinders its removal from the flue gas by electrostatic precipitation.

Various conditioning agents have been used to improve precipitator performance by decreasing the resistivity of the fly ash particles. We chose to use sulfur trioxide (SO_3).

Tests, using SO_3 injection, were conducted at Crawford Generating Station and State Line Station. We have subsequently committed ten units, ranging in size from 120 MW to 620 MW, to SO_3 conditioning by the end of 1976.

Several prerequisites are necessary for successful flue gas conditioning. First, the precipitator must be capable of meeting compliance at design conditions with high sulfur coal or be capable of being modified to improve its performance to a satisfactory level.

Second, the SO_3 must be distributed properly into the flue gas to completely treat the fly ash before it enters the precipitator. Normally, the proper location of the probes and nozzles to obtain optimum distribution requires a flow model study.

The third requirement is that the SO_3 equipment must be simple to operate and capable of automatically controlling the feed depending on boiler load. It must also be capable of being on line from a cold start in less than 4 hours.

The first Commonwealth Edison test of SO_3 injection took place at Crawford Generating Station in 1970. During a test of Big Horn low sulfur (0.5%) coal, sulfur trioxide was injected to determine its effectiveness in reducing fly ash resistivity.

The 225 MW, pulverized coal fired boiler was operated at rated load with no additives. The sulfur dioxide concentrations produced from this fuel ranged from 610 to 720 ppm by volume at the precipitator outlet. During the injection of SO_3 on the third day, the sulfur dioxide concentrations remained basically the same.

The SO_3 concentration sampled in the gas duct about 30 feet downstream of the injection ports started at a rate of about 5 ppm and gradually increased to 22 ppm. The total injection time was 8½ hours when the liquid SO_3 supply was exhausted. During the entire SO_3 injection period, the SO_3 level at the precipitator outlet was of the order of 0.5 ppm or less.

While injecting SO_3, the sulfur content of the fly ash increased by approximately 4%. There was ample calcium oxide in the fly ash to absorb practically all of the SO_3 added during the test period.

The appearance of the stack and dust loading tests at the precipitator outlet indicated no improvement with the addition of SO_3. Since the test program was primarily concerned with the effect of Big Horn coal on boiler operation, the SO_3 injection method was quite crude, using barrels of SO_3 in a heated room which was fed by gravity to the injection probes in the precipitator inlet duct. In addition, the test run was not long enough to reach equilibrium conditions with the fly ash already collected. Later testing at State Line Station indicated several days of treatment are necessary. The simplified injection method did not insure proper distribution of the SO_3 in the flue gas. The test results were inconclusive.

Two SO_3 injection systems were later installed on low sulfur coal burning units previously operated with medium sulfur coal. The first to be operational, was a pilot sulfur burner installed on a 230 MW pulverized coal fired boiler at State Line Station in 1972.

This equipment shown schematically in Figure 1, designed by Research-Cottrell, consists of a liquid sulfur feed to a pan type burner where the sulfur dioxide is formed by combustion. The sulfur dioxide is then passed through an electric heater and a two-pass catalytic converter, with interstage cooling, which converts over 90% of the SO_2 to SO_3.

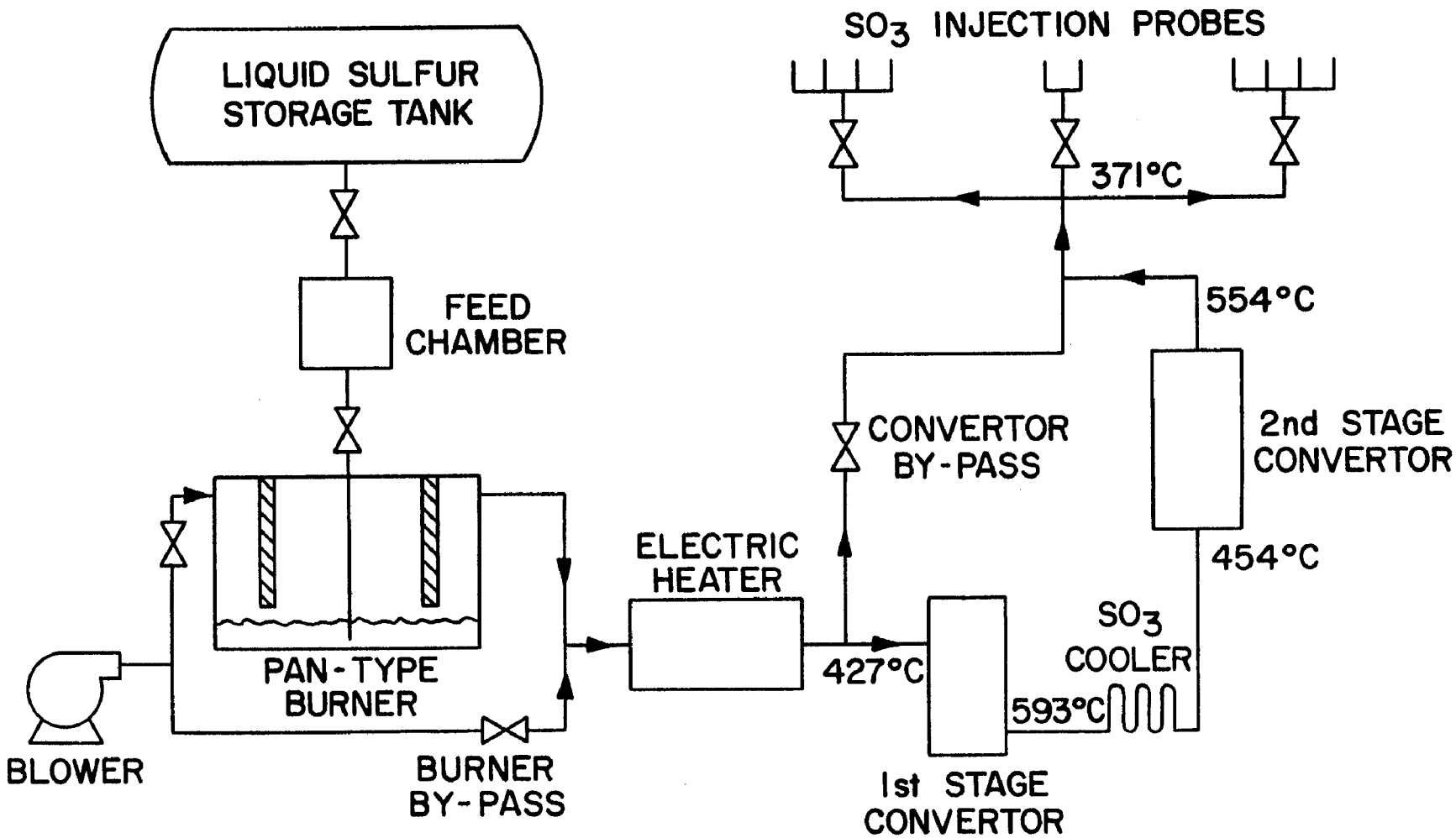

Figure 1. Sulfur burning flue gas conditioning system, State Line Unit 3

The SO_3-air mixture of about 10% SO_3 is then piped through an insulated manifold to the probe and nozzle system located internally in the ducts leading to the electrostatic precipitator.

This R-C prototype gas conditioning system was placed in service in May 1973. The coal burned was Arch Mineral No. 1 (Seminole Mine) from Wyoming which is an extremely poor fuel from a gas cleaning standpoint, having low sulfur and sodium content as shown in the coal and ash analysis in Table 1. It was soon obvious that the capacity of the gas conditioning system was inadequate.

The experimental system had to be modified by reducing the total system pressure drop, and increasing the combustion air rate. This was accomplished by increasing the probe nozzle areas. In addition, provision was made to spike the sulfur dioxide combustion gases with vaporized SO_2 supplied from a liquid SO_2 storage tank.

Testing of the system included measuring particulates, gas composition, fuel and ash analysis and precipitator power input. Difficulty in measuring the SO_3 was encountered using the EPA method 8. The method used to determine the SO_3 concentration was to measure the amount of sulfur burned, determining the temperature rise in the converter, and applying an equilibrium conversion diagram to project the SO_2 conversion. Gas temperatures varied from 144 to 154°C (292 to 345°F) at the precipitator inlet with moisture content ranging from 8.4 to 10.7%. Oxygen content of the gas was 5 to 6%, roughly equivalent to 35% excess air. Particulate inlet loadings ranged from 5.95 g/m^3 stp to 7.32 g/m^3 stp (2.6 to 3.2 gr/scf).

The effect of the SO_3 concentration on precipitator efficiency is shown in Figure 2. An appreciable improvement in efficiency accompanied SO_3 conditioning. The two conditioned runs below 149°C (300°F) exhibited better precipitator efficiencies than similar tests above 149°C (300° F) as would be expected.

The corona power input exhibited a great improvement with flue gas conditioning as shown in Figure 3. Without conditioning, sparking limits the power input level to about 25 watts/1000 acfm. A ten-fold increase in power to about 250 watts/1000 acfm accompanied SO_3 addition to about 40 ppm. Additional

Table 1. TYPICAL COAL AND ASH ANALYSIS
ARCH MINERAL NO. 1

"As received" coal analysis (% by weight)	
Moisture	10.8 - 12.3
Sulfur	0.52 - 0.86
Ash	10.94 - 14.43
Gram-cal./gram (Btu/lb)	5,358 - 5,654 (9,644 - 10,176)
Ash analysis (% by weight)	
Silica	31.6 - 39.7
Alumina	16.9 - 19.0
Iron oxide	10.6 - 18.8
Titanium oxide	0.5 - 0.7
Calcium oxide	15.3 - 18.8
Magnesium oxide	3.0 - 3.6
Potassium oxide	1.0 - 1.6
Sodium oxide	0.64 - 0.74

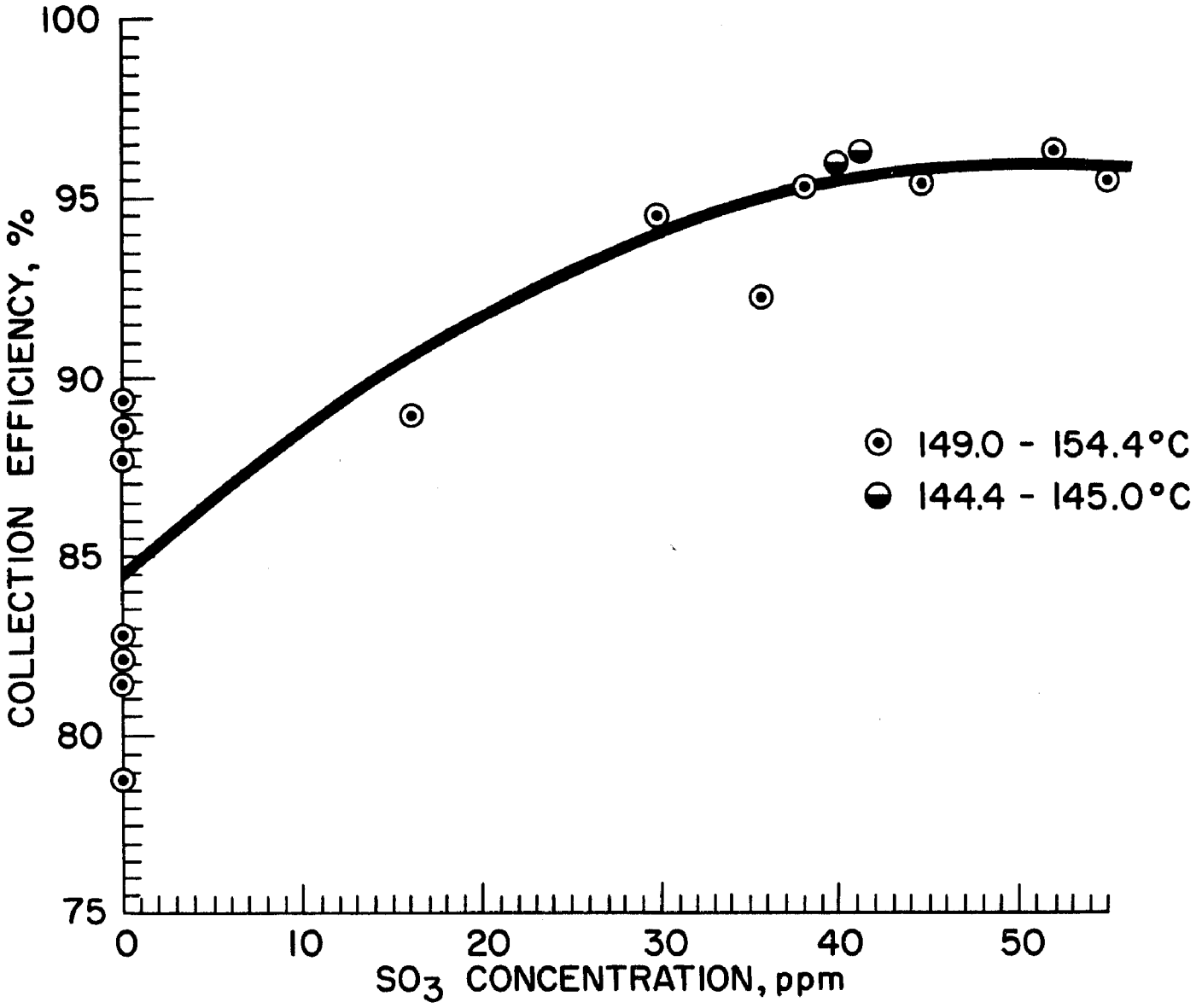

Figure 2. Effect of conditioning level on collection efficiency, State Line Unit 3

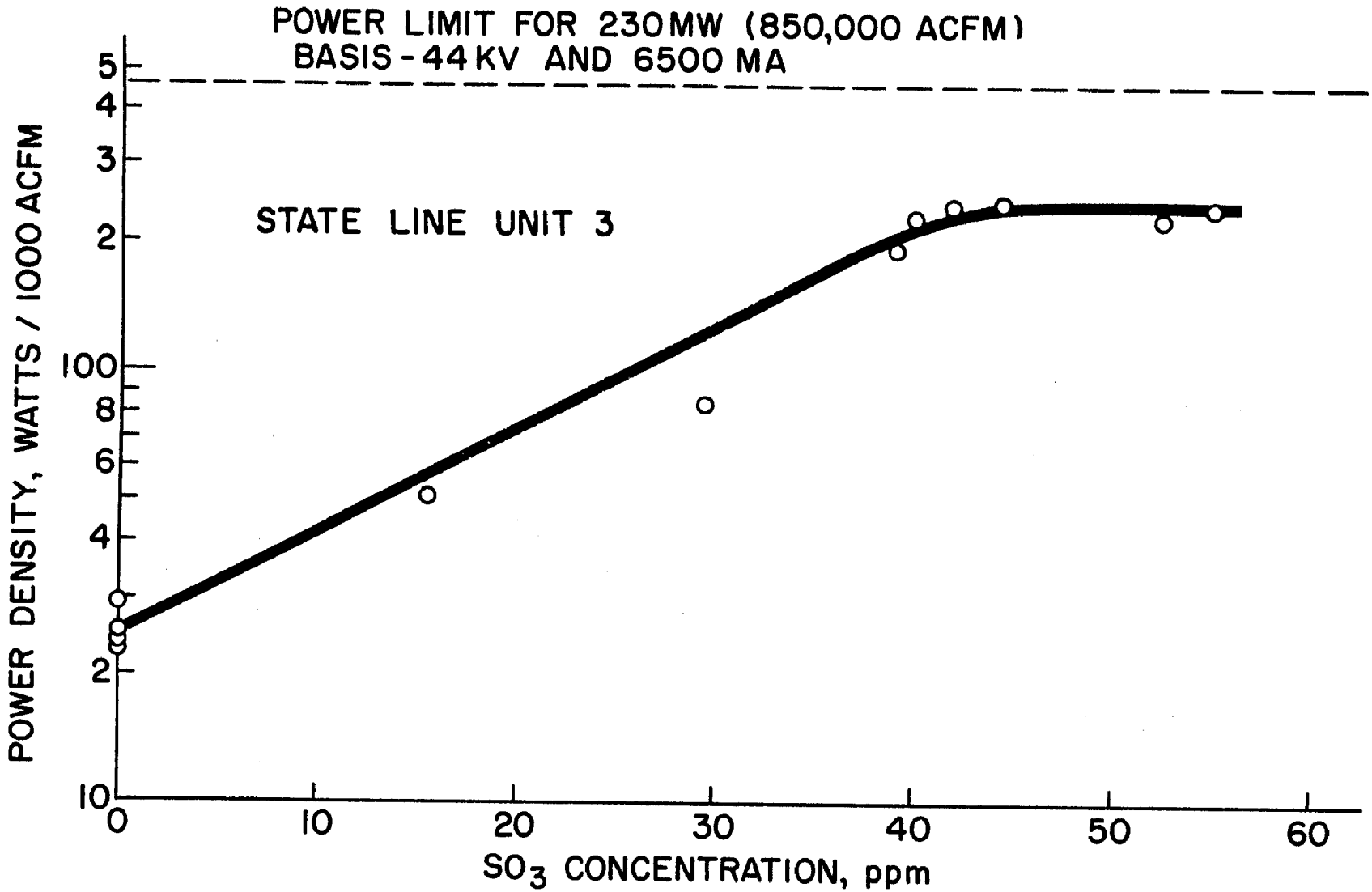

Figure 3. Corona power input as a function of SO_3 addition

SO_3 injection above this level did not appear to improve the power input to the precipitator.

Since the basic purpose of the prototype system was to prove normal precipitator performance could be obtained by SO_3 injection, the test program was considered successful, even if all of the objectives, such as a reliable gas analysis were not obtained.

It was also concluded that increased SO_3 levels are required when treating highly basic fly ash, such as that produced from Arch Mineral coal. Because of uncertainty of coal sources, future systems must be at least capable of injecting SO_3 at the 55 ppm level when at full boiler load.

Since commitments for other flue gas treatment had to be made to the Illinois Environmental Protection Agency and the City of Hammond, Indiana, on an extremely tight schedule, a second system was being designed and built at the same time the State Line system was being tested.

The second installation, a liquid SO_3 system, installed on a pulverized coal fired, 325 MW boiler at Waukegan station, was designed for 20 ppm SO_3 injection. Fortunately, the system was designed with a spare evaporator, which will now be needed to operate at the desired SO_3 concentration. Unfortunately, the piping could not be changed and the system, designed to carry 8% SO_3-air mixture to the probes will be transporting a 15% mixture. This could increase the possibility of a chemical corrosion problem if the dry air system functions marginally.

This system supplied by Chemithon Corporation was placed in operation March 7th of this year and is capable of automatically following the boiler load.

The system, as shown schematically in Figure 4, consists of a pressurized liquid SO_3 storage tank which feeds two electrically heated evaporators. Heated dry air is added in the evaporators and the air and gaseous SO_3 is then routed through a heat traced, insulated pipe to the probe and nozzle system located internally in the ducts before the electrostatic precipitator.

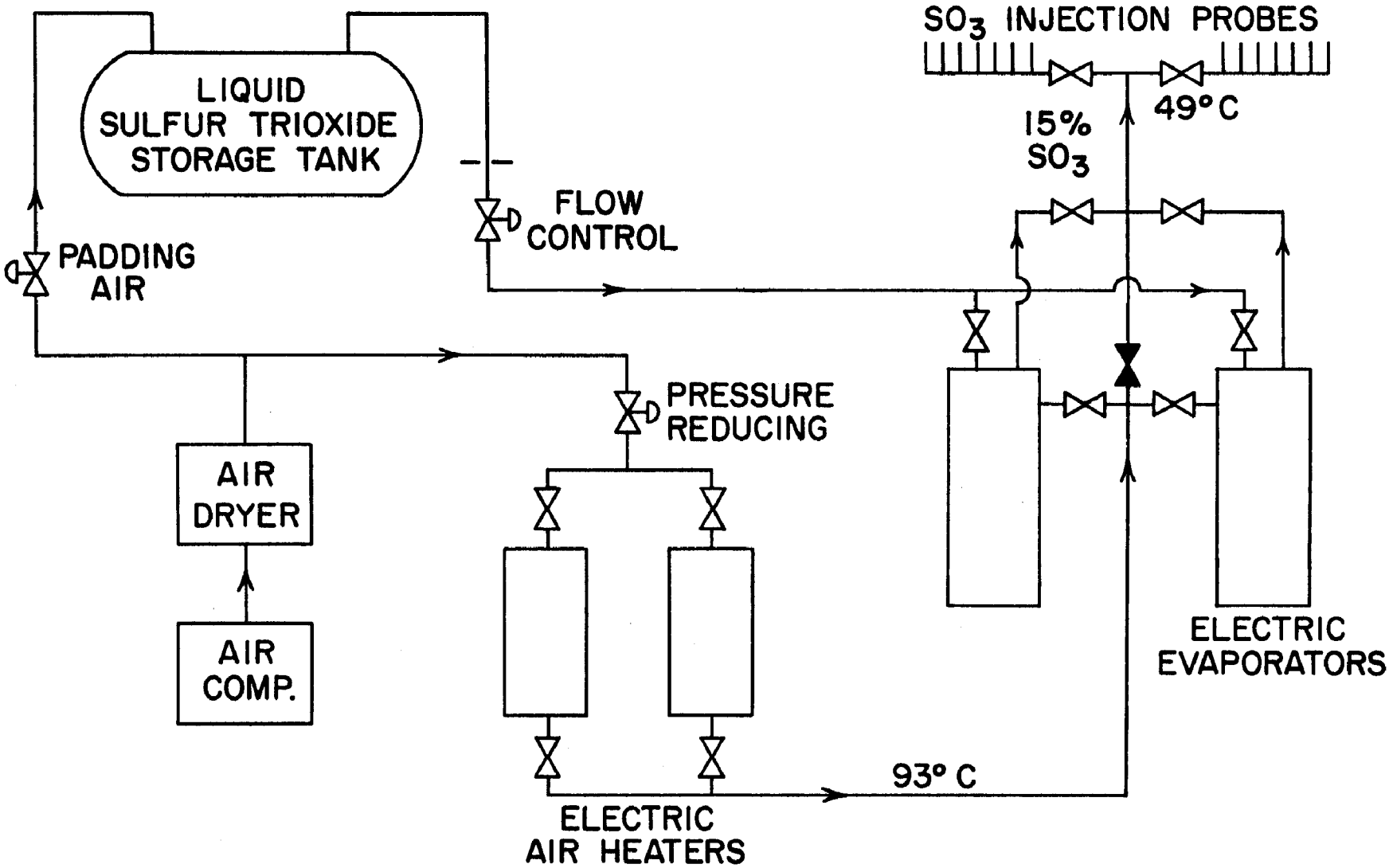

Figure 4. Sulfur trioxide evaporation flue gas conditioning system, Waukegan 8

Although the liquid SO_3 system has operated intermittently for a total of 200 hours and has operated in the automatic mode, actual testing of the system has been delayed, due to boiler operation with fuel gas during the summer.

An inspection of the 316 S.S. injection probes during a unit outage in June revealed considerable chemical attack at some of the nozzles. Newly designed experimental probes will be installed prior to expected testing of the system in October of this year.

Since the installation of the State Line and Waukegan systems, two new flue gas conditioning systems have been purchased and are presently being installed at State Line Station.

An engineering and economic study of the existing systems indicated that a sulfur burner type SO_3 treatment system would be desirable.

Some of the factors considered in arriving at this decision were:

1. Initial cost of installation (about the same for liquid SO_3 and sulfur burning)

2. Operating cost of the system (sulfur burning will reduce cost by ¼)

3. Availability of chemical supply (decided advantage for liquid sulfur)

4. Material storage and handling problem (sulfur is a much safer material)

5. Simplicity of operation (no decided advantage to either system)

The liquid sulfur burner units presently being installed on State Line 3 and 4 are rated at 91 and 136 kg/hr (200 and 300 lbs/hr) of sulfur, respectively. These units will be fully automatic, having a 10-1 turn-down ratio, requiring an operator only for lightoff and twice a shift routine inspection.

The State Line 3 Unit should be operational by December 31, 1974, which will meet our compliance date.

The compliance dates for the remaining seven units are such that they will have to be awarded, and construction started, before the new unit at State Line Station can be tested and evaluated.

APPLICATION OF ELECTROSTATIC PRECIPITATORS FOR THE CONTROL OF FUMES FROM LOW ODOR PULP MILL RECOVERY BOILERS

John E. Paul
The Rust Engineering Co.
Birmingham, Alabama

ABSTRACT

The cellulose pulping industry has long used electrostatic precipitators to collect soda ash entrained in recovery boiler flue gases. At a collection efficiency of 85 to 95 percent, the optimum economic situation is reached where capital outlay and operating expenses balance the value of the chemicals recovered over the life of the equipment. In recent years, however, stringent governmental regulation of particulate emissions has necessitated collection efficiencies above 99 percent. Although economic operation can not be achieved, traditional precipitator design is readily adaptable to these higher collection efficiencies.

The pulp and paper industry in the United States has recently embarked upon a program to eliminate the emission of odorous gases from pulp mills. This involves a totally different operation of the kraft pulping liquor recovery process. Low-odor operation of the recovery boiler results in a particulate emission with different physical properties from those produced by the traditional process. Electrostatic precipitators of the traditional design are incapable of handling this particulate emission. Fundamental changes in precipitator design and application are therefore necessary.

INTRODUCTION

Of the many chemical pulping processes available today, the kraft (alkaline sulfate) process is the most widely used, both on a numerical and a production volume basis. It provides for a closed cycle recovery for spent pulping chemicals. (See Figure 1.) The pulp cooking (lignin separation) process produces weak black liquor as a residue. This liquor, mainly sodium sulfate (Na_2SO_4) and sodium carbonate (Na_2CO_3), is concentrated to the point that it may be burned in the furnace of a recovery boiler. This thermal oxidation reduces the liquor constituents and releases the thermal energy of the organic portion. The reduced chemicals are causticized and returned to the pulping process as fresh cooking liquor.[1] The thermal energy is used to generate steam for process use.

A substantial portion of the reduced soda ash is entrained as particulate in the recovery boiler flue gases. To optimize the recovery process, pulp mills have used electrostatic precipitators to collect a portion of this entrained soda ash for many years. This was done primarily on economic considerations, since the value of the chemicals recovered at a collection efficiency of 85 to 95 percent balanced the required capital outlay and operating expenses over the life of the equipment.

In recent years, growing public concern over environmental pollution has resulted in stringent governmental regulation of particulate emissions. Collection efficiencies above 99 percent are now mandatory in most locations. Due to such favorable media characteristics as acceptable electrical resistivity, the particle charging and deposition process requirements for these high collection efficiencies present relatively few design problems. Until recently, the majority of design effort has been expended on the improvement of component resistance to the highly corrosive atmosphere in which the precipitator must operate.

In the last few years, the pulp and paper industry has made a commitment to eliminate odorous gases escaping from pulp mills. A large part of this odor elimination program centers around the recovery process for kraft pulping liquor. The necessary changes in the recovery process result in particulate emissions from the recovery boiler with different physical properties from those produced by the traditional process. Electrostatic precipitators sized on the basis of empirical information accumulated from operating

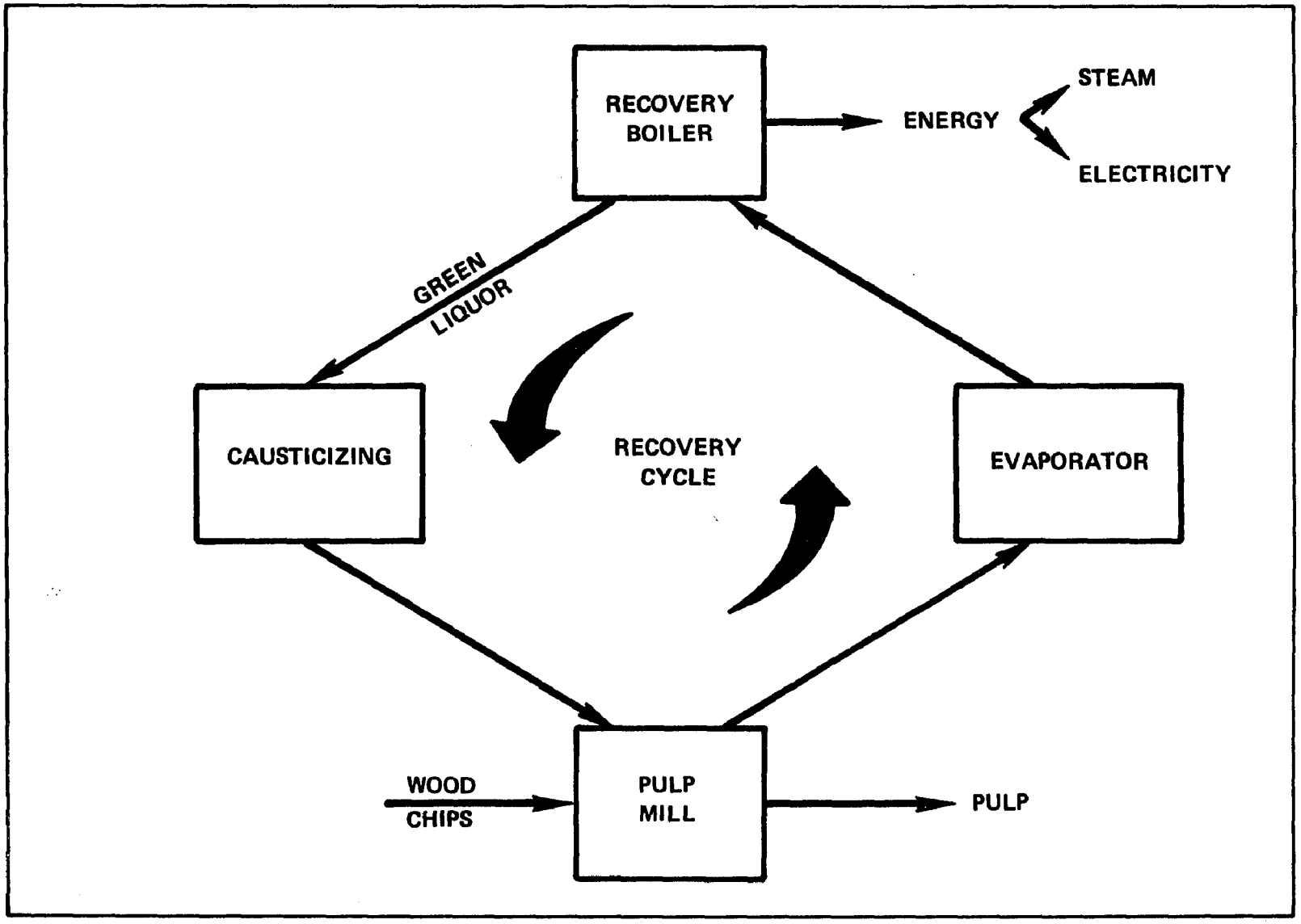

Figure 1. Kraft pulping liquor closed cycle recovery process

facilities on the traditional process are incapable of handling this emission with the required efficiency and operational reliability.

To more fully understand the two processes and what is being done in the design of precipitators for application to the low-odor process, let us look at the basic difference between the traditional recovery process and the low-odor process.

THE TRADITIONAL PROCESS

The feature of greatest interest in the traditional recovery process is a device in which the concentrated black liquor is brought into direct contact with the flue gases from the recovery boiler. (See Figure 2.) This device is either a spray chamber where gas turbulence is created by cyclonic action or a rotary or cascade evaporator. Heat from the flue gases is used for partial evaporation of the moisture content of the black liquor. The solid content is thus increased from approximately 50 percent to 65 percent. Some of the entrained particles are scrubbed from the flue gases, and the temperature is reduced to approximately 150°C (300°F). It has been shown that the black liquor also absorbs sulfur dioxide (SO_2) from the flue gases in the direct contact process.[2] This increases the sulfidity of the liquor which, when fired, generates more sulfur dioxide.

After passing through the direct contact device, the flue gases contain up to 35 percent water vapor by volume. The particulate matter is highly hygroscopic and absorbs a portion of the water vapor. Dry particulate matter has a bulk density of 320 to 480 kg/m^3 (kilogram per cubic meter) — 20 to 30 lb/ft^3 (pounds per cubic foot). This density allows traditional precipitators to be designed so that the collected salt cake is rapped from the collecting electrodes and falls by gravity into a flat-bottom pan containing concentrated black liquor. Motorized agitators provide proper mixing and dissolving of the salts for return to the salt cake mix tank.

Unfortunately, the direct contact device and, to a lesser degree, the wet-bottom precipitator are sources of volatilized hydrogen sulfide (H_2S), mercaptans, and organic sulfides and disulfides. These gases are the offensive odors associated with the kraft pulping liquor recovery process.

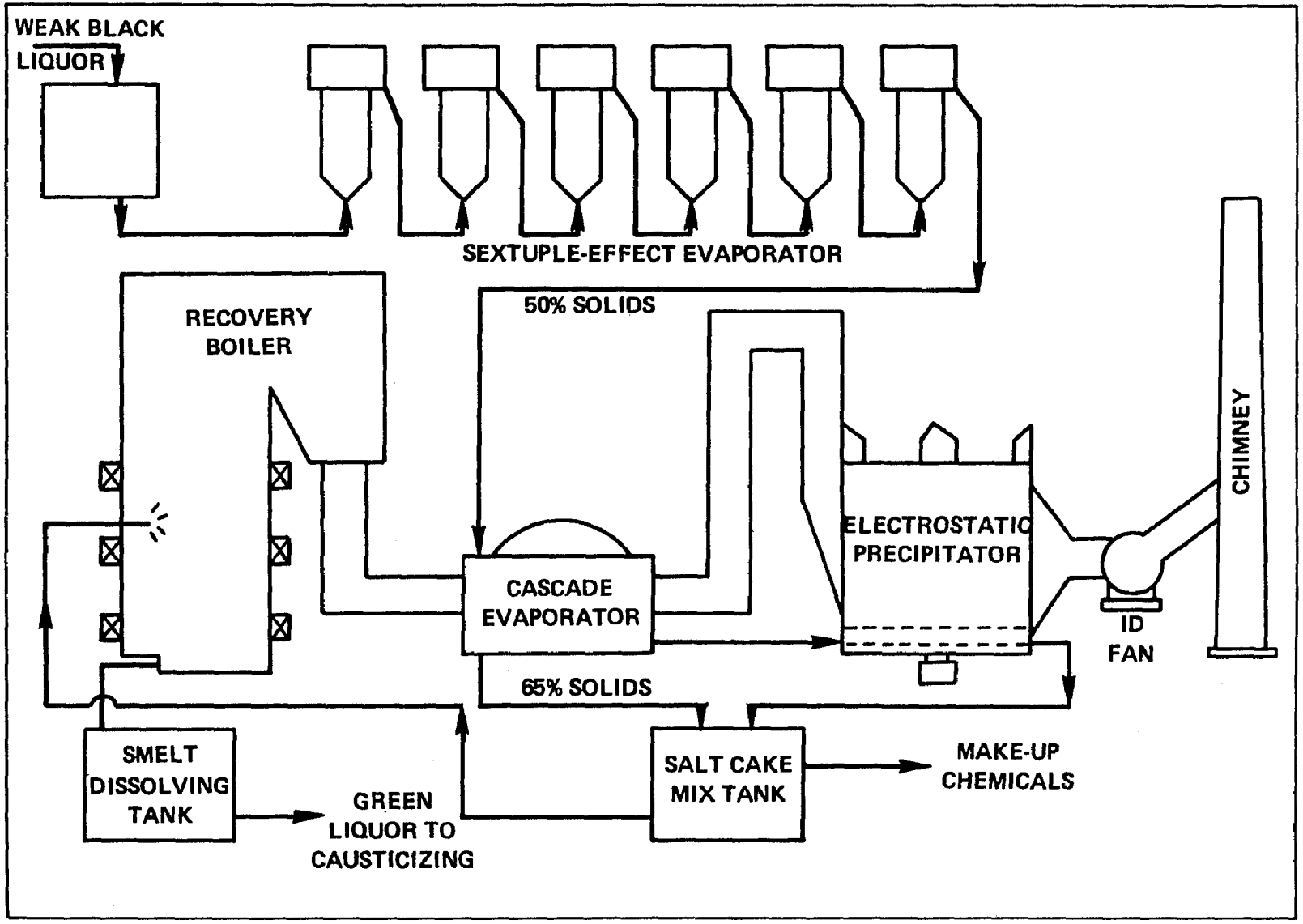

Figure 2. Traditional liquor recovery process

THE LOW-ODOR PROCESS

The low-odor concept of kraft pulping liquor recovery has been used in Europe for some time, but was only recently introduced here in the United States. The primary feature of this process is the elimination of direct contact between the concentrated black liquor and the recovery boiler flue gases. (See Figure 3.) A number of different flow designs are offered for the low-odor process, but, in general, the black liquor leaving the evaporator at 45 to 50 percent solids is further condensed to 60 to 65 percent solids in a concentrator. It is then piped directly to the recovery boiler. The boiler is equipped with an enlarged economizer section or convection-type air pre-heaters or both. This increases the boiler efficiency and insures that the flue gases will enter the precipitator at 175°C (350°F) to 230°C (450°F). Elimination of direct contact between the black liquor and the flue gases reduces the water vapor content to 15 to 20 percent by volume. The wet-bottom pan of the precipitator is replaced with a dry receiving facility that discharges the collected soda ash into an agitated make-down tank. From here, the recovered chemicals are returned to the liquor loop at the salt cake mix tank.

LOW-ODOR PRECIPITATOR DESIGN

Initial application of the precipitator to the new process indicated that substantial differences existed in the physical properties of the particulate matter. This required a fundamental revision of precipitator application design practices. The dust collected on the electrodes of the of the precipitator was found to have a bulk density of 80 to 160 kg/m^3 (5 to 10 lb/ft^3), substantially lower than the traditional process. Particle size was mostly in the three micron and smaller region. (See Figure 4.) In addition, the particles displayed a strong tendency to adhere to each other or any other surface they contacted.

The reason for this change in physical characteristics is not yet fully understood. One theory suggests that the equilibrium of the chemical reactions in the recovery boiler shifts in relation to varying furnace bed temperature.[3] Operating experience indicates that both the quantity and the physical characteristics of the particulate will vary considerably with the mode of recovery boiler operation. Furnace bed temperatures above 1,050°C (1,900°F) prevent the formation of hydrogen sulfide and sulfur dioxide,

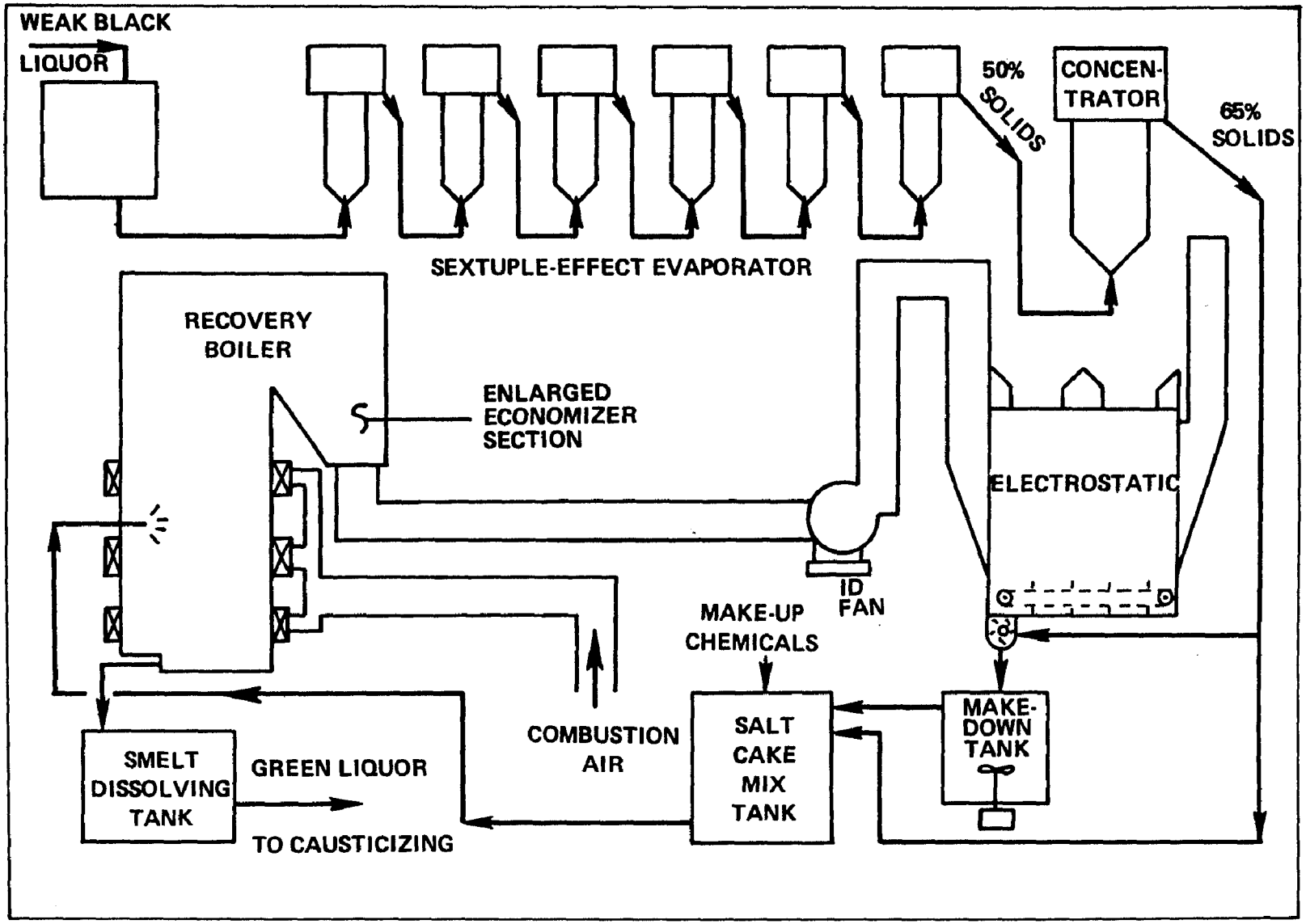

Figure 3. Low-odor liquor recovery process

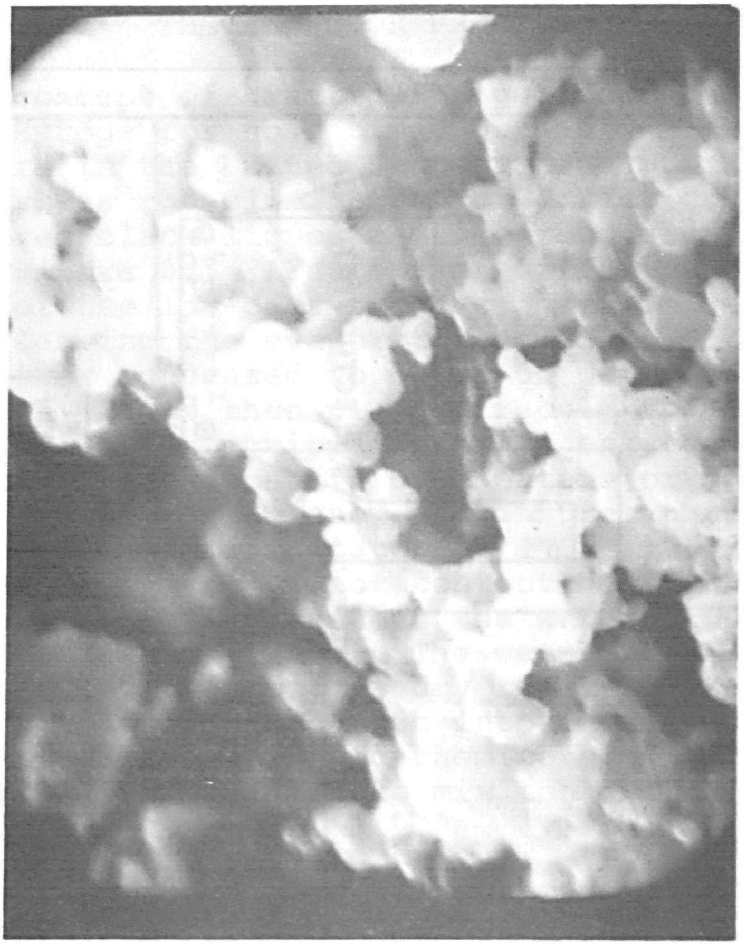

1 micron

Figure 4. 10,000X electron photomicrograph of particulate matter produced by the low-odor process

but they result in the formation of sodium metal—boiling point 875°C (1,600°F). Temperatures above 1,200°C (2,200°F) result in a flue gas that is rich in sodium carbonate and an increased particulate loading to the precipitator.

The particulate produced by the low-odor process results from the complex interaction of volatilized sodium metal with oxygen and sulfur oxides. This dust consists of approximately 90 percent sodium sulfate and 10 percent sodium carbonate fume. With increasing acidity, the particulate appears to become more adherent. The reaction principles of the low-odor process do not differ from those of the traditional process. It must, therefore, be assumed that the conditioning effect of the direct contact evaporation process rendered the particulate acceptable to the precipitator, and a complete understanding of the furnace reaction principles was of little value.

Due to the degenerative nature of the particulate matter, actual quantitative relationships are difficult to establish. Consequently, major design efforts are directed toward improvements in precipitator design to cope with the most adverse operating conditions.

The typical size distribution of particulate matter produced by an operational low-odor recovery boiler is given in Table 1. Four different samples were collected at the precipitator inlet and averaged to give the values in the table. The particulate loading was found to be 2.2 grains/acf (grains per actual cubic foot). Operation difficulties with the collection equipment led to some particles in the 2.40 to 4.08 micron range being collected with those greater than 4.08 microns.

Table 2 shows the typical size distribution of the particulate collected at the precipitator outlet during two different tests. Test 1 gives the size distribution of the particulate collected at an efficiency of 95 percent. The size distribution of that collected at an efficiency of 99 percent is given in Test 2. The results of these two tests are shown graphically in Figure 5.

Under the influence of electrostatic forces, this fine particulate rapidly forms an agglomerate that adheres tenaciously to any surface of electrically attractive potential. (See Figure 6.) The build-up of dust on electrode supporting surfaces and hopper walls can significantly reduce the required clearance, resulting in premature power arcing. The corresponding overall loss of power input to the electrostatic field will seriously impair the efficiency of the precipitator. It has been reported that spiked or

TABLE 1. TYPICAL INLET PARTICLE SIZE DISTRIBUTION

Size interval (μm)	Material collected (milligrams)	Percentage
>4.08	19.1	19.8
2.40 - 4.08	7.3	7.58
1.62 - 2.40	19.6	20.3
0.892- 1.62	25.2	26.1
0.51 - 0.892	12.6	13.6
<0.51	12.8	13.27

TABLE 2. TYPICAL OUTLET PARTICLE SIZE DISTRIBUTION

Size interval (μm)	Material collected (milligrams)	Percentage
	Test I	
>11.8	9.5	44
7.44 - 11.8	3.0	14
6.20 - 7.44	0.1	0
3.96 - 6.20	0.6	3.0
2.18 - 3.96	0.8	3.5
1.12 - 2.18	1.0	4.8
0.67 - 1.12	3.8	17.7
0.45 - 0.67	2.4	11.1
< 0.45	0.4	1.9
	Test II	
> 3.75	7.0	51.5
2.20 - 3.75	1.3	9.6
1.49 - 2.20	1.5	11.0
0.82 - 1.49	2.1	15.4
0.47 - 0.82	1.4	10.3
< 0.47	0.3	2.2

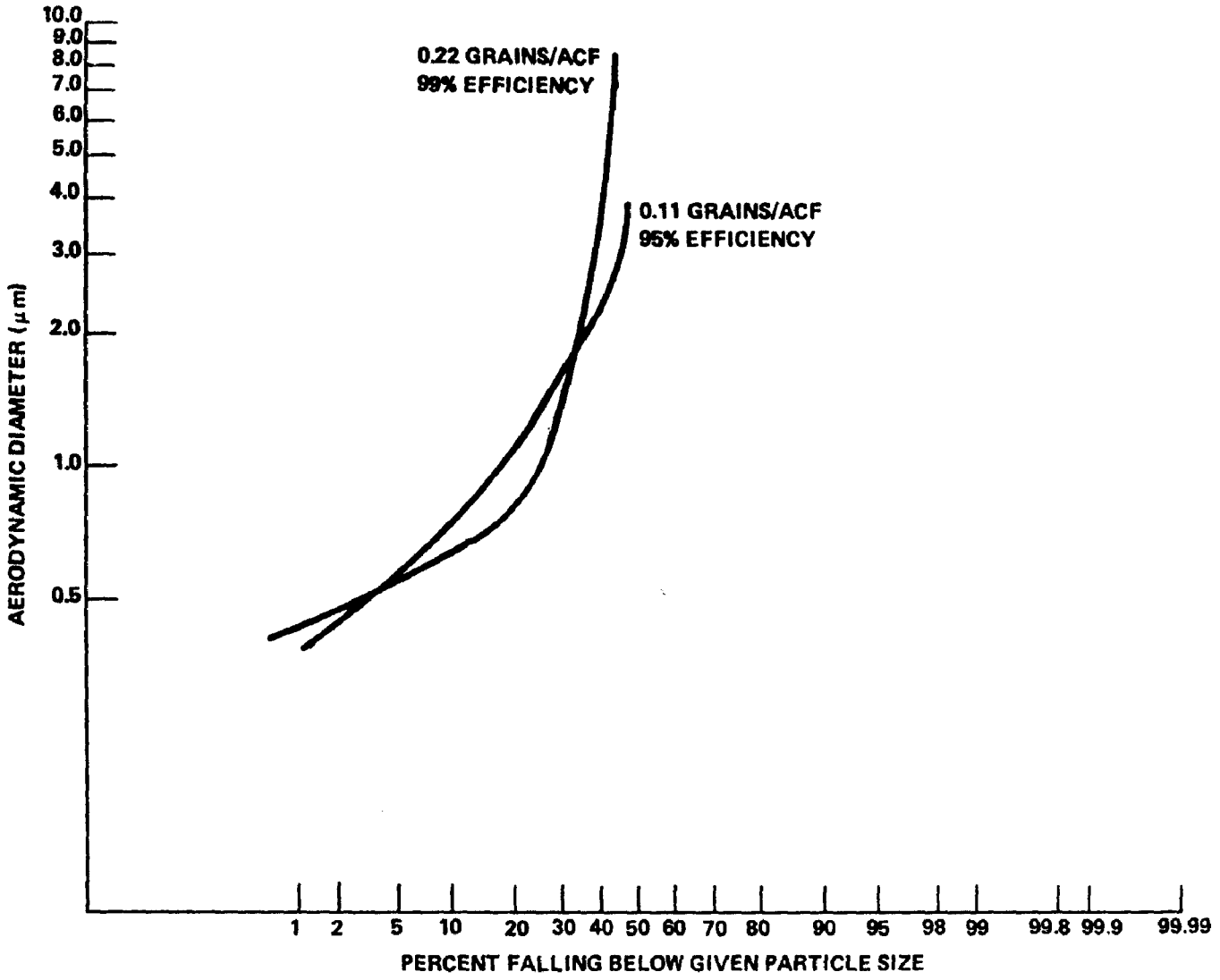

Figure 5. Size distribution of particulate produced by the low-odor process

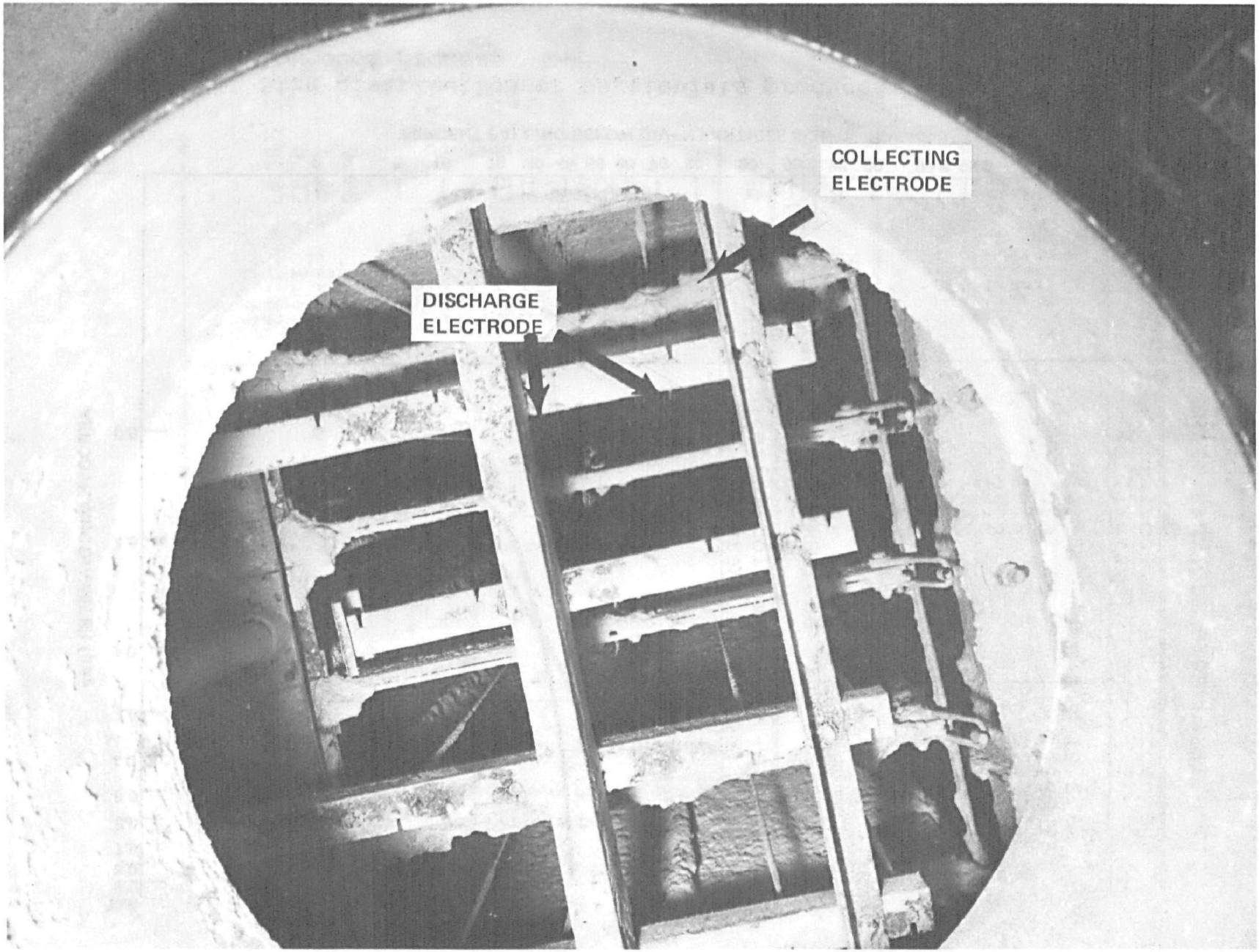

Figure 6. Electrode suspension system showing dust build-up

barbed wire discharge electrodes have achieved superior electrical stability under these conditions.

To dislodge this dust, sufficient rapping forces to produce rapid acceleration parallel to the gas flow (a shear action) must be applied to the collecting surfaces. Over-rapping or vibrations perpendicular to the gas flow will fracture and scatter the agglomerate, resulting in serious re-entrainment of the particulate.

Re-entrainment will also occur if the flue gas velocity in the precipitator treatment zone exceeds approximately 1 m/sec (meter per second)—3.5 ft/sec (feet per second). It is, therefore, of the utmost importance that the treatment zone of the precipitator be designed to uniformly distribute the gas velocity. The series electrical sectionalization and treatment length should be increased to give a minimum collector plate height-to-length aspect ratio of 1-to-1. This will prevent any re-entrained particulate escaping the precipitation system.

Application of traditional precipitators to the low-odor process disclosed that the basic design was incapable of handling build-up such as shown in Figures 7 and 8. The initial approach to this problem was to increase the rapping forces and the addition of rappers to the hopper walls. The forces required to dislodge the dust, however, exceeded the structural limitations of the precipitator design, and damage to the electrode system and the precipitator shell occurred. A new system of electrode suspension and a different method of transmitting the rapping forces had to be found. One design that incorporates the desired features utilized freely-suspended collecting electrode plates and rigid discharge electrode elements mounted in a frame. When rapped, the elements vibrate at high frequencies without shifting their position relative to the collecting electrode plates.

The precipitator hopper should be designed with no sloping sides. When the dust agglomerate is dislodged from the collecting electrode plates by the rapping process, it will settle on a flat hopper bottom. The settled dust will be removed from the hopper bottom by a continuously operating scraper conveyor. This scraper conveyor will discharge the dust into a ribbon mixer located in a trough. (See Figure 9.) The trough is constantly flushed with concentrated black liquor supplied from the main heavy black liquor line. The liquor will dissolve the dust and carry it to the salt cake mix tank.

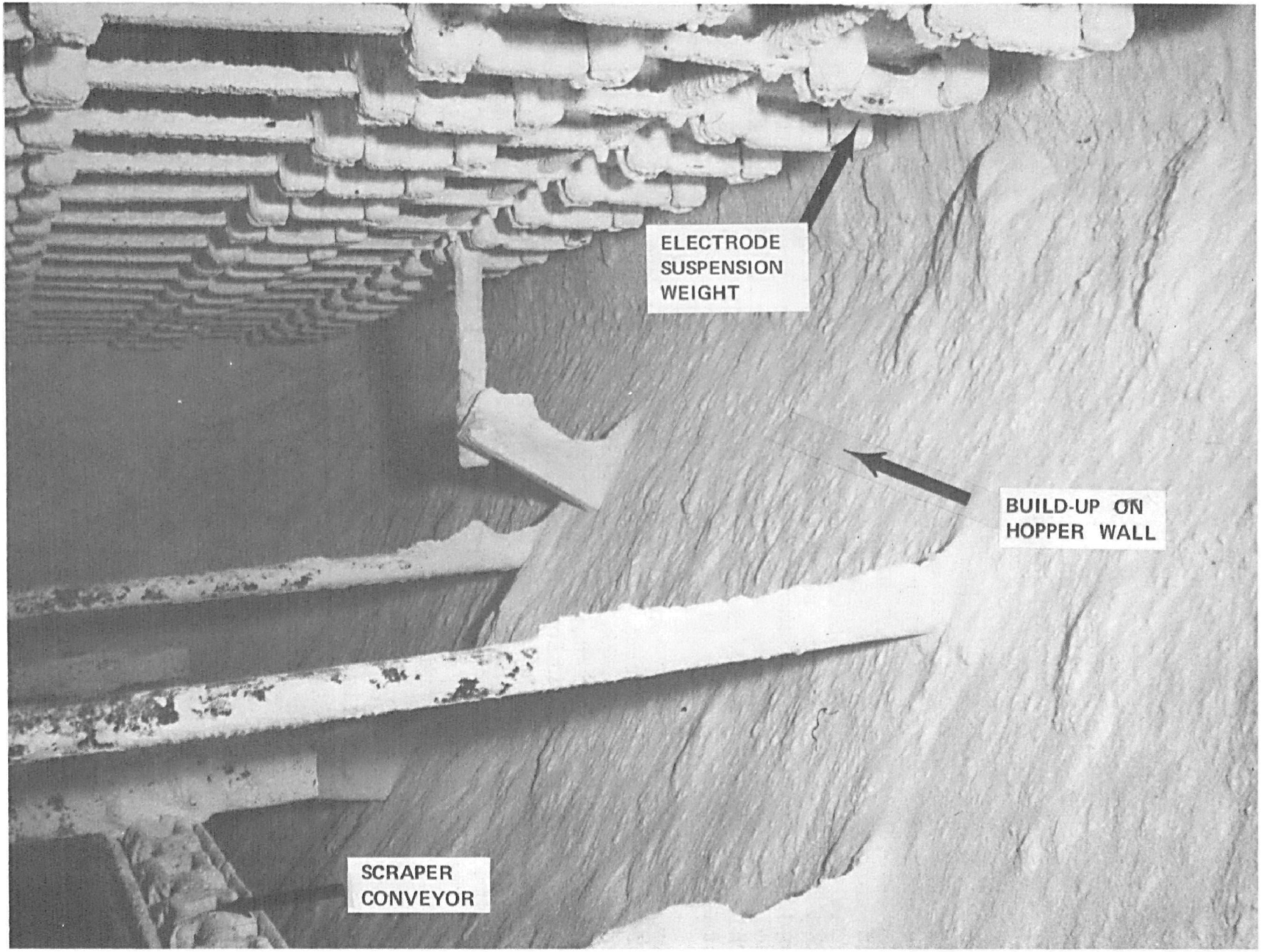

Figure 7. Precipitator hopper showing dust build-up on sloping side

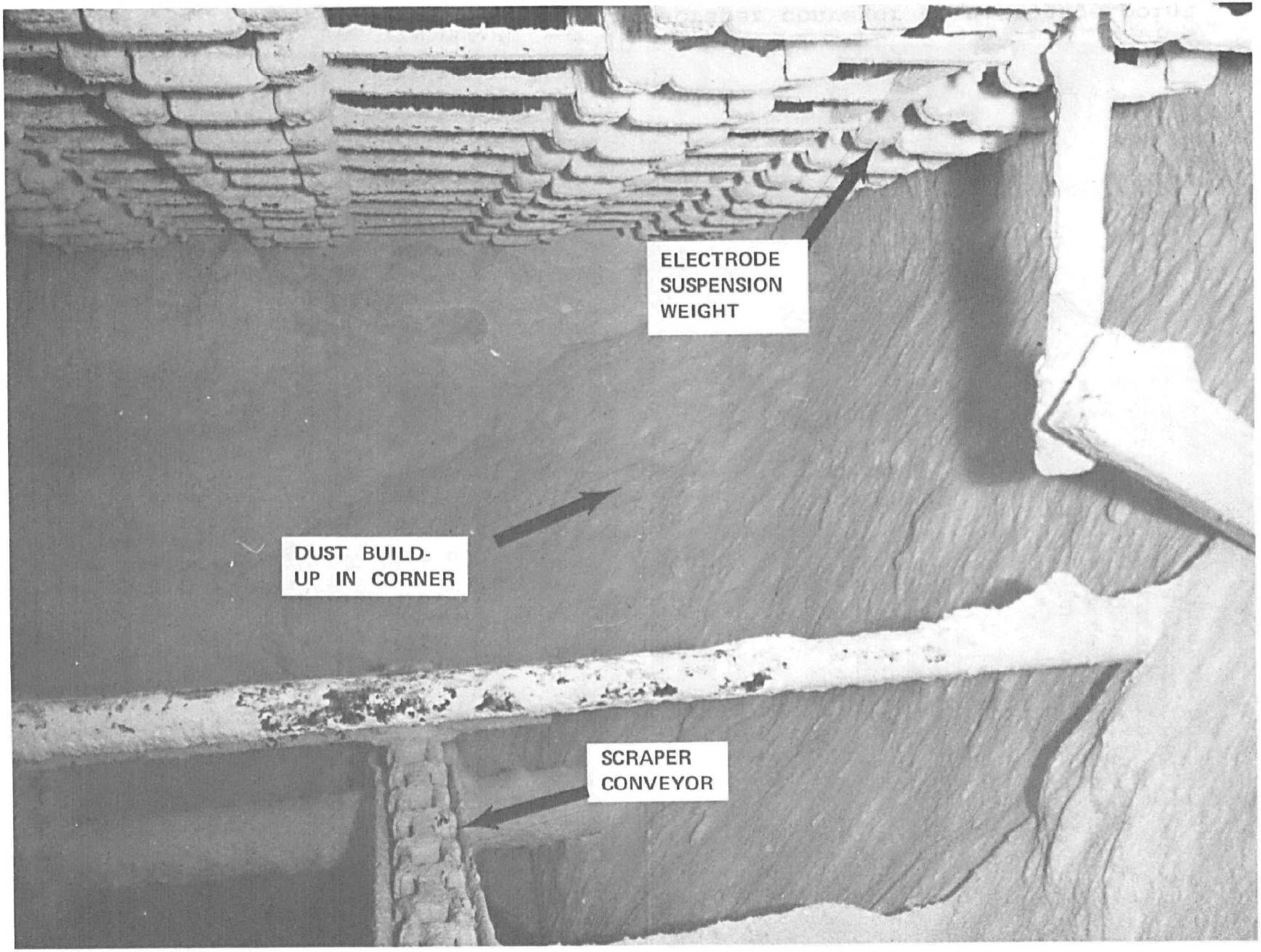

Figure 8. Precipitator hopper showing dust build-up in sloping corner

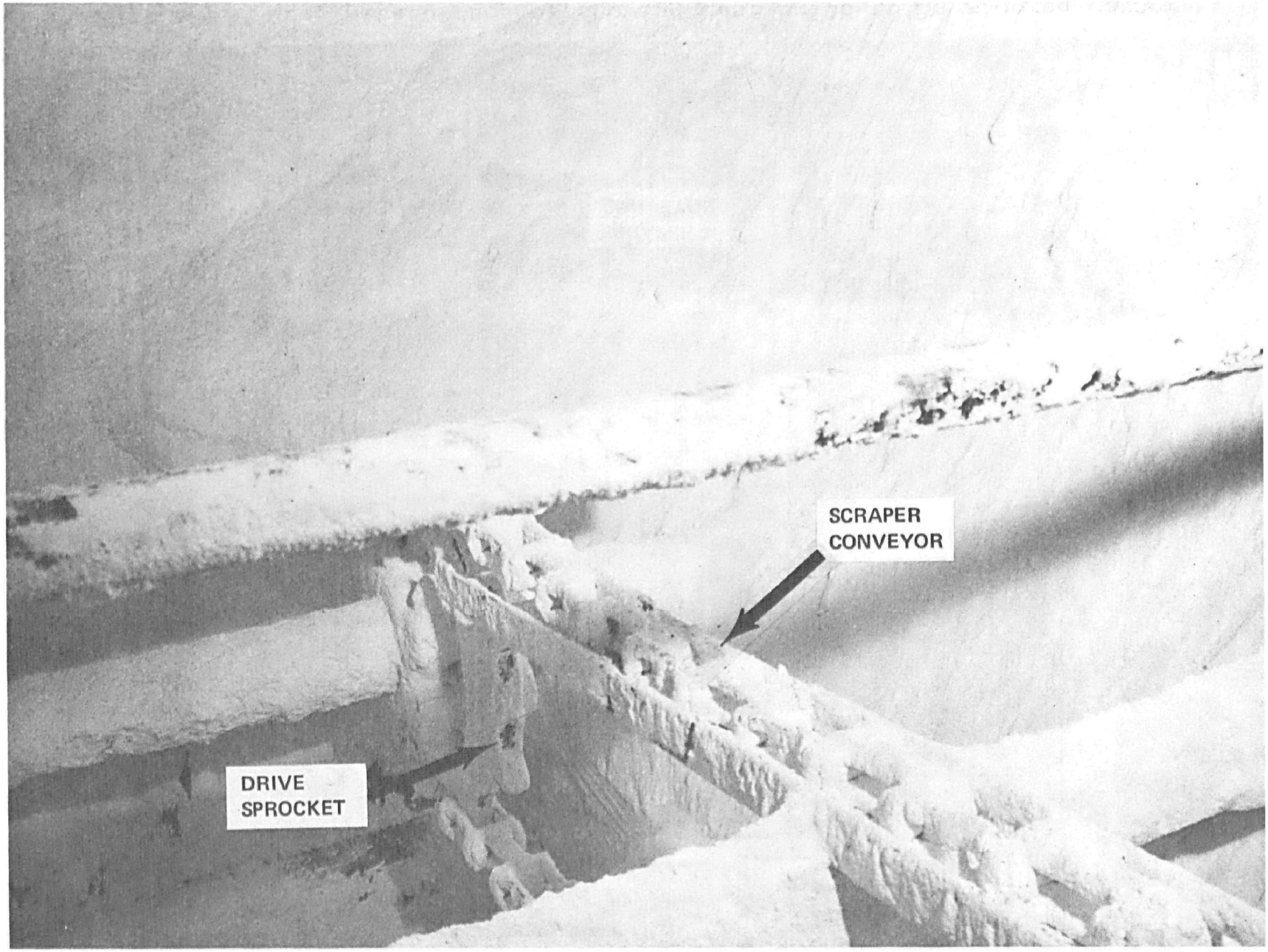

Figure 9. Precipitator hopper showing scraper conveyor at discharge point

Additional design advancements include measures to retard corrosion, such as well-ventilated insulator compartments and a coating of high temperature resistant zinc primer followed by a silicone finish coat on the steel shell of the precipitator. Some vendors also offer a double-shell design with hot air circulating between the inner and outer shells.

Table 3 gives the results of a series of five performance tests conducted on a precipitator after six months' operation on a low-odor recovery boiler. The EPA (Environmental Protection Agency) dry method test was used. The inlet particle loading was not measured, but was arbitratily assumed to be 3.00 gr/scfd (grains per standard cubic foot dry). This is an average value for recovery boilers of the type that was tested. Here, it serves only to establish a relationship.

Additional indication of current precipitator sizing practices is given in Table 4. These are theoretical design criteria for electrostatic precipitator installations of four different manufacturers. Some of these installations will be in operation in the near future. A comparison of the theoretical design criteria and the operational achievements of these installations should prove very valuable to the advancement of low-odor precipitator design.

For today's requirements of collection efficiencies in the 99 percent-plus range, precipitation rate parameters of 5.5 to 6.5 cm/sec should form the basis for sizing the equipment.

ECONOMICS

The capital costs of a 99.5 percent efficient electrostatic precipitator system for application to a low-odor recovery boiler are currently quoted in the range of $5.50 to $6.50 per acfm erected. This is approximately 30 percent higher than the capital outlay required for a traditional electrostatic precipitator system.

Table 3. PERFORMANCE TEST RESULTS FOR AN ELECTROSTATIC PRECIPITATOR ON A LOW-ODOR RECOVERY BOILER

Item	Units	Test 1	Test 2	Test 3	Test 4	Test 5
Gas volume	acfm wet	274,310	292,782	312,178	299,248	294,630
Gas temperature	°F	338	349	361	347	345
Water vapor	% by volume	21.5	22.8	23.1	22.1	22.9
Inlet load	gr/scfd	3.00	3.00	3.00	3.00	3.00
Outlet load	gr/scfd	0.00265	0.00314	0.00242	0.00220	0.00273
Efficiency	percent	99.91	99.89	99.99	99.92	99.91
CE area	ft^2	172,032	172,032	172,032	172,032	172,032
Specific area	CE/vol	0.627	0.587	0.551	0.575	0.584
Velocity	ft/sec	2.68	2.87	3.06	2.93	2.89
Treatment time	sec	14.81	13.83	12.97	13.55	13.73
Migration velocity	cm/sec	5.647	5.885	6.923	6.193	6.063
Emission weight	lb/hr	3.226	4.002	3.358	3.026	3.461

Table 4. DESIGN CRITERIA FOR ELECTROSTATIC PRECIPITATORS

Item	Units	No. 1	No. 2	No. 3	No. 4	No. 5	No. 6	No. 7
Gas volume	acfm wet	559,000	390,000	340,000	422,000	527,000	700,000	300,000
Gas temperature	°F	400	416	415	450	450	475	400
Water vapor	% vol	15		20			10-15	
Inlet load	grains/scfd	8.0	4.87	5.84	8.0	8.0	2-12.0	
Outlet load	grains/scfd	0.016	0.029	0.024	0.024	0.01-0.06		0.08
Efficiency	%	99.8	99.56	99.5	99.7	99.7	99.5	99.0
CE area	ft^2	342,144	181,210	154,500	198,144	249,000	328,320	134,475
Specific area	CE/vol	0.612	0.464	0.454	0.469	0.473	0.469	0.451
Velocity	ft/sec	2.8	2.74	2.94	2.96	2.95	3.07	2.7
Treatment time	sec	16.89	12.8	12.5	12.9	13.0	14.0	12.42
Available current density	mA/ft^2 CE	0.0458	0.05	0.042	0.045	0.043		0.0372
Design parameter	w=cm/sec	5.1	5.92	5.94	6.5	6.25	5.74	5.96

Item	Units	No. 8	No. 9	No. 10	No. 11	No. 12	No. 13	No. 14
Gas volume	acfm wet	325,000	450,000	384,000	700,000	700,000	402,000	400,000
Gas temperature	°F	470	375	400	450	400/475	500	460
Water vapor	% vol					15-25	15-25	20-25
Inlet load	grains/scfd	8.0		2-7.0		2-12.0	6-12	
Outlet load	grains/scfd			0.01-0.035			0.0293	
Efficiency	%	99.5	99.5		99.5	99.5	99.67	99.5
CE area	ft^2	116,928	187,544	147,840	307,037	326,646	176,290	172,032
Specific area	CE/vol	0.3598	0.4167	0.385	0.438	0.466	0.438	0.430
Velocity	ft/sec	3.38	3.34	3.31	2.99	3.08	3.0	3.69
Treatment time	sec	9.94	11.5	10.6				10.756
Available current density	mA/ft^2 CE	0.0372	0.0372	0.0372				
Design parameter	w=cm/sec	6.49	6.46	6.99	6.14	5.77	6.61	6.26

SUMMARY

Electrostatic precipitators have been used for many years to recover soda ash particles entrained in recovery boiler flue gases. Governmental requirements for collection efficiencies in the 99 percent-plus range, while uneconomical, present relatively few design problems. The low-odor concept of kraft pulping liquor recovery results in a particulate emission that is much finer and more adherent than that produced by the traditional process. Insufficient rapping forces lead to dust build-up problems and prevent traditional precipitators from achieving the desired operational reliability. Increasing the rapping forces only aggravates the situation by fracturing and scattering the dust agglomerate. This results in serious re-entrainment. Damage to the electrode system and the precipitator shell may also occur, since the forces required to dislodge the dust exceed the structural limitations of traditional precipitators.

Electrostatic precipitators for application to the low-odor process are designed with freely-suspended collection electrode plates and rigid charging electrode elements. During the rapping process, the elements will not shift their position relative to the collection plates. The series electrical sectionalization and treatment length is increased to give a minimum collector plate height-to-length aspect ratio of 1-to-1. This will prevent re-entrained particles from escaping the precipitator. The treatment zone is also designed for maximum uniform gas velocity distribution to hold particle re-entrainment to an absolute minimum. The precipitator hopper is designed with a flat bottom. This will prevent dust build-up that would occur on the sloping sides of a traditional precipitator.

The recovery boiler operation must be tuned to provide optimum performance, both from the production point of view and the pollution abatement point of view. The precipitator design must be adapted to handle the most difficult dust problems.

REFERENCES

1. Herman, F. J. Kraft Pulp in Theory and Practice. Wenzl Lockwood Publishing Co.

2. Walther, J. E., and H. R. Amberg. Odor Control in the Kraft Pulp Industry. Chem. Eng. Progr. 66:73-80, March 1970.

3. Lang, C. J., G. G. DeHaas, T. W. Gommi, and W. Nelson. Recovery Furnace Operation Parameter Effects on SO_2 Emissions. Tappi 56:115-119, June 1973.

4. Henderson, J. S., and J. E. Roberson. 1971 Precipitator Survey. Tappi 56:91-94, April 1973.

WET ELECTROSTATIC PRECIPITATORS FOR CONTROL OF SUB-MICRON PARTICLES

Even Bakke
MikroPul Division
United States Filter Corporation
Summit, New Jersey

ABSTRACT

The application of wet electrostatic precipitators is rapidly gaining popularity. The emission regulations are becoming more and more stringent and they are being enforced. The emphasis on removal of fine solid particles and organic liquid droplets all in the sub-micron range is increasing. In order to meet the required outlet loadings and opacities, the pressure drops that have to be applied across a conventional scrubber have increased exponentially. The wet electrostatic precipitator is emerging as an economic alternative by the virtue of its very low power consumption and its great potential for removing sub-micron particles with efficiencies in the high nineties. Several applications with the wet electrostatic precipitator will be reviewed in this paper.

INTRODUCTION

The use of the wet electrostatic precipitator (WEP) for collection of fine particles is rapidly increasing. The major reason for this is that the air pollution codes on solid particulates and condensables (e.g. organic droplets) are becoming more and more stringent and they are being enforced to a much greater extent than just a few years ago. Traditionally, the high energy scrubbers and fabric filters have been applied to control of fine particles. However, the high energy scrubber has extremely high energy consumption which in many cases is impossible to sustain. The fabric filter, especially the high energy fabric filter (e.g. pulse jet) gives inherently very high removal efficiencies on fine

particles, however its application is limited by the chemical and physical nature of the particles. If they are hygroscopic and/or have a tendency to solidify on the filter bags, or are wet and thereby stick to the fibers, the fabric filter cannot be used. There are also definite temperature and chemical resistance limitations associated with the fabric filters and normally the fabric filter will not remove gaseous pollutants or uncondensed organic vapors.

The wet electrostatic precipitator overcomes many of the limitations of the high energy scrubber and the fabric filter. It has a relatively low power consumption, typically for a WEP composed of three electrical fields, the total power consumption including fan, pumps, power supplies, and insulator heaters would be 0.8 kW/1000 acfm; this would be equivalent to a scrubber pressure drop of only 5.8 in. water gauge (W.G.) with a liquid to gas ratio of 5 gpm/1000 acfm. The WEP has an electrostatically operated mist eliminator which is much more effective than a mechanical type with chevrons or spin vanes that are normally used with scrubbers.

When comparing the WEP with fabric filters, the WEP performance is to a much less degree affected by the nature of the particles. For example, it will remove the organic fraction that has condensed at the WEP operating temperature which is always the saturation temperature of the gas that is being treated. It follows, therefore, that the performance of the WEP is not very sensitive to the gas temperature, since the gas to be treated must be saturated with water vapor before it enters the first electrostatic field. Further, since the internal components are continuously being washed with water or process liquor, the WEP will also remove gaseous pollutants only limited by the solubility of the gaseous component in the washing liquor. From the above mentioned power consumption for the WEP, it is evident that its power consumption, in terms of equivalent pressure drop, is approximately the same as for a fabric filter; the fabric filter is normally operated in the range from 3 to 6 in. W.G.

The dry electrostatic precipitator performs well only when the dust deposit on the grounded collecting plates has a resistivity greater than approximately 10^7 ohm-cm, but less than 2×10^{10} ohm-cm.[1] If the resistivity is less than 10^7, the electrostatic force holding the dust particles on to the dust layer or plates is very low and reentrainment of particles can become a serious problem during steady operation and during plate and electrode cleaning (e.g. rapping). This will have the overall effect of lowering the collection efficiency. If, on the other hand, the dust layer resistivity is higher than 2×10^{10}, the voltage drop through the dust layer to the grounded plates can become very significant, having

the effect of lowering the field strength in the space between the ion emission electrode and the top of the dust layer. This can cause a breakdown in the field and so-called "back corona" can take place. Both of these effects will lower the collection efficiency.

Since the collecting plates and electrodes in the WEP are cleaned continuously, the above mentioned limitations do not exist. The resistivity of the water film, which is very low, is the governing factor in the dust discharging process, not the resistivity of a dust layer formed by the collected particles.

It therefore follows that the wet electrostatic precipitator on certain applications has many technical and economic advantages when compared to high energy scrubbers, fabric filters and dry electrostatic precipitators. Its use can be generalized to applications where particles to be removed are solids and condensables, with a significant sub-micron range, and where gaseous pollutants also must be removed.

PRINCIPLE OF OPERATION

The principle of operation has been described by Bakke[2,3] and only a very brief description will be presented here.

The wet electrostatic precipitator of the type discussed here can be characterized as a continuously sprayed, horizontal flow, parallel plate, and solid discharge electrode type. In terms of gaseous absorption it can be characterized as a combination of a co-current and cross-flow scrubber. Figure 1 shows a cut-away view of the internal configuration.

On applications using a wet electrostatic precipitator, it is essential that the dust laden gas treated is saturated with water vapor. This prevents the water drops inside the WEP from evaporating which if allowed to occur, causes loss of washing water and wet/dry zones which will cause materials to build up on the internal members. The saturation of the gas can be accomplished by installing a spray tower or scrubber upstream of the WEP, or in the inlet section of the WEP, or both.

To optimize WEP performance, a uniform velocity profile across the inlet section is necessary. This is accomplished by installing "U" shaped baffle (diffuser) members in the inlet. Furthermore, by spraying co-current onto the inlet diffuser members, some of the coarser particles will be removed and the gas absorption process will be started.

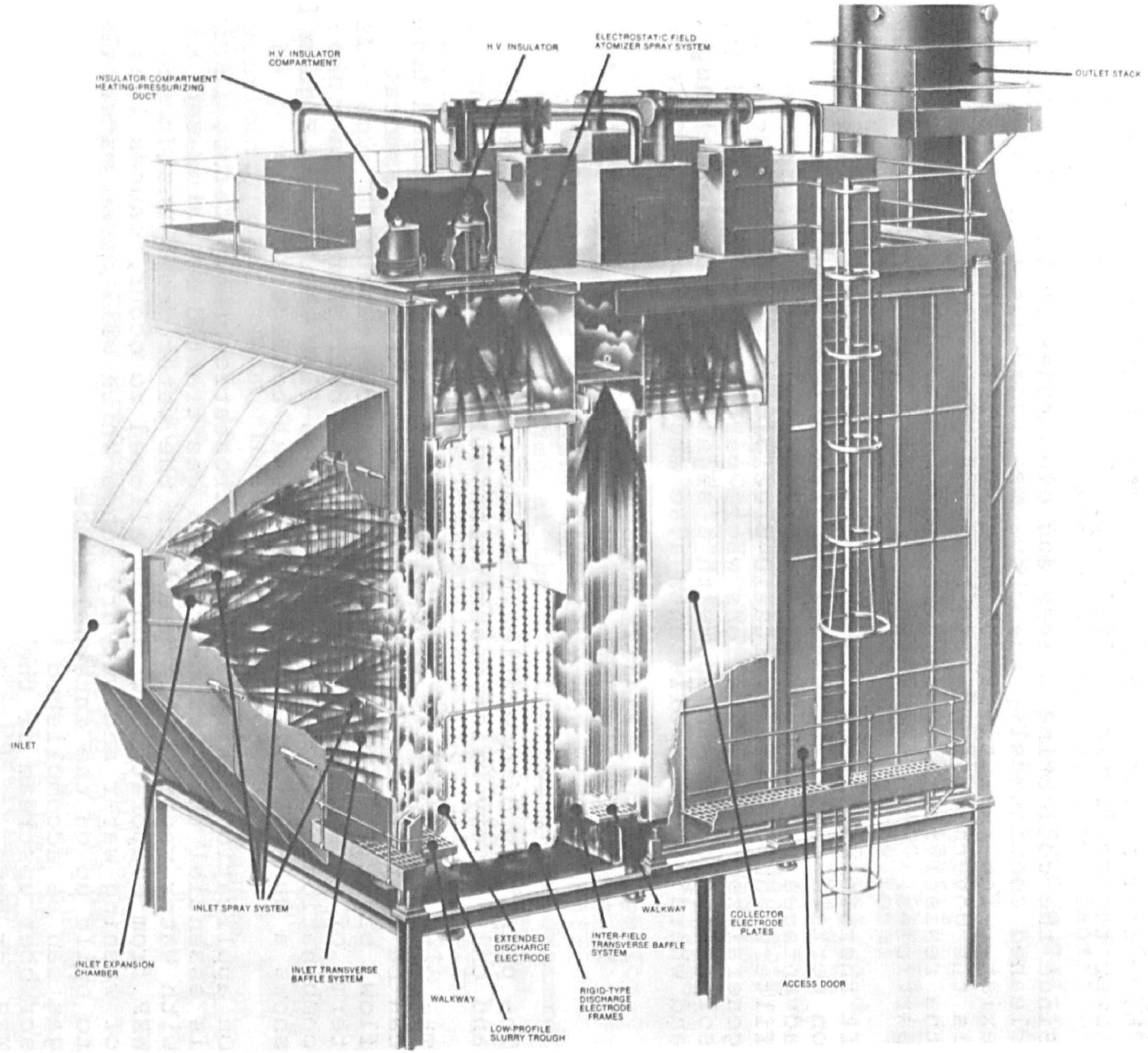

Figure 1. MikroPul Elektrofil wet electrostatic precipitator

After passing through the sections of "U" shaped baffles, the dirty gas stream enters into the first electrostatic field. Water sprays located above the electrostatic field sections introduce evenly distributed water droplets to the gas stream for washing of all internal surfaces. The particulates and the water droplets in the electrostatic field pick up charges and migrate to the collecting plates. The collected water droplets form a continuous downward flowing film over all collecting plates and keep them clean. The water film and the collected particulates flow down the collecting plates into the troughs below which are sloped to a drain.

The transverse baffle gas distribution system combined with an extended electrode, i.e., where the electrode extends beyond the plate in the axial direction, is located upstream and downstream of each field, thereby insuring complete gas flow uniformity from passage to passage, and the collection of particulates and droplets by impingement and electrostatic forces. Also the extended discharge electrode system improves the collection efficiency by increasing effective collection area and treatment time. At the entry of a field, particles are given an advance charge by the forward extended electrode before they come into proximity of the collecting plates. Thus, the electrostatically charged particles immediately start to migrate toward the leading edge of the collection plates.

It has been found that the downstream side of the baffles at the exit of a field collects a considerable amount of material. This can be accounted for by observing that some of the very small charged particles escaping the parallel plate field are pulled into the wake of baffles by the slight vacuum resulting from the turbulent dissipation of energy and are being collected on the grounded backside of the baffles.

The discharge electrode frames are mounted on conventional collar-type high voltage support insulators. Insulator compartments are heated and pressurized to prevent moisture and particulate leakage into the insulator compartment.

In any particulate and/or gaseous removal process where a washing liquid is used, it is important to remove the carry-over liquid drops and mists before the outlet of the equipment, thereby preventing dense plumes. We have found that doing this electrostatically is highly efficient. Hence, the last section of the WEP is operated without continuous sprays, thereby establishing an electrostatic barrier which most of the electrostatically charged liquid droplets cannot penetrate and the mist is collected on the front side of the baffles. However, some small dust particles which penetrate

the fields in the WEP will collect on the downstream baffles. Therefore, this surface is washed intermittently to prevent extraneous build-up of particulates.

There are also other types of wet electrostatic precipitators than the parallel plate type described above. A very old type is the tubular unit with tubes suspended from a tube-sheet with concentric wires as electrodes. The flow is vertically upwards and the washing is done continuously or intermittently by flooding or spraying onto the tubesheet. The water drains down the tubes and washes off collected materials. Another type being used is a parallel plate unit with vertical gas flow. There are also other types available which could be classified as low energy scrubbers with electrostatic sections to enhance the removal efficiency on smaller particles.

All of the above mentioned types have the disadvantage that they are not suited for staging. If a two-stage unit is necessary, two complete units will have to be mounted in series. The tubular type has the disadvantage of only using the inside of the tubes as collection surfaces. Therefore, the cross-sectional area needed for a certain gas flow is much larger than for a parallel plate unit where both sides of the plates are used for collection. In addition, since the outsides of the tubes are not washed, they could be subjected to heavy corrosion and build-up. Bohne[5] compared the performance of tubular and parallel plate units on Soderberg potline applications and concluded that the parallel plate unit was more economical.

As it was discussed above, the operation of the wet electrostatic precipitator is not influenced by the resistivity of the dust layer. The particle charging process is the same as in a dry electrostatic precipitator; however, the electrostatic field has somewhat different characteristics. Since the gas in the WEP is always saturated with water vapor, the theoretical sparkover voltage increases; however, the corona current at a given voltage is lower.[4]

However, there is a practical limit of sparkover voltage in a WEP. Imperfections in spray alignment and spray cones will cause local high droplet concentrations or sheets of water. If the concentration of water drops is too high in the jet or sheet of water, sparks will follow the water and limit the voltage at which the unit can be operated. The effect is exactly the same as if there was a mechanical misalignment; the point acts as a sink for ions and the performance of the field decreases drastically. Spray nozzle selection and positioning is therefore very critical.

The mathematical relationship used to describe the electrostatic force[2] can be represented as:

$$F_e = 12 \frac{\varepsilon}{\varepsilon+2} \pi \varepsilon_0 a^2 \frac{t}{t + 4\varepsilon_0/N_0 e\mu} \left(\frac{dv}{dr}\right)^2 \quad 0.49 \qquad (1)$$

This relationship shows for a given electrostatic field, the effects of the dielectric constant, ε, for the particle and the particle diameter on the electrostatic force, F_e. Since we are not concerned with the resistivity of the dust layer, this equation shows that for a given electrostatic field the two parameters to be concerned with are the dielectric constant and the particle diameter. Based upon Equation 1, the trajectory of the particles can be calculated as a function of size and dielectric constant and the results are shown in Figures 2 and 3. From these log-log plots it can be seen that the time and the horizontal distance needed for a particle to migrate the full field spacing varied considerably with the dielectric constant. For example, for a 1 micron particle to migrate 6 inches, it takes 6.3 seconds or 5.7 meters if the particle has a dielectric constant of 78 (water); however, if the dielectric constant is 2 (typical condensed hydrocarbon, e.g., toluene, C_7H_8 with a boiling point of 110°C) it takes 12 seconds and 11 meters, respectively, or almost twice the time and distance.

This analysis points to the fact that condensable hydrocarbons and other materials with low dielectric constants, i.e., very good electrical insulators, should be more difficult to collect. This effect has been confirmed by field measurements.

APPLICATIONS

Table 1 shows the installation list of the MikroPul wet electrostatic precipitators. All of these are of the parallel plate type with horizontal flow. As it can be seen, the applications span over a wide variety of industrial air pollution sources. Most of these installations are scaled up from initial pilot plant studies. In addition to these installations, the following applications have been piloted:

Tire-Cord Curing Oven
Glass Melting Furnace
Fiberglas Forming Line
Sinter Plant
Secondary Brass Melting Furnace
Phosphorus Reduction Furnace
Borax Dryer

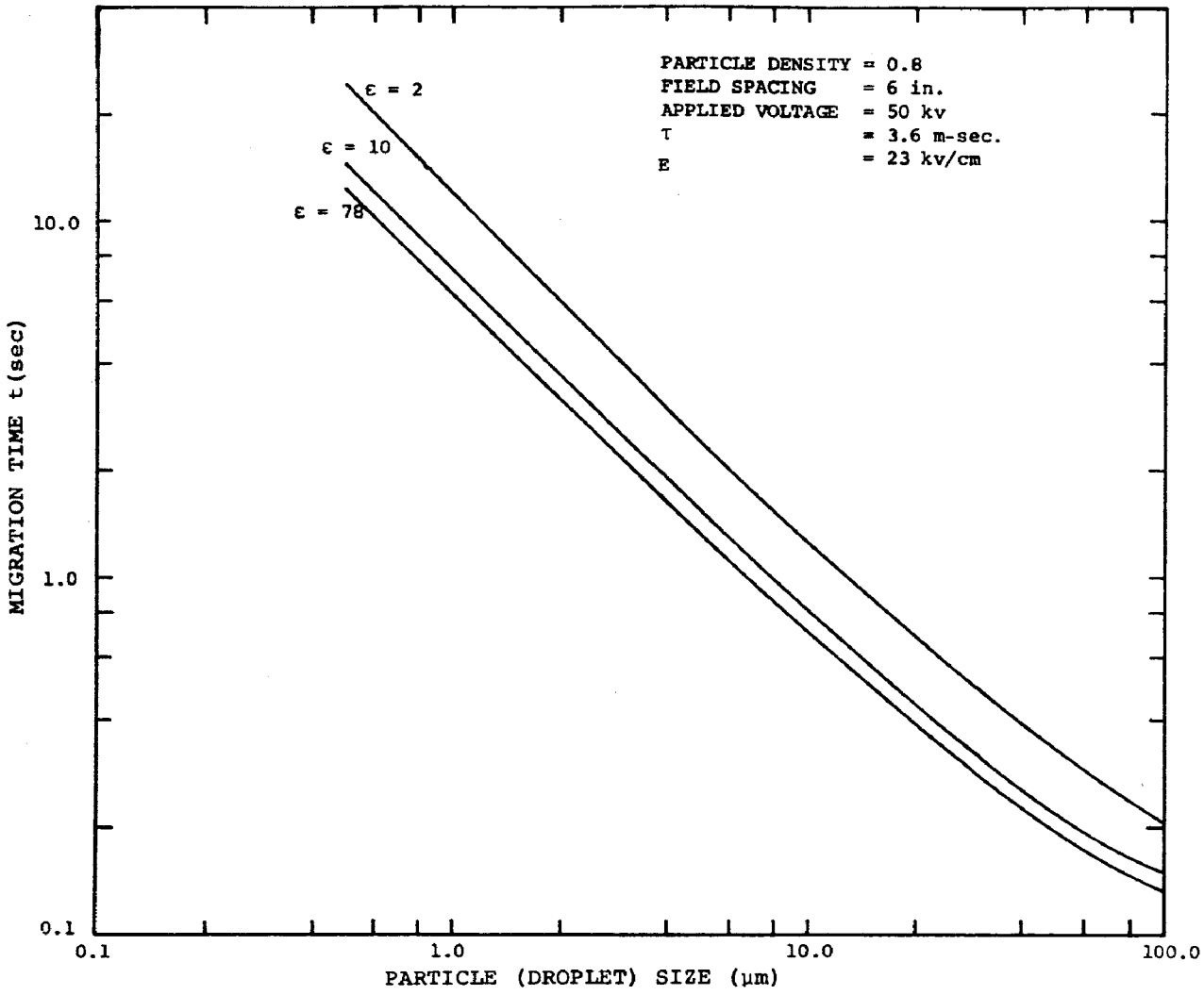

Figure 2. Particle size vs. migration time for collection

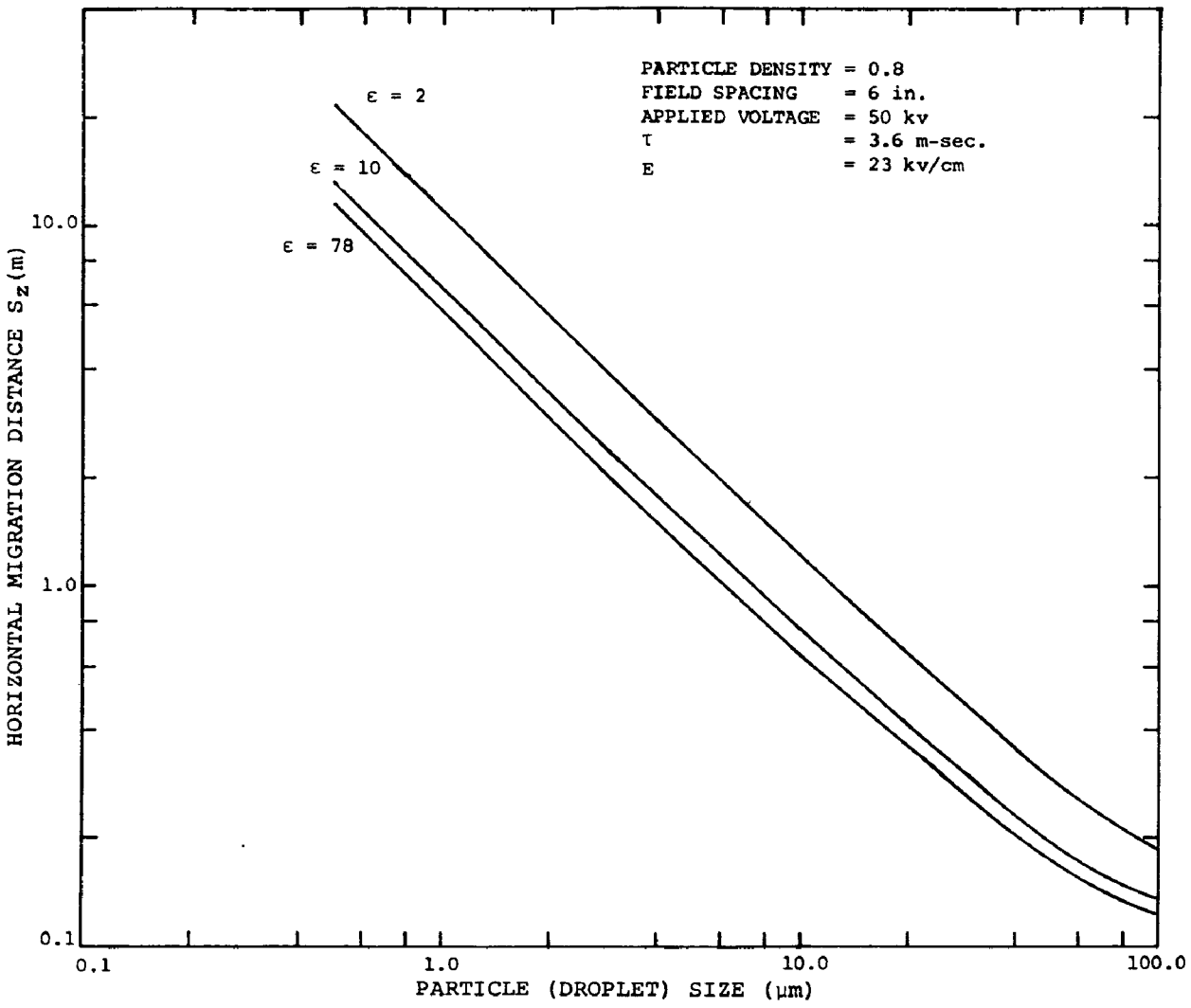

Figure 3. Particle size vs. horizontal migration distance for collection

Table 1. MIKROPUL WET ELECTROSTATIC PRECIPITATOR INSTALLATIONS

Application	No. units	Capacity, cfm	Installation date
Aluminum Potlines			
Martin Marietta Goldendale, Wash. Vertical stud pots	Pilot unit 20	7,500 7,500	1971
Martin Marietta The Dalles, Oregon Vertical stud pots	7 4	12,000 6,000	1972
Reynolds Metals Co. Longview, Wash. Horizontal stud pots	Pilot unit	50,000	Oct. 1971
Phase I	1 4	50,000 100,000	June 1973
Phase II	4 12	50,000 100,000	
Phase III	10	100,000	1974
Fiberglas Forming Lines			
Certain-Teed Products Kansas City, Kansas Phenolic resin application	2	100,000	1973
Carbon Anode Baking Furnace			
Airco Speer Carbon Graphite Niagara Falls, New York Ring furnace	4	9,000	1973
Reynolds Metals Co. Hamburg, Germany Ring furnace, for prebake potlines	1	26,500	1973
Reynolds Metals Co. Troutdale, Oregon Ring furnace, for prebake potlines	2	50,000	1975

(continued)

Table 1 (cont'd.) MIKROPUL WET ELECTROSTATIC PRECIPITATOR INSTALLATIONS

Application	No. units	Capacity, cfm	Installation date
	Oil Mist		
General Motors Corp. Buick Division Flint, Michigan On a mill for grinding oily scrap	1	15,000	1972
	Sodium Sulfite Mist		
Shattuck Chemical co. Denver, Colorado	1	3,500	1972
	Phosphate Rock Dust		
W. R. Grace and Co. Bartow, Florida On the dryer, downstream of low energy scrubbers	2	115,000	1974
	Coke Oven Emissions		
Dominion Foundry and Steel Hamilton, Ontario On a coke side hood	2	150,000	1974-1975
Republic Steel On a coke side hood	2	100,000	1975
	Manganese Arc Furnace		
Diamond Shamrock Kingwood, West Virginia On manganese reduction cells	1	100,000	1975

In general, these applications fall in two categories, (1) removal of fine solid particles, which would otherwise require a high energy scrubber and (2) removal of condensed organic fumes. Because of less stringent air pollution codes, both of these categories could, only a few years ago, be treated with either high or low energy scrubbers.

In terms of advancement in the state of the art, three applications shown in Table 1 stand out. These are the installations on (1) Horizontal Stud Soderberg Potlines, (2) Anode Baking Furnaces and (3) Coke Oven Emissions. These three applications will be discussed below.

HORIZONTAL STUD SODERBERG POTLINES

For this application there are two modes of operation: with or without a low energy scrubber upstream of the WEP. Figure 4 shows a schematic of the system. For Phases I and II existing low energy scrubbers are used for the purpose of gas saturation and pretreatment. For Phase III, the old scrubbers are removed and the gas saturation and pretreatment must be done in the inlet cone. Reference 3 gives a very detailed description of this application, and only the highlights will be discussed here.

For Phases I and II, two scrubbers are connected together on the outlet side to give a total flow of approximately 100,000 acfm into the WEP. At each end of the plant, one scrubber is connected to one WEP which treats 50,000 acfm. The high pH sodium based liquor from the water treatment plant is fed counter current to the gas flow to obtain maximum fluoride removal efficiency. The liquor is returned from the scrubbers back to the water treatment and cryolite recovery plants.

With a liquid to gas ratio of 5 gpm/1000 acfm and the liquor pH between 8 and 9, fluoride removal efficiencies higher than 98% have been measured, i.e., the outlet loading of HF was found to be less than 1 ppm.

Figure 5 shows the particle size distribution of the solid particles, as measured by Raemhild.[6] As it can be seen, the mean particle size to the WEP inlet with scrubbers upstream is 0.22 microns (for Phases I and II) and without scrubber is 0.70 microns (for Phase III). Figure 6 shows the relationship between specific collection area in sq ft per 1000 acfm and collection efficiency in %. Lines of constant migration velocity as calculated from the Deutsch-Anderson equation are also shown. The efficiency curves for solids and hydrocarbons are results from many tests and it is interesting to note that the Deutsch-Anderson equation only applies in a

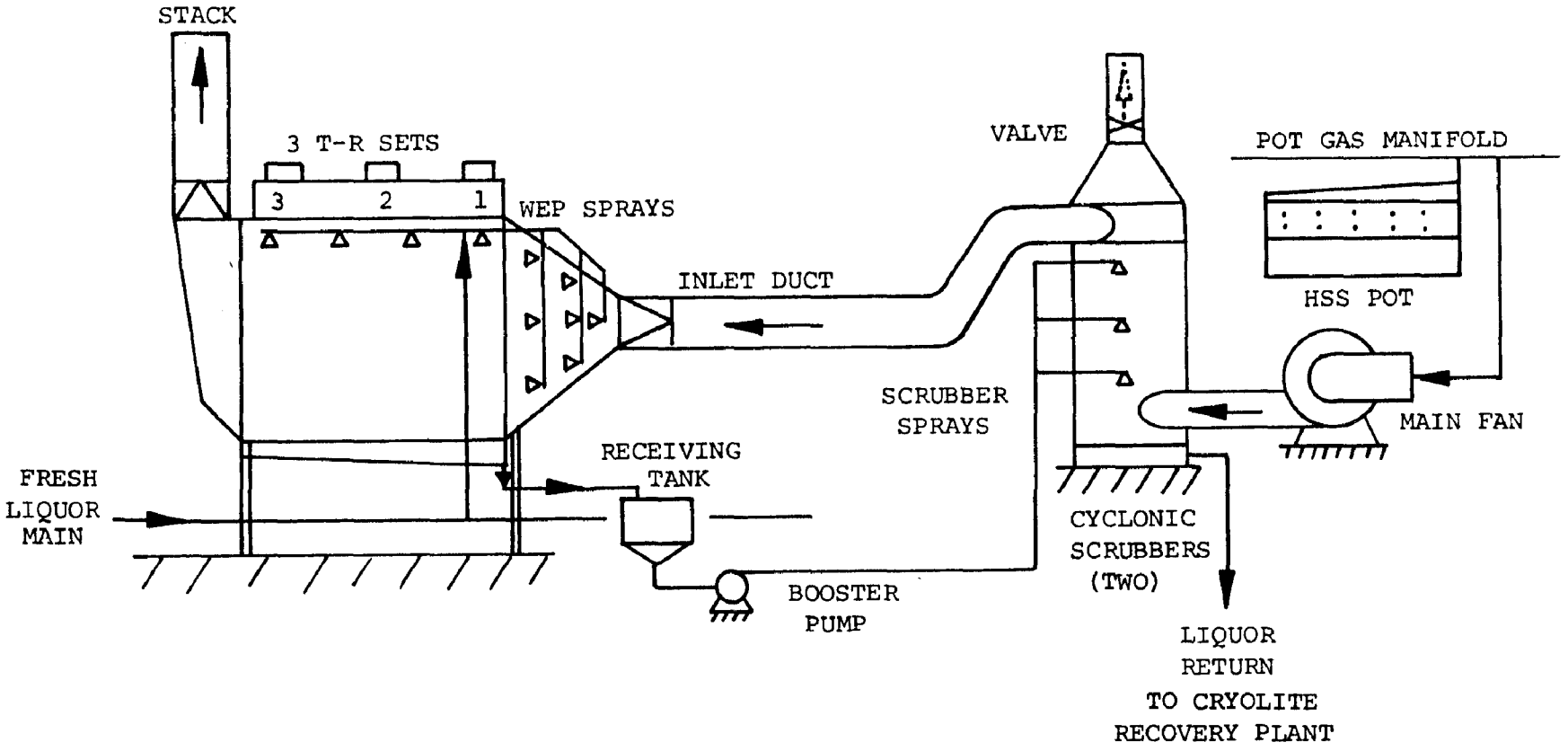

Figure 4. Schematic of primary emission control system, Reynolds Metals Company, Longview, Washington

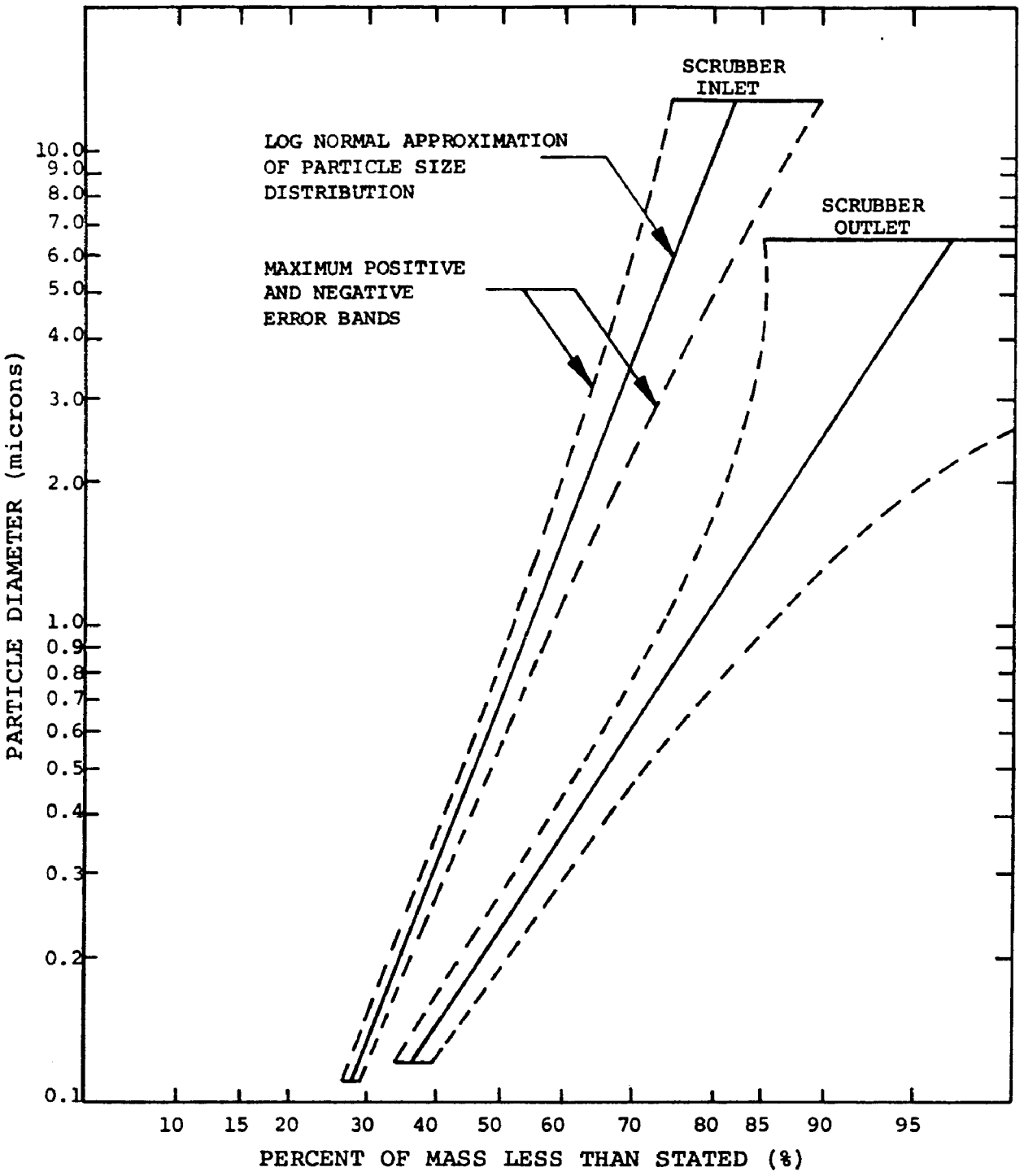

Figure 5. Scrubber inlet and outlet particle size distributions, Reynolds Metals Company, Longview, Washington, Plant[6]

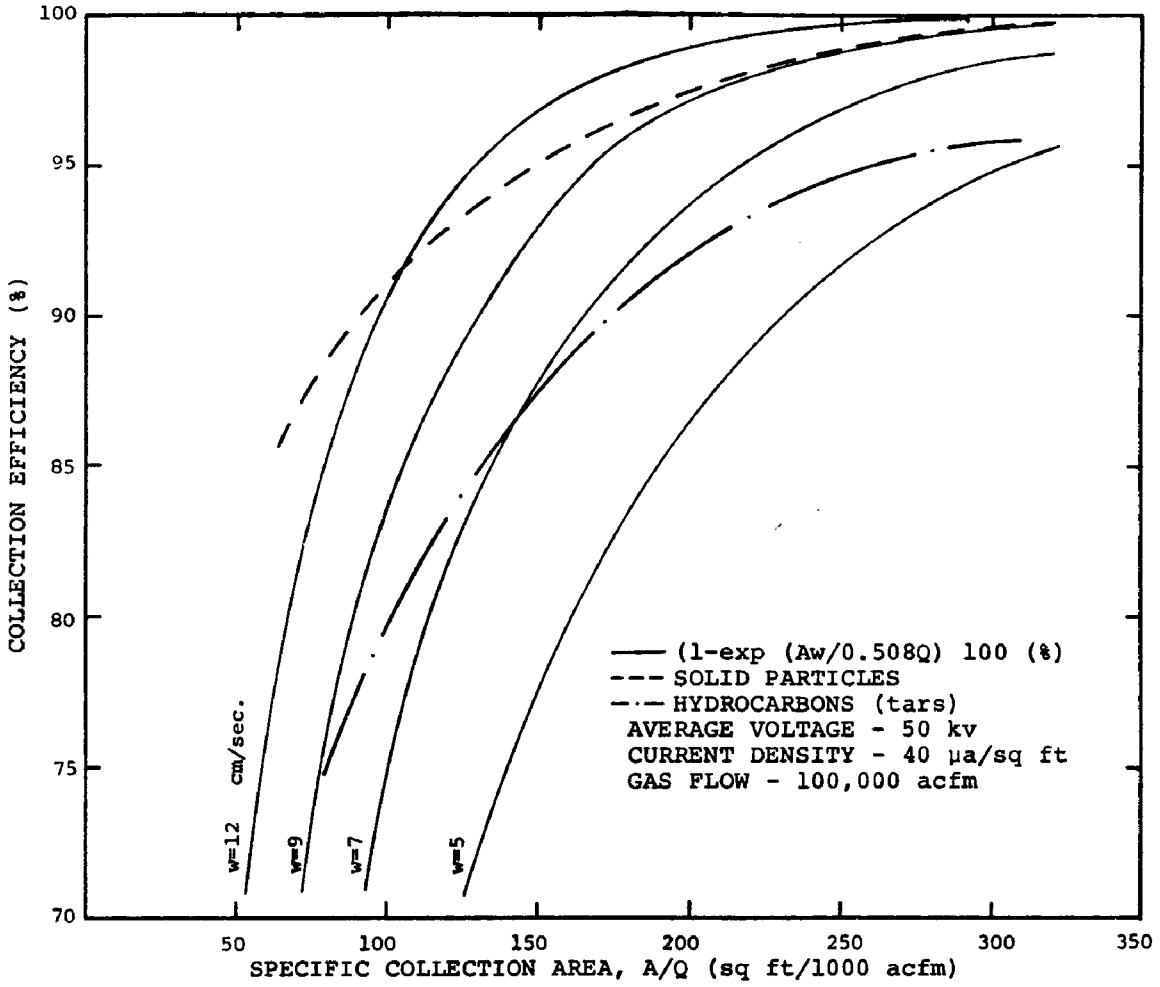

Figure 6. Specific collection area vs. removal efficiency

very narrow range of specific collection areas. The units are designed with three independent electrostatic fields and the normal specific collection area is approximately 300 sq ft per 1000 acfm. Other data points were obtained by shutting down one or two fields upstream of the third field and by varying the gas flow rate. As it can be seen from Figure 6, the migration velocity for the hydrocarbons is much lower than the migration velocity for the solid particles. There are probably two reasons for this: First, as shown above, the tars have a very low dielectric constant, which lowers the electrostatic force. From Equation 1, a particle with $\varepsilon = 2$ will have one-half of the force when compared to a particle with $\varepsilon = 100$ when the ratio $\varepsilon/(\varepsilon+2)$ approaches 1. Second, the condensable tars are probably all smaller than 0.1 micron.

When we compare the economics of the WEP with a high energy scrubber which has to operate with a pressure drop of 50 in. W.G. to show comparable performance, we find that the power consumption for the WEP could produce 45 tons of aluminum per year on a 6000 tons per year production (25 pots) or 0.75% of annual production; however, the power needed for the venturi scrubber could produce 350 tons of aluminum per year or 5.8% of the annual production. For this reason, with the current scarcity of power, the WEP's were selected. When we compare the annual operating cost of the WEP and the venturi scrubber we find that the former's cost is 15% less than the latter; the fixed charges are higher because of a larger investment, but the power costs are much lower.

ANODE BAKING FURNACES (RING TYPE)

In this process, so-called "green" carbon electrodes are baked in oil or gas-fired furnaces. The nature of the fumes depends upon the raw materials and the type of furnace used. The operation of the ring furnace involves a cycle of several steps and different sections of the furnace complex are operated at different steps of the process. During the baking cycle, the temperature reaches about 950°C and large volumes of gases evolve and 30 to 40% of the weight of the "green" electrode is lost. This volatilized pitch must be cooled to condensation before it can be collected in the air pollution control device.

If the inlet concentration of tars is sufficiently high, a dry electrostatic precipitator is justified and applied upstream of the WEP to recover as much of dry tars as possible which can be recycled. There is a fire hazard in the dry unit and proper fire protections must be designed into

the system. There is also a temperature problem. On the one hand, it is desired to operate the dry unit at the lowest possible temperature to condense out as much of the hydrocarbons as possible; however, on the other hand the tar must flow down the collecting plates by itself and the temperature must be higher than the acid dew point. To further reduce the outlet loading and to remove SO_2 and HF in the case of a baking furnace for a prebake aluminum potline, the dry unit is backed up with a WEP.

If the inlet loading is not high enough to justify a dry unit, the gas is pretreated in a low energy scrubber and then treated by the WEP. With two field units, outlet loadings in the range of 0.003 gr/scf, giving a clear stack, have been measured. If the outlet loading increases much above this value, the stack will become visible and this is an indication of the extreme fineness of the condensed tars. They are believed to be all less than 0.1 micron.

At Reynolds Metals in Hamburg, a dry precipitator is used ahead of the WEP and since the gas from it contains a relatively high concentration of SO_2 and a closed loop water treatment system was required, a double alkali water treatment process was selected. This installation has been running for approximately a year.

At Airco Speer, the inlet loadings of both tars and SO_2 are much lower, so the gas is pretreated in a low energy scrubber. The water treatment consists of a large tank with skimmers and bottom scrapers.

For both of these installations, the removal of the hydrocarbon emulsion from the water is very difficult, and improved methods for removal are now being developed.

COKE OVENS

In 1973 MikroPul operated a pilot plant on a coke side hood at the St. Louis Plant of Missouri Coke and Chemicals Division, Great Lakes Carbon Corporation. Great Lakes Carbon had constructed a continuous hood on the coke-side extending the length of a 40-oven battery. The concept is illustrated in Figure 7. The purpose of the hood is to capture smoke emitted during coke pushes and fumes from leaking doors. A baffle construction puts the upcoming hot gases into a swirling motion and the duct in the top of the hood draws off the hot gases with the particles and hydrocarbons. Because of the swirling motion, the amount of hot gas escaping during the push cycle is contained and is gradually drawn off. This reduces the induced amount of ambient air or in other words

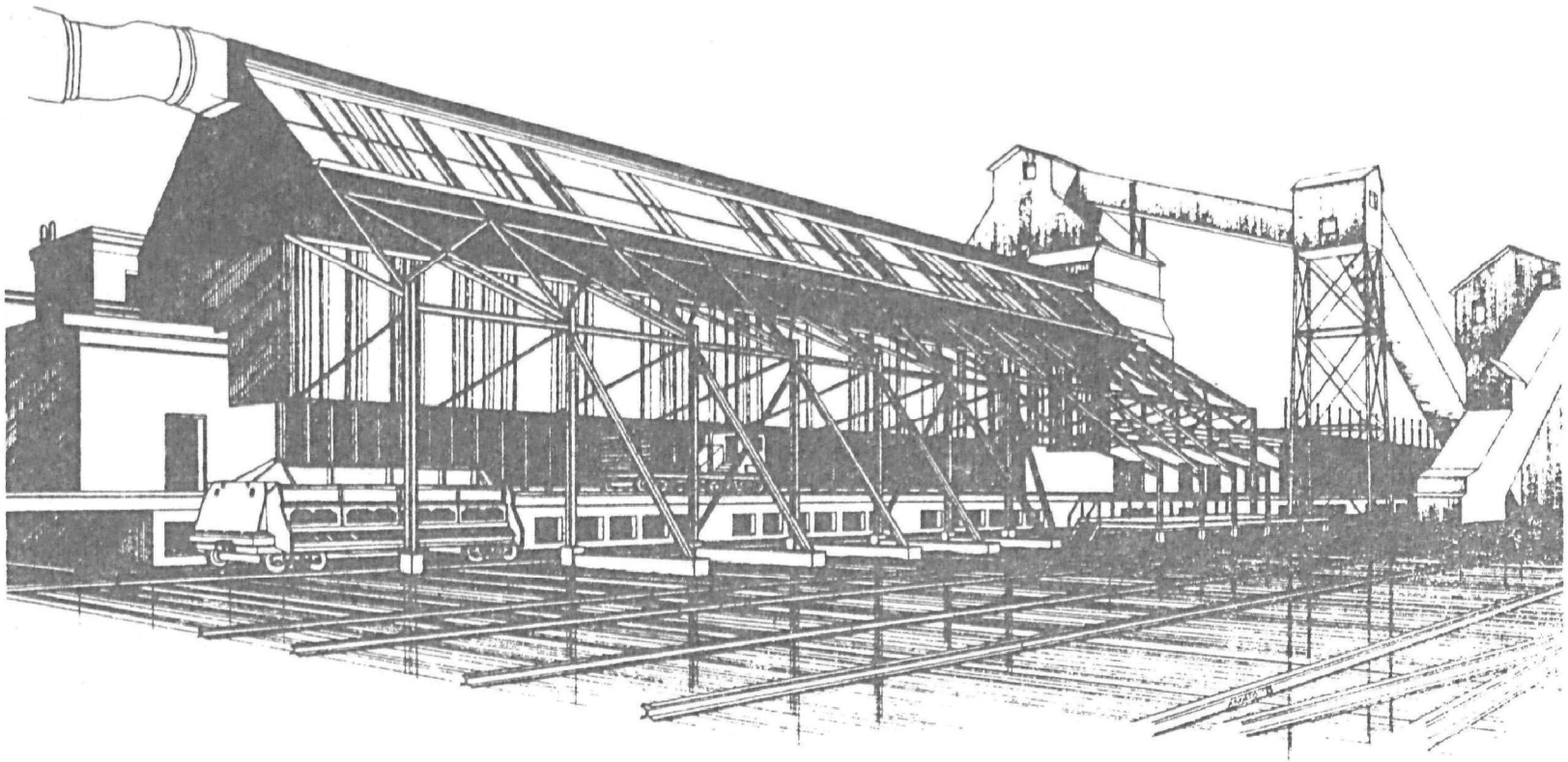

Figure 7. Coke side hood

cuts down the amount of air needed to prevent "spill over" along the tracks at the base of the battery. The WEP is connected with a duct to the system, downstream of the fan and approximately 300,000 acfm is sufficient for an 82-oven battery. This size battery is normally split in two halves with a precipitator, 150,000 acfm, serving each half of the battery.

Tests were run with low energy and high energy scrubbers in parallel with the WEP pilot; however, only the WEP could produce a clear stack during the push cycle and the average particulate outlet loadings are very low, the limiting factor being stack opacity. The particulates consist of a mixture of carbon particles and very small condensed hydrocarbon droplets. The size distribution is typically bimodal with the carbon particles in the range from 3 microns to 30 microns and the condensed hydrocarbons practically all in the sub-micron range. The overall removal efficiency during the coke pushing was found to be consistently higher than 98.5%. The venturi scrubber had to be operated in the range of 25 to 30 in. W.G. in order to even come near the WEP's performance during coke pushing.

As a result of this successful test, MikroPul signed an exclusive agreement with Great Lakes Carbon on the use of the continuous shed and MikroPul has received two orders for hoods and WEP's as shown in Table 1, one for Dominion Foundry and Steel and one for Republic Steel.

WATER TREATMENT

If the liquor is to be recycled through the WEP which in most cases is necessary to save on water consumption, the same water treatment methods used with scrubbers must be applied, i.e., the suspended and dissolved solids must be maintained at an acceptable level. The clarification of solids must be sufficient to minimize spray nozzle plugging and build-up of recycled materials on the internal members of the precipitator. If condensable materials are being collected, means for removing them must be provided, such as skimming devices and/or sludge removal provisions. If too much of the organics are recycled, reentrainment into the gas stream of these components in the precipitator can become a problem.

The dissolved solids concentration must be maintained at a steady and acceptable level either by the right amount of purging or by chemical treatment, or both. The level of dissolved solids which is acceptable must be determined by pilot plant tests.

On some applications it is necessary to neutralize acidic components such as HF and SO_2. By feeding a high pH liquor into the unit such that the pH of the liquor coming out of the WEP is 7 or higher, it has been possible to use mild steel construction and still have satisfactory corrosion rates. However, the decision to use mild steel construction where corrosive gases are present has always been backed up by careful pilot plant studies.

POWER CONSUMPTION AND ECONOMICS

As mentioned in the introduction, the total net power consumption for a WEP with three fields is approximately 0.8 kw/1000 acfm. Included are: 0.5 in.W.G. pressure drop across the unit, insulator heaters for all fields, the high voltage power to the electrodes and the pump power assuming a liquid to gas ratio of 5 gpm/1000 acfm at 50 psig.

The installed cost for a 100,000 acfm module with a specific collection area of 300 sq ft/1000 acfm, mild steel construction is $3 to $4 per acfm.

CONCLUSIONS

Successful use of wet electrostatic precipitators has been demonstrated on many new applications over the last few years. It has been shown that the parallel plate, horizontal flow type wet electrostatic precipitator can remove submicron solid particles and condensable organic materials with very high efficiencies at modest power consumptions. Therefore, the wet electrostatic precipitator is emerging as an economic alternative to high energy scrubbers.

REFERENCES

1. White, H. J. Industrial Electrostatic Precipitation. Reading, Mass., Addison-Wesley, 1963. 376 p.

2. Bakke, E. The Application of Wet Electrostatic Precipitators for Control of Fine Particulate Matter. MikroPul Div., United States Filter Corp. (Presented at Symposium on Control of Fine Particulate Emissions from Industrial Sources, U.S.-U.S.S.R. Working Group, Stationary Source Air Pollution Control Technology. San Francisco. January 15-18, 1974.)

3. Bakke, E. On the Application of Wet Electrostatic Precipitators for Control of Emissions from Soderberg Aluminum Reduction Cells. In: Light Metals 1974. Volume 1, Aluminum Cell Technology and Environmental Control. Proceedings, 103rd Annual Meeting, American Institute of Mining Engineers. Dallas. February 1974. p. 185-206.

4. Oglesby, S., Jr., and G. B. Nichols. A Manual of Electrostatic Precipitator Technology. Southern Research Institute, Contract CPA 22-69-73, National Air Pollution Control Administration. 1970. Part I. Fundamentals. NTIS PB 196380. 322 p.

5. Bohne, P. W. Evaluation of a Prototype Wet Wood Plate Electrostatic Precipitator on Soderberg Aluminum Cell Exhaust Gases. In: Proceedings, 101st Annual Meeting, American Institute of Mining Engineers. San Francisco. February 1972.

6. Raemhild, G. A. Collection of Aerosols from a Horizontal Spike Soderberg Aluminum Reduction Plant by a Wet Cyclonic Spray Scrubber as Related to Scrubber Operating Parameters. M. S. Thesis, University of Washington, Seattle. 1972.

CALCULATION OF THE CHARGING RATE OF FINE PARTICLES BY UNIPOLAR IONS

Wallace B. Smith and Jack R. McDonald
Southern Research Institute
Birmingham, Alabama

ABSTRACT

Theories of particle charging based on boundary value solutions to the diffusional equation may not be applicable to electrostatic precipitators where the ion density is rarely more than an order of magnitude greater than the particle concentration. A new charging equation, based on kinetic theory, is presented which evaluates the charging rate in terms of the probability of collisions between the dust particles and ions. In the presence of an external electric field, the surface of the particle is divided into three charging regions, and separate charging rates are calculated for each region. The total charging rate is the sum of these three individual rates. For large particles and high electric fields, this theory predicts essentially the same charging rate as the classical field charging equation of Rohmann and Pauthenier. For low electric fields, the theory reduces to White's diffusional charging equation. Agreement is within 25 percent of Hewitt's experimental results over the entire range of variables where data is available. For practical charging times, agreement is within 15 percent.

INTRODUCTION

GENERAL

In addition to being an important fundamental physical process, the charging of particles by unipolar ions with an applied electric field is of great practical significance to workers involved in the research and development of charge augmented pollution control devices and electrical particle size analyzers. For example, it is possible to define electrostatic precipitator performance in terms of the terminal velocity of the particles in the laminar boundary region near the collection plates (migration velocity). Since the migration velocity of a given particle is directly proportional to the charge on that particle, a theoretical electrostatic precipitator performance model must include an accurate theory for the charging rate.

Historically, two physical mechanisms have been considered to dominate the charging process. Diffusional charging, the result of collisions between dust particles and ions which have motion due to their thermal kinetic energy, seems to adequately describe the charging rate over a fairly broad range of particle sizes where the external field is low, or equal to zero.

On the other hand, field charging theories agree well with experiments where particle diameters exceed about 1 μm and the applied electric field intensity is moderate to high. In field charging, ions are visualized as drifting along field lines and impacting upon the surface of the particle until enough charge (the saturation charge) is accumulated to repel other ions.

The most difficult charging condition to describe mathematically is one wherein both the field and diffusional charging mechanisms are important. Some of the most important work, related to this aspect of charging, that has been done to date is summarized in the following paragraphs.

PREVIOUS WORK

Hewitt[1]

In 1957, Hewitt published a paper describing his experiments on particle charging. Although limited in scope, these experiments are still the best source of experimental data relating charge or particle mobility to particle size, ion

density, and external electric field. Hewitt covered a range in diameters from 0.1 μm to 1.3 μm using dioctyl phthalate (DOP) spheres which have a dielectric constant of 5.1. All his work was done using a positive corona charging device.

The results of these experiments may be summarized as follows:

- The electrical mobility, which depends on particle size and accumulated charge, is a minimum for particles 0.2-0.4 μm in diameter.
- An external field will affect the charging rate even for very small particles (0.14 μm diameter).
- In the absence of an applied electric field, the classical diffusional charging theory describes the charging process adequately.
- For strong electric fields and larger (>1 μm diameter) particles, field charging is the dominant mechanism and the classical field charging equation is adequate to describe the charging rate.
- From Hewitt's experimental data, the sum of the charges calculated using the classical diffusional and field theories, independently, is in fair agreement with experiment for a range of conditions.

White[2]

White published an extensive review of particle charging theories and experiments prior to 1963, as well as some of his own work. The equations describing field and diffusional charging which we refer to in this paper as the "classical" charging equations are also re-derived. These equations are:

$$dq/dt = N_0 \pi a^2 \bar{v} \exp(-qe/4\pi\varepsilon_0 akT) \quad (1)$$

for diffusional charging, and

$$dq/dt = (N_0 z q_s/4\varepsilon_0)(1-q/q_s)^2 \quad (2)$$

for field charging,

where q = instantaneous charge on the particle (coul),
q_s = saturation charge (coul),
t = time (sec),
T = temperature (°K),
N_0 = free ion density (m^{-3}),
e = electronic charge (1.6×10^{-19} coul),
K = dielectric constant,
k = Boltzmann's constant (1.38×10^{-23} j/°K),
ϵ_0 = permittivity of air ($\sim 8.85 \times 10^{-12}$ F/m),
a = particle radius (m),
$\bar{v}$ = rms thermal speed of ions (m/sec), and
z = electrical mobility of particles ($m^2/V \cdot sec$).

Figure 1, after Liu and Yeh,[3] shows the relative contributions of the diffusional and field charging mechanisms as related to particle size, for two field strengths. Even the unmodified classical equations predict a significant effect on charging by an external electric field for particles as small as 0.05 μm radius.

Murphy, Adler, and Penney[4]

Murphy, et al. attempted a rigorous theoretical treatment of the charging of submicron particles in the presence of an applied electric field. Although they were unsuccessful in deriving a useful expression for the charging rate, except in special cases, they were able to estimate the effect of an electric field upon the ionic distribution near the particle. The basic idea is that an applied field, superimposed on the field due to the charge accumulated on the particle, will cause the ions to crowd nearer the particle on one side ($\theta=0$) and be drawn away from the particle on the opposite side ($\theta=180°$). Because of the exponential nature of the ionic distribution, the increase at $\theta=0$ will be much larger than the decrease at $\theta=180°$. Murphy, et al. estimated an increase in ion density by a factor up to 440 times as large as the normal Maxwell Boltzmann distribution would predict at $\theta=0$, depending on the amplitude of the applied field. At $\theta=180°$, however, the decrease was less than a factor of 3. Thus, the changes in ion density do not cancel, and there is a large net increase in ion density near the particle.

Liu and Yeh[3]

Liu and Yeh published a theory similar in concept to that of Murphy, et al. but much easier to implement. They consider two charging regimes: one where both field charging and diffusional charging are important, and a second where the charge on the particle exceeds the saturation value predicted

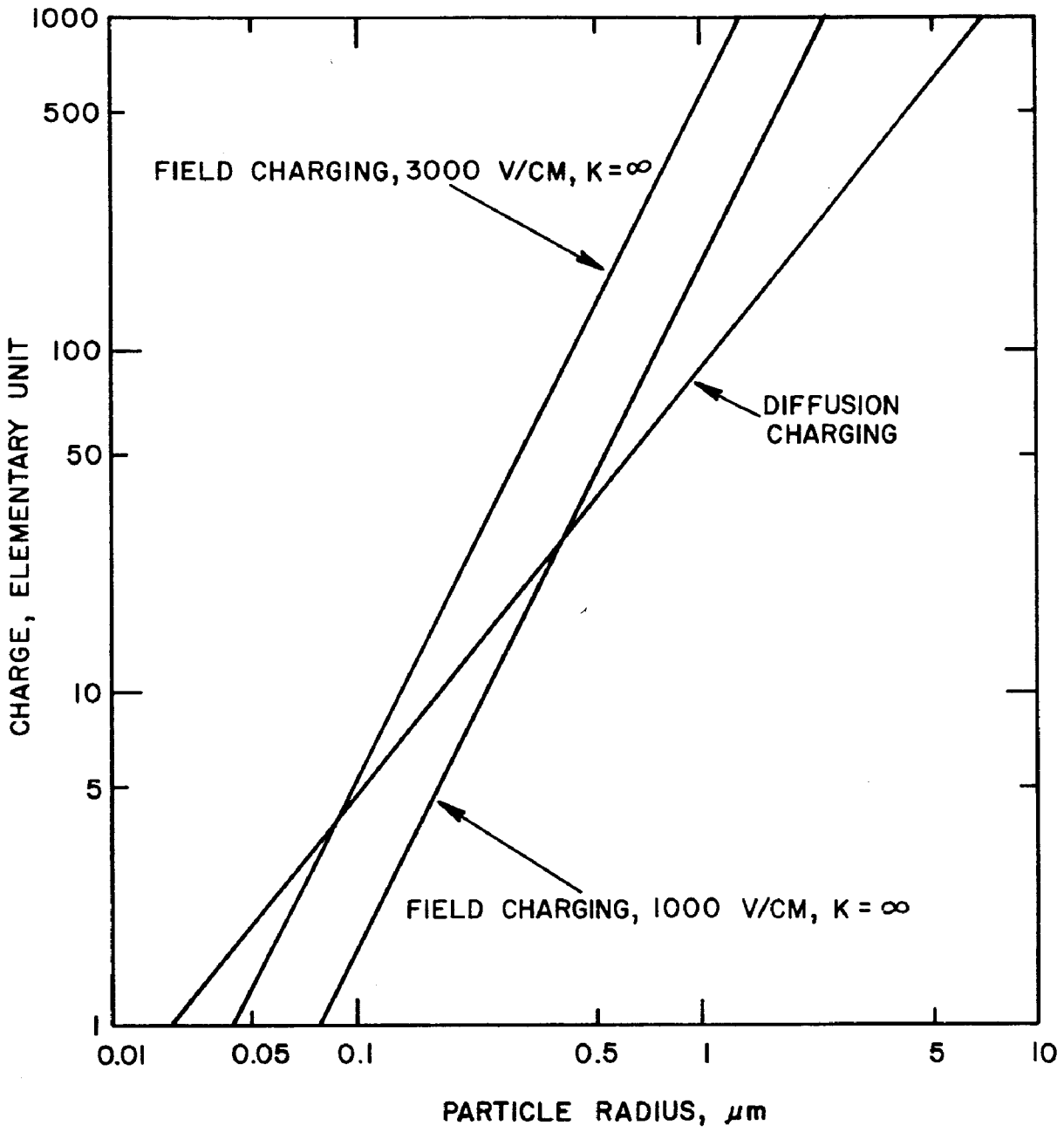

Figure 1. Relative contributions of field and diffusional mechanisms in the charging of small particles.[2] $N_0 t = 10^7$ sec/cm^3

by field charging and only diffusional charging is significant. An integral part of this theory is the assumption that ions form clusters of 16 molecules in a corona discharge so that the electrical mobility and mean thermal speed are much lower than for diatomic oxygen. Using values of 118 m/sec and 1.1 x 10^{-4} $m^2/V \cdot sec$ for the mean thermal speed and electrical mobility, respectively, Liu and Yeh obtain good agreement for small particles over a wide range of applied fields. These values of thermal speed and mobility, however, differ considerably from most values found elsewhere in the literature (mobility $\sim$2.2 x 10^{-4} $m^2/V \cdot sec$ and thermal speed $\sim$475 m/sec).

For particles larger than about 0.5 μm diameter and high electric fields, this theory predicts charging rates much higher than those given by the classical field charging equation. Since field charging is believed to approximately describe the charging process under these conditions, the disparity seems to indicate that the theory is not applicable to larger particles.

In the next section, "Theoretical Discussion and Results", a new theory is introduced which does give satisfactory agreement with experiment. In the case of zero applied field, this theory reduces to the classical diffusional equation. For large particles and high fields, the results are within a few percent of those predicted by the classical field charging equation.

THEORETICAL DISCUSSION AND RESULTS

None of the theories mentioned above are suitable for use in a computer model to simulate unipolar charging in an electrostatic precipitator where a wide range in particle sizes and electric fields is found. It is possible, however, to use certain ideas from kinetic theory to construct a theoretical model which does give an adequate description of the charging process over a wide range of conditions. This approach is similar to that given by White in developing his diffusional charging equation (Equation 1).

Figure 2 shows the two-dimensional physical model which is used as the basis for the theoretical development outlined in the next section. The particle shown in this sketch, and its environment, are considered to be representative of the average of a large number of similar systems which make up

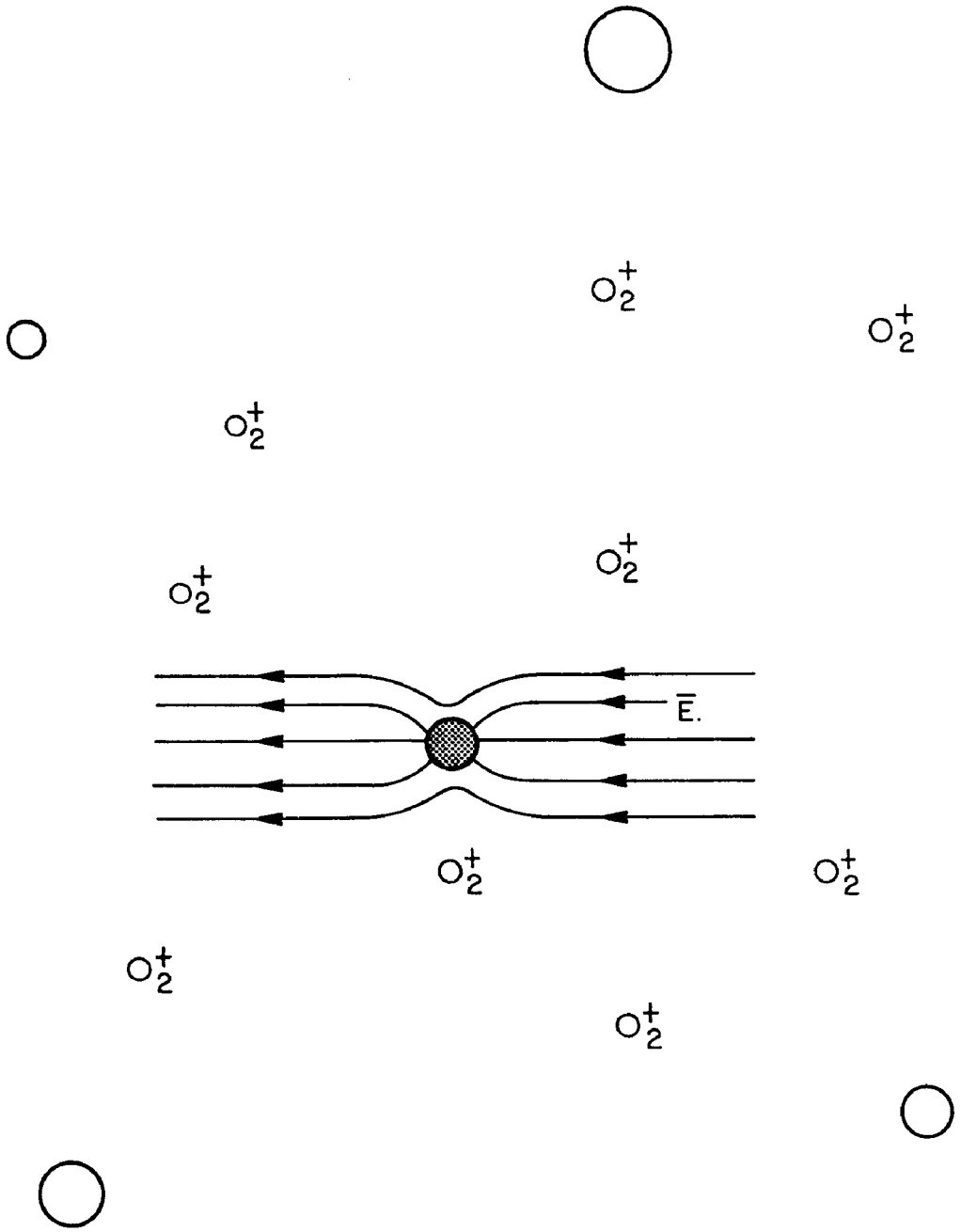

Figure 2. Two dimensional physical model for developing a charging theory

the aerosol under investigation. The following considerations, suggested by this figure, are important when applying classical kinetic theory or statistical thermodynamics to the charging of dust in a flue gas.

The volume of space associated with each particle is equal to N_p^{-1}, where N_p is the average number of particles per unit volume. The linear dimensions of this volume are on the order of $N_p^{-1/3}$ (in most cases, 10-100 μm).

In electrostatic precipitators, the number of ions in the volume N_p^{-1} is equal to N_0/N_p where N_0 is the ion density. N_0/N_p can vary from about 1 to 10, or to 100 at the outlet of a very efficient precipitator.

The mean thermal speed of the ions is at least an order of magnitude greater than their drift velocity. This means that the kinetic energy of the ions due to the applied field is insignificant when compared to their thermal energy.

The majority of collisions suffered by ions are with neutral molecules. Thus, the energy of the ionic system is not conserved and no macroscopic potential function can be defined for the motion of the ions in the electric field.

Because of the low number density of ions relative to the dimensions of the volume, N_p^{-1}, the concept of a single particle in space surrounded by an infinite cloud of ions whose motion is determined by charge or concentration gradients is not valid.

With these considerations in mind, an attempt has been made to develop a new theoretical expression for the charging rate of fine particles in a unipolar ion field.

Figure 3 is a simplified diagram which will be used to define the nomenclature used in the theoretical development. The physical description, however, will be based on the conceptual representation shown in Figure 2, where the particle of interest is surrounded by gas molecules, ions, and other charged particles. The particle is assumed to be spherical, and only components of the electric field due to charge on the particle and the applied field are considered. The external field, E_0, is taken to be uniform and directed along the negative z axis. The dashed line in Figure 3 which is labeled r_0 corresponds to points in space where the radial component of the net electric field is equal to zero. The

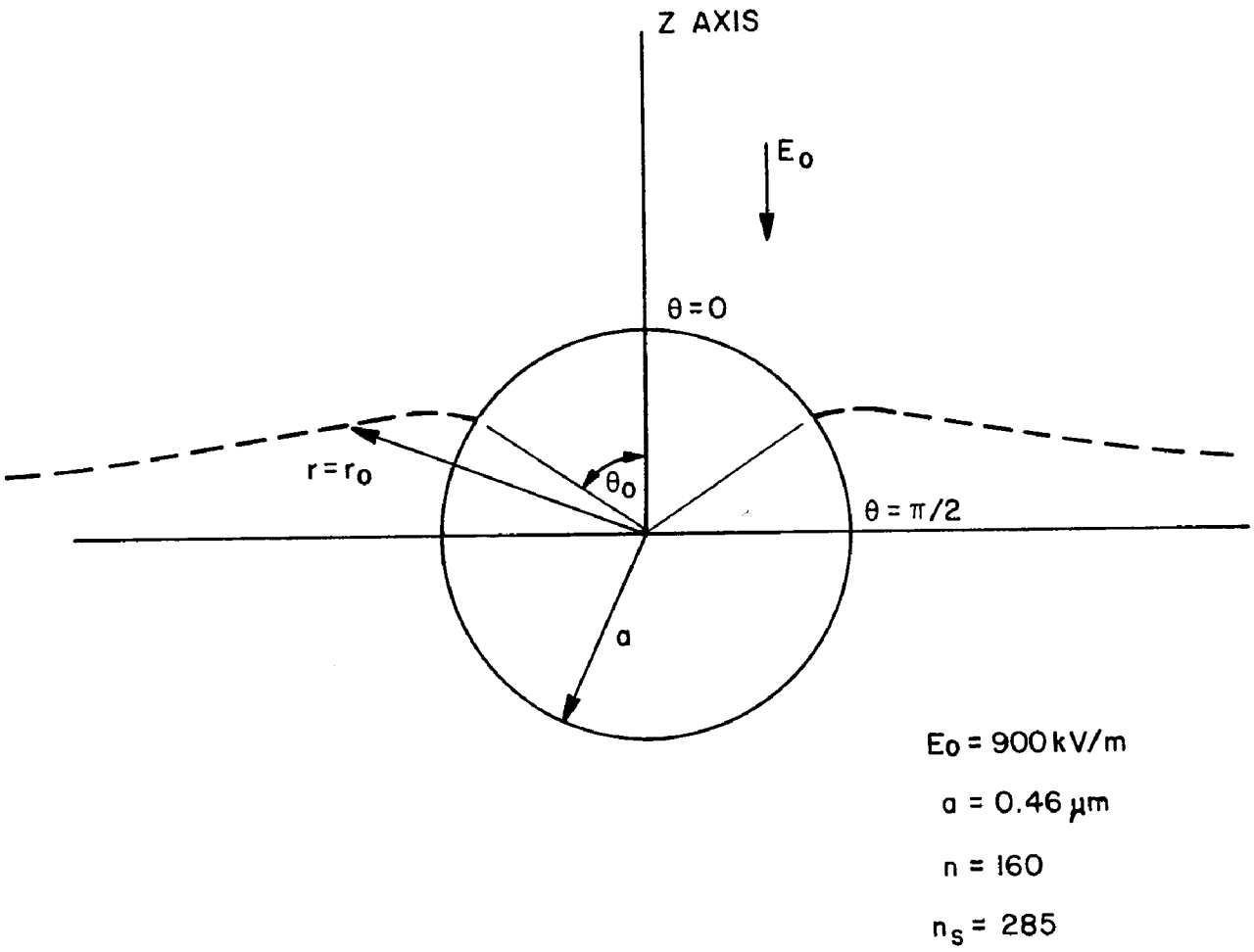

Figure 3. Model for mathematical treatment of charging rate. Along $r=r_0$ and at θ_0, the radial component of the electric field is equal to zero

angle θ_0 corresponds to the azimuthal angle at which r_0 is equal to the particle radius, a. For values of θ greater than θ_0, the electric field is directed outward from the particle surface and ions are repelled. For angles less than θ_0, the electric field is directed inward toward the particle surface and ions are attracted by the particle. θ_0 always lies between 0 and $\pi/2$ radians.

For the purposes of discussion, three areas of interest are defined on the particle surface. One area, designated as Region I, is that bounded by $\theta=0$ and $\theta=\theta_0$; a second region, Region II, is bounded by $\theta=\theta_0$ and $\theta=\pi/2$; and the third region of interest, Region III, is the "dark side" of the particle where $\theta > \pi/2$. Our approach to arriving at an equation for the charging rate, dq/dt, is to quantify the probability that ions can reach the particle surface in each of these three regions.

The rate at which ions reach the particle surface is

$$dn/dt = (1/e)(dq/dt) = P \cdot N_s(E_0,a,\theta,q) \qquad (3)$$

where

P = the probability that a given ion will move in a direction to impact with the particle,

q = the instantaneous charge on the particle, and

$N_s(E_0,a,\theta,q)$ = the ion density at the particle surface.

Mathematically, the problem reduces to the evaluation of N_s over the particle surface. This is most conveniently done by writing the charging rate as the sum of the three individual charging rates for Regions I, II, and III.

$$\frac{dq}{dt} \rightarrow \left(\frac{dq}{dt}\right)_I + \left(\frac{dq}{dt}\right)_{II} + \left(\frac{dq}{dt}\right)_{III}. \qquad (4)$$

The steps involved in transforming equation (3) into a differential equation which can be solved, and the details of the numerical solution, will not be presented in this paper, but the emphasis is placed instead on the particle charging rates predicted by the theory. The complete expression for the charging rates is

$$\frac{dq}{dt} = \frac{N_0 Z n_s e}{4\varepsilon_0}\left(1-\frac{ne}{n_s e}\right)^2$$

$$+ \frac{\pi a^2 \tilde{v} N_0 e}{2} \int_{\theta_0}^{\pi/2} \exp -\left[\left\{\frac{ne^2(r_0-a)}{4\pi\varepsilon_0 kTar_0}\right.\right.$$

$$\left.\left. + \frac{\left[3ar_0^2 - r_0^3(K+2) + a^3(K-1)\right] eE_0\cos\theta}{k\,Tr_0^2(K+2)}\right\}\right] \sin\theta d\theta$$

$$+ \frac{\pi a^2 \tilde{v} N_0 e}{2} \exp\left(-ne^2/4\pi\varepsilon_0 akT\right) \qquad (5)$$

Figures 4 through 13 compare the predictions of this theory with experimental data, and with other theories, for values of E_0 and N_0t which might be found in electrostatic precipitators.

In Figures 4 through 8, conventional values for the mean thermal speed and ion mobility (463 m/sec and 2.2×10^{-4} $m^2/V{\cdot}sec$, respectively) are used in all the equations. Liu *et al.* have measured values considerably lower than these (118 m/sec and 1.1 $m^2/V{\cdot}sec$, respectively), and his theory agrees more closely with experiment when these lower values are used.[5] Figures 9 through 13 are comparisons of the theories with experiment using Liu's values for the ion mean thermal speed and mobility. For this latter series of figures, it can be seen that worse agreement is found for our theory, and also for classical field and diffusional equations under conditions where these should apply. We believe that this is an indication that the low values for ion mobility and mean thermal speed used by Liu *et al.* are not typical of corona discharge.

The agreement between the new theory and Hewitt's experimental data is within 25 percent over the entire range of data that is available. For values of N_0t which are typical of electrostatic precipitation, the agreement is within 15 percent. This degree of accuracy is considered to be adequate for the prediction of precipitator collection efficiencies where such factors as reentrainment, nonideal geometry, sneakage, poorly defined gas flow distributions, etc., introduce much larger uncertainties.

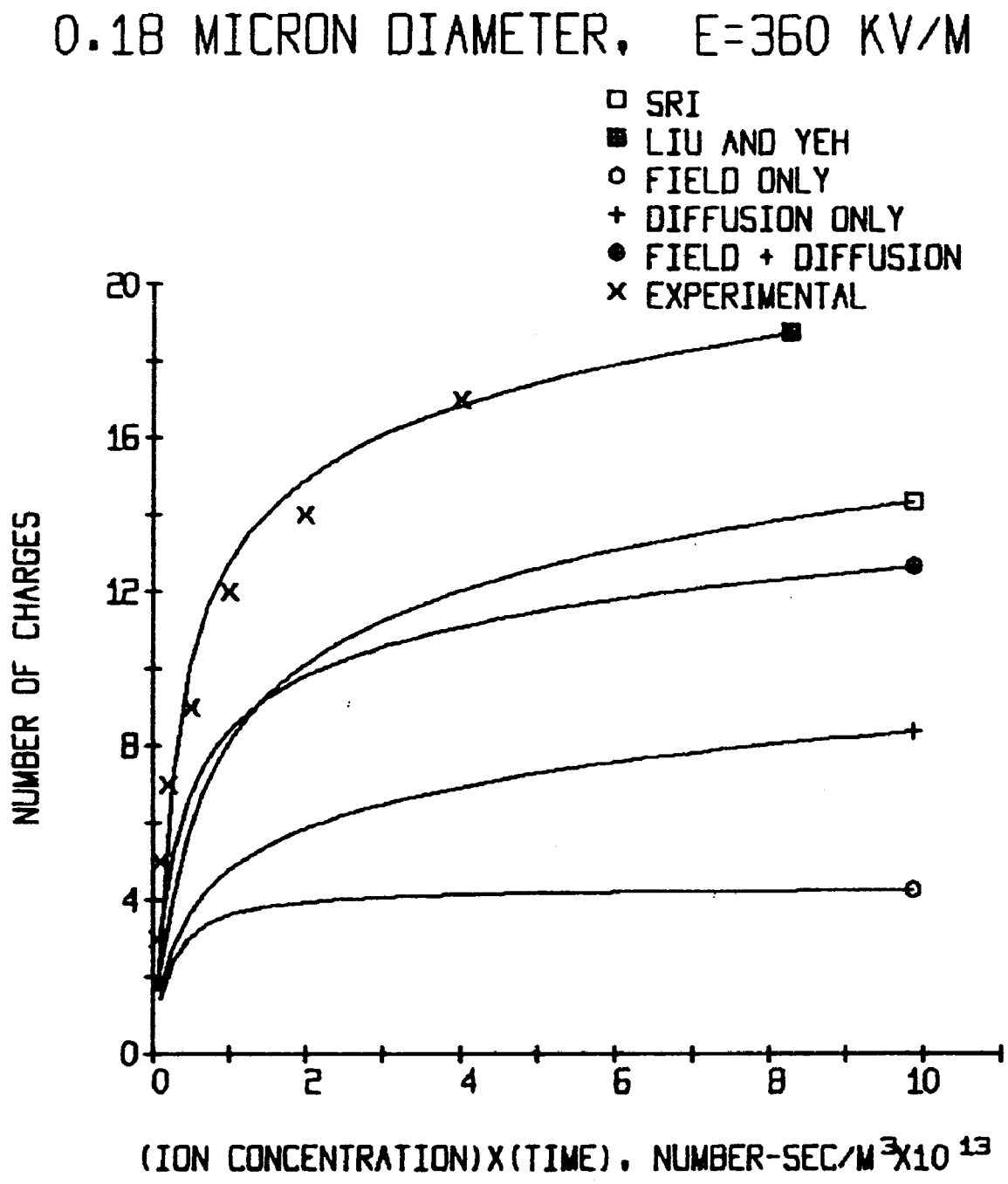

Figure 4. Comparison of theories and Hewitt's experimental data for 0.18 micron diameter particles and medium electric field intensity. In all theories $\bar{v}$ = 463 m/sec and Z = 2.2 x 10^{-4} m^2/V·sec

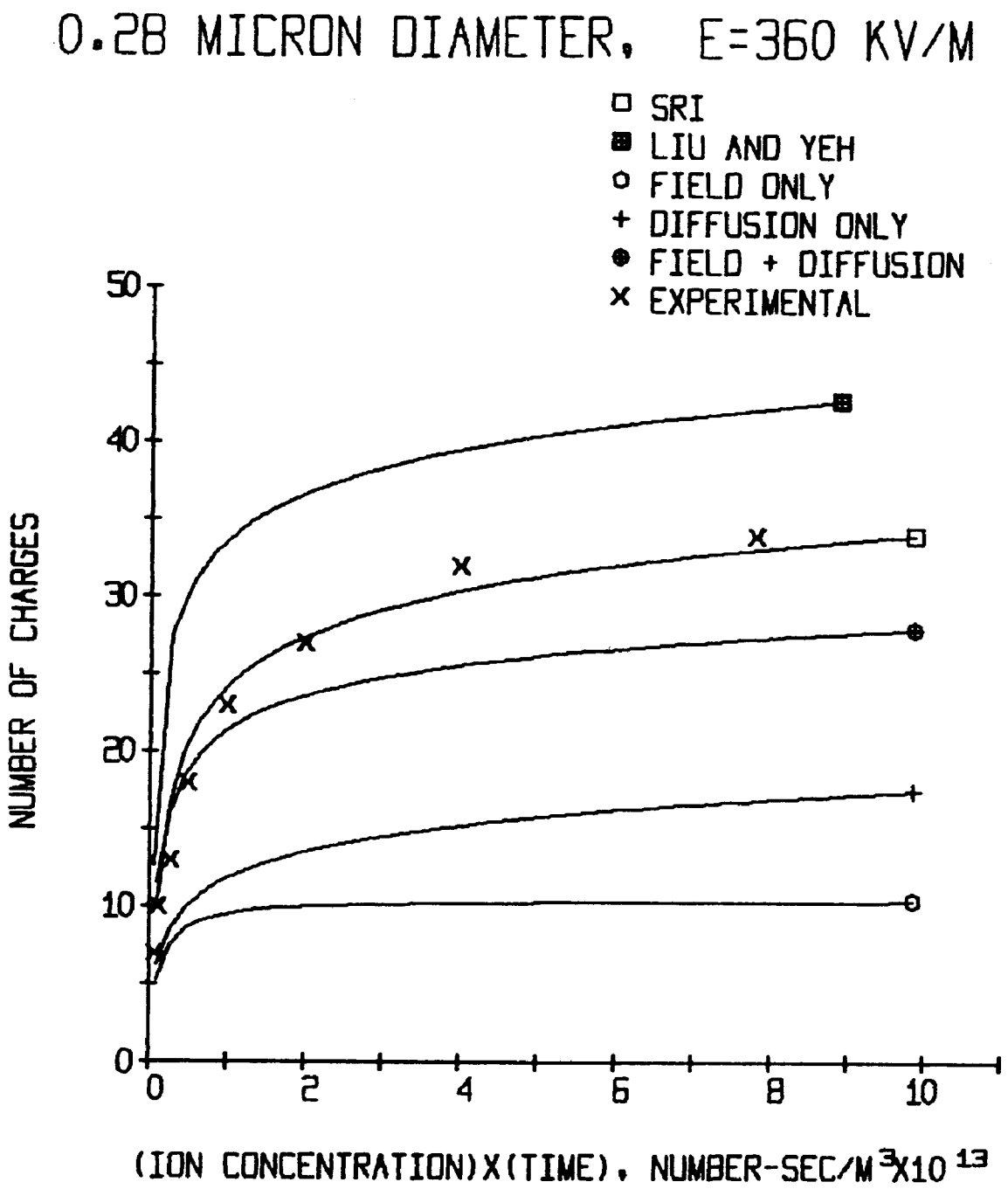

Figure 5. Comparison of theories and Hewitt's experimental data for 0.28 micron diameter particles and medium electric field intensity. In all theories $\tilde{v}$ = 463 m/sec and Z = 2.2 x 10^{-4} m^2/V·sec

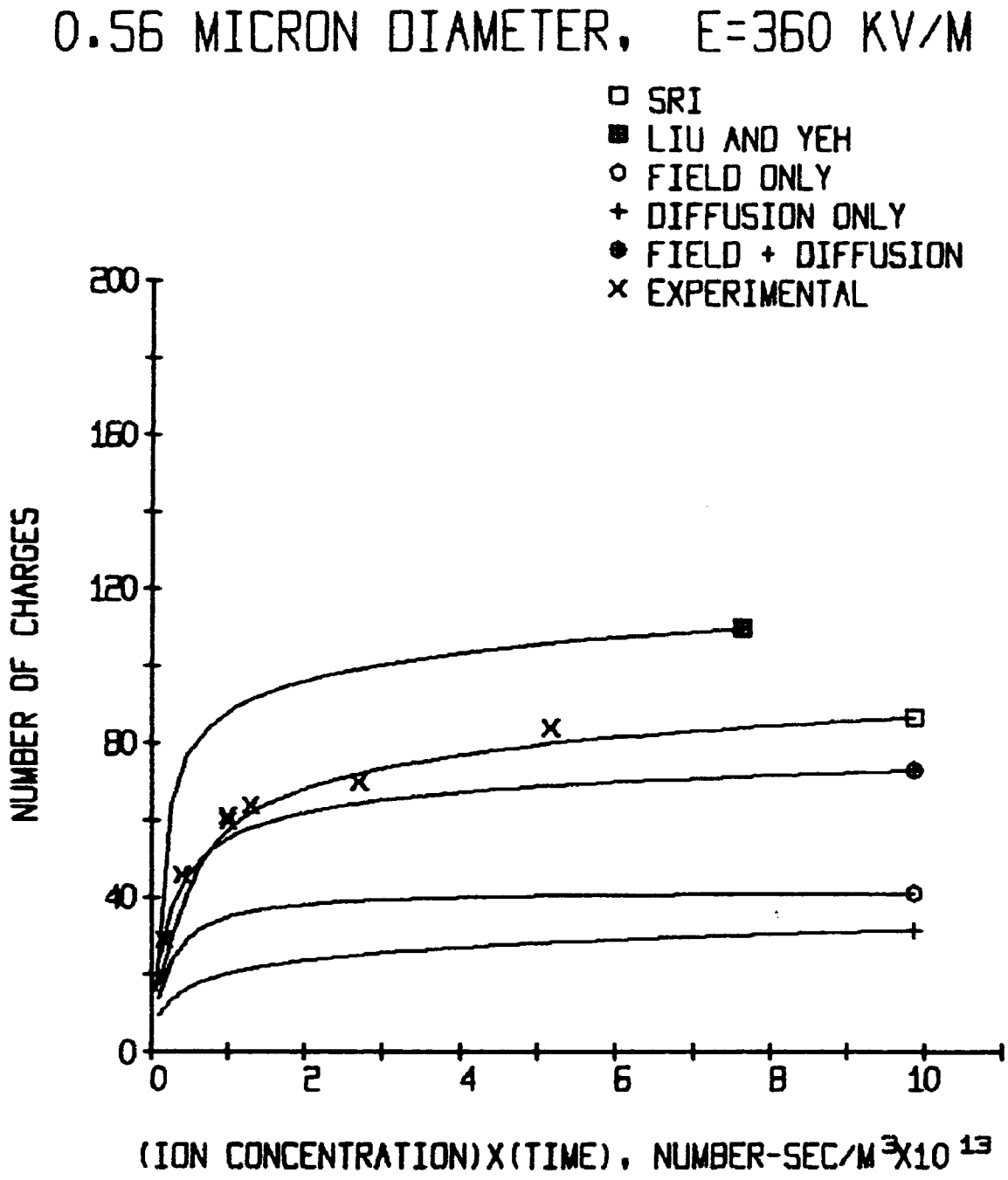

Figure 6. Comparison of theories and Hewitt's experimental data for 0.56 micron diameter particles and medium electric field intensity. In all theories $\bar{v}$ = 463 m/sec and Z = 2.2 x 10^{-4} $m^2/V \cdot sec$

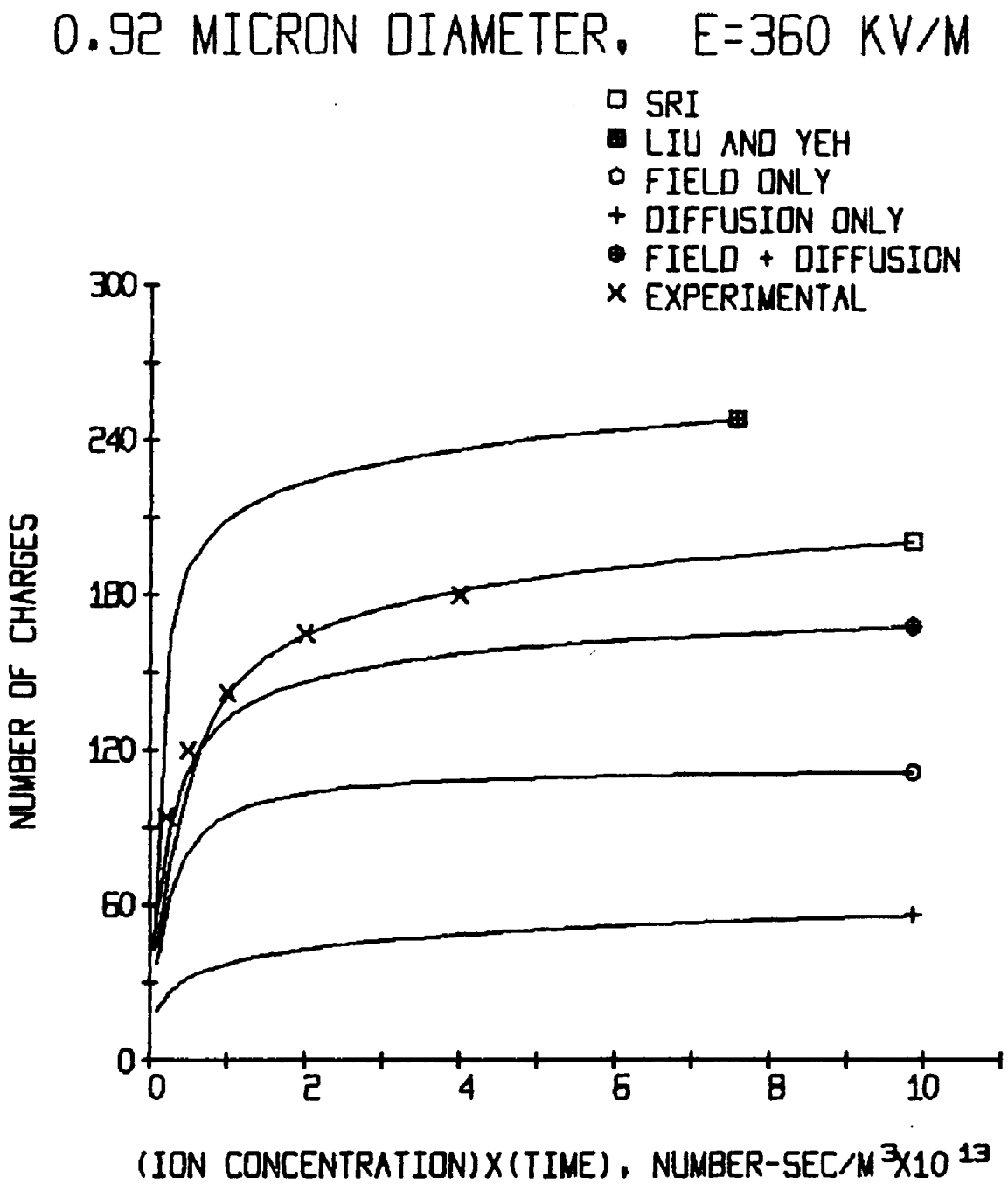

Figure 7. Comparison of theories and Hewitt's experimental data for 0.92 micron diameter particles and medium electric field intensity. In all theories $\bar{v}$ = 463 m/sec and Z = 2.2 x 10^{-4} $m^2/V \cdot sec$

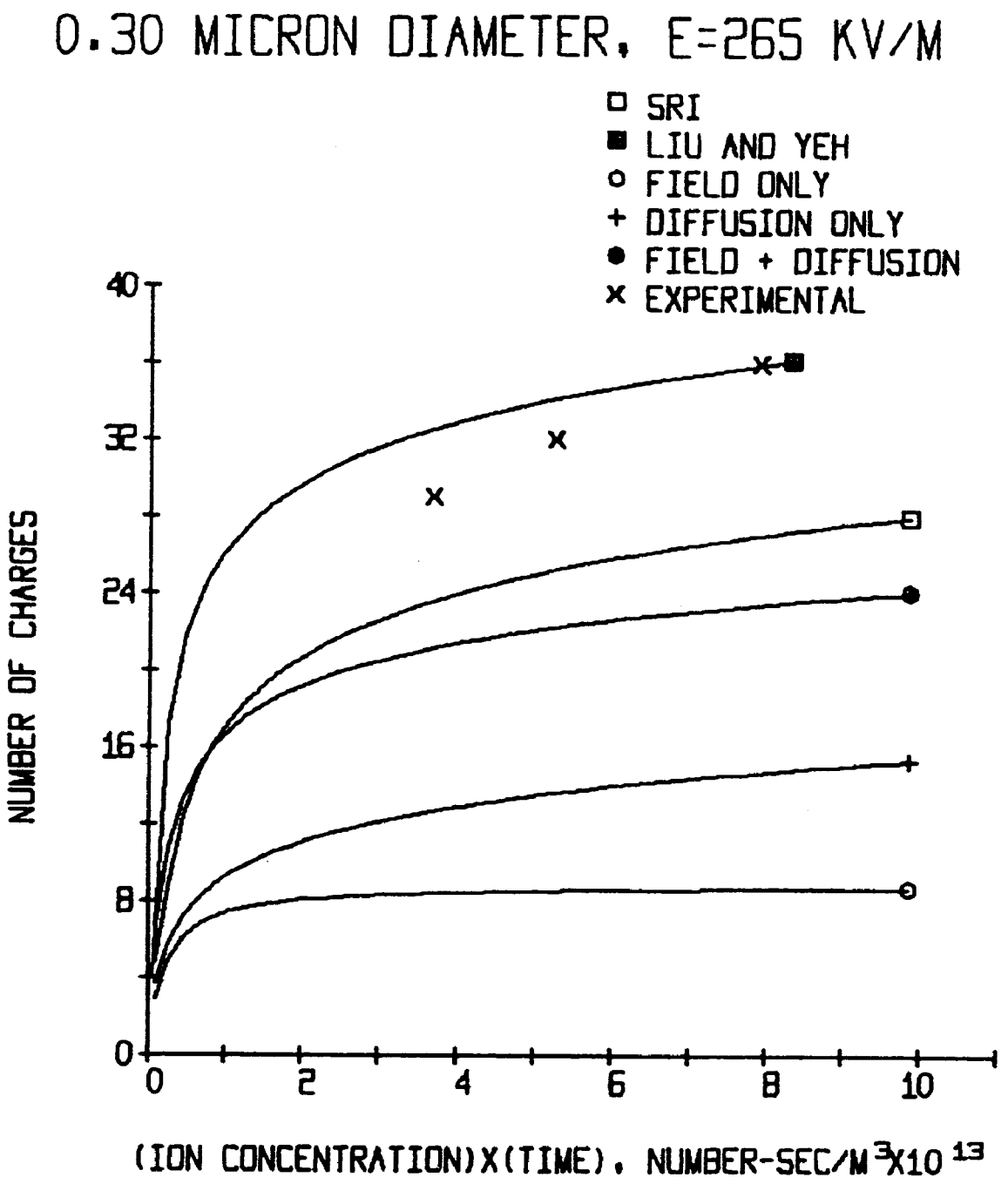

Figure 8. Comparison of theories and experimental data of Penney and Lynch for 0.3 micron diameter particles and medium electric field intensity. In all theories $\tilde{v}$ = 463 m/sec and Z = 2.2 x 10^{-4} $m^2/V \cdot sec$

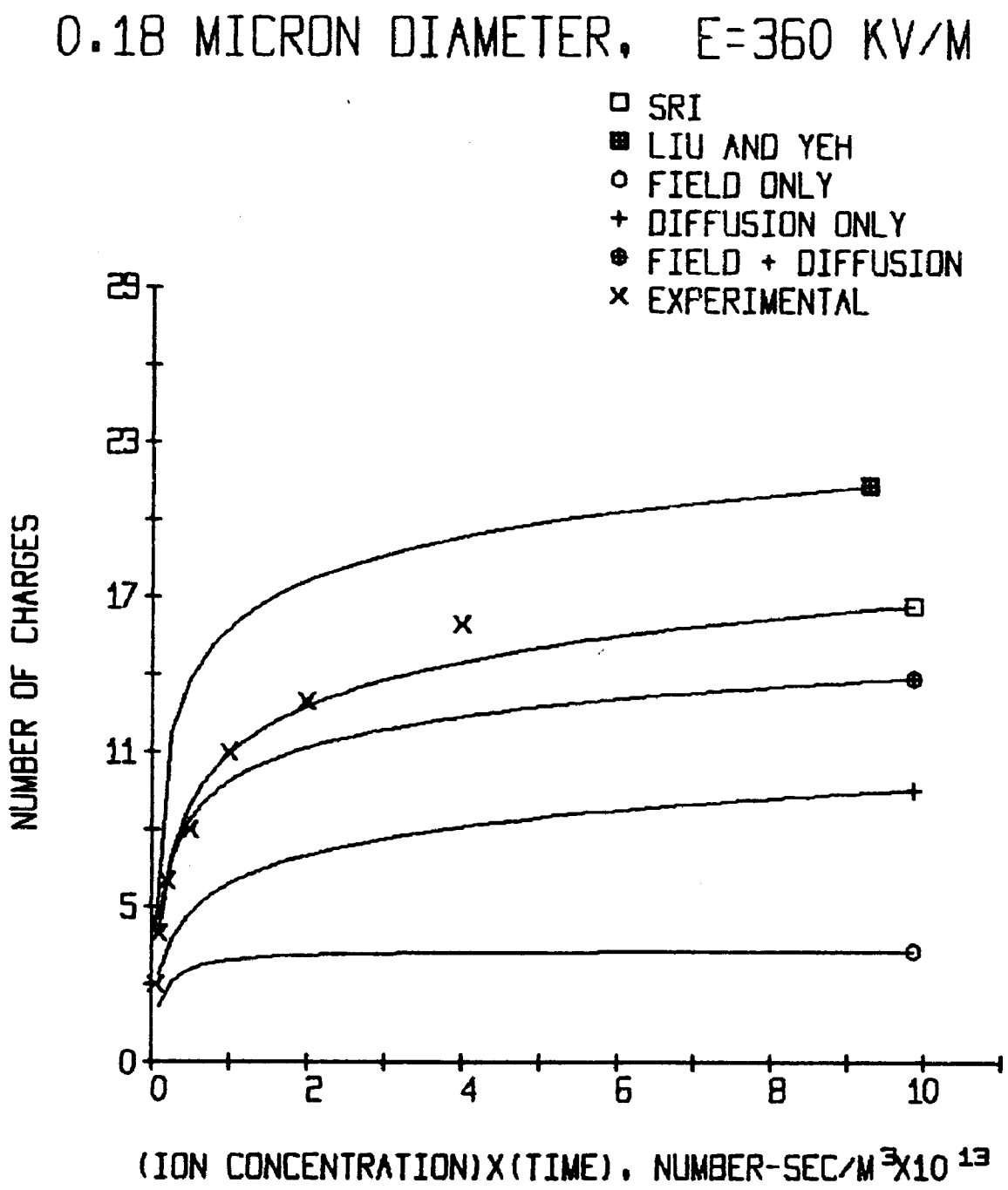

Figure 9. Comparison of theories and Hewitt's experimental data for 0.18 micron diameter particles and medium electric field intensity. In all theories $\tilde{v}$ = 118 m/sec and Z = 1.1 x 10^{-4} $m^2/V \cdot sec$

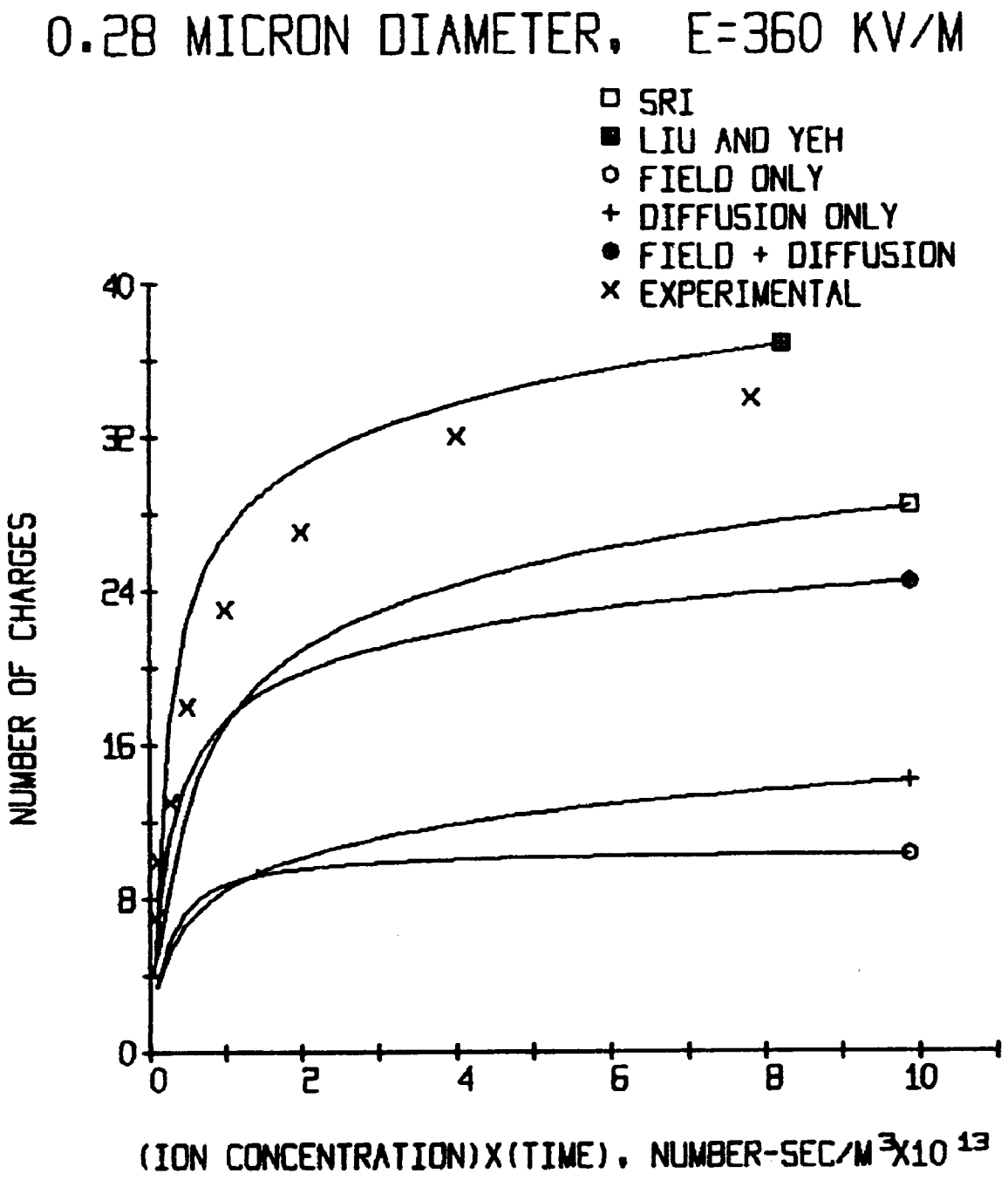

Figure 10. Comparison of theories and Hewitt's experimental data for 0.28 micron diameter particles and medium electric field intensity. In all theories $\bar{v}$ = 118 m/sec and Z = 1.1 x 10^{-4} $m^2/V \cdot sec$

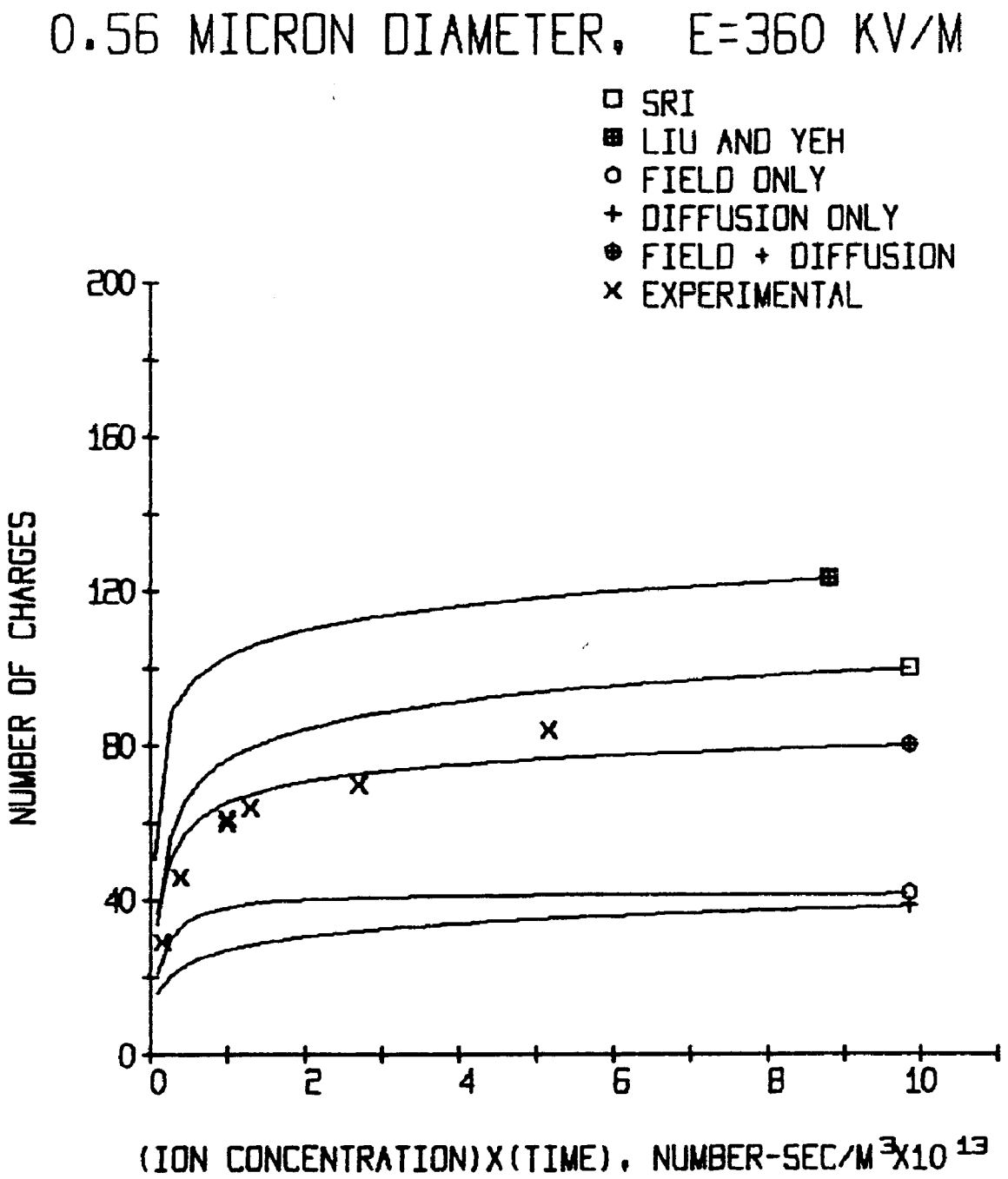

Figure 11. Comparison of theories and Hewitt's experimental data for 0.56 micron diameter particles and medium electric field intensity. In all theories $\tilde{v}$ = 118 m/sec and Z = 1.1 x 10^{-4} $m^2/V \cdot sec$

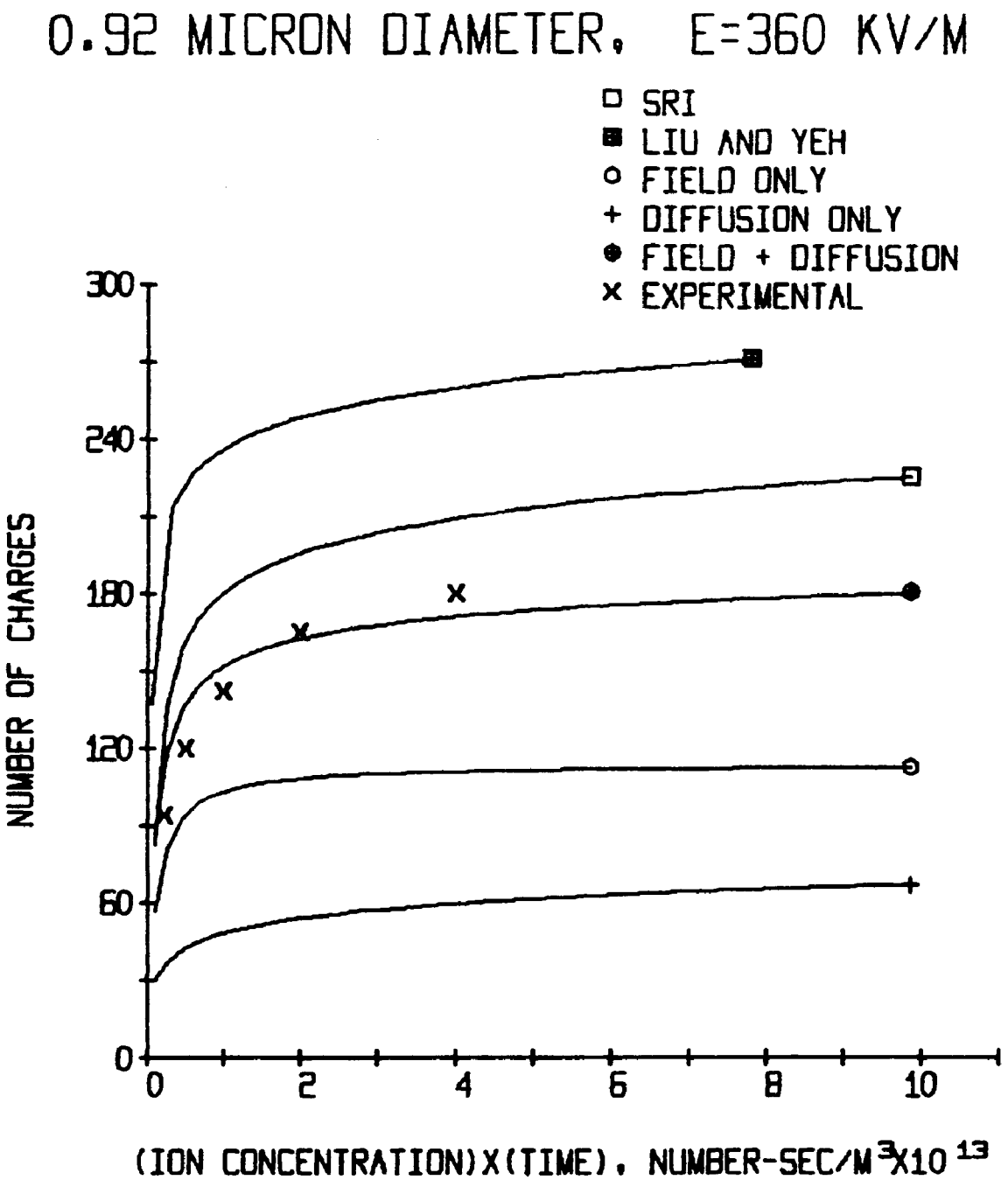

Figure 12. Comparison of theories and Hewitt's experimental data for 0.92 micron diameter particles and medium electric field intensity. In all theories $\tilde{v}$ = 118 m/sec and Z = 1.1 x 10^{-4} $m^2/V \cdot sec$

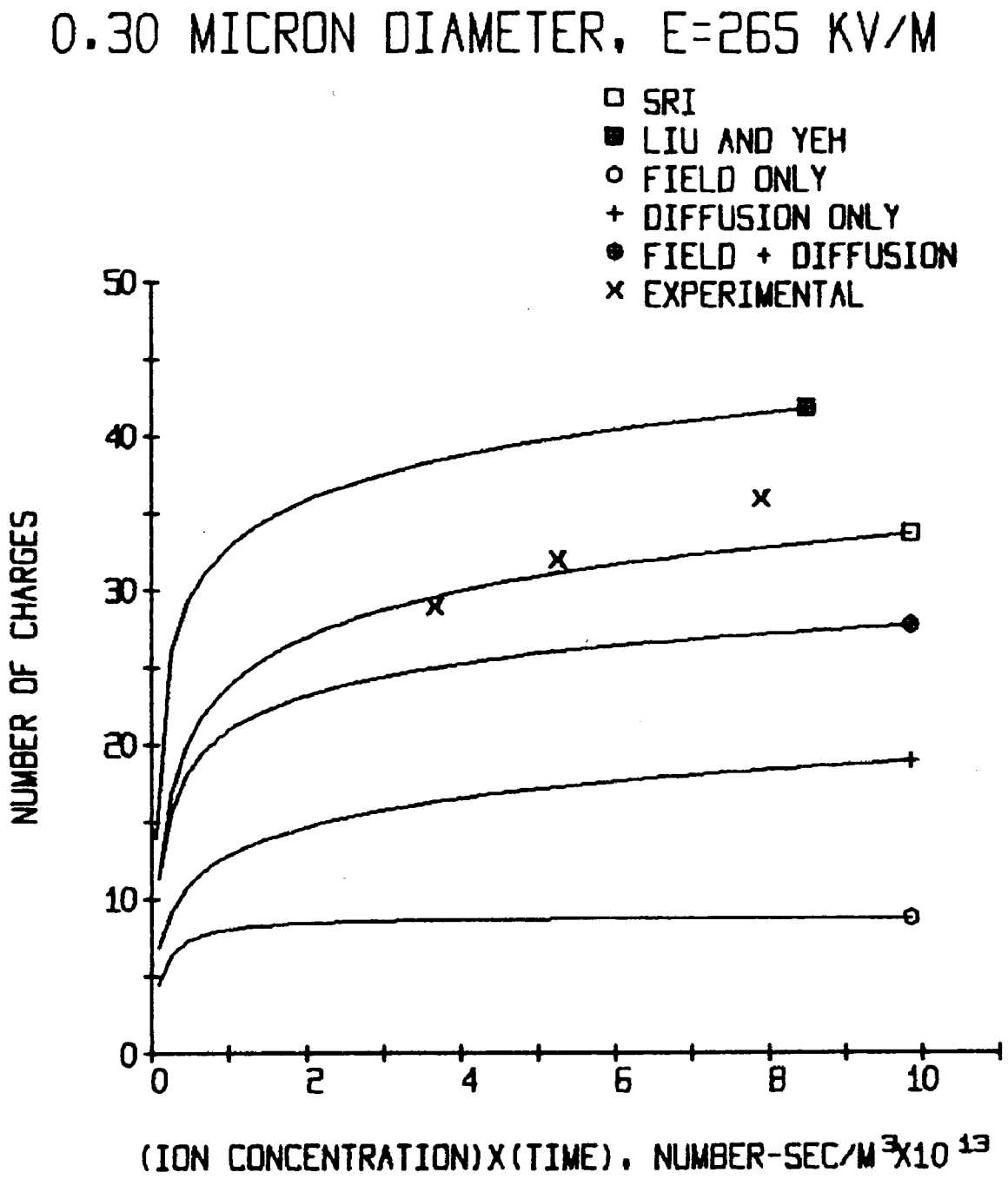

Figure 13. Comparison of theories and experimental data of Penney and Lynch for 0.3 micron diameter particles and medium electric field intensity. In all theories $\tilde{v}$ = 118 m/sec and Z = 1.1 x 10^{-4} $m^2/V \cdot sec$

ACKNOWLEDGMENTS

This work was supported by the Control Systems Laboratory, Environmental Protection Agency, Research Triangle Park, North Carolina, under Contract Number 68-02-1490.

REFERENCES

1. Hewitt, G. W. The Charging of Small Particles for Electrostatic Precipitation. Trans. Amer. Inst. Elec. Eng. 76, Part I:300-306, July 1957.

2. White, H. J. Industrial Electrostatic Precipitation. Reading, Mass., Addison-Wesley, 1963 p. 126-154.

3. Liu, B. Y. H., and H. C. Yeh. On the Theory of Charging of Aerosol Particles in an Electric Field. J. Appl. Phys. 39(3):1396-1402, February 1968.

4. Murphy, A. T., F. T. Adler, and G. W. Penney. A Theoretical Analysis of the Effects of an Electric Field on Charging of Fine Particles. Trans. Amer. Inst. Elec. Eng. 78, Part I:318-326, September 1959.

5. Liu, B. Y. H., K. T. Whitby, and H. H. S. Yu. Diffusion Charging of Aerosol Particles at Low Pressures. J. Appl. Phys. 38(4):1592-1597, March 1967.

THE EFFICIENCY OF ELECTROSTATIC PRECIPITATORS UNDER CONDITIONS OF CORONA QUENCHING

M. B. Awad and G. S. P. Castle
The University of Western Ontario
London, Ontario

ABSTRACT

The suppression of corona by particle space-charge is of considerable importance in electrostatic precipitators dealing with medium concentrations of fine fumes or smokes, or with very heavy concentrations of larger particles. In spite of the practical importance of the problem, the effect of the dust concentration on collection efficiency has found no direct answer in the literature.

In addition to the expected reduction in corona current due to low mobility dust particles, the presence of these charged particles has two other main effects:

(1) The electric field in the vicinity of the discharge electrode is weakened and hence the concentration of ions originating in the ionization zone and forming the charging current is decreased. It then follows that, in the limit, the charge acquired per particle should decrease as the dust concentrations increase for fixed values of applied voltage.

(2) The resulting space-charge build-up causes an increase in the field strength adjacent to the collecting surface of the precipitator.

The importance of each of these effects on the collection efficiency will be dependent on the relative decrease in particle charge as compared to the increase in the collection field.

Experiments have been carried out under both positive and negative corona with aerosol concentrations having specific surfaces in the range 0 to 44 m^2/m^3. The results have shown that the dependence of efficiency on the aerosol concentration at fixed values of voltage may follow one of two regimes:

(1) For low values of corona current densities, as the specific surface area increases, the efficiency decreases. In this case, the charge per particle decreases as the particle concentration increases and becomes far below the normal charge attainable. Here the increase in the collection field is more than counteracted by the large reduction in particle charge.

(2) For higher values of initial corona current densities, as the particle specific surface area increases the efficiency either increases slightly or stays constant, in spite of major reductions in the measured corona current. In this case there should also be a reduction in the charge per particle with the increase in particle concentration; however, this is apparently offset by the increase in the collection field strength.

Analysis of the results, coupled with an interpretation of existing theories, indicates that a major parameter that must be considered is the ratio of the initial corona current density and the specific surface of the particles.

INTRODUCTION

It is well known that the collection efficiency of an electrostatic precipitator shows a strong dependence both upon the properties of the gas and of the particulate material.

As a result, the influence of the type of material has been widely studied and is best characterized by the parameter of resistivity. Detrimental effects occur in two extreme conditions. If the dust resistivity is too high, back corona results; if the resistivity is too low, reentrainment occurs. Both of these effects have their origin in the behavior of the dust once it has been precipitated on the collecting electrode.

However, an additional property of the dust, its space-charge, has its influence prior to the deposition of the dust and results in the phenomenon of corona quenching. Although this effect has been known for many years and has been the subject of considerable interest[1-6], it does not appear to have received the same attention in recent literature as the previous two effects. Since the present trend towards using finely ground, lower grade, coals of high ash content will probably accelerate in the next decade, it seems important to look further at the effect of the particle space-charge on the collection efficiency.

The purpose of the work reported here is two-fold:

(1) To discuss some of the limitations of the assumptions made in the literature regarding particle space-charge effects.

(2) To present some interim experimental results showing the effect of specific surface on the corona current and collection efficiency in a laboratory scale precipitator.

REVIEW OF PREVIOUS WORK

In this section, it is intended to present a brief review of previous work that has been done on particle space-charge and its effect on corona quenching.

Pauthenier and Moreau-Hanot[1] developed the theory of electrical charge imparted to a dust particle in a corona discharge by the ion-bombardment mechanism. Particles larger than approximately 0.5 μm diameter acquire a charge given by:

$$q = (4\pi\varepsilon_0 p E_0 a^2)\ \frac{t}{t+\tau} \tag{1}$$

where $$p = 2\ \left(\frac{\kappa_p - 1}{\kappa_p + 2}\right) + 1 \tag{2}$$

and $$\tau = \frac{4\ \varepsilon_0}{N_0 e K_i} \tag{3}$$

For smaller particles, it is well known that diffusion charging effects must also be considered.

As a result of these mechanisms the suspended dust particles become charged as they enter the ionized corona field in the electrostatic precipitator. In the application of this charging theory in precipitation the electric field intensity E and the ion concentration N are commonly assumed to be uniform throughout the volume of the precipitator. This implies that particles of the same size are charged to the same degree.

The total corona current in a precipitator consists of charges carried by both free ions and charged particles and is given by:

$$J_{ld} = 2\pi rE\ (K_i \rho_i + K_p \rho_p) \tag{4}$$

(Under certain conditions near spark-over in negative corona an electron component may also exist.) As the dust concentration increases, ρ_p increases while ρ_i decreases. However, since the particle mobility K_p is normally 2 to 3 orders of magnitude less than the ion mobility, the measured corona current, although smaller than the measured current with clean gas for the same voltage, may be assumed to be carried essentially by free ions. However, the low mobility particles which are charged with the same sign as the discharge electrode cause an increase in the total space-charge and hence reduce the ionization field in the vicinity of the discharge electrode. In addition, this build-up of space-charge in the gap enhances the collection field at the outer electrode.

From the quantitative point of view, Poisson's equation taking the particle space-charge effect into account is given as:

$$\nabla \cdot \bar{E} = \frac{1}{\varepsilon_0} \left[\rho_i + \rho_p\right] \tag{5}$$

where $$\rho_i = \frac{J_{ld}}{2\pi r K_i E} \tag{5a}$$

$$\rho_p = \varepsilon_0 pES \tag{5b}$$

Solving equation (5) in cylindrical geometry and substituting normally assumed boundary conditions, the field distribution is given by:[1]

$$E(r) = \left\{ \left[\left(\frac{a}{r}\right)^2 E_c^2 + \frac{J_{1d}}{4\pi\varepsilon_0 K_i (pSr)^2} \right] e^{2pSr} - \frac{J_{1d}}{4\pi\varepsilon_0 K_i} \left[\frac{2}{pSr} + \frac{1}{(pSr)^2} \right] \right\}^{\frac{1}{2}} \quad (6)$$

Lowe and Lucas[2] used equation (6) to plot the field intensity across the tube in the presence of dust burden. This plot confirms that the particle space-charge reduces the field near the corona wire and raises it near the wall. However, it is important to realize that this plot is based on several assumptions, the most critical being a uniform distribution of particle space-charge in the gap.

Neglecting the component $(\frac{a}{r})^2 E_c^2$ near the wall and constraining (2pSr) to be much less than 1 in equation (6) the field at the wall becomes:

$$E = \left\{ \frac{J_{1d}}{2\pi\varepsilon_0 K_i} \left(1 + \frac{2pSr}{3}\right) \right\}^{\frac{1}{2}} \quad (7)$$

Winkel and Schuetz[3] equated the field given by equation (7) with the approximate value of the field at the wall with no particle space-charge, i.e.:

$$E = \left\{ \frac{J_{1c}}{2\pi\varepsilon_0 K_i} \right\}^{\frac{1}{2}} \quad (8)$$

and obtained

$$\frac{J_{1c}}{J_{1d}} = 1 + \frac{2pb}{3} S \quad (9)$$

They showed equation (9) to be in a qualitative agreement with their experimental results. This equation predicts that the only dimension affecting the suppression ratio is the radius of the outer electrode. The limitations of the assumptions used in deriving the above equations are discussed elsewhere.[7]

EFFECT ON COLLECTION EFFICIENCY

In the following discussion, cylindrical geometry will be considered and the proposed mechanisms will be dealt with separately under the headings of charging and collection.

THE CHARGING PROCESS

Assume uncharged particles having specific surface area S are placed in a corona discharge having an original field E and ion density N. The gas ions travelling along the field lines will impart charge to the particles, according to the Pauthenier relationship. If the specific surface area is very small or the original corona current is very high the particle space-charge density can be neglected with respect to the ion space-charge density even though significant changes in current may occur. If the specific surface area is increased or the original current density is not high enough so that the particle space-charge density cannot be neglected, then the resulting space-charge will reduce the field in the vicinity of the discharge electrode thus reducing the ionization coefficient and the rate of ion production in the sheath. Therefore, the original values of E and N will be reduced. In addition, as the particle concentration increases, local field interactions will also take place further reducing the effective charging field. This will then result in a lower maximum charge per particle and a longer charging time constant. The corona current generation from the sheath will also be dependent on the axial distance along the corona wire, i.e. as the particles proceed in the corona field they gain more charge and suppress more sheath generation.

In summary, the original corona current during the charging process is reduced by two mechanisms:

(1) The binding of the ions by the low mobility particles, and

(2) The lower ion generation from the sheath.

Note that in equation (5b) the particle space-charge density is based on the assumption that the charging process is completed and the particles are charged to saturation. Therefore, the application of the final field equation (6) must be restricted to outside the region where the charging

process occurs. At the end of the above process, the particles are essentially fully charged and if particle reentrainment is negligible the next stage will be mainly for collection.

THE COLLECTION PROCESS

This process takes much longer than the charging and thus represents the main part of the precipitator. The fully charged particle from the previous stage should not pick up appreciable numbers of ions in this case. Therefore, any reduction in the corona current is due mainly to the field reduction in the ionized generation sheath. If we assume that the previous stage only represents a small component of the total length of the precipitator, then the main part of the reduction in the current in corona quenching is due to the lower generation from the sheath rather than the pick up of ions and the mobility effect. These charged particles will however cause enhancement of the collection field.

The relative magnitudes of both ρ_i and ρ_p in equation (5) will obviously vary with the axial distance and equations (6) and (7) must be applied to a given location in the precipitator. Note that the collection rate will govern the amount of particle space-charge remaining in the gap and hence the corona current in the presence of the particles and the corona current suppression ratio. A deduction from this will be that the corona current suppression ratio J_{1c}/J_{1d} as a function of S will be dependent on:

(1) The applied voltage—As the voltage increases the original corona current increases, the collection rate increases and the suppression ratio J_{1c}/J_{1d} decreases. This has been shown in a previous paper.[7]

(2) The collection area—If one imagined a precipitator where the particles are collected very quickly in a short section of it whereas the remainder stays almost free from the particles, then the suppression ratio will decrease with the increase in collection area.

(3) The flow rate—Decreasing the flow rate results in higher collection efficiency and hence lower corona suppression ratio.

From the above discussion it can be seen that equation (8) which was obtained on the basis of many assumptions (including the assumption of constant electric field at the wall with and without particle space-charge), shows only a qualitative trend that may be suitable only for low values of specific surfaces and it cannot be relied upon for any quantitative comparison.

Thus, in any given situation the question of whether an increase in the specific surface area will result in a decrease or increase in the collection efficiency depends upon the reduction in the charge per particle as compared with the increase in the collection field.

EXPERIMENTAL SET-UP

All experiments were carried out using a cylindrical corona apparatus 7.62 cm (3 in.) diameter and 15.24 cm (6 in.) long with its ends flared to eliminate any end effects and the possibility of back corona. Separate tests were carried out using a corona wire of diameter 0.065 in. under both positive and negative corona.

The length of the precipitator was kept as short as possible to localize the space-charge effects. The total air flow was kept constant at 6.8×10^{-3} m^3/sec (15 cfm) while the specific surface area was varied from zero to 44 m^2/m^3 by changing the amount of the smoke generated from a DOP smoke generator (Royco Model 258WA) and reducing the clean air flow in proportion. The particle size distribution was assumed[8] to obey the log-normal distribution with a geometric mean diameter = 0.36 μm and geometric standard deviation = 1.66. Calculations of the specific surface area are described in detail in reference 7. The collection efficiencies were measured on a mass basis by dissolving a small quantity of sodium fluorescein (6.4×10^{-3} % by wt) in the DOP as a tracer and analyzing the residues collected on millipore filters in a highly sensitive fluorometer (G. K. Turner Associates, Model No. 111).

RESULTS AND DISCUSSION

Figures 1 and 2 show the collection efficiency versus the specific surface area of the suspended material in the gas at fixed total air flow rate for both polarities. The values of the quenched corona current density in mA/m are indicated between brackets at each point with the initial current densities shown under the appropriate voltage. For applied

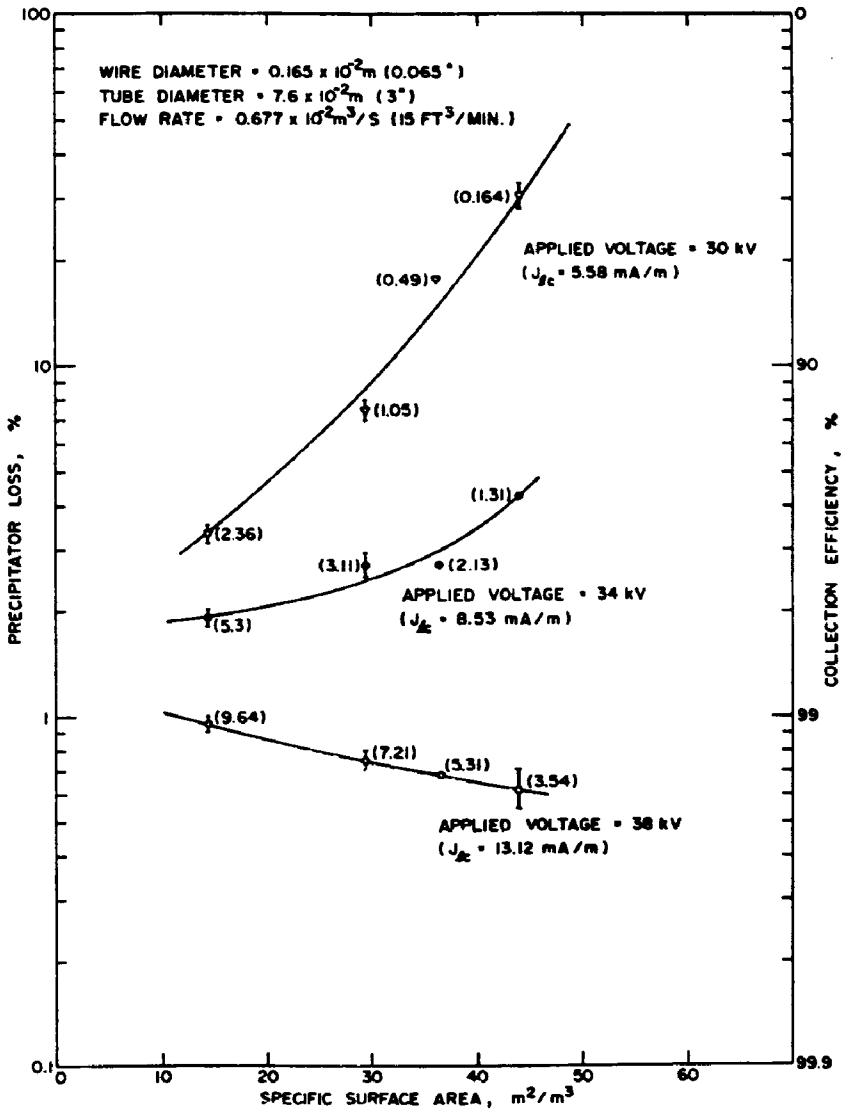

Figure 1. Negative corona collection efficiency vs the specific surface area

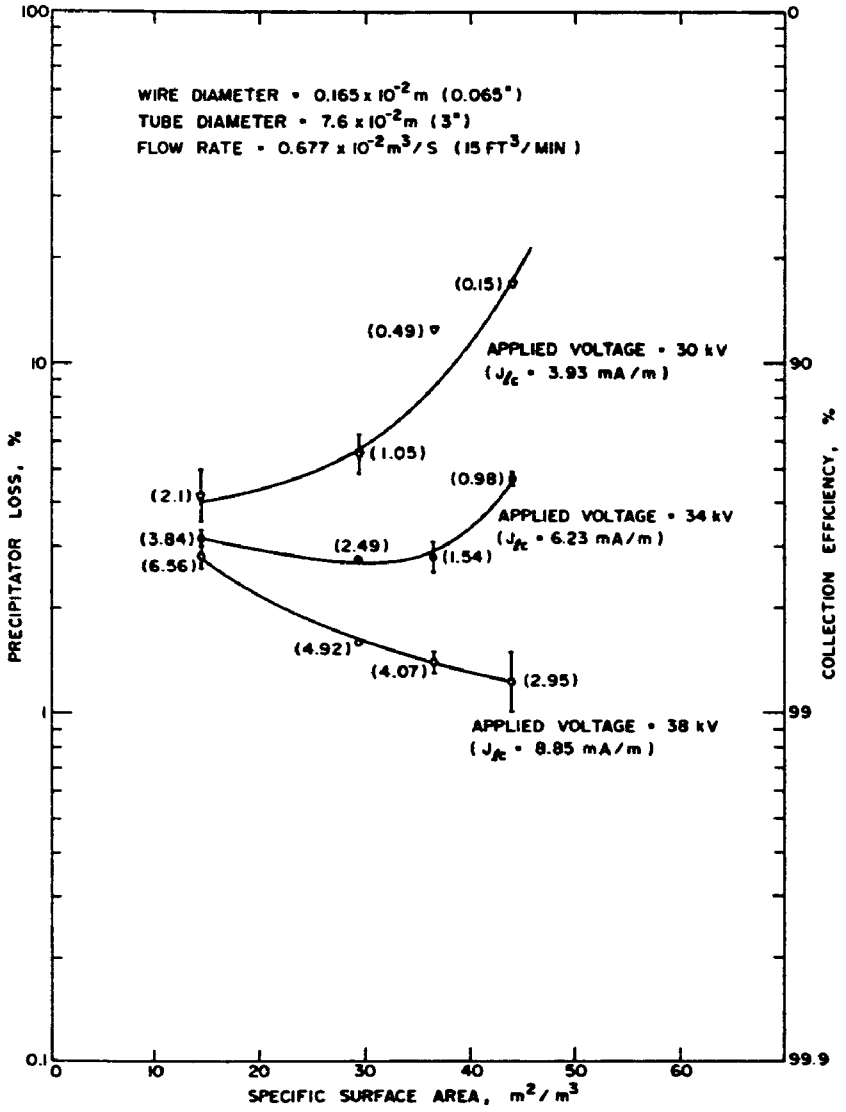

Figure 2. Positive corona collection efficiency vs the specific surface area

voltages of 30 and 34 kV, as the specific surface area increases, the corona current decreases and the efficiency decreases. This can be explained as follows. In the charging process, the charge per particle decreases as the specific surface area increases. In the collection process, the collection field at the outer electrode is not enhanced enough to compensate for the reduction in the charge for the following reason. At these voltages, the original corona current density with clean air in the collection zone was relatively low and the suppression of the current generation from the sheath was relatively large ($21 \leqslant (J_{1c}/J_{1d}) \geqslant 2$). Note that in general, the higher the original current, the lower will be the current suppression because of the faster collection rate. Since the reduction in the ionic current in the presence of the suspended material is large, then the collection field component due to the ionic current is greatly reduced. However, the presence of the charged particles will give another component that adds to the ionic component forming the total collection field. In this case the particle space-charge is small due to the relatively low charge acquired by the particles.

On the other hand, at an applied voltage of 38 kV (i.e. a higher original current than the previous two cases) the corona current suppression is relatively low ($4.4 \leqslant (J_{1c}/J_{1d}) \geqslant 1.4$) and the collection field enhancement at the outer electrode was apparently capable of compensating for the reduction in the charge per particle resulting in an increase in collection efficiency as the specific surface area increases.

Comparison of the results shown in Figures 1 and 2 indicates that for applied voltages of 30 and 34 kV where the corona current density with clean air is relatively low, the negative corona although having higher values of J_{1c} and J_{1d} gives lower efficiency than the positive for the same specific surface area (highest three values only) and the same applied voltage. This is believed to be due to the non-uniformity of the negative corona discharge in the axial direction for low current densities and the creation of gas pockets of low ion space-charge density between the successive localized tufts. These gas pockets should result in lower charging for some portion of the suspended material. With the increase in applied voltage the number of tufts increases and also a free electron component of the current becomes apparent. Therefore, at applied voltage of 38 kV the negative corona with its higher values of both J_{1c} and J_{1d} results in higher efficiency than the positive.

The above discussion and the results in Figures 1 and 2 indicate that a reasonable factor that may be used as an indicator for the relative effect the space-charge may have on the collection efficiency is the current density originally present in the gap with clean gas coupled with the specific surface area of the particles. For this reason, Figures 3 and 4 are plotted showing J_{1c}/S versus the collection efficiency for the same corona wire in negative and positive corona respectively. This indicates that a variation of the specific surface area for a certain original value of J_{1c} such that the ratio is larger than approximately 0.5 mA in the negative case and 0.25 mA in the positive, should not result in a reduction in efficiency. On the other hand, variations of the specific surface area for certain original current J_{1c} such that the ratio is less than these limits should result in a reduction in collection efficiency.

CONCLUSIONS

1. Particles carried in suspension in the gas interact with the partial processes responsible for their transport from the active precipitator space to the collecting electrode. This interaction is much more complex than generally assumed in the literature. The total corona current varies in the axial direction according to the specific surface area of the suspended material, the original corona current with clean air, the total air flow rate and the collection area. Therefore, the corona current suppression ratio versus the specific surface area is dependent on many variables and difficult to be compared with any theory. Furthermore, the electric field distribution in the gap will be a function of both the radial and the axial directions and this distribution will also be dependent on many variables as mentioned above.

2. In the precipitator tested the efficiency of collection for a fixed voltage appears to be primarily dependent on the original current density with clean gas coupled with the specific surface area. This dependence can be classified into two regimes:

   (a) If the ratio of the corona current density with clean gas J_{1c} to the specific surface area of the suspended material S is smaller than approximately 0.5 mA for the negative

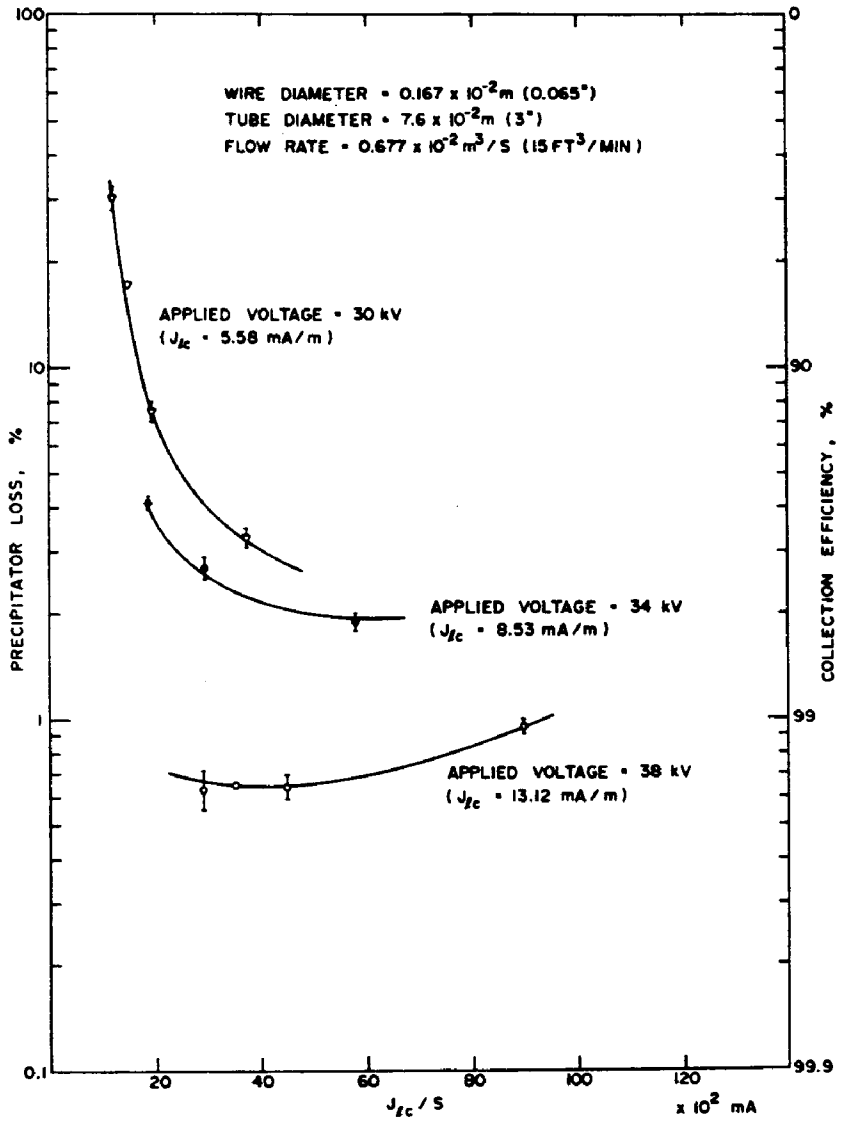

Figure 3. Negative corona collection efficiency vs the corona current density with clean gas per unit specific surface area

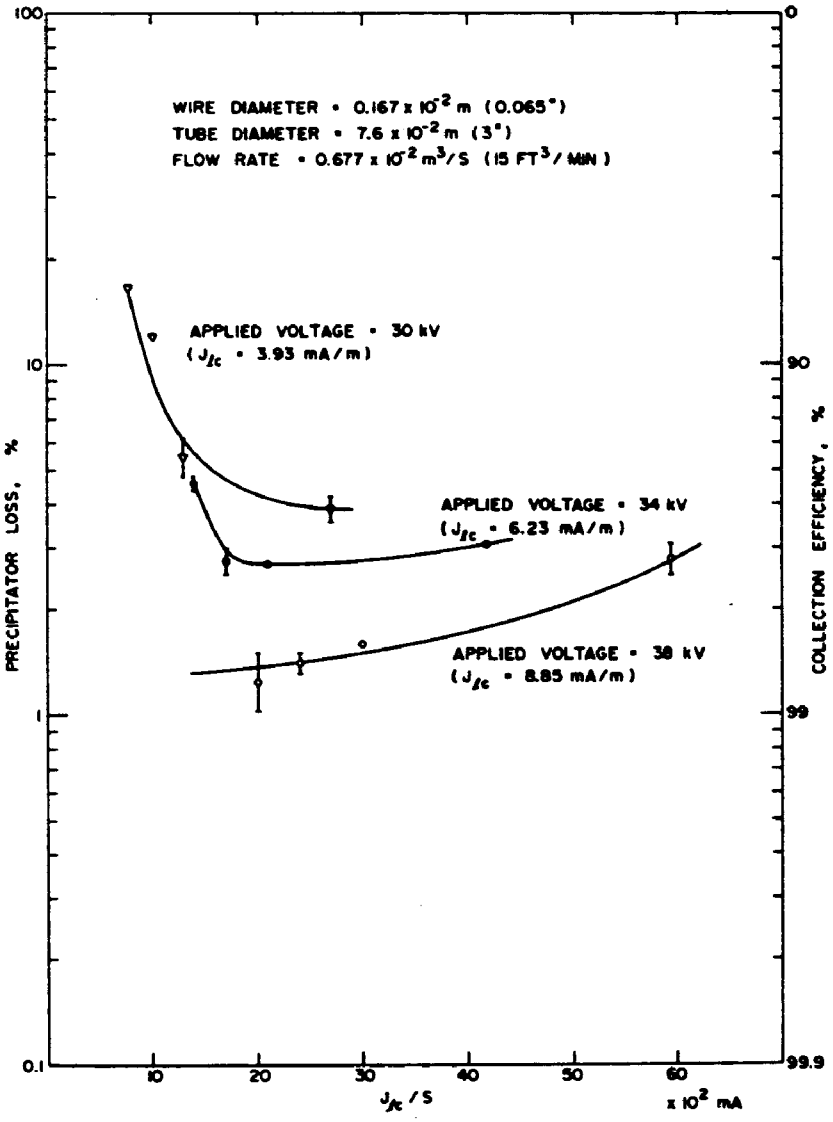

Figure 4. Positive corona collection efficiency vs the corona current density with clean gas per unit specific surface area

corona and 0.25 mA for the positive then an increase in S for a certain original value of J_{lc} should result in a reduction in collection efficiency.

(b) If the ratio J_{lc}/S is higher than the above experimental limits, then the increase in S for a certain original value of J_{lc} should result in a slight increase in the collection efficiency. In this case, it appears that collection field enhancement is occurring.

NOMENCLATURE

a	corona wire radius and particle radius, m
b	radius of the outer cylinder, m
E	electric field, V/m
e	ion charge, coul
E_c	corona starting field with clean gas, V/m
J_{lc}	linear current density in clean gas, A/m
J_{ld}	linear current density in dusty gas, A/m
K_i	ion mobility, $m^2/(V\text{-}sec)$
K_p	particle mobility, $m^2/(V\text{-}sec)$
N	ion density, $ions/m^3$
p	dimensionless parameter = $2\left(\frac{\kappa_p - 1}{\kappa_p + 2}\right) + 1$
q	particle charge, coul
r	radial distance measured from the center of the corona wire, m
S	specific surface area of the particles, m^{-1}
ε_0	permittivity of free space, 8.86×10^{-12} F/m
k_p	relative dielectric constant of particle, dimensionless

ρ_i ion space-charge density, coul/m^3

ρ_p particle space-charge density, coul/m^3

τ charging time constant, sec

REFERENCES

1. Pauthenier, M., and M. Moreau-Hanot. La Charge des Particules Spheriques dans un Champ Ionisé [Charging of Spherical Particles in an Ionized Field]. J. Phys. Radium (Paris). 3:590-615, 1932.

2. Lowe, H. J., and D. H. Lucas. The Physics of Electrostatic Precipitation. Brit. J. Appl. Phys. (London). Suppl. 2:S40-47, 1953.

3. Winkel, A., and A. Schuetz. Elektrische Abscheidung Feindisperser Eisenoxidstaube bei Hoheren Temperaturen unter Besonderer Berücksichtigung des Elektrischen Staubwiderstandes [Electrical Separation of Finely Dispersed Iron Oxide Dust at High Temperatures with Special Consideration to Electrical Resistivity of the Dust]. Staub-Reinhalt. Luft. 22:343, 1962.

4. White, H. J. Industrial Electrostatic Precipitation. Reading, Mass., Addison-Wesley, 1963. p. 114-119.

5. Cooperman, P. Dust Space-Charge in Electrical Precipitators. (Conference paper CP 62-253, presented at American Institute of Electrical Engineers Winter General Meeting. New York. 1962.)

6. Sproull, W. T. Corona Quenching - Its Significance in Electrical Precipitation. J. Air Pollut. Contr. Assoc. 13:617-621, December 1963.

7. Awad, M. B., and G. S. P. Castle. Corona Quenching in Electrostatic Precipitators. University of Western Ontario. (To be presented at Institute of Electrical and Electronics Engineers Annual Meeting. Pittsburgh. 1974.)

8. Prodi, V., C. Melandri, and G. M. Giacomelli. Size Spectrometry of DOP Particles Using Low-Temperature Separation and Replica Technique. Staub-Reinhalt. Luft (in English). 30:31-34, March 1970.

RADIATION CHARGING: A NOVEL WAY TO ELECTRICALLY CHARGE FINE PARTICLES

Robert Jennings Heinsohn, Samuel H. Levine,
Robert A. Fjeld, and Gary W. Malamud
The Pennsylvania State University
University Park, Pennsylvania

INTRODUCTION

The purpose of this paper is to describe a way to electrically charge fine particles without using an electrical corona. We suggest that by using electric and magnetic fields, in conjunction with ionizing radiation, it is technically feasible to electrically charge fine particles. Once charged, they can be removed from the air stream by directly applying transverse electric fields. Thus, radiation charging is obviously applicable to electrostatic collection. In addition, since electrostatic forces can assist filtration and wet collection systems, we suggest that it may be possible to design new and improved filtration and wet scrubber systems using radiation charging. The objectives of this paper are:

a) to present expressions that predict the charge acquired by particles

b) to present the results of preliminary experiments

HISTORICAL REVIEW

The idea of subjecting matter to radiation appears to have originated in a 1929 patent application[1] in which M. J. McCray proposed an "apparatus for activating matter with radiations." It was 1945 before C. W. Jacob[2] proposed a device that used radiation to produce ionization in a gas stream and (using charged plates) to collect the charged particles. More recently, F. J. Meyer[3] patented an "irradiating apparatus" in which x-ray sources were located inside a chamber through which air was passed. The notable part of Meyer's patent was his suggestion of the possibility of replacing the x-ray tubes by radioactive sources. The ion distributions produced by these two schemes would consist of equal concentrations of positive and negative ions uniformly distributed in the gas stream, i.e., a bipolar space charge. Unfortunately, a bipolar space charge actually serves to electrically neutralize, rather than charge, an aerosol[4]. In fact, commercially available particle neutralizers, which use alpha or beta emitters, are based on this principle.

Recognizing the problems of charging particles in a bipolar space charge, F. J. Maas[5] patented an apparatus utilizing an alpha emitting isotope to cause gas ionization and an electric field transverse to the gas flow to produce a unipolar space charge. R. Leupe, et al.[6] reported on a similar device employing an alpha source and an electrode configuration that was also claimed to yield a unipolar space charge. However, due to the extremely low penetration of alpha particles, their practicality to ionize gas is limited.

Recent designs involving Co^{60} gamma sources and an electric field in cylindrical geometry have received attention[7-11]. Gas ionization is produced by Compton scattered electrons from both the walls of the device and the carrier gas. A voltage difference between inner and outer cylindrical electrodes causes a separation of the charge into regions of predominantly one polarity. An instrument discussed by Hasenclever and Siegmann[7] and Coenen[8] based on this design is used as a dust monitor. With no particles passing through the ionization region, a constant current to a central electrode is measured. Particles that pass through the region are charged by the ions, but are not collected by the weak field. Thus, dust laden air decreases the current to the electrode which in turn triggers a warning device.

Mohnen and Holtz[9] describe a similar device that involves two chambers rather than one. Ambient air is passed through one of the chambers while filtered air flows through the other. A comparison of the current to each of the electrodes provides some measure of the particle concentration in the ambient air.

Gamma ionization is applied to a particle collection system by increasing the applied electric field and source intensity. Dickter[10] obtained collection efficiencies of approximately 70% for 0.7 micron diameter salt particles. Using 10,000 Curies of Co^{60} and a stoker-fed coal furnace, Schultz[11] obtained collection efficiencies typical of those obtained in commercial electrostatic precipitators for particles larger than 2 microns and higher efficiencies for smaller particles.

While the results of Schultz's work are promising and the devices of Hasenclever and Siegmann, Coenen, and Mohnen and Holtz have merit, an evaluation of the full range of applicability of the schemes is difficult, if not impossible, without a mathematical description of the physical processes. Furthermore, only a small fraction of the energy of the electrons scattered by the gamma radiation is utilized for ionization. Thus, in systems of realistic size energetic electrons transfer most of their energy to the duct walls, which does not contribute to gas ionization.

RADIATION CHARGING SYSTEM

The major elements of a radiation charging system consist of:

1) a duct containing the dust laden gas stream

2) a radiation source located inside and/or outside the duct

3) a transverse electric field

4) longitudinal or transverse magnetic field.

The location and intensities of the radiation sources and magnetic fields to produce the maximum charging have not been determined. For this initial study, the apparatus shown in Figure 1 was assembled. A schematic portrayal of the phenomena involved in radiation charging is shown in Figure 2. Since the object of the study is to develop and

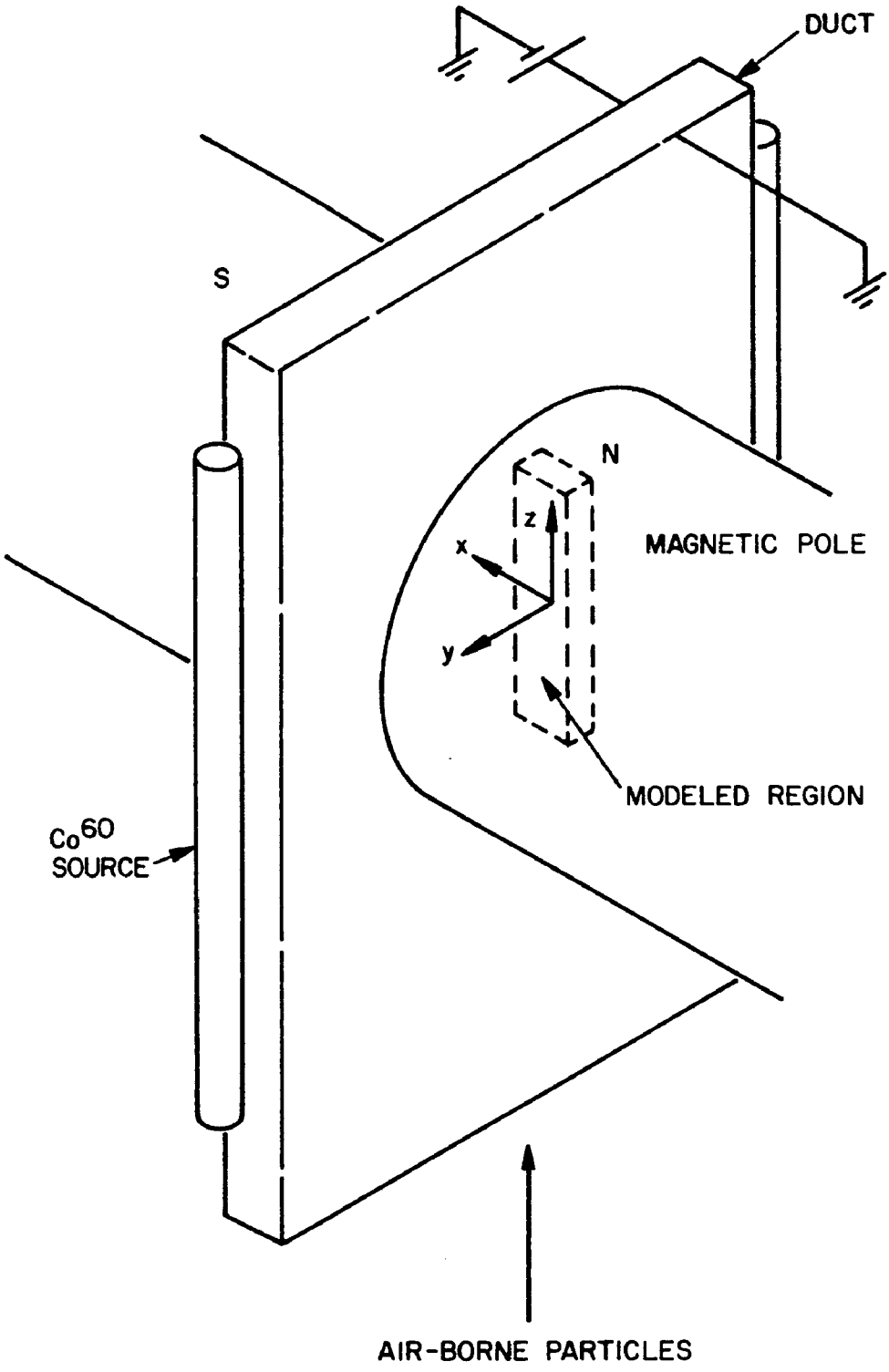

Figure 1. Sketch of the experimental apparatus

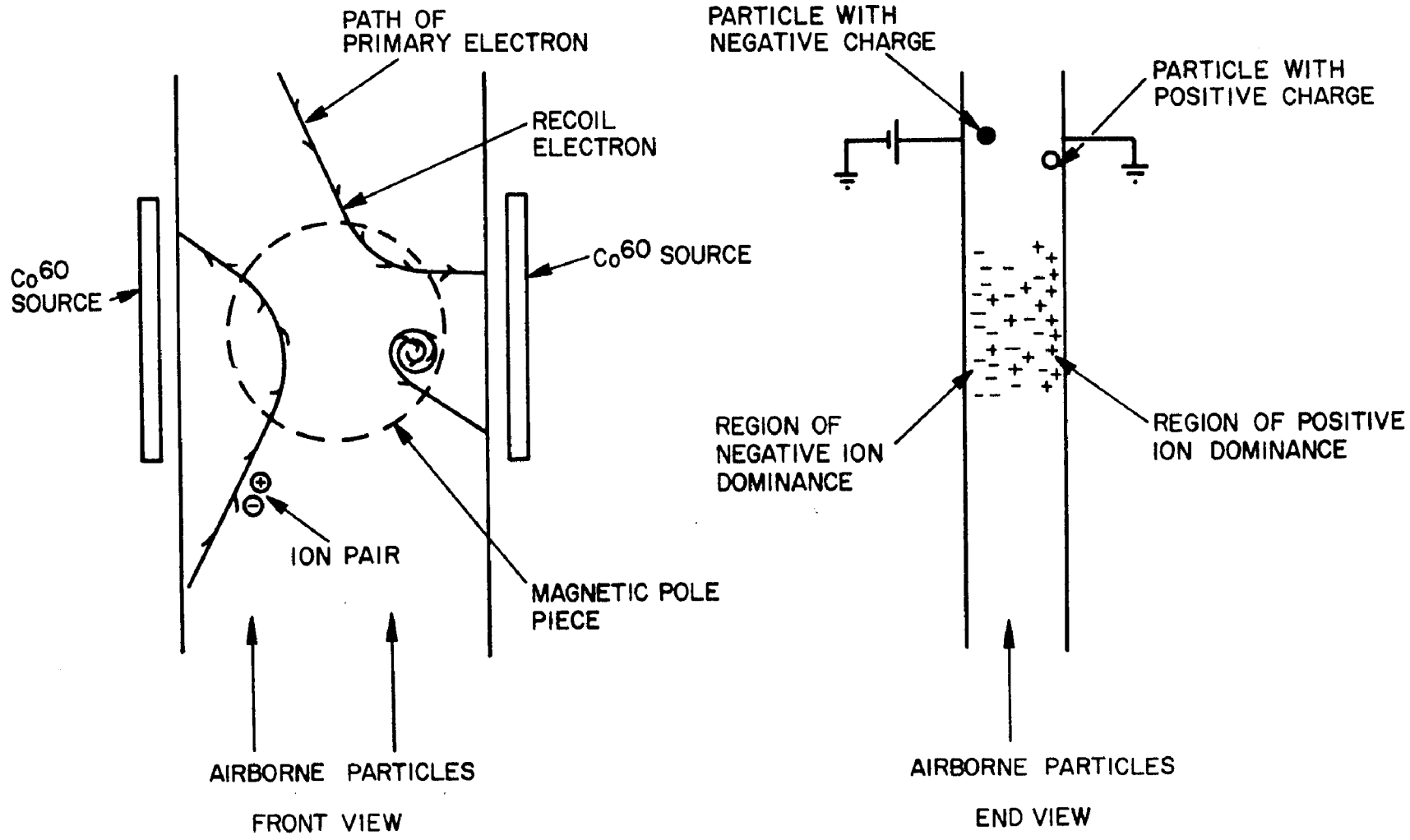

Figure 2. Conceptualization of ion production and particle charging

test an analytical model of charging, rather than to collect particles, the apparatus is designed to facilitate analysis and the execution of preliminary experiments. A uniform flow of a controlled aerosol flows upward in the z-direction and a uniform electric field and magnetic field are applied in the x-direction. The duct is narrow and variations in the y-direction are neglected. The test section is considered to be well inside the periphery of the magnetic pole pieces. Thus, the only spatial variable is in the x-direction.

PHENOMENOLOGICAL DESCRIPTION

A conceptual design of the proposed charging scheme is presented in Figure 2. A radiation source that emits gamma rays is situated outside the duct. Energetic electrons are introduced into the ionization region by Compton scattering of the gammas in air and the walls of the duct. Alternatively, (not shown in Figure 2) energetic electrons can be introduced by stationary beta sources placed inside the duct. The high energy electrons, whether supplied directly by a beta source or indirectly by Compton scattering of gammas, interact with gas molecules in air to create positive and negative ions. In the absence of a magnetic field electrons lose only a small fraction of their energy in the gas. A magnetic field, which is not intense enough to appreciably affect molecular ions, causes the highly energetic electrons to spiral about the field lines and in a well designed system to lose all of their energy in the confined region through which the dust and air pass. This greatly increases ion densities obtainable from a given gamma or beta source. In comparison to the gamma ionization methods discussed earlier, it should be possible to generate ions of comparable concentration with substantially weaker radiation intensities or to produce even higher ion densities, if needed, with the same radiation intensity. It should be noted that the experimental apparatus of Figure 1 was not designed to maximize ion generation, but rather to facilitate preliminary experiments. In fact, it can be seen in Figure 2 that the magnetic field actually serves to divert electrons out of the central portion of the duct.

The electric field is not of sufficient strength to affect the energetic electrons and serves to separate the ions and create regions of predominantly positive ions near the cathode and negative ions near the anode. The ions attach to particles moving through the duct, putting a net positive charge on particles near the cathode and a net negative charge on those near the anode.

ION GENERATION

Prediction of the ion generation rate from knowledge of the radioactive source strength, material and geometrical considerations is a complicated matter, particularly for a gamma source located outside the duct as shown in Figure 1. The first step in the process is to estimate the spectrum of electrons entering the gas stream. For this purpose a brief order of magnitude estimate was made using the following assumptions:

1) Each radioactive source was 75 Curies of Co^{60}, contained in a cylinder, 1 cm in diameter and 25 cm long.

2) The gamma flux leaving the source was solely in the radial direction.

3) Due to the size and location of the source, only 20% of the gammas from the source impinged on the duct (10^9 gammas/sq cm sec). Scattered gamma radiation was neglected.

4) The energy spectrum of the electrons generated by Compton scattering and the subsequent loss of energy as they pass through the duct walls was calculated by assuming the gamma flux was normal to an infinite slab of finite thickness.

On the basis of the above assumptions, the energy spectrum of electrons entering the gas stream was calculated and is shown in Figure 3.

Energetic electrons, produced by Compton scattering, ionize, dissociate and excite molecules in the air stream. Collisions between high energy (primary) electrons and molecules lower the energy of the primary electrons and produce ions and recoil electrons. The process continues until the primary and recoil electrons no longer possess enough energy to ionize gas molecules. In terms of the size of the equipment and gas densities and temperatures involved, it is permissible to deal in averages, which in air at STP result in the eventual production of a positive ion and a thermal electron, i.e., ion pair, each time the primary electron loses 34 eV. Thus, each 1 MeV primary electron produced by Compton scattering eventually produces 2.94×10^4 ion pairs. Ion pairs are assumed to consist primarily of singly charged nitrogen and oxygen molecular ions. Since nitrogen and oxygen molecules are the dominant species in air and have approximately equal mass, the assumption is made that the

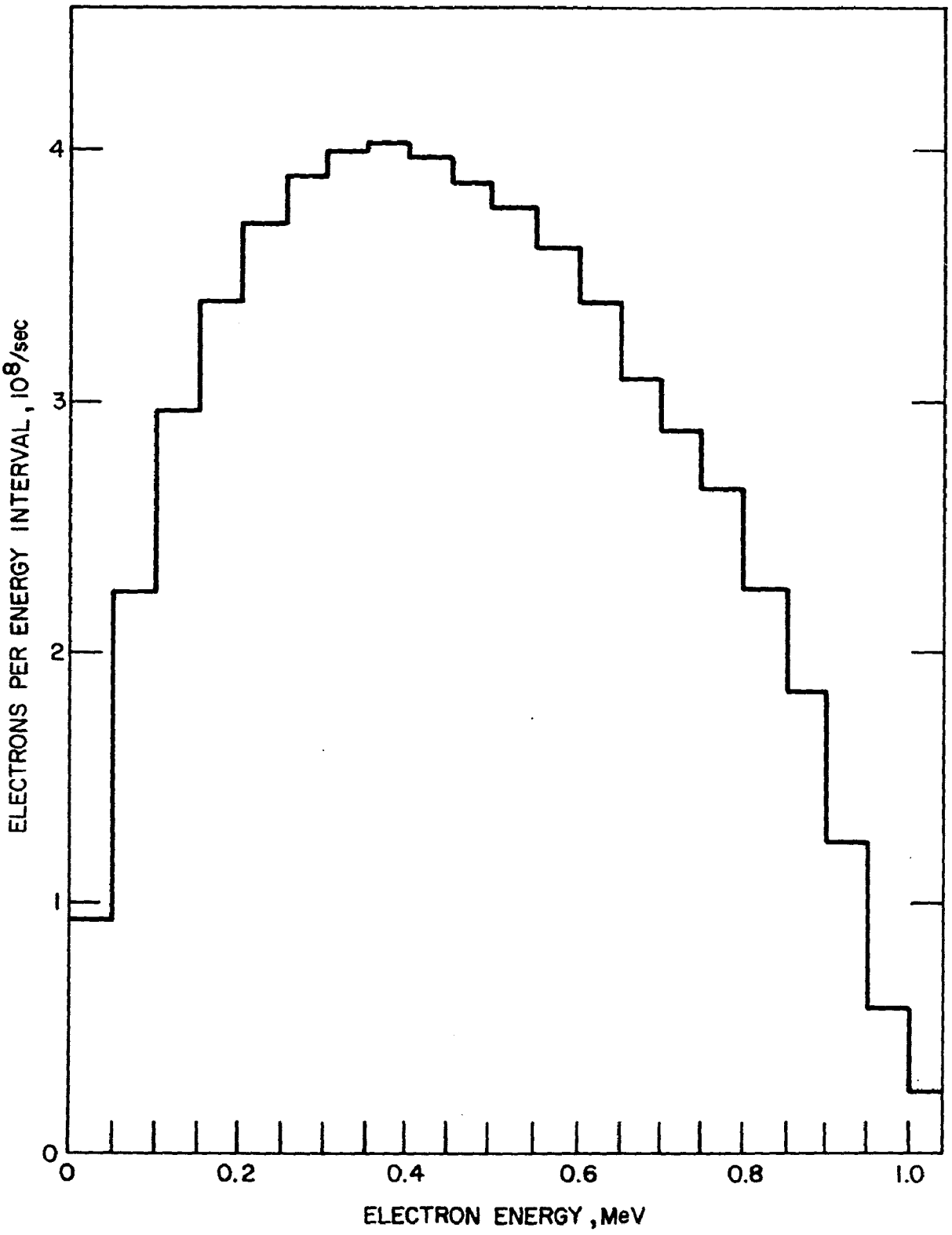

Figure 3. Energy histogram of Compton electrons emitted from the duct wall

end result of collisons of energetic electrons with air is the formation of singly charged positive and negative molecular ions with an atomic mass of approximately thirty amu.

Since the range (distance traveled by an energetic electron before it becomes a thermal electron) of high energy electrons in air is quite large, the maximum production of ion pairs cannot be realized in a confined volume and it is necessary to trap the energetic electrons by using a magnetic field. Table 1 shows the range and the maximum number of ion pairs produced by various energetic electrons. Shown also in Table 1 is the radius of curvature of an electron trapped by a magnetic field.

Table 1. FEATURES OF ENERGETIC ELECTRONS

Electron energy (MeV)	Range in air (cm)	Maximum number of ion pairs produced	Cyclotron radius			
			B(Gauss)	r (cm)	B(Gauss)	r (cm)
0.1	11	2,940	500	2.24	5,000	0.224
0.46	120	13,500	500	5.50	5,000	0.550
0.99	330	29,200	500	9.38	5,000	0.938

The maximum number of ions produced by the energetic electrons entering the duct can be estimated from the following:

$$S = \sum_{i=0}^{N} (n_i)\frac{\Delta E_i}{34} \qquad (1)$$

where N = number of groups in electron energy spectrum (from Figure 3)

ΔE_i = energy deposited in the charging region by an electron in group i

n_i = number of electrons in group i (from Figure 3)

All of the quantities in Equation (1) can be calculated except ΔE_i, the energy deposited in the charging region. Although Landau[12] has developed an analytical expression that accurately describes the loss in electron energy due to ionization in sufficiently thin absorbers, no suitable expression exists for the energy lost due to ionization, excitation, radiation, etc. in thick absorbers. However, an analytical expression for energy loss can be derived from a range-energy relation of the form:

$$R = f(E) \tag{2}$$

where R = range of electron of original energy, E
$f(E)$ = empirical relation describing dependence of R on E

Consider an electron of original energy, E_i, incident on a slab of thickness, S, at point A as indicated in Figure 4. The distance R_i is the range of an electron E_i, while ℓ is the range of an electron of energy E_f. E_f is the energy of the electron as it leaves the slab at point B. Thus,

$$S + \ell = R_i, \text{ or}$$
$$S + f(E_f) = f(E_i) \tag{3}$$

Equation (3) can be solved for E_f,

$$E_f = f^{-1}\left[f(E_i) - S\right]$$

and ΔE_i becomes

$$\Delta E_i = E_i - E_f \tag{4}$$

Katz and Penfold[13] give an empirical expression for $R(E)$ that can be used for an absorber of any density.

$$R(E) = \frac{0.412}{\rho} E^{(1.265 - 0.0954 \ln E)} \tag{5}$$

On the basis of the above, the volumetric ion generation rate is estimated to be 3×10^8 ions/cm^3-sec. In a system designed to completely trap all the electrons, the ion generation rate can be computed from the above by replacing ΔE_i by E_i. The resulting ion generation rate is 4.5×10^{10} ions/cm^3-sec, an increase by a factor of 150.

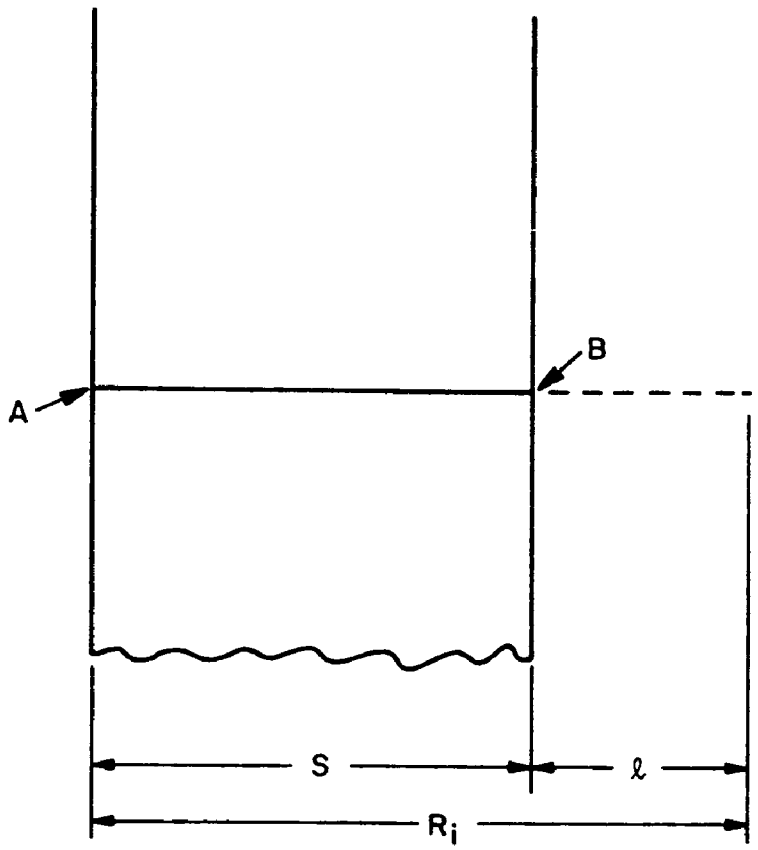

Figure 4. Model employed to estimate electron energy loss

Many gammas pass through the walls and ionize the air directly. This direct ionization of air has been shown to be important[14] in Schultz' gamma ray precipitator, but this effect is neglected in the study.

ION DISTRIBUTION

The concentrations of ions within the duct are controlled by the following processes:

1) ion generation
2) ion recombination
3) diffusion as a consequence of a concentration gradient
4) drift as a consequence of an electric field
5) convection by the bulk motion of the gas
6) acquisition of charge by dust particles

To a first approximation it is assumed that the bulk transport of ions and the rate at which particles acquire charge can be neglected. The ion concentration obtained in this way corresponds to a stationary gas or to a gas moving uniformly in the z-direction when there is no variation in any properties in that direction.

In steady state, the net production of charge equates to the transport of charge, viz.

$$S(\bar{r}) = -\alpha n^+(\bar{r})n^-(\bar{r}) + D^+\nabla^2 n^+(\bar{r}) + \mu^+ \text{ Div } (\bar{E}(\bar{r})n^+(\bar{r})) \tag{6}$$

$$S(r) = -\alpha n^+(r)n^-(r) + D^-\nabla^2 n^-(r) - \mu^- \text{Div } (\bar{E}(\bar{r})\ n^-\ (\bar{r})) \tag{7}$$

The transport term due to the electric field changes sign for negative ions because μ^- is taken as positive and the negative charges are moving "against" the field. Perturbations of the electric field occur where there is a significant space charge due to ions. This is described by Poisson's equation.

$$\text{Div } \bar{E}\ (\bar{r}) = \frac{1}{\varepsilon}\ (n^+(\bar{r}) - n^-\ (\bar{r})) \tag{8}$$

PARTICLE CHARGING

Without an applied electric field, the space charge produced by radiation has negative and positive ion densities that are equal to each other and of little value to charge small particles. The application of an electric field segregates the ions into regions of predominantly one polarity. Dust particles passing through these regions become charged by a combination of the electric field "bombarding" the particles with ions and by the diffusion of ions toward the particles. A considerable body of literature exists on bombardment and diffusion charging. We suggest that in bipolar regions, particles acquire charge in a way similar to that proposed by Liu and Yeh[15] for unipolar charging. Figure 5 depicts a particle of radius a in a region where $n^+ > n^-$ and provides a convenient conceptual understanding of the process. We propose that positive ions are driven along field lines to the front surface (1) and negative ions are driven along field lines to the rear surface (2). At the same time, negative ions diffuse to the front of the particle, surface 1, and positive ions diffuse to the rear surface.

The rate at which the particle acquires a net positive charge is equal to the difference between the rates at which it separately acquires positive and negative charge. Positive ions continue to be driven to the particle by the electric field until such time as the particle's charge produces a local electric field that repels the oncoming stream of positive charge. We define the charging process up to this point as Regime I. Charging does not cease at the end of Regime I, since ions continue to diffuse to the entire particle and negative ions continue to be driven to the entire particle. We define these charging processes as Regime II. While we have modified the theory of Liu and Yeh to include the motion of charges of both polarity, the basic derivation of the equations from first principles remains valid for our process. For a particle located in a region where $n^+ > n^-$

Regime I

$$\left[\frac{dq}{dt}\right]_I = n^+\mu^+\pi a^2\left[1 + \frac{2(D-1)}{(D+2)}\right]E\left(1 - \frac{q}{q_{tr}}\right)^2 + \frac{n^+}{2}v^+_{rms}\,\pi a^2\left[1 + \frac{q}{q_{tr}}\right]$$

$$- n^-\mu^-\pi a^2\left[1 + \frac{2(D-1)}{(D+2)}\right]E\left(1 + \frac{q}{q_{tr}}\right)^2 - \frac{n^-}{2}v^-_{rms}\,\pi a^2\left[1 - \frac{q}{q_{tr}}\right] \quad (9)$$

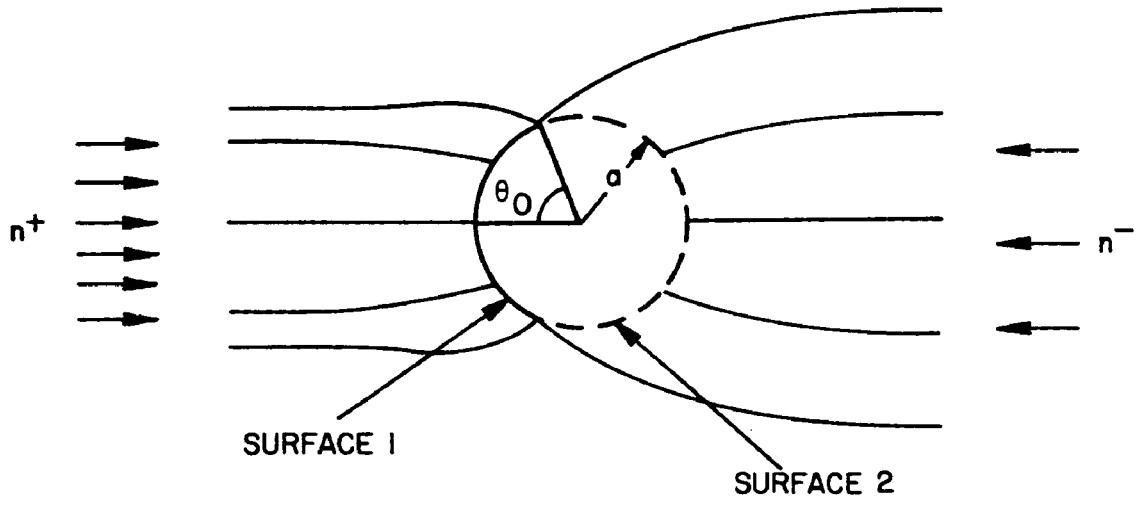

REGIME I, $\theta_o > 0$

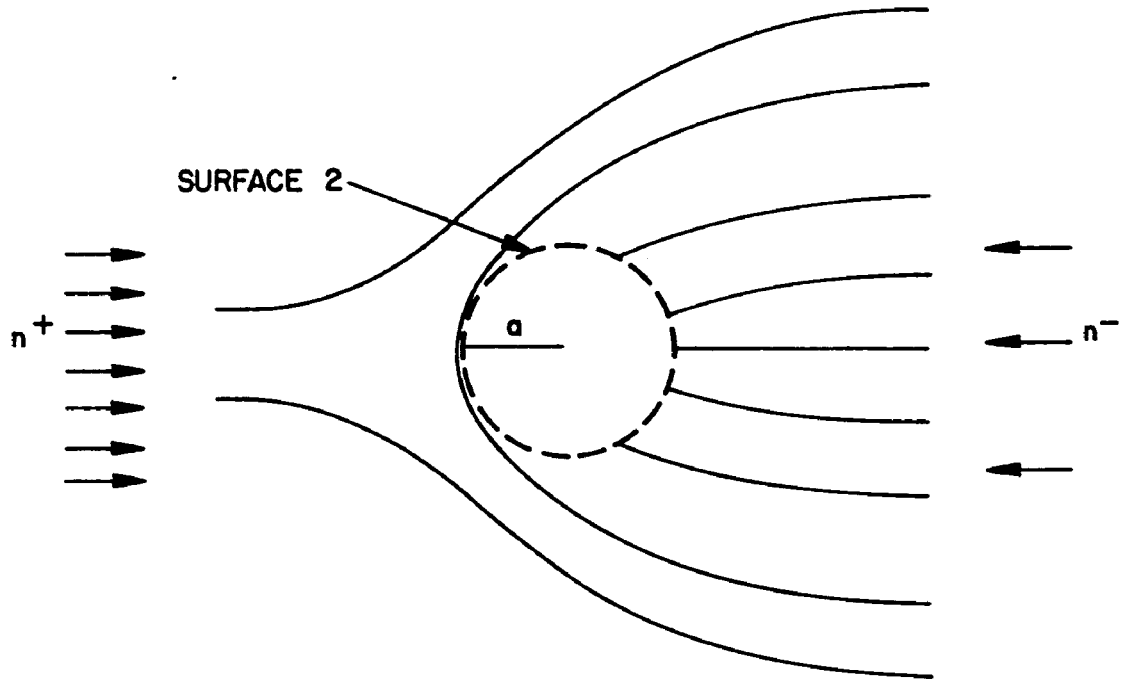

REGIME II, $\theta_o = 0$

Figure 5. Conceptual sketch of unified bipolar charging theory in a region where $n^+ > n^-$

Regime II

$$\left[\frac{dq}{dt}\right]_{II} = \frac{1}{2} v^{+}_{rms} \pi a^2 n^{+} \exp\left[\frac{q(V_a - V)}{kT}\right]$$

$$- n^{-}\mu^{-}\pi a^2 \left[1 + \frac{2(D-1)}{(D+2)}\right] E \left(1 + \frac{q}{q_{tr}}\right) \qquad (10)$$

If the particle is located in a region where $n^{-} > n^{+}$, the above equations should be altered by simply reversing the plus and minus superscripts. The term q_{tr} represents the number of charges on the particle such that the electric field at the surface of the particle (E(a,O)) becomes zero. In Regime I, $q < q_{tr}$ and in Regime II, $q > q_{tr}$.

$$q_{tr} = 4\pi\varepsilon a^2 E \left[1 + \frac{2(D-1)}{(D+2)}\right] \qquad (11)$$

ANALYTICAL PREDICTIONS

Since the long-range goal of the research is to describe the charge particles acquire as they pass through a region of radiation, the earlier equations would have to be modified to include bulk motion of the gas. Prior to doing this, we believe it instructive to solve the equations for physical processes in which there is no motion of the gas or particles. Such solutions will indicate the trends we can later expect and the relative importance of various terms in the equations.

ION DISTRIBUTION

Ion concentrations in the test region are found by solving Equations (6-8) (See Appendix). The mobilities were assumed to be the same, i.e., $\mu^{+} = |\mu^{-}|$ and equal to 1 volt-sec/cm^2. Figure 6 shows the positive ion concentration for several applied fields and a constant ion generation rate (S) of 10^{11} ions/cc sec. A companion curve for negative ions is not shown since it is the mirror image of Figure 6.

For large electric fields, recombination and diffusion are negligible, the electric field is not perturbed and ions are

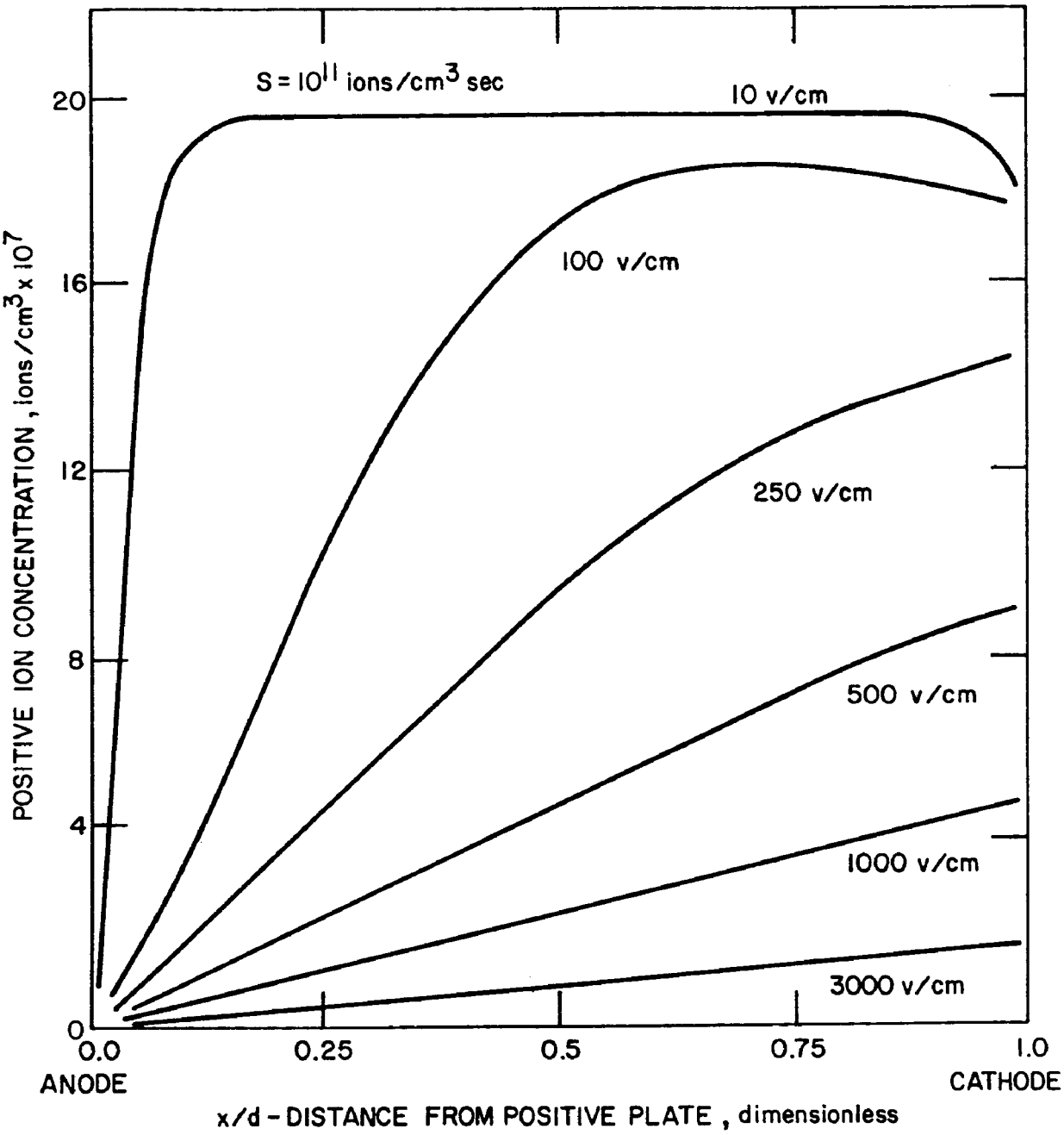

Figure 6. Dependence of positive ion concentration on applied electric field. Note there is a companion negative ion concentration which is the mirror image of the above

rapidly drawn to the electrodes as quickly as they are formed. Thus, when the electric field intensity is large, Equations (6-8) become

$$n^+(x) = Sx/E\mu^+ \tag{12}$$

$$n^-(x) = S(d - x)/E\mu^- \tag{13}$$

$$E(x) = V_0/d \tag{14}$$

As the electric field intensity decreases, recombination assumes greater importance, diffusion increases but remains small and the electric field is perturbed by the ion space charge. As the applied field approaches zero, the ion concentration approaches a constant value, i.e.,

$$n^+(x) = n^-(x) = [S/\alpha]^{\frac{1}{2}} = \text{const} \tag{15}$$

The effect of space charge is graphically presented in Figure 7 where the local values of electric field (E(x)) are plotted for a constant applied voltage (V_0) and various ion generation rates (S). For ion generation rates below 10^{10} ions/cc sec, the electric field is quite high. In the center of the duct the perturbation of the electric field increases with the ion generation rate until the concentration begins to approach $[S/\alpha]^{\frac{1}{2}}$ whereupon it increases slightly.

PARTICLE CHARGING

When small particles pass through a non-uniform space charge shown in Figure 6, and non-uniform electric field as shown in Figure 7, it can be expected that the charge accumulated by the particle will depend on where in the duct it is located as well as the exposure time. Furthermore, a charged particle will also be transported laterally by the electric field and find itself in a region where space charge and electric field have changed.

As a first estimate to this complicated process, solutions are obtained for single particles which are not transported laterally by the electric field. Equations (9) and (10) are solved for a single particle located at a particular location (x/d) in the duct where (n^+/n^-) and E possessed certain constant values.

A steady-state charge is acquired by a particle when the net charging rate is reduced to zero. Plotted in Figure 8 are (dq/dt) versus q and q versus t for a constant value of E (1373 volts/cm) and three different values of (n^+/n^-). The

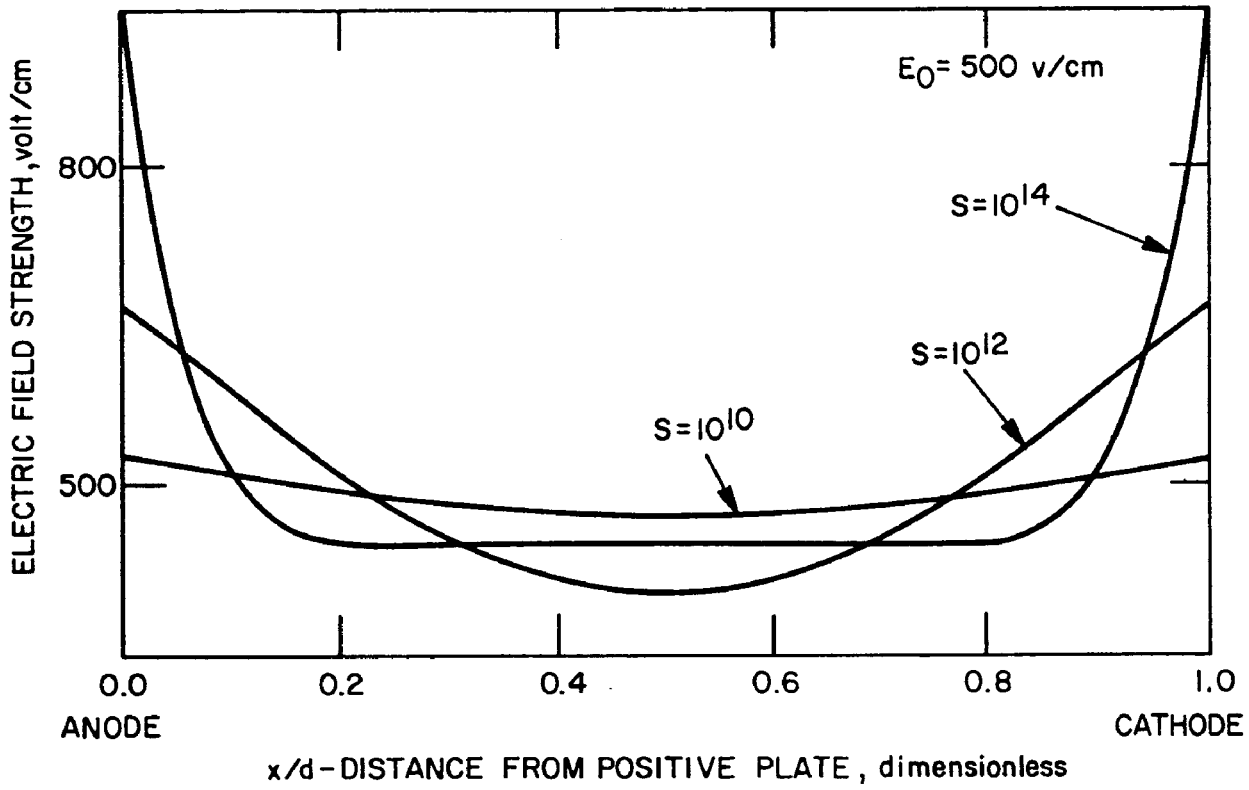

Figure 7. Dependence of electric field and electric potential on ion generation rate

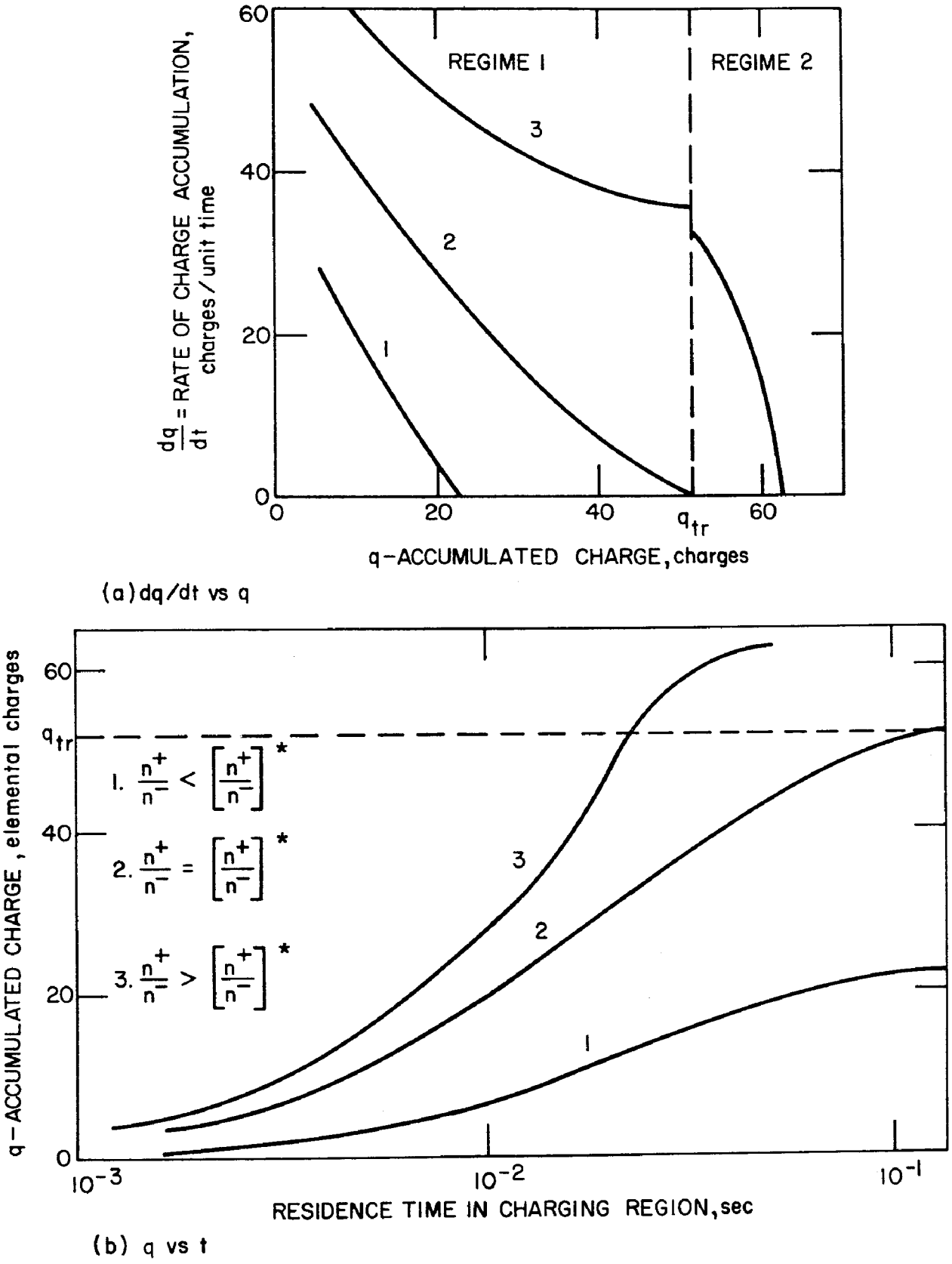

Figure 8. Unified bipolar charging for various values of n^+/n^- and E=1373 V/cm

condition for $(dq/dt) = 0$ at $q = q_{tr}$ can be found from Equation 9 if the mobilities and root-mean-square velocities of positive and negative ions are assumed to be equal, viz.,

$$0 = \frac{n^+}{2} v_{rms} \pi a^2 (1) - n^- \mu \pi a^2 \left[1 + \frac{2(D - 1)}{(D + 2)}\right] (4) E \tag{16}$$

Solving for the particular value of (n^+/n^-) at this condition yields

$$(n^+/n^-)^* = \frac{8 E\mu [1 + \frac{2(D - 1)}{(D + 2)}]}{v_{rms}} \tag{17}$$

Curve 2 in Figure 8 depicts charging when (n^+/n^-) is given by Equation (17). It is seen that the steady-state charge is precisely equal to the transition charge. Physically, this means that, at $q = q_{tr}$, charging by diffusion of positive ions is exactly balanced by negative ions driven to the particle by the electric field. When $(\frac{n^+}{n^-}) < (\frac{n^+}{n^-})^*$, (represented by Curve 1), field charging by negative ions dominates the diffusion of positive ions and the steady-state charge is less than the transition charge. In this case, Regime II is never reached. In Curve 3, it is seen that the higher relative concentrations of positive ions prohibit the attainment of a steady-state charge in Regime I. It is in this case that a flaw in the theory of Liu and Yeh and in the bipolar theory advanced in this paper becomes evident. The value of dq/dt is not continuous at $q = q_{tr}$ because in Regime I the repulsive force between the charged particle and positive ions in the diffusion charging term is ignored for the diffusion charging process, while in Regime II it is considered. Thus, the rate of charging undergoes a discontinuity in moving from Regime I to Regime II. The change in the rate of charging, $\frac{d}{dt}(\frac{dq}{dt})$ is greater in Regime II because of the inclusion of the repulsive force.

Figures 9 and 10 show the steady-state negative charge 0.1 and 0.5 micron DOP (dioctyl phthalate, D=5.1) particles are expected to acquire if located at various positions in the duct. Application of theory predicts an increase in a particle's steady-state charge with increasing electric field intensity in spite of the fact that the separate magnitudes of each concentration decrease with increasing electric field (reference Figure 5). Thus, particle charging is more

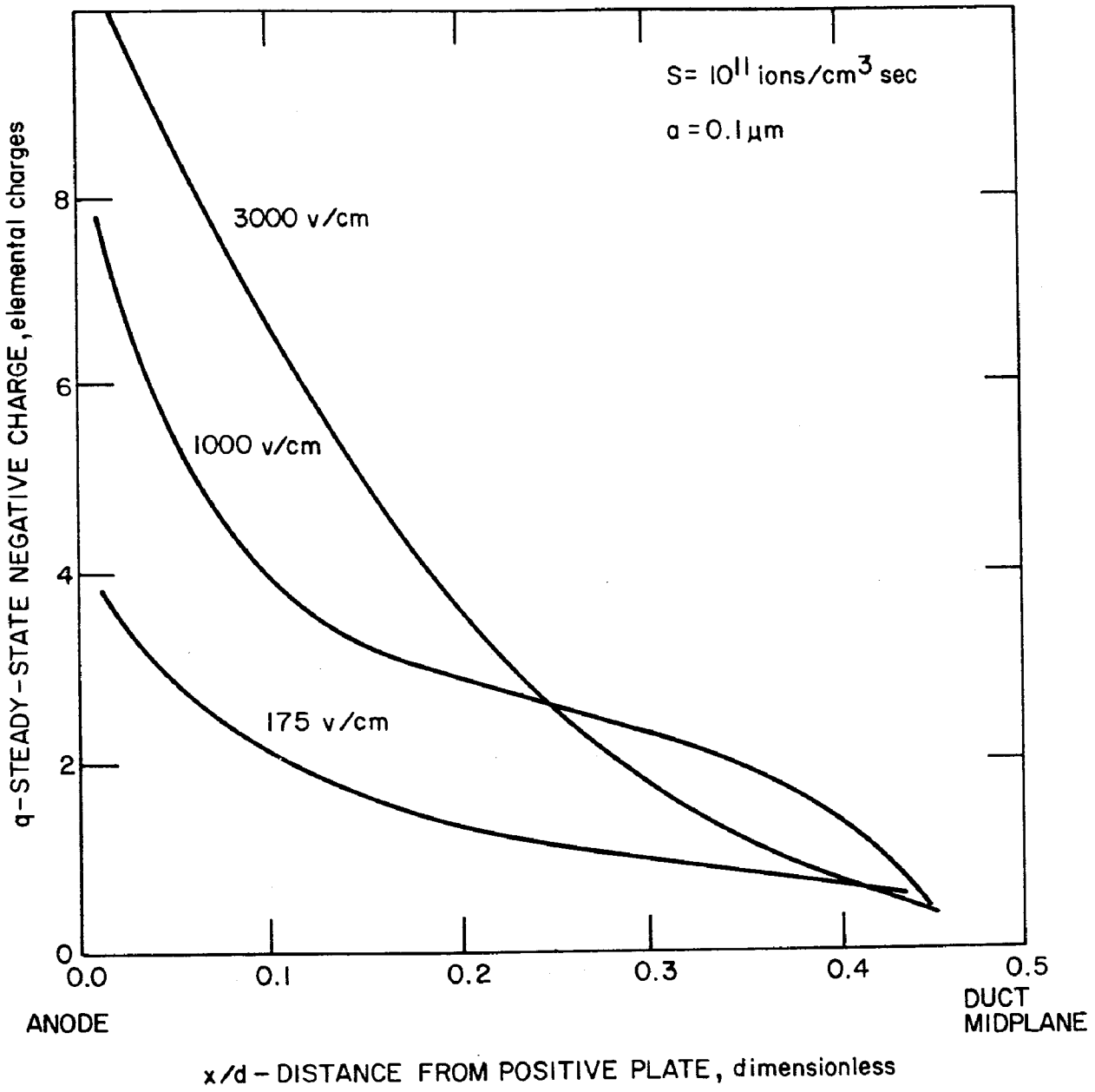

Figure 9. Particle charging as calculated by unified bipolar theory for DOP particles of radius (a) equal to 0.1 μm

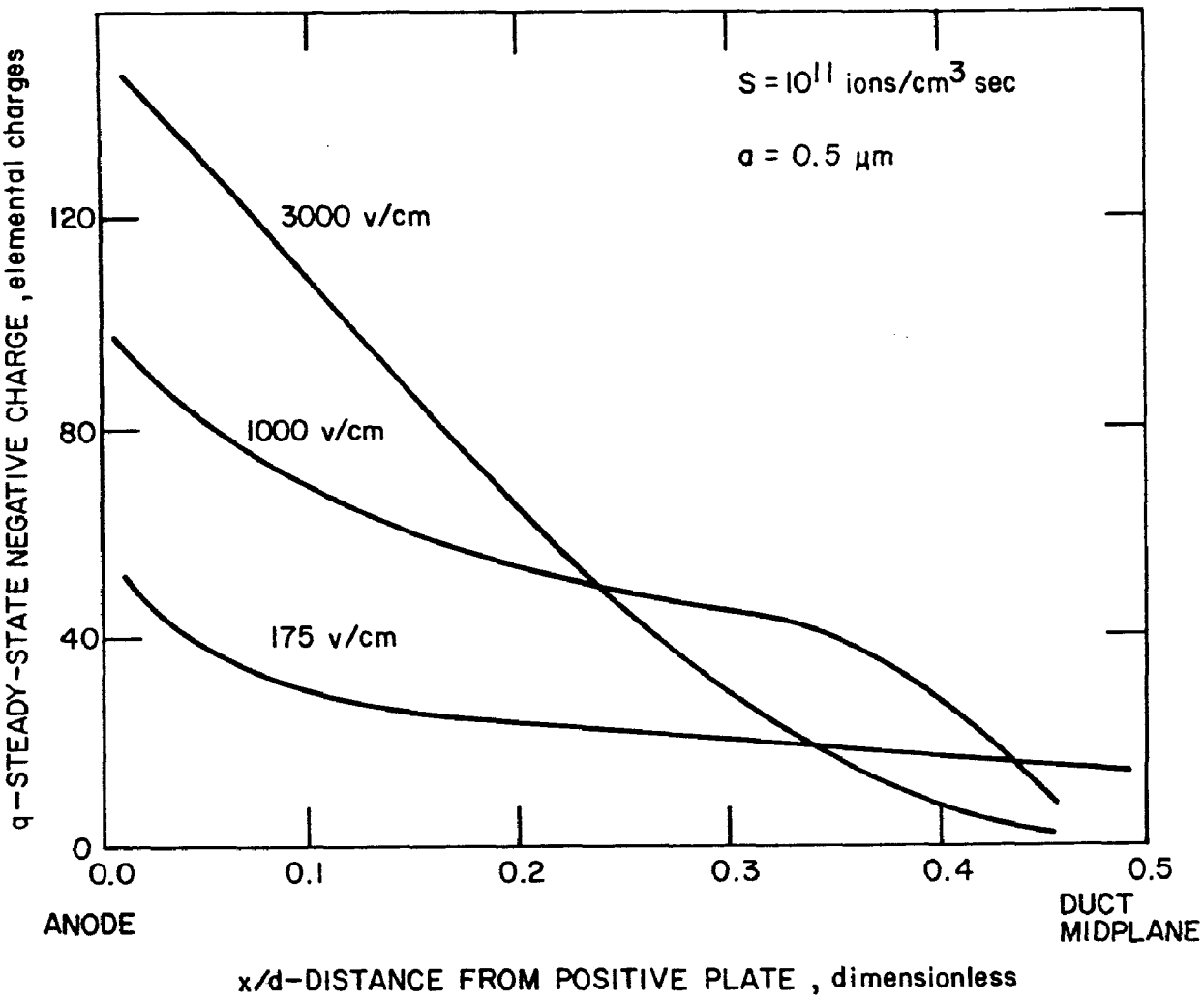

Figure 10. Particle charging as calculated by unified bipolar theory - DOP particle of radius (a) equal to 0.5 μm

strongly governed by changes in the applied electric field than in the accompanying changes in the ion concentration.

A second point worth noting is that because the graphs cross one another, there are regions in the duct where a particle's charge is adversely affected by an increasing electric field. While interesting, the point is somewhat misleading since the analytical model ignores the lateral motion of charged particles. Since the lateral motion will transport a negatively charged particle to the left, particles will drift to regions where the steady-state charge on a particle can be even higher. Thus, if the model is broadened to include the motion of the particle, it is expected that particle charging will be enhanced.

Figure 11 shows the effect of varying the ion generation rate on the steady-state charge acquired by a particle. From Figure 7 it is seen that for a constant applied electric field, an increase in the ion generation rate perturbs the local electric field, which, judging from Figure 6, suggests that the ion concentration will change. Thus it is expected that if a larger radiation source is used, the resulting increase in ion generation will affect, and possibly increase, the steady-state charge on a particle. Figure 11 shows that this is only true in a narrow region adjacent to the duct wall and that in the major portion of the duct the charge on the particle decreases. Thus, for a given ion generation rate, an optimum applied electric field is suggested for maximum charging, and vice versa. However, it should be noted that the effect is small and that a four-fold change in the ion generation rate only alters the steady-state charge by less than 50%.

PRELIMINARY EXPERIMENTS

To examine the accuracy of the conceptual model described earlier, a series of preliminary experiments were conducted using apparatus schematically shown in Figure 12. An aqueous suspension of Dow polystyrene beads, 0.500 microns in diameter (0.0027 standard deviation) was atomized in a collision generator and the particles discharged into the base of a 24 inch diameter, 24 inch high plenum chamber, one foot upstream of test station 2. In the plenum chamber, the aerosol mixed with ambient air in approximately a 1:10 ratio. It was assumed that scattered radiation in the hot cell was sufficient to neutralize any electrostatic charges acquired by the aerosol during atomization. The velocity and concentration profiles were found to be uniform at the test section

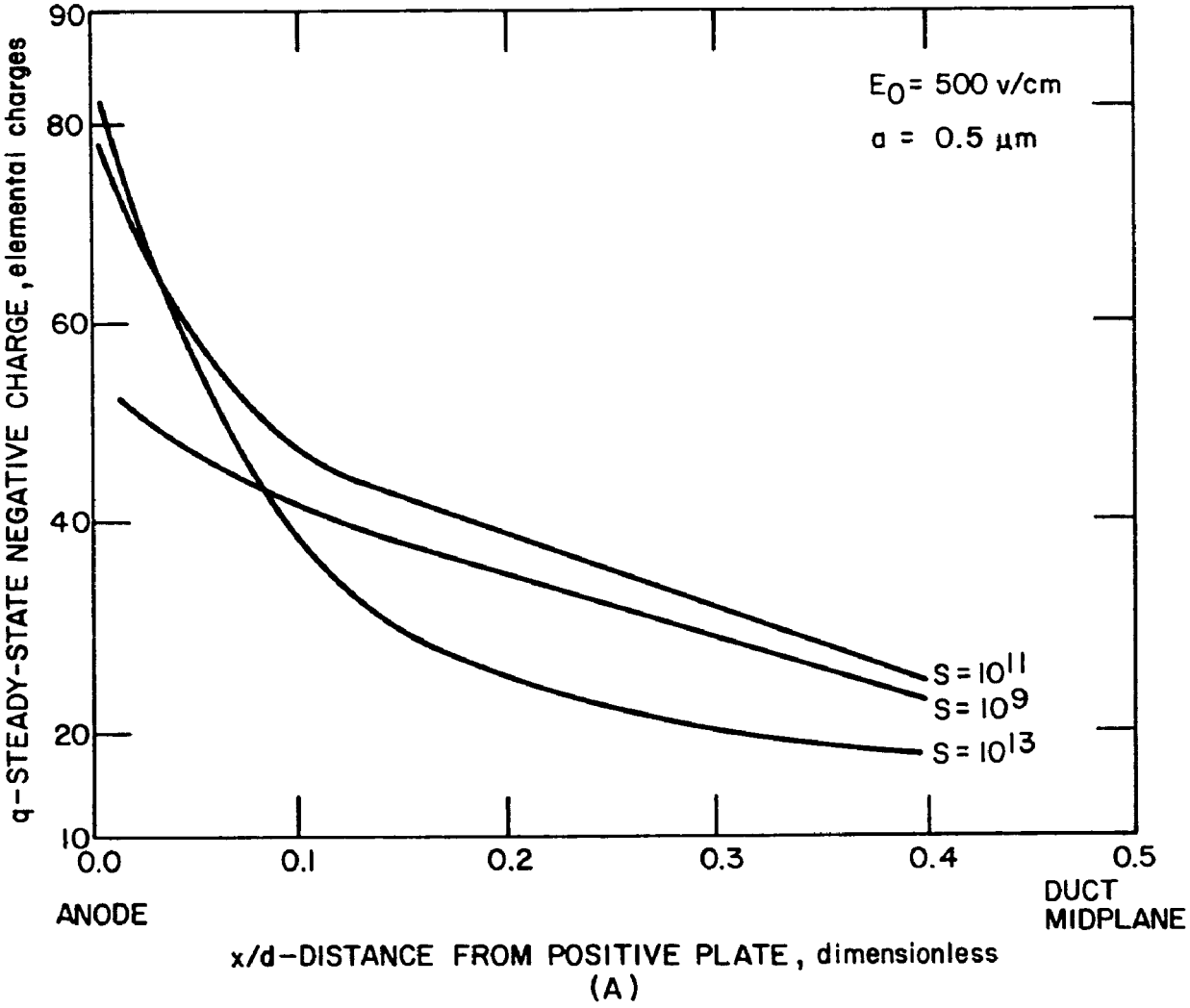

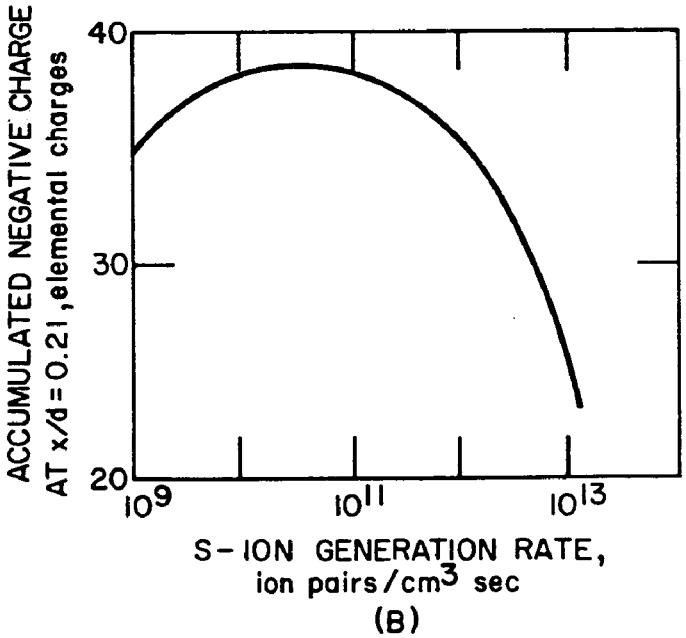

Figure 11. Dependence of unified bipolar charging on ion generation rate

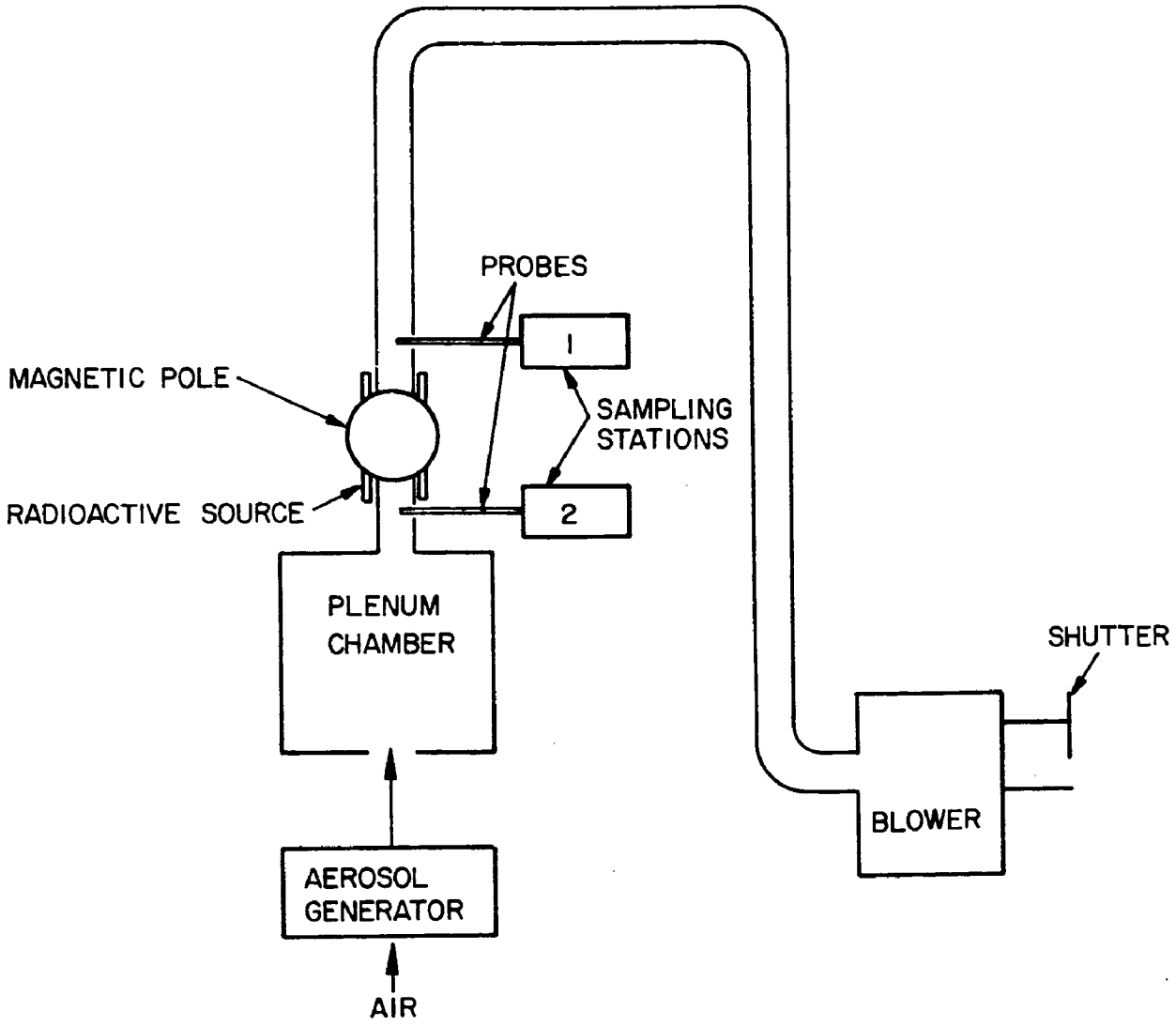

Figure 12. Schematic diagram of test apparatus

and Reynolds numbers based on length were sufficiently high to suggest that boundary layers along the walls were significant.

The magnetic field was produced by an electromagnet with a 7 inch pole piece and was applied across the duct in the x-direction as shown in Figure 1. An electric field was also applied in the same direction and aluminum coated Mylar foil fastened to the inside surface of the duct served as the electrodes. A circular portion of the cathode, 10 sq cm in area, was isolated from the rest of the grounded cathode and the current to it measured by a Keithley electrometer (Figure 13). Two 75 Curie Co^{60} radiation sources were inserted in holders outside the duct. The entire apparatus was assembled inside a "hot cell" at the Breazeale Nuclear Reactor at Penn State. All the instruments were placed outside the hot cell and connecting wires, tubes, etc. fed through access ports in the walls of the hot cell. Experiments were conducted under the following conditions:

average gas velocity, 4.5 and 7.0 ft/sec
gas temperature and pressure, local atmospheric values
average particle concentration, 200 cm^{-3}
magnetic field strength, 0 - 6000 gauss
applied electric field, 0 - 3000 volts
duct dimensions (inside) - 9 inches x 1 inch
duct material (wall thickness - 1/2 inch) - wood

At various constant flow conditions and values of the magnetic field, the applied voltage (V_0) was varied and the current to the circular electrode (hereafter called ionization current) recorded.

IONIZATION CURRENT IN THE ABSENCE OF A FLOWING AEROSOL

In the absence of the aerosol and at zero gas velocity, Figure 14 shows that charge generated by radiation and transported to the cathode by the electric field increases with voltage but ultimately reaches a steady value. The asymptotic value of current corresponds to the condition where the removal of charge by the electric field is faster than the removal by diffusion or recombination. In flame plasmas this value is called the saturation current. The current is limited by the rate at which ions are generated and the average rate of ion generation ($\bar{S}$) can be found from Equation (18).

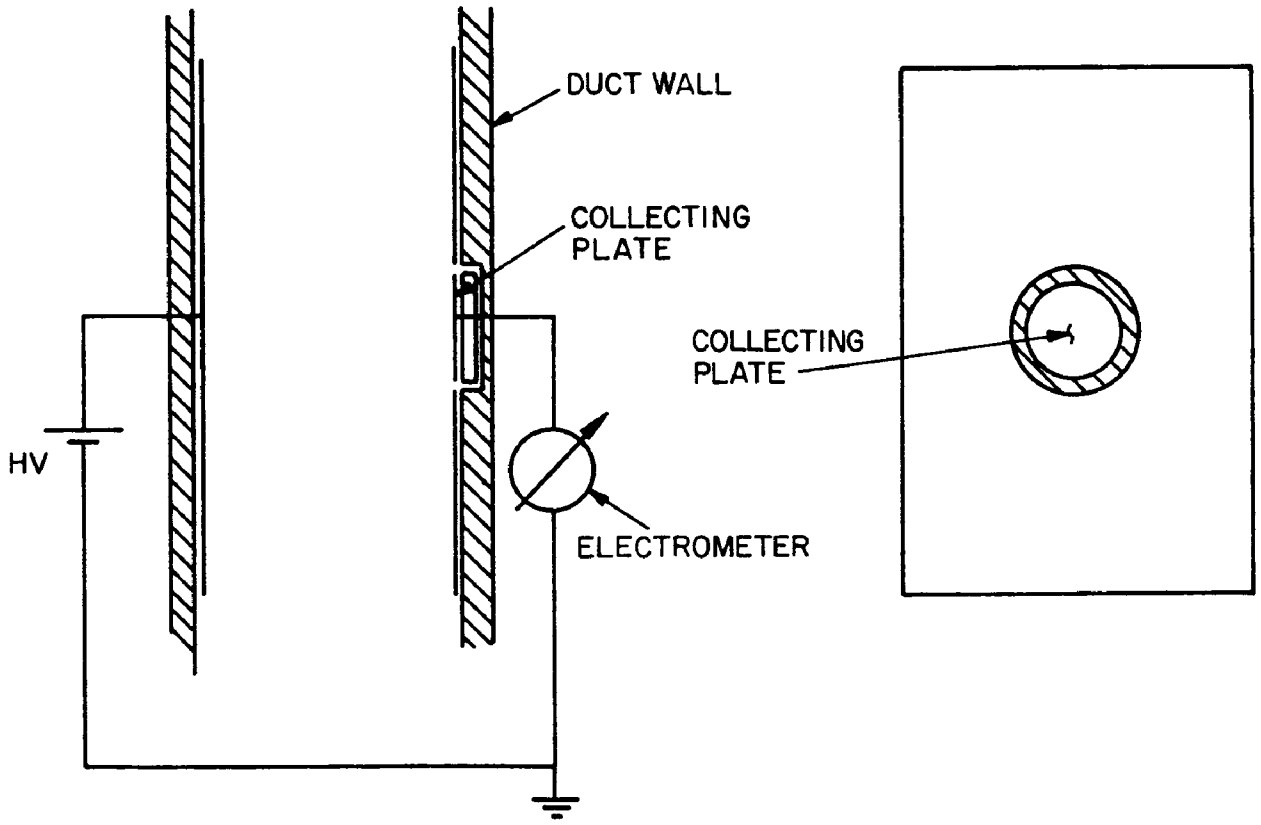

Figure 13. Sketch of collection plate

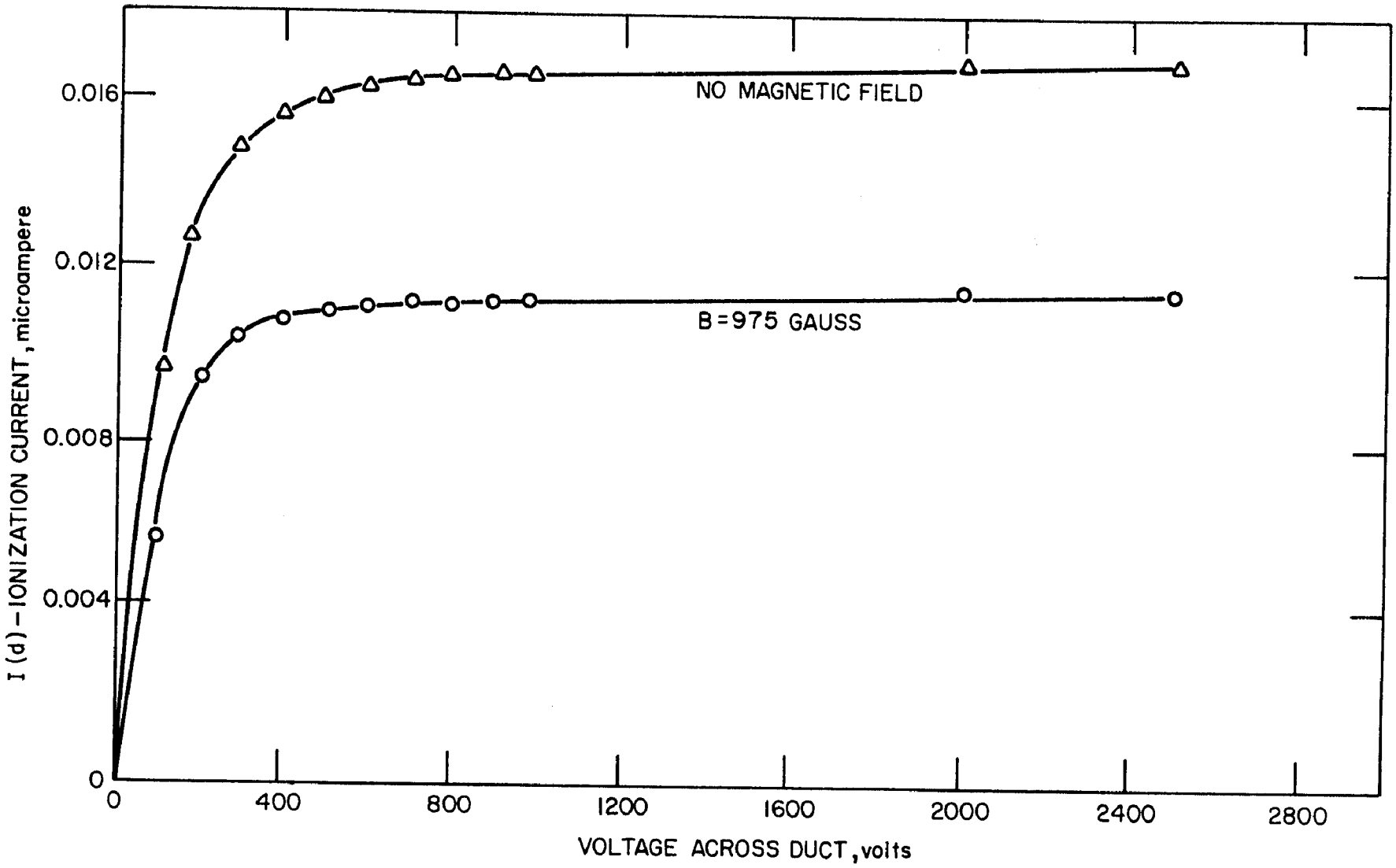

Figure 14. Effect of magnetic field on ionization current under conditions of zero flow velocity and with no addition of small particles

$$I_{sat} = \iiint_V S \, dV = \bar{S}A \int_0^d dx = \bar{S}Ad \qquad (18)$$

From Figure 14,

$\bar{S} = 4.8 \times 10^9$ ions/cm^3 sec, no magnetic field

$\bar{S} = 3.2 \times 10^9$ ions/cm, 975 gauss

Using this value of $\bar{S}$, Equations (6-8) can be solved for a variety of applied voltages and the ion densities predicted. At conditions below saturation, the current through the circular electrode (I(d)) can be predicted from

$$I(d) = An^+(d)E(d)\mu^+ \qquad (19)$$

The upper curve in Figure 14 corresponds to the current predicted by the solution of Equations (6-8, 19) when S is given the value of 4.8×10^9 ions/cm^3 sec. The good agreement between experiment and theory suggests that in the absence of the flowing aerosol the proposed model yields a valid description of the current at the wall.

When a magnetic field of 975 gauss is applied to the test region, the plateau occurs at a lower current as seen by the lower curve in Figure 14. Physically, this implies that in the experimental apparatus, the magnetic field lowers the rate of ion generation. The reduction is significant and expected even though it is contrary to the goals of the research effort. In a well-designed radiation charging system it is believed that a magnetic field can increase the rate of ion generation. The opposite occured in our experiments because the system design was not optimized for ion generation, but rather to facilitate computation and experimental measurements. It is believed that energetic electrons formed at the walls of the duct by Compton scattering were deflected by the magnetic field and never reached the central portion of the duct (see Figure 2). Hence, the total number of ions in the duct was lower with the magnetic field than without it. No direct measurement of the local ion density was made to verify this prediction. In any event, Figure 14 confirms the belief that a magnetic field alters the rate of ion generation.

IONIZATION WITH A FLOWING AEROSOL

Figure 15 shows that the bulk motion of the gas affects ionization but only at voltages (and hence electric fields) below 600 volts. In terms of ion density this suggests that

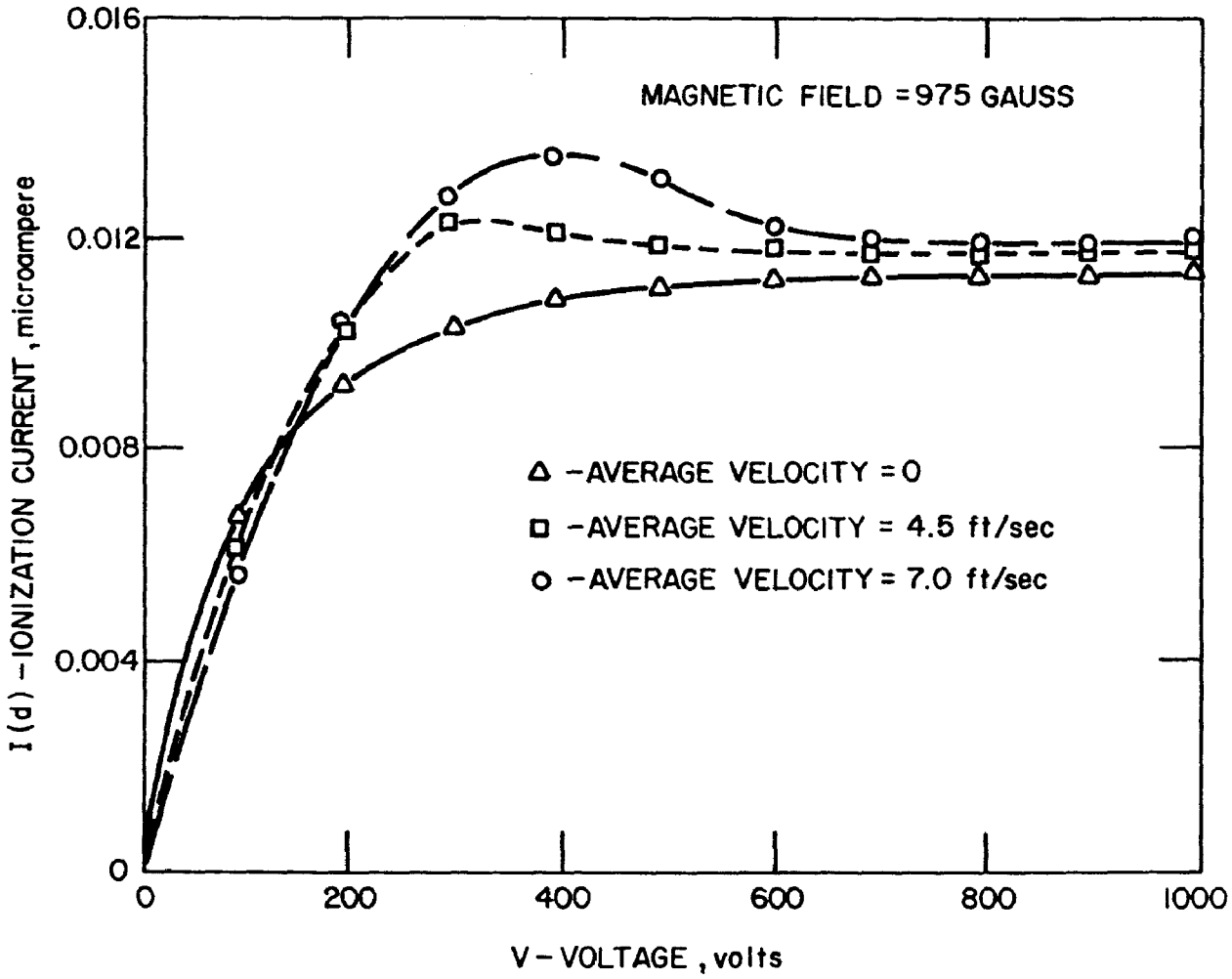

Figure 15. Dependence of ionization on velocity of air in duct with no addition of small particles

at these modest electric fields, the transport of charge cannot be predicted by Equations (6-8) and the model must be modified to include bulk motion. At larger electric fields, the motion of charge by the electric field dominates that by bulk motion. From Figures 16 and 17 it is seen that the presence of low concentrations of particles only slightly increases the transport of charge to the circular electrode. Solutions of Equations (6-10) show that if particle concentration is approximately 200 particles/cm^3, it will not significantly alter the transport of charge.

DISCUSSION AND CONCLUSIONS

ION GENERATION RATE

The average ion generation measured experimentally was an order of magnitude larger than predicted in the absence of trapping. It is believed that the discrepancy is due primarily to the neglect of scattered gamma radiation and to the crude model that was used to predict the ion generation rate. A more sophisticated model must be developed which accurately describes the motion of energetic electrons under the influence of a magnetic field and the various ionization processes that ensue. Further study on radiation charging also requires knowledge of the spatial variation of the ion generation rate in the charging region. The reduction in the ion generation rate following the application of a magnetic field was expected and in order to understand (and hopefully to reverse) the effect, a more sophisticated model must be developed. Once developed, techniques and instruments must be developed that will enable the direct measurement of the spatial variation in the ion generation rate.

ION DENSITIES

Particle charging expressions require knowledge of the local values of the ion and current density. Unfortunately, no direct measurement of these quantities was made and we can only surmise what they are from measurements of the current at the circular electrode. In the absence of a flowing aerosol, the application of the analytical model describing the ion density (Equations 6-8) yields results that are in excellent agreement with the experimental results (Figure 14) and seems to support the accuracy of the model, at least under conditions of a stationary gas. The weakness of the model

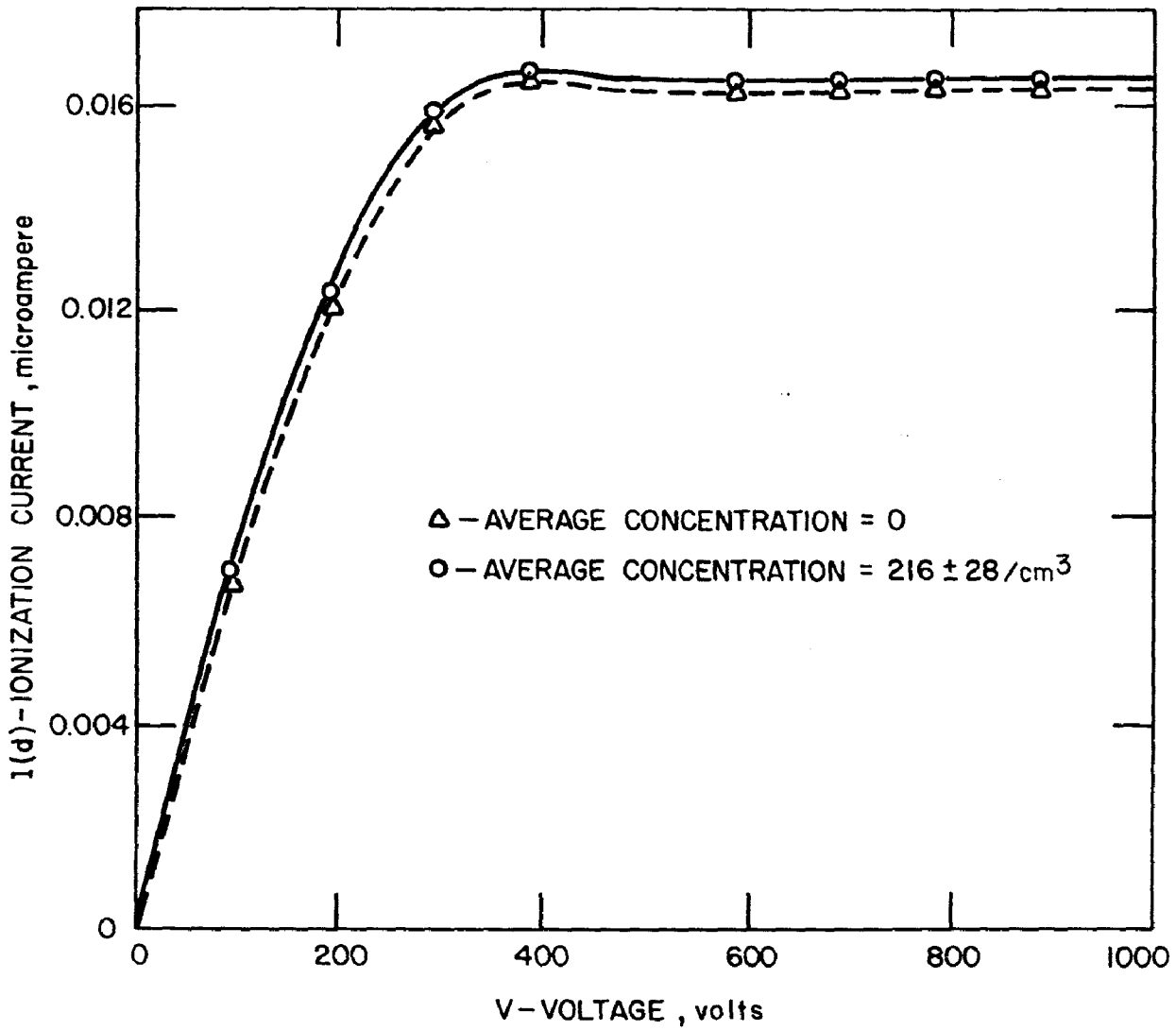

Figure 16. Dependence of current on particles. No magnetic field, average flow velocity = 7 ft/sec

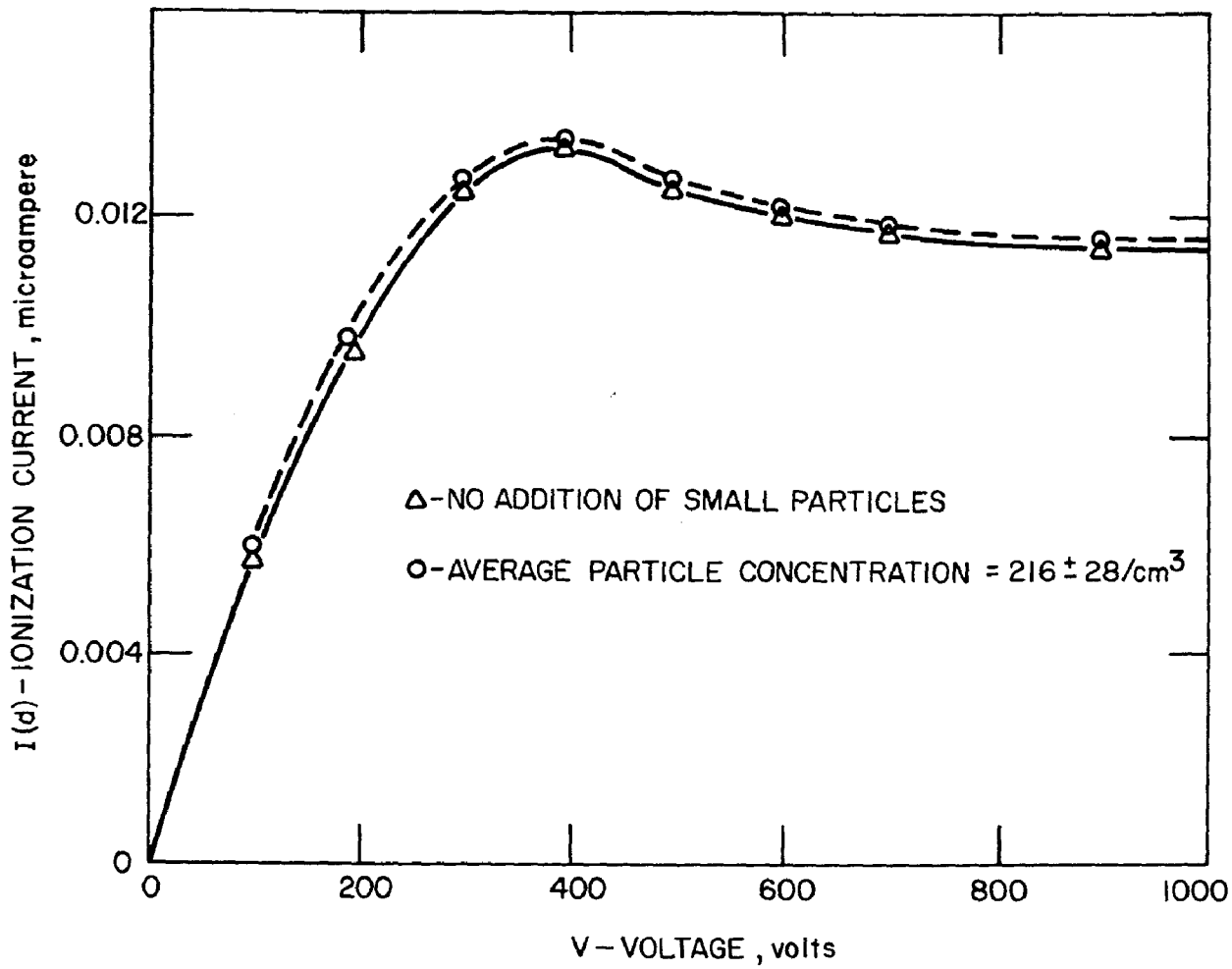

Figure 17. Impact of particles and magnetic field on ionization current. Magnetic field = 975 gauss, flow velocity - 7 ft/sec

lies in its neglect of bulk motion of the gas. Figure 15 clearly indicates that at electric field intensities less than saturation, the motion of the gas cannot be neglected. Limitations in the aerosol generation system prevented the generation of aerosol in sufficient (and realistic) concentration so as to affect the ion density.

PARTICLE CHARGING

We did not experimentally measure the charge acquired by particles and, therefore, cannot verify the predictions of Figures 9-11. Nevertheless, we see no reasons to disbelieve the significance of these predictions. For a particle at any point in the gas stream there are unique values of electric field intensity and ion generation rate to produce a maximum charge per particle. Thus, in the eventual design of equipment using radiation charging, it will not be necessary to use radiation sources of immense intensity (and hence hazard), but rather a judicious combination of source strength and applied electric field.

Two deficiencies in the charging model are evident and require attention in further research. The discontinuity in the charge rate between Regimes I and II requires modification of the conceptual model. More important, however, is modification of the charging model that accounts for the lateral motion of the particle due to its lateral drift produced by the electric field. Since the variables ion density, electric field, and gas velocity appearing in the charging expression are not constants as was assumed in this study, but change due to the particle's lateral motion (i.e. x-direction), it is believed that the lateral motion of the particle will substantially change the rate of charging and increase the eventual charge the particle acquires.

ENGINEERING FEASIBILITY

Study has not progressed to the point where the engineering feasibility can be assessed, but some conclusions can be drawn. Since energetic electrons are ultimately sought for ionization, it is suggested that these can be more easily acquired by beta radiation than by Compton scattering of gamma radiation. The reductions in shielding and radiation hazards are vast. The modest intensities of the magnetic field needed to trap energetic electrons suggest that permanent magnets can be used rather than electromagnets. The savings in electrical power will be significant.

NOMENCLATURE

a	radius of aerosol particle
A	cross-sectional area of collecting electrode
d	distance between anode and cathode
D	dielectric constant of aerosol particle
D^+, D^-	diffusion coefficient of positive and negative ions
$\bar{E}(\bar{r})$	local electric field intensity
$I(d)$	Ionization current measured at collecting electrode
I_{sat}	saturation value of ionization current
k	Boltzmann constant
$n^+(\bar{r})$, $n^-(\bar{r})$	local density of positive and negative ions
q	charge acquired by aerosol particle
q_{tr}	transition charge on aerosol particle (Equation 11)
$\bar{r}$	distance from the origin to the point in question
$S(\bar{r})$	local ion generation rate
$\bar{S}$	average ion generation rate
t	time
T	absolute temperature
v_{rms}	root mean square velocity of gas molecules
V, V_a, V_0	voltage in space, at particle surface, and difference between electrodes
x, y, z	coordinates of a point inside the duct (x is distance normal to electrode surface)

α	ion recombination coefficient
ε	permittivity of gas
θ_0	angle (Figure 2)
μ^+, μ^-	mobility of positive and negative ion

ACKNOWLEDGMENT

This investigation was supported by the Graduate Air Pollution Training Program, Office of Air Programs, Environmental Protection Agency, Grant No. T900011 and Engineering Foundation of the United Engineering Trustees, Inc., United Engineering Center Grant No. RC-A-73-8.

REFERENCES

1. McCray, H. F. Apparatus and Process for Utilizing Emanations from Radioactive Materials. U. S. Patent 1,991,934, September 1929.

2. Jacob, C. W. Electrical Precipitation Apparatus. U. S. Patent 2,381,455, October 1942.

3. Meyer, F. J. Irradiating Apparatus. U. S. Patent 2,980,202, April 1961.

4. Davies, C. N. (ed.). Aerosol Science. New York, Academic Press, 1966.

5. Maas, F. J. Ionizer for Electrostatic Precipitations. U. S. Patent 2,756,840, July 1956.

6. Leupi, R., and J. Schedling. Apparatus for the Electrical Charging by Means of Radioactive Preparations of Matter Suspended in a Gas Stream. U. S. Patent 2,934,648, April 1960.

7. Hasenclever, D., and H. C. Siegmann. A New Method for Dust Measurement by Means of Molecular-ion Attachment. Staub-Reinhalt. Luft (in English). 20:212-218, 1960.

8. Coenen, W. Recording Dust Measurement by the Molecular-Ion Attachment Method. Staub-Reinhalt.Luft (in English). 24:350-353, September 1964.

9. Mohnen, V. A., and P. Holtz. The SUNYA-ASRC Aerosol Detector. J. Air Pollut. Contr. Assoc. 18:667-668, October 1968.

10. Dickter, W. An Investigation of a Device Using Radiation to Charge and Collect Particulate Matter M. S. Thesis, Nuclear Engineering, Pennsylvania State University, University Park, 1969.

11. Schultz, M. A., M. E. Crotzer, and W. R. Knapick. Collection of Particulate Matter from Smokestacks Using Gamma-Ray Ionization. Nucl. Tech. 17:38-48, January 1973.

12. Landau, L. On the Energy Loss of Fast Particles by Ionization. J. Phys. (USSR). 8:201-205, 1944.

13. Katz, L., and A. S. Penfold. Range-Energy Relations for Electrons and the Determination of Beta-Ray Endpoint Energies by Absorption. Rev. Mod. Phys. 24:28-44, January 1952.

14. Bartholet, T. G. Ionization of Air by Gamma Radiation in an Electric Field. M. S. Thesis, Nuclear Engineering, Pennsylvania State University, University Park, 1974.

15. Liu, B. Y. H., and H. C. Yeh. On the Theory of Charging of Aerosol Particles in an Electric Field. J. Appl. Phys. 39:1396-1402, February 1968.

APPENDIX

Equations (6-8) represent three simultaneous, nonlinear second order differential equations in three spatially dependent unknowns: positive and negative ion concentrations and the local electric field. Four of the six boundary conditions necessary to solve the equations are $n^+(0) = 0$, $n^-(1) = 0$, $V(0) = V_0 = 0$. The final two boundary conditions are $n^+(1) = n^+(1)$ and $n^-(0) = n^-(0)$ where $n^+(1)$ and $n^-(0)$ are allowed to depend on $n^+(1 - \frac{x}{d})$ and $n^-(\frac{x}{d})$ respectively, through Equations (A-1) and (A-2).

$$n^+(1) = n^+(1 - \frac{\Delta x}{d}) + \beta \left.\frac{dn^+}{dx}\right|_{(1 - \frac{\Delta x}{d})} \qquad \text{(A-1)}$$

$$n^-(0) = n^-(\frac{\Delta x}{d}) + \beta \left.\frac{dn^-}{dx}\right|_{(\frac{\Delta x}{d})} \qquad \text{(A-2)}$$

where Δx = mesh spacing in finite difference formalism

β = some positive constant

It is found that ion distributions are independent of β for $0 \leq \beta \leq 2$ so it was decided to let $\beta = 1$.

Solutions to the set of equations are obtained by writing finite difference equations for positive and negative ion concentrations at equal intervals in the ionization region. The set of difference equations is solved by the method of tridiagonal matrices. An iterative procedure is required and works as follows. A set of ion concentrations is assumed. The electric field based on these concentrations is then obtained and used to determine new ion concentrations. The procedure is repeated until the electric field and ion concentration do not change in successive iterations. The method of tridiagonal matrices proves to be an efficient means of solving matrix equations and ion distributions are obtained at a reasonable expense of computer time.

COLLECTION OF AEROSOL PARTICLES BY ELECTROSTATIC DROPLET SPRAY SCRUBBERS

Michael J. Pilat
University of Washington
Seattle, Washington

ABSTRACT

Theoretical calculations and experimental measurements show that the collection of small aerosol particles (0.05 to 5 micron diameter range) by water droplets in spray scrubbers can be substantially increased by electrostatically charging the droplets and particles to opposite polarity. Measurements with a 140 acfm two-chamber spray scrubber (7 seconds gas residence time) showed an increase in the overall particle collection efficiency from 68.8% at uncharged conditions to 93.6% at charged conditions, with a dioctyl phthalate aerosol (1.05 micron particle mass mean diameter and 2.59 geometric standard deviation). The collection efficiency for 0.3 micron particles increased from 35% to 87% when charged.

During 1973-1974 a 1,000 acfm pilot plant electrostatic scrubber was constructed inside a 40 ft trailer for evaluation on controlling particulate emissions from pulp mill operations (funded by Northwest Pulp and Paper Association). Field tests performed on the particle emissions exhausting from SO_2 absorption towers treating the gases from a magnesium based sulfite recovery boiler have shown particle collection efficiencies ranging from about 60 to 99% by weight, depending on the electrostatic scrubber operating conditions. Energy requirements for the University of Washington Electrostatic Scrubber are about 0.5 horsepower/1,000 acfm (350 watts/1,000 acfm) including gas pressure drop, water pressure drop, and electrostatic charging of the water spray droplets and the particles.

INTRODUCTION

In the early 1940's an electrostatic droplet spray scrubber consisting of electrically charged water droplets collecting aerosol particles charged to the opposite polarity was proposed by Penney[1]. He patented an "electrified liquid spray dust precipitator" involving particle charging by corona discharge and droplet charging by either ion impactor or induction. With a water flowrate of about 5 gallons/1000 acf, a single spray nozzle charged to 9,000 to 10,000 volts, particle charging with a corona wire in a 3-inch diameter metal cylinder (12,500 volts), and a scrubber chamber 6-3/8 inches in diameter and about 24 inches in length, Penney reported an increase in the dust collection efficiency from 13.8% with no charging to 44.8% with the particles and droplets charged to opposite polarity.

Eyraud et al.[2] reported high particle collection efficiencies with a wet electrostatic scrubber using negatively charged droplets and uncharged aerosol particles generated by the pyrolysis of vulcanized rubber. The scrubber consisted of centrally located water spray tubes inside a one-meter diameter cyclonic spray scrubber 3.5 meters high. The electric potential on the water sprays was 60,000 volts and the liquid to gas flowrate ratio was 45.5 gallons/1000 acf.

An electrostatic space charge scrubber involving water droplets and aerosol particles charged to the same polarity which then precipitate onto the scrubber walls was proposed by Hanson and Wilke[3]. They calculated that 299 gallons of water per minute in the form of 5 micron diameter droplets charged to 10,000 volts would be required for 97% collection efficiency of 1.0 micron diameter particles in a gas flow of 100,000 cfm (2.99 gallons/1000 acf).

THEORETICAL CALCULATION OF PARTICLE COLLECTION EFFICIENCY

For his Ph.D. dissertation research Kraemer[4] theoretically and experimentally investigated the collection of negatively charged dioctyl phthalate aerosol particles (about 0.8 microns diameter) onto positively charged (6,000 volts) metal spheres (0.64 to 1.1 cm diameter). Based on these studies Kraemer and Johnstone[5] predicted a single droplet (50 micron diameter droplet charged negatively at 5,000 volts) collection efficiency of 332,000% for 0.05 micron diameter particles (4 electron units positive charge per

particle). Kraemer and Johnstone's calculations of the single droplet collection efficiency considered only the forces of fluid resistance and of electrostatics (the inertial and Brownian diffusion forces were assumed to be negligible).

Sparks[6] in his Ph.D. dissertation research calculated the efficiency of charged droplets for collecting charged particles of opposite polarity. The calculations involved solving the equation of particle motion for a gas flowing around a sphere as reported by Sparks and Pilat[7]. The Runge-Kutta numerical solution for particles (negative charging voltage of 1,000 volts/cm) flowing near a droplet (positive charging voltage of 1,000 volts/cm) included the forces of Brownian diffusion, inertia, and electrostatics. The calculation results, shown in Figure 1 predict a single droplet collection efficiency of about 275% for 0.05 micron diameter particles and 200 micron diameter droplets with an undisturbed fluid velocity of 100 cm/sec. Recently George and Poehlein[8] and Nielsen and Hill[9] have reported similar theoretical calculation results for the enhancement of particle collection by single droplets with electrostatic charging.

EXPERIMENTAL MEASUREMENTS

ELECTROSTATIC DROPLET SPRAY APPARATUS

The 140 acfm double chamber University of Washington Electrostatic Scrubber is shown schematically in Figure 2. A dioctyl phthalate aerosol was generated by injecting the DOP into an electrically heated aluminum tube 1.5 in. in diameter and 18 in. in length. The DOP condensation aerosol passed through a blower, a corona charging section, and into the first scrubber chamber. The scrubber chamber and ducts were constructed of 1/4 in. thick Lucite. The corona charging sections on both chambers consisted of a single 12 gauge steel rod mounted horizontally in the middle of the rectangular inlet ducts with ground strips of copper and was charged to 27,000 volts. The first chamber (60 inches high by 24 inches wide, rectangular) was counter-current and had a water flow of 1.2 gallons/minute with 20 spray nozzles. The second chamber (45 inches high and 20 inches in diameter, cylindrical) was co-current and had a water flow of 1.0 gallons/minute with 13 spray nozzles. The spray nozzles were Spraying Systems Fogjet 7N4 nozzles. The water droplets were inductively charged positively with a 5 kilovolt power supply.

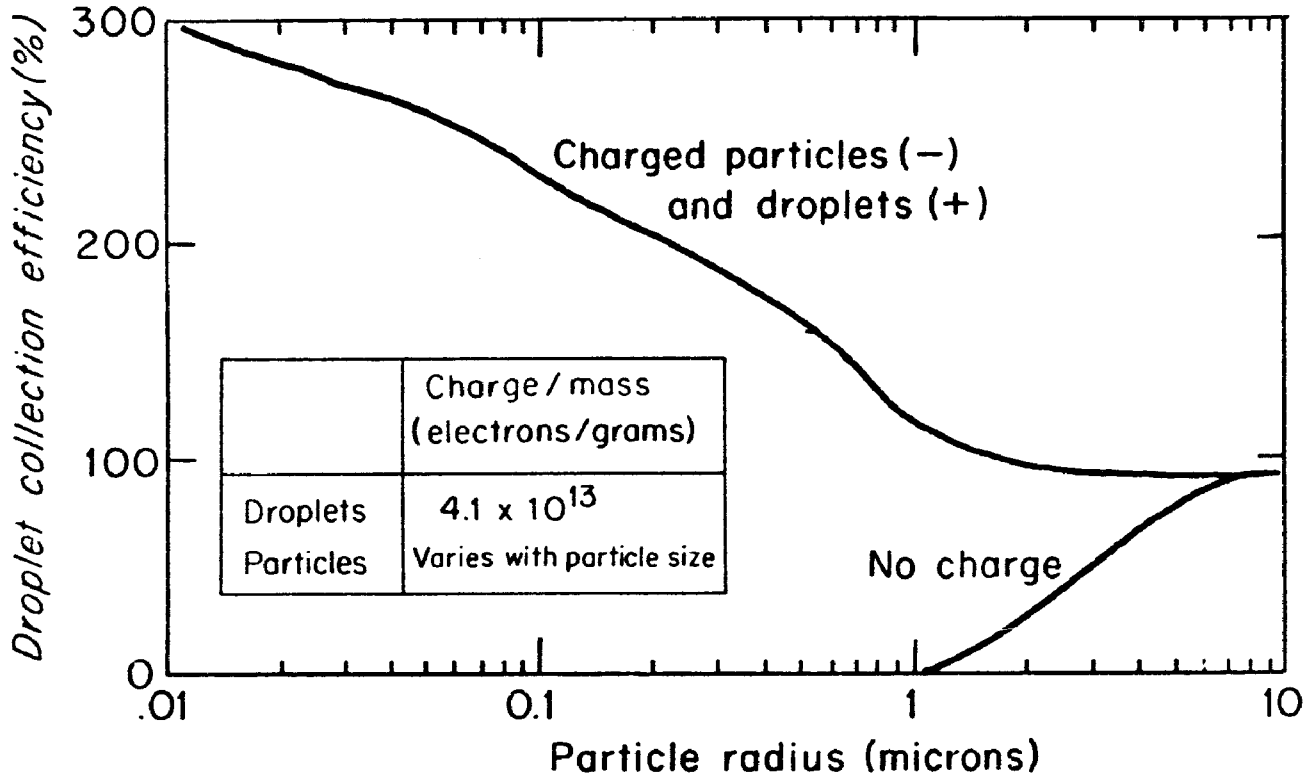

Figure 1. Calculated particle collection efficiencies for a single 200 micron diameter droplet with 100 cm/sec undisturbed fluid velocity

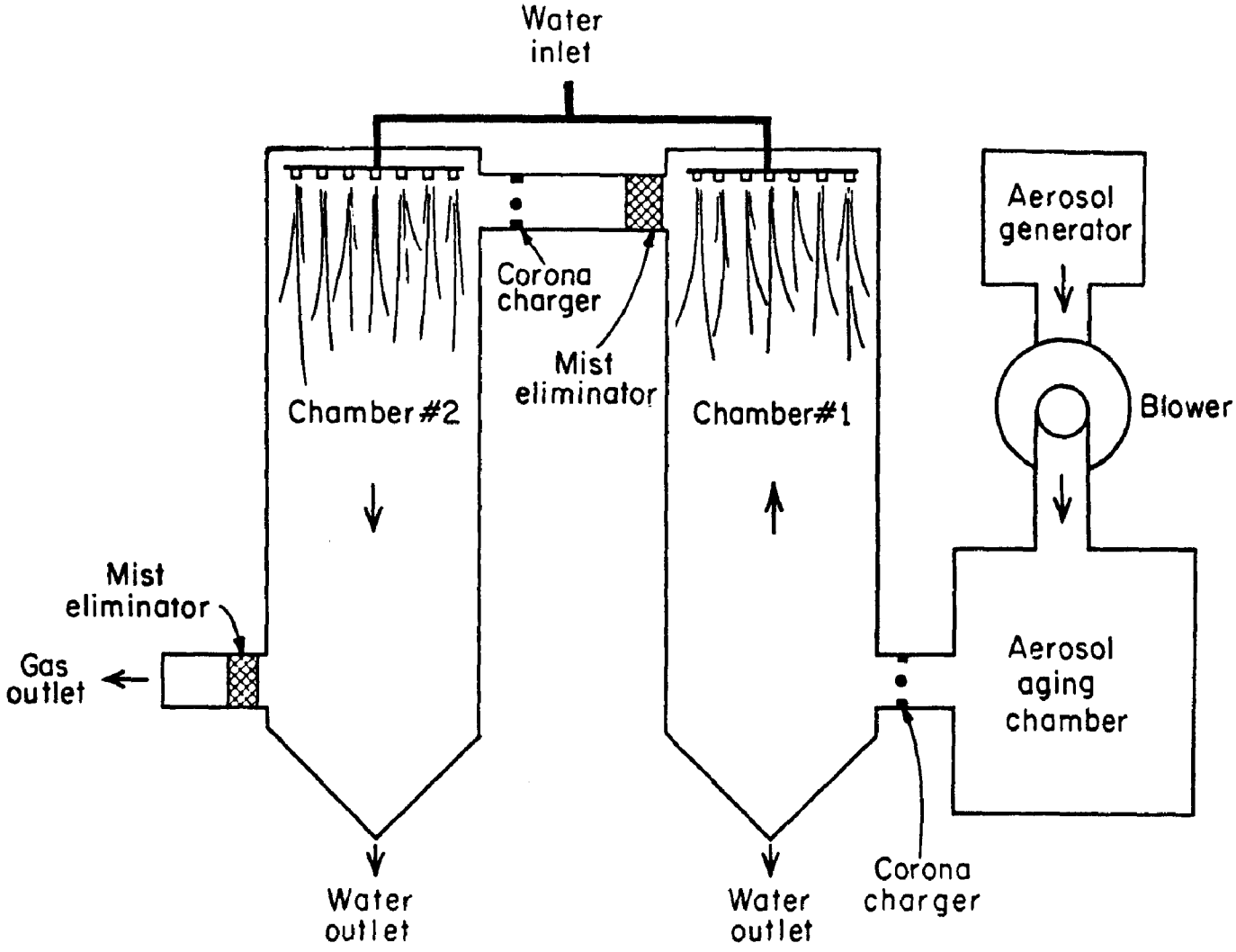

Figure 2. Schematic of electrostatic droplet spray scrubber

MEASUREMENT TECHNIQUES

The particle mass concentration and size distribution were simultaneously measured at the inlet (upstream of the charging section on the first chamber) and outlet of the electrostatic scrubber using Mark III University of Washington Sources Test Cascade Impactors. These cascade impactors are similar to those reported by Pilat, Ensor, and Bosch[10] and are commercially available under a licensing agreement with the University of Washington. The DOP aerosol mass concentration at the inlet to the electrostatic scrubber was typically about 0.15 grains/acf. The particle size distributions at the scrubber inlet and outlet are shown in Figure 3.

The size distribution of the water droplets was measured by collecting the droplets on greased (melted petroleum jelly) glass slides and photographing them as described by Pigford and Pyle[11]. The droplet images on the photomicrographs were sized with a Zeiss particle size analyzer. As the water droplets form hemispheres on the greased slides, a conversion factor of 1.26 was used to correct the flattened diameter to the real droplet diameter. About 700 droplets were sized for each distribution measured. The droplet size distributions at 103 psig and at charged (5,000 volts) and uncharged conditions are shown in Figure 4.

The electrostatic charges of the aerosol particles and the water droplets were measured with a similar device which basically consisted of a sample collection section and a charge measuring circuit. The aerosol charge analyzer involved a 1-inch diameter Gelman filter holder with a Type A glass fiber filter to collect the particles. The filter holder and nozzle (for isokinetic sampling) was electrically insulated from a grounded aluminum shield which protected the filter holder from external electric fields. The aerosol charge to mass ratio was obtained by monitoring the current for a recorded particle sampling time and then weighing the filtered particles. The aerosol charge was typically about 5×10^{-5} coulombs/gram (3.5×10^{14} electrons/gram).

The droplet charge analyzer included a 3-inch square droplet collector (packed with aluminum shavings) connected to a grounded microammeter (10^{-7} to 10^{-8} amps). The droplet charge analysis consisted of placing the collector in the spray droplets, monitoring the current and sampling time, and weighing the amount of water collected. The droplet charge with 5,000 volts inductance charging was typically 5.6×10^{-7} coulombs/gram (3.8×10^{12} electrons/gram).

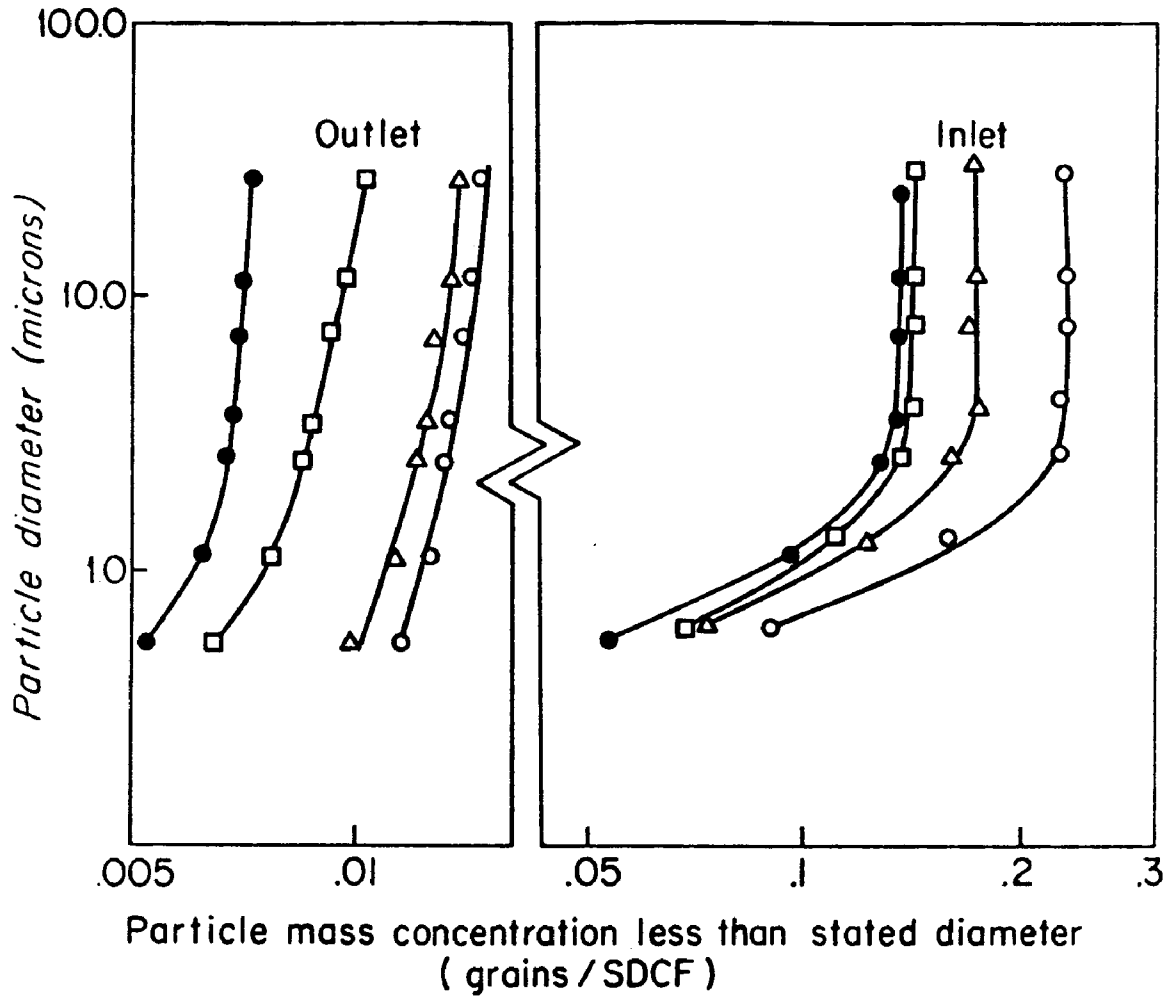

Figure 3. Size distributions of di-octyl phthalate aerosol particles at electrostatic droplet spray scrubber inlet and outlet

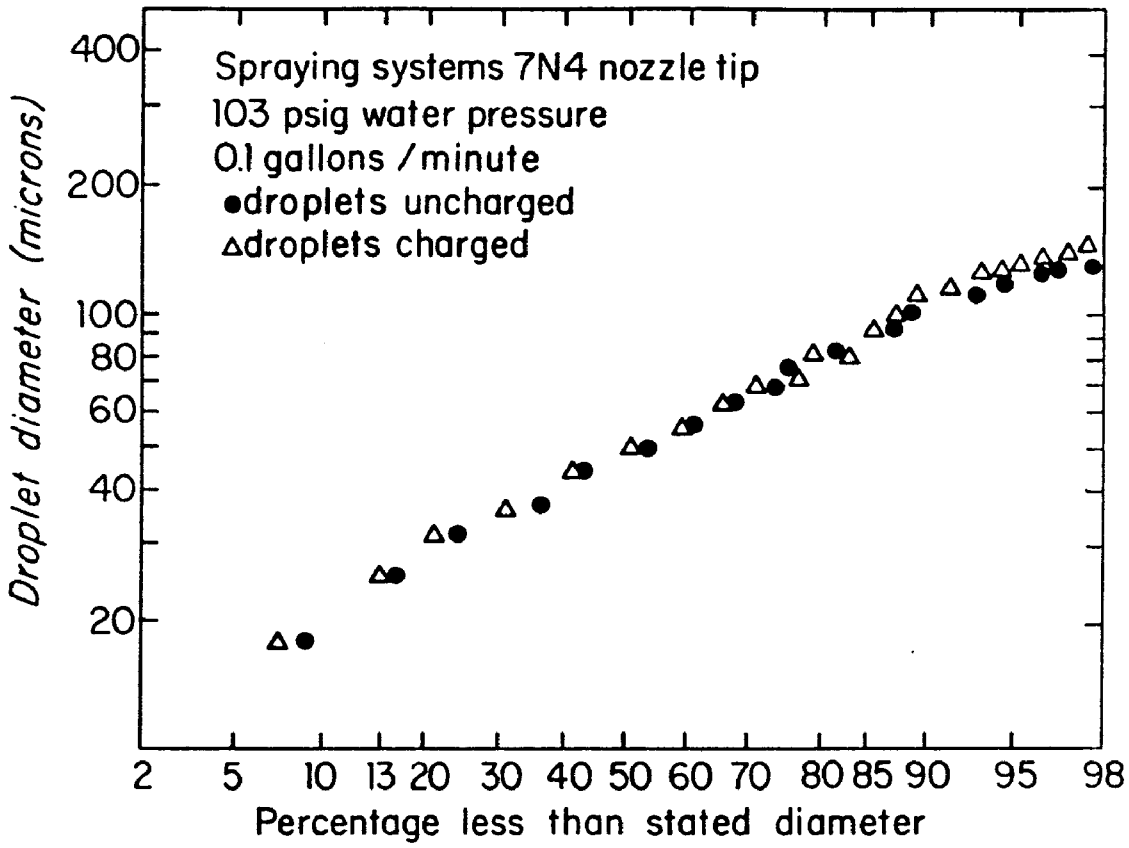

Figure 4. Size distribution of water spray droplets

RESULTS OF LABORATORY TESTS

Simultaneous measurements of the aerosol particle size distribution and mass concentration at the inlet and outlet of the 140 acfm University of Washington Electrostatic Scrubber pilot plant showed that the overall particle collection efficiency increased from 68.8% at uncharged conditions to 93.6% at charged conditions. Four particle collection efficiency as a function of particle size tests were performed at electrostatic charging conditions and three tests at uncharged conditions. Each different symbol in Figure 5 represents a separate particle collection efficiency test. As shown in Figure 5 the collection efficiency for the 0.3 micron diameter particles increased from 35% at uncharged condition to 87% when charged.

A 1,000 acfm University of Washington Electrostatic Scrubber pilot plant was constructed in the laboratory and tested in 1973 providing improved particle collection efficiencies at lower water to gas flow rate ratios. The tests on the 1,000 acfm pilot plant were conducted in order to determine the possible effects of scaling up such a system.

FIELD TESTING OF U. OF W. ELECTROSTATIC SCRUBBER

During 1973-1974 a 1,000 acfm U. of W. Electrostatic Scrubber was constructed in a 40 ft trailer for field tests on controlling particle emissions for pulp mill operations. The initial field tests of this pilot plant were conducted at the University of Washington coal-fired power boiler in order to check out the system on hot (about 350^{0}F) gases. Exhaust gases from the coal-fired boiler were obtained upstream of the electrostatic precipitator at right angles to the gas flow (non-isokinetic sampling) and passed through the U. of W. Electrostatic Scrubber. The particle collection efficiency at 877 acfm was measured to be 98.2% (inlet 0.153 grains/sdcf, outlet 0.0028 grains/sdcf) at a water flow of 2.2 gpm, particle charge voltage of 30 kilovolts and water charge voltage of 2 kilovolts. The inlet particle mass concentration was somewhat low at 0.153 grain/sdcf as it was measured downstream of a water spray cooler which lowered the gas temperature from about 350°F to 200°F in order to protect the fiberglassed plywood ducting. It is expected that considerably higher particle collection efficiencies could be obtained with this Electrostatic Scrubber on coal-fired boilers because

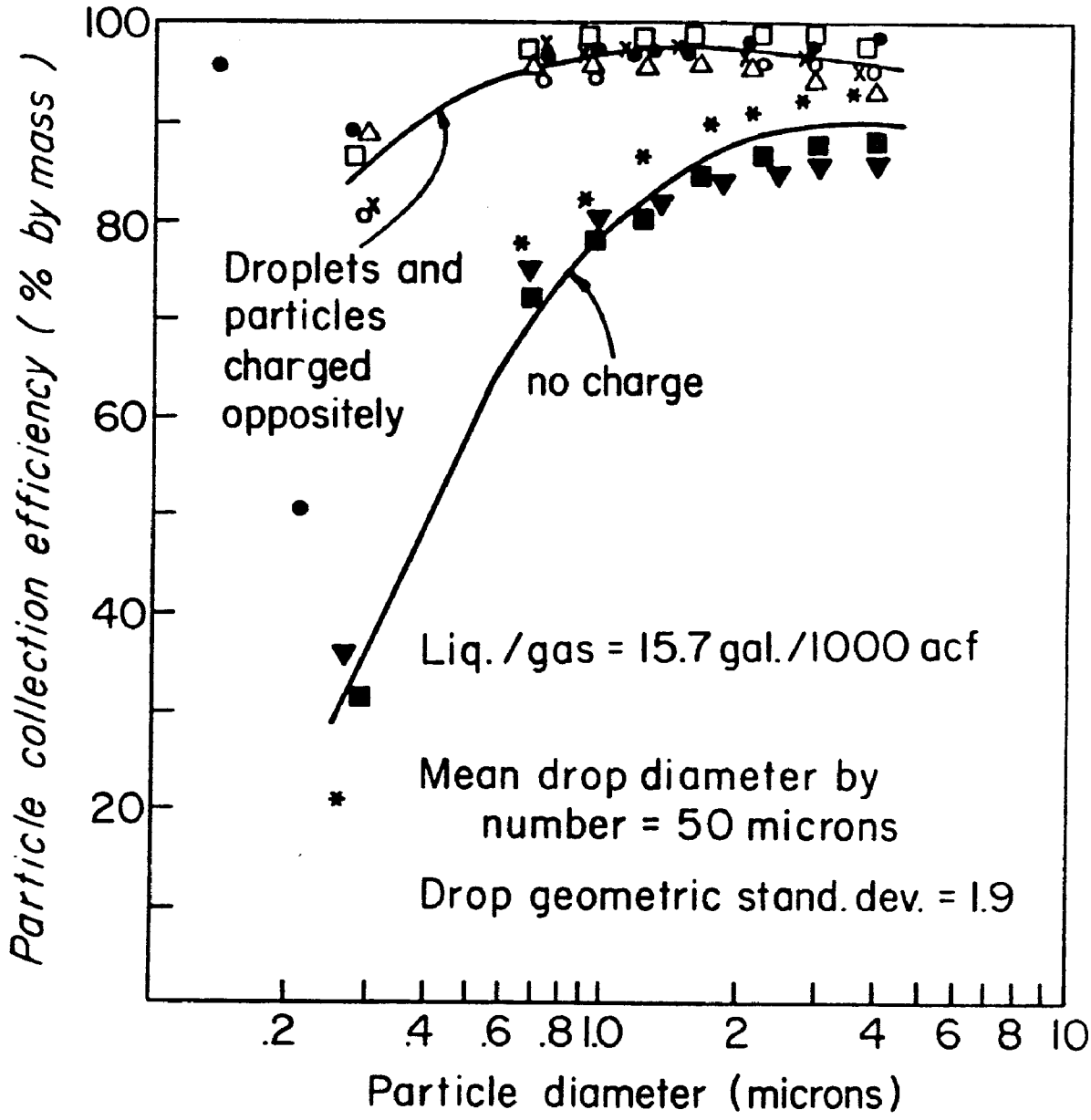

Figure 5. Particle collection efficiency of electrostatic spray droplet scrubber as a function of particle size

the system has been improved considerably since these first tests. After the one week of testing at the U. of W. power plant the U. of W. Electrostatic Scrubber pilot plant trailer was shipped to a sulfite pulp mill where tests have been conducted on the emissions from the SO_2 absorption tower treating the gases exhausting from a magnesium sulfite recovery boiler. Particle collection efficiencies ranging from about 60 to 99% by weight have been measured depending on the electrostatic scrubber operating conditions. At high particle collection efficiencies the energy requirements for the U. of W. Electrostatic Scrubber are about 0.5 horsepower/1,000 acfm (350 watts/1,000 acfm) including gas pressure drop, water pressure drop, and electrostatic charging of the water spray droplets and the aerosol particles.

It is intended that future research work at the University of Washington on electrostatic scrubbers will include field testing of particle collection of emissions from pulp mill operations and coal-fired boilers and particle-single droplet theoretical and experimental studies. Because of the great potential for combined SO_2 and particle collection by the electrostatic scrubber, research efforts should also be started on this application.

ACKNOWLEDGMENTS

This research was supported in part by the University of Washington and by research grants from Reynolds Metals Company (Longview, Washington), Alaska Lumber and Pulp Company (Sitka, Alaska), Ketchikan Pulp Company (Ketchikan, Alaska), and the Northwest Pulp and Paper Association.

REFERENCES

1. Penney, G. W. Electrified Liquid Spray Dust Precipitator. U. S. Patent 2,357,354, September 1944.

2. Eyraud, C., J. Joubert, R. Morel, C. Henry, and B. Roumesy. Study of a New Dust Collector Using Electrostatically Sprayed Water. In: Proceedings, Part I, International Clean Air Congress. London. October 4-7, 1966. p. 129-130.

3. Hanson, D. N., and C. R. Wilke. Electrostatic Precipitator Analysis. Ind. Eng. Chem. Process Des. Develop. 8(3):357-364, July 1969.

4. Kraemer, H. F. Collection of Aerosol Particles by Charged Droplets. Ph.D. Dissertation, University of Illinois, Urbana, 1954.

5. Kraemer, H. F., and H. F. Johnstone. Collection of Aerosol Particles in the Presence of Electric Fields. Ind. Eng. Chem. 47:2426-2434, December 1955.

6. Sparks, L. E. The Effect of Scrubber Operating and Design Parameters on the Collection of Particulate Air Pollutants. Ph.D. Dissertation, University of Washington, Seattle, 1971.

7. Sparks, L. E., and M. J. Pilat. Effect of Diffusiophoresis on Particle Collection by Wet Scrubbers. Atmos. Environ. (Oxford, England). 4(6):651-660, 1970.

8. George, H. F., and G. W. Poehlein. Capture of Aerosol Particles by Spherical Collectors. Electrostatic, Inertial, Interception, and Viscous Effects. Environ. Sci. Technol. 8:46-49, January 1974.

9. Nielsen, K. A., and J. C. Hill. Effect of Electrical Forces on Target Efficiencies for Spheres. ERI Project 947 Report, Engineering Research Institute, Iowa State University, Ames, 1974.

10. Pilat, M. J., D. S. Ensor, and J. C. Bosch. Source Test Cascade Impactor. Atmos. Environ. (Oxford, England). 4(6):671-679, 1970.

11. Pigford, R. L., and C. Pyle. Performance Characteristics of Spray-Type Absorption Equipment. Ind. Eng. Chem. 43:1649-1666, July 1951.

CHARGED DROPLET SCRUBBING FOR FINE PARTICLE CONTROL

C. W. Lear, W. F. Krieve, and E. Cohen
Systems Group of TRW Inc.
Redondo Beach, California

ABSTRACT

Some basic mechanisms of interaction of highly charged scrubbing droplets with fine particulate are studied. In the 1.0-0.1 micron particulate size range, the most effective mechanisms are electrically augmented impact scrubbing and charge exchange without impact. A charged droplet scrubber using electrohydrodynamically sprayed droplets and an applied field to achieve electrical impact scrubbing is described. It is shown that such scrubbers are capable of high densities of droplets in the 100-micron size range, and charged to near their upper stability limit. Collection efficiencies of 30 to 50 percent per stage are demonstrated in the sub-micron particulate size range.

INTRODUCTION

Charged droplet scrubbing is similar to conventional scrubbing methods in that it removes particulate and fumes from contaminated gas by means of interaction of droplets of scrubbing liquor with the particles of dirt or fume. Beyond this, the similarity ends. Because of their unusual electrical interaction mechanisms, which are not yet fully understood, charged droplet scrubbers are still considered as novel and experimental devices in industrial pollution control. In the charged droplet scrubber the electrical interaction mechanisms exist in addition to the normal impact and diffusional scrubbing mechanisms. These dominate in the 0.1 to 1.0 micron particulate size range, where the normal mechanisms lack effectiveness.

As the name "charged droplet scrubbing" implies, the scrubbing droplets, usually water, will generally carry a high electrical charge which is induced during or after their formation. The droplets may move under the influence of electric fields, either deliberately applied or existing by virtue of the ambient space charge. The particulate may also be electrically charged. All these conditions may contribute to the electrical interaction aspects of charged droplet scrubbers.

This report describes work done at TRW Systems to determine the applicability of charged droplet scrubbing specifically to the control of fine particulate. A large portion of the work was done under contract to the Environmental Protection Agency. Throughout this report, the reference to fine particulate will indicate the general range of 0.1 to 1.0 micron in diameter. The work described here includes studies of the effectiveness of various charged droplet scrubbing mechanisms, as well as direct measurements of the performance of a charged droplet scrubber.

CHARGED DROPLET SCRUBBING DEVICES

Charged droplet scrubbing concepts may be broadly classified according to droplet formation techniques, as well as according to droplet-particle interaction mechanisms.

DROPLET FORMATION

The various alternatives for forming charged droplets have been presented previously by Melcher et al.[1] Perhaps the two most commonly used methods are electrohydrodynamic spraying and mechanical spraying followed by corona charging. Of these two, the former is capable of giving the highest droplet surface charge density. It is usually desired to maximize the droplet charge density.

The size of droplets formed by electrohydrodynamic spraying is a function of the size of the liquid streamers issuing from the spray tube. These streamers break up into columnar segments, which subsequently break into droplets under the action of electrostatic forces. The size of the liquid column is determined by the spray tube size, the local electric field, and the liquid fluid properties.

The maximum charge density on the surface of a liquid column is determined from the local atmospheric breakdown limit with Peek's correction for cylindrical electrodes.[2,3]

$$E_b = E_0 \delta \left[1 + \frac{0.0308}{\sqrt{\delta S}} \right] \qquad (1)$$

where E_0 = normal breakdown strength for the medium at standard conditions. $E_0 = 3 \times 10^6$ volts/meter for normal air

δ = gas density relative to standard conditions

S = electrode radius, meters

The columns thus formed break up into segments of length nominally 4.508 times their diameter according to the Rayleigh stability criterion.[4,5] The surface charge density on the droplets thus formed has been calculated[3] and is shown in Figure 1 for water droplets in air at standard conditions.

The upper limit of charge density on a droplet surface is either the corona breakdown limit or the Rayleigh limit. The latter is stability limit determined by the balance between electrostatic forces and surface tension forces on the droplet surface. The two limits are close. Above 40 micron radius, the Rayleigh limit governs for water. It is given by

$$E_b = 2\left(\frac{\sigma}{\varepsilon_0 S}\right)^{\frac{1}{2}} \qquad (2)$$

where ε_0 = permittivity of free space, 8.854×10^{-12} coul/volt-meter

σ = surface tension of liquid, newtons/meter

This limit is also shown in Figure 1. The figure indicates that the droplets are charged to a value below their Rayleigh limit at formation. The droplets will evaporate without loss of charge, and approach the Rayleigh limit.

Droplet evaporation not only affects the total droplet charge and charge release to ambient air, but also the useful droplet lifetime. This is not a significant problem for a droplet radius over 50 microns or so, but may be serious for

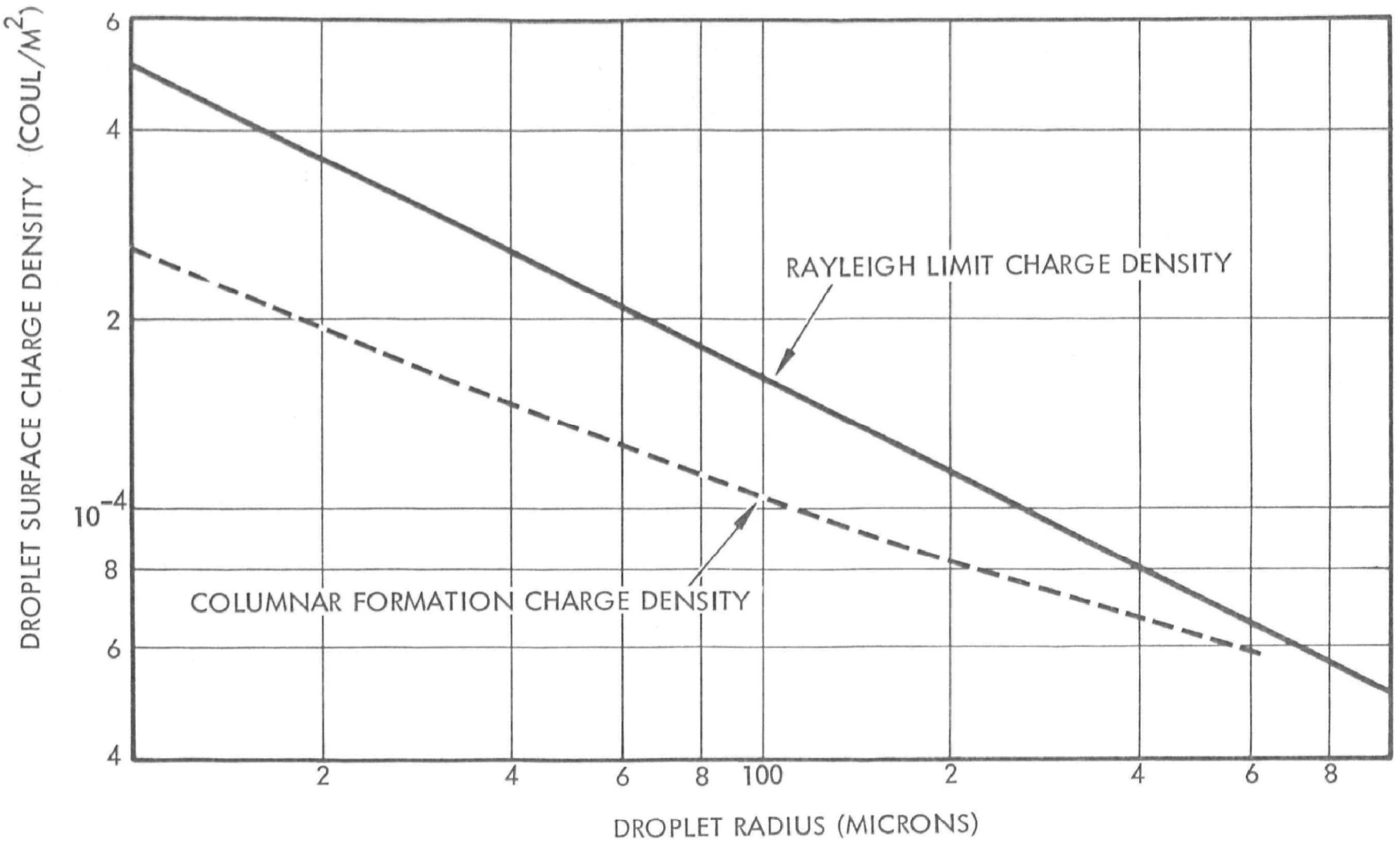

Figure 1. Limits of surface charge densities on water droplets (Rayleigh limit) and columnar segments of water

droplets smaller than 5 or 10 microns. Droplet evaporation lifetimes were calculated for water droplet in air at atmospheric pressure and 100°C for various values of relative humidity. These are shown in Figure 2.

PARTICULATE REMOVAL MECHANISMS

The removal of sub-micron size particulate from a gas stream has proven to be difficult to accomplish. This is due in part to low mobility and unfavorable inertial properties of the small particulate. One basic problem is that of establishing a significant relative velocity between a particle to be removed and the collecting surface (in this case, droplets). For smaller particulate, this becomes harder to do, and requires considerably more energy input to the gas stream or the collecting surfaces, or both.

If a significant relative velocity can be established, the particulate can be made to impinge upon some collecting surface and thereby be removed from the gas stream. Such a collecting surface may be a stationary or moving part of the hardware, as in a precipitator device, or it may be a moving liquid surface, as in a scrubber.

Inertial impact scrubbing is effective for particle sizes down to about 1 micron. Particulates above 0.01 micron in size are still too massive to be moved about much by anything except the strongest turbulent forces. Below the 0.01 micron limit, they begin to be increasingly affected by molecular forces, and random Brownian motion will be observed. Very fine particulate may then diffuse freely and rapidly to the collecting surfaces.

In a sufficiently humid environment, fine particulate may act as nucleation sites for the growth of water droplets, which are more easily removed from the gas stream once they are large enough.

The particulate size range between about 1.0 and 0.1 micron remains relatively unaffected by either impact or diffusion mechanisms. Because electrical interactions are effective in this size range, charged droplet scrubbing is of great interest here.

The addition of electrical forces gives rise to electrically augmented impact scrubbing, which is produced by an enhancement of relative velocity between droplet and particle. Induced charging occurs when charge is transferred from a droplet to a particle through electrical breakdown on a near

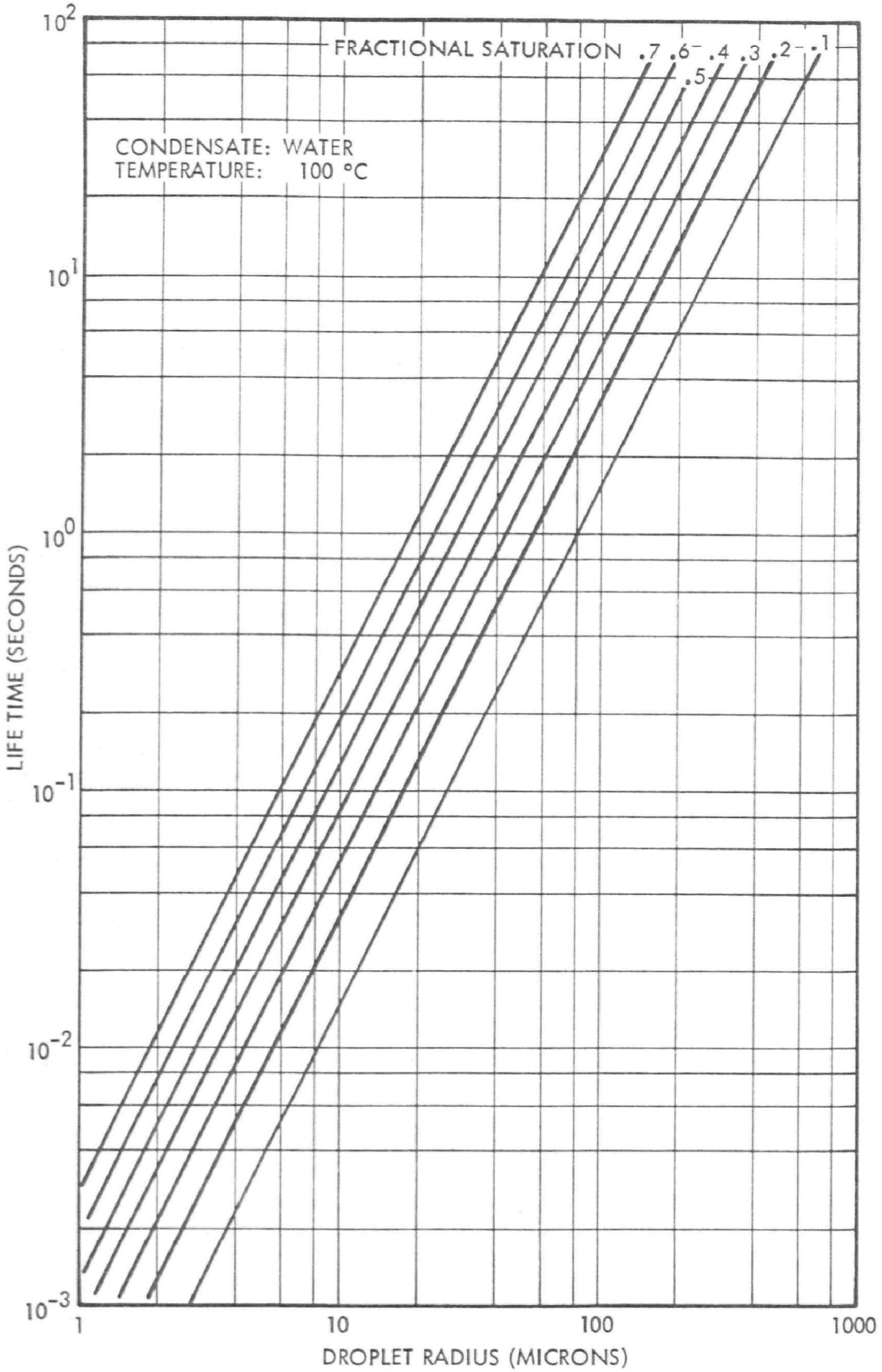

Figure 2. Water droplet evaporation lifetimes as a function of initial droplet radius and relative humidity

miss. If charge is released locally by droplet evaporation, it will lead to enhanced field charging of particulate. In addition, corona charging will always be present to some degree.

Computations have been made to obtain cross sections for collisional capture and induced charging of particulate by a droplet. The geometry of the derivation is shown in Figure 3. The model assumed is one in which a relatively large droplet is introduced into the carrier gas within which a small particle is at rest. The droplet moves at a drift velocity U which is assumed constant for purposes of the derivation. As the droplet moves within the gas, a "wake" flow field is generated which gives rise to accelerations on the particle, and which, if sufficiently strong, can sweep the particle out of the direct path of the droplet.

As the droplet moves through the gas, it sweeps out a volume equal to its path length times its projected area. Particles within this volume which are not swept out by aerodynamic forces as the droplet moves along its trajectory are collected on the droplet by agglomeration.

Particles within a concentric cylinder of radius S+D may remain within this cylinder as the droplet passes. If a particle passes with its center within a distance D of the droplet surface, it is assumed to have interacted with the droplet strongly enough to be collected by induced charging.

Particles originally residing within a concentric cylinder of radius Z*, as indicated in Figure 3, will remain in the interaction cylinder. A particle starting from radius Z* will follow a grazing trajectory as shown in Figure 3, and this radius defines an interaction boundary.

The analysis given in the present work is in terms of a collection efficiency which is consistent with common usage. The basis of its definition is the cross section of the complete interaction cylinder.

$$p = \left(\frac{Z^*}{S+D}\right)^2 \tag{3}$$

The portion of this efficiency due to induced charging depends on an impact parameter defined by

$$A = \frac{D}{S} \tag{4}$$

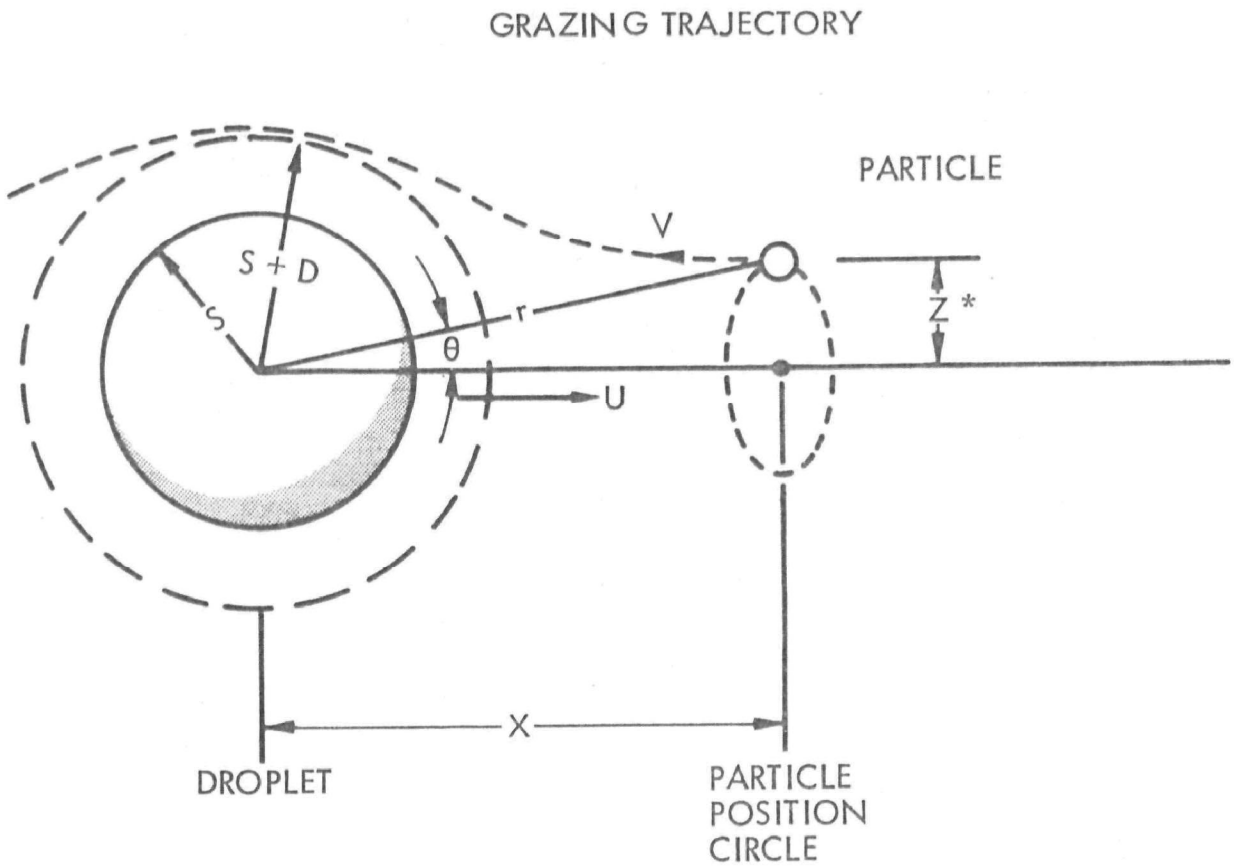

Figure 3. Droplet-particle interaction model

Induced charging impact parameters were calculated in two ways, and are shown in Figure 4 as a function of particle radius. The dashed line shows values of A for which corona breakdown will occur at the surface of a spherical particle. The droplet is assumed to be spherical and charged to the Rayleigh limit. The surrounding medium is air at standard conditions. The electric field enhancement is caused by the induced polarization of the particle.

If the droplet surface charge is at the Rayleigh limit, then a field perturbation at the surface may cause a Rayleigh-type or corona breakdown.[3] A quantity of charge is transferred to the particle, neutralizing the field perturbation. The particle charge was calculated, and the resulting drift velocity of the particle in a field of 5 kV/cm was calculated assuming Stokes' law drag. A series of curves are shown in Figure 4, as solid lines, for various drift times over a 10-centimeter distance. Larger impact parameters result in smaller particle charges, thus longer drift times.

Droplet collection efficiencies were obtained by solving the full equations of motion of a particle in a Stokes' flow field surrounding the droplet. Again, Stokes' law drag was assumed on the particle. The analysis was programmed for a computer. The collision effectiveness probability was found to depend on three parameters, physically corresponding to droplet velocity, droplet surface charge, and induced charging impact parameter. These parameters are U/Uc, E_{0D}/Ec and A, where E_{0D} is the droplet surface field, and the characteristic velocity and field are

$$Uc = \frac{9\mu S}{2\rho R^2} \tag{5}$$

where μ = viscosity of carrier gas, kg/m-sec

ε = true particulate density, kg/m^3

and

$$E_c = \frac{3\mu}{2\varepsilon_0} \cdot \frac{\varepsilon+2}{\varepsilon-1} \cdot \frac{S}{R^2} \cdot \frac{Uc}{E_{0D}} \tag{6}$$

A parametric study of the collection efficiency is shown in Figure 5. The most variability occurs with the parameter U/Uc. The results are presented on log-probability scales and approach straight lines for large U/Uc. There is little variability with impact parameter, except for values of A over 0.5, and at the lower end of the velocity scale.

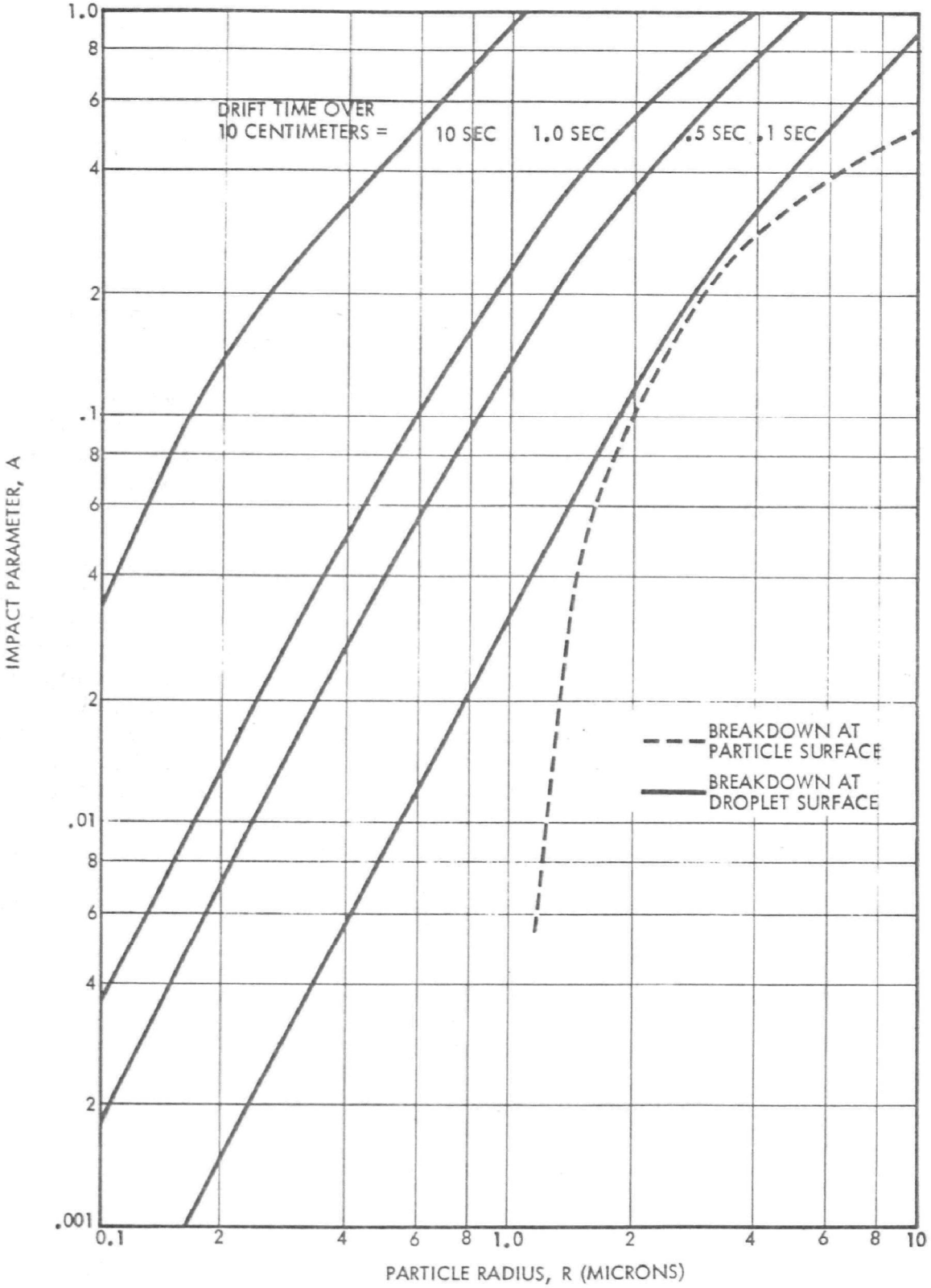

Figure 4. Induced charging impact parameters for particle and droplet surface breakdown. A sequence of drift times is plotted. Droplet radius is 60 microns. Particulate is spherical with $\varepsilon = 5$. $E_{0D} = 2.3 \times 10^7$ volts/meter, the Rayleigh limit

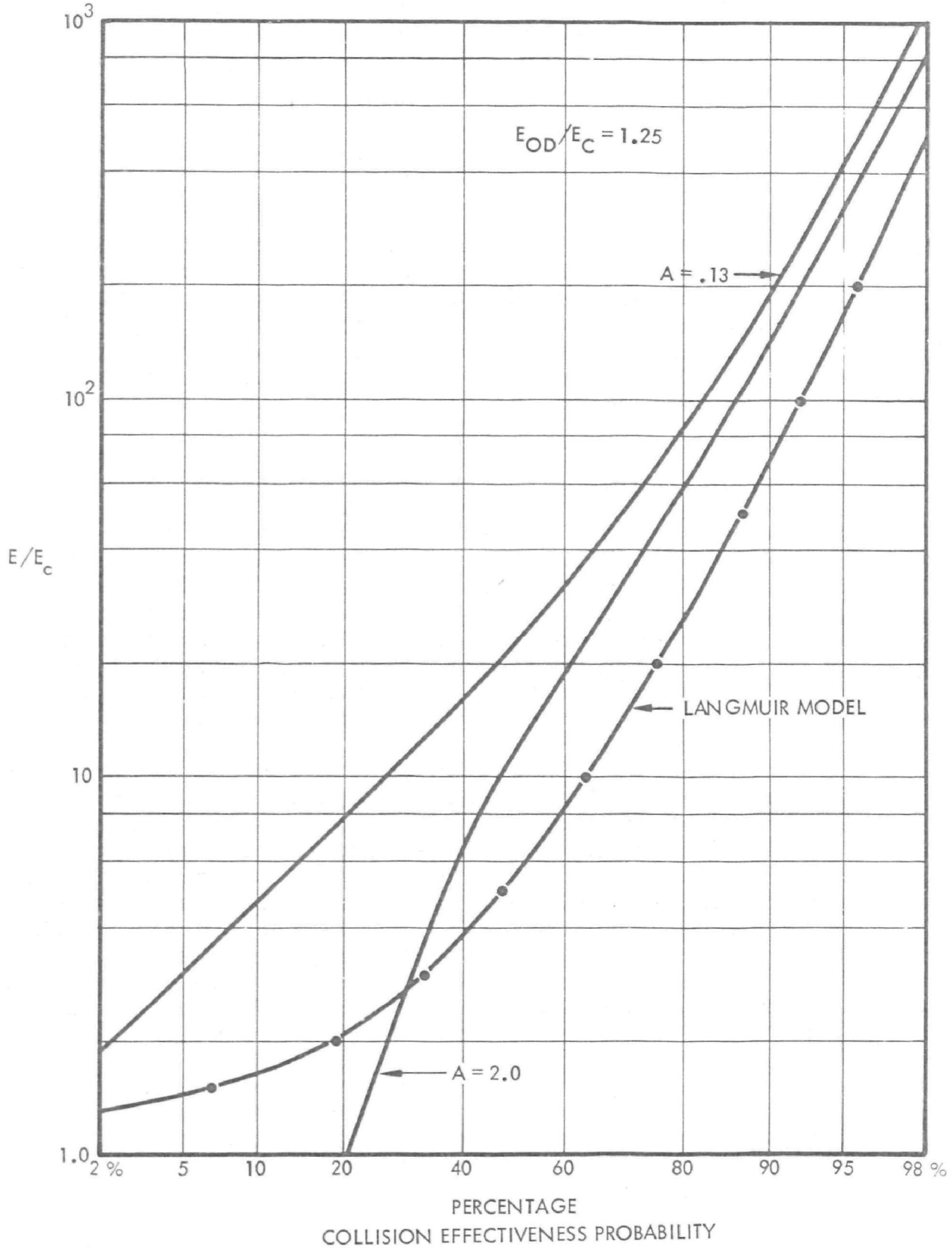

Figure 5. Parametric study of collision effectiveness probability for $E_{0D}/Ec = 1.25$

Also shown in Figure 5 for comparison is Langmuir's empirical model for the collection efficiency of raindrops.[6] This model is a single parameter model, depending only on U/Uc, with electrical effects neglected.

EXPERIMENTAL APPROACH

The TRW Charged Droplet Scrubber (CDS) was chosen as an experimental device with which to explore the effectiveness of various charged droplet scrubbing mechanisms. Data have also been obtained for overall collection efficiency. The TRW/CDS was chosen because it uses the strongest and most effective mechanisms studied. Its main merit is in the enhancement of collection efficiencies realized by high droplet velocities.

The TRW Charged Droplet Scrubber is an electrical scrubber device in which the droplets are relatively large and charged, the particulate is generally uncharged, and an ambient electric field is externally imposed. The electric field is used both to form charged droplets hydrodynamically and to move them through the scrubbing volume. A high droplet velocity through the scrubbing volume is achieved by means of the high electric field forces. The large relative velocity between droplets and particulates results in a high droplet collection efficiency.

Figure 6 is a diagrammatic sketch of the TRW/CDS showing its operating principle. The scrubbing liquor, generally fresh water, is raised from a ground potential to high voltage (about 40 kV) by flowing through a long electrical resistance path in the form of an insulating tubing. Electrical isolation is achieved through the resistance of the water itself. The water is then introduced into a hollow electrode which contains a series of hollow, elongated spray tubes. Emerging at the tips of these spray tubes, the water sees a high electric field force. Droplets are formed here by the joint action of electrical and surface tension forces, in a classical electrohydrodynamic spraying process. The droplets thus formed are highly charged, their surface field being near the local corona limit or Rayleigh stability limit. They move swiftly through the scrubbing volume under the influence of the ambient electric field between the electrode and the collecting walls.

Because of the high droplet velocities (around 30 m/sec) induced by the ambient electric field, there is a large relative motion between droplets and particulate. This large relative velocity produces sufficient inertia in the small

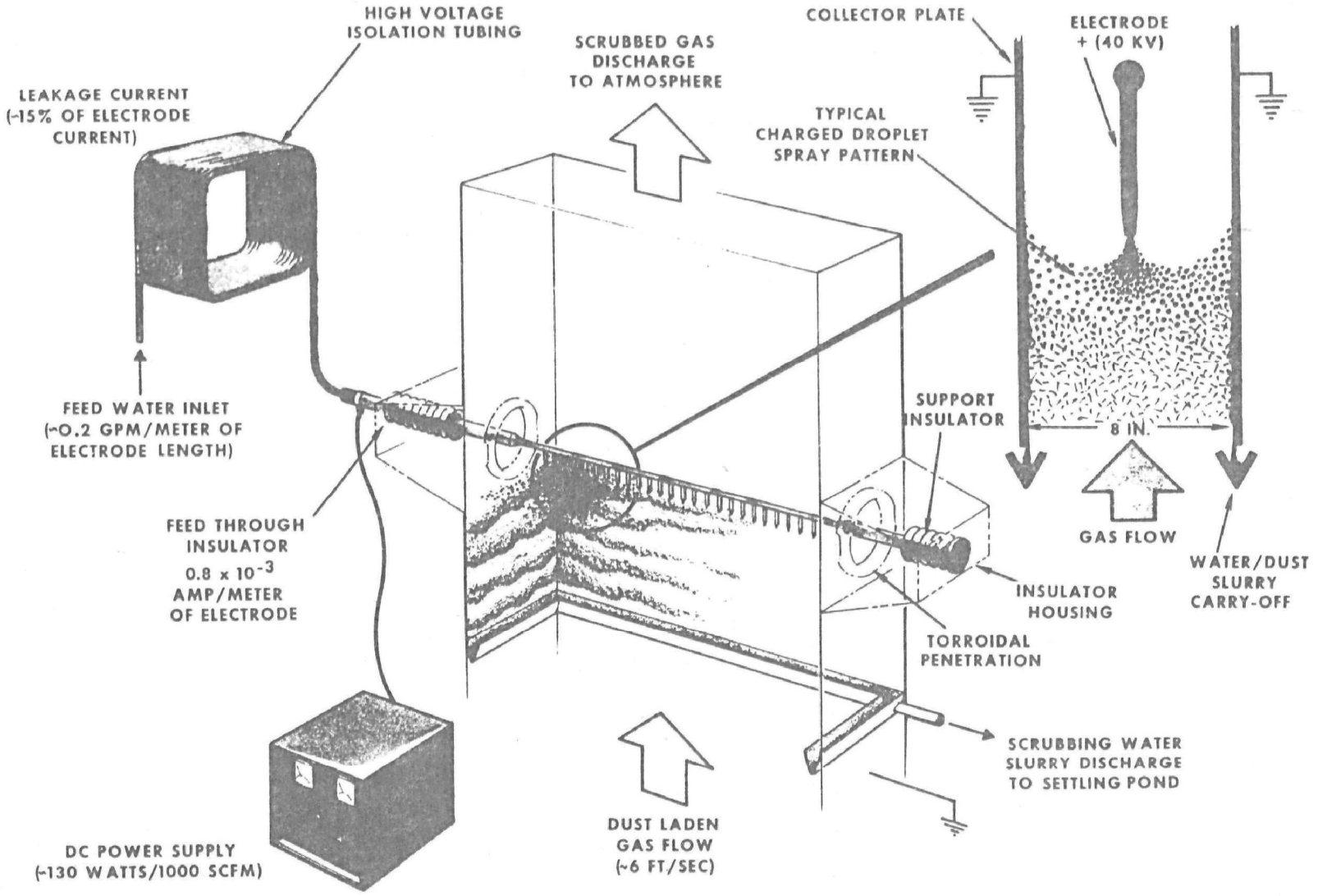

Figure 6. TRW Systems Charged Droplet Scrubber operating principle

particles to overcome aerodynamic forces which would normally sweep them around the droplet with the flow stream. As a result of the forces, they are able to approach the droplet more closely and thus interact. This close approach leads to enhancement of particulate collection by agglomeration and by electrical interaction. The result is an improvement of overall efficiency as compared to conventional scrubbing devices.

Table 1 shows a set of design parameters and operating conditions for a 1000 acfm TRW Charged Droplet Scrubber. These operating conditions are nominal, and represent unspecified operating conditions for results presented in this paper. Figure 7 shows the general configuration of a three-stage, three-module CDS mounted for preliminary testing.

Table 1. OPERATING CONDITIONS FOR TRW/CDS

Number of stages	3
Volume flow	1000 acfm (1700 m^3/hr)
Flue velocity	5 ft/sec (1.5 m/sec)
Duct cross section	3.6 sq ft (0.33 m^2)
Spray nozzle spacing	1.75 inch (4.5 cm)
Active electrode length	128 inch (3.25 m)
Electrode-to-wall spacing	3 inch (8 cm)
Spray nozzle o.d.	0.050 inch (1.25 mm)
Operating voltage	45 kV
Operating current	6 milliamp
Electrode inlet pressure	4 inch H_2O (1000 N/m^2)
Scrubbing water flow	0.4 gpm (1.5 liter/min)
Wall wash flow	1.2 gpm (4.5 liter/min)
Water conductivity	400-700 μmho/cm
Leakage resistance	>10 megohm

RESULTS

Experimental results were obtained on three different scales. Research scale measurements were made on a small, fully instrumented unit in the lab. These measurements included droplet formation and distribution photography, droplet velocity measurements, and current density measurements. A larger bench scale unit was used to directly measure collection efficiencies of a lab-generated, size-controlled fume. Finally, pilot scale measurements have been made to determine collection efficiencies in a field environment.

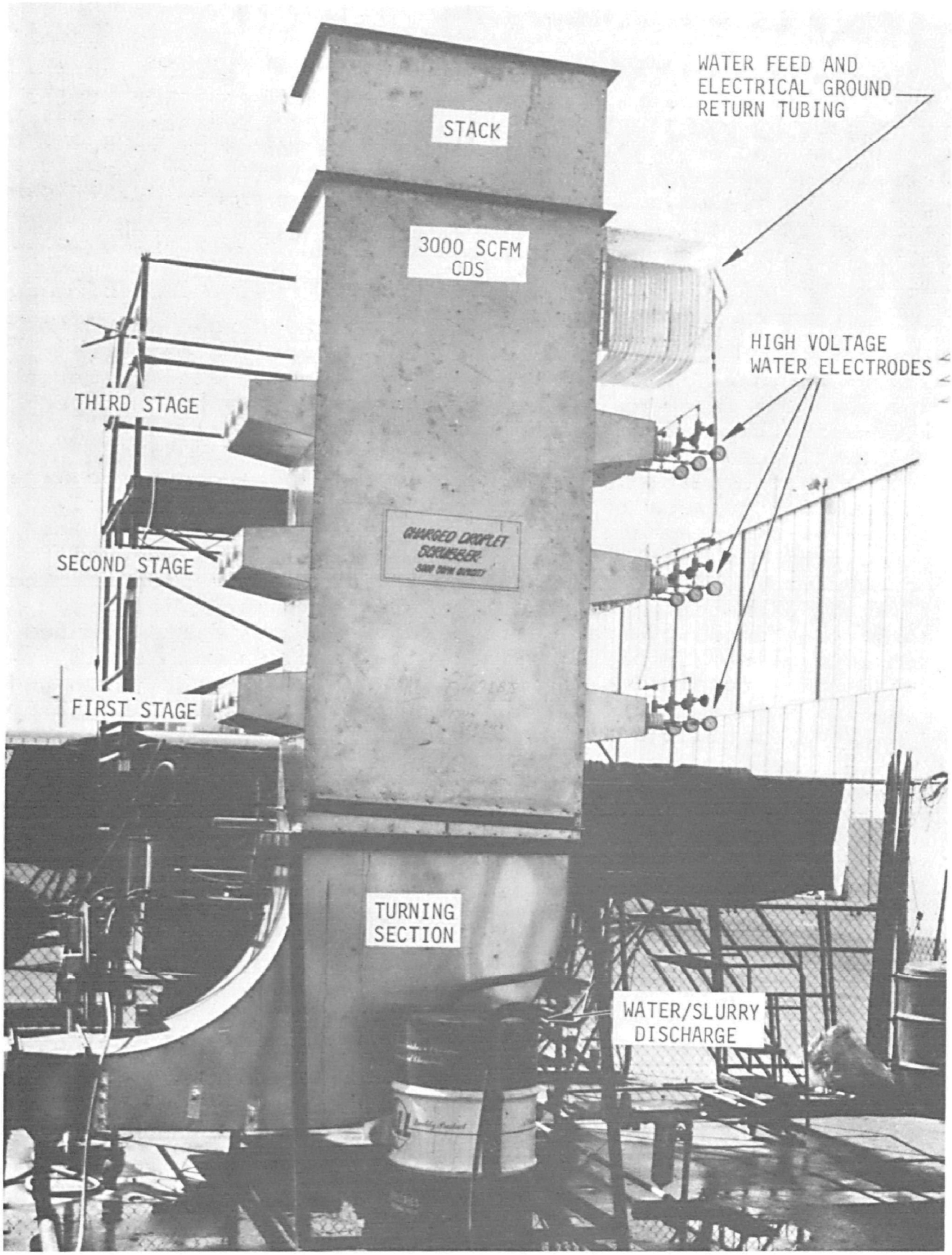

Figure 7. 3000 acfm (5100 m^3/hr) Charged Droplet Scrubber, pilot scale

RESEARCH SCALE MEASUREMENTS

Enlarged photographs of the scrubbing volume around a spray tube tip were made in a research scale scrubber. The photos were made by backlighting the scene with a flash lamp of 1-microsecond exposure time. A five-tube array of spray tubes was used, both for 18 and 22 gauge tube sizes. The extracting field was at the corona breakdown limit and the average field through the scrubbing volume was 5 kV/cm. The nominal water flow rate through a 22 gauge spray tube was 0.066 cc/sec, and through an 18 gauge tube was 0.22 cc/sec.

The photographs reveal mechanisms by which charged droplets are formed in electrohydrodynamic spraying. The water is drawn out in a filament from the spray tube by electrostatic forces. The filament is formed from a meniscus which generally wets the outside of the spray tube. The filament is constantly changing position and configuration as it is driven by fluctuations in the local field due to space charge. This action is seen in Figure 8. Figure 9 shows the early stages of disintegration of a portion of filament that separated from the main column. Charged droplets are sprayed off the ends of the column and from kinks in the middle. The filament diameter may change size at the kinks. Figure 10 shows the remnants of a liquid column that has disintegrated completely into droplets. Figure 11 was taken with an 18 gauge spray tube and shows several very large, weakly charged droplets. This figure has many examples of filament break-up processes, including Rayleigh instability.

These photographs and others were counted for droplet number density and size distribution. The size distributions were found to be approximated by log-normal, with a most-probable size near that of a particle with a Rayleigh limited surface charge density and a formation field near corona breakdown. This confirmed earlier conjectures concerning droplet size. Table 2 gives log-normal distribution parameters for typical sample counts from 22 gauge and 18 gauge spray tubes.

The photographs were also counted for number density distribution. The overall number density for nominally operating 22 gauge spray tubes was 42 droplets per cubic centimeter, with a rather large standard deviation of 30. The average number density from 18 gauge spray tube pictures was 19 ±4 droplets per cubic centimeter.

Droplet velocities in the scrubber were measured using a helium-neon laser velocimeter of the type described by Farmer.[7] Droplet size could not be correlated with velocity

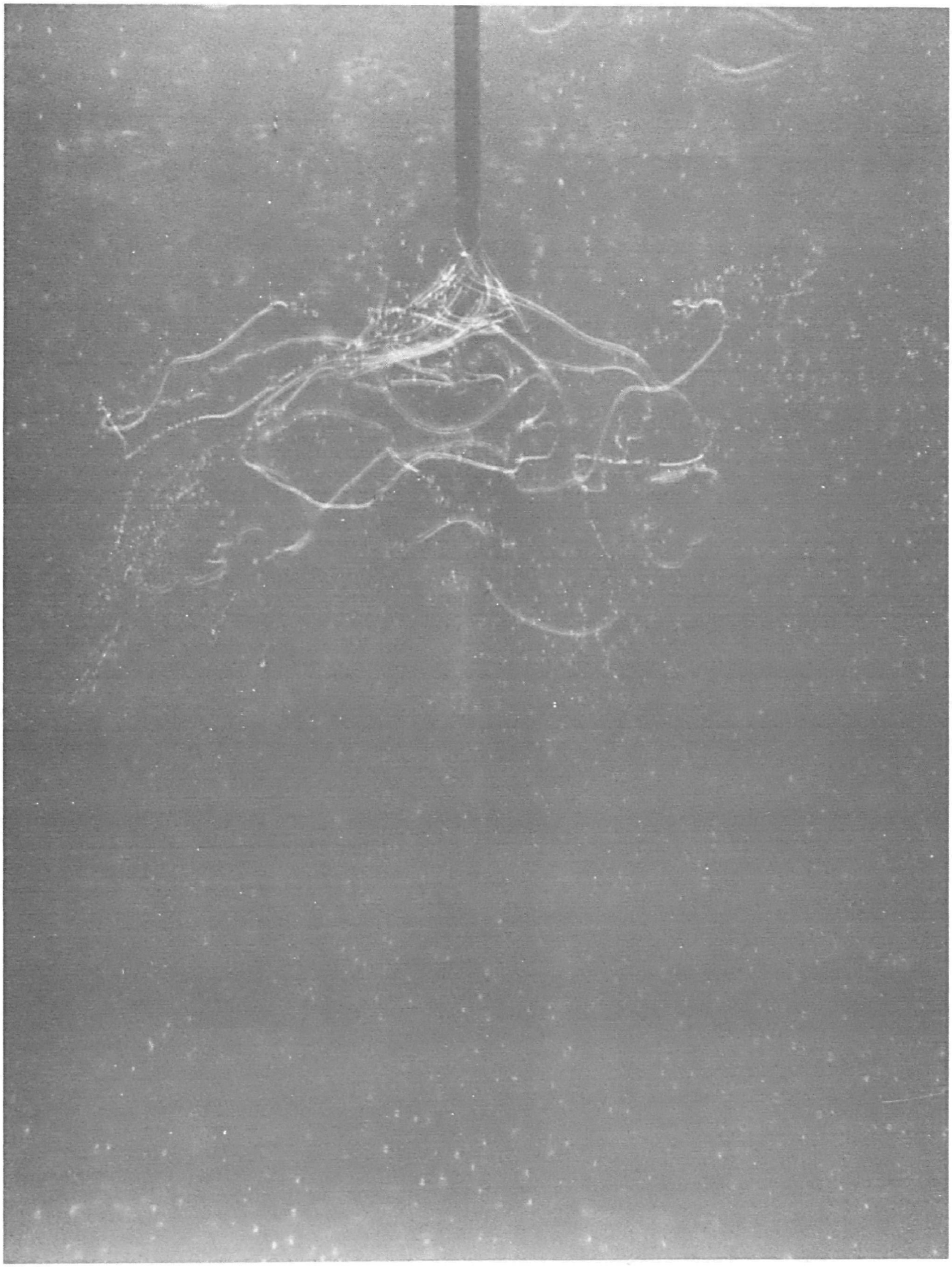

Figure 8. Droplet formation by electrohydrodynamic spraying, 22 guage spray tube, 4 exposures at 1/15-second intervals

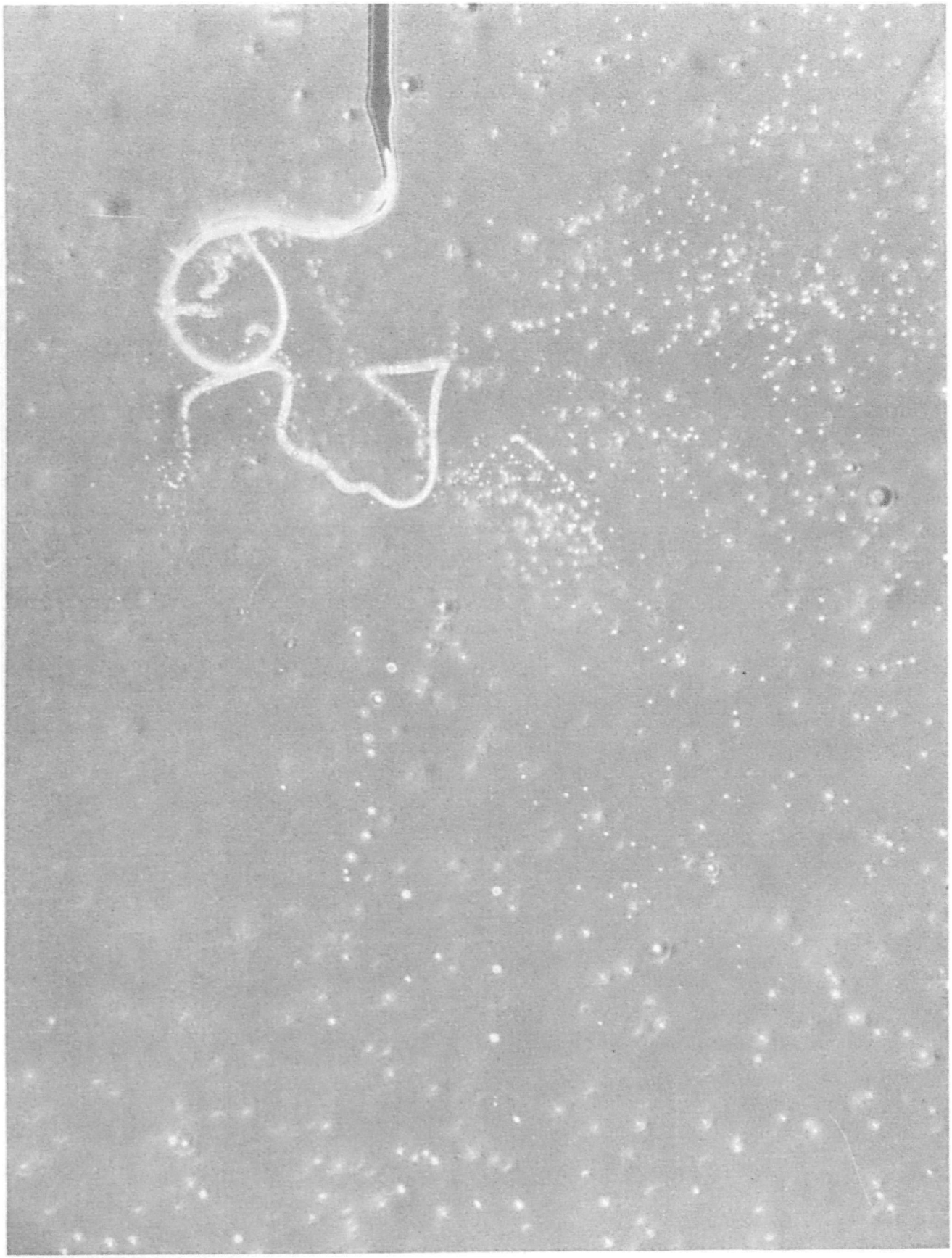

Figure 9. Droplet formation, early stages, 22 gauge spray tube

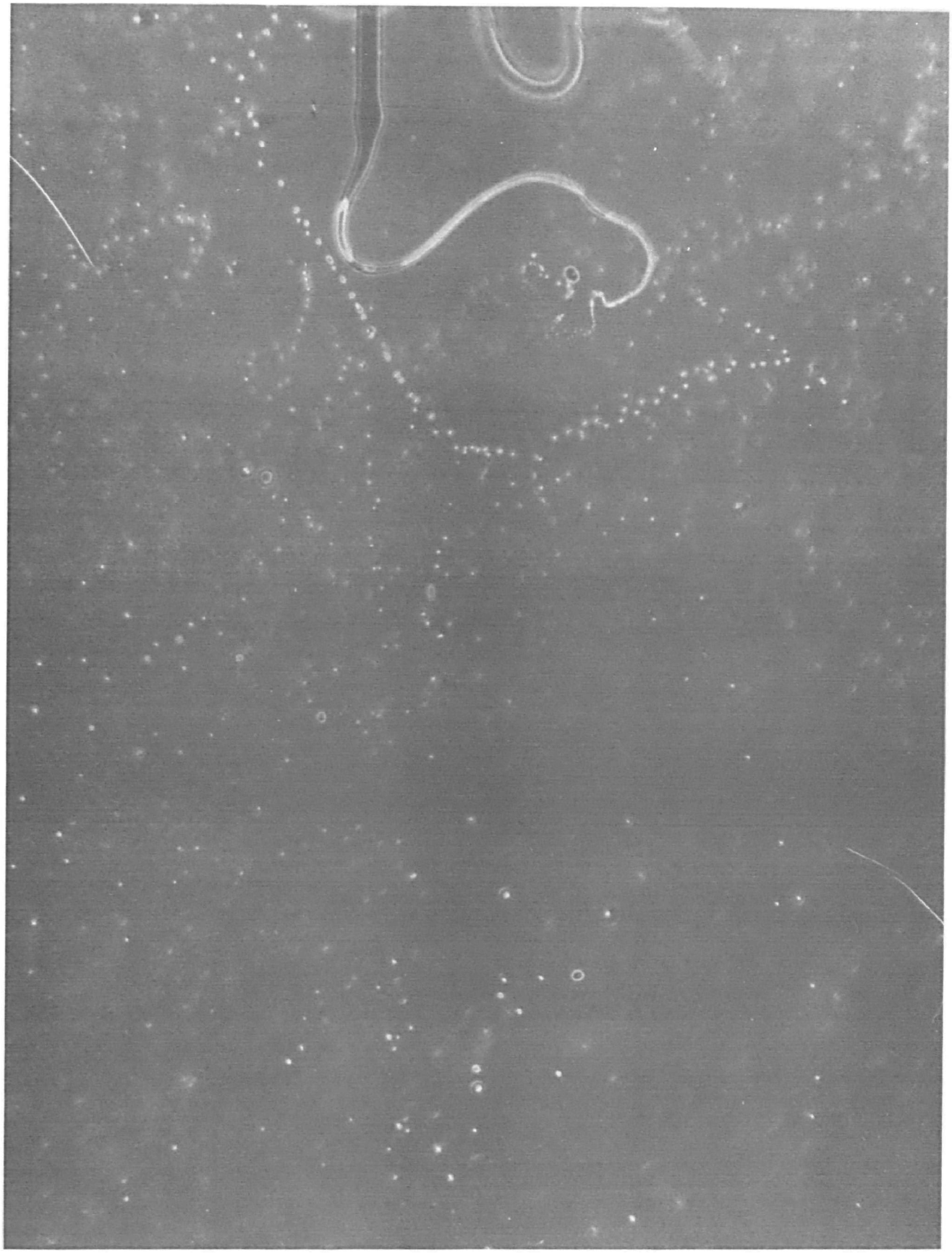

Figure 10. Droplet formation, later stages, 22 gauge spray tube

Figure 11. Droplet formation, filament breakup, 18 gauge spray tube

Table 2. LOG-NORMAL DISTRIBUTION PARAMETERS FOR TWO SIZE DISTRIBUTIONS OF CHARGED DROPLETS

Spray tube size	22 Gauge	18 Gauge
Modal radius (microns)	59.	88
Mass-mean radius (microns)	156.	212
Geometric mean radius (microns)	88.	125
Mean radius (microns)	105.	149
Geometric standard deviation	1.86	1.81
Sample size	165	79
Spray tube o.d. (mm)	0.712	1.27
Spray tube i.d. (mm)	0.39	0.84

in this experiment. For each experimental condition, the maximum velocity component in the velocimeter plane (normal to the scrubber collecting walls) was found. This was assumed to be the maximum velocity of the most effective, most frequently occurring droplets.

The maximum velocity component seen for both the 120-micron droplets and the 180-micron droplets was about 30 m/sec. The maximum measured velocity component was also the most prevalent. The velocity was about one-tenth that expected for Stokes' law drag, and showed that the droplet motion is governed by a drag coefficient in the intermediate flow regime. Stokes' law drag is

$$C_D = \frac{24}{N_{RE}}$$

where N_{RE} is the Reynolds number of the droplet. The velocity trajectories of both droplets were then calculated using the appropriate intermediate drag law:

$$C_D = \frac{18.5}{N_{RE}^{0.6}}$$

Over a path length of 0.1 meter (half the scrubber width) the smaller droplets just reach their terminal velocity of 32 m/sec, while the larger droplets reach the same velocity while still accelerating, but strike the collecting wall.

A typical current density profile, in the direction of gas flow, is shown in Figure 12. The current density profiles were measured with a series of electrically isolated collecting strips embedded in the scrubber wall.

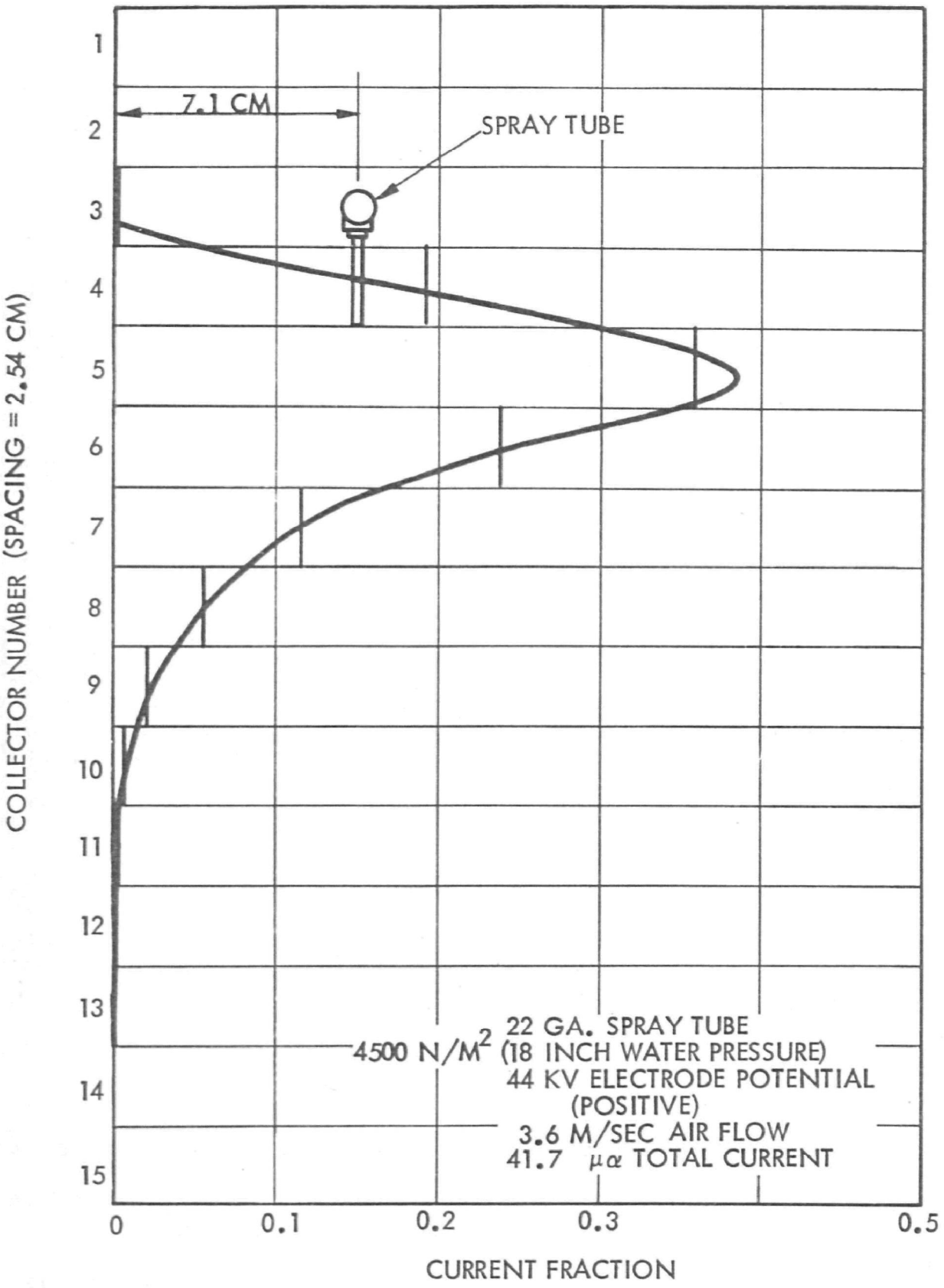

Figure 12. Typical current density profile on the wall of the scrubber

There was little change in the current collected with and without water flowing, but at the same voltage, for two reasons. One is that the droplet formation field is very close to corona breakdown, and the other is that the mobility of the droplets is no greater than that of ions. The data thus give little information about the relative droplet and corona current. Corona-to-droplet current ratios were previously estimated at about 30 percent.[3] The current profile data also indicate effective scrubbing lengths on the order of 15 centimeters.

COLLECTION EFFICIENCY MEASUREMENTS

Measurements of total and fractional collection efficiency of a TRW Charged Droplet Scrubber have been made both on a bench test scale and on a pilot plant scale. Scrubber collection efficiency was found by simultaneously sampling the inlet and outlet of the scrubber to determine the average loadings. In most cases, the loading was obtained with a direct measurement of weight. In others, a particulate number count was obtained.

A single stage, single module device with 15 spray tubes, equally spaced at 1 inch, was run at about 900 m^3/hr volume flow rate to obtain bench scale efficiency measurements. The gas stream was pre-loaded with newly dispersed aerosol from an electric-arc fume generator. The fume was zinc oxide formed from an arc between a carbon electrode and a melted zinc surface. Samples of the fume were collected and examined under an electron microscope. The particle size is a few tenths of a micron.

Total and fractional collection efficiencies were measured by filter samples taken through 0.2-micron nominal filters. The samples were weighed and were then given an individual particle count in a Royco counter. The highest measured efficiency was 70 percent at a 10 centimeter electrode-to-wall spacing and a 1 meter/sec flue velocity. This efficiency was achieved over a broad range of inlet loadings, from 0.001 to 0.01 grain per cubic foot (0.0023 to 0.023 milligram per liter). Degradation of efficiency occurs at higher loadings with the smaller spray tubes (22 gauge) because of space charge effects. The most marked effect on efficiency was found to be with collector plate spacing. Efficiency dropped to about 35 percent with a 30 percent increase in plate spacing.

The Royco particle counter was used to obtain fractional efficiencies in size categories down to 1 micron. Fractional efficiency was found to be uniform and independent of

particle size. A pair of Anderson eight-stage samplers were used to obtain efficiencies in the sub-half micron size range. These proved to be slightly degraded, an efficiency of 50 percent being measured at the 1 meter/sec flue velocity.

Several pilot plant tests have been conducted with CDS units rated at 1700 nm^3/hr (1000 scfm). Such tests have been conducted both in the field and under simulated process conditions.

A series of tests were run by redispersing a size-graded talc into a temperature-controlled airstream. The talc was graded by the manufacturer (United Sierra) at 1.8-micron mean size. It was analyzed to have about 40 percent by weight of the distribution under 2 microns in diameter. The particulate was metered by a speed-controlled auger and aspirated into the process air stream.

Table 3 shows performance data obtained during these tests. Scrubbing efficiency was obtained by simultaneously sampling the inlet and outlet dust loadings of the scrubber. Inlet sampling was done isokinetically with a 1/2-inch probe followed by a 1.0-micron nominal ceramic filter, a water vapor condenser, and a dry gas meter. The scrubber outlet was sampled super-isokinetically with a high volume sampler and a 0.2-micron paper filter.

The data show that collector plate spacing or, perhaps more appropriately, specific collection area has a very significant effect on performance. This effect is due to a lower mean drift time for the particulate to the collection plate. Increasing specific water flow improves the efficiency within the range investigated. Increasing velocity tends to degrade it. The data also show there may be an advantage to operating at negative potential if the increased specific power can be tolerated.

SUMMARY

Because normal scrubbing mechanisms are augmented by electrostatic mechanisms, charged droplet scrubbers are important devices for control of particulates in the 0.1 to 1.0 micron range. Among the more beneficial effects are electrically augmented impact scrubbing and charge exchange without impact. Both these effects are enhanced by a large electrically induced relative velocity between droplets and particles.

Table 3. THREE-STAGE CDS PERFORMANCE DATA - UNITED SIERRA TALC (1.8 MICRON MEAN SIZE)

Test no.	Gas temp. (°C)	Gas velocity (m/sec)	Collector spacing (m)	Voltage (kV)	Collector current (mA)	Inlet loading (g/m^3)	Specific power ($W/m^3/hr$)	Specific water flow (l/m^3)	Scrubbing efficiency (%)
1	61	1.22	0.15	41	3.0	0.796	0.147	0.093	97.6
2	61	1.22	0.15	41	3.1	0.796	0.153	0.093	98.7
3	61	1.22	0.15	41	3.1	0.796	0.153	0.093	99.5
4	61	1.22	0.15	-50	6.0	0.796	0.365	0.093	99.7
5	61	1.22	0.15	-50.5	6.3	0.796	0.388	0.093	99.8
6	21	1.22	0.10	42.5	6.0	1.60	0.470	0.150	99.91
7	21	1.22	0.10	42.5	6.0	1.60	0.470	0.150	99.93
8	24.3	1.22	0.10	20	1.0	2.69	0.037	0.158	99.59
9	24.3	1.22	0.10	30	2.5	2.69	0.139	0.158	99.94
10	23.8	2.13	0.10	30	2.3	0.40	0.072	0.088	97.63
11	81.5	1.22	0.15	43	3.5	0.704	0.182	0.111	97.38
12	81.5	1.22	0.15	50	4.8	0.704	0.294	0.108	96.40

Electrohydrodynamic spraying is capable of giving high densities of droplets in the 100-micron size range, and charged to near their upper stability limit. The droplet distribution is stable, and the most probably occurring droplet is the most highly charged. Scrubbing efficiencies of 30 to 70 percent per stage have been demonstrated in the sub-micron particulate size range. The scrubbing efficiency is a strong function of the collector plate spacing.

REFERENCES

1. Melcher, J. R., and K. S. Sachar. Charged Droplet Technology for Removal of Particulates from Industrial Gases. Final Report. Massachusetts Institute of Technology, Contract 68-002-001, Environmental Protection Agency. August 1, 1971.

2. Peek, F. W., Jr. Dielectric Phenomena in High-Voltage Engineering. 3rd ed. New York, McGraw-Hill, 1929. Chapter 4.

3. Lear, C. W., W. F. Krieve, and E. Cohen. Application of Charged Droplet Scrubbing to Fine Particle Control. TRW Systems Group, Contract 68-02-1345, Environmental Protection Agency. Report to be issued.

4. Rayleigh, Lord. Proc. Roy. Soc. (London) 29 (71):1879.

5. Rayleigh, Lord. Proc. London Math. Soc. 10 (4):1878.

6. Suits, C. G. (ed.). Collected Works of Irving Langmuir, Volume 2, Cloud Nucleation. New York, Pergamon, 1962.

7. Farmer, W. M. Measurement of Particle Size, Number Density, and Velocity Using a Laser Interferometer. Appl. Opt. 11:2603-2612, November 1972.

CLOSING COMMENTS

Dennis C. Drehmel
Environmental Protection Agency
Research Triangle Park, North Carolina

Historically, electrostatic precipitators have been reliable and effective particulate abatement devices for controlling more than 90% of the mass of particles in power generation and non-ferrous smelter effluent gas streams. However, the fine particles (those with diameters less than 3 microns) constitute a major portion of those particles which are not controlled. As observed by Dr. Burchard, it is these particles which cause poor visibility, constitute a health hazard, act as transport vehicles for gaseous pollutants, and may be active chemically and catalytically. As increasingly higher efficiencies have been required for recent precipitator designs, the removal of fine particles has improved. Mr. McCain reported fractional efficiency data for full scale electrostatic precipitators which show at least 85% removal in the submicron range with the minimum efficiency at 0.3 to 0.5 micron. This minimum is predictable from theory. Besides theoretical limitations, collection efficiencies are low in field installations because the precipitator is not operated in accord with the original design or is not designed to avoid power supply or gas flow distribution problems.

With the advent of SO_2 emission standards, the burning of low sulfur coals for power generation has accrued increasing interest. Unfortunately, such coals are often high in ash with a high resistivity at normal ESP operating temperatures. Since high resistivity degrades precipitator performance, several approaches have been proposed: careful designs of larger cold precipitators; hot precipitators; flue gas conditioning. During the panel discussion on this topic it was agreed that each application must be considered individually for selecting the proper approach. Cold-side precipitators have the clear advantage of treating a lower

gas volume while hot-side precipitators are relatively insensitive to ash resistivity changes because of, for example, coal compositional changes.

While power generation accounts for a third of the less than 3 micron particulate emissions, sources such as iron and steel mills, Kraft pulp mills, and ferro-alloy plants are also important submicron particulate emitters. Consequently, in the Control Systems Laboratory (CSL) of EPA there is interest in new applications of improved precipitator designs or in new concepts which will extend the applicability of electrostatic devices. Approaches utilizing new charging techniques, wet precipitators, or electrostatic scrubbers, as described at this symposium, are part of a body of technology which is not yet fully developed and utilized. It was the intent of CSL in sponsoring this symposium to stimulate the identification and development of this body of new technology. By means of an active program of identification and development of new concepts, the high fine particle removal efficiencies available for high sulfur fly ash will become technically and economically feasible for most other important sources of fine particles.

METRIC CONVERSION FACTORS

Non-Metric	Multiplied by:	Yields Metric
inches, U. S. (in.)	2.540	centimeters (cm)
feet, U. S. (ft)	0.3048	meters (m)
square inches, U. S. ($in.^2$)	6.452	square centimeters (cm^2)
square feet, U. S. (ft^2)	0.09290	square meters (m^2)
cubic feet, U. S. (ft^3)	0.02832	cubic meters (m^3)
tons, short	0.9072	tons, metric
pounds, avoirdupois (lb)	0.4536	kilograms (kg)
grains (gr)	0.06480	grams (g)
gallons, U. S. (gal)	3.785	liters (l)
feet/minute (ft/min)	0.005080	meters/second (m/sec)
cubic feet/minute (ft^3/min)	0.0004720	cubic meters/second (m^3/sec)
grains/cubic foot (gr/ft^3)	2.289	grams/cubic meter (g/m^3)
pounds/square inch (psi)	0.06805	atmospheres (atm)
inches of water [at 4°C (39.2°F)]	0.002458	atmospheres (atm)
horsepower (hp)	0.7457	kilowatts (kW)
degrees Fahrenheit (°F)	$\frac{5}{9}$(°F - 32)	degrees Centigrade (°C)

TECHNICAL REPORT DATA *(Please read Instructions on the reverse before completing)*		
1. REPORT NO. EPA-650/2-75-016	2.	3. RECIPIENT'S ACCESSION NO.
4. TITLE AND SUBTITLE Symposium on Electrostatic Precipitators for the Control of Fine Particles		5. REPORT DATE January 1975 6. PERFORMING ORGANIZATION CODE
7. AUTHOR(S) Charles E. Feazel (Editor)		8. PERFORMING ORGANIZATION REPORT NO. SORI-EAS-75-056 Project 3294-1
9. PERFORMING ORGANIZATION NAME AND ADDRESS Southern Research Institute 2000 Ninth Avenue South Birmingham, Alabama 35205		10. PROGRAM ELEMENT NO. 1AB012; ROAP 21ADL-034 11. CONTRACT/GRANT NO. 68-02-1308 (Task 14)
12. SPONSORING AGENCY NAME AND ADDRESS EPA, Office of Research and Development NERC-RTP, Control Systems Laboratory Research Triangle Park, NC 27711		13. TYPE OF REPORT AND PERIOD COVERED Proceedings 14. SPONSORING AGENCY CODE
15. SUPPLEMENTARY NOTES		

16. ABSTRACT The papers in these proceedings, prepared by investigators active in research on electrostatic precipitators (ESPs), describe recent advances in ESP technology, especially in the control of fine particles (those less than 1-2 micrometers in diameter) in industrial emissions. Data such as fractional collection efficiency measurements are presented that can be used to help define the capability of ESPs for the control of fine particles. Techniques for the sizing and design of ESPs, including a theoretically based mathematical model of ESP performance, and the selection of power supplies to improve performance and reliability are discussed. Methods for combatting the problem of collection high-resistivity fly ash from the combustion of low-sulfur coal that are described include the operation of ESPs at both lower and higher than usual flue-gas temperatures, and the conditioning of fly ash by injection of sulfur trioxide, ammonia, or sulfamic acid into the flue gas. Performance data are presented on ESPs for the control of fumes from kraft pulp mill recovery boilers and on wet ESPs in aluminum reduction plants and other industrial applications. Research on electrostatic and radiation charging of fine particles, on corona quenching by particle space charge, and on charged-droplet scrubbers is discussed.

17. KEY WORDS AND DOCUMENT ANALYSIS			
a. DESCRIPTORS		b. IDENTIFIERS/OPEN ENDED TERMS	c. COSATI Field/Group
Air Pollution Electrostatic Precipitators Dust Control Measurement Mathematical Models Power Supplies Fly Ash		Air Pollution Control Stationary Sources Fine Particles Fractional Collection Efficiency	13B 21B 09C 14B 12A
18. DISTRIBUTION STATEMENT Unlimited		19. SECURITY CLASS *(This Report)* Unclassified 20. SECURITY CLASS *(This page)* Unclassified	21. NO. OF PAGES 501 22. PRICE

EPA Form 2220-1 (9-73)